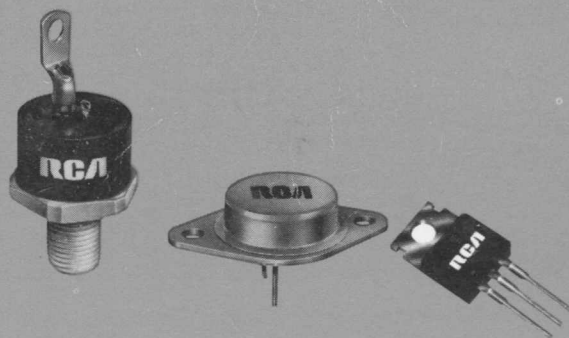


Thyristor and Rectifier Manual

RCA Solid
State



TRM-445

\$5.00 Optional Price



Thyristor and Rectifier Manual

This Manual is intended as a guide to the selection and use of silicon rectifiers and thyristors (triacs and silicon controlled rectifiers) for a variety of power switching and control applications. It covers the general physical theory, maximum ratings, electrical characteristics, packages, and handling and mounting of silicon rectifiers, silicon controlled rectifiers, and triacs. The main emphasis, however, is on circuit applications of these devices. Device selection criteria and design examples are given for a broad range of circuits, including dc power supplies, voltage regulators, ac power controls, television horizontal-deflection systems, and ignition systems. An up-to-date listing of thyristors and rectifiers currently available from RCA Solid State Division as standard commercial products is also included.

This Manual is a basic reference text that will be found useful by engineers, technicians, educators, students, hobbyists, and other interested in the operation, capabilities, and circuit applications of thyristors and rectifiers.

RCA Solid-State Division Somerville, N.J. 08876

*Copyright 1975 by RCA Corporation
(All rights reserved under Pan-American Copyright Convention)*

Printed in U.S.A. 8/75

Contents

	Page
General Physical Theory	3
Semiconductor Materials, P-N Junctions, Basic Energy Relationships, Rectifier Potential-Energy Analysis, Thyristor Potential-Energy Analysis, Thyristor Equivalent-Model Analysis	
Thermal Considerations	29
Basic Thermal System, Thermal-Stability Requirements, Thermal Impedance, Selection of External Heat Sinks, Thermal-Fatigue Considerations	
Packages, Handling, and Mounting	52
General Considerations, Low- and Medium-Power Rectifier Packages, Flexible-Lead Thyristor Packages, Flanged-Case Thyristor Packages, Stud Packages, Press-Fit Packages, VERSAWATT Thyristor Packages	
Silicon Rectifiers	70
Electrical Characteristics, Maximum Ratings, Multiple Rectifier Connections, Fast-Recovery Rectifiers, Other Special-Function Rectifiers	
Basic Thyristor Design and Rating Factors	99
Pellet Structures, Principal Voltage-Current Characteristics, Effect of Gate Signal on Breakover Voltage, Ratings and Limiting Characteristics, Reliability, Product Matrices	
Thyristor Gating and Switching Requirements	138
Gate Characteristics, Trigger-Circuit Requirements, Switching Characteristics, Snubber Networks	
Thyristor Triggering	177
Phase Control, Zero-Voltage Switching, Basic Triggering Techniques, Triggering Devices, Isolated Trigger Circuits, Integrated-Circuit Zero-Voltage Switch	
Heating Controls	206
Incandescent Lighting Controls	223
Motor Controls	237
Triac Controls for Three-Phase Power Systems	253
DC Power Supplies	262
Rectifier Circuits, Filter Networks, Regulated DC Power Supplies Using Thyristor Pass Elements	
AC Voltage Regulator	292
Circuit Operation, Heater-Voltage Regulator, Line-Voltage-Regulated DC Power Supply	
SCR Inverters and Converters	301
SCR Horizontal Deflection Systems	314
Standards for Scanning and Synchronization, Analysis of Basic Deflection Circuit, Auxiliary Deflection-System Functions, Functional Description of SCR Deflection System, SCR Deflection Circuits for Color TV Receivers, SCR Deflection System for Monochrome TV Receivers	
Capacitive-Discharge Ignition Systems	350
Basic Considerations for Automotive Systems, Basic Capacitive-Discharge Systems, Types of Capacitive-Discharge Systems, Automotive Ignition System	
Index to RCA Thyristors and Rectifiers	368

Information furnished by RCA is believed to be accurate and reliable. However, no responsibility is assumed by RCA for its use; nor for any infringements of patents or other rights of third parties which may result from its use. No license is granted by implication or otherwise under any patent or patent rights of RCA.

General Physical Theory

Silicon rectifiers and thyristors (silicon controlled rectifiers and triacs) are, in essence, merely solid-state switches. A rectifier is a simple unidirectional device that acts as an open switch in one direction and as a closed switch in the other direction. A silicon controlled rectifier is designed to operate as an open switch in one direction and, depending on circuit operating conditions, as either an open or a closed switch in the other direction. A triac is a completely bidirectional switch that, as demanded by circuit logistics, may be either open or closed in either direction.

Silicon rectifiers and thyristors are widely used in the rectification, switching, and control of ac power in applications such as dc power supplies, switching regulators, converters and inverters, lamp dimmers and flashers, heating controls, motor speed controls, capacitive-discharge ignition systems, and horizontal deflection systems for television receivers. These solid-state devices offer the advantage of low cost, light weight, small package size, excellent voltage and current capabilities, and reliability which

exceeds that of their electron-tube and electromechanical counterparts. The basic voltage-current relationships that permit silicon rectifiers and thyristors to provide the switching action required in such a broad range of power applications can be explained by a brief review of the properties of semiconductor materials and junctions and an analysis of the potential energies across the junctions formed by the layers of semiconductor material used in the construction of these devices.

SEMICONDUCTOR MATERIALS

Unlike other electron devices, which depend for their functioning on the flow of electric charges through a vacuum or a gas, solid-state devices make use of the flow of current in a solid. In general, all materials may be classified into three major categories—conductors, semiconductors, and insulators,—depending upon their ability to conduct an electric current. As the name indicates, a semiconductor material has poorer conductivity than a conductor, but better conductivity than an insulator.

The materials most often used in semiconductor devices is silicon.

Resistivity

The ability of a material to conduct current (conductivity) is directly proportional to the number of free (loosely held) electrons in the material. Good conductors, such as silver, copper, and aluminum, have large numbers of free electrons; their resistivities are of the order of a few millionths on an ohm-centimeter. Insulators such as glass, rubber, and mica, which have very few loosely held electrons, have resistivities as high as several million ohm-centimeters.

Silicon lies in the range between these two extremes, as shown in Fig. 1.

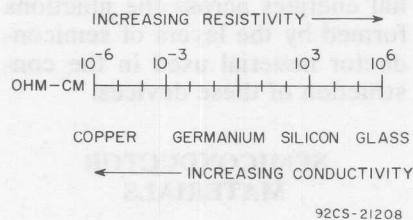


Fig. 1—Resistivity of typical conductor, semiconductor, and insulator.

Pure silicon has a resistivity, in the order of 60,000 ohm-centimeters at room temperature (this resistivity decreases rapidly as the temperature rises). As used in solid-state devices, however, silicon contains carefully controlled amounts of certain impurities which reduce its resistivity to values in the range from 0.01 to 1000 ohm-centimeters, depending upon the application.

Impurities

Carefully prepared semiconductor materials have a crystal structure. In this type of structure, which is called a lattice, the outer or valence electrons of individual atoms are tightly bound to the electrons of adjacent atoms in electron-pair bonds, as shown in Fig. 2. Because such a

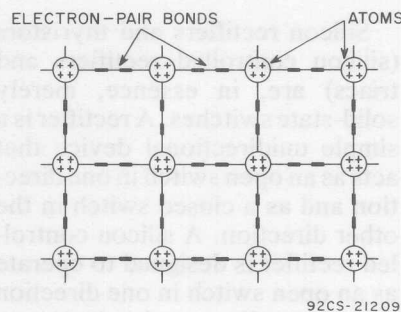


Fig. 2—Crystal lattice structure.

structure has no loosely held electrons, semiconductor materials are poor conductors under normal conditions. In order to separate the electron-pair bonds and provide free electrons for electrical conduction, it would be necessary to apply high temperature or strong electric fields.

Another way to alter the lattice structure and thereby obtain free electrons, however, is to add small amounts of other elements having a different atomic structure. By the addition of almost infinitesimal amounts of such other elements, called **impurities**, the basic electrical properties of pure semiconductor materials can be modified and controlled. The ratio of impurity to the semi-

conductor material is usually extremely small, in the order of one part in ten million.

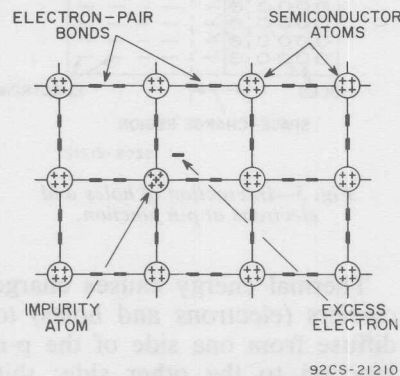
When the impurity elements are added to the semiconductor material, impurity atoms take the place of semiconductor atoms in the lattice structure. If the impurity atoms added have the same number of valence electrons as the atoms of the original semiconductor material, they fit neatly into the lattice, forming the required number of electron-pair bonds with semiconductor atoms. In this case, the electrical properties of the material are essentially unchanged.

When the impurity atom has one more valence electron than the semiconductor atom, however, this extra electron cannot form an electron-pair bond because no adjacent valence electron is available. The excess electron is then held very loosely by the atom, as shown in Fig. 3, and requires only slight excita-

tion to break away. Consequently, the presence of such excess electrons increase the conductivity of the material, i.e., its resistance to current flow is reduced.

Impurity elements which are added to silicon crystals to provide excess electrons include phosphorus, arsenic, and antimony. When these elements are introduced, the resulting material is called **n-type** because the excess free electrons have a negative charge. (It should be noted, however, that the negative charge of the electrons is balanced by an equivalent positive charge in the center of the impurity atoms. Therefore, the net electrical charge of the semiconductor material is not changed.)

A different effect is produced when an impurity atom having one less valence electron than the semiconductor atom is substituted in the lattice structure. Although all the valence electrons of the impurity atom form electron-pair bonds with electrons of neighboring semiconductor atoms, one of the bonds in the lattice structure cannot be completed because the impurity atom lacks the final valence electron. As a result, a vacancy or **hole** exists in the lattice, as shown in Fig. 4. An electron from an adjacent electron-pair bond may then absorb enough energy to break its bond and move through the lattice to fill the hole. As in the case of excess electrons, the presence of holes encourages the flow of electrons in the semiconductor material; consequently, the conductivity is increased and the resistivity is reduced.



92CS-21210

Fig. 3—Lattice structure on n-type material.

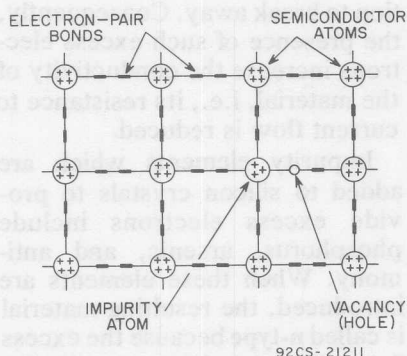


Fig. 4—Lattice structure of p-type material.

The vacancy or hole in the crystal structure is considered to have a positive electrical charge because it represents the absence of an electron. (Again, however, the net charge of the crystal is unchanged.) Semiconductor material which contains these holes or positive charges is called **p-type** material. P-type materials are formed by the addition of boron, aluminum, gallium, or indium.

Although the difference in the chemical composition of n-type and p-type materials is slight, the differences in the electrical characteristics of the two types are substantial, and are very important in the operation of solid-state devices.

P-N JUNCTIONS

When n-type and p-type materials are joined together, as shown in Fig. 5, an unusual but very important phenomenon occurs at the interface where the two materials meet (called the **p-n junction**). An interaction

takes place between the two types of material at the junction as a result of the holes in one material and the excess electrons in the other.

When a p-n junction is formed, some of the free electrons from the n-type material diffuse across the junction and recombine with holes in the lattice structure of the p-type material; similarly, some of the holes in the p-type material diffuse across the junction and recombine with free electrons in the lattice structure of the n-type material. This interaction or diffusion is brought into equilibrium by a small space-charge region (sometimes called the **transition region** or **depletion layer**). The p-type material thus acquires a light negative charge and the n-type material acquires a slight positive charge.

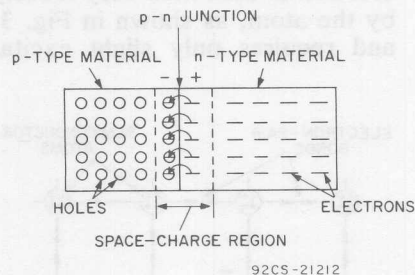
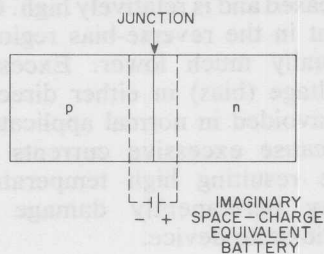


Fig. 5—Interaction of holes and electrons at p-n junction.

Thermal energy causes charge carriers (electrons and holes) to diffuse from one side of the p-n junction to the other side; this flow of charge carriers is called **diffusion current**. As a result of the diffusion process, however, a

potential gradient builds up across the space-charge region. This potential gradient can be represented, as shown in Fig. 6, by an imaginary battery connected across the p-n junction. (The battery symbol is used merely to illustrate internal effects; the potential it represents is not directly measurable.) The potential gradient causes a flow of charge carriers, referred to as **drift current**, in the opposite direction to the diffusion current.



92CS-21213

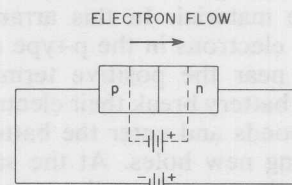
Fig. 6—Potential gradient across space-charge region.

Under equilibrium conditions, the diffusion current is exactly balanced by the drift current so that the net current across the p-n junction is zero. In other words, when no external current or voltage is applied to the p-n junction, the potential gradient forms an **energy barrier** that prevents further diffusion of charge carriers across the junction. In effect, electrons from the n-type material that tend to diffuse across the junction are repelled by the slight negative charge induced in the p-type material by the potential gradient, and holes from the p-type material are repelled by the slight positive charge induced in

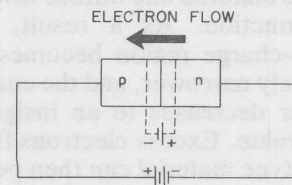
the n-type material. The potential gradient (or energy barrier, as it is sometimes called), therefore, prevents total interaction between the two types of materials, and thus preserves the differences in their characteristics.

Current Flow

When an external battery is connected across a p-n junction, the amount of current flow is determined by the polarity of the applied voltage and its effect on the space-charge region. In Fig. 7(a), the positive terminal of the battery is connected to the n-type material and the negative terminal to the p-type material. In this arrangement, the free electrons in the n-type material are attracted toward the positive terminal of the battery and away from the junction. At the same



(a) REVERSE BIAS



(b) FORWARD BIAS

92CS-21214

Fig. 7—Electron current flow in biased p-n junctions.

time, holes from the p-type material are attracted toward the negative terminal of the battery and away from the junction. As a result, the space-charge region at the junction becomes effectively wider, and the potential gradient increases until it approaches the potential of the external battery. Current flow is then extremely small because the space-charge region is essentially devoid of free charge carriers and, therefore, acts as an insulator. Consequently, almost all the applied voltage is dropped across the space-charge region, and a negligible voltage difference (electric field) exists across either the p-type or the n-type region. Under these conditions, the p-n junction is said to be **reverse-biased**.

In Fig. 7(b), the positive terminal of the external battery is connected to the p-type material and the negative terminal to the n-type material. In this arrangement, electrons in the p-type material near the positive terminal of the battery break their electron-pair bonds and enter the battery, creating new holes. At the same time, electrons from the negative terminal of the battery enter the n-type material and diffuse toward the junction. As a result, the space-charge region becomes effectively narrower, and the energy barrier decreases to an insignificant value. Excess electrons from the n-type material can then penetrate the space-charge region, flow across the junction, and move by way of the holes in the p-type material toward the positive terminal of the battery. This electron

flow continues as long as the external voltage is applied. Under these conditions, the junction is said to be **forward-biased**.

Voltage-Current Characteristic

The generalized voltage-current characteristic for a p-n junction in Fig. 8 shows both the reverse-bias and forward-bias regions. In the forward-bias region, current rises rapidly as the voltage is increased and is relatively high. Current in the reverse-bias region is usually much lower. Excessive voltage (bias) in either direction is avoided in normal applications because excessive currents and the resulting high temperatures may permanently damage the solid-state device.

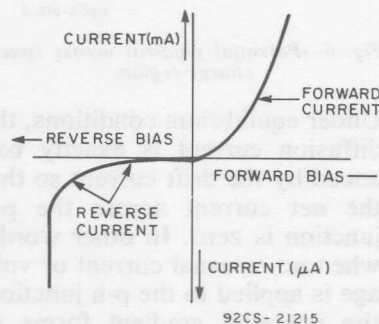


Fig. 8—Voltage-current characteristic for a p-n junction.

Rectifier Diode

The simplest type of solid-state junction device is the **rectifier diode**, which is represented by the symbol shown in Fig. 9(a). Structurally, the rectifier diode is

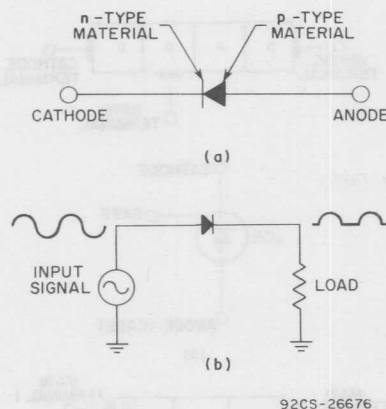


Fig. 9-(a) Schematic symbol for a solid-state diode; (b) simple diode rectifying circuit.

basically a p-n junction similar to those shown in Fig. 7. The n-type material which serves as the negative electrode is referred to as the **cathode**, and the p-type material which serves as the positive electrode is referred to as the **anode**. The arrow symbol used for the anode represents the direction of "conventional current flow" mentioned above; electron current flows in a direction opposite to the arrow.

Because the junction diode conducts current more easily in one direction than in the other, it is an effective rectifying device. If an ac signal is applied, as shown in Fig. 9(b), electron current flows freely during the positive half cycle, but little or no current flows during the negative half cycle.

One of the most widely used types of solid-state diodes is the **silicon rectifier**. These devices are available in a wide range of current capabilities, ranging

from tenths of an ampere to several hundred amperes, and are capable of operation at voltages as high as 1000 volts or more. Parallel and series arrangements of silicon rectifiers permit even further extension of current and voltage limits.

Thyristor Structures

If two p-type and two n-type semiconductor materials are arranged in a series array that consists of alternate n-type and p-type layers, a device is produced which behaves as a conventional rectifier in the reverse direction and as a series combination of an electronic switch and a rectifier in the forward direction. Conduction in the forward direction can then be controlled or "gated" by operation of the electronic switch. These devices, called **thyristors**, have control characteristics similar to those of thyatron tubes; more specifically, they are solid-state switches whose bistable state depends on the regenerative feedback associated with a p-n-p-n structure. Basically, this group includes any bistable solid-state device that has three or more junctions (i.e., four or more semiconductor layers) and can be switched from a high-impedance (off) state to a low-impedance (on) state, and from a low-impedance state to a high-impedance state, within at least one quadrant of the principal voltage-current characteristic.

There are several types of thyristors; these types differ primarily in the number of electrode

terminals and in the operating characteristics in the third (negative) quadrant of the voltage-current characteristic, as shown in Table I. Reverse-blocking triode thyristors, commonly called **silicon controlled rectifiers (SCR's)**, and bidirectional triode thyristors, referred to as **triacs**, are the most popular types. Fig. 10 shows the junction diagrams and schematic symbols for the SCR and the triac.

Table I—Different Types of Thyristors

No. of Terminals	Third-Quadrant Operation		
	Blocking	Conducting	Switching
2	Reverse-blocking diode thyristor	Reverse-conducting diode thyristor	Bidirectional diode thyristor
3	Reverse-blocking triode thyristor (SCR)	Reverse-conducting triode thyristor	Bidirectional triode thyristor (triac)

Silicon Controlled Rectifiers—

An SCR is a four-layer p-n-p-n device designed to provide bistable switching when operated in the forward-bias mode. As shown in Fig. 10(a), this device has three electrodes, referred to as the **cathode**, the **anode**, and the **gate**. For operation in the forward-bias mode, the anode potential must be positive with respect to the cathode. During normal operation, the SCR is turned on by application of a positive voltage to the gate electrode. The SCR then remains on,

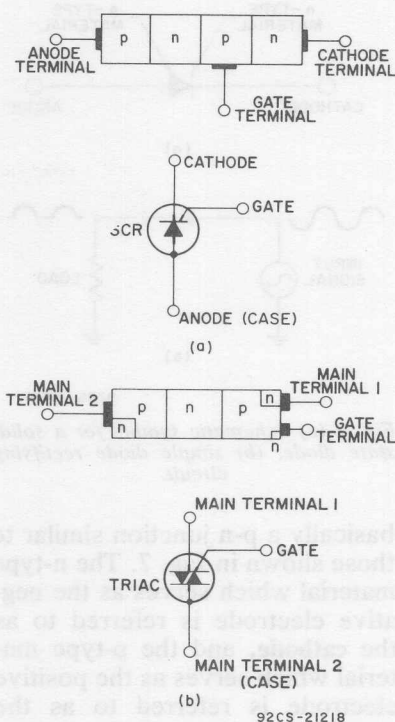


Fig. 10—Junction diagrams and schematic symbols for (a) SCR's and (b) triacs.

even though the gate voltage is removed or made negative, until the anode-to-cathode voltage is reduced to a value below that required to sustain the regenerative action necessary for forward conduction. Faster turn off can be achieved by reversal of the forward current flow.

Gate Turn-off SCR's (GTO's)—

In certain types of SCR's, interruption of main-terminal current (turn-off) can be accomplished by application of a bias voltage to the gate that is the reverse of that required to turn on the

SCR so that it removes rather than injects charge carriers. These types, which are referred to as gate-turn-off SCR's (GTO's) employ the same basic four-layer, three-junction regenerative semiconductor structure and exhibit a pulse turn-on capability similar to that of conventional SCR's. GTO devices, however, differ from conventional SCR's in that they are designed to turn off with the application of a reverse bias to the gate electrode.

Because the current-voltage characteristics of the GTO is significantly different from those of conventional SCR's a separate schematic symbol has been created for the GTO. Fig. 11 shows this symbol.

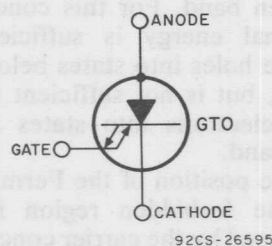


Fig. 11—Schematic symbol for a gate-turn-off SCR.

Triacs—A triac is an n-p-n-p-n device that is designed to provide bilateral switching characteristics for either polarity of applied voltage. This device as shown in Fig. 10(b), also has three electrodes, which are referred to as **main terminal No. 1**, **main terminal No. 2**, and the **gate**. The gate is specially designed so that either a positive or a negative gate voltage can trigger the triac into conduction for either polarity of the vol-

tage across the main terminals. As with conventional SCR's, however, once the triac is turned on, the gate has no further control. The device remains in the on state until the voltage across the main terminals is reduced below the value required to sustain conduction. Unlike the SCR, the triac cannot be turned off by reversal of the polarity of the voltage across the main terminals. A rapid reversal of this voltage merely causes current to flow in the opposite direction.

BASIC ENERGY RELATIONSHIPS

The electrons in a solid occupy specific electron states. Each state is defined by a precise physical location and a specific energy level and, therefore, can be occupied by only one electron at any given time. The solid contains only a finite number of electron states. Some of these states are occupied (full); others are empty. The **Fermi energy level**, E_F , is the dividing line above which most of the existing electron states are empty and below which most states are full. Conduction in a solid occurs only by movement of free charge carriers, i.e., free electrons or free holes. A free electron is one at an energy level for which most of the existing states are empty. A free hole is an empty state at an energy level for which most of the existing states are filled. Free electrons exist, therefore, only at energy levels above E_F , and free holes exist only at levels below E_F . Because electrons and holes tend

to seek the lowest available energy levels, they both move toward E_F , which is the zero energy level for both types of charge carriers. In relation to the Fermi level, therefore, electrons always tend to "fall", and holes always tend to "rise". If the charge carriers were not affected by outside influences, all free electrons and holes would eventually reach the Fermi level and disappear. A distribution of electrons above the Fermi level is maintained, however, because the thermal energy of the lattice constantly agitates the electrons to non-zero energy levels.

In the metal contact regions of a solid-state device, there is a continuous distribution of electrons about the Fermi energy level so that free holes and free electrons exist simultaneously side by side. In the semiconductor regions, there is a band of energy, called the **forbidden-energy region**, in which no electron states exist. As a free carrier tries to move through the system of metal to semiconductor to metal, it can move freely through the metal; when the carrier reaches the semiconductor, however, it encounters an obstacle, the forbidden-energy region. The carrier must either go over or under this region depending upon whether it is a free electron or a free hole. The carrier must obtain sufficient energy so that it is displaced far enough from the Fermi level to go over or under the forbidden region. If sufficient energy, such as thermal agitation or an applied voltage, is not available, the carrier is reflected back to its origin.

In silicon crystal, the forbidden region is wide enough so that at ordinary temperatures, there is not sufficient thermal energy available to distribute carriers both above and below the band. If the Fermi energy level is close to the top of the band, thermal energy is sufficient to lift electrons into states on top of the forbidden region, but is not sufficient to push holes into states below this region. As a result, the material contains many free electrons and is referred to as an n-type semiconductor because it contains mostly negative-charge carriers.

Similarly, a p-type region in the semiconductor, which contains mostly positive-charge carriers, results when the Fermi level is close to the bottom of the forbidden band. For this condition, thermal energy is sufficient to excite holes into states below the band, but is not sufficient to excite electrons into states above the band.

The position of the Fermi level in the forbidden region is determined by the carrier concentration. This concentration, in turn, is determined by both the dopant concentration and the concentration of injected carriers.

At the metal-to-semiconductor interfaces, the dopant concentration is very high. At such interfaces, the carrier concentration cannot be changed significantly by injected carriers, and the position of the Fermi level in the forbidden region is firmly fixed. In the inner semiconductor regions and near the junctions, the dopant concentration is rela-

tively low so that the total carrier concentration and, therefore, the position of the Fermi level in the forbidden region can be changed by injection of carriers from surrounding regions. These factors make the forbidden-energy region appear flexible within the body of the semiconductor but rigid at the metal-to-semiconductor contacts. This rigidity of the potential hill at the contacts prevents electrons in the metal from entering the p-type semiconductor, but allows holes to circulate freely between the metal and the p-type region; similarly, electrons can circulate freely between metal and the n-type region but holes cannot cross the metal-to-n-type-semiconductor interface.

The basic relationships and energy states described in the preceding paragraphs define the behavior of a solid-state device in the equilibrium condition, i.e., with no external bias voltages applied to the device terminals. The operation of silicon rectifiers and thyristors can be conveniently explained by analyses of the potential-energy distribution across the devices for different biasing conditions. These basic equilibrium relationships, however, point out two basic factors that must be considered in potential-energy analyses of the operation of rectifiers and thyristors under both forward- and reverse-bias conditions, as follows:

(1) The shape of the forbidden-energy region is rigid at the metal-to-semiconductor contact. The shape is determined by the

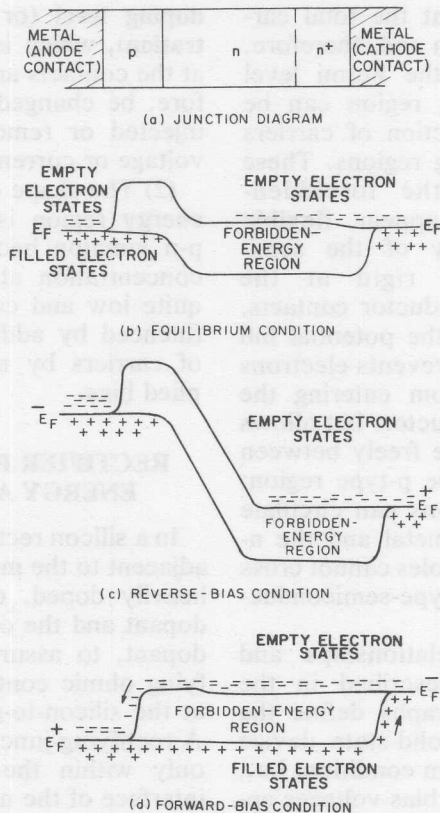
doping level (or carrier concentration), which is extremely high at the contacts and cannot, therefore, be changed by the carriers injected or removed by applied voltage or current.

(2) The shape of the forbidden-energy region is flexible at the p-n junction because the carrier concentration at the junction is quite low and can be readily influenced by addition or removal of carriers by means of an applied bias.

RECTIFIER POTENTIAL-ENERGY ANALYSIS

In a silicon rectifier, the regions adjacent to the metal contacts are heavily doped, one with p-type dopant and the other with n-type dopant, to assure that nonrectifying ohmic contacts are formed at the silicon-to-metal interfaces. A rectifying junction should exist only within the silicon, at the interface of the n-type and p-type regions. A lightly doped n-type region between the heavily doped n- and p-type regions provides the high blocking-voltage capability required of the rectifier. Because of this lightly doped region, the more heavily doped n-type region adjacent to the metal contact is referred to as the n^+ region. The silicon rectifier, therefore, is a p-n- n^+ structure.

The operation of a p-n- n^+ junction may be visualized in terms of the potential-energy diagrams shown in Fig. 12. In these diagrams, the vertical scale represents energy. An increase in electron energy is indicated by the



92CM-21220

Fig. 12—Potential-hill diagrams for various stages of rectifier operation (upward direction indicates increasing electron energy; downward direction indicates increasing hole energy).

upward direction from the Fermi energy level (E_F line), and an increase in hole energy is indicated by the downward direction from this level. Electrons are always above the E_F line and holes are always below this line, which represents the ground state or zero energy level for both types of carriers. Both electrons and holes tend to “fall” toward this level unless there is some source of energy to move them away from it. In the diagrams, free

electrons are indicated by minus (−) signs and free holes by plus (+) signs.

Fig. 12(a) shows the junction diagram for the basic p-n-n+ rectifier structure, and Fig. 12(b) shows the shape of the forbidden-energy region in the equilibrium condition. For this condition, the charge carriers do not have sufficient energy to overcome this potential barrier, except for the few electrons and holes that are normally displaced above and

below the Fermi level by the thermal energy from the silicon crystal.

Reverse-Bias Conditions

Under reverse-bias conditions, the potential energy of electrons is increased on the negatively biased side of the junction so that the energy at this end is higher, as shown in Fig. 12(c). Although the applied bias is such that it tends to push electrons from the metal into the p-type region and holes from the metal into the n-type region, no current flows because the rigidity of the forbidden-energy region at the contacts prevents such movements of the charge carriers. The applied voltage simply increases the height of the potential hill at the junction because there are no carriers available to move in the direction that the field would cause them to move. On both sides, the carriers have an "uphill" climb to the junction.

Forward-Bias Conditions

The application of a positive voltage to the p-type region and a negative voltage to the n-type region raises the electrons to a higher potential energy on the n-type side of the junction, as shown in Fig. 12(d). Because the forbidden-energy region is flexible only at the junction, the applied bias causes the height of the built-in potential hill to be reduced, as shown in Fig. 12(d). As a result, many electrons now have sufficient thermal energy to get over the hill, and many holes have

sufficient thermal energy to get under it. Because the height of the hill is equivalent to about one electron-volt, a forward bias of one volt is sufficient to allow electrons and holes to move unimpeded across the junction; the current is then limited only by the ohmic resistance of the external circuit.

THYRISTOR POTENTIAL-ENERGY ANALYSIS

The bistable action of a thyristor can be explained by analysis of the potential-energy conditions in the p-n-p-n structure of an SCR. This analysis can be directly related to each operating quadrant of a triac because, as will be explained subsequently, a triac is essentially equivalent to two SCR's in an inverse parallel connection. The forward-blocking and forward-conducting states that occur in the forward-voltage (first) quadrant of an SCR are exhibited by a triac in both the first and third quadrants of the principal voltage-current characteristic, and the potential-energy conditions for the corresponding stable states and the transitions between them are identical in both types of devices.

The electron-hole interactions that make possible the switching transitions in p-n-p-n semiconductor structures are represented graphically by the diagrams shown in Figs. 13, 14, and 15. These diagrams show the potential-energy conditions and the approximate equivalent charge-carrier distributions for the var-

ious biasing conditions and switching states of a thyristor. In these diagrams, free electrons are represented by minus (-) signs and free holes by plus (+) signs.

Forward-Blocking State

The sequence of diagrams in Fig. 13 illustrates the transition of the thyristor from the equilibrium (zero-bias) condition to the forward-blocking state. In the equilibrium condition, the concentration of charge carriers (electrons and holes) is determined primarily by dopant concentrations. For this condition, which is represented by the diagram shown in Fig. 13(b), there is approximately one free carrier for each dopant atom.

When the cathode side of the thyristor is biased negatively with respect to the anode side, the potential energy of the electrons is increased in the cathode region and that of the holes is increased in the anode region. Because of the difference in energy level from cathode to anode, the shape of the forbidden-energy region is altered in the most lightly doped section (i.e., the n-type base) so that the height of the potential hill of the central junction is increased. As shown in Fig. 13(c), any electrons that exist in this region "fall down" the resultant hill, and any holes in this region "rise" to the top of the hill. In this way, all free charge carriers are removed, and the hill becomes a depletion region, as shown in Fig. 13(d).

The movement of charge carriers with an increase in the for-

ward voltage results in a charging, or displacement, current similar to the current ($i = Cdv/dt$) that charges a capacitor. This displacement current ceases when the forward voltage reaches a steady value because there are no additional carriers for the field to move. Although there are many electrons available on the cathode side of the thyristor and many holes available on the anode side, these carriers cannot enter the depletion region because they do not have sufficient energy to "climb" the 0.8- to 1.0-volt potential hills at junctions J_1 and J_3 .

The current and voltage waveforms during the transition from the equilibrium to the forward-blocking state are shown in Fig. 13(e).

Forward-Conducting State

The transition in a thyristor from the forward-blocking state to the forward-conducting state is illustrated by the potential-hill diagrams shown in Fig. 14. When a thyristor is in the forward-blocking state, shown in Fig. 14(b), application of a positive bias to the gate causes the potential energy of electrons in this region to be reduced so that the height of the potential hill at junction J_1 is decreased, as shown in Fig. 14(c). A positive gate bias of 0.8 to 1.0 volt reduces the barrier of J_1 sufficiently so that electrons from the n-type emitter can move across the p-type base into the depletion region. The electric field then sweeps them across this region, as indicated in Fig. 14(c).

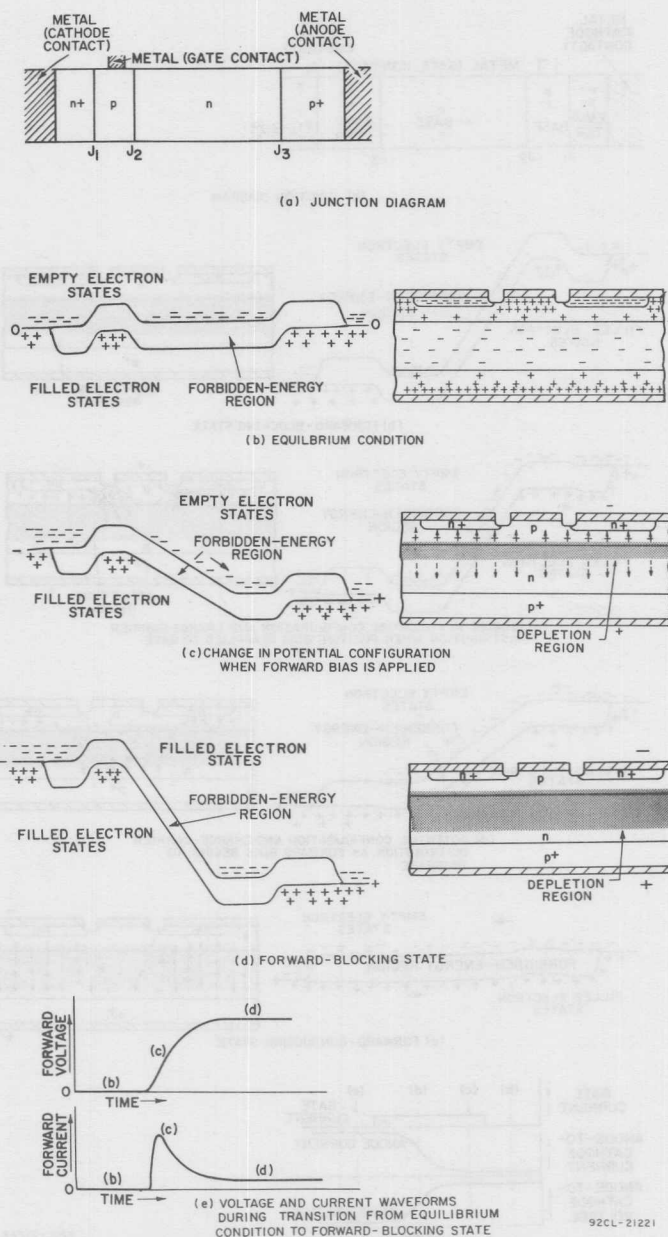
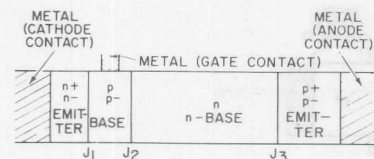
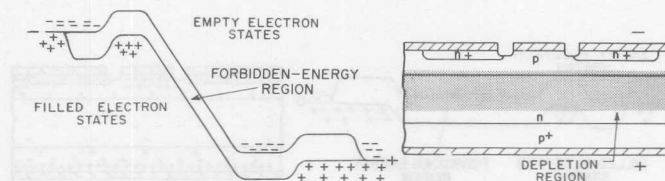


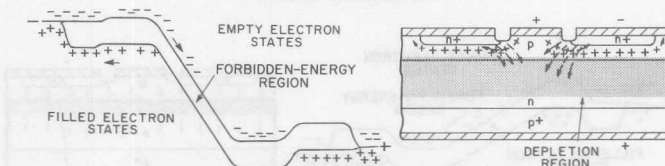
Fig. 13—Potential-hill diagrams for various stages of thyristor transition from equilibrium condition to forward-blocking condition (electron energy increases upward, hole energy increases downward).



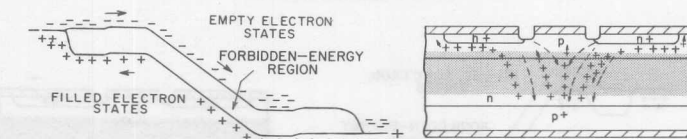
(a) JUNCTION DIAGRAM



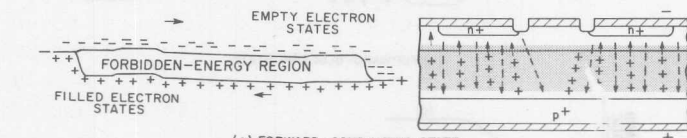
(b) FORWARD-BLOCKING STATE



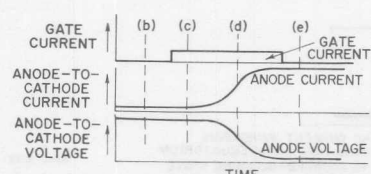
(c) CHANGE IN POTENTIAL CONFIGURATION AND CHARGE-CARRIER DISTRIBUTION WHEN POSITIVE BIAS IS APPLIED TO GATE



(d) POTENTIAL CONFIGURATION AND CHARGE-CARRIER DISTRIBUTION AS FORWARD BIAS BEGINS TO INCREASE



(e) FORWARD-CONDUCTING STATE



(f) CURRENT AND VOLTAGE WAVEFORMS DURING TURN-ON TRANSITION

92CL-21222

Fig. 14—Potential-hill diagrams and charge-carrier distribution for various stages of thyristor transition from forward-blocking state to forward-conducting state.

Electrons accumulate in the "well" at the bottom of the depletion region until their combined negative charge increases the potential electron energy sufficiently to cause the potential hill at junction J_3 to disappear. Holes can then move from the p-type emitter across the n-type base into the depletion region. These holes then immediately "climb" the potential hill at J_2 , as shown in Fig. 14(d).

The increased supply of holes to the p-type base further depresses the potential hill at J_1 so that the n-type emitter can inject an even greater number of electrons into the depletion layer. This action, in turn, increases the injection of holes from the p-type emitter. As a result of these regenerative effects, the current through the thyristor increases rapidly, and the depletion region collapses to complete the transition to the forward-conducting state. Fig. 14(e) illustrates this condition. In this state, the concentrations of both holes and electrons are greatly increased over the equilibrium concentrations. The conductivities of the base regions are then determined by the concentration of injected carriers rather than by the concentration of dopant atoms.

A comparison of Fig. 14(e) with Fig. 12(d) shows that the forbidden-energy region of a thyristor in the conducting state is essentially identical to that of a forward-biased rectifier. As a result, the forward voltage drops of the two types of devices are approximately the same. The thyristor

can be sustained in the forward-conducting state by an anode-to-cathode forward-voltage drop of approximately 1 volt, and the thyristor current, like that of the rectifier, is limited only by the impedance of the external circuit.

The current and voltage waveforms during the transition from the forward-blocking to the forward-conducting state are shown in Fig. 14(f).

Turn-off

The transition in the thyristor from the forward-conducting state back to the forward-blocking state is illustrated in Fig. 15. This transition is accomplished either by momentary reduction of the anode current to zero, or (SCR's only) by momentary reversal of the anode-to-cathode voltage.

In the conducting state, carrier concentrations far in excess of the equilibrium level are injected into the n- and p-type regions. These excess carriers remain for a finite time after the anode current is reduced to zero. If the forward bias is re-applied before these excess carriers are removed, the device simply returns to the conducting state and does not switch to the blocking condition. After the excess carriers are removed and the device is returned to equilibrium, the potential hills rebuild, and the device can return to the forward-blocking state, as shown in Fig. 13.

The removal of excess carriers can be accomplished if the anode current is reduced to zero until the excess carriers recombine or move out of the depletion region.

This removal corresponds to a direct transition from the conditions shown in Fig. 15(c) to those shown in Fig. 15(g) or 13(b). The potential hill at junction J_1 rebuilds first because it is in the more heavily doped region of the device, but the hills at J_2 and J_3 also rebuild as the excess carriers disappear during the zero-anode-current condition.

For SCR's, a more rapid removal of the excess carriers can be accomplished by a momentary reversal of the anode-to-cathode voltage. This transition is shown in Figs. 15(d) through 15(f). As the reverse voltage increases, carriers are pulled out of the device in the direction opposite to that in which they were injected so that a substantial reverse current results.

The removal of carriers is aided as a potential hill and a depletion

region begin to build at junction J_3 , as shown in Fig. 15(d). As the remaining quantity of excess carriers is reduced, the reverse current decreases, and reverse voltage builds up. At the stage shown in Fig. 15(e), the reverse depletion region has built up, but the undepleted n-type base region still contains some excess carriers which prevent the potential hill at J_2 from rebuilding, and which continue to flow out as reverse current. At the stage shown in Fig. 15(f), the excess carriers have all been removed, and device has reached its steady-state reverse-blocking condition. In Fig. 15(g), the reverse bias has been removed, all regions return to the equilibrium zero-bias carrier concentrations, and the device is ready for return to the forward-blocking condition.

Fig. 16 shows the current and

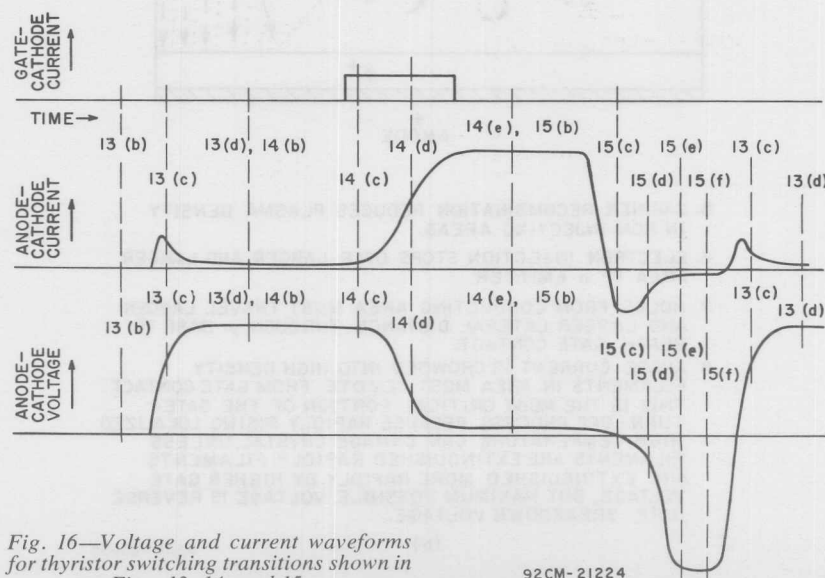


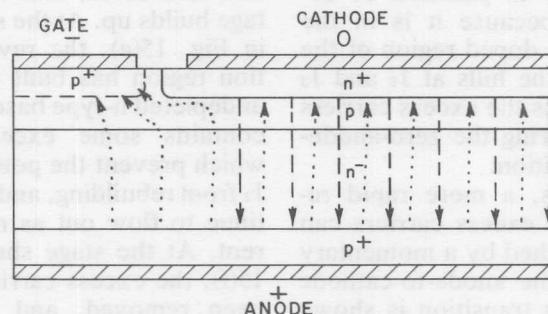
Fig. 16—Voltage and current waveforms for thyristor switching transitions shown in Figs. 13, 14, and 15.

92CM-21224

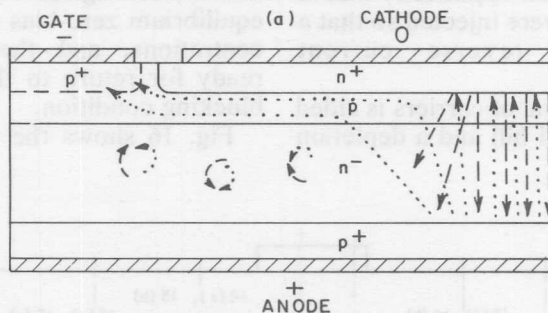
voltage waveforms that correspond to the various conditions described in Figs. 13, 14, and 15.

Gate-Controlled Turn-off

Fig. 17 shows the sequence of actions in the gate-controlled



1. NEGATIVE BIAS APPLIED TO GATE.
2. HOLES FROM ANODE ARE REMOVED THROUGH GATE.
3. ELECTRON INJECTION STOPS IN AREA ADJACENT TO GATE
4. GATE DRAWS HOLES FROM MORE REMOTE AREAS AS AREA CLOSER TO GATE IS DEPLETED OF CARRIERS



5. CARRIER RECOMBINATION REDUCES PLASMA DENSITY IN NON-INJECTING AREAS.
6. ELECTRON INJECTION STOPS OVER LARGER AND LARGER AREA OF n EMITTER
7. HOLES FROM CONDUCTING AREA MUST TRAVEL LARGER AND LARGER LATERAL DISTANCE THROUGH p BASE TO REACH GATE CONTACT.
8. ANODE CURRENT IS CROWDED INTO HIGH DENSITY FILAMENTS IN AREA MOST REMOTE FROM GATE CONTACT. THIS IS THE MOST CRITICAL PORTION OF THE GATE-TURN-OFF PROCESS BECAUSE RAPIDLY RISING LOCALIZED HIGH TEMPERATURE CAN DAMAGE CRYSTAL, UNLESS FILAMENTS ARE EXTINGUISHED RAPIDLY. FILAMENTS ARE EXTINGUISHED MORE RAPIDLY BY HIGHER GATE VOLTAGE, BUT MAXIMUM POSSIBLE VOLTAGE IS REVERSE GATE BREAKDOWN VOLTAGE.

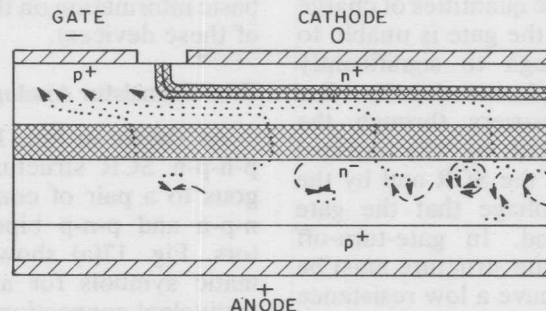
(b)

92CM-25539

Fig. 17—Gate-controlled turn-off in GTO devices. (Cont'd on page 23)

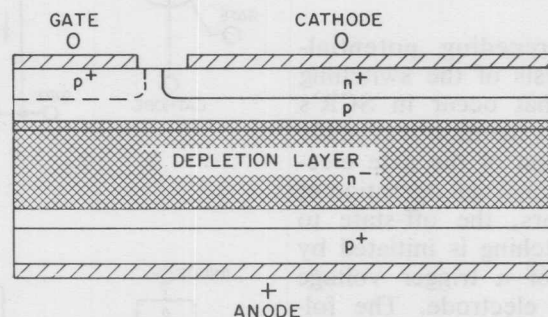
turn-off of GTO devices. Any SCR exhibits some gate-turn-off capability, but the maximum cur-

rent that can be interrupted in this way in conventional SCR's is only slightly greater than the main-



9. AS FINAL FILAMENTS ARE EXTINGUISHED, ELECTRON INJECTION STOPS AND DEPLETION LAYER BUILDS ON GATE-CATHODE JUNCTION.
10. DEPLETION LAYER BEGINS TO BUILD ON FORWARD BLOCKING JUNCTION.
11. CATHODE CURRENT STOPS, BUT ANODE-TO-GATE CURRENT CONTINUES TO FLOW AS CARRIERS FROM n BASE PLASMA DIFFUSE INTO DEPLETION LAYER. ANODE-TO-GATE CURRENT DECAYS EXPONENTIALLY AS PLASMA CONCENTRATION IS REDUCED BY RECOMBINATION.

(c)



12. ANODE VOLTAGE APPROACHES STEADY-STATE VALUE AS DEVICE IMPEDANCE INCREASES.
13. NEGATIVE GATE BIAS CAN BE REMOVED WHEN PLASMA CONCENTRATION HAS FALLEN BELOW REGENERATIVE VALUE, AND ANODE VOLTAGE IS CLOSE TO STEADY STATE VALUE.

(d)

NOTE : DOTS REPRESENT POSITIVE CHARGE CARRIERS (HOLES)
DASHES REPRESENT NEGATIVE CHARGE CARRIERS (ELECTRONS)

92CM-25540

Fig. 17-Gate-controlled turn-off in GTO devices. (Cont'd from page 22)

terminal current at which the SCR will turn off of its own accord with zero gate bias and is well below the normal operating currents of the SCR. The main terminals inject such large quantities of charge carriers that the gate is unable to remove enough to significantly reduce the plasma density. Removal of carriers through the gate is limited by the internal resistance of the SCR and by the maximum voltage that the gate can withstand. In gate-turn-off SCR's, the gate structure must be designed to have a low resistance to the lateral flow of carriers within the device and a high reverse breakdown voltage.

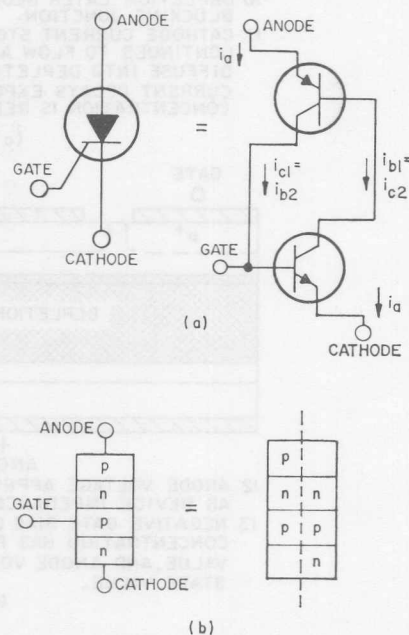
THYRISTOR EQUIVALENT-MODEL ANALYSES

In the preceding potential-energy analysis of the switching transitions that occur in SCR's and triacs, no mention was made of the function of the gate electrode. During normal operation of these thyristors, the off-state to on-state switching is initiated by application of a trigger voltage to the gate electrode. The following equivalent-model analyses illustrate the role of the gate electrode in the operation of both SCR's and triacs. (These analyses assume that the reader has a basic knowledge of the operation of bipolar transistors. Readers that are not familiar with bipolar transistors should refer to the **RCA Solid-State Designer's Handbook**, Technical Series SP-52; the

RCA Transistor, Thyristor, and Diode Manual, Technical Series SC-16; **RCA Power Transistors Manual**, Technical Series PM-82, or any other text that provides basic information on the operation of these devices).

Two-Transistor Analogy of an SCR

As shown in Fig. 18, the basic p-n-p-n SCR structure is analogous to a pair of complementary n-p-n and p-n-p bipolar transistors. Fig. 17(a) shows the schematic symbols for an SCR and equivalent connection of the complementary pair of transistors,



92CS-25295

Fig. 18—Two-transistor analogy of an SCR: (a) schematic symbols of an SCR and the equivalent two-transistor model; (b) structure of an SCR and of the equivalent two-transistor model.

and Fig. 17(b) shows the equivalent relationship of the p-n-p-n SCR structure and the interconnected transistor structures. The n-p-n and p-n-p transistors in the equivalent model are interconnected so that regenerative action occurs when a proper gating signal is applied to the base of the n-p-n transistor.

When the two-transistor model is connected in a circuit to simulate normal SCR operation, the emitter of the p-n-p transistor is returned to the positive terminal of a dc supply through a limiting resistor R_2 , and the emitter of the n-p-n transistor Q_2 is returned to the negative terminal of the dc supply to provide a complete electrical path, as shown in Fig. 19. When the model is in the off state, the initial value of principal-current flow is zero. If a positive pulse is then applied to the base of the n-p-n transistor, the transistor turns on and forces the collector (which is also the base of the

p-n-p transistor) to a low potential; as a result, a current I_a begins to flow. Because the p-n-p transistor Q_1 is then in the active state, its collector current flows into the base of the n-p-n transistor ($I_{c1} = I_{b2}$) and sets up the conditions for regeneration. If the external gate drive is removed, the model remains in the on state as a result of the division of currents associated with the two transistors, provided that sufficient principal current (I_a) is available.

Theoretically, the model shown in Fig. 18 remains in the on state until the principal current flow is reduced to zero. Actually, turn-off occurs at some value of current greater than zero. This effect can be explained by observation of the division of currents as the value of the limiting resistor is gradually increased. As the principal current is gradually reduced to the zero current level, the division of currents within the model can no longer sustain the required regeneration, and the model reverts to the blocking state.

The two-transistor model illustrates three features of thyristors: (1) a gate trigger current is required to initiate regeneration, (2) a minimum principal current (referred to as "latching current") must be available to sustain regeneration, and (3) reduction of principal-current flow results in turn-off at some level of current flow (referred to as "holding current") that is slightly greater than zero.

Fig. 20 shows the effects of a

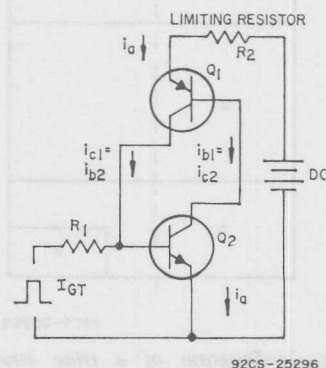


Fig. 19—Two-transistor model connected to show a complete electrical path.

resistive termination at the base of the n-p-n transistor on the latching and holding currents. The collector current through the p-n-p transistor must be increased to supply both the base current for the n-p-n transistor and the shunt current through the terminating resistor. Because the principal-current flow must

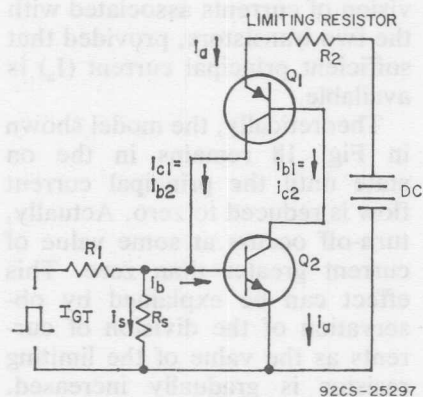


Fig. 20—Two-transistor model of SCR with resistive termination of the n-p-n transistor base.

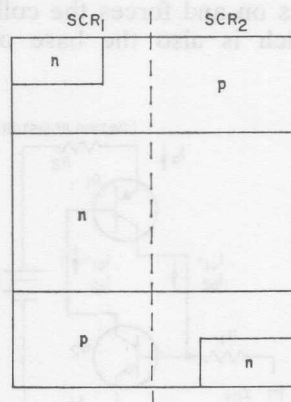
be increased to supply this increased collector current, latching- and holding current requirements also increase. The use of the two-transistor model provides a more concise meaning to the mechanics of thyristors. In thyristor fabrication, it is generally good practice to use a low-beta p-n-p unit and to include internal resistance termination for the base of the n-p-n unit. Termination of the n-p-n provides immunity from "false" (non-gated) turn-on, and the use of the low-beta p-n-p units permits a wider base region to be used to support the high voltage

encountered in thyristor applications.

The two-transistor model of a conventional SCR, shown in Fig. 19, can also be used to represent a gate-turn-off SCR. In the GTO, however, the internal resistance is reduced and a lower-beta input (n-p-n) unit with a high emitter-base breakdown capability is employed. These design changes are required to achieve effective gate turn-off control, but also result in a reduction in the high regenerative gain inherent in conventional SCR's with an attendant effect on other device characteristics.

Two-SCR Analogy of a Triac

Functionally, a triac may be considered as two parallel SCR (p-n-p-n) structures oriented in opposite directions, as shown in Fig. 21. The same approach used to explain gating, latching, and



92CS-25299

Fig. 21—Diagram of a triac structure which shows that this device is basically two SCR structures in an inverse parallel arrangement.

holding currents in the SCR can be extended to include the two-SCR model of a triac.

In triacs, the gate-trigger-pulse polarity is usually measured with respect to main terminal No. 1, which is comparable to the cathode terminal of an SCR. The triac can be triggered by a gate-trigger pulse which is either positive or negative with respect to main terminal No. 1 when main terminal No. 2 is either positive or negative with respect to main terminal No. 1. The triac, therefore, can be triggered in any of four operating modes, as summarized in Table II. The quadrant designations refer to the operating quadrant on

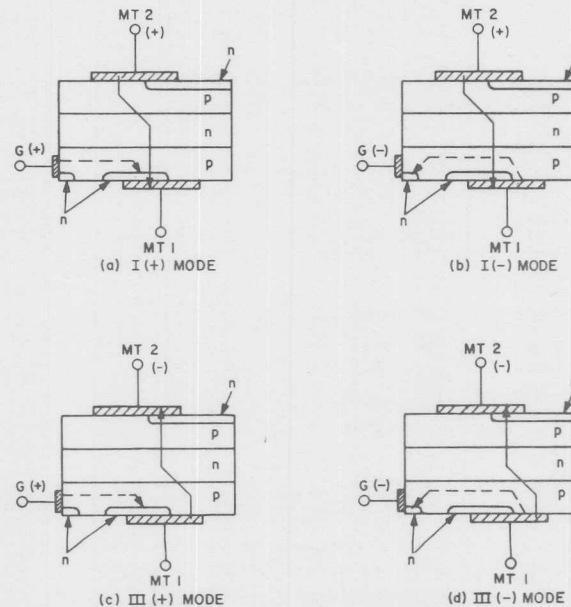
Table II—Triac Triggering Modes

Gate-to-Main-Terminal-No. 1 Voltage	Main-Terminal-No. 2-to-Main-Terminal-No. 1 Voltage	Operating Quadrant *
Positive	Positive	I (+)
Negative	Positive	I (-)
Positive	Negative	III (+)
Negative	Negative	III (-)

*Positive (+) and negative (-) signs indicate polarity of gate trigger pulse.

the principal voltage-current characteristics (either I or III), and the polarity symbol represents the gate-to-main-terminal-No. 1 voltage. Fig. 22 shows the flow of current in a triac for each of the four triggering modes.

The gate-trigger requirements of the triac are different in each



92CS-25300

Fig. 22—Current flow in a triac for each triggering mode.

operating mode. The I (+) mode (gate positive with respect to main terminal No. 1 and main terminal No. 2 positive with respect to main terminal No. 1), which is comparable to equivalent SCR operation, is usually the most sensitive. The smallest gate current is required to trigger the

triac in this mode. The other three operating modes require larger gate-trigger currents. For RCA triacs, the maximum trigger-current rating in the published data is the largest value of gate current that is required to trigger the selected device in any operating mode.

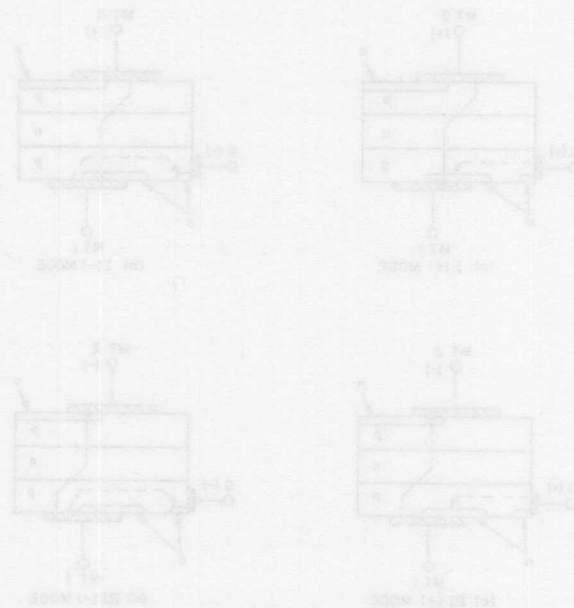


Fig. 12—Current flow in a triac for each triggering mode.

Thermal Considerations

The maximum allowable power dissipation in a silicon rectifier or thyristor is limited by the temperature of the semiconductor pellet (i.e., the junction temperature). An important factor that assures that the junction temperature remains below the specified maximum value is the ability of the associated thermal circuit to conduct heat away from the device. For this reason, all solid-state power devices should be mounted on a good thermal base (usually copper), and means should be provided for the efficient transfer of heat from this base to the surrounding environment.

When a silicon rectifier or thyristor is mounted in free air, without a heat sink, the steady-state thermal circuit is defined by the **junction-to-free-air thermal resistance** given in the published data on the device. Thermal considerations require that there be a free flow of air around the device and that the power dissipation be maintained below that which would cause the **junction temperature** to rise above the maximum rating. When the device is mounted on a heat sink, however, care must be taken to assure that

all portions of the thermal circuit are considered.

Silicon rectifiers and thyristors may also be adversely affected by temperature variations that result from changes in power dissipation during operation or in the temperature of the ambient environment. Such temperature variations produce cyclic mechanical stresses at the interface of the semiconductor pellet and the copper base to which the pellet is attached because of the different thermal-expansion coefficients of these materials. These thermally induced cyclic stresses may eventually lead to a wearout type of failure referred to as **thermal fatigue**.

BASIC THERMAL SYSTEM

When current flows through a solid-state device, power is dissipated in the semiconductor pellet that is equal to the product of the voltage across the junction and the current through it. As a result, the temperature of the pellet increases. The amount of the increase in temperature depends on the power level and how fast the heat can flow away from the

junction through the device structure to the case and the ambient atmosphere. The rate of heat removal depends primarily upon the thermal resistance and capacitance of the materials involved. The temperature of the pellet rises until the rate of heat generated by the power dissipation is equal to the rate of heat flow away from the junction; i.e., until thermal equilibrium has been established.

Although silicon rectifiers and thyristors can operate at high temperatures, the actual pellet of silicon is quite small and has a very low thermal capacity. During normal operation, a silicon p-n junction dissipates approximately 1 watt of power for each ampere of forward current. The temperature of the junction rises rapidly during high-current operation. An increase in junction temperature beyond rated capabilities, as a result of either high currents or excessive ambient temperatures, may cause device failure, either directly because of irreversible material damage as a result of the high temperature or indirectly because of the effect of the increased temperature on the off-state blocking capability, as described later. The heat dissipated in the silicon pellet must be removed rapidly, therefore, so that the temperature of the junction is not allowed to rise above the safe operating value of 125°C. For this reason, the silicon pellet is mounted between heavy copper parts in a symmetrical direct-soldered arrangement that results in uniform distribution of thermal

stresses, minimum thermal fluctuations, and low thermal resistance.

Fig. 23 shows cross-sectional diagrams of a typical high-current silicon rectifier (stud package) and thyristor (press-fit package). Because of the way in which these devices are constructed, there is always a thermal "drop" between the silicon pellet and the outside of the case. This thermal "drop", which is analogous to the voltage drop across the various components of an electrical circuit, is caused by the **thermal impedances** of the various components of the internal rectifier or thyristor structure. These impedances include both **thermal resistance** and **thermal capacitance**. For example, in the stud-type package shown in Fig. 23(a) the lower side of the silicon pellet is soldered directly to a heavy copper stud that provides a low-thermal-resistance path between the pellet and the rectifier heat sink. The upper side of the pellet is soldered to a heavy copper block which, together with the stud, forms a thermal capacitor.

Thermal resistance can be compared to electrical resistance. Just as electrical resistance is the extent to which a material resists the flow of electricity, thermal resistance is the extent to which a material resists the flow of heat. A material that has a low thermal resistance is said to be a good thermal conductor. In general, materials which are good electrical conductors are good thermal conductors, and vice versa.

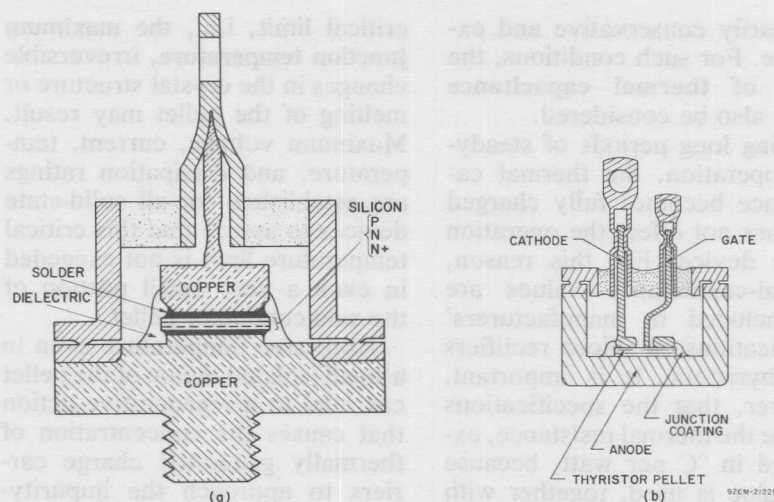


Fig. 23—Cross-sectional diagrams of (a) a silicon rectifier mounted in a stud package and (b) a thyristor mounted in a press-fit package.

The methods of rating solid-state power devices under steady-state conditions are indicated by the following definition of thermal resistance: The thermal resistance of a solid-state device is the ratio of the temperature drop to the heat generated through internal power dissipation under steady-state conditions; the temperature drop is measured between the region of heat generation and some reference point.

The over-all thermal resistance of an assembled device is usually expressed as the rise in junction temperature above the case temperature per unit of power dissipated in the device. This information, together with the maximum junction-temperature rating, enables the user to determine the maximum power level at

which the device can be safely operated for a given case temperature. Subtraction of the case temperature from the maximum junction temperature indicates the allowable internal temperature rise. If this value is divided by the specified thermal resistance of the device, the maximum allowable power dissipation is determined.

It should be noted that thermal resistance is defined for steady-state conditions. If a uniform temperature over the entire semiconductor junction is assumed, the power dissipation required to raise the junction temperature to a predetermined value, consistent with reliable operation, can be determined. Under conditions of intermittent or switching loads, however, such a design is un-

necessarily conservative and expensive. For such conditions, the effect of **thermal capacitance** should also be considered.

During long periods of steady-state operation, the thermal capacitance becomes fully charged and does not affect the operation of the device. For this reason, thermal-capacitance values are not included in manufacturers' specifications on silicon rectifiers and thyristors. It is important, however, that the specifications include the thermal resistance, expressed in °C per watt, because this value is used, together with the power dissipated by the device, to determine the rise in junction temperature above the case temperature.

The thermal capacitance incorporated into the device structure becomes extremely important when the silicon pellet is subjected to sudden changes in current, such as may occur during a fault condition. This capacitance absorbs heat produced by high-current pulses and allows the heat to flow through the pellet and copper block (low-thermal-resistance path) during periods of low current. In this way, fluctuations in junction temperature are held to a minimum.

THERMAL-STABILITY REQUIREMENTS

As mentioned earlier, power is dissipated in the semiconductor material of a solid-state device in the form of heat. If the temperature of the semiconductor material is allowed to exceed some

critical limit, i.e., the **maximum junction temperature**, irreversible changes in the crystal structure or melting of the pellet may result. Maximum voltage, current, temperature, and dissipation ratings are established for all solid-state devices to assure that this critical temperature limit is not exceeded in even a very small portion of the semiconductor pellet.

Excessive temperature even in a small isolated region of the pellet can lead to a regenerative action that causes the concentration of thermally generated charge carriers to approach the impurity-carrier concentration. When the condition becomes extreme, device voltage drops collapse to a very low value, and the current increases abruptly and is limited only by the voltage and impedance of the external circuit. This extreme condition is referred to as **thermal runaway**.

Thermal runaway is a condition that can occur in any solid-state device because of the regenerative relationship between junction temperature T_j and power dissipation P_D . A rise in junction temperature causes a corresponding increase in power dissipation. The increase in power dissipation then causes a further rise in junction temperature and thereby results in an additional increase in dissipation. At high junction temperatures, this regenerative action occurs at such a rapid rate that no point of stable operation can be achieved. The increased temperature that results during thermal runaway may or may not destroy a solid-state device de-

pending upon how far the regenerative action is allowed to proceed. In general, thermal runaway is not a cause of device failure because this condition can be avoided by selection of devices that have adequate ratings, careful control of maximum circuit voltages and currents, and use of recommended thermal mounting techniques. Figs. 24 through 27 illustrate graphical techniques that can be used to define thermal-stability requirements in circuit applications of solid-state devices.

Fig. 24(a) shows a basic thermal-equilibrium curve that illustrates the linear relationship between junction temperature and

power dissipation. The inverse slope of this linear curve defines the total steady-state thermal resistance from the semiconductor junction to the ambient atmosphere. If the junction-to-ambient thermal resistance $R_{\theta JA}$ is low, the slope of the equilibrium curve is very steep, but becomes progressively less steep as the thermal resistance is increased. Fig. 24(b) shows a typical heat-dissipation curve for a solid-state device. This curve, which is independent of thermal resistance, indicates the device dissipation when the junction temperature is maintained at any specific value by some external means. The

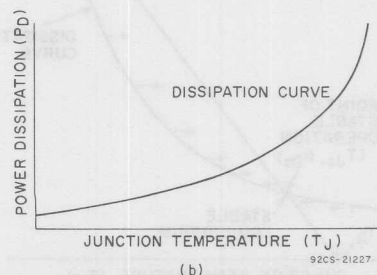
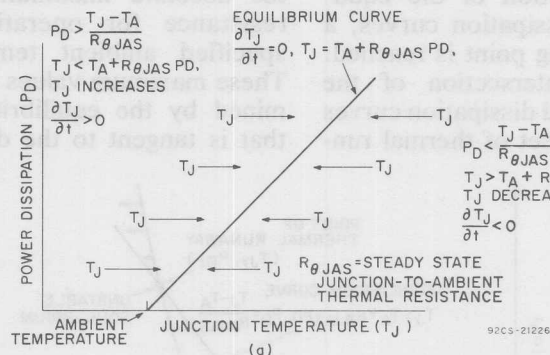


Fig. 24—Power dissipation as a function of temperature: (a) thermal-equilibrium curve; (b) power dissipation curve.

basic curves shown in Fig. 24 can be combined to obtain graphical solutions to the thermal-stability problem.

The equilibrium curve and the dissipation curve may be combined, as shown in Fig. 25, to determine a stable thermal operating point for a solid-state device. The junction temperature and the power dissipation in a solid-state device define an operating point that lies on the dissipation curve. This operating point tends to move toward a point of constant temperature on the thermal-equilibrium curve. If the junction temperature of the device is maintained below the value that corresponds to the upper intersection of the equilibrium and dissipation curves, a stable operating point is reached. The upper intersection of the equilibrium and dissipation curves defines the onset of thermal run-

away. If the junction temperature exceeds the thermal-runaway value, the operating point still tries to move toward the equilibrium curve; however, the regenerative relationship between temperature and dissipation in this region causes both junction temperature and dissipation to increase at such a rapid rate that no upper equilibrium point can be reached.

Thermal-equilibrium and power dissipation curves may also be combined to determine the absolute maximum ambient temperature T_A in which it is permissible to operate a solid-state device that has a specific thermal resistance $R_{\theta J-A}$ or to determine the absolute maximum thermal resistance for operation in a specified ambient temperature. These maximum values are determined by the equilibrium curve that is tangent to the dissipation

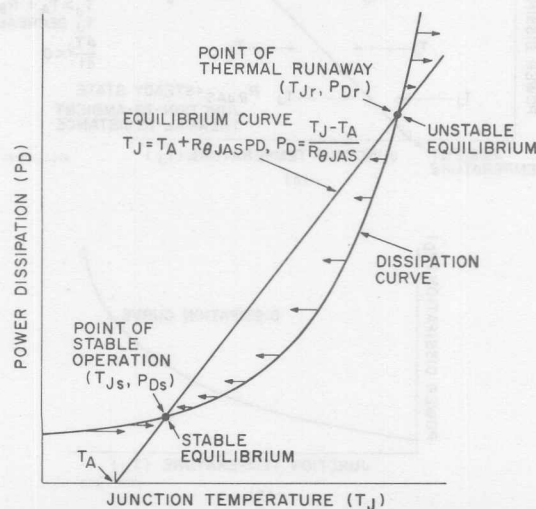


Fig. 25—Equilibrium and dissipation curves plotted on same scale.

curve, as shown in Figs. 26 and 27. The point of tangency defines the absolute maximum values. Any further increase in ambient temperature or junction-to-ambient thermal resistance would result in equilibrium curves that have no point of intersection with the dissipation curve.

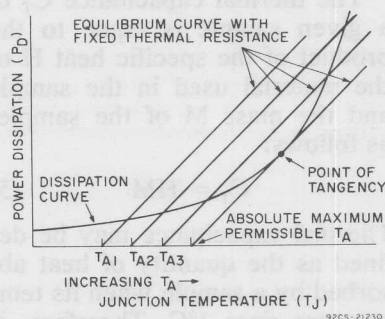


Fig. 26—Graphical solution for maximum ambient temperature permissible for a fixed thermal resistance.

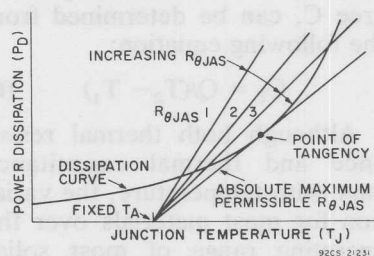


Fig. 27—Graphical solution for maximum thermal resistance permissible for a fixed ambient temperature.

Theoretically, a curve of power dissipation P_D as a function of junction temperature T_J can be derived to describe the dissipation curve. This equation can be determined from the circuit load line and the theoretical current-

voltage/junction-temperature characteristics of a solid-state device. If such a dissipation equation can be obtained, the points of stable operation and of thermal runaway and the maximum permissible values for ambient temperature T_A and junction-to-ambient thermal resistance $R_{\theta JA}$ can be determined analytically by simultaneous solution of the dissipation equation with the equilibrium equation. In many cases, a mathematical equation for the dissipation curve is very difficult, or impossible, to obtain. In such instances, however, the requirements for thermal stability can always be determined by application of graphical techniques to an empirical power-dissipation curve, as shown in Figs. 25 through 27.

THERMAL IMPEDANCE

The temperature of the semiconductor pellet (i.e., the junction temperature T_J) of a solid-state device is related to the temperatures of the various other elements surrounding it by mathematical relationships similar to those that define the properties of an electrical circuit that contains resistance and capacitance. It is convenient, therefore, to describe the thermal properties of a solid-state device in terms of thermal impedance, thermal resistance, and thermal capacitance.

General Mathematical Relationships

Fig. 28 shows a layer of thermally conductive material that

has a constant cross-sectional area A , a thickness d , and a thermal conductivity K . (The thermal conductivity K is a basic property of the material itself and is independent of geometry.) If the surface S_1 is maintained at a temperature T_1 and the surface S_2 is

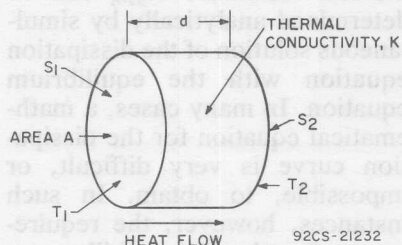


Fig. 28—Diagram of a layer of thermally conductive material.

maintained at a higher temperature T_2 , a given quantity of heat Q flows through the layer in a time t . The rate of heat flow P through the layer is expressed by the following relationship:

$$P = Q/t \quad (1)$$

The thermal conductance G_T of the layer can be determined from the physical dimensions of the layer and the thermal conductivity of the layer material, as follows:

$$G_T = KA/d \quad (2)$$

The thermal resistance R_θ is the reciprocal of thermal conductance G_T and, therefore, is given by

$$R_\theta = d/KA \quad (3)$$

The thermal resistance of the layer can be measured experimentally by determination of the

time rate of heat flow ($P = Q/t$) and the difference between the temperatures T_1 and T_2 . The following equation defines the thermal resistance, expressed in degrees C per watt, in terms of these quantities:

$$R_\theta = (T_2 - T_1)/P \quad (4)$$

The thermal capacitance C_T of a given sample is equal to the product of the specific heat H of the material used in the sample and the mass M of the sample, as follows:

$$C_T = HM \quad (5)$$

Thermal capacitance may be defined as the quantity of heat absorbed by a sample when its temperature rises 1°C . Therefore, if a given sample absorbs a quantity of heat Q when its temperature is increased from T_1 to T_2 , the thermal capacitance of the sample, expressed in watt-seconds per degree C, can be determined from the following equation:

$$C_T = Q/(T_2 - T_1) \quad (6)$$

Although both thermal resistance and thermal capacitance vary with temperature, the variation for most materials over the operating range of most solid-state devices is small enough so that it may usually be neglected in thermal calculations.

Junction-to-Case Thermal Impedance

The thermal properties of any solid-state power device may be represented by an electrical analog circuit, such as that shown in

Fig. 29, which consists of a current generator connected to a series of resistors that have capacitance to ground distributed along their length. The power P dissipated within the crystal of a solid-state device results in a flow of heat outward from the crystal. This flow of heat (dis-

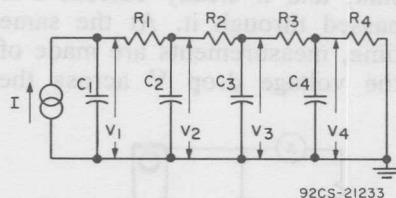


Fig. 29—Electrical analog circuit used to describe thermal properties of a solid-state device.

sipated power P in calories per second or in watts) in a solid-state device is analogous to the flow of charge (electrical current I in coulombs per second or amperes) in such a circuit. Thermal resistances and thermal capacitances of the device are analogous to the electrical resistances and capacitances shown in the circuit. The potential difference or voltage between any two points in the electrical analog circuit is analogous to the temperature difference between the corresponding two points of the device it represents. Table III shows the relationship between various electrical quantities and their corresponding thermal quantities.

Thermal impedance Z_T , like electrical impedance Z , is a complex variable because of the time dependence associated with the thermal capacitance C_T .

In the electrical or thermal-

analog circuit shown in Fig. 29, the thermal resistances closest to the heat source are large because the cross section of the semiconductor pellet is small (all the heat generated flows through a small area). As shown in Eq. (3), thermal resistance varies inversely with cross-sectional area. In general, thermal resistances become progressively smaller as distance from the semiconductor element increases.

Table III—Comparison of Various Electrical Quantities and Corresponding Thermal Quantities

Electrical	Thermal
Current generator	Heat generator (semiconductor crystal)
Resistance R (ohms or volts/ampere)	Thermal Resistance R_θ ($^{\circ}\text{C}/\text{watt}$)
Capacitance C (ampere-second/volt)	Thermal Capacitance (C_T (watt-second/ $^{\circ}\text{C}$))
Potential difference $V^1 - V^2$ (volts)	Temperature difference $T^1 - T^2$ ($^{\circ}\text{C}$)
Potential above ground $V - V_G$ (volts)	Temperature above ambient $T - T_A$ ($^{\circ}\text{C}$)
Current I (amperes)	Power dissipation P (watts)
Impedance Z (volts/ampere)	Thermal impedance Z_T ($^{\circ}\text{C}/\text{watt}$)

Eq. (5) indicates that thermal capacitance varies directly with both mass and specific heat. Therefore, the small mass of the semiconductor element of a device causes the thermal capacitance to be smallest at the heat source and to become progressively larger as distance from the heat source increases. The final thermal capacitance in the series must be considered as an infinite

capacitance, which electrically is the same as a direct short across the end of the line.

In the electrical-analog circuit shown in Fig. 29, resistance can be determined by application of a steady known current I through the resistors and measurement of the voltage drop E across them. Thus, the resistances are given by

$$R_2 = \frac{V_1 - V_2}{I}, R_3 = \frac{V_2 - V_3}{I} \dots \quad (7)$$

In the analogous thermal circuit, thermal resistance is measured by application of a steady known amount of heat, or power P , through the resistors and measurement of the temperature difference $(T_1 - T_2)$ across the thermal resistance R_{θ} . Thermal resistances are then given by

$$R_{\theta_2} = \frac{T_1 - T_2}{P}$$

$$R_{\theta_3} = \frac{T_2 - T_3}{P} \dots \quad (8)$$

In the electrical analog circuit, a steady current is essential for accurate measurement because any changes in current are accompanied by charging or discharging of the capacitors, which causes an unknown value of current to flow through the resistors. Because the equation $R = V/I$ is used to solve for resistance, both V and I must be known.

Similarly, in the thermal circuit, there must be a steady heat flow because any charging or discharging of the thermal capaci-

tances produces an unknown variation in the value of P . For example, if the thermal resistance between the junction and the outer case of a thyristor or rectifier stud package is to be measured, the arrangement shown in Fig. 30 might be used. The device is mounted on a suitable heat sink, and a steady current I is passed through it. At the same time, measurements are made of the voltage drop V across the

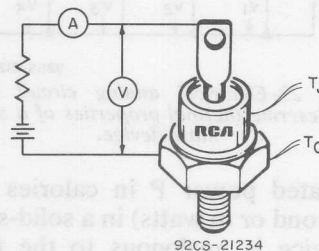


Fig. 30—Suitable arrangement for measuring the thermal resistance of a solid-state device.

device, the temperature T_J at the junction, and the temperature T_C at the case. The power P dissipated as heat within the device, and hence the power that passes out through the thermal resistances, is given by $P = IV$ (watts). The thermal resistance $R_{\theta_{J-C}}$ of the device is then given by

$$R_{\theta_{J-C}} = \frac{T_J - T_C}{P} (^{\circ}\text{C}/\text{watt}) \quad (9)$$

Such a simple measurement of thermal resistance is applicable to measurement with a constant heat input only. If there is any change or fluctuation in heat-input rate, the change in temperature difference lags behind the

change in heat input because some of the heat flows into or out of the thermal capacitances.

If a step function of power is applied to the device (i.e., if the power input at time t_1 increases from $P = 0$ to $P = P_1$), the temperature difference between junction and case rises as shown in Fig. 31, and approaches temperature T_1 asymptotically. This temperature-rise curve is similar to the voltage-rise curve which would be obtained in the analogous resistance-capacitance electrical circuit.

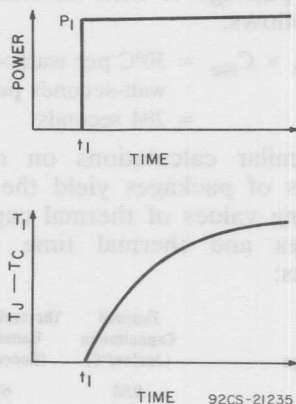


Fig. 31—Temperature-rise curve obtained with step function of power.

The exact shape of the curve depends upon the magnitudes of the thermal-resistance and thermal-capacitance components of the device. Fig. 32 shows a typical thermal-response curve for a solid-state power device. This curve indicates that solid-state devices have multiple thermal time constants.

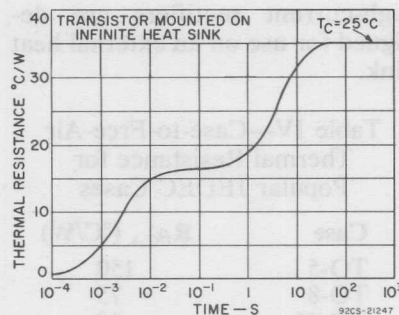


Fig. 32—Graphical representation of transient thermal response (i.e., thermal-impedance) curve.

Case-to-Ambient Thermal Resistance

The thermal equivalent circuits for a solid-state device discussed in the preceding section considered only the thermal paths from junction to case. For devices, such as thyristors and silicon rectifiers in which the silicon pellet is mounted directly on the header or pedestal, the total internal thermal resistance from junction to case $R_{\theta J-C}$ varies from 50°C per watt to less than 1°C per watt. If the device is not mounted on a heat sink, the thermal resistance from case to ambient air $R_{\theta C-A}$ is so large in comparison to that from junction to case that the net over-all thermal resistance from junction to ambient air is primarily the result of the $R_{\theta C-A}$ term. Table IV lists values of case-to-air thermal resistance for popular thyristor JEDEC cases. Beyond the limit of a few hundred milliwatts, it becomes impractical to increase the size of the case to make the $R_{\theta C-A}$ term comparable to the $R_{\theta J-C}$ term. As a result, thyristors and

high-current rectifiers are designed for use on an external heat sink.

Table IV—Case-to-Free-Air
Thermal Resistance for
Popular JEDEC Cases

Case	$R_{\theta_{C-A}}$ ($^{\circ}\text{C}/\text{W}$)
TO-5	150
TO-8	75
TO-66	60
TO-3	30

Case-to-Ambient Thermal Capacitance

The thermal capacitance of the over-all package is also an important factor in the thermal circuit of a solid-state power device. The thermal capacitance of a package is calculated relatively easily. First, the material constituents of the package are determined. The thermal capacitances of these materials are then calculated and added together to obtain the thermal-capacitance value for the over-all package. For example, the RCA copper-button TO-3 thyristor package contains about 4 grams of copper and 12 grams of steel. The other constituents of this package have negligible thermal capacitance.

The thermal capacitance of any material is equal to the product of its mass and specific heat. The calculations of the thermal capacitances (C_{Cu} and C_S) for the copper button and the steel case yield the following results:

$$\begin{aligned} C_{Cu} &= 4 \text{ grams} \times 0.093 \\ &= 0.37 \text{ cal per } ^{\circ}\text{C} \\ C_S &= 12 \text{ grams} \times 0.105 \\ &= 1.26 \text{ cal per } ^{\circ}\text{C} \end{aligned}$$

The following summation then provides the total thermal capacitance of the over-all package:

$$\begin{aligned} C_{pkg} &= C_{Cu} + C_S \\ &= 1.63 \text{ cal per } ^{\circ}\text{C} \end{aligned}$$

Expressed in terms of watt-seconds per $^{\circ}\text{C}$, this value becomes

$$\begin{aligned} C_{pkg} &= 1.63 \text{ cal per } ^{\circ}\text{C} \times 4.18 \\ &\quad \text{cal per joule} \\ &= 6.8 \text{ joules per } ^{\circ}\text{C} \\ &= 6.8 \text{ watt-seconds per } ^{\circ}\text{C} \end{aligned}$$

The thermal resistance from case to the ambient air of the copper-button TO-3 package is approximately 20°C per watt. The thermal-cooling time constant for this package is then determined as follows:

$$\begin{aligned} R_{\theta_{C-A}} \times C_{pkg} &= 30^{\circ}\text{C per watt} \times 6.8 \\ &\quad \text{watt-seconds per } ^{\circ}\text{C} \\ &= 204 \text{ seconds} \end{aligned}$$

Similar calculations on other types of packages yield the following values of thermal capacitances and thermal time constants:

Package	Thermal Capacitance (Joules/ $^{\circ}\text{C}$)	Thermal Time Constant (Seconds)
TO-5	0.58	69
TO-66 (no button)	2.56	128
TO-8	1.84	110
TO-3 (Cu button)	6.8	204

These values can be used to calculate temperature effects of pulses on devices that are not mounted on heat sinks. The thermal time constants can be used to estimate how long units must be cooled between tests to avoid temperature changes. For example, the application of a 150-watt pulse for 1 second results in a temperature rise in the TO-3

package determined as follows:

$$\begin{aligned} T_{\text{rise}} &= 150 \text{ watts}/6.8 \text{ Joules}/^{\circ}\text{C} \\ &= 22^{\circ}\text{C} \end{aligned}$$

The time required to cool the package to within 3°C of room temperature can be determined as follows:

$$\begin{aligned} T &= 22e^{-t/204} \\ 3 &= 22e^{-t/204} \\ \ln 3/22 &= -t/204 \\ t &= 6.1 \text{ minutes} \end{aligned}$$

Effect of External Heat Sink

In the preceding discussion, the sources of thermal resistance within silicon rectifiers and thyristors were explained, and the thermal properties of free-air-mounted devices were described. This section explains the use of heat sinks to increase the power-handling capability of these devices.

The primary purpose of a heat sink is to increase the effective heat-dissipation area. The effect on the thermal equivalent circuit is shown in Fig. 33. From the electrical analog, the effective resistance of the two parallel thermal paths is smaller than that of either of the paths. The effect of the heat sink is to provide an additional low-thermal-

resistance path from case to ambient air. The heat-sink thermal resistance actually consists of two series elements, the thermal resistance from case to heat sink that results from conduction ($R_{\theta CS}$) and the thermal resistance from heat sink to ambient air caused by convection and radiation ($R_{\theta SA}$).

In practice, the case must be electrically isolated from the heat sink except for grounded-anode circuits. The thermal resistance from case to heat sink, therefore, includes two components. One component is caused by surface irregularities and can be minimized by use of silicone grease compounds; the other component is introduced by the electrical insulating washer required. The thermal capacitance of these two elements is very small and can be neglected.

If the full power-handling capability of a solid-state device, as determined by $R_{\theta JC}$, is to be realized, there should be no temperature differential between the case and ambient air. This condition can occur only when the thermal resistance of the heat sink is zero, i.e., when the device is mounted on an infinite heat sink. Although an infinite heat sink can never be realized in practice, the greater the ratio $R_{\theta JC}/R_{\theta CA}$, the closer is the approximation, and the nearer the maximum power limit defined by $R_{\theta JC}$ can be approached. When a silicon rectifier or thyristor is used with a heat sink, the heat loss by convection and radiation through the case is very small compared to

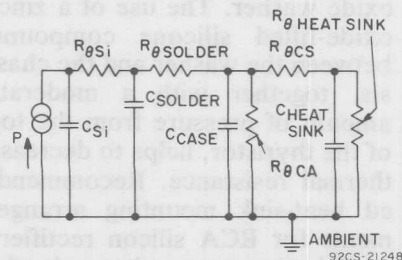


Fig. 33—Thermal equivalent circuit for a thyristor or rectifier mounted on a heat sink.

the loss through the heat sink. If $R_{\theta_{case}}$ and C_{case} are neglected, or at worst combined with $R_{\theta_{heat\ sink}}$ and $C_{heat\ sink}$, the thermal equivalent circuit for the device can be represented as shown in Fig. 34.

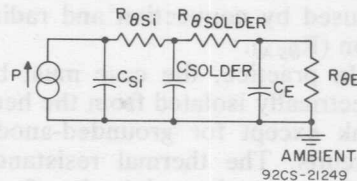


Fig. 34—Simplified thermal equivalent circuit for a thyristor or rectifier mounted on a heat sink.

Effect of Heat-Sink Insulators

As pointed out previously, when solid-state devices are to be mounted on heat sinks, some form of electrical isolation must be provided between the case and the heat sink. Unfortunately, however, good electrical insulators usually are also good thermal insulators. It is difficult, therefore, to provide electrical insulation without introduction of significant thermal resistance between case and heat sink. The best materials for this application are mica, beryllium oxide (Beryllia) and anodized aluminum. A comparison of the properties of these three materials for case-to-heat-sink isolation of the TO-3 package is shown in Table V. If the area of the seating plane, the thickness of the material, and the thermal conductivity are known, the case-to-heat-sink thermal resistance $R_{\theta_{c-s}}$ can be readily calculated by use of Eq. (10). In

all cases, this calculation should be experimentally verified. Irregularities on the bottom of the

Table V—Comparison of Insulating Washers Used for Electrical Isolation of Thyristor TO-3 Case from Heat Sink

Material	Thickness (inches)	$R_{\theta_{c-s}}$ ($^{\circ}\text{C}/\text{W}$)
Mica	0.002	0.4
Anodized Aluminum	0.016	0.35
Beryllia	0.063	0.25

device seating plane or on the face of the heat sink or insulating washer may result in contact over only a very small area unless a filling compound is used. Although silicone grease has been used for years, recently newer compounds with zinc oxide fillers (e.g., Dow Corning #340 or Wakefield #120) have been found to be even more effective.

For a JEDEC TO-5 thyristor package, a good method for electrical isolation of the anode from a metal chassis or printed-circuit board is by means of a beryllium-oxide washer. The use of a zinc-oxide-filled silicone compound between the washer and the chassis, together with a moderate amount of pressure from the top of the thyristor, helps to decrease thermal resistance. Recommended heat-sink mounting arrangements for RCA silicon rectifiers and thyristors are shown in the section on **Packages, Handling, and Mounting**.

SELECTION OF EXTERNAL HEAT SINKS

Consideration of the thermal problems involved in the mounting of silicon rectifiers and thyristors is synonymous with consideration of the best heat sink for a particular application. A variety of heat-sink configurations and mounting arrangements that have resulted from these basic considerations are described in the section on **Packages, Handling, and Mounting**. In general, selection of the optimum heat sink for a specific application depends upon an understanding of the basic mechanisms of heat transfer and the internal and external thermal impedances of the device to be mounted and adherence to some simple guidelines.

Heat-Transfer Methods

Heat may be transferred by three basic processes: conduction, convection, and radiation. Each of these processes is used in the removal of heat from silicon rectifiers and thyristors.

Conduction is a process of heat transfer in which heat energy is passed from one atom to the next, while the actual atoms involved in the transfer remain in their original positions. If a known amount of power flows through a material, the thermal resistance which may be attributed to conduction is determined by the following equation:

$$R_{\theta_{\text{cond}}} = d/4.186 KA \text{ } ^\circ\text{C per watt} \quad (10)$$

where d is the length of the thermal path in centimeters, K is the thermal conductivity in cal/(sec) (cm) ($^\circ\text{C}$), A is the area perpendicular to the thermal path t in square centimeters, and the conversion factor 4.186 is given in (watt) (sec)/cal. This equation is merely another form of Eq. (3) in which the conversion factor is used to obtain the result in $^\circ\text{C}$ per watt.

Convection is a term applied to the transfer of heat by the physical motion of hot material. In forced convection, the medium of heat transfer is moved by a fan. In natural convection, the medium moves because of differences in density. Both forced and natural convection are used for thyristor and rectifier cooling. The following equation defines the thermal resistance of vertical plates freely suspended in free air at ground level:

$$R_{\theta_{\text{conv}}} = (2300/A) (L/T_s - T_{\text{amb}})^{1/4} \quad (11)$$

where A is the total exposed area (twice the area of one side) in square centimeters, T_s is the surface temperature of the heat sink in $^\circ\text{C}$, T_{amb} is the ambient temperature in $^\circ\text{C}$, and L is the height of the heat sink in centimeters.

The third process by which heat may be transferred is **radiation**. The rate of emission from a surface can be found from Stefan's law. In accordance with this law, the equation for radiation thermal resistance may be written as follows:

$$R_{\theta_{\text{rad}}} = \frac{1793 \times 10^8}{AE (T_s^2 - T_{\text{amb}}^2)} (T_s - T_{\text{amb}})$$

where A is the total exposed area in square centimeters, E is the emissivity (a function of the surface finish), T_s is the surface temperature in $^{\circ}\text{C}$, and T_{amb} is the ambient temperature in $^{\circ}\text{C}$.

Physical Criteria

The sources of thermal resistance both internal and external to solid-state devices have been discussed, and the processes which may be used for heat removal have been explained briefly. Solid-state power devices are normally designed to be used with an external heat sink.

Most practical heat sinks for thyristors and rectifiers used in modern, compact equipment are the result of experiments with heat transfer through convection, radiation, and conduction in a given application. Although there are no set design formulas that provide exact heat-sink specifications for a given application, there are a number of simple rules that reduce the time required to evolve the best design for the job. These simple rules are as follows:

- (1) The surface area of the heat sink should be as large as possible to provide the greatest possible heat transfer. The area of the surface is dictated by case-temperature requirements and the environment in which the device is to be placed.

- (2) The heat-sink surface should have an emissivity value near unity for optimum heat transfer by radiation. A value approaching unity can be obtained if the heat-sink surface is painted flat black.

- (3) The thermal conductivity of the heat-sink material should be such that excessive thermal gradients are not established across the heat sink.

Although these rules are followed in conventional heat-sink systems, the size and cost of such systems often become restrictive in compact, mass-produced solid-state power circuits. The use of mass-produced prepunched parts, direct soldering, and batch-soldering techniques eliminates many of the difficulties associated with heat sinks by making possible the use of a variety of simple, efficient, readily fabricated heat-sink configurations that can be easily incorporated into the mechanical design of equipment. Detailed recommendations on heat-sink mounting of RCA thyristors and rectifiers are given in the section on **Packages, Handling, and Mounting**.

Types of Heat Sinks

Heat sinks are produced in various sizes, shapes, colors, and materials; the manufacturer should be contacted for exact design data. It is convenient for discussion purposes to group heat sinks into three categories as shown below:

1. **Flat vertical-finned types** are normally aluminum extrusions with or without an anodized black finish. They are unexcelled for natural convection cooling and provide reasonable thermal resistance at moderate air-flow rates for forced convection.

aluminum with an anodized black finish. They are used when maximum cooling in minimum lateral displacement is required, using natural convection.

3. Cylindrical horizontal-finned types are normally fabricated from sheet-metal rings and have a painted black matte finish. They are used in confined spaces for maximum cooling in minimum displaced volume.

It is also common practice to use the existing mechanical structure or chassis as a heat sink. The design equations and curves for such heat sinks based upon convection and radiation are shown in Figs. 35, 36, and 37.

vection and radiation is given⁴⁵ in Fig. 38. This nomograph applies for natural bright finish on the copper or aluminum. The family of curves shown in Fig. 39 may also be used as a guide to the determination of the required heat-sink area. These curves apply to square copper or aluminum heat sinks that have a dull finish.

Performance Criteria

The performance that may be expected from a commercial heat sink is normally specified by the manufacturer, and the information supplied in the design curves shown in Figs. 35, 36 and 37 pro-

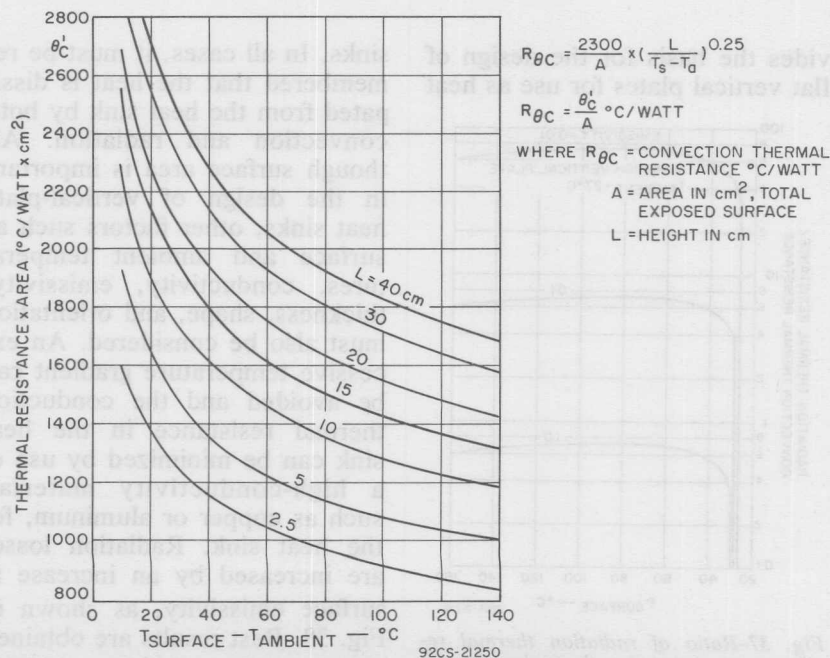


Fig. 35—Convection thermal resistance as a function of temperature drop from the surface of the heat sink to free air for heat sinks of various heights.

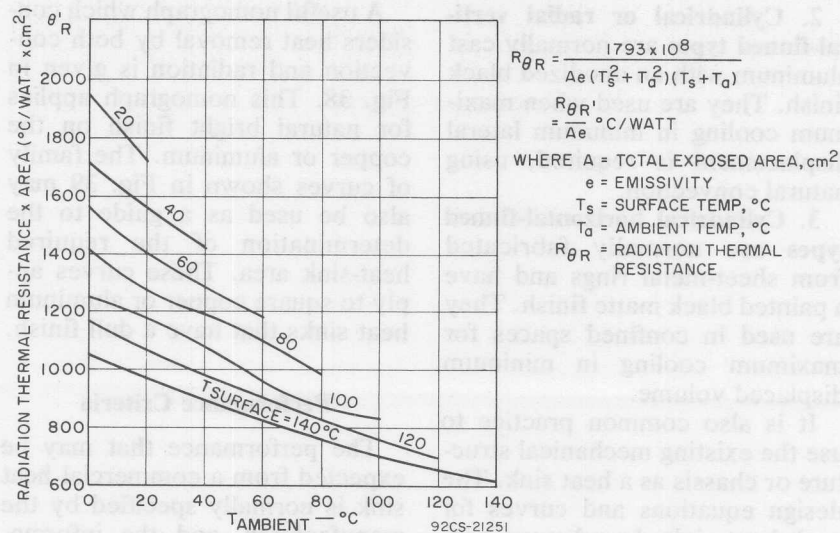


Fig. 36—Radiation thermal resistance as a function of ambient temperature for various heat-sink surface temperatures.

vides the basis for the design of flat vertical plates for use as heat

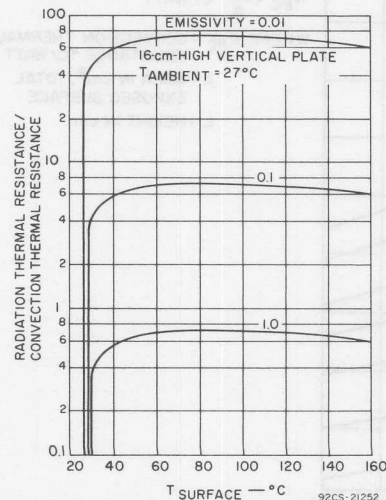


Fig. 37—Ratio of radiation thermal resistance to convection thermal resistance as a function of heat-sink surface temperature for various surface emissivities.

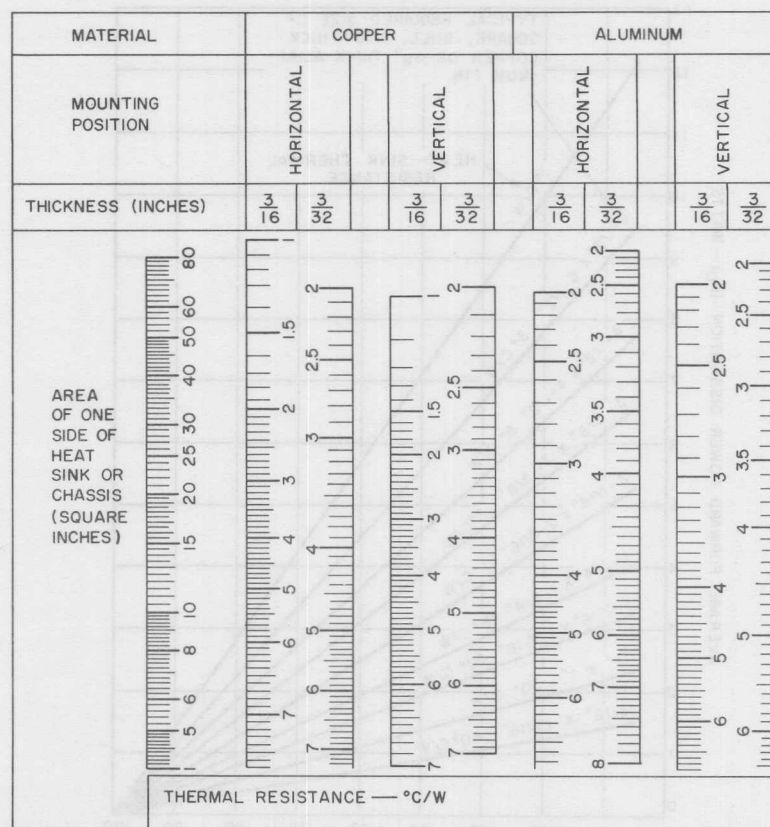
sinks. In all cases, it must be remembered that the heat is dissipated from the heat sink by both convection and radiation. Although surface area is important in the design of vertical-plate heat sinks, other factors such as surface and ambient temperatures, conductivity, emissivity, thickness, shape, and orientation must also be considered. An excessive temperature gradient can be avoided and the conduction thermal resistance in the heat sink can be minimized by use of a high-conductivity material, such as copper or aluminum, for the heat sink. Radiation losses are increased by an increase in surface emissivity, as shown in Fig. 38. Best results are obtained when the heat sink has a black matte finish for which the emis-

sivity is at least 0.9. When free-air convection is used for heat removal, a vertically mounted heat sink provides a thermal resistance that is approximately 30 per cent lower than that obtained with horizontal mounting.

In restricted areas, it may be necessary to use forced-convection cooling to reduce the effective thermal resistance of the heat

sink. On the basis of the improved reliability of cooling fans, it can be shown that the over-all reliability of a system may actually be improved by use of forced-convection cooling because the number of components required is reduced.

Economic factors are also important in the selection of heat sinks. It is often more economical



92CS-21253

Instruction for use: Select the heat-sink area at left and draw a horizontal line across the chart from this value. Read the value of maximum thermal resistance depending on the thickness of the material, type of material, and mounting position.

Fig. 38—Thermal resistance as a function of heat-sink dimensions.

to use one heat sink with several properly placed devices than to use individual heat sinks. It can be shown that the cooling efficiency increases and the unit cost decreases under such conditions.

Typical Examples

The curves shown in Fig. 39 are designed for use with the power-dissipation curves shown

in the technical bulletins describing the various RCA thyristors. These curves are conservative and can be used directly for thyristors having junction-to-case thermal-resistance ratings ($R_{\theta JC}$) of 5°C per watt or less. The curves shown in Fig. 40 represent the power-dissipation characteristics of a typical thyristor. As an example of the use of Figs. 39 and

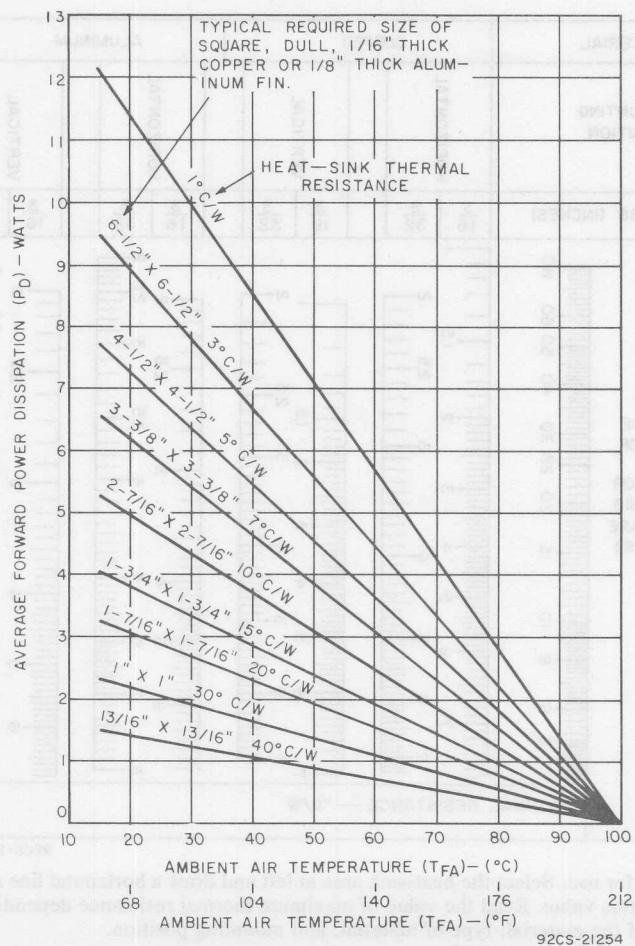


Fig. 39—Guide to heat-sink area determination.

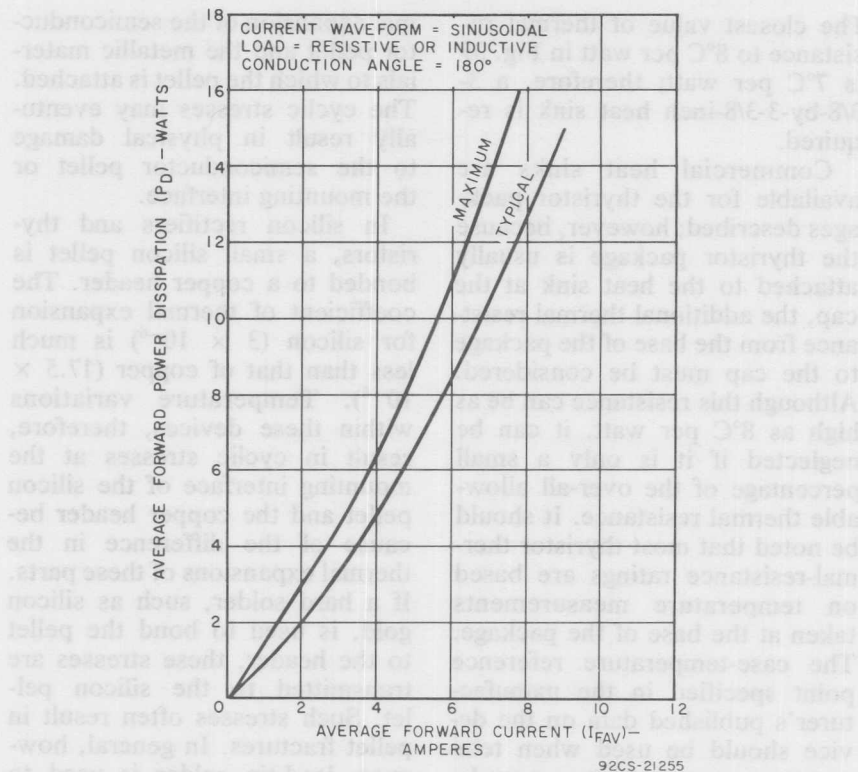


Fig. 40—Typical thyristor power-dissipation curves.

40, it is assumed that an appropriate heat sink must be found for a thyristor that is to conduct a current of 2 amperes, operate at an air temperature of 37°C, and be soldered to the heat sink at the base of the package. From Fig. 40, the maximum power dissipation in the thyristor is found to be 3 watts. Fig. 39 shows that the maximum allowable thermal resistance of the heat sink at this level of power dissipation is 15°C per watt, and that a square, dull, 1/16-inch-thick copper or 1/8-inch-thick aluminum heat sink with an area of at least 1-3/4 by 1-1/4 inches is required.

The curves of Fig. 39 can also be used with thyristors that have junction-to-case thermal-resistance ratings greater than 5°C per watt. However, the difference between the higher thermal-resistance value of the thyristor and the value of 5°C per watt upon which the curves are based must be subtracted from the thermal-resistance values shown in Fig. 39. For example, if it is assumed that the conditions are the same as those stated previously except that the junction-to-case thermal resistance of the device is 13°C, per watt the difference in thermal-resistance values is 8°C per watt.

The closest value of thermal resistance to 8°C per watt in Fig. 39 is 7°C per watt; therefore, a 3-3/8-by-3-3/8-inch heat sink is required.

Commercial heat sinks are available for the thyristor packages described; however, because the thyristor package is usually attached to the heat sink at the cap, the additional thermal resistance from the base of the package to the cap must be considered. Although this resistance can be as high as 8°C per watt, it can be neglected if it is only a small percentage of the over-all allowable thermal resistance. It should be noted that most thyristor thermal-resistance ratings are based on temperature measurements taken at the base of the package. The case-temperature reference point specified in the manufacturer's published data on the device should be used when temperature measurements are made. A low-mass temperature probe or thermocouple equipped with wire leads no larger than AWG No. 26 should be employed for systems with thermal-resistance values less than 50°C per watt. For systems with thermal-resistance values greater than 50°C per watt, smaller wire (such as AWG No. 36) is preferred.

THERMAL-FATIGUE CONSIDERATIONS

When a solid-state device is alternately heated and allowed to cool, cyclic mechanical stresses are produced within the device because of differences in the ther-

mal expansion of the semiconductor pellet and the metallic materials to which the pellet is attached. The cyclic stresses may eventually result in physical damage to the semiconductor pellet or the mounting interface.

In silicon rectifiers and thyristors, a small silicon pellet is bonded to a copper header. The coefficient of thermal expansion for silicon (3×10^{-6}) is much less than that of copper (17.5×10^{-6}). Temperature variations within these devices, therefore, result in cyclic stresses at the mounting interface of the silicon pellet and the copper header because of the difference in the thermal expansions of these parts. If a hard solder, such as silicon gold, is used to bond the pellet to the header, these stresses are transmitted to the silicon pellet. Such stresses often result in pellet fractures. In general, however, lead-tin solder is used to bond the silicon pellet to the copper header. The cyclic thermal stresses then are absorbed by non-elastic deformation of the soft lead solder, and very little stress is transmitted to the pellet.

The continuous flexing that results from cyclic temperature changes may eventually cause fatigue failures in a conventional lead solder system. Such failures are a function of the amount of change in temperature at the mounting interface, the difference in the thermal-expansion coefficients of the silicon pellet and the material to which the pellet is attached, and the maximum dimensions of the mounting interface.

Fatigue failures occur whenever the cyclic stresses damage the solder to the point at which the transfer of heat between the pellet and the surface to which it is mounted becomes impaired. This condition, which is indicated by a significant rise in junction-to-case thermal resistance, may exist in only a small portion of the pellet. This portion, however, overheats, and device failure results because of regenerative conditions that lead to thermal runaway.

Thermal-fatigue failures are accelerated because of dislocation "pile-ups" that result from impurities in the lead solder. RCA has developed a process that substantially reduces the amount of impurities introduced into the solder. Use of this proprietary "**Controlled Solder Process**" makes it possible to avoid the microcracks that propagate to cause fatigue failures and, therefore, greatly increases thermal-cycling capability.

The performance of any solid-state device is critically dependent upon the thermal capabilities of the device. This factor, together with the wide diversity of circuit requirements and associated considerations, has given rise to a large variety of thyristor and rectifier packages in many different configurations and a wide range of power-dissipation capabilities to meet the requirements of the numerous types of applications in which these devices may be used. In selecting a thyristor or rectifier for a particular circuit, the designer should ascertain that the thermal capability of the package is adequate for the application and should observe mounting and handling recommendations and precautions to assure achievement of the high degree of reliability and performance of which the device is capable.

The small size of most solid-state devices offers obvious advantages to the designer of electronic equipment. Designers should realize, however, that these compact devices usually provide only a relatively small insulation area between adjacent leads and the metal envelope. When solid-state devices are used in moist or contaminated environments, therefore, supplementary protection must be provided to prevent development of electrically conductive paths across the relatively small insulating surfaces. Specific information on "voltage creepage" is given in references such as JEDEC Standard No. 7, "Suggested Standard on Thyristors," and JEDEC Standard No. K212, "Standards for Silicon Rectifiers, Diodes and Stacks."

GENERAL CONSIDERATIONS
The small size of most solid-state devices offers obvious advantages to the designer of

Packages, Handling, and Mounting

The performance of any solid-state device is critically dependent upon the thermal capabilities of the device. This factor, together with the wide diversity of circuit layout requirements and economic considerations, has given rise to a large variety of thyristor and rectifier packages in many different configurations and a wide range of power-dissipation capabilities to meet the requirements of the numerous types of applications in which these devices may be used. In selecting a thyristor or rectifier for a particular circuit, the designer should ascertain that the thermal capability of the package is adequate for the application and should observe mounting and handling recommendations and precautions to assure achievement of the high degree of reliability and performance of which the device is capable.

GENERAL CONSIDERATIONS

The small size of most solid-state devices offers obvious advantages to the designers of

electronic equipment. Designers should realize, however, that these compact devices usually provide only a relatively small insulation area between adjacent leads and the metal envelope. When solid-state devices are used in moist or contaminated atmospheres, therefore, supplemental protection must be provided to prevent development of electrically conductive paths across the relatively small insulating surfaces. Specific information on "voltage creepage" is given in references such as JEDEC Standard No. 7, "Suggested Standard on Thyristors," and JEDEC Standard No. RS282, "Standards for Silicon Rectifier Diodes and Stacks."

The metal shells of some rectifiers and of most thyristors operate at the anode voltage. Consideration should be given, therefore, to the possibility of shock hazard if the shells are to be operated at voltages appreciably above or below ground potential. In general, in any application in which devices are operated at high voltages, suitable precautionary

vent direct contact with these devices.

Devices should not be connected into or disconnected from circuits with the power on because high transient voltages may cause permanent damage to them.

Recommended Soldering Methods

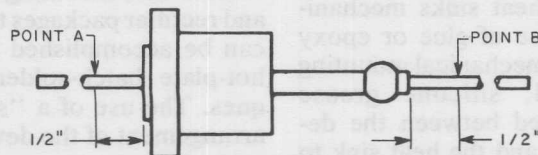
Some thyristor and rectifier packages have flexible leads; the leads of such packages are usually soldered to the circuit elements. In all soldering operations, some slack or expansion elbow should be provided in each lead to prevent excessive tension on the leads. Excessive heat should be avoided during the soldering operation to prevent possible damage to the devices. Some of the heat can be absorbed if the flexible lead of the device is grasped between the case and the soldering point with a pair of pliers.

When dip soldering is employed in the connection of a thyristor or rectifier onto a printed-circuit board, the temperature of the solder should be limited to about 225°C to 250°C for a maximum immersion period of 10 seconds. Moreover, the leads should not be dip-soldered too close to the package case. Fig. 41 shows the

should not extend on a silicon-rectifier DO-1 package.

Lead-Bending Techniques

Flexible leads can be bent into almost any configuration to fit any mounting requirement. These leads, however, are not intended to take repeated bending; repeated bending at the point at which the lead enters the case, in particular, should be avoided. Although the leads are not especially brittle at this point, the sharp edge of the case results in an excessively small radius in a bend made at the case. Repeated bending with a small radius of curvature at a fixed point will eventually cause fatigue and breakage in any material. For this reason, right-angle bends should be made at least 0.20 inch from the case. This practice enables sharp bends to be avoided and permits sufficient electrical isolation to be maintained between lead connections and the device header. A safe bend can be assured if the lead is gripped with pliers close to the case and is then bent the required amount with the fingers, as shown in Fig. 42. When the leads of a number of devices are to be bent into a particular



92CS-26582

Fig. 41—Diagram showing areas beyond which dip-soldering should not extend.

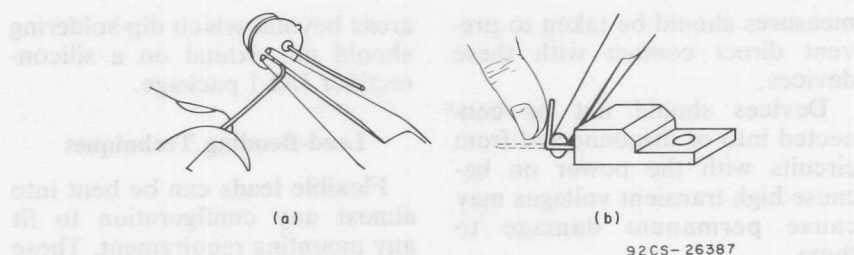


Fig. 42—Method of bending leads on thyristor packages: (a) JEDEC TO-5 hermetic package; (b) JEDEC TO-220AB (Versawatt) molded-plastic package.

configuration, it may be advantageous to use a lead-bending fixture to assure that all leads are bent to the same shape and in the correct place the first time so that no repeated bending of the leads is required.

General Procedures for Heat-Sink Mounting

When thyristors and rectifiers are operated at high power levels (at dissipations greater than the free-air rating), they should be mounted on heat sinks. Methods used to select the proper size and type of heat sink are discussed in the section on **Thermal Considerations** given earlier in this Manual.

For most efficient heat transfer, the heat sink should be in intimate contact with at least one-half the device package. Thyristor and rectifier packages can be mounted on heat sinks mechanically or by use of glue or epoxy adhesives. If mechanical mounting is employed, silicone grease should be used between the device package and the heat sink to eliminate surface voids, to prevent insulation build up because of oxidation, and to help conduct

heat across the interface. The use of glues and epoxy adhesives for mounting provides good bonding, but also increases the thermal resistance at the interface. The rise in the interface thermal resistance can be minimized by use of an adhesive material that has a low thermal resistance, such as Hysol Epoxy Patch Material No. 6C or Wakefield Delta Bond No. 152.*

Some packages, such as the TO-5 types can be attached to the heat sink by soldering. This method is low in cost and results in a permanent bond in which the interface thermal resistance can easily be maintained below 1°C per watt under normal soldering conditions. Typical mounting arrangements for TO-5 thyristor packages are shown in the subsequent discussion on **Flexible-Lead (TO-5 Style) Thyristor Packages**.

Low-cost mounting of thyristor and rectifier packages to heat sinks can be accomplished by oven or hot-plate batch-soldering techniques. The use of a "self-jigging" arrangement of the device and the

*Products of Hysol Corporation, Olean, New York, and Wakefield Engineering, Inc. Wakefield, Massachusetts, respectively.

heat sink and a 60-40 solder preform are recommended for batch-soldering operations. If each unit is soldered individually with a flame or electric soldering iron, the heat source should be held on the heat sink, and the solder should be applied to the unit. Heat should be applied only long enough to permit the solder to flow freely. For packages adaptable to soldering, the body is tin-plated, and maximum solder-wetting is easily obtained without over-heating the devices.

LOW- AND MEDIUM-POWER RECTIFIER PACKAGES

The maximum forward-current ratings for low-current RCA silicon rectifiers supplied in axial-lead packages apply specifically for operation in free air (natural convection cooling) with specified temperatures at the attachment point on the lead. The average (dc) forward-current and the peak recurrent-forward-current capabilities of these rectifiers are increased by use of short lead lengths to the soldering point. The small power dissipation in these rectifiers do not generally cause a substantial increase in the temperature at the mounting point.

RCA low-current packages include the two-lead and axial-lead versions of the JEDEC TO-1 package and the axial-lead JEDEC DO-26 and the DO-15 (molded plastic version of the DO-26) packages shown in Fig. 43. RCA axial-lead rectifiers intended for higher currents (up to 2 amperes) are supplied in the flanged-case,

JEDEC DO-1 package shown in Fig. 44. Fig. 45 shows two methods that may be used for mechanical attachment of this type of package to a heat sink. Rectifiers

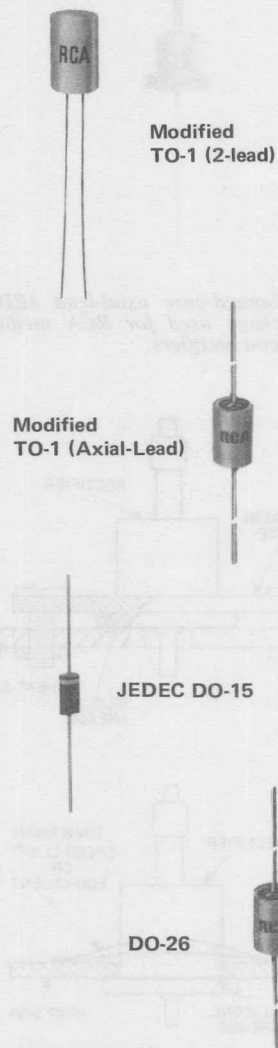
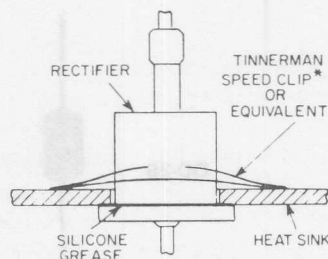
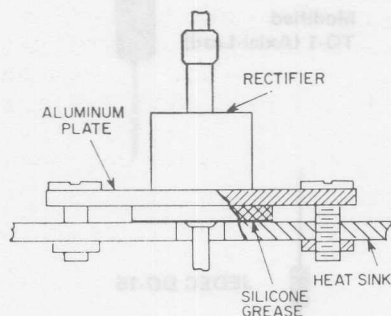


Fig. 43—Packages for RCA low-power silicon rectifiers.



Fig. 44—Flanged-case axial-lead JEDEC DO-1 package used for RCA medium-power silicon rectifiers.



92CS-21267

Fig. 45—Suggested methods for attachment of JEDEC DO-1 flanged-case axial-lead rectifier packages to heat sinks.

intended for use at currents from 6 to 40 amperes are supplied in DO-4 or DO-5 stud packages. Recommended mounting arrangements for rectifier and thyristor stud packages are described later in this section.

FLEXIBLE-LEAD (TO-5-STYLE) THYRISTOR PACKAGES

Fig. 46 shows flexible-lead packages used for RCA thyristors. This group includes the basic JEDEC TO-5 package and low-profile modifications of this basic packages.

Thyristors should be mounted on heat sinks when they are operated at high power levels. An efficient heat-sink method for thyristor in JEDEC TO-5 and modified TO-5 packages is to provide intimate contact between the heat sink and at least one-half of the base of the device opposite the leads. TO-5 packages can be mounted to the heat sink mechanically, with glue or an epoxy adhesive; soldering, however, is preferable for thyristors. Not only is the solder bond both permanent and most efficient, but the thermal resistance $R_{\theta_{CS}}$ from the case to the heat sink is easily kept below 1°C per watt under normal soldering conditions. Oven or hot-plate batch-soldering techniques are recommended because of their low cost.

FLANGED-CASE THYRISTOR PACKAGES

The mounting flanges of thyristor packages such as the JEDEC TO-3 and TO-66 serve as the anode

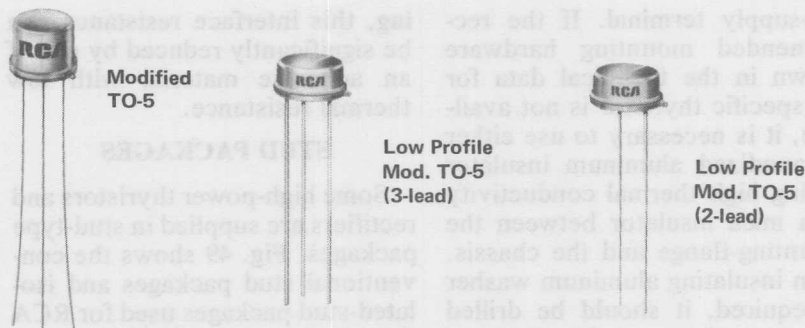


Fig. 46—TO-5 style thyristor packages.

terminal. In such cases, the mounting flange must be securely fastened to the heat sink, which may be the equipment chassis. Under no circumstances, however, should the mounting flange be soldered directly to the heat sink or chassis because the heat of the soldering operation may cause permanent damage to the device.

Fig. 47 shows photographs of the JEDEC TO-3, TO-8 and TO-66 thyristor packages. These pack-

ages can be installed in commercially available sockets. Electrical connections may also be made by soldering directly to the terminal pins. The connections may be soldered to the pins close to the pin seals provided that care is taken to conduct excessive heat

away from the seal; otherwise, the heat from the soldering operation may crack the pin seals and thereby cause permanent damage to the device. During operation, the mounting-flange temperature is higher than the ambient temperature by an amount which depends on the heat sink used. The heat sink must provide sufficient thermal conduction to the ambient environment to assure that the tem-



Fig. 47—RCA flanged-case thyristor packages.

perature of the device mounting flange does not rise above the rated value. The heat sink or chassis may be connected to either the positive or negative supply. In many applications, the chassis is connected to the volt-

age can be installed in commercially available sockets. Electrical connections may also be made by soldering directly to the terminal pins. The connections may be soldered to the pins close to the pin seals provided that care is taken to conduct excessive heat

perature of the device mounting flange does not rise above the rated value. The heat sink or chassis may be connected to either the positive or negative supply. In many applications, the chassis is connected to the volt-

age-supply terminal. If the recommended mounting hardware shown in the technical data for the specific thyristor is not available, it is necessary to use either an anodized aluminum insulator having high thermal conductivity or a mica insulator between the mounting-flange and the chassis. If an insulating aluminum washer is required, it should be drilled or punched to provide the two mounting holes for the terminal pins. The burrs should then be removed from the washer and the washer anodized. To insure that the anodized insulating layer is not destroyed during mounting, it is necessary to remove the burrs from the holes in the chassis.

It is also important that an insulating bushing, such as glass-filled nylon, be used between each mounting bolt and the chassis to prevent a short circuit. However, the insulating bushing should not exhibit shrinkage or softening under the operating temperatures encountered. Otherwise the thermal resistance at the interface between the package and the heat sink may increase as a result of decreasing pressure.

Fig. 48 shows methods of mounting flanged packages. Zinc-oxide-filled silicone grease should be used between the device and the heat sink to eliminate surface voids and help conduct heat across the interface. Although glue or epoxy adhesive provides good bonding, a significant amount of thermal resistance may exist at the interface. As discussed in the section on **General Procedures for Heat-Sink Mount-**

ing, this interface resistance can be significantly reduced by use of an adhesive material with low thermal resistance.

STUD PACKAGES

Some high-power thyristors and rectifiers are supplied in stud-type packages. Fig. 49 shows the conventional stud packages and isolated-stud packages used for RCA thyristors and rectifiers. In conventional stud packages, the stud is directly connected to main terminal No. 2 in triacs, to the anode in SCR's, and to the cathode in conventional forward-polarity or to the anode in reverse-polarity rectifiers. In isolated-stud packages, the stud is isolated from the device electrodes by a ceramic insulator that permits these packages to withstand a voltage difference between the stud and the device electrodes that typically can be as high as 3000 volts. (**WARNING:** The RCA isolated-stud packages should be handled with care. The ceramic portions of these packages contain **beryllium oxide** as a major ingredient. Do not crush, grind, or abrade these portions of the devices because the dust resulting from such action may be hazardous if inhaled.)

Connection of stud packages to the chassis or heat sink should be made at the flat surface of the package perpendicular to the threaded stud. A large mating surface should be provided to avoid hot spots and high thermal drop. The hole for the stud should be only as large as necessary for clearance and should contain no burrs or ridges on its perimeter.

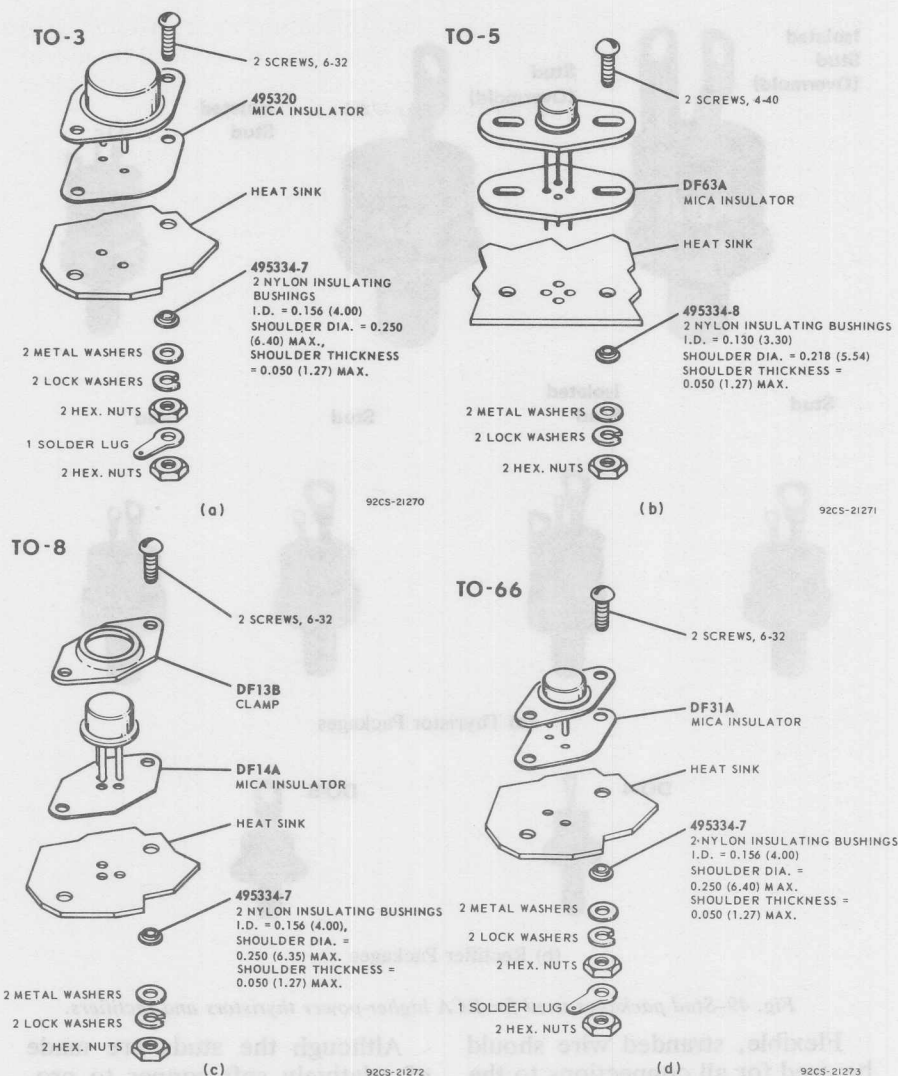


Fig. 48—Methods of mounting flanged packages.

As mentioned in the discussion of flanged packages, the use of a zinc-oxide-filled silicone grease between the device and the heat sink eliminates surface voids, prevents insulation buildup due to oxidation, and helps conduct

heat across the interface. Care must be taken to avoid the application of too much torque lest the semiconductor junction be damaged. Maximum limitations are given in the technical data for the particular devices.

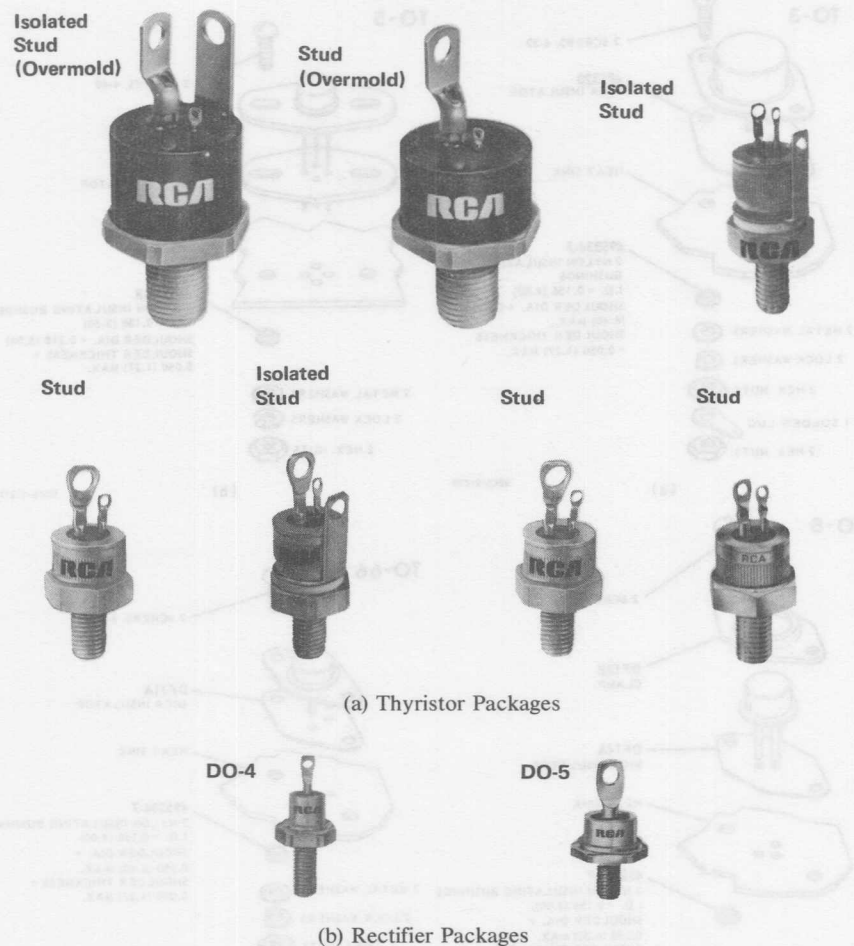
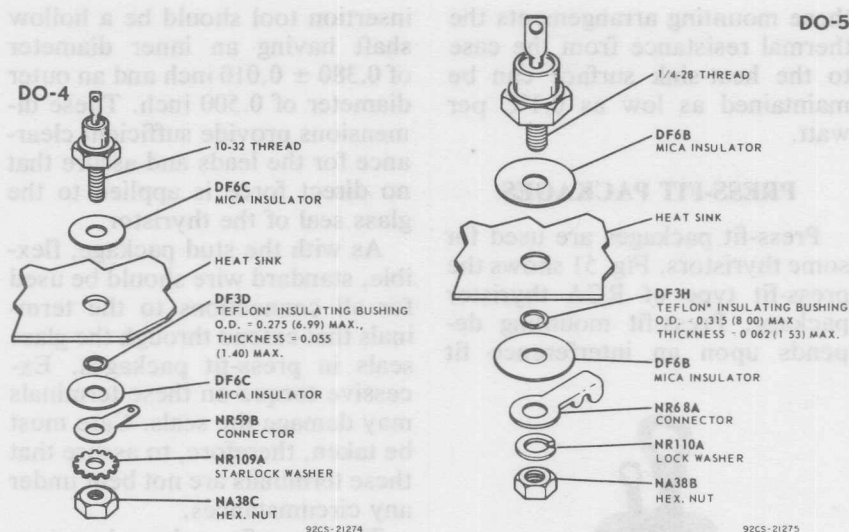


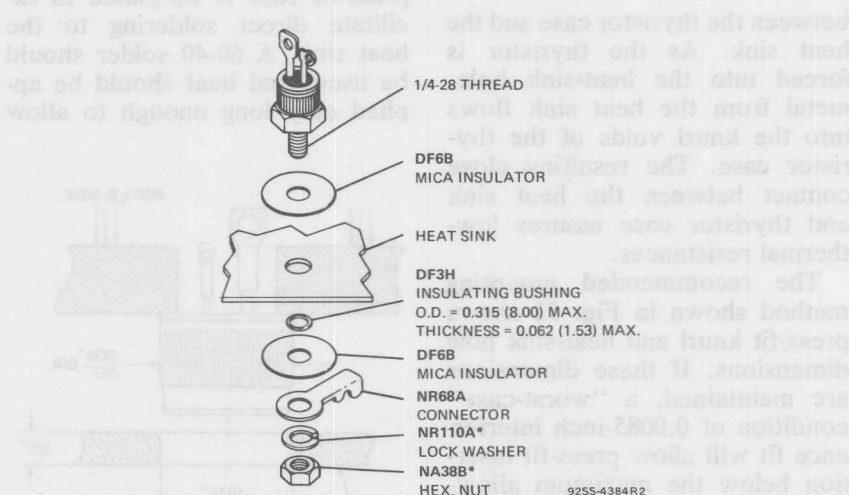
Fig. 49—Stud packages used for RCA higher-power thyristors and rectifiers.

Flexible, stranded wire should be used for all connections to the terminals that extend through the glass seals in stud packages. Excessive torque on these terminals may damage the seals and cause a loss in package hermeticity, which leads to premature device failure. These terminals, therefore, should not be bent under any circumstances.

Although the studs are made of relatively soft copper to provide high thermal conductivity, the threads cannot be relied upon to provide a mating surface. The actual heat transfer must take place on the underside of the hexagonal part of the package. Fig. 50 shows suggested mounting arrangements of the higher-current-type stud packages. With



(a) Rectifier Stud Packages



* Only hardware required for isolated-stud package.

(b) Thyristor Stud and Isolated-Stud Packages

Fig. 50—Suggested mounting arrangements for RCA thyristors and rectifiers supplied in stud packages.

these mounting arrangements the thermal resistance from the case to the heat-sink surface can be maintained as low as 0.1°C per watt.

PRESS-FIT PACKAGES

Press-fit packages are used for some thyristors. Fig. 51 shows the press-fit type of RCA thyristor package. Press-fit mounting depends upon an interference fit



Fig. 51—Press-fit package.

between the thyristor case and the heat sink. As the thyristor is forced into the heat-sink hole, metal from the heat sink flows into the knurl voids of the thyristor case. The resulting close contact between the heat sink and thyristor case assures low-thermal resistances.

The recommended mounting method shown in Fig. 52 shows press-fit knurl and heat-sink hole dimensions. If these dimensions are maintained, a "worst-case" condition of 0.0085-inch interference fit will allow press-fit insertion below the maximum allowable insertion force of 800 pounds. A slight chamfer in the heat-sink hole will help center and guide the press-fit package properly into the heat sink. The

insertion tool should be a hollow shaft having an inner diameter of 0.380 ± 0.010 inch and an outer diameter of 0.500 inch. These dimensions provide sufficient clearance for the leads and assure that no direct force is applied to the glass seal of the thyristor.

As with the stud package, flexible, standard wire should be used for all connections to the terminals that extend through the glass seals in press-fit packages. Excessive torque on these terminals may damage the seals. Care must be taken, therefore, to assure that these terminals are not bent under any circumstances.

The press-fit package is not restricted to a single mounting arrangement; direct soldering and the use of epoxy adhesives have been successfully employed. The press-fit case is tin-plated to facilitate direct soldering to the heat sink. A 60-40 solder should be used, and heat should be applied only long enough to allow

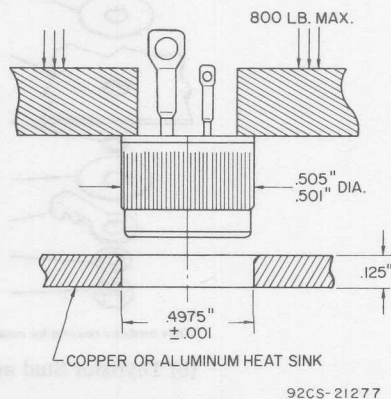


Fig. 52—Recommended mounting method for press-fit packages.

the solder to flow freely. Table VI shows how the case-to-heat-sink thermal resistance of a press-fit thyristor package can vary for different mounting arrangements.

Some RCA press-fit and stud-

type thyristor packages are also available with flexible leads, if desired. Fig. 53 shows the RCA 80-ampere press-fit thyristor package with flexible leads attached.

Table VI – Case-to-Heat-Sink Thermal Resistance of the RCA 80-Ampere Press-Fit and Stud Thyristor Packages.

Package	Type of Mounting Employed	Thermal Resistance-°C/W
	Press-fitted into heat sink. Minimum required thickness of heat sink = 0.25 in (6.35 mm)	0.4
Press-Fit	Soldered directly to heat sink. (60-40 solder which has a melting point of 188°C should be used. Heating time should be sufficient to cause solder to flow freely).	0.15 to 0.3
Stud	Directly mounted on heat sink with or without the use of heat-sink compound.	0.2 to 0.4

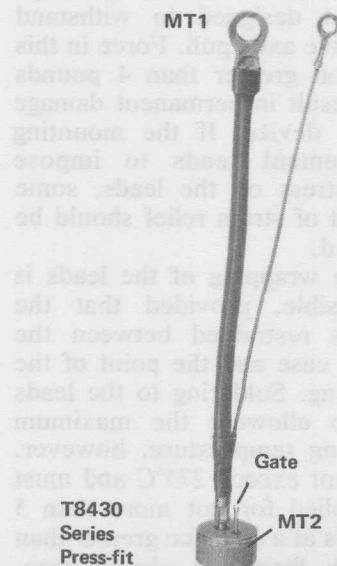


Fig. 53—RCA 80-ampere press-fit thyristor package with flexible leads.

VERSAWATT (MOLDED-PLASTIC) THYRISTOR PACKAGES

RCA thyristors are also available in the VERSAWATT type of molded-silicone-plastic packages. Thyristors supplied in these packages are intended for medium-power applications. Fig. 54 shows the basic configuration for the RCA VERSAWATT thyristor packages.

Lead-Forming Techniques

RCA VERSAWATT plastic packages are both rugged and versatile within the confines of commonly accepted standards for such devices. Although these

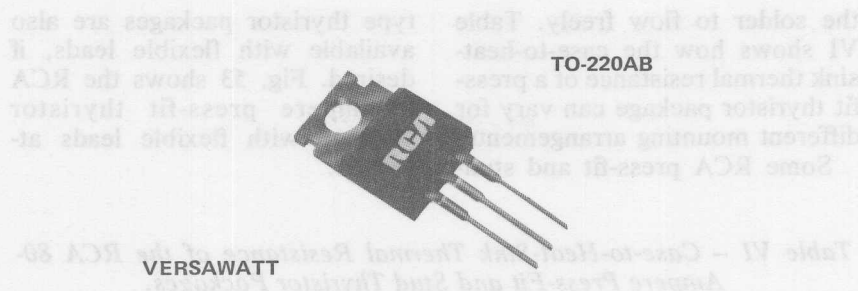


Fig. 54—RCA VERSAWATT (molded-plastic) package for medium-power thyristors.

versatile packages lend themselves to numerous arrangements, provision of a wide variety of lead configurations to conform to the specific requirements of many different mounting arrangements is highly impractical. However, the leads of the VERSAWATT in-line package can be formed to a custom shape, provided that they are not indiscriminately twisted or bent. Although these leads can be formed, they are not flexible in the general sense, nor are they sufficiently rigid for unrestrained wire wrapping. When the leads of a VERSAWATT package are to be formed, the recommended lead-bending techniques given earlier in this section should be followed.

When the leads of an in-line plastic package are to be formed, whether by use of long-nosed pliers or a special bending fixture, the following precautions must be observed to avoid internal damage to the device:

(1) Restrain the lead between the bending point and the plastic case to prevent relative movement between the lead and the case.

(2) When the bend is made in the plane of the lead (spreading),

bend only the narrow part of the lead.

(3) When the bend is made in the plane perpendicular to that of the leads, make the bend at least $\frac{1}{8}$ inch from the plastic case.

(4) Do not use a lead-bend radius of less than $\frac{1}{16}$ inch.

(5) Avoid repeated bending of leads.

The leads of the TO-220AB VERSAWATT in-line package are not designed to withstand excessive axial pull. Force in this direction greater than 4 pounds may result in permanent damage to the device. If the mounting arrangement tends to impose axial stress on the leads, some method of strain relief should be devised.

Wire wrapping of the leads is permissible, provided that the lead is restrained between the plastic case and the point of the wrapping. Soldering to the leads is also allowed; the maximum soldering temperature, however, must not exceed 275°C and must be applied for not more than 5 seconds at a distance greater than $\frac{1}{8}$ inch from the plastic case. When wires are used for connections, care should be exercised to

assure that movement of the wire does not cause movement of the lead at the lead-to-plastic junctions.

Mounting

Fig. 55 shows recommended mounting arrangements and suggested hardware for the VERSAWATT thyristors. The rectangular washer (NR231A) shown in Fig. 55(a) is designed to minimize distortion of the mounting flange when the thyristor is fastened to a heat sink. Excessive distortion of the flange could cause damage to the thyristor. The washer is particularly important when the size of the mounting hole exceeds 0.140 inch (6-32 clearance). Larger holes are needed to accommodate insulating bushings; however, the holes should not be larger than necessary to provide hardware clearance and, in any case, should not exceed a diameter of 0.250 inch. Flange distortion is also possible if excessive torque is used during mounting. A maximum torque of 8 inch-pounds is specified. Care should be exercised to assure that the tool used to drive the mounting screw never comes in contact with the plastic body during the driving operation. Such contact can result in damage to the plastic body and internal device connections. An excellent method of avoiding this problem is to use a spacer or combination spacer-isolating bushing which raises the screw head or nut above the top surface of the plastic body, as shown in

Fig. 56. The material used for such a spacer or spacer-isolating bushing should, of course, be carefully selected to avoid "cold flow" and consequent reduction in mounting force. Suggested materials for these bushings are diallphthalate, fiberglass-filled nylon, or fiberglass-filled polycarbonate. Unfilled nylon should be avoided.

Special Thermal Considerations

Fig. 57 shows a set of curves of typical case-to-heat-sink thermal resistance of the plastic VERSAWATT thyristor packages as a function of mounting torque for several mounting arrangements. Curves A through D show typical case-to-heat-sink thermal resistance for the mounting arrangements shown in Figs. 55(a) through 55(d). Curves E and F are representative of a VERSAWATT thyristor mounted over a heat-sink mounting hole that has a diameter of 0.140 inch (No. 6 screw clearance). Curve E shows the wide variation in thermal resistance with torque when the thyristor is mounted dry. Curve F shows the effect on contact thermal resistance of a thin layer of Dow Corning No. 340 silicone grease applied between thyristor and heat sink. For torques within the recommended range of 4 to 8 inch-pounds, contact thermal resistance is reduced to between 18 and 25 per cent of the dry values.

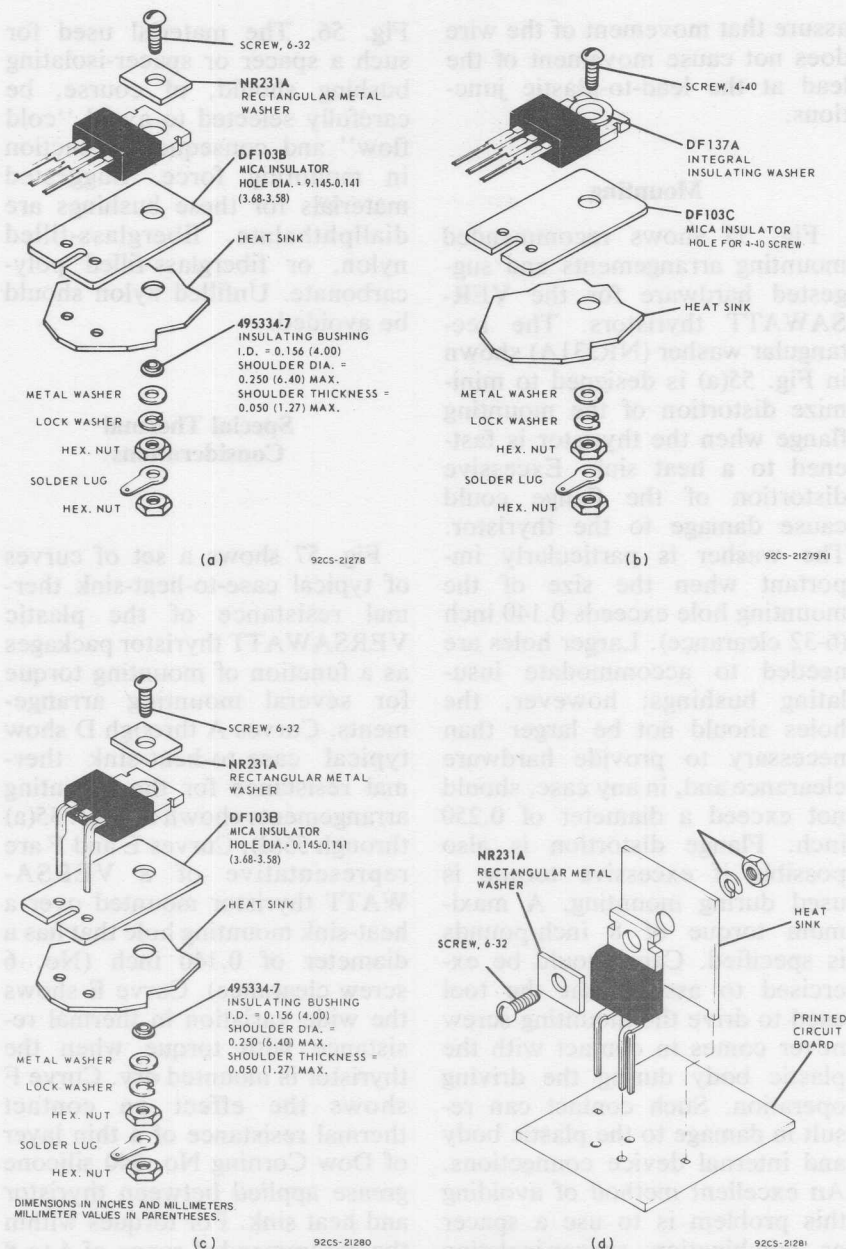


Fig. 55—Mounting arrangements for VERSAWATT thyristor packages: (a) and (b) in-line-lead mounting; (c) chassis mounting; (d) formed-lead vertical mounting on printed-circuit boards.

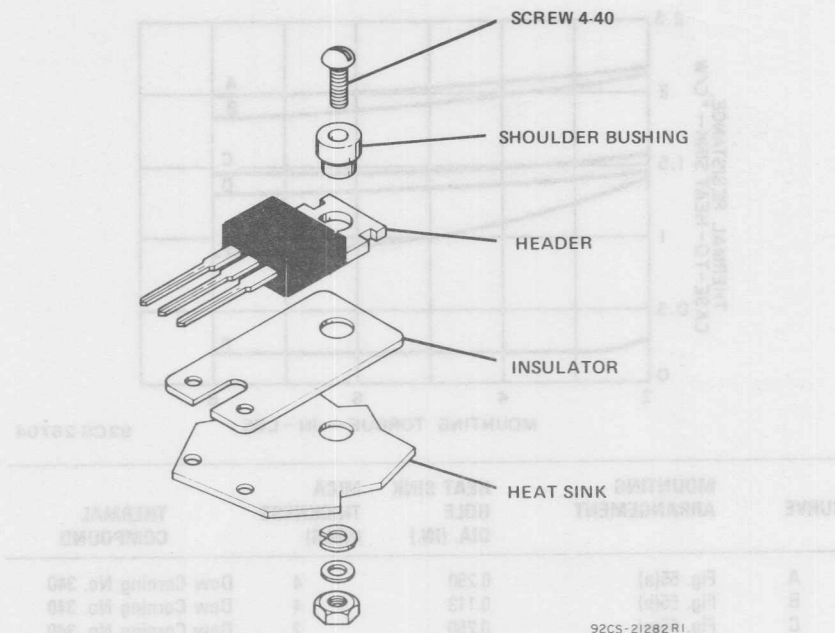


Fig. 56—Mounting arrangement in which an isolating bushing is used to raise the head of the mounting screw above the plastic body of the VERSAWATT package.

When permitted by the thyristor maximum junction-temperature rating, operation of the VERSAWATT thyristor packages with heat-sink temperatures of 100°C or greater results in some shrinkage of the insulating bushing normally used to mount thyristors. The degradation of contact thermal resistance (refer to Fig. 57) is usually less than 25 per cent if a good thermal compound is used.

During the mounting of RCA molded-plastic solid-state power devices, the following special precautions should be taken to assure efficient heat transfer from case to heat sink:

(1) Mounting torque should be between 4 and 8 inch-pounds.

(2) The mounting holes should be kept as small as possible.

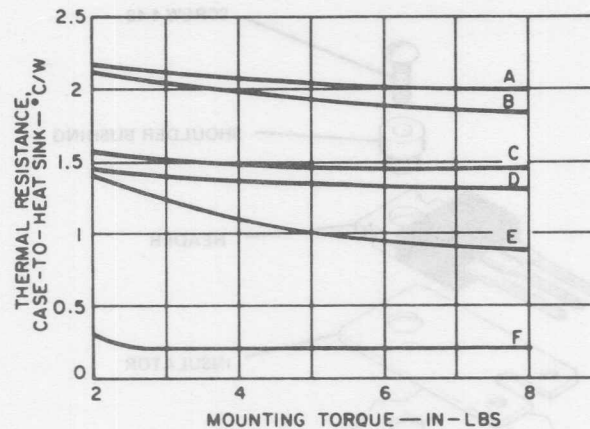
(3) Holes should be drilled or punched clean with no burrs or ridges, and chamfered to a maximum radius of 0.010 inch.

(4) The mounting surface should be flat within 0.002 inch/inch.

(5) Thermal grease (Dow Corning 340 or equivalent) should always be used (on both sides of the insulating bushing normally used to mount power thyristors).

(6) Thin insulating washers should be used (thickness of factory-supplied mica washers ranges from 2 to 4 mils).

(7) A lock washer or torque washer should be used, together with materials that have sufficient



92CS-26704

CURVE	MOUNTING ARRANGEMENT	HEAT SINK HOLE DIA. (IN.)	MICA THICKNESS (MILS)	THERMAL COMPOUND
A	Fig. 55(a)	0.250	4	Dow Corning No. 340
B	Fig. 55(b)	0.113	4	Dow Corning No. 340
C	Fig. 55(a)	0.250	2	Dow Corning No. 340
D	Fig. 55(b)	0.113	2	Dow Corning No. 340
E	—	0.140	None	None
F	—	0.140	None	Dow Corning No. 340

Fig. 57—Typical case-to-heat-sink thermal resistance as a function of mounting torque for an RCA VERSAWATT thyristor package.

creep strength to prevent degradation of heat-sink efficiency during life.

Cleaning After Mounting

A wide variety of solvents is available for degreasing and flux removal. The usual practice is to submerge components in a solvent bath for a specified time. From a reliability standpoint, however, it is extremely important that the solvent, together with other chemicals in the solder-cleaning system (such as flux and

solder covers), not adversely affect the life of the component. This consideration applies to all non-hermetic and molded-plastic components.

It is, of course, impractical to evaluate the effect on long-term thyristor life of all cleaning solvents, which are marketed under a variety of brand names with numerous additives. Chlorinated solvents, gasoline, and other hydrocarbons cause the inner encapsulant to swell and damage the thyristors. Alcohols are acceptable solvents and are recommended for flux removal when-

ever possible. Several examples of suitable alcohols are listed below:

- (1) methanol
- (2) ethanol
- (3) isopropanol
- (4) blends of the above

When considerations such as solvents flammability are of concern, selected Freon-alcohol blends are usable when exposure is limited. Solvents such as those listed below should be safe when used for normal flux removal

operations, but care should be taken to assure their suitability in the cleaning procedure:

- (1) Freon TE
- (2) Freon TE-35
- (3) Freon TP-35 (Freon PC)

These solvents may be used for a maximum of 4 hours at 25°C or for a maximum of 1 hour at 50°C.

Care must also be used in the selection of fluxes in the soldering of leads. Rosin or activated-rosin fluxes are recommended; organic fluxes are not.

Table VII -- Rectifier Product Matrix

Model	Part Number	00-1				00-25			
		100V	200V	300V	400V	100V	200V	300V	400V
1N4001	1N4001	✓	✓	✓	✓	✓	✓	✓	✓
1N4002	1N4002	✓	✓	✓	✓	✓	✓	✓	✓
1N4003	1N4003	✓	✓	✓	✓	✓	✓	✓	✓
1N4004	1N4004	✓	✓	✓	✓	✓	✓	✓	✓
1N4005	1N4005	✓	✓	✓	✓	✓	✓	✓	✓
1N4006	1N4006	✓	✓	✓	✓	✓	✓	✓	✓
1N4007	1N4007	✓	✓	✓	✓	✓	✓	✓	✓
1N4008	1N4008	✓	✓	✓	✓	✓	✓	✓	✓
1N4009	1N4009	✓	✓	✓	✓	✓	✓	✓	✓
1N4010	1N4010	✓	✓	✓	✓	✓	✓	✓	✓
1N4011	1N4011	✓	✓	✓	✓	✓	✓	✓	✓
1N4012	1N4012	✓	✓	✓	✓	✓	✓	✓	✓
1N4013	1N4013	✓	✓	✓	✓	✓	✓	✓	✓
1N4014	1N4014	✓	✓	✓	✓	✓	✓	✓	✓
1N4015	1N4015	✓	✓	✓	✓	✓	✓	✓	✓
1N4016	1N4016	✓	✓	✓	✓	✓	✓	✓	✓
1N4017	1N4017	✓	✓	✓	✓	✓	✓	✓	✓
1N4018	1N4018	✓	✓	✓	✓	✓	✓	✓	✓
1N4019	1N4019	✓	✓	✓	✓	✓	✓	✓	✓
1N4020	1N4020	✓	✓	✓	✓	✓	✓	✓	✓
1N4021	1N4021	✓	✓	✓	✓	✓	✓	✓	✓
1N4022	1N4022	✓	✓	✓	✓	✓	✓	✓	✓
1N4023	1N4023	✓	✓	✓	✓	✓	✓	✓	✓
1N4024	1N4024	✓	✓	✓	✓	✓	✓	✓	✓
1N4025	1N4025	✓	✓	✓	✓	✓	✓	✓	✓
1N4026	1N4026	✓	✓	✓	✓	✓	✓	✓	✓
1N4027	1N4027	✓	✓	✓	✓	✓	✓	✓	✓
1N4028	1N4028	✓	✓	✓	✓	✓	✓	✓	✓
1N4029	1N4029	✓	✓	✓	✓	✓	✓	✓	✓
1N4030	1N4030	✓	✓	✓	✓	✓	✓	✓	✓
1N4031	1N4031	✓	✓	✓	✓	✓	✓	✓	✓
1N4032	1N4032	✓	✓	✓	✓	✓	✓	✓	✓
1N4033	1N4033	✓	✓	✓	✓	✓	✓	✓	✓
1N4034	1N4034	✓	✓	✓	✓	✓	✓	✓	✓
1N4035	1N4035	✓	✓	✓	✓	✓	✓	✓	✓
1N4036	1N4036	✓	✓	✓	✓	✓	✓	✓	✓
1N4037	1N4037	✓	✓	✓	✓	✓	✓	✓	✓
1N4038	1N4038	✓	✓	✓	✓	✓	✓	✓	✓
1N4039	1N4039	✓	✓	✓	✓	✓	✓	✓	✓
1N4040	1N4040	✓	✓	✓	✓	✓	✓	✓	✓
1N4041	1N4041	✓	✓	✓	✓	✓	✓	✓	✓
1N4042	1N4042	✓	✓	✓	✓	✓	✓	✓	✓
1N4043	1N4043	✓	✓	✓	✓	✓	✓	✓	✓
1N4044	1N4044	✓	✓	✓	✓	✓	✓	✓	✓
1N4045	1N4045	✓	✓	✓	✓	✓	✓	✓	✓
1N4046	1N4046	✓	✓	✓	✓	✓	✓	✓	✓
1N4047	1N4047	✓	✓	✓	✓	✓	✓	✓	✓
1N4048	1N4048	✓	✓	✓	✓	✓	✓	✓	✓
1N4049	1N4049	✓	✓	✓	✓	✓	✓	✓	✓
1N4050	1N4050	✓	✓	✓	✓	✓	✓	✓	✓
1N4051	1N4051	✓	✓	✓	✓	✓	✓	✓	✓
1N4052	1N4052	✓	✓	✓	✓	✓	✓	✓	✓
1N4053	1N4053	✓	✓	✓	✓	✓	✓	✓	✓
1N4054	1N4054	✓	✓	✓	✓	✓	✓	✓	✓
1N4055	1N4055	✓	✓	✓	✓	✓	✓	✓	✓
1N4056	1N4056	✓	✓	✓	✓	✓	✓	✓	✓
1N4057	1N4057	✓	✓	✓	✓	✓	✓	✓	✓
1N4058	1N4058	✓	✓	✓	✓	✓	✓	✓	✓
1N4059	1N4059	✓	✓	✓	✓	✓	✓	✓	✓
1N4060	1N4060	✓	✓	✓	✓	✓	✓	✓	✓
1N4061	1N4061	✓	✓	✓	✓	✓	✓	✓	✓
1N4062	1N4062	✓	✓	✓	✓	✓	✓	✓	✓
1N4063	1N4063	✓	✓	✓	✓	✓	✓	✓	✓
1N4064	1N4064	✓	✓	✓	✓	✓	✓	✓	✓
1N4065	1N4065	✓	✓	✓	✓	✓	✓	✓	✓
1N4066	1N4066	✓	✓	✓	✓	✓	✓	✓	✓
1N4067	1N4067	✓	✓	✓	✓	✓	✓	✓	✓
1N4068	1N4068	✓	✓	✓	✓	✓	✓	✓	✓
1N4069	1N4069	✓	✓	✓	✓	✓	✓	✓	✓
1N4070	1N4070	✓	✓	✓	✓	✓	✓	✓	✓
1N4071	1N4071	✓	✓	✓	✓	✓	✓	✓	✓
1N4072	1N4072	✓	✓	✓	✓	✓	✓	✓	✓
1N4073	1N4073	✓	✓	✓	✓	✓	✓	✓	✓
1N4074	1N4074	✓	✓	✓	✓	✓	✓	✓	✓
1N4075	1N4075	✓	✓	✓	✓	✓	✓	✓	✓
1N4076	1N4076	✓	✓	✓	✓	✓	✓	✓	✓
1N4077	1N4077	✓	✓	✓	✓	✓	✓	✓	✓
1N4078	1N4078	✓	✓	✓	✓	✓	✓	✓	✓
1N4079	1N4079	✓	✓	✓	✓	✓	✓	✓	✓
1N4080	1N4080	✓	✓	✓	✓	✓	✓	✓	✓
1N4081	1N4081	✓	✓	✓	✓	✓	✓	✓	✓
1N4082	1N4082	✓	✓	✓	✓	✓	✓	✓	✓
1N4083	1N4083	✓	✓	✓	✓	✓	✓	✓	✓
1N4084	1N4084	✓	✓	✓	✓	✓	✓	✓	✓
1N4085	1N4085	✓	✓	✓	✓	✓	✓	✓	✓
1N4086	1N4086	✓	✓	✓	✓	✓	✓	✓	✓
1N4087	1N4087	✓	✓	✓	✓	✓	✓	✓	✓
1N4088	1N4088	✓	✓	✓	✓	✓	✓	✓	✓
1N4089	1N4089	✓	✓	✓	✓	✓	✓	✓	✓
1N4090	1N4090	✓	✓	✓	✓	✓	✓	✓	✓
1N4091	1N4091	✓	✓	✓	✓	✓	✓	✓	✓
1N4092	1N4092	✓	✓	✓	✓	✓	✓	✓	✓
1N4093	1N4093	✓	✓	✓	✓	✓	✓	✓	✓
1N4094	1N4094	✓	✓	✓	✓	✓	✓	✓	✓
1N4095	1N4095	✓	✓	✓	✓	✓	✓	✓	✓
1N4096	1N4096	✓	✓	✓	✓	✓	✓	✓	✓
1N4097	1N4097	✓	✓	✓	✓	✓	✓	✓	✓
1N4098	1N4098	✓	✓	✓	✓	✓	✓	✓	✓
1N4099	1N4099	✓	✓	✓	✓	✓	✓	✓	✓
1N4100	1N4100	✓	✓	✓	✓	✓	✓	✓	✓

Silicon Rectifiers

As explained in the section on **General Physical Theory**, silicon rectifiers are essentially cells containing a simple p-n junction. As a result, they have low resistance to current flow in one (forward) direction, but high resistance to current flow in the opposite (reverse) direction. They can be operated at ambient temperatures up to 200°C, current levels as high as hundreds of amperes, and voltage levels greater than 1000 volts. In addition, they can be used in parallel or series arrangements to provide higher current or voltage capabilities. The **Rectifier Product Matrix**,

shown in Table VII, points out the broad range of current and voltage capabilities and the variety of package structures that can be selected from the extensive line of RCA rectifiers.

Because of their high forward-to-reverse current ratios, silicon rectifiers can achieve rectification efficiencies greater than 99 per cent. When properly used, they have excellent life characteristics which are not affected by aging, moisture, or temperature. They are very small and light in weight, and can be made impervious to shock and other severe environmental conditions.

Table VII — Rectifier Product Matrix

RCA Rectifiers	Mod. TO-1	DO-1				DO-26			
	0.25A	0.75A	0.75A	1A	1A	0.75A	0.75A Insulated	1A	1A Insulated
I _{FSM}	30A	15A	15A	35A	35A	35A	35A	50A	50A
V _{RRM(V)}	50		1N536		1N2858A				
	100	D1300A	1N440B	1N537	1N2859A				
	200	D1300B	1N441B	1N538	1N2860A	1N3193	1N3253	1N5211	1N5215
	300		1N442B	1N539	1N2861A				
	400	D1300D	1N443B	1N540	1N1763A	1N2862A	1N3194	1N3254	1N5212
	500		1N444B	1N1095	1N1764A	1N2863A			
	600		1N445B	1N547		1N2864A	1N3195	1N3255	1N5213
	800						1N3196	1N3256	1N5214
	1000						1N3563		1N5218
File No.	794	5	3	89	91	41	41	245	245

Table VII — Rectifier Product Matrix (cont'd)

RCA Rectifiers		DO-15		DO-4		DO-5	
I_O		1A	1.5A	6A	12A	20A	40A
I_{FSM}		30A	50A	160A	240A	350A	800A
$V_{RRM(V)}$	50	D1201F	1N5391	1N1341B	1N1199A	1N248C	1N1183A
	100	D1201A	1N5392	1N1342B	1N1200A	1N249C	1N1184A
	200	D1201B	1N5393	1N1344B	1N1202A	1N250C	1N1185A
	300		1N5394	1N1345B	1N1203A	1N1195A	1N1187A
	400	D1201D	1N5395	1N1346B	1N1204A	1N1196A	1N1188A
	500		1N5396	1N1347B	1N1205A	1N1197A	1N1188A
	600	D1201M	1N5397	1N1348B	1N1206A	1N1198A	1N1190A
	800	D1201N	1N5398				
	1000	D1201P	1N5399				
	File No.	495	478	58	20	6	38

Fast-Recovery Types

RCA Rectifiers		DO-26		DO-15		DO-4		DO-5			
I_O		1A	1A	6A	6A	12A	12A	20A	20A	30A	40A
I_{FSM}		35A	50A	75A	125A	150A	250A	225A	300A	300A	700A
$V_{RRM(V)}$	50	D2601F	D2201F	1N3879	D2406F	1N3889	D2412F	1N3899	D2520F	1N3909	D2540F
	100	D2601A	D2201A	1N3880	D2406A	1N3890	D2412A	1N3900	D2520A	1N3910	D2540A
	200	D2601B	D2201B	1N3881	D2406B	1N3891	D2412B	1N3901	D2520B	1N3911	D2540B
	300			1N3882	D2406C	1N3892	D2412C	1N3902	D2520C	1N3912	
	400	D2601D	D2201D	1N3883	D2406D	1N3893	D2412D	1N3903	D2520D	1N3913	D2540D
	500										
	600	D2601M	D2201M		D2406M		D2412M		D2520M		D2540M
	800	D2601N	D2201N								
	1000										
Reverse Recovery Time t_{rr}											
	Typ.	200 ns.	200 ns.	—	200 ns.	—	200 ns.	—	200 ns.	—	200 ns.
	Max.	500 ns.	500 ns.	200 ns.	350 ns.	200 ns.	350 ns.	200 ns.	350 ns.	200 ns.	350 ns.
	File No.	723	629	726	663	727	664	728	665	729	580

For Horizontal-Deflection Circuits

RCA Rectifiers		DO-26		DO-1		DO-15
I_O		0.5*	1.6*	1.9*	—	1A
I_{FSM}		30A	70A	70A	30A	50A
Trace			D2601M	D2103SF		D2201M
Commutating			D2601E	D2103S		D2201M
Linearity						D2201B
Regulator						D2201B
Clamp	D2600M				D2101S	
File No.		839	839	522	522	629

* $I_F(RMS)$ value

NOTE: The file numbers listed in the matrix charts indicate the RCA technical data bulletins that provide detailed technical data on RCA rectifiers.

ELECTRICAL CHARACTERISTICS

Fig. 58 shows the basic current-voltage characteristic for a silicon rectifier. As explained in the potential-hill analyses in the section on **General Physical Theory**, the forward current is many times larger than the re-

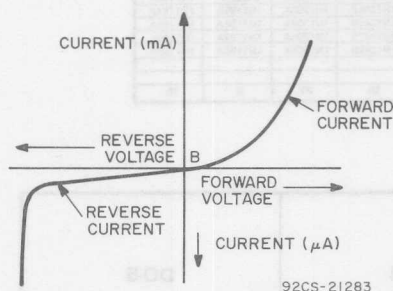


Fig. 58—Current-voltage characteristic of a silicon rectifier.

verse current over the normal operating range of the rectifier. The small reverse (leakage) current gradually rises with an increase in reverse voltage. This increase in reverse current eventually leads to junction breakdown, as indicated by an abrupt increase in reverse current at high reverse voltages. Another important feature of the rectifier characteristic is that the forward voltage drop remains small up to the maximum rated current. The basic characteristic curve shown in Fig. 58 serves as a model in the development of the characteristics data given in the manufacturer's specifications on silicon rectifiers.

Characteristics data given for silicon rectifiers are based on the

manufacturer's determination of the inherent qualities and traits of the device. These data, which are usually obtained by direct measurements, provide information that a circuit designer needs to predict the performance capabilities of his circuit and form the basis for the ratings that define the safe operating limits for the rectifier.

Forward Voltage Drop

The major source of power loss in a silicon rectifier arises from the forward-conduction voltage drop. This characteristic, therefore, is the basis for many of the rectifier ratings.

A silicon rectifier usually requires a forward voltage of 0.4 to 0.8 volt, depending upon the temperature and impurity concentration of the p-n junction, before a significant amount of current flows through the device. As shown in Fig. 59, a slight rise in the forward voltage beyond this point causes a sharp increase in the forward current. The slope of

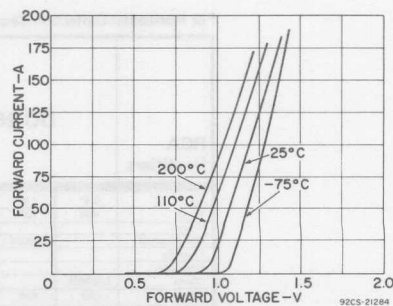


Fig. 59—Typical forward characteristics of a silicon rectifier.

the voltage-current characteristic at voltages above this threshold value represents the **dynamic resistance** of the rectifier. Losses that result from this resistance characteristic increase as the square of the current and thus increase rapidly at high current levels. The dynamic resistance is dependent upon the construction of the rectifier junction and is inversely proportional to the area of the silicon pellet.

Fig. 59 also shows that, at any reasonable current level, the value of forward voltage required to initiate current flow through the rectifier decreases as the temperature of the rectifier junction increases. This voltage-temperature dependence has a compensatory effect in rectifiers operated at high currents, but it is a source of difficulty when rectifiers are operated in parallel, as explained later in this section in the discussion of **Multiple Rectifier Connections**.

Reverse Current

When a reverse-bias voltage is applied across a silicon rectifier, a limited amount of reverse current flows through the rectifier. This current is in the order of only a few microamperes, as compared to the milliamperes or amperes of forward current produced when the rectifier is forward-biased. Initially, as shown in Fig. 60, the reverse current increases slightly as the blocking (reverse-bias) voltage increases, but then tends to remain relatively constant, even though the blocking voltage is increased signifi-

cantly. The figure also indicates that an increase in operating temperature causes a substantial increase in reverse current for a given reverse voltage. **Reverse-blocking thermal runaway** may occur because of this characteristic if the reverse dissipation becomes so large that, as the junction temperature rises, the losses increase faster than the rate of cooling.

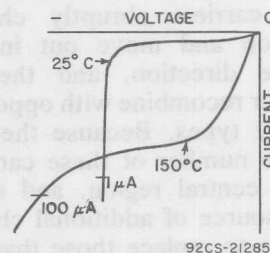


Fig. 60—Typical reverse characteristics of a silicon rectifier.

If the reverse blocking voltage is continuously increased, it eventually reaches a value (which varies for different types of silicon rectifiers) at which a very sharp increase in reverse current occurs. This voltage is called the **breakdown** or **avalanche** (or **zener**) voltage. Although rectifiers can operate safely at the avalanche point, the rectifier may be destroyed as a result of thermal runaway if the reverse voltage increases beyond this point or if the temperature rises sufficiently (e.g., a rise in temperature from 25°C to 150°C increases the current by a factor of several hundred).

Reverse Recovery Time

After a silicon rectifier has been operated under forward-bias

conditions, some finite time interval (in the order of a few microseconds) must elapse before it can return to the reverse-bias condition. This reverse-recovery time is a direct consequence of the greatly increased concentration of charge carriers in the central region that occurs during forward-bias operation. If the bias is abruptly reversed, some of these carriers abruptly change direction and move out in the reverse direction, and the remainder recombine with opposite-polarity types. Because there is a finite number of these carriers in the central region, and there is no source of additional charge carriers to replace those that are removed, the device will eventually go into the reverse-bias condition. During the removal period, however, the charge carriers constitute a reverse current known as the **reverse-recovery current**.

Fig. 61 shows the current waveform obtained when a sinusoidal voltage is applied across a silicon rectifier. During the positive alternation of the input voltage, the rectifier conducts and accumulates stored charge. When the supply voltage reverses polarity, the reverse recovery cur-

rent flows through the rectifier until all the stored charge is removed.

The reverse-recovery time imposes an upper limit on the frequency at which a silicon rectifier may be used. Any attempt to operate the rectifier at frequencies above this limit results in a significant decrease in rectification efficiency and may also cause severe overheating and resultant destruction of the rectifier because of power losses during the recovery period.

MAXIMUM RATINGS

Ratings are established for solid-state devices to help circuit and equipment designers use the performance and service capabilities of each type to maximum advantage. They define the limiting conditions within which a device must be maintained to assure satisfactory and reliable operation in equipment applications. A designer must thoroughly understand the constraints imposed by the device ratings if he is to achieve effective, economical, and reliable equipment designs. Reliability and performance considerations dictate that he select devices for which no ratings will be exceeded by any operating conditions of his application, including equipment malfunction. He should also realize, however, that selection of devices that have overly conservative ratings may significantly add to the cost of his equipment.

Three systems of ratings (the **absolute maximum system**, the

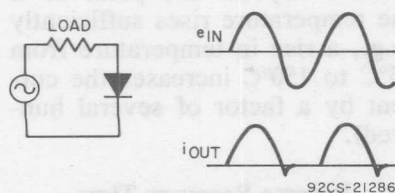


Fig. 61—Test circuit and output current waveform obtained when a sinusoidal voltage is applied across a silicon rectifier.

design center system, and the design maximum system) are currently in use in the electronics industry. The ratings given in the technical data for solid-state devices are based on the absolute maximum system. A definition for this system of ratings has been formulated by the **Joint Electron Devices Engineering Council (JEDEC)** and standardized by the **National Electrical Manufacturers Association (NEMA)** and the **Electronic Industries Association (EIA)**, as follows:

“**Absolute-Maximum** ratings are limiting values of operating and environmental conditions applicable to any electron device of a specified type as defined by its published data, and should not be exceeded under the worst probable conditions.

“The device manufacturer chooses these values to provide acceptable serviceability of the device, taking no responsibility for equipment variations, environmental variations, and the effects of changes in operating conditions due to variations in device characteristics.

“The equipment manufacturer should design so that initially and throughout life no absolute-maximum value for the intended service is exceeded with any device under the worst probable operating conditions with respect to supply-voltage variation, equipment component variation, equipment control adjustment, load variation, signal variation, environmental conditions, and variations in device characteristics.”

Ratings are given for those stress factors that careful study and experience indicate may lead to severe degradation in performance characteristics or eventual failure of a device unless they are constrained within certain limits. Table VIII lists the critical rating factors and limiting characteristics and indicates the symbols used to specify the safe operating capabilities of silicon rectifiers.

Ratings for silicon rectifiers are determined by the manufacturer on the basis of extensive testing. These ratings express the manufacturer's judgment of the maximum stress levels to which the rectifiers may be subjected without endangering the operating capability of the unit. The most significant factors for which silicon rectifiers must be rated are: peak reverse voltage, forward current, surge (or fault) current, operating and storage temperatures, amperes squared-seconds, and mounting torque.

Peak Reverse Voltage

Excessive off-state voltage potentials produce high leakage (or reverse) currents in solid-state devices. In silicon rectifiers, the high reverse currents that result from excessive reverse-bias voltages can lead to crystal breakdown and consequent destruction of the devices.

Peak reverse voltage (V_{RM}) is the rating used by the manufacturer to define the maximum allowable reverse voltage that can be applied across a rectifier. This

Table VIII—Ratings and Limiting Characteristics for Silicon Rectifiers

Quantity	Symbol	Quantity	Symbol
Ambient temperature	T_A	Reverse current:	
Case temperature	T_C	Total rms value	$I_{R(RMS)}$
Junction temperature	T_J	DC value, no alternating component	I_R
Storage temperature	T_{stg}	DC value, with alternating component	$I_{R(AV)}$
Thermal Resistance	R_θ	Instantaneous total value	I_{RM}
Junction to ambient	$R_{\theta J-A}$	Reverse recovery time	t_{rr}
Junction to case	$R_{\theta J-C}$	Reverse voltage:	
Case-to-ambient	$R_{\theta C-A}$	Total rms value	$V_{R(RMS)}$
Case-to-heat sink	$R_{\theta C-S}$	DC value, no alternating component	V_R
Transient thermal impedance	$R_{\theta(t)}$	DV value, with alternating component	$V_{R(AV)}$
Junction-to-ambient	$R_{\theta J-A}(t)$	Instantaneous total value	v_R
Junction-to-case	$R_{\theta J-C}(t)$	Maximum (peak) total value	V_{RM}
Delay time	t_d	Working peak	V_{RWM}
Rise time	t_r	Repetitive peak	V_{RRM}
Fall time	t_f	Non-repetitive peak	V_{RSM}
Forward current:		Reverse breakdown voltage:	
Total rms value	$I_{F(RMS)}$	DC value, no alternating component	$V_{(BR)R}$
DC value, no alternating component	I_F	Instantaneous total value	$v_{(BR)R}$
DC value, with alternating component	$I_{F(AV)}$	Forward Power Loss:	
Instantaneous total	i_F	DC value, no alternating component	P_F
Maximum (peak) total value	I_{FM}	DC value, with alternating component	$P_{F(AV)}$
Repetitive peak	I_{FRM}	Instantaneous total value	p_F
Surge (non-repetitive)	I_{FSM}	Maximum (peak) total value	P_{FM}
Forward voltage:		Reverse power loss:	
Total rms value	$V_{F(RMS)}$	DC value, no alternating component	P_R
DC value, no alternating component	V_F	DC value, with alternating component	$P_{R(AV)}$
DC value, with alternating component	$V_{F(AV)}$	Instantaneous total value	p_R
Instantaneous total value	v_F	Maximum (peak) total value	P_{RM}
Maximum (peak) value	V_{FM}		

rating is less than the avalanche breakdown level on the reverse characteristic. With present-day diffused-junction devices the power dissipation at peak reverse voltage is a small percentage of the total losses in the rectifier for operation at the maximum rated current and temperature levels. The reverse dissipation may increase sharply, however, as temperature or blocking voltage is increased to a point beyond that for which the device is capable of reliable operation. It is important, therefore, to operate within ratings.

A transient reverse voltage rating may be assigned when it has been determined that increased

voltage stress can be withstood for a short time duration provided that the device returns to normal operating conditions when the overvoltage is removed. This condition is illustrated in Fig. 62.

Peak-reverse voltage ratings for single-junction silicon rectifiers range from 50 to 1500 volts and for multiple-junction silicon-recti-

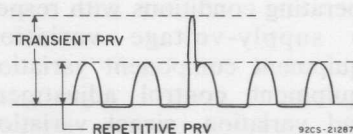


Fig. 62—Typical waveform of repetitive and transient reverse voltages applied across a silicon rectifier.

fier assemblies may be as high as several hundred thousands of volts.

Forward Current

If the current in a solid-state device becomes sufficiently large, the semiconductor pellet could be melted by the excessive junction temperatures that result. Maximum current ratings, however, are not usually based on the current-carrying capacity of the semiconductor pellet. Such ratings are usually based on the degradation of specific device performance characteristics that result when the current density exceeds a critical value or on the fusing current of an internal connecting wire.

The current rating assigned to a rectifier is expressed as a maximum value of forward current at a specific case temperature. For these conditions, the power dissipation and internal temperature gradient through the thermal impedance from junction to case are such that the junction is at or near the maximum operating temperature for which the blocking-voltage rating can be maintained. At current levels above this maximum rating, the internal and external leads and terminals of the device may experience excessive temperatures, regardless of the heat sink provided for the pellet itself. The current rating can be described more fully in the form of a curve such as that shown in Fig. 63.

Because the current through a rectifier is not normally a smooth flow, current ratings are usually

expressed in terms of average current (I_{AV}), peak current (I_M), and rms current (I_{RMS}). Each of these currents may be expressed in terms of the other two currents.

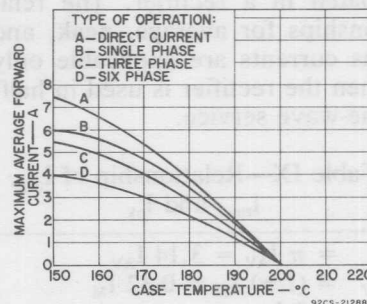


Fig. 63—Current rating chart for a 12-ampere silicon rectifier.

The **average current** through a rectifier in half-sine-wave service is related to the peak current by the following equation:

$$I_{AV} = \left[\frac{\int_0^{\pi} I_M \sin \omega t \, d(\omega t)}{2\pi} \right]$$

$$= I_M / \pi \quad (13a)$$

or

$$I_M = \pi I_{AV} \quad (13b)$$

The relationship between the **peak current** and **rms current** of a rectifier in half-sine-wave service can be expressed as follows:

$$I_{RMS} = \left[\frac{\int_0^{\pi} I_M^2 \sin^2 \omega t \, d(\omega t)}{2\pi} + \frac{\pi}{2\pi} I_M^2 \right]^{1/2}$$

$$= \frac{1}{2} I_M \quad (14a)$$

or

$$I_M = 2 I_{RMS} \quad (14b)$$

Table IX summarizes the relationships expressed by Eqs. (13) and (14). As discussed later, certain of these relationships are used to determine the power dissipated in a rectifier. The relationships for average, peak, and rms currents are applicable only when the rectifier is used in half-sine-wave service.

Table IX—Relationship of I_{avg} , I_{rms} , and I_{pk}

I_M	$= \pi I_{AV} = 3.14 I_{AV}$
I_{AV}	$= (1/\pi) I_M = 0.32 I_M$
I_M	$= 2 I_{RMS}$
I_{RMS}	$= 1/2 I_M$
I_{AV}	$= (2/\pi) I_{RMS} = 0.64 I_{RMS}$
I_{RMS}	$= (\pi/2) I_{AV} = 1.57 I_{AV}$

Published data for rectifiers usually list maximum limits for average current and for repetitive peak current. The **maximum average forward-current rating** $I_{F(AV)}$ is the maximum average value of current that is allowed to flow through the rectifier in the forward direction under stated conditions. The **repetitive peak forward-current rating** I_{FRM} is the maximum instantaneous value of repetitive forward current permitted under stated conditions. The dual maximum ratings are required because, under certain conditions (e.g., when a highly capacitive load is used), it is possible for the average current to be low and for the peak current to be high enough to cause overheating of the rectifier. The approximate expression for power losses P in a silicon rectifier,

given by the following equation, can be used to explain how this type of operation is possible:

$$P_{(watts)} = (V_{dc} I_{dc}) + (I_{RMS}^2 R_{dyn}) \quad (15)$$

where the voltage V_{dc} is 0.4 to 0.8 volt depending upon the junction temperature; the direct current I_{dc} is equivalent to the average current I_{AV} ; the current I_{RMS} is the true rms current and, for a fixed average current, increases as the peak current increases; and R_{dyn} is the dynamic resistance of the rectifier over the current range considered.

An analysis of Eq. (15) shows that if the peak current is increased and the conduction time is decreased so that the average current is held constant, the rms current and, therefore, the power dissipated in the rectifier ($I_{RMS}^2 R_{dyn}$) are also increased. This behavior explains why the maximum permissible value of average current in multiple-phase circuits is reduced as the number of phases is increased and the conduction period is reduced. Fig. 63 shows the effect of the number of phases on the variation in average current with case temperature.

Surge Current

A third maximum-current limit given in the manufacturer's data on silicon rectifiers is the surge (or fault) current rating I_{FSM} . During operation, unusually high surges of current may result at turn-on, load switching, and short circuits. A rectifier can absorb a limited amount of increased dis-

sipation that results from short-duration high surges of current without any effect except a momentary rise in junction temperature. If the surges become too high, however, the temperature of the junction may be raised beyond the maximum capability of the device. The rectifier may then be driven into thermal runaway and, consequently, be destroyed. Fig. 64 shows a typical surge-current rating curve for a silicon rectifier.

If the value and duration of anticipated current surges exceed the rating of the rectifier, impedance may be added to the circuit to limit the magnitude of the surge current, or fuses may be used to limit the duration of the surges. (The procedure used to calculate the value of the surge limiting resistance is explained in the discussion of capacitive load circuits in the section on DC Power Supplies.) In some cases,

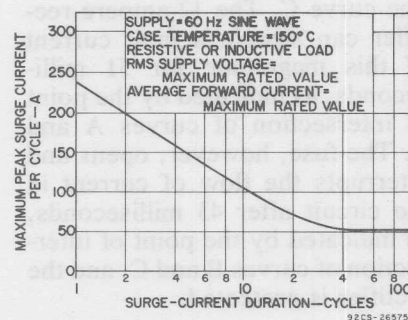


Fig. 64—Peak-surge-current rating chart for a 12-ampere silicon rectifier.

a rectifier that has an average-current rating higher than that required by the circuit must be used to meet surge requirements

of the circuit. The technique eliminates the need for additional circuit impedance elements or special fusing.

If fuses are used to protect the rectifiers, a coordination chart, such as that shown in Fig. 65, should be constructed. This chart

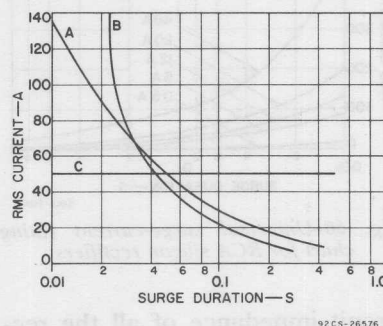


Fig. 65—Coordination chart that relates rectifier surge-current rating (curve A), opening characteristics of circuit fuses (curve B), and maximum available surge current in a circuit (curve C).

shows the surge rating of the rectifier (curve A), the opening characteristics of the fuse (curve B), and the maximum surge current available in the circuit (curve C). In the construction of a coordination chart for a particular rectifier, the rms value of the surge current can be obtained from a universal surge-rating chart, such as that shown in Fig. 66. The opening characteristics of the fuse can be obtained from the manufacturer's published data, and the maximum surge current can be calculated.

The coordination chart shown in Fig. 65 was prepared for a 12-ampere silicon rectifier operated in half-wave service from a

220-volt rms ac source and protected by a fuse having opening characteristics as shown by curve B. If the total short-

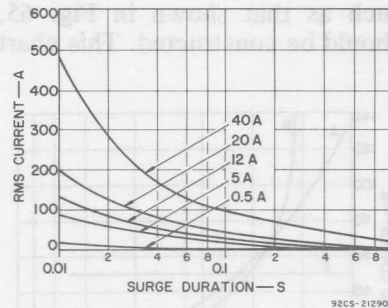


Fig. 66—Universal surge-current rating chart for RCA silicon rectifiers.

circuit impedance of all the rectifier elements is determined to be 2.25 ohms, the peak surge current I_s for full-wave operation can be calculated as follows:

$$I_s = \frac{220 V_{RMS} \times 1.41}{2.25} \\ = 137.6 \text{ amperes}$$

For half-wave service, the peak surge current ($I_s = I_{FSM}$) can be converted to rms current by use of the relationships given in Table VIII, as follows:

$$I_{RMS} = \frac{1}{2} I_{FSM} \\ = \frac{137.6}{2}, \text{ or } 68.8 \text{ amperes}$$

Curve A of Fig. 65, which is merely a reproduction of the 12-ampere curve on the universal rating chart shown in Fig. 66, gives

the surge-current rating of the 12-ampere silicon rectifier, but does not consider the normal rms value of current that the rectifier can handle. This normal value of rms current must be subtracted from the total surge current to determine the actual overcurrent of the fault. First, the relationships in Table IX are used to convert the average-current rating of the rectifier to the normal rms value, as follows:

$$I_{RMS} = 1.57 I_{AV} \\ = 1.57 \times 12, \text{ or } 18.8 \text{ amperes}$$

The overcurrent is then determined from the following calculation:

$$I_{\text{surge}} - I_{\text{normal}} = 68.8 - 18.8, \\ \text{or } 50 \text{ amperes}$$

The 50-ampere fault current is represented on the coordination chart in Fig. 65 by the straight-line curve C. The 12-ampere rectifier can sustain a fault current of this magnitude for 51 milliseconds, as indicated by the point of intersection of curves A and C. The fuse, however, opens and interrupts the flow of current in the circuit after 43 milliseconds, as indicated by the point of intersection of curves B and C, and the rectifier is protected.

Amperes Squared-Seconds (I^2t)

The amperes-squared-seconds (I^2t) rating for silicon rectifiers is a useful figure of merit that provides important information

for fuse coordination. This rating indicates the energy, E , required to melt the fusible material of a particular fuse; it is based on the following familiar power relationship:

$$P = I^2 R \quad (16)$$

where R is the resistance of the fuse element and I is the rms value of the current in the fuse.

The above equation can be expressed in terms of energy ($E = Pxt$) as follows:

$$E = I^2 Rt \quad (17)$$

The resistance R is constant for a given fuse material; this term is dropped from the equation to obtain the figure of merit I^2t that is directly proportional to the energy required to melt the fuse material.

The I^2t rating for a particular silicon rectifier can be determined directly from the surge-current curves for the device. For example, the I^2t rating for a rectifier operated with a 60-Hz ac input can be calculated from the following relationship:

$$I^2t = \frac{\text{one-cycle surge-current rating}}{2} \times 16.67 \times 10^{-3} \quad (18)$$

In this relationship, the factor 16.67×10^{-3} represents the time in seconds for one cycle of operation at 60-Hz, and the peak surge-current value is divided by 2 to obtain the rms value (i.e., $I_{\text{rms}} = I_{\text{pk}}/2$).

The peak value of surge current that can be sustained by a 12-ampere silicon rectifier is 240 amperes, as indicated by the curves shown in Fig. 65(a). The I^2t rating for the rectifier is calculated as follows:

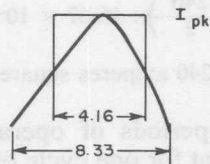
$$\begin{aligned} I^2t &= \left(\frac{240}{2} \right)^2 \times 16.67 \times 10^{-3} \\ &= 240 \text{ amperes squared-seconds} \end{aligned}$$

For periods of operation less than that for one cycle of a 60-Hz sine wave (i.e., for subcycle time periods), the manufacturer's data does not specify the exact surge-current capability of a rectifier. Under such conditions, a somewhat different procedure is required for fuse coordination. In this procedure, consideration must be given to two important factors.

First, the worst-case condition for fusing results from the application of a square wave of current. If other current waveforms are converted into an equivalent square wave, a conservative fusing rating can be obtained. For example, a half-sine wave of 60-Hz current has a duration of 8.3 milliseconds. The duration of an equivalent square wave having the same peak amplitude is 4.16 milliseconds, as indicated in Fig. 67.

Second, because of fundamental differences in thermal and structural characteristics, the surge-current capabilities of solid-state devices and fuses also differ. For fuses, this capability is a constant proportional to I^2t . For a solid-state device this capability

is proportional to I^2t , where x is some value between 2 and 3. A safe approximation for a rectifier surge-current failure curve would result from the use of I^3t to define the upper energy limit.



92CS-25674

Fig. 67—Square-wave equivalent of a half sine-wave of 60-Hz current.

The two factors discussed above are taken into account in the subcycle surge-current rating chart shown in Fig. 68. In this chart, the peak surge-current that can be sustained by a rectifier for a subcycle period is normalized by the peak one-cycle surge-current rating (I^2t) and plotted as a cubic function of time. The normalized I^2t value for the single-cycle surge (which is equivalent to a 4.16 millisecond square wave) is assigned the value of 1, and a line that has a slope of $1/3$ is drawn through this point (1, 4.16 ms.) on a log-log graph to define the subcycle surge-current capability of a silicon rectifier. Use of this curve is illustrated by the following example, in which the I^2t rating is to be determined for a 1 millisecond duration.

The subcycle surge-current rating curve in Fig. 68 shows that the normalizing factor at 1 millisecond is 0.62. The 1-millisecond

I^2t value is then determined as follows:

$$I^2t_{(1 \text{ ms})} = 0.62 I^2t_{(\text{single-cycle surge})} \quad (19)$$

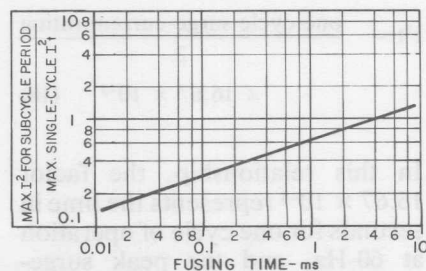
For a 12-ampere silicon rectifier, which has a single-cycle surge capability of 240 amperes squared-seconds, this value becomes

$$\begin{aligned} I^2t_{(1 \text{ ms})} &= (0.62) 240 \text{ A}^2\text{s} \\ &= 149 \text{ A}^2\text{s} \end{aligned}$$

For the 12-ampere silicon rectifier, therefore, the I^2t rating for a time period of 1 millisecond is 149 amperes squared-seconds. This value can then be used to calculate the peak square-wave current allowable for a 1-millisecond period as follows:

$$\begin{aligned} I_{pk(1 \text{ ms})} &= \left(\frac{149}{1 \times 10^{-3}} \right)^{1/2} \\ &= 386 \text{ amperes} \end{aligned}$$

The I^2t fusing rating may be determined by an alternate approach if the peak available short-circuit current is known. Fig. 69 shows a relationship between



92CS-25675

Fig. 68—Subcycle surge-current rating chart.

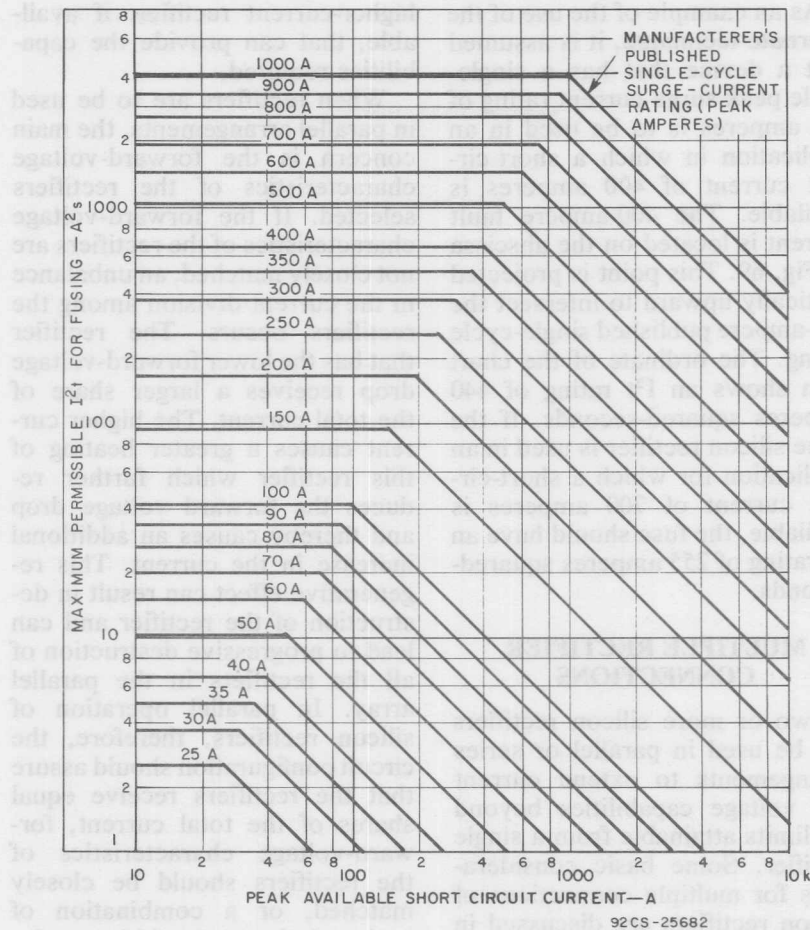


Fig. 69—Maximum permissible I^2t as a function of peak available short-circuit current.

short-circuit currents and published single-cycle I^2t ratings. This chart, like that shown in Fig. 68, is based on a constant I^3t so that for peak currents that exceed the single-cycle rating, the I^2t capability is inversely proportional to the peak current, as

indicated by the following relationship:

$$I^3t = K$$

$$I^2t = K/I$$

(20)

As an example of the use of the alternate technique, it is assumed that a device that has a single-cycle peak surge-current rating of 350 amperes is to be used in an application in which a short-circuit current of 400 amperes is available. The 400-ampere fault current is located on the abscissa of Fig. 69. This point is projected vertically upward to intersect the 350-ampere published single-cycle rating. The ordinate of the chart then shows an I^2t rating of 440 amperes squared-seconds. If the same silicon rectifier is used in an application for which a short-circuit current of 700 amperes is available, the fuse should have an I^2t rating of 255 amperes squared-seconds.

MULTIPLE RECTIFIER CONNECTIONS

Two or more silicon rectifiers can be used in parallel or series arrangements to extend current and voltage capabilities beyond the limits attainable from a single rectifier. Some basic considerations for multiple connections of silicon rectifiers are discussed in the following paragraphs.

Parallel Arrangements

When two or more silicon rectifiers are connected in parallel, the current-handling capability of the combined units is substantially greater than that of a single rectifier of the same type. It is often more practical, however, to obtain the greater current capability by use of a multiphase circuit or by selection of a single

higher-current rectifier, if available, that can provide the capabilities required.

When rectifiers are to be used in parallel arrangements, the main concern is the forward-voltage characteristics of the rectifiers selected. If the forward-voltage characteristics of the rectifiers are not closely matched, an unbalance in the current division among the rectifiers occurs. The rectifier that has the lower forward-voltage drop receives a larger share of the total current. The higher current causes a greater heating of this rectifier which further reduces the forward voltage drop and thereby causes an additional increase in the current. This regenerative effect can result in destruction of the rectifier and can lead to progressive destruction of all the rectifiers in the parallel array. In parallel operation of silicon rectifiers, therefore, the circuit configuration should assure that the rectifiers receive equal shares of the total current, forward-voltage characteristics of the rectifiers should be closely matched, or a combination of both techniques should be used.

An equal division of current among the rectifiers can be forced by use of resistors or balancing inductors in series with each rectifier. The major disadvantage to the use of series resistors is that they introduce large power losses that reduce rectifier efficiency. The major disadvantage of balancing reactors is the relatively high cost of these components.

The best method to assure equal division of current through

parallel rectifiers is to select rectifiers on the basis of matched forward-voltage characteristics. This selection can be made more easily when a large number of parallel circuits is to be constructed, because the rectifiers can then be graded into different voltage-drop categories and units from only one category selected for a given parallel circuit. Because the forward voltage drop of a silicon rectifier is dependent upon the temperature, rectifiers used in a parallel array should be maintained at the same temperature. One technique that may be used to assure that temperature deviations among the rectifiers will be held to a minimum is to mount all the units in the parallel array on the same heat sink.

When silicon rectifiers are connected in parallel arrangements, all contacts should have a low resistance, the wires used should be large enough so that their resistance is negligible, and in high-current arrays the wiring should be arranged so that a minimum unbalance in inductive effects is achieved.

Series Arrangements

Two or more silicon rectifiers may be connected in series arrangements when voltage requirements exceed the capabilities of a single rectifier. The main concern when rectifiers are to be operated in series is that the reverse voltage be divided equally across each rectifier. The use of resistance-capacitance equalizing networks and the selection of rectifiers that have matched reverse

characteristics are the two most common techniques employed to assure equal voltage division.

A third technique that may be employed when rectifiers are connected in series is the use of transformers that have multiple secondary windings. Each secondary winding is connected across one of the rectifiers in the series array. This technique is practical when only a few rectifiers are to be connected in series. For a large number of rectifiers, the cost and complexity of the multiple-secondary approach become prohibitive.

FAST-RECOVERY RECTIFIERS

As pointed out earlier, in the discussion of **Electrical Characteristics**, the reverse-recovery time of a silicon rectifier imposes a finite limit on the maximum frequency at which the device may be used. In most rectifier applications that require fast-recovery rectifiers, the rectifiers are not used as conventional high-frequency rectifiers. Most requirements for rectifiers capable of very rapid forward-to-reverse current switching include the following types of applications:

- high-speed inverters and converters
- switching regulators
- television high-voltage power supplies
- "free wheeling" diodes in chopper supplies

Table X shows significant characteristics and ratings for RCA fast-recovery silicon rectifiers.

Table X — Fast-Recovery Silicon Rectifiers

RCA TYPE	Forward Current				Voltage V_{RRM} V	Temp. Range Operating °C	Voltage Drop		Rev. Recovery Time		
	RMS $I_F(RMS)$ A	Av. I_O A	Surge I_{FSM} A	Temp.- T_A °C			V_F V	I_F A	t_{rr} μs	I_{FM} A	T_C °C

D21 types

D2103SF	3	—	70	150 ^{••}	750	-30 to 80	1.4	4	0.5	3.14	25
D2103S	3	—	70	150 ^{••}	700	-30 to 80	1.4	4	0.5	3.14	25
D2101S	1	—	30	45	700	-30 to 80	1.5	4	0.7	3.14	25

•• Junction Temperature

D22 types

D2201F	1.5	1	50 [•]	100 ^m	50	-40 to 150	1.9	4	0.5	3.14	25
D2201A	1.5	1	50 [•]	100 ^m	100	-40 to 150	1.9	4	0.5	3.14	25
D2201B	1.5	1	50 [•]	100 ^m	200	-40 to 150	1.9	4	0.5	3.14	25
D2201D	1.5	1	50 [•]	100 ^m	400	-40 to 150	1.9	4	0.5	3.14	25
D2201M	1.5	1	50 [•]	100 ^m	600	-40 to 150	1.9	4	0.5	3.14	25
D2201N	1.5	1	50 [•]	100 ^m	800	-40 to 150	1.9	4	0.5	3.14	25

• At Junction Temperature (T_J) = 150°C ■ Lead Temperature**D26 types**

D2600M	0.5	—	30	45	600	-40 to 80	2	4	0.7	20	25
D2601E	1.6	—	70	150 [•]	500	-40 to 80	1.9	4	0.5	20	25
D2601M	1.9	—	70	150 [•]	600	-40 to 80	1.9	4	0.5	20	25

D2601F	1.5	1	35 [•]	100 ^m	50	-40 to 150	1.9	4	0.5	20	25
D2601A	1.5	1	35 [•]	100 ^m	100	-40 to 150	1.9	4	0.5	20	25

D2601B	1.5	1	35 [•]	100 ^m	200	-40 to 150	1.9	4	0.5	20	25
D2601D	1.5	1	35 [•]	100 ^m	400	-40 to 150	1.9	4	0.5	20	25
D2601M	1.5	1	35 [•]	100 ^m	600	-40 to 150	1.9	4	0.5	20	25
D2601N	1.5	1	35 [•]	100 ^m	800	-40 to 150	1.9	4	0.5	20	25

• At Junction Temperature (T_J) = 165°C ■ Lead Temperature • Junction Temperature**D24 Types**

D2406F	9	6	125	100	50	-40 to 150	1.4	6	0.35	19	25
D2406A	9	6	125	100	100	-40 to 150	1.4	6	0.35	19	25
D2406B	9	6	125	100	200	-40 to 150	1.4	6	0.35	19	25
D2406C	9	6	125	100	300	-40 to 150	1.4	6	0.35	19	25
D2406D	9	6	125	100	400	-40 to 150	1.4	6	0.35	19	25
D2406M	9	6	125	100	600	-40 to 150	1.4	6	0.35	19	25
1N3879	9	6	75	100	50	-65 to 150	1.4	6	0.20	1	25
1N3880	9	6	75	100	100	-65 to 150	1.4	6	0.20	1	25
1N3881	9	6	75	100	200	-65 to 150	1.4	6	0.20	1	25
1N3882	9	6	75	100	300	-65 to 150	1.4	6	0.20	1	25
1N3883	9	6	75	100	400	-65 to 150	1.4	6	0.20	1	25

D2412F	18	12	250	100	50	-40 to 150	1.4	12	0.35	38	25
D2412A	18	12	250	100	100	-40 to 150	1.4	12	0.35	38	25
D2412B	18	12	250	100	200	-40 to 150	1.4	12	0.35	38	25
D2412C	18	12	250	100	300	-40 to 150	1.4	12	0.35	38	35
D2412D	18	12	250	100	400	-40 to 150	1.4	12	0.35	38	25
D2412M	18	12	250	100	600	-40 to 150	1.4	12	0.35	38	25

Table X — Fast Recovery Silicon Rectifiers (cont'd)

RCA TYPE	Forward Current				Voltage V_{RRM} V	Temp. Range Operating °C	Voltage Drop		Rev. Recovery Time		
	RMS $I_F(RMS)$ A	Av. I_O A	Surge I_{FSM} A	Temp- T_C °C			V_F V	i_F A	t_{rr} μs	I_{FM} A	T_C °C

D24 Types (cont'd)

1N3889	18	12	150	100	50	-65 to 150	1.4	12	0.20	1	25
1N3890	18	12	150	100	100	-65 to 150	1.4	12	0.20	1	25
1N3891	18	12	150	100	200	-65 to 150	1.4	12	0.20	1	25
1N3892	18	12	150	100	300	-65 to 150	1.4	12	0.20	1	25
1N3893	18	12	150	100	400	-65 to 150	1.4	12	0.20	1	25

D25 types

D2520F	30	20	300	100	50	-40 to 150	1.4	20	0.35	63	25
D2520A	30	20	300	100	100	-40 to 150	1.4	20	0.35	63	25
D2520B	30	20	300	100	200	-40 to 150	1.4	20	0.35	63	25
D2520C	30	20	300	100	300	-40 to 150	1.4	20	0.35	63	25
D2520D	30	20	300	100	400	-40 to 150	1.4	20	0.35	63	25
D2520M	30	20	300	100	600	-40 to 150	1.4	20	0.35	63	25
1N3899	30	20	225	100	50	-65 to 150	1.4	20	0.20	1	25
1N3900	30	20	225	100	100	-65 to 150	1.4	20	0.20	1	25
1N3901	30	20	225	100	200	-65 to 150	1.4	20	0.20	1	25
1N3902	30	20	225	100	300	-65 to 150	1.4	20	0.20	1	25
1N3903	30	20	225	100	400	-65 to 150	1.4	20	0.20	1	25

1N3909	45	30	300	100	50	-65 to 150	1.4	30	0.20	1	25
1N3910	45	30	300	100	100	-65 to 150	1.4	30	0.20	1	25
1N3911	45	30	300	100	200	-65 to 150	1.4	30	0.20	1	25
1N3912	45	30	300	100	300	-65 to 150	1.4	30	0.20	1	25
1N3913	45	30	300	100	400	-65 to 150	1.4	30	0.20	1	25

D2540F	60	40	700	165	50	-40 to 150	1.8	100	0.35	125	25
D2540A	60	40	700	165	100	-40 to 150	1.8	100	0.35	125	25
D2540B	60	40	700	165	200	-40 to 150	1.8	100	0.35	125	25
D2540D	60	40	700	165	400	-40 to 150	1.8	100	0.35	125	25
D2540M	60	40	700	165	600	-40 to 150	1.8	100	0.35	125	25

‡ Reverse-polarity versions available

Types of Recovery Characteristics

During forward conduction, a silicon rectifier accumulates minority charge carriers that result in the build-up of a stored charge in the device. If forward conduction is immediately followed by the application of reverse voltage (as normally occurs in most circuits), the rectifier cannot instantaneously block the flow of reverse current. The stored charge must first be removed before the

rectifier can recover its reverse blocking capability. In the removal of the stored charge, the minority carriers are "swept out" by the reverse current and are eliminated by recombination with majority carriers. Conventional silicon rectifiers accumulate a significant amount of stored charge, and the minority carriers have a relatively long lifetime. Consequently, the amount of time required for the rectifier to recover its reverse blocking capa-

bility, i.e., the rectifier reverse-recovery time, is relatively long, as shown in Fig. 70.

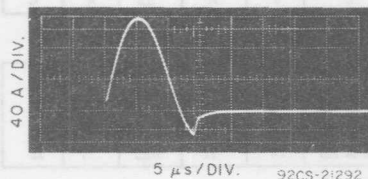


Fig. 70—Reverse-recovery characteristics of a conventional silicon rectifier.

In the design and fabrication of silicon rectifiers, the basic rectifier structure can be modified to reduce the lifetime of minority carriers. In such cases, the reverse-recovery time of the rectifiers is dramatically decreased, as shown in Fig. 71. The exact

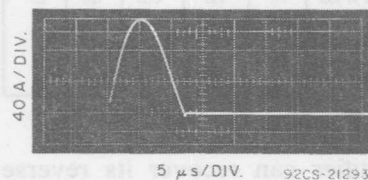


Fig. 71—Reverse-recovery characteristics of a silicon rectifier specially designed for fast recovery of its reverse blocking capability.

shape of the recovery characteristics of fast-recovery rectifiers is a function of both device processing and the circuit in which the device is used, and these characteristics may differ significantly for different rectifier types or for the same rectifiers used in dif-

ferent circuit configurations. In general, however, the basic forms of the recovery characteristics for fast-recovery rectifiers are as shown in Fig. 72.

Fig. 72(a) shows the normal "soft" characteristic desired in most applications that require fast-recovery rectifiers. Although the reverse-current recovery is rapid, it occurs smoothly with no abrupt discontinuities. A minimum of ringing or rf radiation is produced by this type of recovery characteristic. Fig. 72(b) shows a "snap" type of recovery characteristic. The reverse cur-

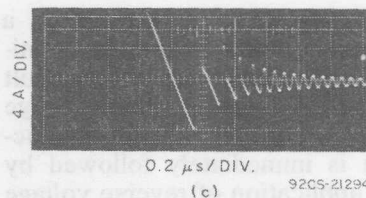
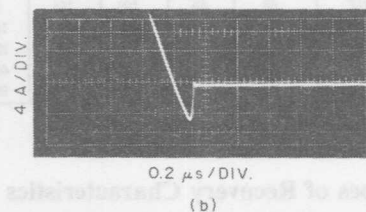
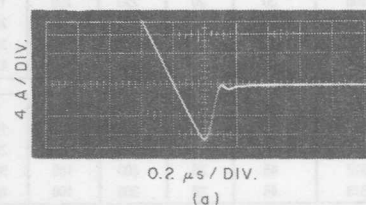


Fig. 72—Basic forms of recovery characteristics for fast-recovery rectifiers: (a) normal "soft" characteristic; (b) "snap" characteristic; (c) "snap" characteristic with ringing oscillations.

rent rises to a peak value in the normal way, but then decays (snaps off) almost instantaneously to a value very near zero. If the peak value of the reverse current is relatively high, an appreciable amount of energy is contained in the harmonics generated by the snap-off. These harmonics may then produce radio-frequency interference in any sensitive, nearby radio or television receiving equipment. In addition, if the inductance of the rectifier lead connection is significant, the snap-off may induce ringing in the lead inductance that may result in circuit malfunction. In severe cases, the rate of change of current through the lead inductance may be so rapid that the voltage induced may be large enough to destroy the rectifier.

The recovery characteristics shown in Fig. 72(c) represent the extreme case of snap-off. The snap-off is so rapid that very high ringing voltages are induced. On the positive alternation of the ringing voltage, the rectifier is again driven into forward conduction, and the device goes through another reverse-recovery period when the current passes through zero. The cycle is repeated several times with a gradually decaying magnitude until the positive alternations of the induced ringing voltage is too small to drive the rectifier into forward conduction. The ringing, therefore, decays gradually somewhat like a damped sine wave.

RCA fast-recovery rectifiers are designed to have a reverse-recovery characteristic similar to

that shown in Fig. 72(a). This type of characteristic is achieved by use of carefully controlled gold-doping to reduce the lifetime of minority carriers and design of the junction geometry to prevent abrupt decreases in the peak negative current.

Recovery-Time Test Circuit

Fig. 73(a) shows a circuit recommended by the JEDEC Committee (JC-22) on Power Rectifiers for use in the measurement of rectifier recovery time. In this circuit, capacitor C is charged during the positive alternation of the input ac voltage. During the negative half-cycle, the silicon

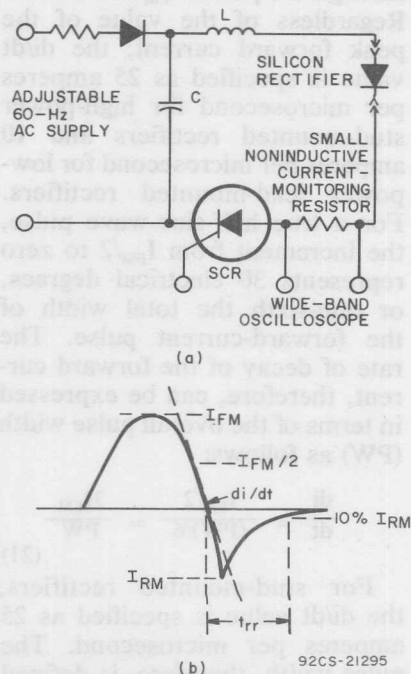


Fig. 73—JEDEC test circuit and waveform for rectifier reverse-recovery-time measurement.

controlled rectifier (SCR) is triggered, and capacitor C discharges through inductor L and the rectifier on which the recovery-time measurements is being made. The resultant test-current waveform is shown in Fig. 73(b). Inductor L and capacitor C form a series resonant circuit so that the forward current through the rectifier is very nearly a half sine wave. The peak forward current I_{FM} is specified as π times the average rated value of the half-sine-wave current through the rectifier. The rate of decay of the forward current ($-di/dt$) is specified as the slope of a straight line that passes through the points $I_{FM}/2$ and zero. Regardless of the value of the peak forward current, the di/dt value is specified as 25 amperes per microsecond for high-power stud-mounted rectifiers and 10 amperes per microsecond for low-power lead-mounted rectifiers. For a true half-sine-wave pulse, the increment from $I_{FM}/2$ to zero represents 30 electrical degrees, or one-sixth the total width of the forward-current pulse. The rate of decay of the forward current, therefore, can be expressed in terms of the overall pulse width (PW) as follows:

$$\frac{di}{dt} = \frac{I_{FM}/2}{(PW)/6} = \frac{3I_{FM}}{PW} \quad (21)$$

For stud-mounted rectifiers, the di/dt value is specified as 25 amperes per microsecond. The pulse width, therefore, is defined by the following relationship:

$$PW = 3I_{FM}/25 = 0.12I_{FM} \quad (22)$$

For lead-mounted rectifiers, the di/dt value is specified as 10 amperes per microsecond, and the expression for the pulse width becomes

$$PW = 3I_{FM}/10 = 0.3I_{FM} \quad (23)$$

The desired width of the current pulse is obtained by selection of the proper values for L and C in the test circuit. The values of these components are determined from the following relationships:

$$PW = \pi(LC)^{1/2} \quad (24)$$

$$C = I_{FM}(PW)/\pi V_p \quad (25)$$

where V_p is the peak voltage across the capacitor.

The relationships expressed above all assume zero circuit losses. Some adjustment of the calculated values of L and C may be required to compensate for these losses.

A typical practical circuit for measurement of the recovery time of a fast-recovery rectifier is shown in Fig. 74. The diode in parallel with the S6431M SCR in this circuit carries the reverse current through the LC circuit so that the reverse recovery characteristics of the rectifier are not affected by the reverse recovery characteristic of the SCR.

Many other circuits have been used for measuring reverse recovery time. Fig. 75 shows one method which has been used as the basis for reverse-recovery data by some manufacturers. In this circuit, the forward-current

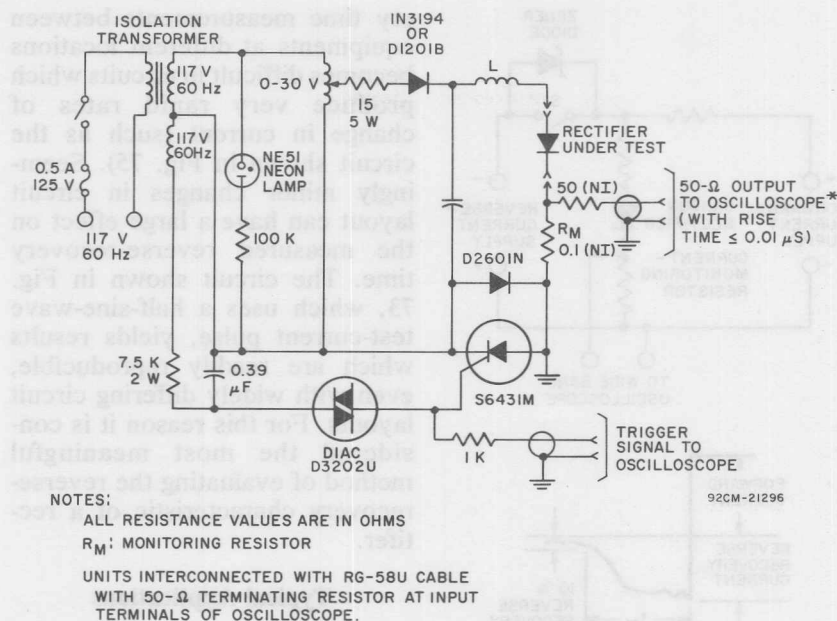


Fig. 74—Test circuit for measurement of reverse-recovery time in which a bypass diode is used to assure that the recovery characteristic of the silicon rectifier is not affected by recovery characteristic of the SCR.

supply and the associated resistors are adjusted to provide a specified value of forward current. The reverse-current supply is adjusted to supply a specified value of reverse-recovery current when switch S is closed. In some cases, the switch S and the reverse-current supply are replaced by a pulse generator.

Fig. 76 shows another circuit that is used by many manufacturers for measurement of rectifier reverse-recovery characteristics. This circuit is basically a modification of the circuit shown in Fig. 75. The resistor R_1 and the forward-current supply are selected to produce a specified value of forward current, and the resis-

tor R_2 and the reverse-current supply are selected to produce a specified value of reverse current.

Unfortunately, most of the different methods of measuring reverse recovery time yield widely varying results. The values obtained depend on many factors, including the magnitude of forward current, the magnitude of reverse-recovery current, the point on the waveform at which recovery time is measured (usually 10 per cent of peak reverse current), and the rate at which forward current decays toward zero (usually a function of circuit layout, stray capacitance, and inductance).

Correlation of reverse-recov-

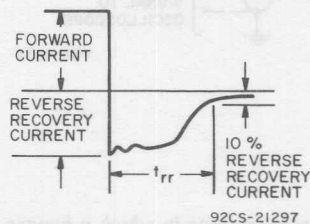
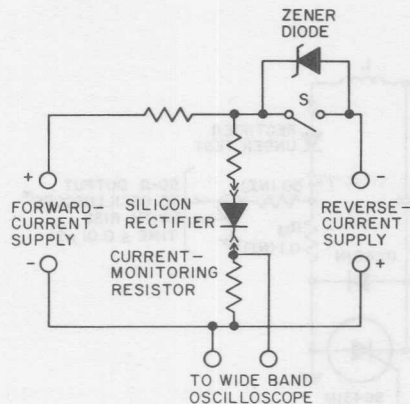


Fig. 75—Recover-time test circuit in which the forward-current supply and associated resistors are adjusted for a specified value of forward current.

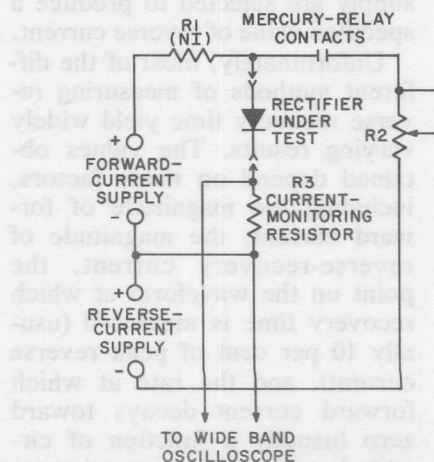
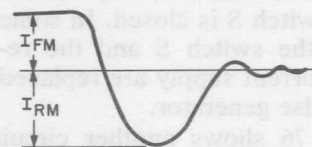


Fig. 76—Recovery-time test circuit in which the forward-current supply and reverse-current supply are adjusted for specified values of forward and reverse current, respectively.

ery time measurements between equipments at different locations becomes difficult in circuits which produce very rapid rates of change in current (such as the circuit shown in Fig. 75). Seemingly minor changes in circuit layout can have a large effect on the measured reverse-recovery time. The circuit shown in Fig. 73, which uses a half-sine-wave test-current pulse, yields results which are readily reproducible, even with widely differing circuit layouts. For this reason it is considered the most meaningful method of evaluating the reverse-recovery characteristic of a rectifier.

Typical Applications

Fast-recovery rectifiers are useful in a wide variety of applications. Perhaps the simplest use of these devices is as high-frequency rectifiers in applications such as



92CS-21298

portable power supplies and television receivers. The rectification efficiency of a high-frequency rectifier is directly dependent upon the reverse-recovery characteristics of the device. In high-frequency high-voltage supplies that require use of several series-connected rectifier p-n junctions, the problem becomes more complex than simply the achievement of maximum rectification efficiency. As described in the discussion of **Multiple Rectifier Connections**, when the applied voltage across such a series-connected rectifier assembly goes negative, the rectifier junction that has the fastest recovery time will turn off first. This junction must then withstand the entire peak inverse voltage applied across the entire series combination until the second fastest and then other rectifier junctions turn off. As pointed out previously, matched rectifier combinations or voltage equalizing networks must be used to minimize the probability of rectifier failures because of variations in recovery times. When current requirements are very small and rectifier recovery times are very short, it may be practical not to use any special voltage-equalization techniques. In such cases, the first rectifier junction to turn off operates in a non-destructive avalanche mode until succeeding slower junctions turn off.

Another common use of fast-recovery rectifiers is as "free-wheeling" diodes. In this type of application, a rectifier is normally connected across an inductive

load and conducts current proportional to the energy stored in the inductance. This current flows when no power is supplied to the load and continues to flow until all energy stored in the inductor has been removed or until energy is again supplied to the inductance from the power source. Other names used for the free-wheeling diode include **dumper diode**, **flyback diode**, **feedback diode**, and **flywheel diode**.

Fig. 77 illustrates a common application of a free-wheeling diode. This figure shows a high-

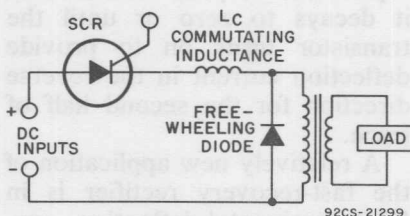


Fig. 77—High-frequency chopper circuit that uses a free-wheeling diode.

frequency chopper circuit that uses a free-wheeling diode to maintain current flow through the load during the off period of the SCR and to prevent the development of excessive voltage across the load.

The dumper diode in a television receiver is another application of the use of a fast-recovery rectifier to maintain current through an inductive load when no power is supplied to the load from the power supply. Fig. 78 shows the diode connection for this type of application. During the first half of trace (left half

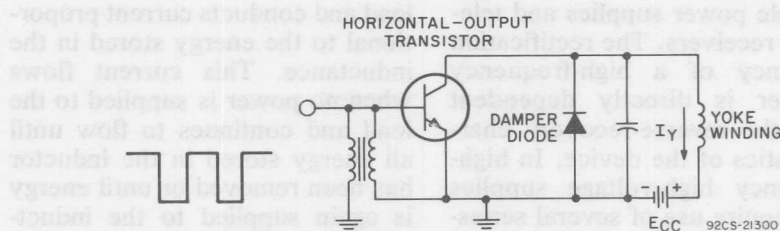


Fig. 78—Transistor horizontal output stage that uses a fast-recovery rectifier as the damper diode.

of raster), the horizontal output transistor does not conduct, but current flows through the yoke inductance in the direction indicated. The damper diode provides a path for the yoke current until it decays to zero or until the transistor turns on to provide deflection current in the reverse direction for the second half of trace.

A relatively new application of the fast-recovery rectifier is in SCR horizontal-deflection systems for television receivers. Fig. 79 shows the basic circuit

configuration for this type of application. Fast-recovery rectifiers are used for both the trace diode D_t and the commutating diode D_c . (A detailed analysis of the basic circuit is given later in this Manual in the section on **SCR Horizontal-Deflection Systems**.) Briefly, the basic function of the trace diode D_t is much the same as that of the damper diode in the transistor deflection circuit. In addition, this diode conducts a portion of the commutating current from the commutating SCR for a short period just prior to

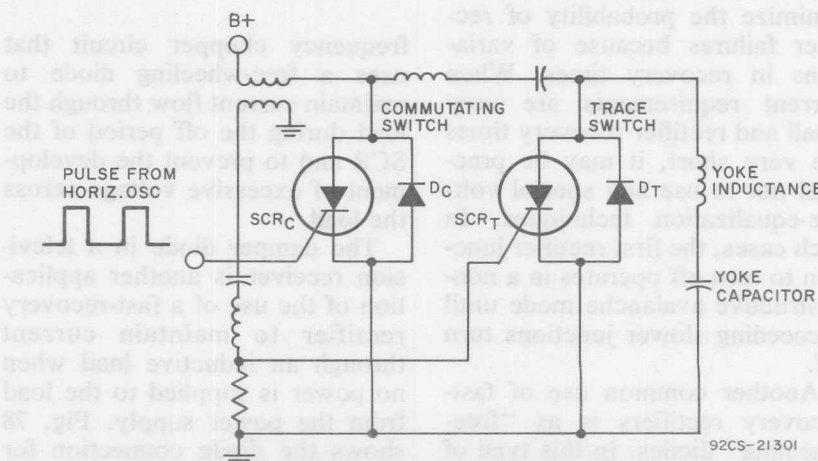


Fig. 79—SCR horizontal-deflection circuit that uses fast-recovery rectifiers to aid in the trace and retrace switching functions.

the start of retrace to allow the trace SCR to recover its forward-blocking capability. During the second half of retrace, the energy stored in the yoke capacitor is returned to the yoke inductance through the commutating diode D_c . During this period, the commutating SCR recovers its forward-blocking capability.

Fast-recovery rectifiers are also frequently used in high-frequency inverters, especially those operated with inductive loads, to improve circuit efficiency. Fig. 80 shows an example of this application of fast-recovery rectifiers.

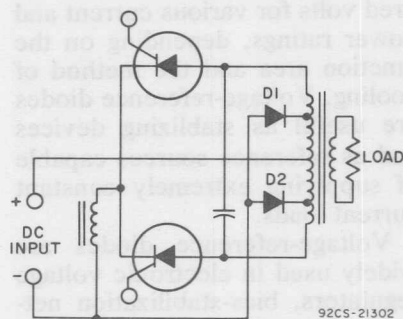


Fig. 80—High-frequency inverter that uses fast-recovery rectifier to increase circuit efficiency.

In this circuit, fast-recovery rectifiers D_1 and D_2 feed back reactive power to the dc power supply. If the load is inductive, the energy stored in the load at the end of each half-cycle of ac voltage is returned to the power supply at the start of the next half-cycle. If the load is capacitive, the energy stored in the load at the start of each half-cycle is returned to the power supply during the

second half of the same half-cycle. A complete inverter that employs this basic technique is described in detail in the section on **SCR Inverters and Converters**.

OTHER SPECIAL-FUNCTION RECTIFIERS

In addition to fast-recovery types, other rectifiers that exhibit unique characteristics can be obtained by special contouring of the basic silicon-rectifier junction structure, by use of special processing techniques, or by selective testing. This group includes controlled-avalanche rectifiers, voltage-reference (zener) diodes, and compensating diodes.

Controlled-Avalanche Rectifiers

Controlled-avalanche types are recommended for silicon-rectifier applications in which the ability to withstand high-voltage transients is an important design consideration. In controlled-avalanche rectifiers, the voltage at which avalanching occurs is predetermined during manufacture by precise control of the resistivities (i.e., doping-impurity concentrations) in the junction areas and by careful attention to the geometry of the silicon pellet.

In the manufacture of controlled-avalanche rectifiers, special care is taken to assure exceptional regularity of the silicon pellet and an even distribution of impurities in both the n- and p-type regions of the semiconductor junction. In addition, the

edges of the silicon p-n junction are shaped to reduce the intensity of localized electric fields at the junction surface. These conditions assure that breakdown will be uniform across the entire junction area rather than concentrated at weak spots close to the junction surface. Such uniform avalanching, when maintained within acceptable limits, is not destructive.

Extensive tests of controlled-avalanche rectifiers permit precise predictions of the behavior of these devices under high-reverse-voltage conditions. The rectifiers are tested to determine their ability to withstand high-voltage transients and are subjected to life tests to determine their capability for sustained operation in the avalanche region. The slope of the current-voltage curve in the avalanche region defines the dissipation level at the onset of avalanche breakdown and also the maximum dissipation level that the rectifiers are rated to withstand under reverse-bias conditions.

Within the specified ratings, controlled-avalanche rectifiers can safely absorb large bursts of energy, such as may result from abrupt switching of inductive circuits.

Voltage-Reference Diodes

Voltage-reference or zener diodes are silicon rectifiers in which the reverse current remains small until the breakdown voltage is reached and then increases rapidly with little further increase in voltage. The sche-

matic symbol for a zener diode is shown in Fig. 81; a typical zener

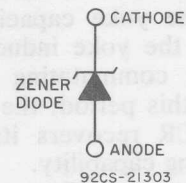


Fig. 81—Schematic symbol for a zener diode.

characteristic curve is shown in Fig. 82. The breakdown voltage is a function of the diode material and construction, and can be varied from one volt to several hundred volts for various current and power ratings, depending on the junction area and the method of cooling. Voltage-reference diodes are useful as stabilizing devices and as reference sources capable of supplying extremely constant current loads.

Voltage-reference diodes are widely used in electronic voltage regulators, bias-stabilization networks for audio power amplifiers,

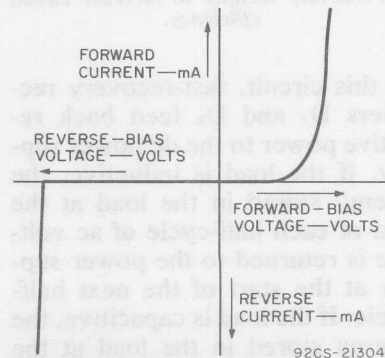


Fig. 82—Typical characteristic curve for a zener diode.

and other applications that require a fixed voltage reference. Fig. 83 illustrates the use of a zener diode as the voltage-reference element in a simple voltage regulator that consists merely of a transistor, a resistor, and the zener diode.

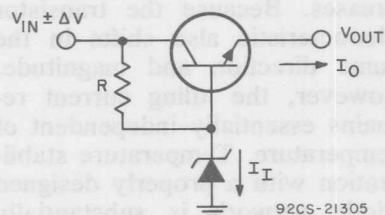


Fig. 83—Simple transistor voltage regulator that uses a zener diode as the voltage-reference element.

The zener diode maintains the base of the transistor at a constant voltage, and changes in the output can result only from variations in the transistor base-to-emitter voltage with current and temperature. If large currents are drawn from the transistor, a zener diode that has a high current rating is required for this application.

Compensating Diodes

Low-power silicon rectifiers, such as the RCA D1300 series, are frequently used as compensating diodes in bias stabilization networks for transistor amplifier and oscillator circuits. Excellent stabilization of collector current for variations in both supply voltage and temperature can be obtained by the use of a compensating diode operating in the forward direction in the bias network of amplifier or oscillator circuits.

Fig. 84 shows the transfer characteristics of a transistor; Fig. 85 shows the forward characteristics of a compensating diode. In a typical circuit, the diode is biased in the forward direction; the operating point is represented on the diode characteristics by the dashed horizontal line. The diode current at this point determines a bias voltage which establishes the transistor idling current. This bias voltage shifts with varying temperature in the same direction and magnitude as the transistor characteristic, and thus provides an idling current that is essentially independent of temperature.

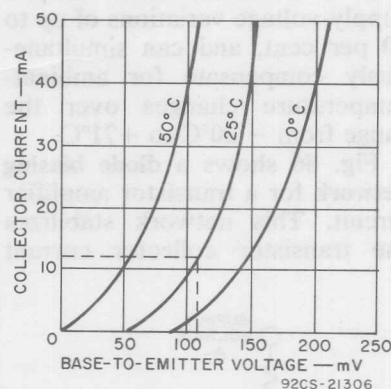


Fig. 84—Transfer characteristics of transistor.

The use of a compensating diode also reduces the variation in transistor idling current as a result of supply-voltage variations. Because the diode current changes in proportion with the supply voltage, the bias voltage to the transistor changes in the same proportion and idling-current changes are minimized. Compensating diodes can maintain tran-

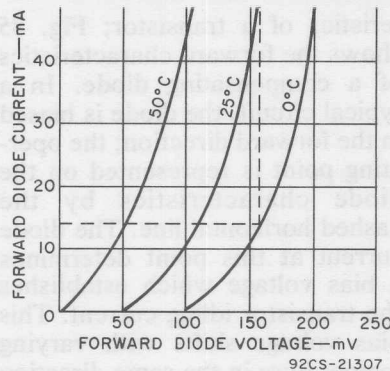


Fig. 85—Forward characteristics of compensating diode.

sistor bias voltages within ± 0.015 volt of a desired value despite supply-voltage variations of up to 40 per cent, and can simultaneously compensate for ambient-temperature changes over the range from -20°C to $+71^{\circ}\text{C}$.

Fig. 86 shows a **diode biasing network** for a transistor amplifier circuit. This network stabilizes the transistor collector current

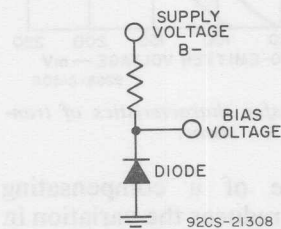


Fig. 86—Transistor bias network that uses a voltage-compensating diode.

and supply voltage. The forward-biased diode current determines a bias voltage which establishes the transistor **idling** current (collector current under no-signal conditions). As the temperature increases, this bias voltage decreases. Because the transistor characteristic also shifts in the same direction and magnitude, however, the idling current remains essentially independent of temperature. Temperature stabilization with a properly designed diode network is substantially better than that provided by most thermistor bias networks. Any temperature-stabilizing element should be thermally close to the transistor being stabilized.

In addition, the diode bias current varies in direct proportion with changes in supply voltage. The resultant change in bias voltage is small, however, so that the idling current also changes in direct proportion to the supply voltage. Supply-voltage stabilization with a diode biasing network reduces current variation to about one-fifteenth that obtained when resistor or thermistor bias is used for a silicon transistor.

The diode bias network shown in Fig. 86 is generally used in class B circuits. The bias resistor values for class B circuits are generally much lower than those for class A circuits.

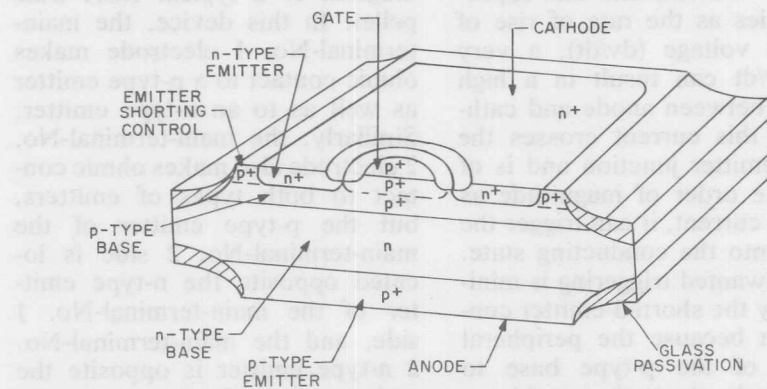
Basic Thyristor Design and Rating Factors

The basic potential-energy relationships that make possible the bistable switching in SCR's, gate-turn-off SCR's (GTO's), and triacs were explained in the section on **General Physical Theory**. In essence, the SCR is a unidirectional device that may be used for both ac and dc functions, and the triac is a bidirectional device that is used mainly for ac functions. The GTO differs from the conventional SCR in that it is designed to turn off with the application of a negative voltage to the

gate electrode, without reducing anode voltage.

PELLET STRUCTURES

Fig. 87 shows a cross-sectional diagram of a typical RCA SCR pellet. The shorted-emitter construction used in RCA SCR's can be recognized by the metallic cathode electrode in direct contact with the p-type base layer around the periphery of the pellet. The gate, at the center of the pellet, also makes direct metallic



92CS-21309

Fig. 87—Cross section of a typical SCR pellet.

contact to the p-type base so that the portion of this layer under the n-type emitter acts as an ohmic path for current flow between gate and cathode. Because this ohmic path is in parallel with the n-type emitter junction, current preferentially takes the ohmic path until the IR drop in this path reaches the junction threshold voltage of about 0.8 volt. When the gate voltage exceeds this value, the junction current increases rapidly, and injection of electrons by the n-type emitter reaches a level high enough to turn on the device.

In addition to providing a precisely controlled gate current, the shorted-emitter construction also improves the high-temperature and dv/dt (maximum allowable rate of rise of off-state voltage) capabilities of the device. The junction depletion layer acts as a parallel-plate capacitor which must be charged when blocking voltage is applied. Because the charging, or displacement, current ($i = Cdv/dt$) into this capacitor varies as the rate of rise of forward voltage (dv/dt), a very high dv/dt can result in a high current between anode and cathode. If this current crosses the n-type emitter junction and is of the same order of magnitude as the gate current, it can trigger the device into the conducting state. Such unwanted triggering is minimized by the shorted-emitter construction because the peripheral contact of the p-type base to the cathode electrode provides a large-area parallel path by which the dv/dt current can reach the

cathode electrode without crossing the n-type emitter junction. (The critical dv/dt value for thyristors is discussed more fully in a subsequent paragraph.)

The center-gate construction of the SCR pellet provides fast turn-on and high di/dt capabilities i.e., maximum rate of rise of forward current. (Thyristor turn-on characteristics and di/dt capabilities are explained later in this section.) In an SCR, conduction is initiated in the cathode region immediately adjacent to the gate contact and must then propagate to the more remote regions of the cathode. Switching losses are influenced by the rate of propagation of conduction and the distance conduction must propagate from the gate. With a large central gate, all regions of the cathode are in close proximity to the initially conducting region so that propagation distance is significantly decreased; as a result, switching losses are minimized.

Fig. 88 shows a cross-sectional diagram of a typical RCA triac pellet. In this device, the main-terminal-No. 1 electrode makes ohmic contact to a p-type emitter as well as to an n-type emitter. Similarly, the main-terminal-No. 2 electrode also makes ohmic contact to both types of emitters, but the p-type emitter of the main-terminal-No. 2 side is located opposite the n-type emitter of the main-terminal-No. 1 side, and the main-terminal-No. 2 n-type emitter is opposite the main-terminal-No. 1 p-type emitter. The net result is two four-layer switches in parallel, but

point, the current through the device is extremely small, and the thyristor is effectively an open switch. When the voltage across the main terminals increases to a value exceeding the breakover point, the thyristor switches to its high-conduction state and is effectively a closed switch. The thyristor remains in the on state until the current through the main terminals drops below a value which is called the **holding current**. At this point, the thyristor reverts back to the high-impedance off state.

SCR Characteristic

Fig. 89 shows the principal voltage-current characteristic curve for an SCR. This curve shows that the operation of an SCR under reverse-bias conditions (anode negative with respect to cathode) is very similar to that of reverse-biased silicon rectifiers or other solid-state diodes. In this bias mode, the SCR exhibits a very high internal impedance, and only a slight amount of reverse current, called the **reverse blocking**

current, flows through the p-n-p-n structure. This current is very small until the reverse voltage exceeds the reverse breakdown voltage; beyond this point, however, the reverse current increases rapidly. The value of the reverse breakdown voltage differs for individual SCR types.

During forward-bias operation (anode positive with respect to cathode), the p-n-p-n structure of the SCR is electrically bistable and may exhibit either a very high impedance (forward-blocking or off state) or a very low impedance (forward-conducting or on state). In the forward-blocking state, a small forward current, called the forward off-state current, flows through the SCR. The magnitude of this current is approximately the same as that of the reverse-blocking current that flows under reverse-bias conditions. As the forward bias is increased, a voltage point is reached at which the forward current increases rapidly, and the SCR switches to the on state. This value of voltage is called the **forward breakover voltage**.

When the forward voltage exceeds the breakover value, the voltage drop across the SCR abruptly decreases to a very low value, referred to as the **forward on-state voltage**. When an SCR is in the on state, the forward current is limited primarily by the impedance of the external circuit. Increases in forward current are accompanied by only slight increases in forward voltage when the SCR is in the state of high forward conduction.

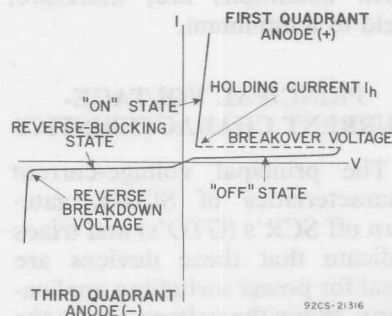


Fig. 89—Principal voltage-current characteristic for an SCR.

GTO Characteristic

Fig. 90 shows the anode-to-cathode voltage-current characteristic and the gate-to-cathode voltage-current characteristic of a GTO.

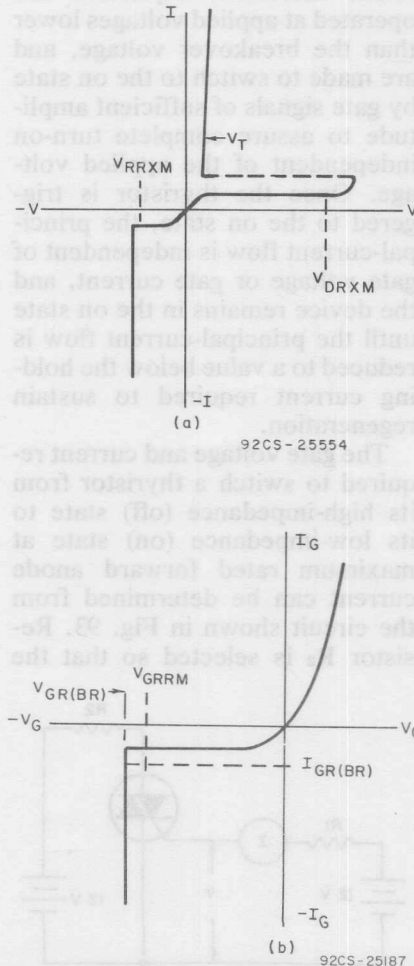


Fig. 90—(a) anode-to-cathode voltage-current characteristic, and (b) gate-to-cathode voltage-current characteristic of a gate-turn-off SCR.

Triac Characteristic

A triac exhibits the forward-blocking, forward-conducting, voltage-current characteristic of a p-n-p-n structure for either direction of applied voltage, as shown in Fig. 91. This bidirectional switching capability results because, as mentioned previously, a triac consists essentially of two p-n-p-n devices of opposite orientation built into the same crystal. The device, therefore, operates basically as two SCR's connected in parallel, but with the anode and cathode of one SCR connected to the cathode and

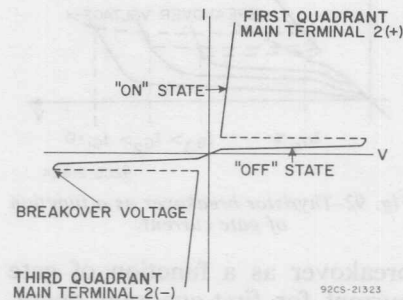


Fig. 91—Principal voltage-current characteristic for a triac.

anode, respectively, of the other SCR. As a result, the operating characteristics of the triac in the first and third quadrants of the voltage-current characteristics are the same, except for the direction of current flow and applied voltage. The triac characteristics in these quadrants are essentially identical to those of an SCR operated in the first quadrant. For the triac, however, the high-impedance state in the third

quadrant is referred to as the off state rather than as the reverse-blocking state. Because of the symmetrical construction of the triac, the terms forward and reverse are not used in reference to this device.

EFFECT OF GATE SIGNAL ON BREAKOVER VOLTAGE

The breakover voltage of a thyristor can be varied, or controlled, by injection of a signal at the gate terminal. Fig. 92 shows curves of

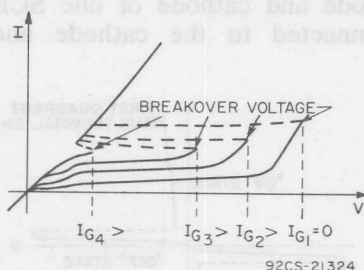


Fig. 92—Thyristor breakover as a function of gate current.

breakover as a function of gate current for first-quadrant operation of an SCR. A similar set of curves can be drawn for both the first and the third quadrant to represent triac operation.

When the gate current I_g is zero, the applied voltage must reach the breakover voltage of the SCR or triac before switching occurs. As the value of gate current is increased, however, the ability of a thyristor to support applied voltage is reduced and there is a certain value of gate current at which the behavior of the thyristor closely resembles that of a rectifier. Because thyristor turn-

on, as a result of exceeding the breakover voltage, can produce instantaneous power dissipation during the switching transition, the device may be damaged unless the magnitude and rate of rise of principal current is restricted to tolerable levels. For normal operation, therefore, thyristors are operated at applied voltages lower than the breakover voltage, and are made to switch to the on state by gate signals of sufficient amplitude to assure complete turn-on independent of the applied voltage. Once the thyristor is triggered to the on state, the principal-current flow is independent of gate voltage or gate current, and the device remains in the on state until the principal-current flow is reduced to a value below the holding current required to sustain regeneration.

The gate voltage and current required to switch a thyristor from its high-impedance (off) state to its low-impedance (on) state at maximum rated forward anode current can be determined from the circuit shown in Fig. 93. Resistor R_2 is selected so that the

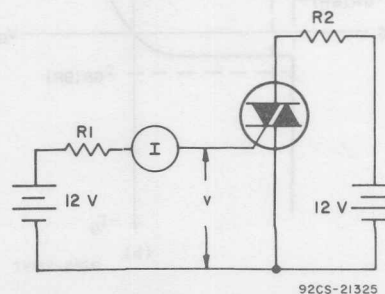


Fig. 93—Circuit used to measure thyristor gate voltage and current switching threshold.

anode current specified in the manufacturer's ratings flows when the device latches into its low-impedance or on state. The value of R_1 is gradually decreased until the device under test is switched from its off state to its low-impedance or on state. The values of gate current and gate voltage immediately prior to switching are the values required to trigger the thyristor. For an SCR, there is only one mode of gate firing capable of switching the device into the on state, a positive gate signal for a positive anode voltage. If the gate polarity is reversed (negative voltage), the reverse current flow is limited by the value of R_2 and the gate-cathode internal shunt. The value of power dissipated for the reverse gate polarity is restricted to the maximum power-dissipation limit imposed by the manufacturer.

A triac can be triggered by either a positive or a negative gate signal regardless of the polarity of the voltage across the main terminals of the device. The direction of the principal current, however, influences the gate trigger current; as a result, the magnitude of current required to trigger the triac differs for each triggering

mode. The triggering modes in which the principal current is in the same direction as the gate current require less gate current than the triggering modes in which the principal current is in opposition to the gate current. The directions of the gate current and the principal current for each triggering mode are indicated in the junction diagrams shown in Fig. 21 in the section on **General Physical Theory**. For convenience, Fig. 94 shows these current directions in relation to the schematic symbol of a triac.

RATINGS AND LIMITING CHARACTERISTICS

Thyristors must be operated within the maximum ratings specified by the manufacturer to assure best results in terms of performance, life, and reliability. (The ratings specified by thyristor manufacturers are based on the **absolute maximum system**. **Absolute maximum ratings** are defined in the section on **Silicon Rectifiers**.) These ratings define limiting values, determined on the basis of extensive tests, that represent the best judgment of the manufacturer of the safe operating capability of the device. The manufacturer also

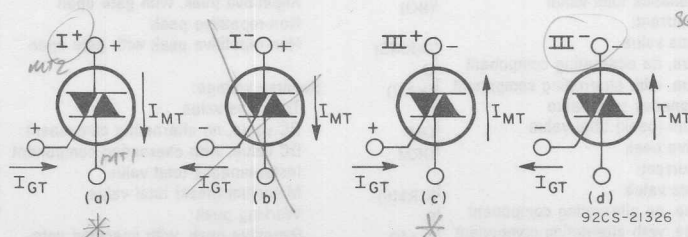


Fig. 94—Gating conditions for each of the four triggering modes of a triac.

specifies a number of device characteristics, which are directly measurable properties that define the inherent qualities and traits of the thyristor. Some of these characteristics are important factors in the determination of the maximum ratings and in the prediction of the performance, life, and reliability that the thyristor can provide in a given application. Table XI lists the important ratings and limiting characteristics and indicates the symbols normally used to specify the safe operating capabilities of thyristors.

Voltage Breakdown

All thyristor structures consist of one relatively wide, lightly doped base region between two more heavily doped regions of opposite impurity type. This lightly doped base region supports the main blocking voltage in both directions. The choice of design parameters (width and doping) for this base has the most fundamental effect on all thyristor electrical properties because blocking voltages, on-state voltage, power dissipation, and

Table XI — Ratings and Limiting Characteristics for Thyristors

Quantity	Symbol	Quantity	Symbol
Ambient temperature	T_A	Maximum (peak) total value	I_{RM}
Case temperature	T_C	Repetitive peak	I_{RRM}
Junction temperature	T_J	Reverse breakdown current:	
Storage temperature	T_{stg}	DC value, no alternating component	$I_{(BR)R}$
Thermal Resistance	R_θ	Instantaneous total	$I_{(BR)R}$
Junction to ambient	$R_{\theta J-A}$	On-state voltage:	
Junction to case	$R_{\theta J-C}$	Total rms value	$V_{T(RMS)}$
Case-to-ambient	$R_{\theta C-A}$	DC value, no alternating component	V_T
Case-to-heat sink	$R_{\theta C-S}$	DC value, with alternating component	$V_{T(AV)}$
Transient thermal impedance	$R_{\theta(t)}$	Instantaneous total value	V_T
Junction-to-ambient	$R_{\theta J-A} (t)$	Maximum (peak) total value	V_{TM}
Junction-to-case	$R_{\theta J-C} (t)$	Breakover voltage:	
On-state current:		DC value, no alternating component	$V_{(BO)}$
Total rms value	$I_{T(RMS)}$	Instantaneous total value	$V_{(BO)}$
DC value, no alternating component	I_T	Off-state voltage:	
DC value, with alternating component	$I_{T(AV)}$	Total rms value	$V_{D(RMS)}$
Instantaneous total value	I_T	DC value, no alternating component	V_D
Maximum (peak) total value	I_{TM}	DC value, with alternating component	$V_{D(AV)}$
Surge (non-repetitive)	I_{TSM}	Instantaneous total value	V_D
Overload	$I_{T(OV)}$	Maximum (peak) total value	V_{DM}
Breakover current:		Working peak	V_{DWM}
DC value, no alternating component	$I_{(BO)}$	Repetitive peak	V_{DRM}
Instantaneous total value	$I_{(BO)}$	Repetitive peak, with gate open	V_{DROM}
Off-state current:		Non-repetitive peak	V_{DSM}
Total rms value	$I_{D(RMS)}$	Non-repetitive peak with gate open	V_{DSOM}
DC value, no alternating component	I_D	Reverse voltage:	
DC value, with alternating component	$I_{D(AV)}$	Total rms value	$V_{R(RMS)}$
Instantaneous total value	I_D	DC value, no alternating component	V_R
Maximum (peak) total value	I_{DM}	DC value, with alternating component	$V_{R(AV)}$
Repetitive peak	I_{DRM}	Instantaneous total value	V_R
Reverse current:		Maximum (peak) total value	V_{RM}
Total rms value	$I_{R(RMS)}$	Working peak	V_{RWM}
DC value, no alternating component	I_R	Repetitive peak, with specified gate-to-cathode resistance	V_{RRM}
DC value, with alternating component	$I_{R(AV)}$		
Instantaneous total value	I_R		

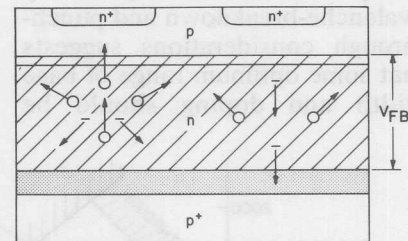
Table XI—Ratings and Limiting Characteristics for Thyristors (Cont'd)

Quantity	Symbol	Quantity	Symbol
Repetitive peak, with gate open	V_{RRM}	Gate non-trigger current:	
Non-repetitive peak, with specified gate-to-cathode resistance	V_{RSM}	DC value, no alternating component	I_{GD}
Non-repetitive peak, with gate open	V_{RSOM}	Maximum (peak) total value	I_{GDM}
Reverse breakdown voltage:		Gate voltage:	
DC value, no alternating component	$V_{(BR)R}$	DC value, no alternating component	V_G
Instantaneous total	$V_{(BR)R}$	Maximum (peak) total value	V_{GM}
Holding current:		Gate trigger voltage:	
DC value, no alternating component	I_H	DC value, no alternating component	V_{GT}
Instantaneous total value	I_H	Instantaneous total value	V_{GT}
Latching current:		Maximum (peak) total value	V_{GTM}
DC value, no alternating component	I_L	Gate non-trigger voltage:	
Instantaneous total value	I_L	DC value, no alternating component	V_{GD}
Gate current:		Instantaneous total value	V_{GD}
DC value, no alternating component	I_G	Maximum (peak) total value	V_{GDM}
DC value, with alternating component	$I_{G(AV)}$	Gate power dissipation:	
Maximum (peak) total value	I_{GM}	DC value, no alternating component	P_G
Gate trigger current:		DC value, with alternating component	$P_{G(AV)}$
DC value, no alternating component	I_{GT}	Instantaneous total value	P_G
Maximum (peak) total value	I_{GTM}	Maximum (peak) total value	P_{GM}

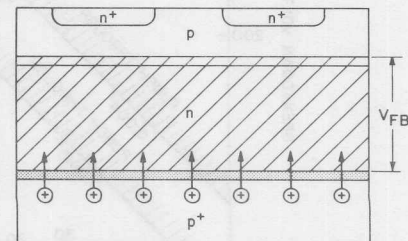
switching speeds all stem from the design of this region.

Voltage breakdown is the most important design criterion for a thyristor. Voltage initiated turn-on can occur as a result of avalanche breakdown or voltage punch-through. (An excessive rate of rise of off-state voltage can also initiate thyristor turn-on, as explained subsequently in the discussion on **Critical Rate of Rise of Off-state Voltage**.)

Avalanche breakdown occurs when the electric field in the depletion region reaches the critical field at which carriers traveling in the field gain sufficient energy between collisions to generate additional carriers when collision occurs. Avalanche voltage increases with lighter doping. Fig. 95(a) illustrates the avalanche-breakdown condition.



(a)



(b)

92CS-21327

Fig. 95—(a) Avalanche-breakdown and (b) voltage punch-through conditions.

Fig. 95(b) provides a diagrammatic representation of **voltage punch-through**. Punch-through may occur with an excess blocking voltage of a polarity for which turn-on is possible. The blocking voltage causes the depletion region to spread to such an extent that it encompasses the p-type emitter. When this spreading occurs, a free flow of holes into the depletion region is possible, and turn-on results. In contrast to avalanche breakdown, punch-through voltage is increased by heavier doping and wider base widths. In a transistor, punch-through is always destructive; in a thyristor, it may not be.

The conflicting demands on impurity concentration imposed by avalanche-breakdown and punch-through considerations suggests that some optimum range of base width and doping should be

selected for any specific design-voltage objective. Fig. 96 shows a basic design chart that may be used to determine this optimum range. In this chart, the impurity concentration is shown on the horizontal axis, and the breakdown voltage is shown on the vertical axis. Optimum ranges of material resistivity and base width are shown for various punch-through values. The maximum voltage for any range chosen is limited by avalanche considerations. The chart shows that avalanche breakdown voltage increases with a reduction in impurity concentration, but that punch-through voltage is decreased for this condition.

The important point illustrated by the chart is that for a practical range of base-material resistivity, a specific base width is required for each voltage class. Thus, a small SCR intended for

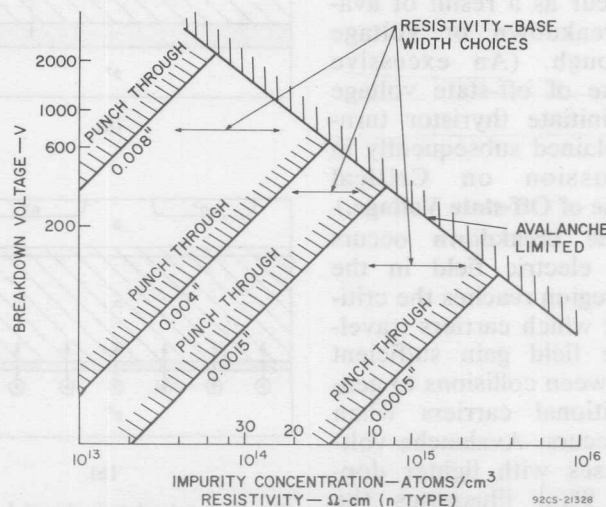


Fig. 96—Basic design chart used to determine optimum range of base width and doping.

logic applications below 200 volts might have an acceptable base width of 1.5 mils and a base-material resistivity in the neighborhood of 10 ohm-centimeters. A 1500-volt device would require a base thickness of 8 mils or more and a base-material resistivity of 50 ohm-centimeters or more. Because the wider base width increases on-state voltage, power dissipation, and thermal resistance, and decreases surge rating and switching speeds, this choice is a fundamental consideration and must be optimized for each voltage class, as a compromise between voltage and other characteristics.

Off-State Voltage Ratings

The voltage ratings of thyristors are given for both steady-state and transient operation and for forward- and (SCR only) reverse-blocking conditions. For SCR's, voltages are considered to be in the forward or positive direction when the anode is positive with respect to the cathode. Negative voltages for SCR's are referred to as reverse-blocking voltages. For triacs, voltages are considered to be positive when main terminal No. 2 is positive with respect to main terminal No. 1. Alternatively, this condition may be referred to as operation in the first quadrant.

When the voltage applied to a thyristor is in the polarity for which switching to the on state is possible, the voltage-blocking capability of the device is temperature-sensitive. The maximum

junction temperature for thyristors is usually between 100°C and 150°C. The selection of the maximum operating temperature represents a compromise which assures that a sufficient number of devices provide the required blocking-voltage capability (for which a low junction temperature is desirable) and which allows the highest possible current rating for the thyristors (for which a high junction temperature is desirable). Increases in junction temperature above this maximum value result in a greater reliability stress and adversely affect the switching characteristics of thyristors.

Peak OFF/State Voltages —The **repetitive peak off-state** voltage V_{DROM} is the maximum value of off-state voltage that the thyristor should be required to block under the stated conditions of temperature and gate-to-cathode resistance. If this voltage is exceeded, the thyristor may switch to the on state. The circuit designer should make sure that the rating is not exceeded to assure proper operation of the thyristor.

The effect of increased temperature is accentuated in thyristors because of the regenerative action upon which the operation of these devices is dependent. Thermally generated currents tend to be multiplied. If this blocking current crosses the gate-to-cathode junction, its effect on the thyristor is similar to that of the gate current and thus tends to reduce the breakover voltage V_{BO} . For this reason, off-state voltage ratings

are specified at the maximum rated junction temperature.

A gate-to-cathode shunting resistance can be used to provide a path for the blocking current that bypasses the gate-to-cathode junction. The use of this shunt resistance improves the off-state blocking capability, but reduces the gate sensitivity. Off-state voltage ratings, therefore, are usually specified with the gate open to represent worst-case conditions.

Under relaxed conditions of temperature or gate impedance, or when the blocking capability of the thyristor exceeds the specified rating, it may be found that a thyristor can block voltages far in excess of its repetitive peak off-state voltage rating V_{DSOM} . Because the application of an excessive voltage to a thyristor may damage it, an absolute upper limit should be imposed on the amount of voltage that may be applied to the main terminals of the device. This voltage rating is referred to as the **nonrepetitive peak off-state voltage** V_{DSOM} . It should be noted that the maximum (peak) total off-state voltage V_{DM} has a single rating irrespective of the voltage grade of the thyristor. This rating is a function of the construction of the thyristor and of the surface properties of the pellet. The V_{DM} rating should not be exceeded under either continuous or transient conditions.

Fig. 97 shows a simple, inexpensive test circuit that may be used to value the off-state voltage capabilities of thyristors. (The circuit may also be used for

reverse-blocking and leakage tests of thyristors.) Resistor R_1 and capacitor C_1 are included in the test circuit to limit the rate of rise of applied voltage to the thyristor under test. Resistor R_2 limits the discharge of capacitor C_1 through the thyristor in the event that the thyristor is turned on during the test. Resistor R_3 provides a discharge path for capacitor C_1 .

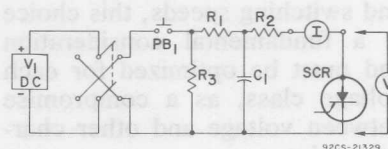


Fig. 97—Test circuit used to determine dc forward- and reverse-voltage-blocking capabilities and leakage current of thyristors.

The GTO provides less regenerative gain than most conventional SCR's; the high-temperature blocking capability of the GTO, therefore, is less sensitive to leakage currents that tend to reduce the breakover-voltage value and inadvertently cause the device to switch to the on state. The GTO, therefore, also has improved dv/dt characteristics, i.e., can withstand a faster rate of rise of off-state voltage without inadvertent switching to the on state.

Reverse Voltages (For SCR's)—Reverse-voltage ratings are given for SCR's to provide operating guidance in the third quadrant, or reverse-blocking mode.

The **repetitive peak reverse voltage** V_{RSOM} is the maximum allow-

able value of reverse voltage, including all repetitive transient voltages, that may be applied to the SCR or GTO. Because reverse power dissipation is small at this voltage, the rise in junction temperature because of this reverse dissipation is very slight and is accounted for in the rating of the SCR.

The **nonrepetitive peak reverse voltage** V_{RSOM} is the maximum allowable value of any nonrepetitive transient reverse voltage which may be applied to the SCR. These nonrepetitive transient voltages are allowed to exceed the steady-state ratings, even though the instantaneous power dissipation can be significant. While the transient voltage is applied, the junction temperature may increase, but removal of the transient voltage in a specified time allows the junction temperature to return to its steady-state operating temperature before a thermal runaway occurs.

The test circuit shown in Fig. 97 may be used for reverse voltage tests of an SCR.

Maximum Junction Temperature

The maximum junction temperature is the second most important consideration in thyristor design. Several factors must be considered in determination of a maximum junction-temperature rating, as indicated in Fig. 98.

At the upper end of the temperature scale, the maximum allowable junction temperature is restricted by material limits defined not so much by the silicon, but by peripheral materials such as the solders used on the pellet in lead attachments, encapsulating resins, and plastic package materials, where used. Temperature excursions into this area cause material and structural damage.

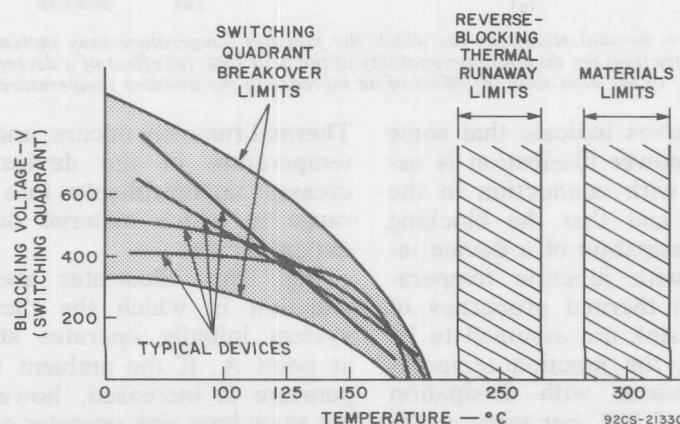
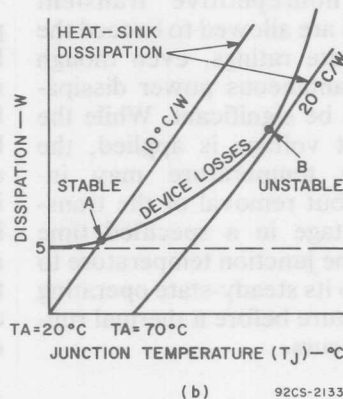
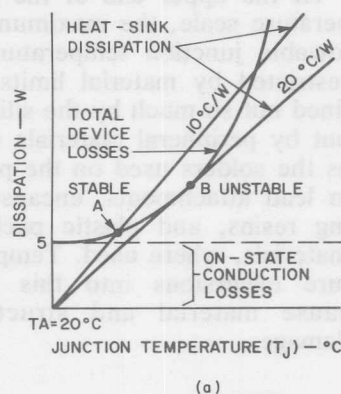


Fig. 98—Basic design chart used to select maximum junction-temperature rating for a thyristor.

The next lower range of limiting temperature is determined by thermal runaway of the reverse-blocking junction in SCR's. This runaway is the familiar mechanism in which reverse-blocking losses generated in the junction increase with junction temperature at a faster rate than the dissipation capability of the heat sink, as described in the section on **Thermal Considerations**. Fig. 99 illustrates thermal-runaway conditions for two common situations.

tem at point A with some temperature rise. If a smaller heat sink is used or if the air flow is constricted in some way, the rate of increase in junction temperature rises. A new slope is then required to represent the characteristic of the heat sink. This situation is indicated by the 20°C-per-watt slope shown in Fig. 99(a). For this condition, the point of operation of the device-and-heat-sink combination shifts from A to B. This point is an unstable one for the thermal system.



92CS-21331

Fig. 99—Two thermal situations for which the junction temperature may increase at a rate greater than the dissipation-capability of the heat sink: (a) effect of a decrease in the size of the heat sink; (b) effect of an increase in the ambient temperature.

The curves indicate that some level of power dissipation is associated with conduction in the on state and that the blocking power dissipation of a device increases with junction temperature. The thermal properties of the heat sink are assumed to be such that the junction temperature increases with dissipation at a rate of 10°C per watt. A device operating in this condition operates stably as a thermal sys-

tem. Thermal runaway occurs, and the temperature of the device increases uncontrollably into the range in which material degradation occurs.

Fig. 99(b) illustrates another situation in which the thermal system initially operates stably at point A. If the ambient temperature is increased, however, the same heat sink operates along a new dissipation curve. The operating point of the thermal

system shifts to point B and beyond. Again, because of the rapid increase in device temperature, limiting temperatures for material degradation are reached.

The lowest range of thyristor temperature limits, as shown in Fig. 98, is defined by the temperature sensitivity of the blocking capability in a switching quadrant. In practice, various devices within a design family exhibit a range of temperature sensitivity. At temperatures greater than 200°C, very few thyristors retain their blocking capability. The temperature sensitivity is improved greatly by decreasing gate sensitivity or by emitter shorting.

It should be noted that turn-on induced by temperature is not in itself damaging, because it results from the excess generation of hole-electron pairs that forward-bias the cathode emitter in much the same manner as a gate signal. Device problems from over-temperature turn-on arise when the "gating" signal is too low in magnitude for the rate of rise of load current (di/dt) required. Temperature-induced turn-on is usually an application problem, therefore, because control of the load is lost.

For a given range of blocking capability, a junction-temperature rating is selected to provide adequate yield of devices that have the required voltage ratings. Typically, for thyristors, junction-temperature ratings have been selected in the range from 100°C to 125°C.

It is also necessary to assure

the adequacy of other parameters of the device which are temperature-sensitive, such as commutation capability in triacs, turn-off time in fast-switching SCR's, and static dv/dt ratings for all thyristors.

On-State Current Ratings (SCR's and Triacs)

Thyristor current ratings define maximum values for normal or repetitive currents and for surge or nonrepetitive currents. These maximum ratings are determined on the basis of the maximum junction-temperature rating, the junction-to-case thermal resistance, the internal power dissipation that results from the current flow through the thyristor, and the ambient temperature. The effect of these factors in the determination of current ratings is illustrated by the following example.

Fig. 100 shows curves of the maximum average forward power dissipation for the RCA-2N3873 SCR as a function of average forward current for dc operation and for various conduction angles. For the 2N3873, the junction-to-case thermal resistance $R_{\theta J-C}$ is 0.92°C per watt and the maximum operating junction temperature T_J is 100°C. If the maximum case temperature $T_{C(max)}$ is assumed to be 65°C, the maximum average forward power dissipation can be determined as follows:

$$P_{AV(max)} = \frac{T_{J(max)} - T_{C(max)}}{R_{\theta J-C}} \quad (26)$$

$$= 0.92 \text{ }^{\circ}\text{C/watt}$$

$$= 38 \text{ watts}$$

The maximum average forward current rating for the specified conditions can then be determined from the rating curves shown in Fig. 100. For example, if a conduction angle of 180 degrees is assumed, the average forward current rating for a maximum dissipation of 38 watts is found to be 22 amperes.

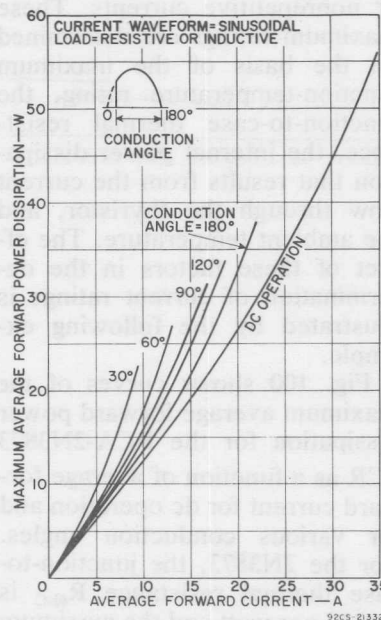


Fig. 100—Power-dissipation rating chart for the RCA-2N3873 SCR.

These calculations assume that the temperature is uniform throughout the pellet and the case. The junction temperature, however, increases and decreases under conditions of transient loading or periodic currents, depending

sipated within the thyristor. The current rating must take these variations into account.

The on-state current ratings for a thyristor indicate the maximum values of average, rms, and peak (surge) current that should be allowed to flow through the main terminals of the device, under stated conditions, when the thyristor is in the on state. For heat-sink-mounted thyristors, these maximum ratings are based on the case temperature; for lead-mounted thyristors, the ratings are based on the ambient or tie-point temperature.

Steady-State Ratings—The example used to show the effect of various factors on maximum current ratings pointed out that these ratings are determined on the basis of the internal power dissipation, the junction-to-case thermal resistance, and the difference between the maximum operating junction temperature and the maximum case temperature. Because the maximum operating junction temperature is fixed, the maximum on-state current ratings may be given by curves that relate current to case temperature. The maximum allowable current approaches zero as the case temperature approaches the maximum operating junction temperature because this current is directly proportional to the ratio of the difference between case and junction temperatures to the junction-to-case thermal resistance.

The basic ratings for thyristors

define the boundary conditions for a basic current/case-temperature rating chart, such as that shown in Fig. 101. The various limits for a specific design rating are indicated by curves 1 through 5. The first item is the choice of junction-temperature rating, as has been described, to assure an adequate yield of devices with useful voltage ratings. This first choice sets the upper boundary on the rating chart.

leads attached to the top of the thyristor, that is, to the cathode of the SCR or main terminal No. 1 of the triac, are not thermally connected to the heat sink of the thermal system that maintains the case temperature. The thermal limit of these leads sets an upper rms current limit for the package, as shown by curve 4.

The case temperature of the thyristor is derated from point 1 as current is increased to main-

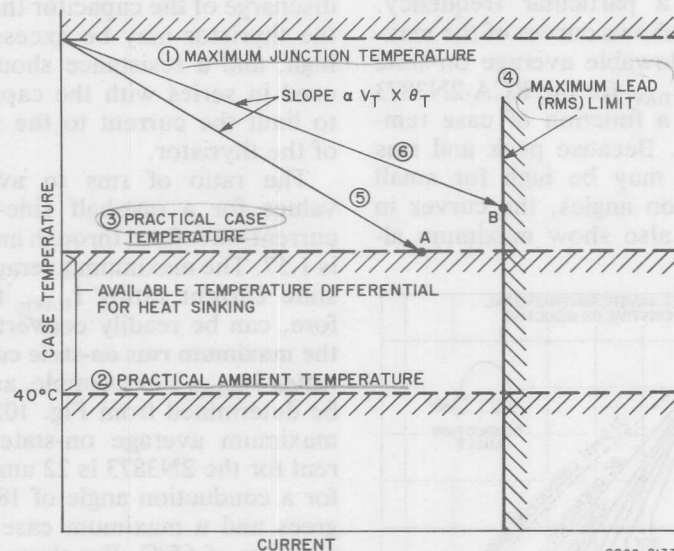


Fig. 101—Basic current/case-temperature rating chart for thyristors.

There is a practical level of ambient temperature, represented by curve 2, which must be allowed for in the design of equipment. Also, in the design of equipment, there must be some differential between the ambient and the case temperature. These considerations set the two lower boundaries, curves 2 and 3. The

tain a constant junction temperature. The slope of the derating, shown by curve 5, is proportional to the on-state dissipation and the junction-to-case thermal resistance. Both of these values are inversely proportional to pellet area. The device defined by derating curve 5 should be terminated in its current rating at point

A for practical heat-sink arrangements and ambient conditions.

A device defined by curve 6 may have a larger chip area, a lower-thermal-resistance package, or a narrower base width in comparison to a device defined by curve 5. This particular device is terminated at the maximum rms current capability of the lead materials.

The **maximum average on-state current rating** is usually specified for a half-sine-wave current at a particular frequency. Fig. 102 shows curves of the maximum allowable average on-state current $I_{T(AV)}$ for the RCA-2N3873 SCR as a function of case temperature. Because peak and rms currents may be high for small conduction angles, the curves in Fig. 102 also show maximum al-

lowable average currents as a function of conduction angle. The maximum operating junction temperature for the 2N3873 is 100°C. The rating curves indicate, for a given case temperature, the maximum average on-state current for which the average temperature of the pellet will not exceed the maximum allowable value. The rating curves may be used for only resistive or inductive loads. When capacitive loads are used, the currents produced by the charge or discharge of the capacitor through the thyristor may be excessively high, and a resistance should be used in series with the capacitor to limit the current to the rating of the thyristor.

The ratio of rms to average values for a one-half sine-wave current waveform through an SCR is 1.57. The maximum average on-state current rating $I_{T(AV)}$, therefore, can be readily converted to the **maximum rms on-state current rating** $I_{T(RMS)}$. For example, as may be determined from Fig. 102, the maximum average on-state current for the 2N3873 is 22 amperes for a conduction angle of 180 degrees and a maximum case temperature of 65°C. For these same conditions, the rms current rating may be determined as follows:

$$\begin{aligned} I_{T(RMS)} &= I_{T(AV)} \times 1.57 \\ &= 22 \text{ amperes} \times 1.57 \\ &= 35 \text{ amperes} \end{aligned}$$

WR
ITAV for DC.

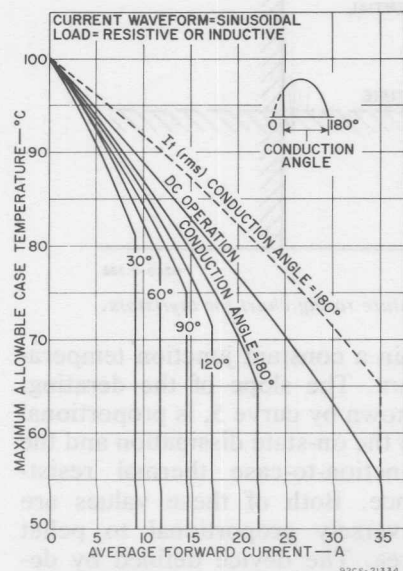


Fig. 102—Current rating chart for the RCA-2N3873 SCR.

The dashed-line curve in Fig. 102 shows the rms current rating for

the 2N3873 as a function of case temperature for a conduction angle of 180 degrees.

The on-state current rating for a triac is given only in rms values because these devices normally conduct alternating current. Fig. 103 shows an rms on-state current rating curve for a typical triac as a function of case temperature.

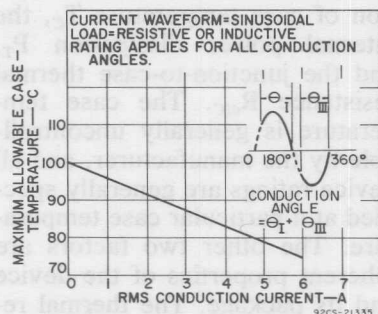


Fig. 103—Current-rating curve for a typical RCA triac.

As with the SCR, the triac curve is derated to zero current when the case temperature rises to the maximum operating junction temperature. Triac current ratings are given for full-wave conduction under resistive or inductive loads. Precautions should be taken to limit the peak current to tolerable levels when capacitive loads are used.

Surge Ratings—the surge on-state current rating I_{TMS} indicates the maximum peak value of a short-duration current pulse that should be allowed to flow through a thyristor during one on-state cycle, under stated conditions. This rating is applicable for any rated load condition.

During normal operation, the junction temperature of a thyristor may rise to the maximum allowable value; if the surge occurs at this time, the maximum limit is exceeded. For this reason, a thyristor is not rated to block off-state voltage immediately following the occurrence of a current surge. Sufficient time must be allowed to permit the junction temperature to return to the normal operating value before gate control is restored to the thyristor. Fig. 104 shows a surge-current rating curve for the 2N3873 SCR. This curve shows peak values of half-sine-wave forward (on-state) current as a function of overload duration measured in cycles of the

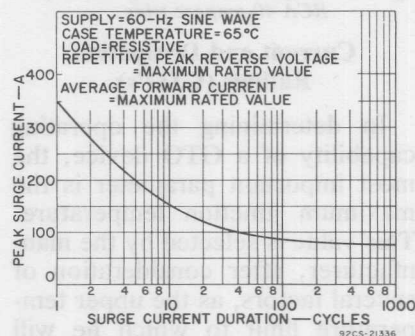


Fig. 104—Surge-current rating curve for the RCA-2N3873 SCR.

60-Hz current. Fig. 105 shows surge-current rating curves for an RCA 40-ampere triac. For triacs, the rating curve shows peak values for a full-sine-wave current as a function of the number of cycles of overload duration. Multicycle surge curves are the basis for the selection of circuit breakers and fuses that are

used to prevent damage to the thyristor in the event of accidental short-circuit of the device. The number of surges permitted over the life of the thyristor should be limited to prevent device degradation.

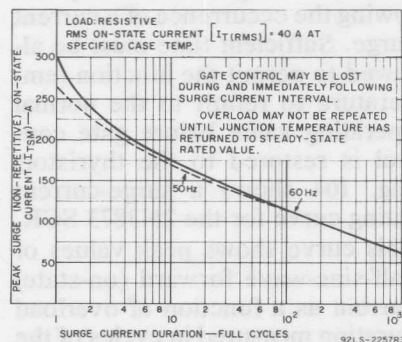


Fig. 105—Surge-current rating chart for RCA 40-ampere triac.

Current and Dissipation Ratings (GTO's)

In determining the operating capability of a GTO device, the most important parameter is the maximum junction temperature. This value is selected by the manufacturer, after consideration of several factors, as the upper temperature limit to which he will guarantee device operation. The **maximum steady-state current rating** is determined on the basis of the upper boundary of the internal junction temperature that the manufacturer will allow. The current rating of a GTO then is based on the maximum junction temperature which, in turn, is a function of three factors as outlined in the following equation:

$$T_{J(\max)} = T_C + P_T R_{\theta JC} \quad (27)$$

where $T_{J(\max)}$ is the maximum average junction temperature, T_C is the case temperature, P_T is the average internal power dissipation, and $R_{\theta JC}$ is the steady-state junction-to-case thermal resistance.

If the junction temperature T_J is maintained at a constant value, then the steady-state current rating of the GTO becomes a function of case temperature T_C , the internal power dissipation P_T , and the junction-to-case thermal resistance $R_{\theta JC}$. The case temperature is generally uncontrollable by the manufacturer, and all device ratings are generally specified at a particular case temperature. The other two factors are inherent properties of the device and its package. The thermal resistance is determined by the type of package and the pellet size, and the power dissipation is a function of the on-state voltage drop across the main terminals of the device that results from the current flow. Fig. 106 shows a typical curve of on-state current as a function of on-state voltage.

The on-state voltage specified in the published data for RCA GTO devices is the maximum value that will be allowed for that particular family of devices. Because this voltage is a maximum, it represents the worst-case power dissipation for steady-state current flow. Fig. 107 shows curves of this power dissipation as a function of peak on-state current for different duty factors.

When the internal power dissipation is known and the maximum allowable junction temperature

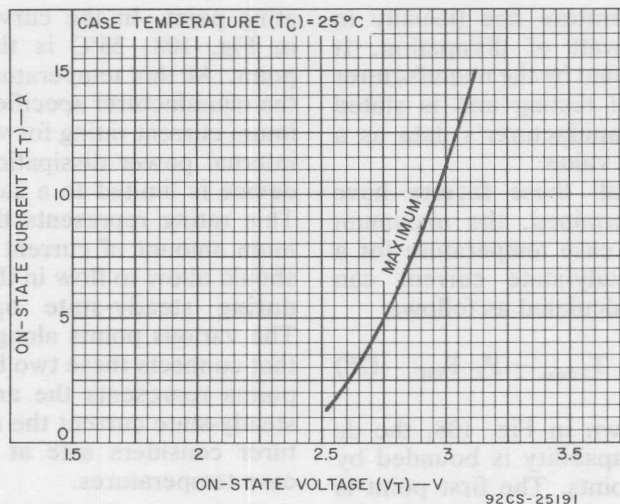


Fig. 106—On-state current as a function of on-state voltage.

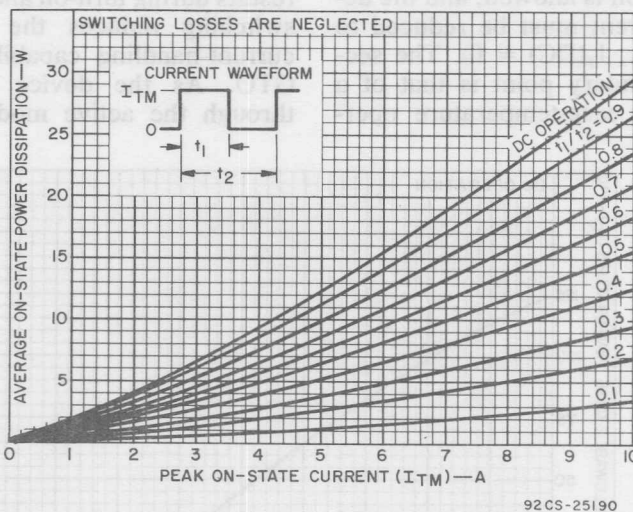


Fig. 107—Maximum average power dissipation.

has been determined, the thermal resistance of the device is the only remaining factor in the case-temperature equation. This factor

represents the amount of temperature rise that occurs in the device for a given power dissipation. The thermal resistance is a measure of

the temperature rise (usually in °C) per watt of dissipation. It is determined by the manufacturer by careful testing and is stated on the manufacturer's data as a maximum value.

When all these factors have been determined, the maximum allowable case temperature for a given steady-state current can then be calculated as follows:

$$T_C = T_{J(max)} - P_T R_{\theta JC} \quad (28)$$

As shown in Fig. 108, the dc current capability is bounded by several points. The first point is that at which the maximum case temperature is equal to the maximum allowable junction temperature. At this point, no internal dissipation is allowed, and the device current must be reduced to zero (i.e., $I_T(DC) = 0$). The second boundary point is that of a practical case-temperature oper-

ating point. In the curve shown in Fig. 108, 25°C is the cutoff point. At this temperature value, the manufacturer specifies a maximum current rating for which the internal power dissipation of the device is limited to a safe value. This rating represents the maximum amount of current the user should allow to flow in the device during steady-state operation. The various points along the line that connects these two boundary points represents the amount of steady-state current the manufacturer considers safe at different case temperatures.

The ratings specified for steady-state operation must be derated during **switching operation**. The additional power dissipation that results during turn-on and turn-off switching reduces the on-state current-handling capability of a GTO. As the device switches through the active mode during

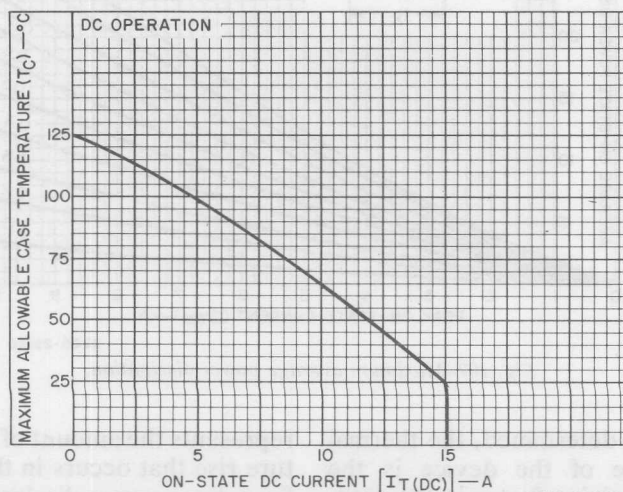


Fig. 108—Maximum allowable case temperature as a function of on-state current.

turn-on and turn-off, the resulting dissipation must be taken into account to assure that the maximum average junction temperature limit will not be exceeded.

As previously stated, the thermal resistance, the maximum junction temperature, and the power dissipated determine the operating case temperature. If the power dissipation is increased by switching losses, the operating case temperature must be lowered, the on-state current must be decreased, or the duty factor must be reduced. During switching operation, the device power dissipation (P_T), which includes both switching losses and on-state losses, may be expressed as follows:

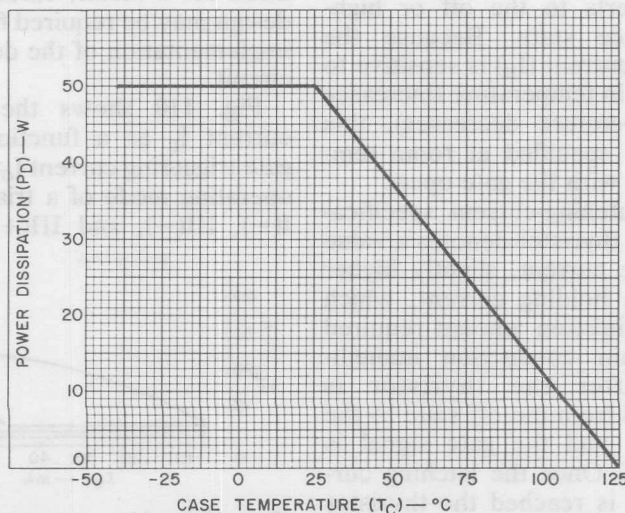
$$P_T = P_{SS} + P_{SW} \quad (29)$$

where P_{SS} is the power dissipation during steady-state operation

and P_{SW} is the power dissipation during the switching mode.

Fig. 109 shows a curve of the power dissipation a GTO device can withstand for a given case temperature. This curve is shown for a constant maximum junction temperature of 125°C. The slope of the curve is the negative reciprocal of the thermal resistance of the device. If the case temperature at which the device is to be operated is known, the power dissipation capability of the device can be determined directly from the curve. This curve represents the total average power dissipation, which must include both switching and steady-state losses to assure that the maximum junction temperature is not exceeded.

For a given current and duty factor, the steady-state dissipation can be determined from Fig. 107. The value of steady-state dissipation is then subtracted from



92CS-25188

Fig. 109—Average power dissipation as a function of case temperature.

the resultant is the amount of power dissipation that can be tolerated as switching losses. These losses are comprised of losses incurred during both the turn-on and turn-off intervals. Factors such as anode supply voltage, load inductance, and gate drive affect the dissipation during these active modes. The over-all effect of these losses is to reduce the current-handling capability of the device.

Holding and Latching Currents

After a thyristor has been switched to the on-state condition, a certain minimum value of anode current is required to maintain the thyristor in this low-impedance state. If the anode current is reduced below this critical holding-current value, the thyristor cannot maintain regeneration and reverts to the off or high-impedance state. Because the holding current (I_H) is sensitive to changes in temperature (increases as temperature decreases), this rating is specified at room temperature with the gate open.

The latching-current specification of a thyristor denotes a value of anode current, slightly higher than the holding current, which is the minimum amount required to sustain conduction immediately after the thyristor is switched from the off state to the on state and the gate signal is removed. Once the latching current (I_L) is reached the thyristor remains in the on, or low-impedance, state until its anode

ing-current rating is an important consideration when a thyristor is to be used with an inductive load because the inductance limits the rate of rise of the anode current. Precautions should be taken to insure that, under pulse-gating conditions, the gate signal is present until the anode current rises to the latching value so that complete turn-on of the thyristor is assured.

Although general considerations for holding and latching currents discussed in the preceding paragraphs are also valid for gate-turn-off SCR's, it should be noted that the holding and latching currents are influenced by the basic design tradeoffs that are inherent in a gate-turn-off SCR. The tradeoffs result in the gate-turn-off SCR having higher holding and latching currents than a comparably rated conventional SCR. As a result, careful circuit design may be required for proper implementation of the device in a circuit.

Fig. 110 shows the latching current I_L as a function of the gate triggering current I_{GT} for each operating mode of a triac. In the I(+), III(-), and III(+) modes,

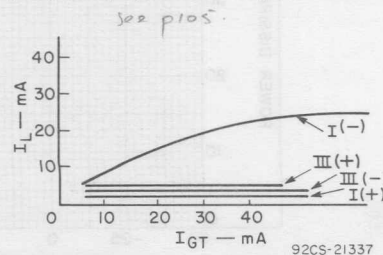


Fig. 110—Latching current as a function of gate current for each triggering mode of a triac.

the latching-current value remains relatively constant with changes in the gate current. In the $I(-)$ mode, however, larger values of latching current are required as the amount of gate current driven into the triac is increased. "Starved" gating in the $I(-)$ mode, therefore, can be a problem because of the dependence of the latching-current value upon the amount of gate current. This dependence is one of the reasons that a triac should be overdriven whenever possible.

Fig. 111 shows a simple test circuit that may be used to determine the holding and latching

For the latching-current test, toggle switches S_1 and S_2 are closed to select the triggering mode, potentiometer R_{GT} is adjusted for the desired value of gate current [usually the $I_{GT}(\text{max})$ value for the device being tested], and the pushbutton switches PB_1 and PB_2 are held closed as potentiometer R_L is adjusted to some value for which the triac is maintained in the off state. The value of R_L is then gradually decreased in small increments until the gate signal injected at each R_L setting by depression of PB_1 turns on the triac. The reading on meter M_1

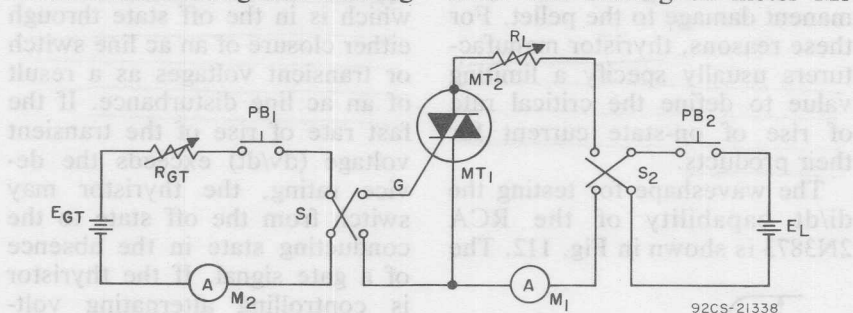


Fig. 111—Test circuit used to determine holding and latching currents of thyristors.

currents of a triac. For the holding-current test, the triac is gated on by closing the toggle switches S_1 and S_2 , depressing the pushbutton switches PB_1 and PB_2 , and adjusting potentiometer R_L to a low value. The pushbutton switch PB_1 is then opened, and the value of potentiometer R_L is increased until the triac turns off. The current reading indicated on the meter M_1 just prior to complete turn-off is the holding-current value.

indicates the latching-current value. The pushbutton switch PB_1 should be alternately opened and closed for this value of R_L to assure that the triac was originally off.

Critical Rate of Rise of On-State Current (di/dt)

When a thyristor is turned on by application of a gate trigger pulse, conduction does not instantly occur throughout the en-

tire pellet. The initial flow of current is concentrated in very small areas near the gate contact. A short interval of time is required for the current to spread sufficiently so that the entire pellet is in conduction. If the rate at which the load current increases is high in comparison to the rate at which current spreads laterally across the pellet, considerable energy will be concentrated in the turned-on areas, and localized high-temperature regions (hot spots) may develop. These hot spots may adversely affect other characteristics of the thyristor or, in extreme cases, may cause permanent damage to the pellet. For these reasons, thyristor manufacturers usually specify a limiting value to define the critical rate of rise of on-state current for their products.

The waveshape for testing the di/dt capability of the RCA 2N3873 is shown in Fig. 112. The

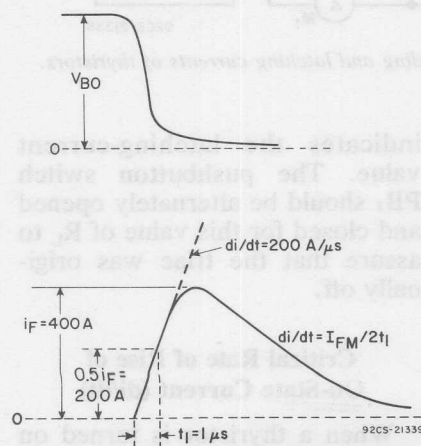


Fig. 112—Voltage and current waveforms used to determine di/dt rating of the RCA-2N3873 SCR.

critical rate of rise of on-state current is dependent upon the size of the cathode area that begins to conduct initially, and the size of this area is increased for larger values of gate trigger current. For this reason, the di/dt rating is specified for a specific value of gate trigger current.

Critical Rate of Rise of Off-State Voltage (dv/dt)

An important parameter for thyristors is the "critical rate of rise of off-state voltage." A source voltage can be suddenly applied to an SCR or a triac which is in the off state through either closure of an ac line switch or transient voltages as a result of an ac line disturbance. If the fast rate of rise of the transient voltage (dv/dt) exceeds the device rating, the thyristor may switch from the off state to the conducting state in the absence of a gate signal. If the thyristor is controlling alternating voltage, "false" (non-gated) turn-on resulting from a transient imposed voltage is limited to no more than half the applied voltage because turn-off occurs during the zero current crossing. However, if the source voltage suddenly applied to the off thyristor is a dc voltage, the device may switch to the on state and turn-off could then be achieved only by circuit interruptions. The switching from the off state is caused by the internal capacitance of the thyristor. A steep-rising voltage impressed across the terminals of a thyristor

causes a capacitance-charging current to flow through the device. This charging current ($i = Cdv/dt$) is a function of the rate of rise of applied off-state voltage. If the rate of rise of voltage exceeds a critical value, the capacitance-charging current exceeds the gate trigger current and causes device turn-on. Operation at elevated junction temperatures reduces the thyristor ability to support a steep-rising (high- dv/dt) voltage because less gate current is required for turn-on. The effect of temperature on the critical rate of rise of off-state voltage is shown in Fig. 113.

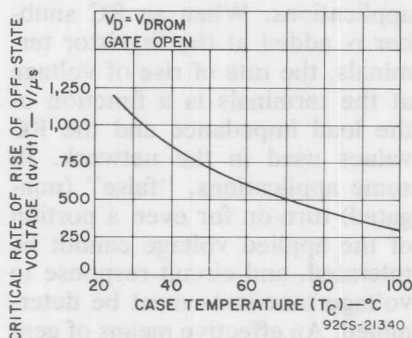


Fig. 113—Critical rate of rise of off-state voltage as a function of case temperature.

The use of the shorted emitter construction in RCA thyristors has resulted in a substantial increase in the dv/dt capability of these devices by providing a shunt path around the gate-to-cathode junction. Typical units can withstand rates of voltage rise up to 200 volts per microsecond under worst-case conditions. The dv/dt

capability of a thyristor decreases as the temperature rises and is increased by the addition of an external resistance from gate to reference terminal. The dv/dt rating, therefore, is given for the maximum junction temperature with the gate open, i.e., for worst-case conditions.

Fig. 114(a) shows a simple test circuit that may be used to determine the dv/dt capability of a thyristor. The curves in Fig. 114(b) define the critical values for linear and exponential rates of increase in reapplied forward off-state voltage for an SCR. The critical value for the exponential rate of rise of forward voltage is the rating given in the manufacturer's test specifications.

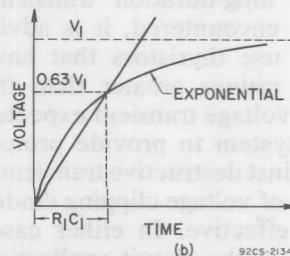
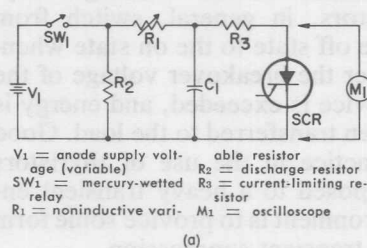


Fig. 114—(a) Test circuit and (b) waveforms used to determine dv/dt capability of a thyristor.

This rating is determined from the following equation:

$$\frac{dv}{dt} = \frac{V_{\text{DROM rating}}}{\text{RC time constant}} \times 0.632 \quad (24)$$

- * The dv/dt specification allows a circuit designer to design an RC time-constant network that can be used to limit the rate of rise of a transient voltage below the critical value of the thyristor.

Voltage transients which occur in electrical systems as a result of disturbance on the ac line caused by various sources such as energizing transformers, load switching, solenoid closure, contactors, and the like may generate voltages which are above the ratings of thyristors and result in spike voltages that exceed the critical rate of rise of off-state voltage. Thyristors, in general, switch from the off state to the on state whenever the breakover voltage of the device is exceeded, and energy is then transferred to the load. Good practice in the use of thyristors exposed to a heavy transient environment is to provide some form of transient suppression.

For applications in which low-energy, long-duration transients may be encountered, it is advisable to use thyristors that have voltage ratings greater than the highest voltage transient expected in the system to provide protection against destructive transients. The use of voltage clipping diodes is also effective. In either case, analysis of the circuit application will reveal the extent to which suppression should be employed. In an SCR application in which

there is a possibility of exceeding the reverse-blocking voltage rating, it is advisable to add a clipping diode or to use an SCR with a higher reverse-blocking voltage rating to minimize power dissipation in the reverse mode. Because triacs generally switch to a low conducting state, if the di/dt buildup of the principal current flow after turn-on is within device ratings it is safe to assume that reliable operation will be achieved under the specified conditions.

The use of an RC snubber is most effective in reducing the effects of the high-energy short-duration transients more frequently encountered in thyristor applications. When an RC snubber is added at the thyristor terminals, the rate of rise of voltage at the terminals is a function of the load impedance and the RC values used in the network. In some applications, "false" (non-gated) turn-on for even a portion of the applied voltage cannot be tolerated, and circuit response to voltage transients must be determined. An effective means of generating fast-rising transients and observing the circuit response to such transients is shown in Fig. 115. This circuit makes use of a mercury-wetted relay to transfer a capacitor charge to the input terminals of a control circuit. This approach permits generation of a transient of known magnitude whose rate of rise of voltage can easily be displayed on an oscilloscope. For a given load condition, the values in the RC snubber network can be adjusted so that the

transient voltage at the device terminals is suppressed to a tolerable level. This approach affords the circuit designer with meaningful information as to how a control

make an independent assessment of the inherent reliability of each type of thyristor under conditions that simulate the most stringent type of service in which the device may be employed for any recommended application.

The natural boundaries of a reliability-assurance program are "time" and "the number of available units." A technique used to obtain meaningful information in a reasonable time from a limited number of samples is accelerated testing. In this type of testing, the devices are subjected to stresses that exceed rated or normal conditions for a relatively short period in order to generate failures that would normally occur at typical conditions over a longer stress period. The results are then extrapolated to predict the mean time to failure (MTTF) under typical operating conditions. The chart shown in Fig. 116 outlines the various types of tests to which RCA thyristors are subjected during reliability evaluations.

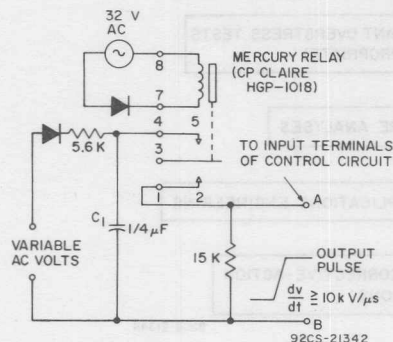


Fig. 115—Circuit used to generate fast-rising transients.

circuit will respond in a heavy transient environment. The circuit is capable of generating transient voltages in excess of 10 kilovolts per microsecond, which exceeds industrial generated transients.

RELIABILITY

Reliability is a prime consideration at each stage in the design, production, and application of RCA thyristors. Thorough research by applications engineers defines the circuit requirements and specifies in detail the necessary device parameters. Design engineers develop devices that meet the objective specifications with sufficient margin for process variations. The specifications define electrical, package, and reliability requirements. Quality-and-reliability-assurance engineers

Reliability Testing

The most important factors in the control of manufacturing defects arise through knowledge of the device design and close process control in manufacture. Nothing that can be done in terms of statistics or testing comes close to the importance of good process control in manufacture. This control is complemented by reliability testing to monitor product capability. During the development phase, various reliability tests are conducted by the product development group. During the

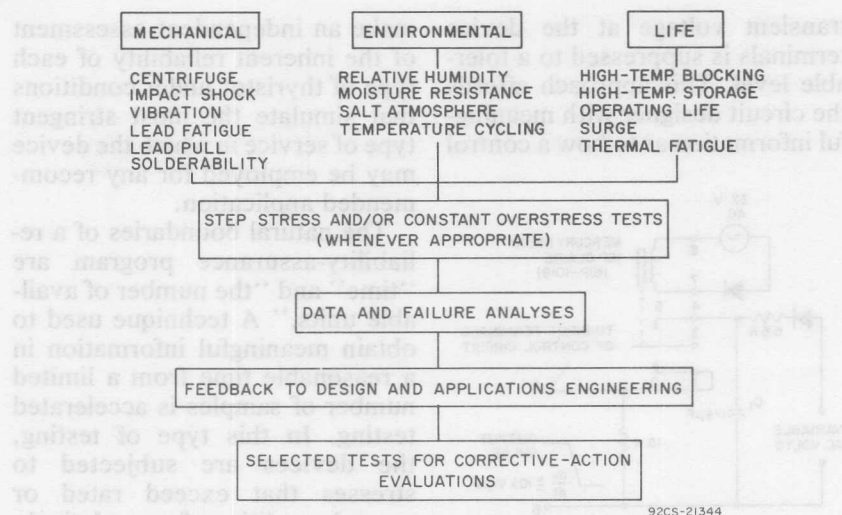


Fig. 116—Outline of reliability evaluations performed on RCA thyristors.

early production phase, the device capability is monitored by an engineering reliability group. During normal production, the manufacturing-plant quality-control department regularly performs the following types of life tests:

- High-temperature blocking
- Thermal fatigue
- Operating life
- High-temperature storage
- Temperature cycling
- Surge
- Vibration
- Shock

The high-temperature blocking test exposes the device to the maximum blocking voltage and the maximum operating temperature. The blocking test is followed by thermal-fatigue testing during which the rated current is passed

through the thyristor, and the resulting power dissipation is used to heat the device to the maximum junction temperature. The current is then interrupted, and the thyristor is cooled rapidly. Thousands of thermal cycles are accumulated to verify the mechanical soundness of the pellet and its mounting system.

During the operating life tests, synthetic switching circuits simultaneously apply maximum current and maximum voltage (at the normal line frequency) to the device at the maximum rated case temperature. This type of testing simulates actual operating conditions. High-temperature storage is used to accentuate any instability that may exist at the surface of the device. Temperature cycling, surge, vibration, and shock are the familiar environmental tests used to assess the

mechanical robustness of the package, the pellet, and the lead-attachment system. Surge testing stresses the ohmic contact system of the device to assure that low thermal resistance and even heat distribution are maintained under the surge condition.

During the development phase, these tests are generally performed on a step stress basis. During the quality-control phase, they are conducted at rated conditions. The data obtained from life testing can provide some statistical representation of failure rate. Fig. 117 shows an example of a method used to represent failure rate in the United States Military Handbook on "Reliability of Electronic Components." The curves shown present failure rates for transistors as a function of temperature. However, because the

blocking junctions in thyristors typically form a p-n-p transistor structure, use of these derating curves for thyristors is justified when sufficient test data are available. Different failure rates have been projected from the statistical summing of experimental data. A derating curve that describes the failure rate of an RCA-2N5442 40-ampere triac is superimposed (dashed line) on the family of transistor derating curves shown in Fig. 117. As indicated by this curve, the failure rate of the 2N5442 triac, and of other thyristors that have been studied, is similar to that for other silicon power devices.

Failure Analysis

A manufacturer has a responsibility to provide the necessary service to determine the causes of

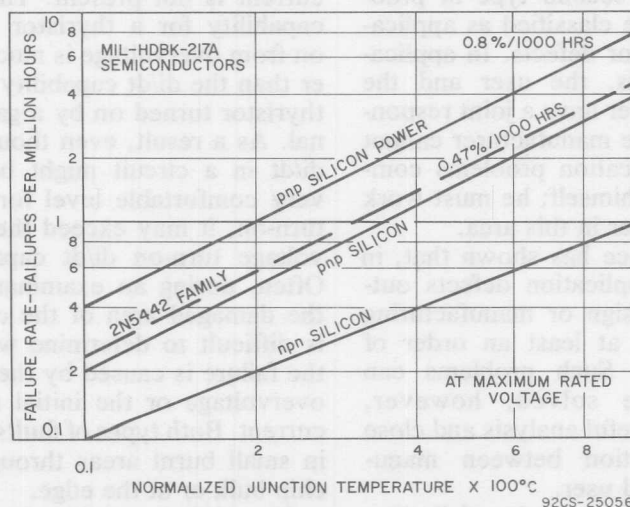


Fig. 117—Failure rates (in failures per 10^6 hours) for MIL-S-19500, transistors, (for power transistors, 1 watt or greater at $T_A = 25^\circ\text{C}$ multiply values shown by two), and for the RCA-2N5442 40-ampere triac (dashed line).

failure of his devices and to provide feedback to the customer or the manufacturing facilities to initiate correction procedures. The various problems encountered with thyristors may be categorized into two basic groups:

1. Manufacturing Defects
2. Application Faults
 - Overvoltage, surface or bulk di/dt , overvoltage turn-on
 - di/dt Turn-on
 - Gated turn-on
 - Gate noise turn-on
 - Gate dissipation, forward-reverse interchanged cathode
 - Surge
 - Overload
 - Hermeticity

The first group includes problems that result from manufacturing defects; the required corrective actions are clearly the responsibility of the device manufacturer. The second type of problem may be classified as application faults or defects. In application defects, the user and the manufacturer have a joint responsibility. The manufacturer cannot solve application problems completely by himself; he must work with the user in this area.

Experience has shown that, in general, application defects outnumber design or manufacturing defects by at least an order of magnitude. Such problems can usually be solved, however, through careful analysis and close communication between manufacturer and user.

Applications faults fall into several general categories. The first and most prevalent is that

arising from overvoltage. Overvoltage damage can occur in the bulk of the device (at defects in the crystal or at diffusion irregularities) or at localized spots on the surface. The concentration of power dissipation at these small areas causes material degradation in either the silicon or the encapsulating materials at the edge. Closely associated with overvoltage turn-on is a di/dt stress that results from turn-on initiated by the overvoltage. If overvoltage turn-on is accomplished without damage within the chip, a danger is still present in that the current resulting from the thyristor turn-on is concentrated in the small area within which turn-on began. Such localized current conduction can result in over-temperature in a small area. In turn-on initiated from overvoltage, the mechanism to cause spreading of the current is not present. The di/dt capability for a thyristor turned on from overvoltage is much lower than the di/dt capability of the thyristor turned on by a gate signal. As a result, even though the di/dt in a circuit might be at a very comfortable level for gated turn-on, it may exceed the overvoltage turn-on di/dt capability. Often, during an examination of the damaged area of the chip, it is difficult to determine whether the failure is caused by the initial overvoltage or the initial rise of current. Both types of faults result in small burnt areas through the chip bulk or at the edge.

The di/dt capability for gated turn-on is high but it can still be exceeded, particularly with

very low values of gate drive. A gated di/dt failure in RCA devices occurs at the inside edge of the n-type emitter, which is the area where conduction begins. This type of failure results in a small area of molten silicon. Such a failure mechanism is easily seen in the chip. Most users today are conscious of the fact that adequate gate signal must be provided, particularly in applications involving fast-rising pulses of large magnitude. However, di/dt failures caused by inadequate gate signal frequently occur. In such circuits, turn-on is probably initiated by noise in the gate circuit, and the designer of the equipment must neutralize these unwanted signals.

Failure may also result because of gate over-dissipation. RCA thyristors have relatively large gates and robust gate leads, so that a good deal of dissipation is acceptable. A triac will operate as a triac when the gate lead is inadvertently interchanged with the Main Terminal No. 1. Because the gate area is much smaller than the main terminal No. 1 area, the gate may be damaged if full current flows. Triac gate damage often destroys blocking voltage in the first quadrant without damage to the blocking voltage in the third quadrant. A consistent failure of first-quadrant blocking voltage, therefore, suggests gate damage.

Short-time surge failure generally results from a gross melting of silicon over much of the cathode or Main Terminal areas. In some RCA packages for lower-current

devices, the internal leads fuse at several hundred amperes of short-circuit current. When the internal leads of a failed device are fused it may be assumed that a momentarily shorted load condition existed. Overload results from a long duration of current in excess of the steady-state rated current which causes a gradual heat build up. The first area to be attacked is the ohmic contact system. In an overload failure, the high-temperature solder used on the chip melts and flows out from under the chip. This flow, which occurs prior to a resulting gross degradation of the ohmic contact system and pellet, characterizes over-load failure.

Hermeticity failures on hermetic devices generally lead to the presence of ionizable material in the encapsulating resin next to the surface. This condition leads to surface current, surface inversion layers, a reduction in a device blocking-voltage capability, and increased blocking leakage current because of the high surface current. Therefore, it is particularly important to maintain hermeticity on hermetically sealed devices. If a device fails because of degraded blocking characteristics, a gross-leak and time-leak check should be performed before any inspection for other possible defects.

PRODUCT MATRICES

The product matrices shown in tables XII and XIII indicate the wide range of operating voltages

types of RCA thyristors are given in the RCA Solid State DATA-BOOK Series SSD-206, "Thyristors, Rectifiers, and Triacs," or in the RCA technical data bulletins on each device.

Table XII—SCR Product Matrix

RCA SCR's		TO-8		TO-66								TO-66 With Heat Rad.	
1T(RMS) TSM (60 Hz) V _{PROM} V _{RROM} (V)	2A 60A	4.5A 200A	5A 60A	FTO* 5A 80A	FTO* 5A 80A	FTO* 5A 80A	FTO* 5A 75A ¹ PM	FTO* 5A 80A	FTO* 5A 80A	5A 80A	FTO* 5A 80A		
15													
25													
30													
50													
100		\$2400A				S3704A					S3714A		
150													
200	2N3528	\$2400B	2N322B		S3700B	S3704B				\$2710B	S3714B		
250													
300													
400	2N3529	\$2400D	2N3525		S3700D	S3704D				\$2710D	S3714D		
500				S3706E									
600	2N4102	\$2400M	2N4101	S3705M	S3700M	S3704M	S3701M			\$2710M	S3714M		
700						S3704S					S3714S		
750								S3702S					
800									S3703SF				
I _{GT} (mA)	15	15	15	30	40	40	35	45	40	15	40		
V _{GT} (V)	2	2	2	4	3.5	3.5	4	4	4	2	3.5		
File No.	114	567	114	839	306	690	476	522	522	266	690		

* FTO – Fast Turn-Off

RCA SCR's	Low Pro- file Mod. TO-5	TO-5 With Heat Rad.	TO-5 With Heat Sprdr.	TO-220AB VERSAWATT						Stud	TO-220AB VERSA- WATT
T _{IRMS}	7A	3.3A	7A	4A	4A	4A	8A	10A	FTO* 10A	12	
T _{ISM} (60 Hz)	100A	100A	100A	35A	35A	35A	100A	100A	90A	125	
V _{RRM}				S2060Q	S2061Q	S2062Q					
V _{RRM} (V)	15										
	25										
	30			S2060Y	S2061Y	S2062Y					
	40			S2060F	S2061F	S2062F	S122F	S2800F		2N6394	
	100			S2060A	S2061A	S2062A	S122A	S2800A		2N6395	
	200	S2600B	S2610B	S2620B	S2060B	S2061B	S2062B	S122B	S2800B	S5210B	2N6396
	250										
	300			S2060C	S2061C	S2062C		S2800C			S6000C
	400	S2600D	S2610D	S2620D	S2060D	S2061D	S2062D	S122D	S2800D	S5210D	2N6397
	500			S2060E	S2061E	S2062E		S2800E			S6000E
	600	S2600M	S2610M	S2620M	S2060M	S2061M	S2062M	S122M	S2800M	S5210M	2N6398
	700							S122S	S2800S		S6000S
	800										
I _{GT} (mA)	15	15	15	0.2	0.5	2	25	15	40	30	
V _{GT} (V)	1.5	1.5	1.5	0.8	0.8	0.8	1.5	1.5	3.5	1.5	
File No.	496	496	496	654	654	654	889	890	737	891	

* FTO – Fast Turn-Off

Table XII—SCR Product Matrix (cont'd)

RCA SCR's	TO-3	Press Fit		Stud	Isolated Stud		Press-Fit, Flex. Leads on ISOSTUD				
		12.5	16		20A	35A	20A	35A	20A	35A	
$I_T(\text{RMS})$	200A	160	200A	350A	200A	350A	200A	350A	200A	350A	
$I_{TSM}(60\text{ Hz})$											
V_{DRM}	15										
$V_{RRM}(V)$	25										
	30										
	50	2N6400									
	100	2N3668	2N6401	S6200A	2N3870	S6210A	2N3896	S6220A	S6420A	S6230A	S6430A
	150										
	200	2N3669	2N6402	S6200B	2N3871	S6210B	2N3897	S6220B	S6420B	S6230B	S6430B
	250										
	300		S6100C								
	400	2N3670	2N6403	S6200D	2N3872	S6210D	2N3898	S6220D	S6420D	S6230D	S6430D
	500		S6100E								
	600	2N4103	2N6404	S6200M	2N3873	S6210M	2N3899	S6220M	S6420M	S6230M	S6430M
	700		S6100S								
	750										
	800			S6400N		S6410N		S6420N		S6430N	
$I_{GT}(\text{mA})$	40	30	15	40	15	40	15	40	15	40	40
$V_{GT}(V)$	2	1.5	2	2	2	2	2	2	2	2	2
File No.	116	892	418	578	418	578	418	578	877	877	877

RCA SCR's	Press-Fit, Isolated on TO-3 Flange	Press-Fit, Flex. Leads, Isolated on TO-3 Flange	TO-48							
$I_T(\text{RMS})$	20A	35A	20A	35A	16A	25A	Pulse Modulator 35A	FTO* 35A	FTO* 35A	
$I_{TSM}(60\text{ Hz})$	200A	350A	200A	350A	125A	150A	150A	180A	250A	
V_{DRM}	15									
$V_{RRM}(V)$	25				2N1842A	2N681				
	30									
	50				2N1843A	2N682			2N3654	
	100	S6240A	S6440A	S6250A	S6450A	2N1844A	2N683	2N3650	2N3655	
	150					2N1845A	2N684			
	200	S6240B	S6440B	S6250B	S6450B	2N1846A	2N685	2N3651	2N3656	
	250					2N1847A	2N686			
	300					2N1848A	2N687	2N3652	2N3657	
	400	S6240D	S6440D	S6250D	S6450D	2N1849A	2N688	2N3653	2N3658	
	500					2N1850A	2N689			
	600	S7240M	S6440M	S6250M	S6450M		2N690	S6493M	S7410M	S7412M
	700									
	750									
	800		S6440N		S6450N					
$I_{GT}(\text{mA})$	15	40	15	40	45	25	80	180	180	
$V_{GT}(V)$	2	2	2	2	3.5	3	2	3	2	
File No.	877	877	877	877	28	96	247	408	724	

* FTO - Fast Turn-Off

Table XII—SCR Product Matrix (cont'd)

For Horizontal-Deflection Circuits

RCA ITR's *	TO-66		TO-220AB VERSAWATT	
	Trace	Commutating (Retrace)	Trace	Commutating (Retrace)
$I_T(\text{RMS})$	5A	5A	8A	8A
$I_{TSM}(60\text{ Hz})$	60A	60A	100A	100A
$V_{DRM}(\text{V})$	300			TAS3901C*
	400	S3900D		TAS3901D*
	450		TAS3900DE*	
	500	S3800E	TAS3900E*	
	550		S3800EF	TAS3901EF*
	600	S3800M		TAS3901M*
	650	S3800MF	TAS3900MF*	TAS3901MF*
	700	S3800S	TAS3900S*	TAS3901S*
	750	S3800SF	TAS3900SF*	
$I_{GT}(\text{mA})$	40	45	30	45
$V_{GT}(\text{V})$	4	4	4	4
File No.	639	639	—	—

* Integrated Thyristor/Rectifier

* Developmental Types

RCA GTO's	TO-3		
	8.5A	8.5A	8.5A
$I_T(\text{DC})$	50A	50A	50A
$I_{TSM}(60\text{ Hz})$			
$V_{DRM}(\text{V})$	100	G5001A G5002A G5003A	
	200	G5001B G5002B G5003B	
	400	G5001D G5002D G5003D	
	600	G5001M G5002M G5003M	
Turn-on Time	t_d	1 μs 1.5 μs 1.5 μs	
t_{gt}	t_r	1 μs 1.5 μs 1.5 μs	
Turn-off Time	t_s	1 μs 3 μs 10 μs	
t_q	t_f	1 μs 3 μs 10 μs	
File No.		867 867 867	

Table XIII—Triac Product Matrix

RCA Triacs		Modified TO-5				Mod. TO-5 With Heat Radiator				TO-66		TO-66 Heat Rad.
STANDARD	I _T (RMS)	2.5A	2.5A	2.5A	2.5A	2.5A	2.5A	2.5A	2.5A	6A	15A	6A
	I _{TSM} (60 Hz)	25A	25A	25A	25A	25A	25A	25A	25A	100A	100A	100A
	V _{DROM} (V)	100	T2300A	T2301A	T2302A	2N5754	T2310A	T2311A	T2312A	T2313A		
	200	T2300B	T2301B	T2302B	2N5755	T2310B	T2311B	T2312B	T2313B	T2700B	T4700B	T2710B
	400	T2300D	T2301D	T2302D	2N5756	T2310D	T2311D	T2312D	T2313D	T2700D	T4700D	T2710D
	450											
	600				2N5757				T2313M			
	800											
	I _{GT} (mA)	I ⁺ , III ⁺	3	4	10	25	3	4	10	25	30	25
	I ⁺ , III ⁺	3	4	10	40	3	4	10	40	40	80	40
ZERO VOLTAGE SWITCH	V _{GT} (V)	All Modes	2.2	2.2	2.2	2.2	2.2	2.2	2.2	2.2	2.5	2.2
	File No.	470	431	470	414	470	431	470	414	351	300	351
	V _{DROM} (V)	100			T2306A				T2316A			
	200				T2306B				T2316B	T2706B	T4706B	T2716B
	400				T2306D				T2316D	T2706D	T4706D	T2716D
	450											
	600											
	I _{GT} (mA)	I ⁺ , III ⁺			45				45	45	45	45
	V _{GT} (V)	I ⁺ , III ⁺			1.5				1.5	1.5	1.5	1.5
	File No.				406				406	406	406	406
60-HZ OPERATION	I _T (RMS)			0.5A	0.5A							
	V _{DROM} (V)	200		T2304B	T2305B							
	400			T2304D	T2305D							
	I _{GT} (mA)	I ⁺ , III ⁺		10	25							
	I ⁺ , III ⁺			10	40							
	V _{GT} (V)	All Modes		2.2	2.2							
	File No.			441	441							
	I _T (RMS)											
	V _{DROM} (V)											
	I _{GT} (mA)											

RCA Triacs		TO-220AB VERSAWATT				Press Fit				Stud	
STANDARD	I _T (RMS)	6A	6A	8A	8A	ISOWATT*				10A	10A
	I _{TSM} (60 Hz)	60A	80A	100A	100A	100A				100A	100A
	V _{DROM} (V)	100				T2805A					
	200	T2500B	T2801B	T2800B	T2802B	T2805B				2N5569	2N5573
	300		T2801C	T2800C	T2802C						
	400	T2500D	T2801D	T2800D	T2802D	T2805D				2N5570	2N5574
	500		T2801E	T2800E	T2802E						
	600			T2800M	T2802M						
	800										
	I _{GT} (mA)	I ⁺ , III ⁺	25	80	25	50	25			25	50
ZERO VOLTAGE SWITCH	V _{GT} (V)	I ⁺ , III ⁺	60		60	60	40	80		40	80
	V _{GT} (V)	All Modes	2.5	4*	2.5	2.5*	2.5	2.5		2.5	2.5
	File No.	615	837	838	838	540	457	458		457	458
	V _{DROM} (V)	100									
	200	T2506B			T2806B	T2856B	T4107B	T4106B		T4117B	T4116B
	400	T2506D			T2806D	T2856D	T4107D	T4106D		T4117D	T4116D
	450										
	600						T4107M	T4106M		T4117M	T4116M
	I _{GT} (mA)	I ⁺ , III ⁺	45			45	45	45		45	45
	V _{GT} (V)	I ⁺ , III ⁺	1.5			1.5	1.5	1.5		1.5	1.5
60-HZ OPERATION	File No.	406			406	406		406	406	406	406
	I _T (RMS)						6A	10A	15A	6A	10A
	V _{DROM} (V)										
	200						T4105B	T4104B	T4103B	T4115B	T4114B
	400						T4105D	T4104D	T4103D	T4115D	T4114D
	I _{GT} (mA)	I ⁺ , III ⁺					50	50	50	50	50
	I ⁺ , III ⁺						80	80	80	80	80
	V _{GT} (V)	All Modes					2.5	2.5	2.5	2.5	2.5
	File No.						443	443	443	443	443
	I _T (RMS)										

* ISOWATT - Mounting tab electrically isolated from electrodes

* I⁺, III⁺ only

Table XIII—Triac Product Matrix (cont'd)

RCA Triacs		Isolated Stud		Press-Fit, Flex. Leads on ISOSTUD		Press-Fit on TO-3 Flange	
STANDARD	I_T (RMS)	10A	15A	10A	15A	10A	15A
	I_{TSM} (60 Hz)	100A	100A	100A	100A	100A	100A
	V_{DROM} (V)	100					
	200	T4121B	T4120B	T4131B	T4130B	T4141B	T4140B
	400	T4121D	T4120D	T4131D	T4130D	T4141D	T4140D
	450						
	600	T4121M	T4120M	T4131M	T4130M	T4141M	T4140M
	800						
	I_{GT} (mA)						
	I ⁺ , III ⁻	25	50	25	50	25	50
ZERO VOLTAGE SWITCH	I ⁻ , III ⁺	40	80	40	80	40	80
	V_{GT} (V)						
	All Modes	2.5	2.5	2.5	2.5	2.5	2.5
	File No.	457	458	878	878	878	878
	V_{DROM} (V)						
	100						
	200	T4127B	T4126B				
	400	T4127D	T4126D				
	450						
	600	T4127M	T4126M				
400 Hz OPERATION	I_{GT} (mA)						
	I ⁺ , III ⁺						
	V_{GT} (V)						
	I ⁺ , III ⁺						
	File No.	406	406				
	I_T (RMS)						
	V_{DROM} (V)	200					
	400						
	I_{GT} (mA)						
	I ⁺ , III ⁻						
	I ⁻ , III ⁺						
	V_{GT} (V)						
	All Modes						
File No.							

RCA Triacs		Press-Fit, Flex. Leads on TO-3 Flange		Press Fit		Stud		
STANDARD	I _T (RMS)	10A	15A	30A	40A	30A	40A	
	I _{TSM} 160 Hz	100A	100A	300A	300A	300A	300A	
	V _{DROM} (V)	100						
	200	T4151B	T4150B	T6401B	2N5441	T6411B	2N5444	
	400	T4151D	T4150D	T6401D	2N5442	T6411D	2N5445	
	450							
	600	T4151M	T4150M	T6401M	2N5443	T6411M	2N5446	
	800				T6400N		T6410N	
	I _{GT} (mA)							
	I ⁺ , III ⁻	25	50	50	50	50	50	
I ⁻ , III ⁺	40	80	80	80	80	80		
V _{GT} (V)	All Modes	2.5	2.5	2.5	2.5	2.5	2.5	
	File No.	878	878	459	593	459	593	
ZERO VOLTAGE SWITCH	V _{DROM} (V)							
	100							
	200			T6407B	T6406B	T6417B	T6416B	
	400			T6407D	T6406D	T6417D	T6416D	
	450							
	600			T6407M	T6406M	T6417M	T6416M	
	I _{GT} (mA)							
	I ⁺ , III ⁺			45	45	45	45	
	V _{GT} (V)							
	I ⁺ , III ⁺			1.5	1.5	1.5	1.5	
	File No.			406	406	406	406	
400-Hz OPERATION	I _T (RMS)			25A	40A	25A	40A	
	V _{DROM} (V)	200		T6405B	T6404B	T6415B	T6414B	
	400			T6405D	T6404D	T6415D	T6414D	
	I _{GT} (mA)							
	I ⁺ , III ⁻			80	80	80	80	
	I ⁻ , III ⁺			120	120	120	120	
	V _{GT} (V)	All Modes						
		File No.			3	3	3	3
					487	487	487	487

Table XIII—Triac Product Matrix (cont'd)

RCA Triacs		Isolated Stud		Press-Fit, Flex. Leads on ISOSTUD		Press-Fit Isolated on TO-3 Flange	
STANDARD	I_T (RMS)	30A	40A	30A	40A	30A	40A
	I_{TSM} (60 Hz)	300A	300A	300A	300A	300A	300A
	$V_{DROM}(V)$	100					
		200	T6421B	T6420B	T6431B	T6430B	T6441B
		400	T6421D	T6420D	T6431D	T6430D	T6441D
		450					
		600	T6421M	T6420M	T6431M	T6430M	T6441M
		800		T6420N		T6430N	T6440N
	$I_{GT}(mA)$						
	I ⁺ , III ⁻	50	50	50	50	50	50
ZERO VOLTAGE SWITCH	I ⁺ , III ⁺	80	80	80	80	80	80
	$V_{GT}(V)$						
	All Modes	2.5	2.5	2.5	2.5	2.5	2.5
	File No.	459	593	878	878	878	878
	$V_{DROM}(V)$	100					
		200	T6427B	T6426B			
		400	T6427D	T6426D			
		450					
		600	T6427M	T6426M			
	$I_{GT}(mA)$						
	I ⁺ , III ⁺	45	45				
	$V_{GT}(V)$						
	I ⁺ , III ⁺	1.5	1.5				
	File No.	406	406				

RCA Triacs		Press-Fit, Flex. Leads, Isolated on TO-3 Flange		Stud		Isolated Stud	
STANDARD	I_T (RMS)	30A	40A	60A	80A	60A	80A
	I_{TSM} (60 Hz)	300A	300A	600A	850A	600A	850A
	$V_{DROM}(V)$	100					
		200	T6451B	T6450B	T8411B	T8410B	T8421B
		400	T6451D	T6450D	T8411D	T8410D	T8421D
		450					
		600	T6451M	T6450M	T8411M	T8410M	T8421M
		800		T6450N			T8420M
	$I_{GT}(mA)$						
	I ⁺ , III ⁻	50	50	75	75	75	75
ZERO VOLTAGE SWITCH	I ⁺ , III ⁺	80	80	150	150	150	15
	$V_{GT}(V)$						
	All Modes	2.5	2.5	2.8	2.5	2.8	2.5
	File No.	878	878	725	894	725	894
	$V_{DROM}(V)$	100					
		200					
		400					
		450					
		600					
	$I_{GT}(mA)$						
	I ⁺ , III ⁺						
	$V_{GT}(V)$						
	I ⁺ , III ⁺						
	File No.						

Thyristor Gating and Switching Requirements

SCR's, gate-turn-off SCR's (GTO's), and triacs have unique characteristics and capabilities that make them ideally suited for power-switching and power-control applications in which low cost, small package size, device reliability, and circuit simplicity are important considerations. In most circuit applications, these devices are switched between two stable states (full off and full on) to control the application of power to the load. SCR's, GTO's and triacs are specifically designed to be triggered from the off state to the on state by application of a signal to the gate terminal. A basic understanding of gate-triggering requirements and switching characteristics of these devices, therefore, is essential to assure successful use of them in circuit applications.

The manufacturer's published data on the gating and switching characteristics of SCR's, GTO's and triacs enables a circuit designer to determine more easily the circuit conditions required to assure positive triggering (i.e., full turn on) and facilitates his selec-

tion of devices that have switching characteristics compatible with the requirements of his circuit. In addition, a knowledge of the basic gating and switching actions in SCR's, GTO's and triacs helps the designer to determine circuit requirements for suppression of transient effects that may result in inadvertent triggering or possible damage to the devices.

GATE CHARACTERISTICS

The manufacturer's specifications indicate the magnitudes of gate current and voltage required to turn on SCR's, GTO's and triacs. Gate characteristics, however, vary from device to device even among devices within the same family. For this reason, manufacturer's specifications on gating characteristics provide a range of values in the form of characteristic diagrams. A diagram such as that shown in Fig. 118 is given to define the limits of gate currents and voltages that may be used to trigger any given device of a specific family. The

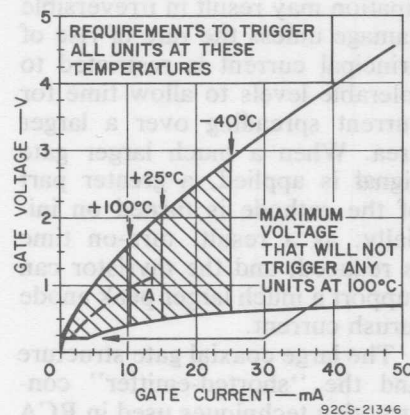


Fig. 118—Gate-characteristic curves for a typical RCA SCR.

boundary lines of maximum and minimum gate impedance on this characteristic diagram represent the loci of all possible triggering points for thyristors in this family. The curve OA represents the gate characteristic of a specific device that is triggered within the shaded area.

Trigger Level

The magnitude of gate current and voltage required to trigger a thyristor varies inversely with junction temperature. As the junction temperature increases, the level of gate signal required to trigger the thyristor becomes smaller. Worst-case triggering conditions occur, therefore, at the minimum operating junction temperature.

The maximum value of gate voltage below the level required to trigger any unit of a specific thyristor family is also an important gate characteristic. At

high operating temperatures, the level of gate voltage required to trigger a thyristor approaches the minimum value, and undesirable noise signals may inadvertently trigger the device. The maximum nontriggering gate voltage at the maximum operating junction temperature of the device, therefore, is a measure of the noise-rejection level of a thyristor.

The gate voltage and current required to switch a thyristor to its low-impedance state at maximum rated forward anode current can be determined from the circuit shown in Fig. 119. The value of resistor R_2 is chosen so that maximum anode current, as specified in the manufacturer's current rat-

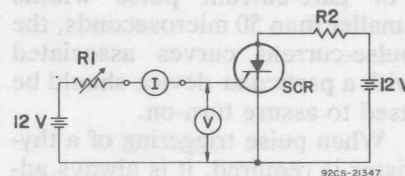


Fig. 119—Test circuit used to determine gate-trigger-pulse requirements of thyristors.

ing, flows when the device latches into its low-impedance state. The value of resistor R_1 is gradually decreased until the device under test is switched from its high-impedance state to its low-impedance state. The values of gate current and gate voltage immediately prior to switching are the gate voltage and current required to trigger the thyristor.

The **gate nontrigger voltage** V_{GD} is the maximum dc gate voltage that may be applied between

gate and cathode of the thyristor for which the device can maintain its maximum rated blocking voltage. This voltage is usually specified at the rated operating temperature (100°C) of the thyristor. Noise signals in the gate circuit should be maintained below this level to prevent unwanted triggering of the thyristor.

Pulse Triggering

The gate current specified in published data for thyristors is the dc gate trigger current required to switch an SCR or triac into its low-impedance state. For practical purposes, this dc value can be considered equivalent to a pulse current that has a minimum pulse width of 50 microseconds. For gate-current pulse widths smaller than 50 microseconds, the pulse-current curves associated with a particular device should be used to assure turn-on.

When pulse triggering of a thyristor is required, it is always advantageous to provide a gate-current pulse that has a magnitude exceeding the dc value required to trigger the device. The use of large trigger currents reduces variations in turn-on time, increases di/dt capability, minimizes the effect of temperature variation on triggering characteristics, and makes possible very short switching times. When a thyristor is initially triggered into conduction, the current is confined to a small area which is usually the more sensitive part of the cathode. If the anode-current magnitude is great, the localized instantaneous power dis-

sipation may result in irreversible damage unless the rate of rise of principal current is restricted to tolerable levels to allow time for current spreading over a larger area. When a much larger gate signal is applied, a greater part of the cathode is turned on initially; as a result, turn-on time is reduced, and the thyristor can support a much larger peak anode inrush current.

The large coaxial gate structure and the "shorted-emitter" construction techniques used in RCA thyristors has extended the range of limiting gate characteristics well beyond that required for normal triggering. Advantage can be taken of the higher peak-power capability of the gate to improve dynamic performance, increase di/dt capability, minimize interpulse jitter, and reduce switching losses. This higher peak-power capability also allows greater interchangeability of thyristors in high-performance applications.

When a thyristor is triggered by a gate signal just sufficient to turn on the device, the entire junction area does not start to conduct instantaneously. Instead, as pointed out in the discussion on **Critical Rate of Rise of On-State Current**, the device current is confined to a small area, which is usually the most sensitive part of the cathode. The remaining cathode area turns on as the anode current increases. When a much larger signal is applied to the gate, a greater part of the cathode is turned on initially and the time to complete the turn-on process is reduced. The

peak amplitude of gate-trigger currents must be large, therefore, when thyristors have to be turned on completely in a short period of time. Under such conditions, the peak gate power is high, and pulse triggering is required to keep the average gate dissipation within the values given in the manufacturer's specifications.

The forward gate characteristics for thyristors, shown in Fig. 120, indicate the maximum allow-

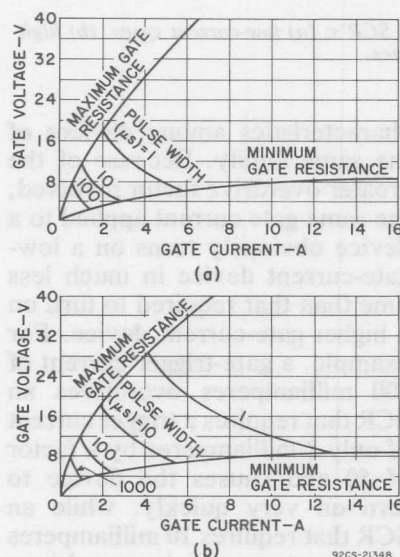


Fig. 120—Forward-gate characteristics for pulse triggering of RCA SCR's: (a) low-current types, (b) high-current types.

able pulse widths for various peak values of gate input power. The pulse width is determined by the relationship that exists between gate power input and the increase in the temperature of the thyristor pellet that results from the application of gate power. The

curves shown in Fig. 120(a) are for RCA SCR's that have relatively small current ratings (2N4101, 2N4102, and S2600D types), and the curves shown in Fig. 120(b) are for RCA SCR's that have larger current ratings (2N3670, 2N3873, and 2N3899 types). Because the higher-current thyristors have larger pellets, they also have greater thermal capacities than the smaller-current devices. Wider gate trigger pulses can therefore be used on these devices for the same peak value of gate input power.

Because of the resistive nature of the "shorted-emitter" construction, similar volt-ampere curves can be constructed for reverse gate voltages and currents, with maximum allowable pulse widths for various peak-power values, as shown in Fig. 121. These curves indicate that reverse dissipations do not exceed the maximum allowable power dissipation for the device.

TRIGGER-CIRCUIT REQUIREMENTS

The basic gate trigger circuit for a thyristor can be represented by a voltage source and a series resistance, as shown in Fig. 122. The series resistance should include both the external circuit resistance and the internal generator resistance. With this type of equivalent circuit, the conventional load-line approach to gate trigger-circuit design can be used. With pulse triggering, it is assumed initially that the turn-on time required to trigger all thyris-

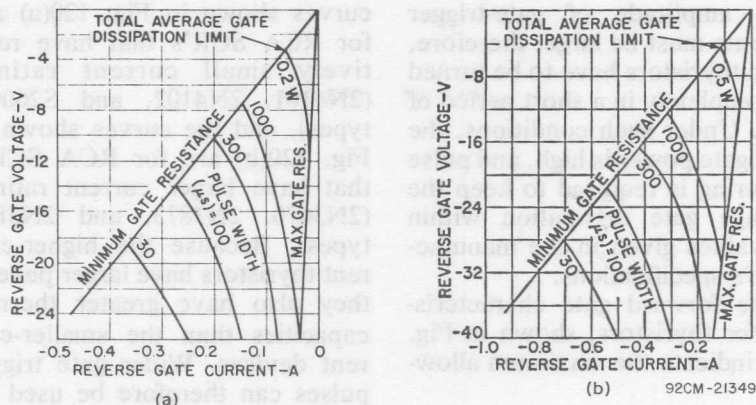


Fig. 121—Reverse gate characteristics of RCA SCR's: (a) low-current types, (b) high-current types.

tors of the same type is known, and that the maximum allowable gate trigger-pulse widths for specific gate-power inputs are to be determined.

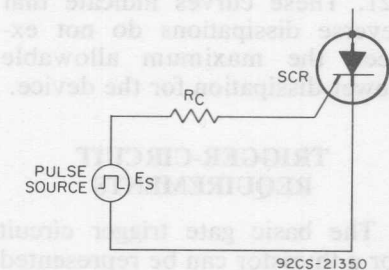


Fig. 122—Equivalent diagram of the basic gate-trigger circuit for a thyristor.

The magnitude of gate-trigger current required to turn on all SCR's of a given type can be determined from the turn-on characteristics shown in Fig. 123. The spread or band of turn-on characteristics for the same gate current results from the variation of gate-trigger

characteristics among devices of the same family. Because of the greater overdrive factor involved, the same gate current applied to a device obviously turns on a low-gate-current device in much less time than that required to turn on a higher-gate-current device. For example, a gate-trigger current of 100 milliamperes overdrives an SCR that requires a trigger current of only 2 milliamperes by a factor of 50 and causes the device to turn on very quickly, while an SCR that requires 10 milliamperes of trigger current is overdriven by a factor of 10 and is turned on more slowly. As the gate current increases, the band of turn-on characteristics becomes narrower, and an increase in gate current does not effectively decrease the turn-on time.

The turn-on characteristics shown in Fig. 123 indicate that a gate-trigger current of 1 ampere is required to assure that all devices of this type will turn on in

the upper curve at 500 milliamperes). In addition, the width of the gate-trigger pulse should be at least 2.5 microseconds to ensure that the SCR remains on after

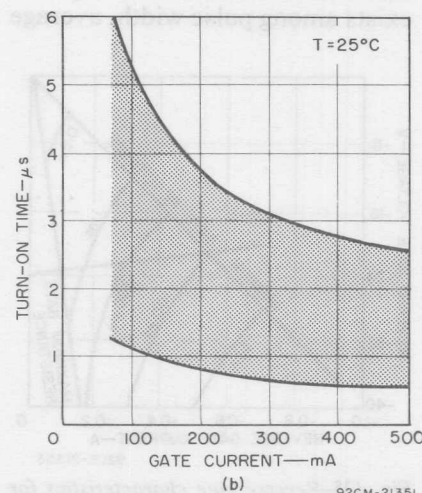
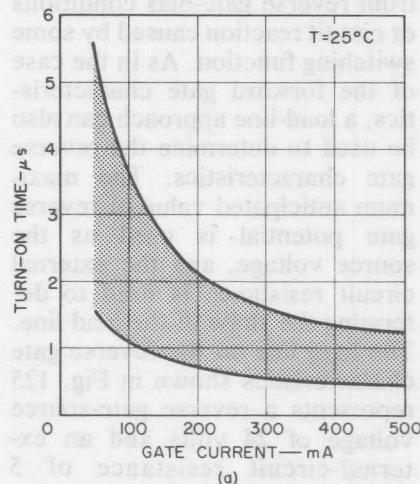


Fig. 123—Typical turn-on time distribution among RCA SCR's: (a) low-current types, (b) high-current types.

width be wide enough for the SCR anode current to achieve the latching value. Conservative design, however, requires the pulse width to be at least equal to the turn-on time. For inductive loads, the turn-on time is larger than indicated in the characteristics curves because of the slow rise of current through the inductance.

A straight load line can then be plotted on the pulse triggering characteristics, as shown in Fig. 124. The two points that determine the position of this line are the source voltage (20 volts) and a point slightly above the intersection of the required gate current (500 milliamperes) and the curve of maximum gate resistance. The load line should lie below the pulse-width curve required to trigger all SCR's (in this example, the 2.5-microsecond curve). The maximum allowable pulse width is obtained by estimation of the pulse-width curve tangent to the load line. In this example, the pulse width is estimated to be 30 microseconds (the pulse-width curves are logarithmically spaced). The load line intersects the abscissa at the 4-ampere point. The maximum circuit resistance, therefore, is 5 ohms. The peak gate power is the product of gate voltage and gate current at the point of tangency of the pulse-width curve, and is approximately 20 watts (10 volts \times 2 amperes).

When gate pulses are used to trigger SCR's, the maximum allowable operating frequency f is dependent upon the average

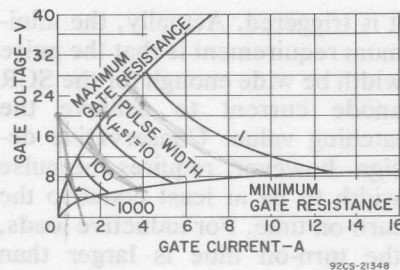


Fig. 124—Forward gate characteristics of typical RCA SCR's showing load line for a source of 20 volts and a required gate current of 1 ampere.

power rating of the gate $P_{g(av)}$ and can be determined from the following equation:

$$f = P_{g(av)} / P_{g(pk)} \times PW_g \quad (30)$$

where $P_{g(pk)}$ is the peak gate power and PW_g is the gate pulse width.

If it is assumed that only half the total average gate-dissipation rating, or 0.25 watt, is used to trigger the device, this value is used in the frequency calculation. For example, if this value is 0.25 watt for the SCR selected, then the maximum allowable operating frequency is determined as follows:

$$f = \frac{0.25 \text{ W}}{20 \text{ W} \times 2.5 \times 10^{-6} \text{ second}} = 5000 \text{ Hz}$$

If there is no reverse gate power dissipation, the maximum allowable frequency can be 10,000 Hz. If the maximum allowable pulse width is 30 microseconds, the maximum allowable operating frequency is proportionately reduced to 416 Hz.

The trigger-circuit design is usually fixed by the requirements for reliable triggering, and reverse gate dissipation is considered after the values of source voltage and circuit resistance have been determined. Reverse gate power dissipation results from reverse gate-bias conditions or circuit reaction caused by some switching function. As in the case of the forward gate characteristics, a load-line approach can also be used to determine the reverse gate characteristics. The maximum anticipated value of reverse gate potential is used as the source voltage, and the external circuit resistance is used to determine the slope of the load line. The load line on the reverse gate characteristics shown in Fig. 125 represents a reverse gate-source voltage of 24 volts and an external-circuit resistance of 5 ohms. From the relationship that exists among pulse width, average

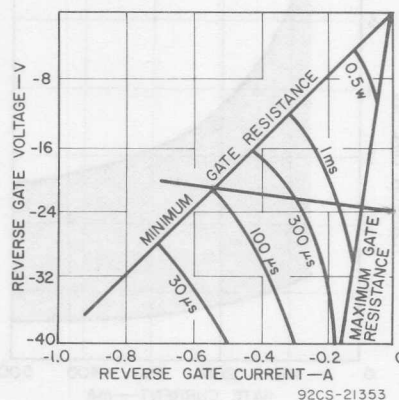


Fig. 125—Reverse gate characteristics for typical RCA SCR's showing load line for a reverse gate-source voltage of 24 volts and an external circuit resistance of 5 ohms.

gate power, peak gate power, and frequency, a maximum pulse width can be calculated for the actual operating frequency. For a reverse gate dissipation of 0.25 watt, peak gate power of 10 watts, and a frequency of 5000 Hz, the maximum allowable pulse width PW is calculated as follows:

$$PW = \frac{0.25 \text{ W}}{5000 \text{ Hz} \times 10 \text{ W}} \quad (31)$$

$$= 5 \text{ microseconds}$$

This reverse gate-pulse width should be less than the maximum allowable pulse width, as determined by the curve that lies just below the load line on Fig. 125. In this example, the maximum allowable pulse width for reverse dissipation is 100 microseconds.

The total average dissipation caused by gate-trigger pulses is the sum of the average forward and reverse dissipations. This total dissipation should correspond to the average gate power dissipation shown in the published data for the selected SCR. If the average gate dissipation exceeds the maximum published value, as the result of high forward gate-trigger pulses and transient or steady-state reverse gate biasing, the maximum allowable forward-conduction-current rating of the device must be reduced to compensate for the increased rise of junction temperature caused by the increased gate power dissipation.

The trigger-circuit design considerations described for RCA SCR's also apply to RCA triacs. Although both types of devices

are triggered in the same manner, the triac can be triggered by either positive or negative gate-trigger pulses independent of the polarity of the voltage between the main terminals.

SWITCHING CHARACTERISTICS

The ratings of thyristors are based primarily upon the amount of heat generated within the device pellet and the ability of the device package to transfer the internal heat to the external case. For high-frequency applications or for high-performance applications that require large peak values but narrow current pulses, the energy lost during the turn-on process may be the main cause of heat generation within the thyristor. The switching properties of the device must be known, therefore, to determine power dissipation which may limit the device performance.

Turn-on Time

When a thyristor is triggered by a gate signal, the turn-on time of the device consists of two stages, a delay time t_d and a rise time t_r , as shown in Fig. 126. The total turn-on time t_{gt} is defined as the time interval between the initiation of the gate signal and the time when the resulting current through the thyristor reaches 90 per cent of its maximum value with a resistive load. The **delay time** t_d is defined as the time interval between the 10-per-cent point of the leading edge of the gate-trigger voltage and the 10-

per-cent point of the resulting current with a resistive load. The **rise time** t_r is the time interval required for the principal current to rise from 10 to 90 per cent of its maximum value. The **total turn-on time**, therefore, is the sum of both the delay and rise times of the thyristor.

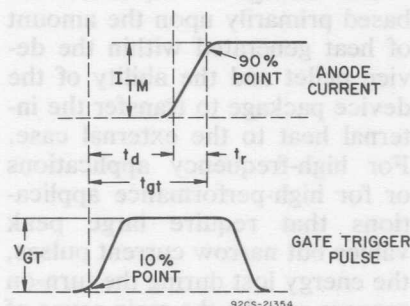


Fig. 126—Gate current and voltage turn-on waveforms for a thyristor.

Conventional SCR's and Triacs—Although the turn-on time of an SCR or a triac is affected to some extent by the peak off-state voltage and the peak on-state current level, it is influenced primarily by the magnitude of the gate-trigger current pulse. Fig. 127 shows the variation in turn-on time with gate-trigger current for the RCA-2N3873 SCR. When larger currents are available from the gate-trigger pulses, the delay time portion of the turn-on period is reduced, and the over-all turn-on time is decreased. When it is desirable to reduce the variation in turn-on time among devices of the same type, higher gate-drive signals should be used. Turn-on time is specified by the thyristor manu-

facturer at the rated blocking voltage.

When a thyristor is turned on by a gate-current pulse, current does not start to flow throughout the entire junction instantaneously; instead, the current is confined initially to a small area adjacent to the gate. The voltage drop across the thyristor at this time is large because the current density in the small area that is turned on is high. As the conduction area increases, the current density is reduced, and the voltage drop across the thyristor becomes smaller. Eventually, the boundaries of the high-current-density region propagate across the entire junction area. The time required for completion of this spreading action is considerably longer than that defined by turn-on time specifications. For resistive loads, the turn-on time can be defined as the time interval between the 10-percent point at the beginning of the gate voltage and the instant at which the applied blocking voltage decreases to 10-percent of its original value.

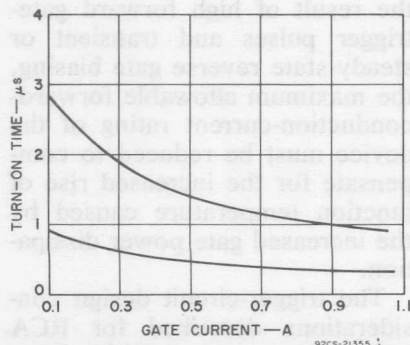


Fig. 127—Turn-on time characteristics for the RCA-2N3873 SCR.

For thyristors operated at low blocking voltages, the 10-per-cent value for the on-state voltage drop is insignificant from the standpoint of device dissipation. For thyristors operated at blocking voltages in the order of hundreds of volts, however, an on-state voltage equal to 10 per cent of the blocking voltage may result in an appreciable amount of device dissipation. Moreover, the typical turn-on time, as defined for adequate gate drives, may be in the order of 2 to 3 microseconds, while the time required for conduction to spread over the entire junction area may be in the order of 20 microseconds.

During the spreading time, the dynamic voltage drop is high, and the current density can produce localized hot spots in the pellet area in conduction. In order to guarantee reliable operation and to provide guidance for equipment designers in applications having short conduction periods, published data for RCA thyristors give the voltage drop at a given instantaneous forward current and at a specified time after turn-on from an off-state condition. The wave shapes for the initial on-state voltage for the RCA-2N3873 SCR are shown in Fig. 128. This initial voltage, together with the time required for reduction of the dynamic forward voltage drop during the spreading time, is an indication of the current-switching capability of the thyristor.

When the entire junction area of a thyristor is not in conduction, the current through that fraction

of the pellet area in conduction may result in large instantaneous power losses. These turn-on switching losses are proportional to the current and the voltage from cathode to anode of the device, together with the repetition rate of the gate-trigger pulses.

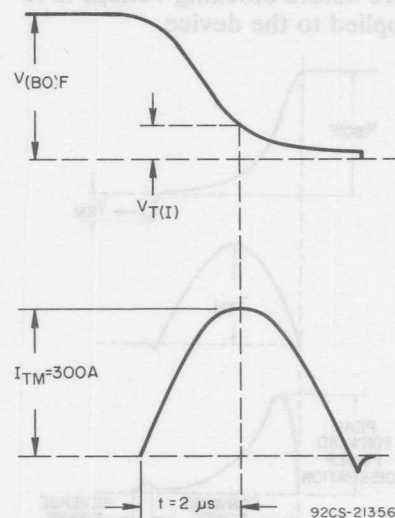


Fig. 128—Initial on-state voltage and current waveforms for the 2N3873 SCR.

The instantaneous power dissipated in a thyristor under such conditions is shown in Fig. 129. The curves shown in this figure indicate that the peak power dissipation occurs in the short interval immediately after the device starts to conduct, usually in the first microsecond. During this time interval, the peak junction temperature may exceed the maximum operating temperature given in the manufacturer's data; in this case, the thyristor should not be required to block voltages immediately after the conduction

interval. If the thyristor must block voltages immediately following the conduction interval, the junction-temperature rating must not be exceeded, and sufficient time must elapse to allow the junction temperature to decrease to the operating temperature before blocking voltage is re-applied to the device.

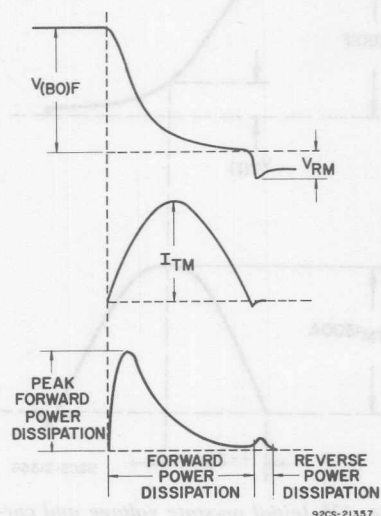


Fig. 129—Instantaneous power dissipation in a thyristor during turn-on.

The transient temperature rise may have a major effect on the turn-off time of a thyristor. As a result, when transient effects have to be considered, turn-off time measurements should be made under pulsed conditions.

GTO Devices—The GTO can be turned on, in a manner similar to that of conventional SCR's, by pulsing the gate positive with respect to its cathode. As positive current is applied to the gate, the voltage current relationship resembles that of a forward biased

p-n junction until the point is reached at which the loop gain becomes unity and regeneration takes over to switch the GTO "on". The GTO, however, behaves differently from a conventional SCR during the turn-on process. Because of design compromises to achieve fast gate-turn-off capability, the high regenerative gain inherent in conventional SCR's is reduced in the GTO design. Essentially, the GTO incorporates the regenerative properties of the two-transistor models for SCR's, but loop gain is reduced, so as to achieve turn-off control at the gate. The gate must be able to divert enough carriers away from the cathode to enable the complete GTO to revert to the "off" state upon imposition of a negative gate-to-cathode bias. As a result of this requirement, some of the normal SCR trigger or turn-on properties are modified.

In effect, turn-on in a GTO is similar to that in a desensitized SCR. If sufficient gate drive is applied during turn-on, satisfactory performance can be achieved. Fig. 130 shows the effect of increased values of gate current on anode-current rise time for two values of on-state anode current.

The on-state voltage of the GTO is a function of the regenerative properties of the device; the transient on-state voltage drop, therefore, can be reduced by use of an increased gate drive, as indicated in Fig. 131. Fig. 132 shows the typical anode voltage-current waveforms during the turn-on process.

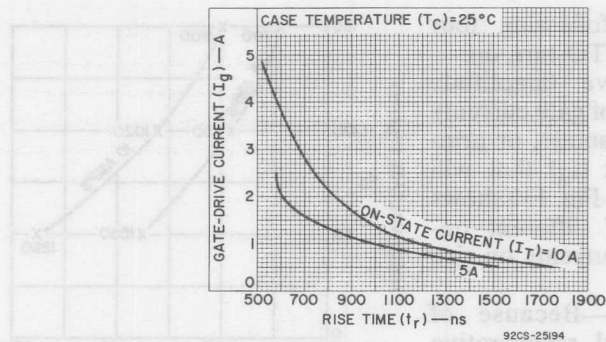


Fig. 130—Gate-drive current as a function of anode-current rise time for on-state currents of 5 and 10 amperes.

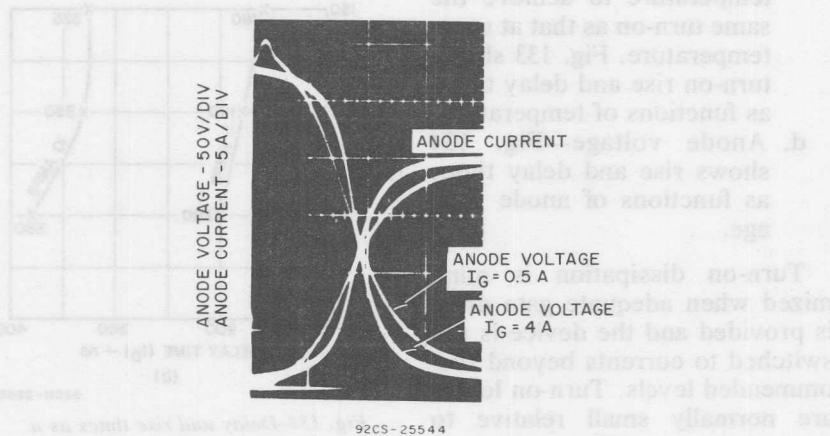


Fig. 131—Effect of forward gate drive on anode transient forward voltage drop during GTO turn-on.

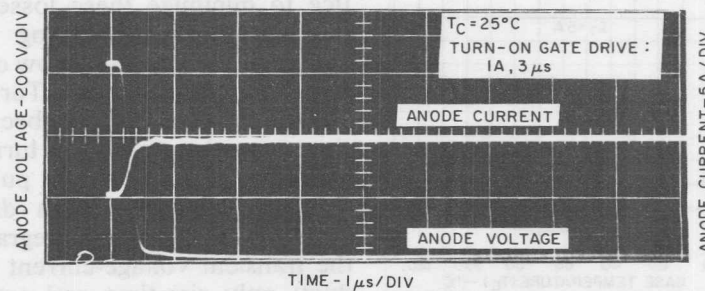
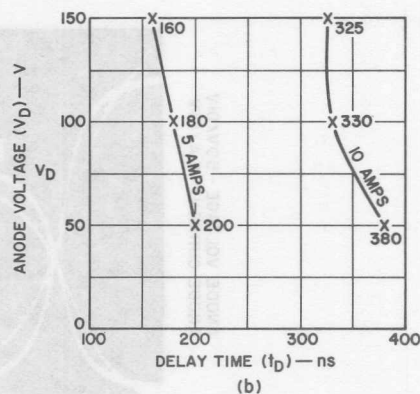
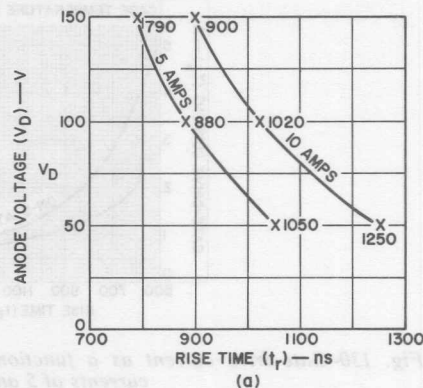


Fig. 132—Typical anode voltage and current waveforms during GTO turn-on.

Basically, the following four factors influence GTO turn-on:

- Forward drive (amplitude and rise time of gate current)
- The level of anode, or principal, current (I_A) that will be switched—Fig. 130 shows the effect of different on-state anode currents on rise time.
- Temperature—Because of the controlled regenerative properties of the GTO, more drive is needed at lower temperature to achieve the same turn-on as that at room temperature. Fig. 133 shows turn-on rise and delay times as functions of temperature.
- Anode voltage—Fig. 134 shows rise and delay times as functions of anode voltage.

Turn-on dissipation is minimized when adequate gate drive is provided and the device is not switched to currents beyond recommended levels. Turn-on losses are normally small relative to



92CM-26667

Fig. 134—Delay and rise times as a function of anode voltage.

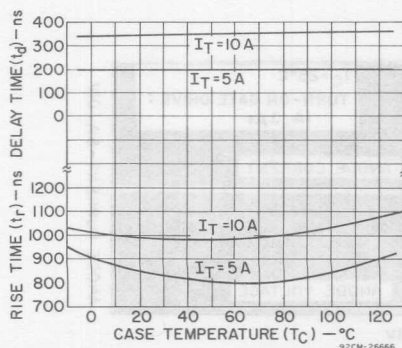


Fig. 133—Turn-on rise and delay times as a function of case temperature.

turn-off losses, but it is good practice to minimize these losses to prevent localized heating (hot spots) and to maintain a low overall junction temperature. Turn-on hot spots are significant because they may adversely affect turn-off for short-duration current pulses. Turn-on dissipation is a direct function of the time integral of the transient voltage-current product; only rise-time and saturation-time losses, therefore, contribute to this dissipation.

Turn-off Time (for SCR's)

Turn-off time of a thyristor is associated only with SCR's. In triacs, a reverse voltage cannot be used to provide circuit-commutated turn-off voltage because a reverse voltage applied to one half of the triac structure would be a forward voltage for the other half.

When the forward current of an SCR is reduced to zero at the end of the conduction period, the application of forward voltage between the anode and the cathode terminals must be delayed for a definite length of time if the device is expected to block the reapplied forward voltage. This required minimum amount of time is referred to as the **turn-off time** of the SCR. In most practical applications, the forward current is removed from the SCR by the reversal of current flow in the circuit with a gradual, controlled rate of change. The decreasing forward current passes through zero and becomes negative before the SCR ceases to conduct and blocks the reverse voltage impressed on the device by the circuit. The **turn-off time** t_q is measured from the time at which the decreasing forward current I_T passes through zero to the point at which the reverse voltage blocked by the SCR passes through zero and becomes positive, as shown in Fig. 135.

After forward conduction, the reverse current in the circuit will continue to flow through the SCR until a depletion layer has developed across the reverse-blocking junction. The reverse current

reaches a peak value (I_{RRM}) and then starts to decay to zero, as

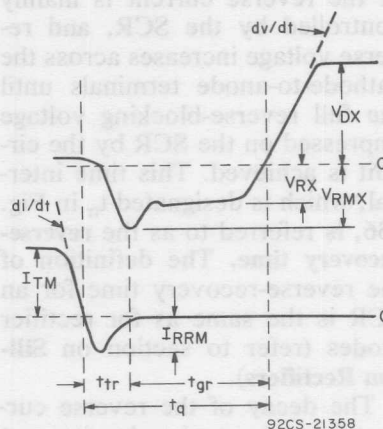


Fig. 135—Circuit-commutated turn-off voltage and current waveforms for an SCR.

shown in Fig. 136. Before the reverse current starts to decay, the rate of change of this current ($-di/dt$) is controlled by the circuit, and a positive voltage is maintained across the terminals

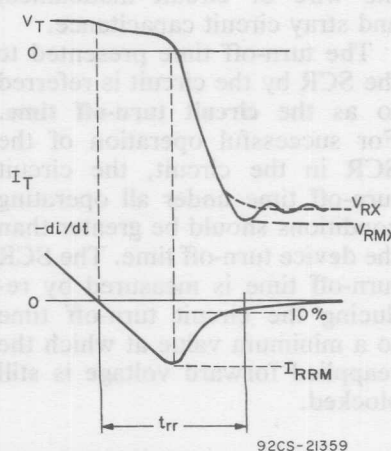


Fig. 136—SCR voltage and current waveforms during the recovery of the reverse-blocking junction.

by the stored charges in the SCR. During decay, the rate of change of the reverse current is mainly controlled by the SCR, and reverse voltage increases across the cathode-to-anode terminals until the full reverse-blocking voltage impressed on the SCR by the circuit is achieved. This time interval, which is designated t_{rr} in Fig. 136, is referred to as the **reverse-recovery time**. The definition of the reverse-recovery time for an SCR is the same as for rectifier diodes (refer to section on Silicon Rectifiers).

The decay of the reverse current from the peak value in most SCR's is fast and produces an under-damped oscillation superimposed on the reverse blocking voltage. The amplitude and frequency of this oscillation depend mainly on the "snap-off" characteristics of the reverse recovery current, the reverse-blocking junction capacitance of the SCR, the wire or circuit inductance, and stray circuit capacitance.

The turn-off time presented to the SCR by the circuit is referred to as the **circuit turn-off time**. For successful operation of the SCR in the circuit, the circuit turn-off time under all operating conditions should be greater than the device turn-off time. The SCR turn-off time is measured by reducing the circuit turn-off time to a minimum value at which the reapplied forward voltage is still blocked.

Dependence of SCR Turn-off Time on Operating Conditions—For a given SCR, the turn-off

time varies significantly with different waveforms and temperatures presented to the device. For reliable operation, it is essential during circuit design that the variations in turn-off time as a function of operating conditions be taken into account. With the proper anticipation of the operating conditions and SCR turn-off time, the circuit turn-off time may be selected without excessive margin that would result in poor utilization efficiency of the SCR.

Temperature: Among all the parameters, temperature has the greatest effect on the turn-off time. The turn-off time of the SCR increases with increasing junction temperature. Fig. 137 shows turn-off time as a function

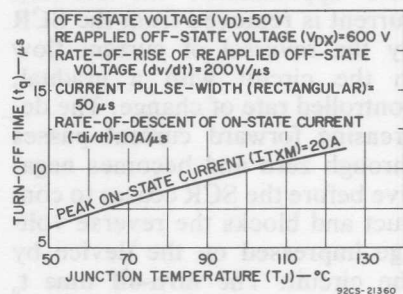


Fig. 137—Typical variation of turn-off time with junction temperature (rectangular pulse).

of junction temperature for a typical RCA SCR. Turn-off time is normally measured at elevated temperatures.

On-state current: An increase in on-state current causes a corresponding increase in the turn-off time. The effect of the on-state

current on turn-off time is somewhat greater at higher temperatures, as shown in Fig. 138. Turn-off time is also affected by the

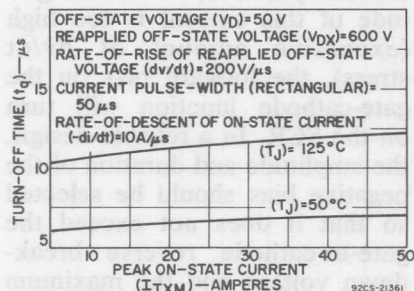


Fig. 138—Typical variation of turn-off time with on-state current.

rate of change of on-state current prior to turn-off. In other words, the SCR "remembers" the on-state current history for several microseconds prior to turn-off. For example, the turn-off time measured for on-state current waveforms such as (a) and (b) in Fig. 139 may be shorter than that measured for the waveform (c). The prior-to-turn-off history of the on-state current (c) in Fig. 139 is more severe than that of the currents (a) and (b). The sensi-

tivity of the SCR's to on-state current history varies from device to device.

Magnitude and rate of rise of reapplied forward voltage: If the rate of rise (dv/dt) of the reapplied forward blocking voltage is held constant, the turn-off time increases with increasing forward blocking voltage. The rate of increase of turn-off time as a function of reapplied forward-blocking voltage becomes greater at higher dv/dt values, as shown in Fig. 140. The SCR turn-off time is affected to a greater degree by variation in the dv/dt of the reapplied forward blocking voltage. The effect of increased dv/dt on the device turn-off time may be off-set by the application of negative bias to the gate of the SCR.

Negative gate bias: Normally during the turn-off time measurement, the gate of the SCR is connected to zero voltage which is applied through a specified gate resistor. If a negative bias is applied to the gate, the turn-off time of the SCR may be reduced (as shown in Fig. 141), and the dv/dt capability improved. The effect of

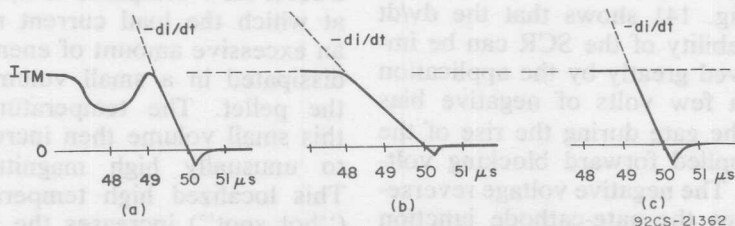


Fig. 139—Waveforms showing effect of the rate of change of on-state current prior to turnoff on turnoff time.

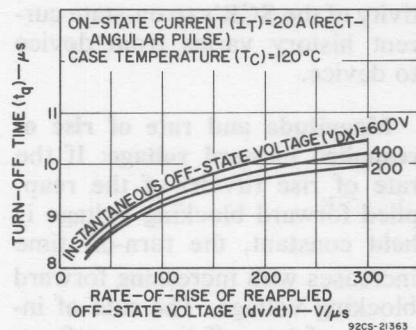


Fig. 140—Typical variation of turn-off time with rate of rise of reapplied off-state voltage (rectangular pulse).

negative bias on turn-off time is more pronounced at higher junction temperatures. At higher bias voltages, the effectiveness of the negative bias slowly diminishes.

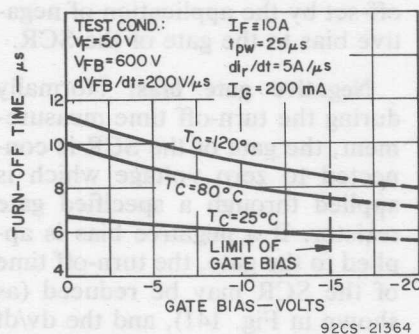


Fig. 141—Typical variation of turn-off time as a function of negative gate bias.

Fig. 141 shows that the dv/dt capability of the SCR can be improved greatly by the application of a few volts of negative bias to the gate during the rise of the reapplied forward blocking voltage. The negative voltage reverse-biases the gate-cathode junction and provides a path for the displacement current that charges

the forward-blocking junction capacitance. Without the negative bias, the displacement current flows through the shorted-emitter resistor (and through the gate-cathode junction). If the magnitude of this current is too high (excessive amount of dv/dt stress), the forward bias on the gate-cathode junction will turn on the SCR. In a reliable design, the amplitude and duration of the negative bias should be selected so that it does not exceed the gate-to-cathode reverse breakdown voltage and the maximum allowable gate power dissipation.

Reverse blocking voltage: The effect of the reverse voltage impressed on the anode-to-cathode terminals on the turn-off time becomes minor above a certain voltage level. Normally, the turn-off time decreases with increasing reverse voltage.

Concentrated turn-on losses: If the SCR is stressed beyond its capability during turn on, some hot spots may be generated in the device, as explained in the section on **Critical Rate of Rise of On-State Current**. If the rate at which conduction spreads in the SCR is slow compared to the rate at which the load current rises, an excessive amount of energy is dissipated in a small volume of the pellet. The temperature in this small volume then increases to unusually high magnitudes. This localized high temperature ("hot spot") increases the turn-off time of the device. The interaction of the turn-on capability

of the device with the turn-off capability may be indicated by the appropriate selection of test conditions. A narrow pulse width with high peak current at rated voltage maximizes the turn-on stresses on the device. The narrow pulse width also prevents the hot spots from cooling down before the blocking voltage is re-applied, as shown in Fig. 142. For applications in which turn-on stresses are not encountered, the turn-off time of the device may be measured with a wide square wave current pulse that turns on the SCR from a low supply voltage. The low voltage will minimize the turn-on dissipation, and

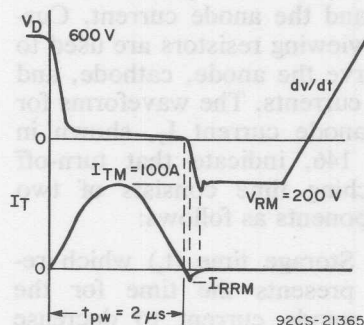


Fig. 142—Waveforms used to test the turn-off time of an SCR with severe turn-off stresses.

the wide current pulse allows time for any "hot spots" to cool. The waveforms shown in Fig. 143 illustrate this condition.

Turn-off Time Test Circuit—Because the turn-off time of an SCR depends upon a number of circuit parameters, the manufacturer's turn-off time specification

is meaningful only if these critical parameters are listed and the test circuit used for the measurement is indicated.

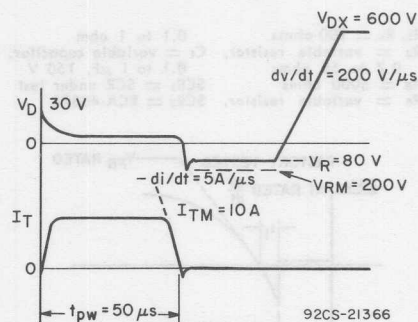
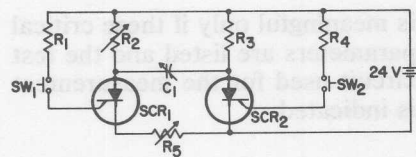


Fig. 143—Waveforms used to test the turn-off time for an SCR for wide square-wave applications and applications in which turn-on stresses are negligible.

Fig. 144 shows a simple test circuit used to measure turn-off time. The circuit subjects the SCR to current and voltage waveforms similar to those encountered in most typical applications. In the circuit diagram, SCR₁ is the device under test. Initially, both SCR's are in the off-state; push-button switch SW₁ is momentarily closed to start the test. This action turns on SCR₁ and load current flows through this SCR and resistor R₂. Capacitor C₁ charges through resistor R₃ to the voltage developed across R₂. If the second push-button switch SW₂ is then closed, SCR₂ is turned on. SCR₁ is then reverse-biased by the voltage across capacitor C₁. The discharge of this capacitor causes a short pulse of reverse current to flow through SCR₁ until this device recovers its reverse-blocking capability. At some time



$R_1, R_4 = 100$ ohms
 $R_2 =$ variable resistor, 0.1 to 1 ohm
 0.7 to 50 ohms
 $R_3 = 5000$ ohms
 $R_5 =$ variable resistor,
 $C_1 =$ variable capacitor,
 0.1 to 1 μ F, 150 V
 $SCR_1 =$ SCR under test
 $SCR_2 =$ RCA-40378

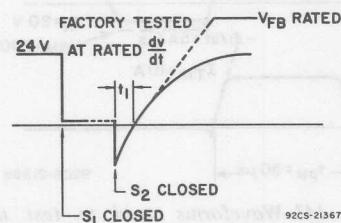


Fig. 144—Test circuit and voltage waveforms used to determine turn-off times of thyristors.

t_1 , the anode-to-cathode voltage of SCR_1 passes through zero and starts to build up in a forward direction at a rate dependent upon the time constant of C_1 and R_2 . The peak value of the reverse current during the recovery period can be controlled by adjustment of potentiometer R_5 . If the turn-off time of SCR_1 is less than the time t_1 , the device will turn off. The turn-off interval t_1 can be measured by observation of the anode-to-cathode voltage of SCR_1 with a high-speed oscilloscope. A typical waveform is shown in Fig. 144.

Turn-off Switching (for GTO's)

An important consideration in the application of gate-turn-off SCR's is the switching dissipation that occurs during the turn-off

period. During this switching interval, the device is in the active mode of operation during which it switches from a low-voltage, high-current state to a high-voltage, low-current state. The switching performance of the GTO is a direct function of the ability of the device to get rid of the heat generated during this switching interval. The switching dissipation is a direct result of the speed at which the device can turn off and the effect that this speed has on inductive elements in the rest of the circuit.

Fig. 145 shows a typical test circuit used to measure the switching times of a gate-turn-off SCR, and Fig. 146 shows the waveforms for the gate-drive voltage and the anode current. Current-viewing resistors are used to observe the anode, cathode, and gate currents. The waveforms for the anode current I_T , shown in Fig. 146, indicate that turn-off switching time consists of two components as follows:

1. Storage time (t_s) which represents the time for the anode current to decrease from its on value to 90 percent of its on value after the turn-off gate pulse is applied.
2. Fall time (t_f) which represents the time for the anode current to decrease from 90 percent of its on value to 10 percent of its on value.

Turn-off time, therefore, is defined by the following equation:

$$T_{gq} = t_s + t_f \quad (32)$$

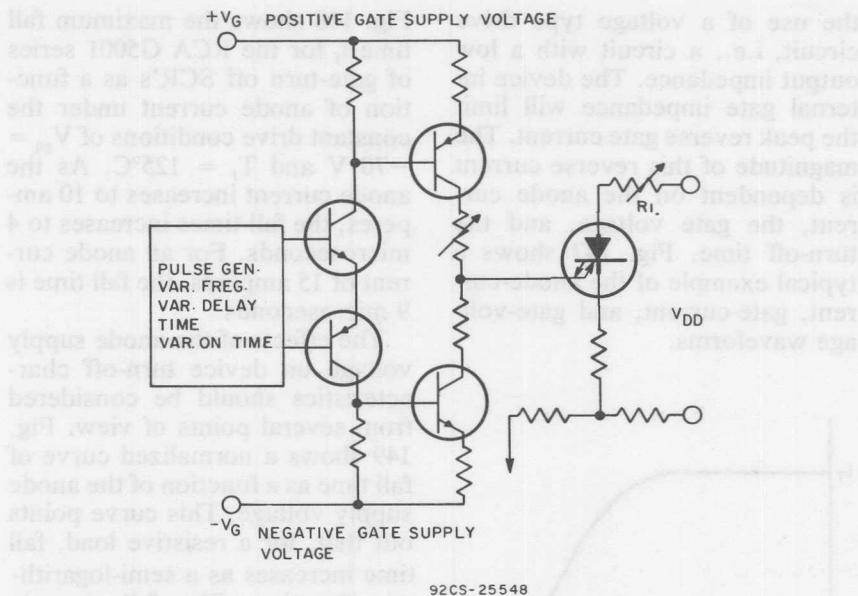


Fig. 145—Test circuit used to measure switching times in gate-turn-off SCR's.

Switching times are dependent on circuit drive and anode conditions. The turn-off times, which are the most critical, are very temperature dependent. Because worst-case turn-off times occur

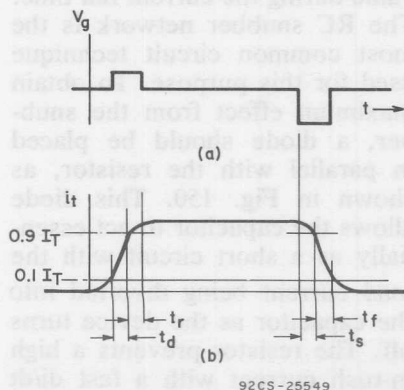


Fig. 146—Gate-drive voltage (a) and anode-current (b) waveforms.

at the maximum junction temperature, characterization at this temperature provides the most useful information about device switching performance. One way, and perhaps the most convenient way, to determine turn-off dissipation is to heat the case of the device to a value equal to the maximum rated junction temperature. The device is then turned on to the current level at which the turn-off time is to be investigated, and the device is turned off. For this test, the device must be operated under low-duty-cycle conditions to prevent further substantial heating of the junction. The gate drive is also an important circuit condition with respect to turn-off dissipation. Optimum operation of the device requires

the use of a voltage type drive circuit, i.e., a circuit with a low output impedance. The device internal gate impedance will limit the peak reverse gate current. The magnitude of this reverse current is dependent on the anode current, the gate voltage, and the turn-off time. Fig. 147 shows a typical example of the anode-current, gate-current, and gate-voltage waveforms.

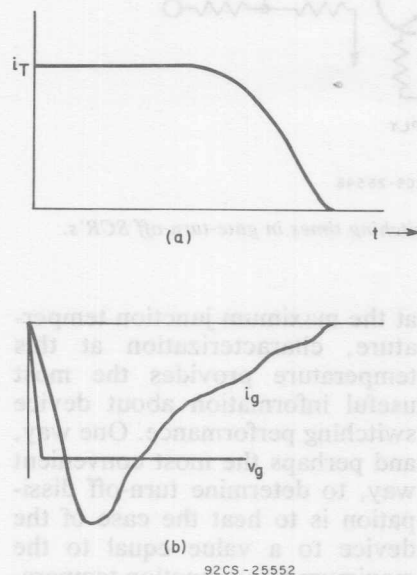


Fig. 147—Anode-current (a), gate-voltage, and gate-current (b) waveforms.

As previously mentioned, the turn-off characteristics are dependent not only on drive conditions, but also on anode circuit conditions. Because fall time represents the interval during which most of the dissipation occurs, the first consideration is how the fall time changes with anode current.

Fig. 148 shows the maximum fall time t_f for the RCA G5001 series of gate-turn off SCR's as a function of anode current under the constant drive conditions of $V_{gq} = -70$ V and $T_J = 125^\circ\text{C}$. As the anode current increases to 10 amperes, the fall times increases to 4 microseconds. For an anode current of 15 amperes, the fall time is 9 microseconds.

The effects of the anode supply voltage on device turn-off characteristics should be considered from several points of view. Fig. 149 shows a normalized curve of fall time as a function of the anode supply voltage. This curve points out that, for a resistive load, fall time increases as a semi-logarithmic function. The fall time is normalized to 1 for a supply voltage V_{DD} of 100 volts. The normalized value increases 2.65 times for a device that turns off into a 1000-volt anode source. The normalized curve also indicates that the device can be turned off faster if the anode voltage across the device is maintained at a low value during the current fall time. The RC snubber network is the most common circuit technique used for this purpose. To obtain maximum effect from the snubber, a diode should be placed in parallel with the resistor, as shown in Fig. 150. This diode allows the capacitor to act essentially as a short circuit with the load current being diverted into the capacitor as the device turns off. The resistor prevents a high in-rush current with a fast di/dt from damaging the device when it is turned back on.

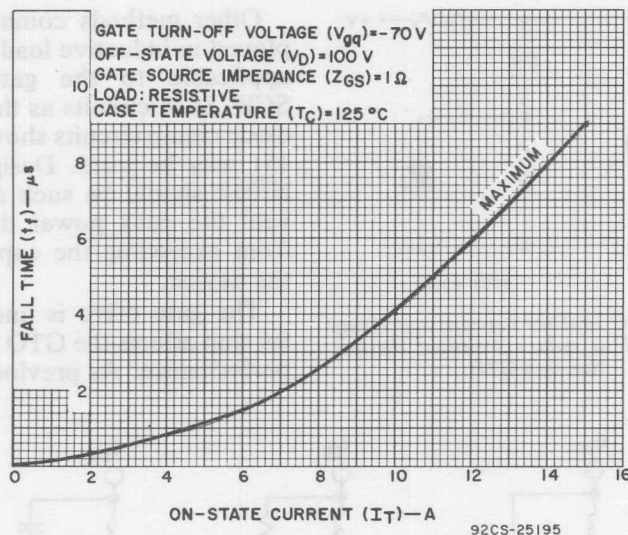


Fig. 148—Maximum fall time as a function of on-state current.

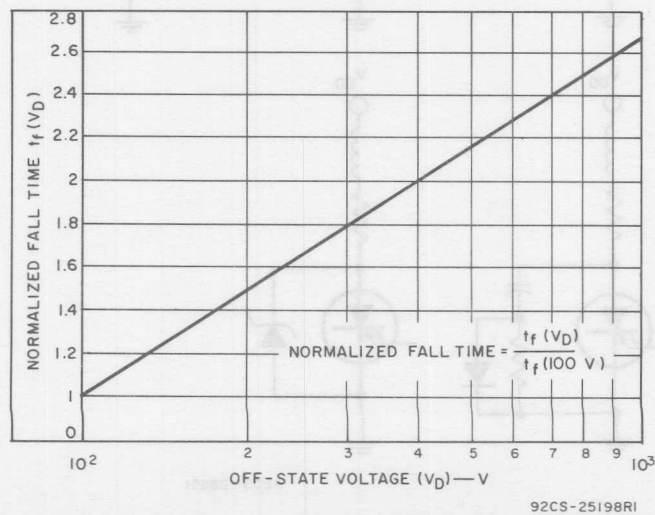


Fig. 149—Normalized fall time as a function of off-state anode voltage.

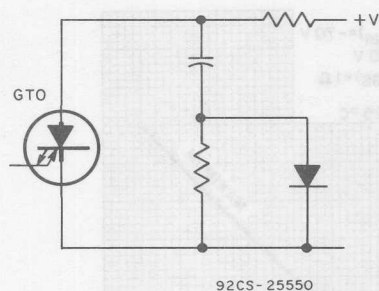


Fig. 150—RC snubber network and clamp diode used to reduce transient dissipation in a GTO.

Other methods commonly employed in inductive loads are also applicable to the gate-turn-off SCR. Such circuits as the various diode clamp circuits shown in Fig. 151 may be used. Design of the circuit should be such as to prevent the peak power dissipation from exceeding the capability of the device.

The gate drive is another factor that affects the GTO switching performance. As previously men-

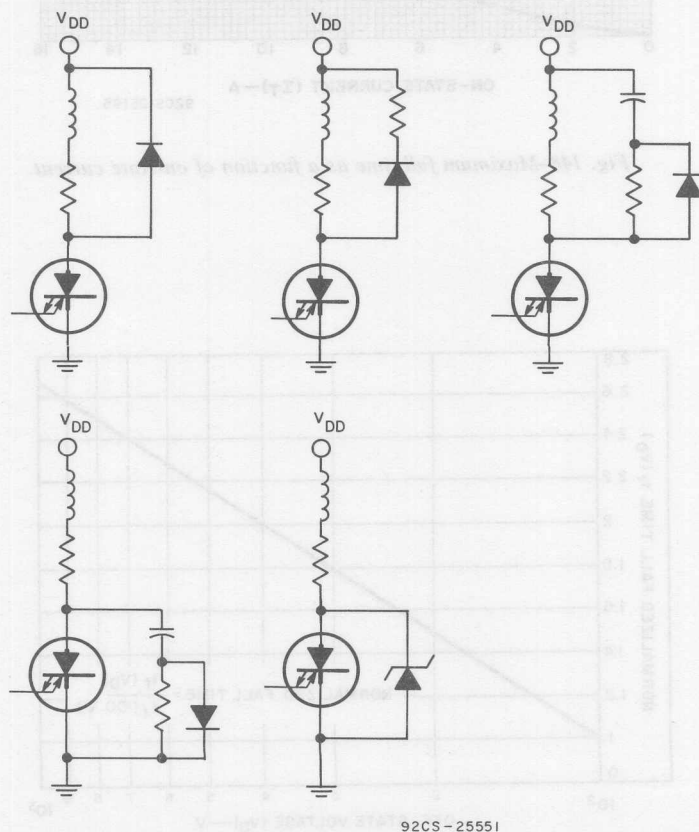


Fig. 151—Circuit diagrams that illustrate different ways of limiting the peak voltage during turn-off.

tioned, best turn-off is obtained when the GTO is driven from a constant voltage source. Fig. 152 shows a normalized curve of fall time as a function of gate-turn-off

tor cannot be great enough to cause the voltage on the gate to drop below the recommended minimum value for the time required. Constant-current drives,

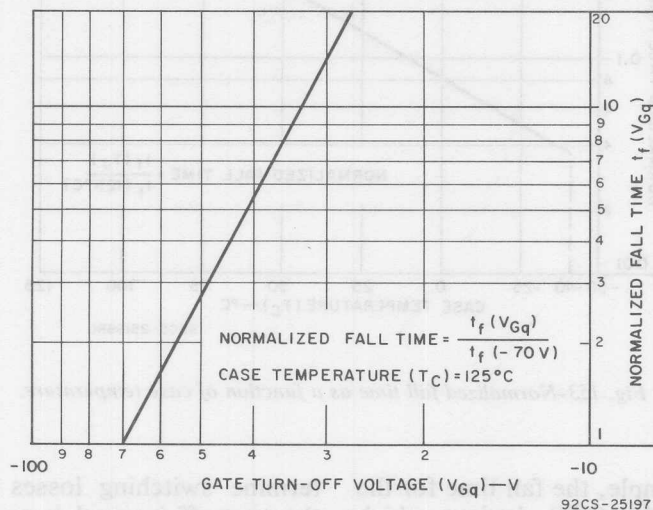


Fig. 152—Normalized fall time as a function of gate-turn-off voltage.

voltage. This curve points out that the fall time of the device increases to about 2.6 times its 70-volt value when the device is driven off with a drive of only 50 volts and 12.5 times for a drive of 30 volts.

When other types of drive circuits are used, several restrictions are imposed by the GTO. First, the reverse gate-breakdown voltage must never be exceeded. If this breakdown voltage is exceeded, loss of gate-control capability can result. Second, the drive circuit must be able to supply sufficient voltage at the end of the turn-off period. For example, under capacitive types of drive, the discharge of the capaci-

tor cannot be great enough to cause the voltage on the gate to drop below the recommended minimum value for the time required. Constant-current drives, if used, must be voltage-clamped below the gate-breakdown voltage under all gate-impedance conditions. As previously mentioned, the gate impedance limits the peak current that can be extracted for a given set of drive conditions.

One of the most important parameters which determine the turn-off speed of the GTO is junction temperature. As the GTO heats up, internal mechanisms tend to cause the device to turn off more slowly. Fig. 153 shows this effect in a curve that is normalized to 125°C . This curve shows that the fall time is shortened as the junction temperature is decreased from the maximum rated value.

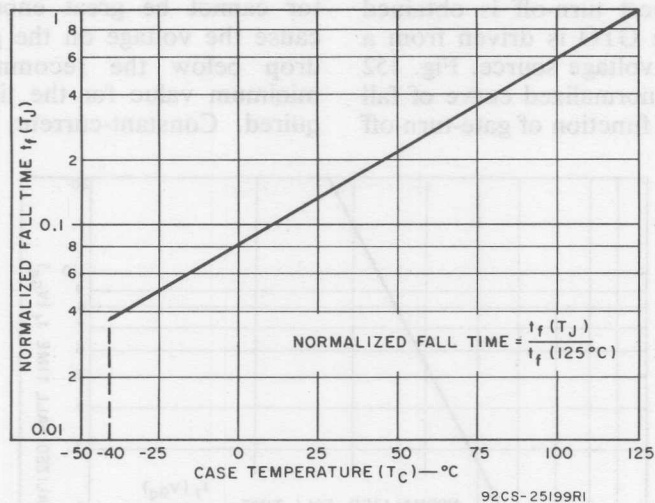


Fig. 153—Normalized fall time as a function of case temperature.

For example, the fall time for the RCA-G5001 GTO devices, which is specified as 1 microsecond maximum for a junction temperature of 125°C, is reduced to 0.6 microsecond for a junction temperature of 100°C.

Turn-off switching performance as outlined above is the result of many factors; all these factors must be taken into consideration to determine the effect that the power dissipation during turn-off has on the operation of the device. It is this dissipation that determines the true switching performance of the GTO. Switching through a high-dissipation load line results in losses that restrict the device with respect to both the average-power limit and the peak-power limit imposed by the localized heating during turn-off.

The most accurate way to de-

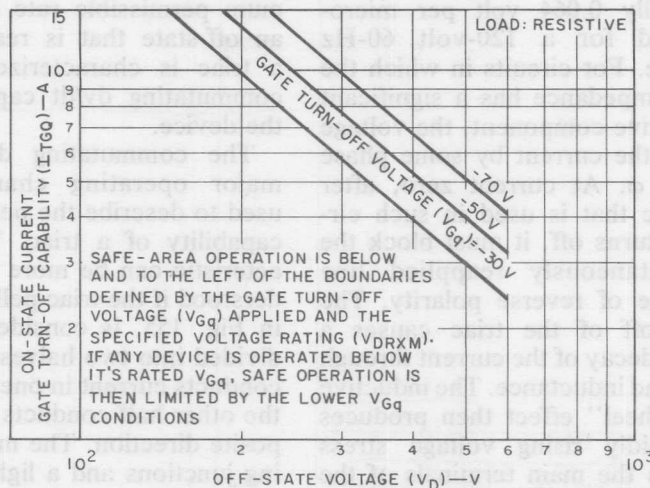
termine switching losses during the turn-off interval is to obtain the actual voltage and current waveforms and perform an integration of their product. This integration would yield the switching losses for that cycle and, when multiplied by the frequency, would give the average turn-off power dissipation. This value then could be used in conjunction with the losses that result from the steady-state conduction to determine the maximum case temperature allowable for the device operating conditions.

To assure that the GTO will switch reliably, care must be taken to prevent the device from becoming damaged during the turn-off interval; that is, the device must not be stressed in excess of its capabilities during turn-off. Fig. 154 shows safe-operating-

area curves that will help the circuit designer assure that the dissipation capabilities of the GTO are not exceeded during turn-off.

Commutating dv/dt Capability (of Triacs)

Turn-off time as associated with SCR's and GTO's is not an important characterization for triacs.



92CS-25196

Fig. 154—Safe-operating-area curves.

These curves indicate the maximum current that can be switched when the GTO is turning off into a given anode voltage supply under the give gate-drive conditions. For example, a GTO that operates from a 400-volt supply and that is driven with a 70-volt gate signal can turn off 6.8 amperes. If the gate is driven by 50 volts, however, only 5.4 amperes can be switched. Points below and to the left of the gate-voltage line can be switched safely. The safe-operating-area curves shown in Fig. 154, however, do not take into account the effects that the turn-off dissipation has on the average power dissipation in the device.

The need to support (block) a reapplied voltage in the opposite quadrant becomes the important consideration in triac applications. The ability of a triac to support this voltage after conduction is characterized as the **critical rate of rise of commutation voltage**, or more simply as the commutating dv/dt .

In triac ac power-control applications, if the gate drive is removed, the triac turns off, or commutates, at the next zero current crossing. At that time, the voltage impressed across the main terminals of the triac is dependent, to a large extent, upon the type of load impedance. For resistive loads, the voltage is in phase with

the current, and the voltage that is reappplied at the zero current crossing is the source voltage. If the stray inductance of the circuit wiring is minimal, the rate of reapplication of voltage is low, typically 0.064 volt per micro-second for a 120-volt 60-Hz source. For circuits in which the load impedance has a significant inductive component, the voltage leads the current by some phase angle ϕ . At current zero, after a triac that is used in such circuits turns off, it must block the instantaneously reappplied line voltage of reverse polarity. The turn off of the triac causes a rapid decay of the current through the load inductance. The inductive "flywheel" effect then produces a rapidly rising voltage stress across the main terminals of the triac. If the rate of rise of this voltage exceeds some critical value, the triac can be turned

back on. In general, this method of turn on does not cause any damage to the triac, but it does result in the loss of control over the power delivered to the load. As stated previously, the maximum permissible rate of rise of an off-state that is reappplied to a triac is characterized as the commutating dv/dt capability of the device.

The commutating dv/dt is a major operating characteristic used to describe the performance capability of a triac. The characteristic can be more easily understood if the triac pellet, shown in Fig. 155, is considered to be divided into two halves. One half conducts current in one direction, the other half conducts in the opposite direction. The main blocking junctions and a lightly doped n-type base region in which charge can be stored are common to both halves of the triac pellet.

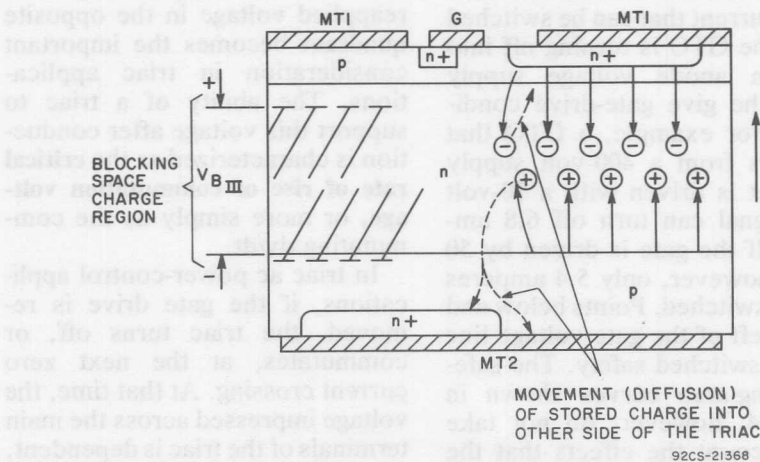


Fig. 155—Junction diagram of a typical triac pellet showing current flow in the first-quadrant (I) side and creation of the blocking space-charge region on the third-quadrant (III) side.

Charge is stored in the n-type base when current is conducted in either direction. The amount of charge stored at the end of conduction depends on the **commutating di/dt** , i.e., the rate of decrease of load current as commutation is approached. The junction capacitance of the triac at commutation is a function of the remaining charge at that time. The greater the di/dt , the more remaining charge, and the greater the junction capacitance. When the circuit voltage changes direction, the current in the conducting half of the triac reduces to zero, and reverse recovery current flows until a depletion layer is established. The device voltage then reverses direction, and the remaining charge may diffuse into the opposite half of the triac structure, as indicated by the dashed line in Fig. 155. The rate of rise of this voltage (commutating dv/dt) in conjunction with the junction capacitance results in a current flow that is similar in its effect to the gate current. This current flow, if large enough, can cause the triac to revert to the conducting state in the absence of a gate signal.

The commutating dv/dt capability is specified in volts per microsecond for the following conditions:

1. the maximum rated on-state current [$I_{T(RMS)}$];
2. the maximum case temperature for the rated value of on-state current;
3. the maximum rated off-state voltage (V_{DROM});
4. the maximum commutating

di/dt (where $di/dt = I_{pk} \sin \omega t$ and $\omega = 2\pi f$);

5. zero gate bias (worst-case, zero-power-factor load).

Commutating dv/dt can be understood as a function of a practical circuit and related to the above conditions by consideration of a simple triac circuit that consists of an inductive load such as a motor. This circuit is shown in Fig. 156, together with waveforms for the circuit. If a gate signal that allows continuous conduction is applied to the triac, the load current (I_L) lags the line voltage (V_{LINE}) by approximately 90 degrees for the inductive load. During the triac on-state conduction, the voltage across the triac (V_T) is in phase with the line current I_L and typically will have an amplitude of ± 1.5 volts.

When the gate signal is removed, the triac begins to commute off near the end of the half-cycle, when the load current drops to a value below the holding current (I_H) of the triac. At the instant the triac commutates off, the voltage (V_T) reverses direction and climbs toward the peak of the line voltage (V_{LINE}), its rate of rise (commutating dv/dt) and overshoot being a characteristic of the circuit components. After the triac successfully commutates off, the voltage (V_T) is in phase with the line voltage. If the commutating dv/dt of the circuit is greater than the commutating dv/dt capability of the triac, the triac does not turn off, but reverts to the on-state. With no gate signal applied, the triac again attempts to turn off in the next

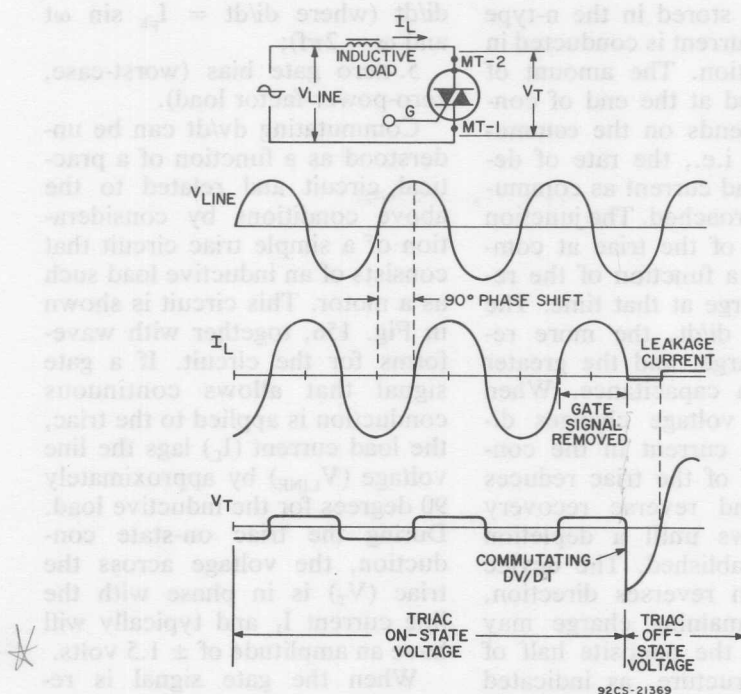


Fig. 156—Waveforms for simple triac circuit with inductive load.

half-cycle (opposite polarity). If it succeeds, it remains off; if its capability is again exceeded, it remains on until the circuit power is interrupted.

In Fig. 157, the last half-cycle of triac conduction current (I_L) has been superimposed on the commutating dv/dt capability. This diagram indicates that the circuit capability exceeds the device capability; therefore, the triac will not commute off. An additional "snubber network", consisting of a resistor and a capacitor, placed across the main terminals of the triac will reduce the commutating dv/dt of the circuit

to within the capability of the device, and thus allow the triac to commute off. A detailed analysis of and design procedures for snubber networks are given later in this section.

As pointed out earlier, the rate of change of main-terminal current immediately before a triac is required to support a reverse voltage has an important bearing on the commutating dv/dt capability of the device. Consequently, as indicated in Fig. 158, the commutating dv/dt capability is affected by both the magnitude and frequency of the pre-blocking-condition current, because the

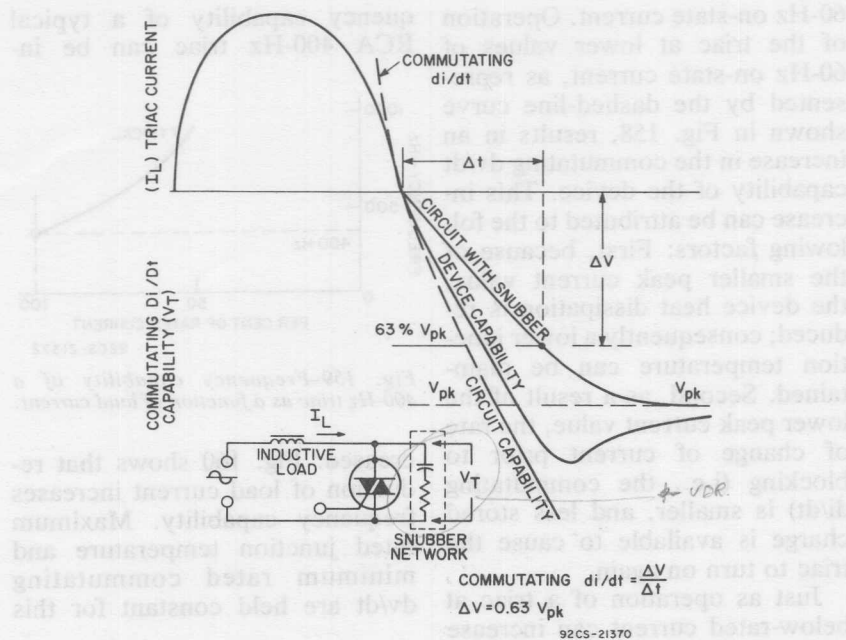


Fig. 157—Use of snubber network to reduce commutating dv/dt of circuit.

rate of change of current varies proportional with each of these factors.

Any triac has a specific commutating dv/dt capability which is specified for a particular value of

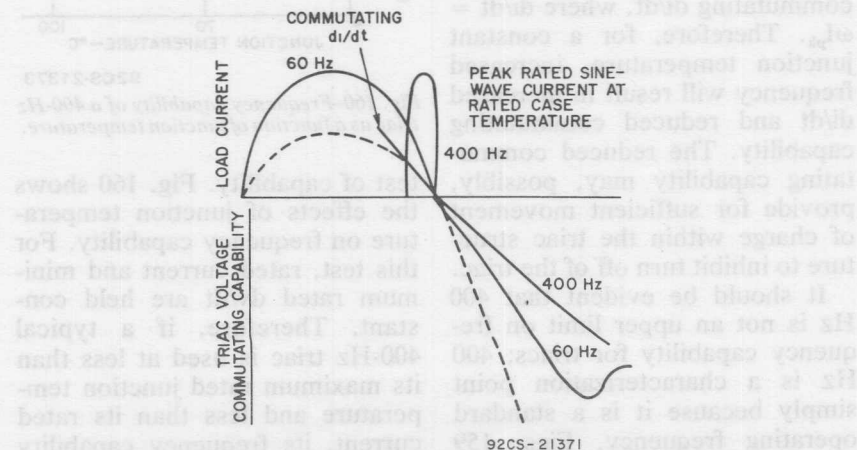


Fig. 158—Dependence of triac commutating capability on current and frequency.

60-Hz on-state current. Operation of the triac at lower values of 60-Hz on-state current, as represented by the dashed-line curve shown in Fig. 158, results in an increase in the commutating dv/dt capability of the device. This increase can be attributed to the following factors: First, because of the smaller peak current value, the device heat dissipation is reduced; consequently a lower junction temperature can be maintained. Second, as a result of the lower peak current value, the rate of change of current prior to blocking (i.e., the commutating di/dt) is smaller, and less stored charge is available to cause the triac to turn on again.

Just as operation of a triac at below-rated current can increase the commutating capability, operation at a frequency greater than rated frequency (60-Hz for most triacs) can reduce the commutating capability. Commutating dv/dt is a function of two basic parameters, junction temperature and commutating di/dt , where $di/dt = \omega I_{pk}$. Therefore, for a constant junction temperature, increased frequency will result in increased di/dt and reduced commutating capability. The reduced commutating capability may, possibly, provide for sufficient movement of charge within the triac structure to inhibit turn off of the triac.

It should be evident that 400 Hz is not an upper limit on frequency capability for triacs; 400 Hz is a characterization point simply because it is a standard operating frequency. Figs. 159 and 160 indicate how the fre-

quency capability of a typical RCA 400-Hz triac can be in-

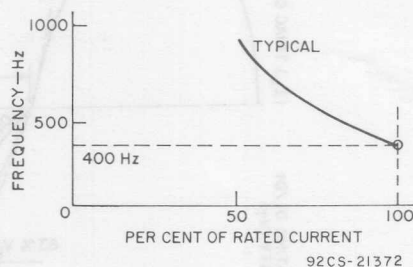


Fig. 159—Frequency capability of a 400-Hz triac as a function of load current.

quency capability of a typical RCA 400-Hz triac can be increased. Fig. 160 shows that reduction of load current increases frequency capability. Maximum rated junction temperature and minimum rated commutating dv/dt are held constant for this

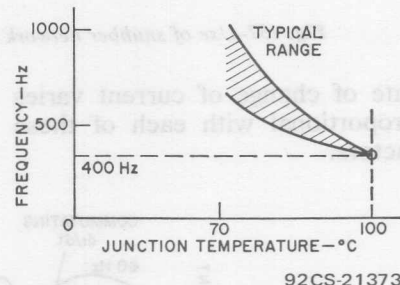


Fig. 160—Frequency capability of a 400-Hz triac as a function of junction temperature.

test of capability. Fig. 160 shows the effects of junction temperature on frequency capability. For this test, rated current and minimum rated dv/dt are held constant. Therefore, if a typical 400-Hz triac is used at less than its maximum rated junction temperature and less than its rated current, its frequency capability is greatly enhanced. Table XIV

Table XIV — RCA Triacs Characterized For Operation at 400-Hz

RCA TYPE	Current			Voltage V _{DRM} V	Temp. Range Operating— °C	Max. Gate Trigger Current I _{GT} -mA Modes				Critical Rate of Rise of:			Thermal Resistance R _{θJC} °C/W			
	I _T (RMS) A	I _{TSM} A	Temp. T _C °C			I+	III—	I—	III+	Commutation Voltage dv/dt - V/μs		Off-State Voltage dv/dt - V/μs				
										Min.	Typ.	T _C -°C		Min.	Typ.	T _C -°C
T23 types																
T2304B	0.5	25	90	200	-50 to 100	10	10	10	10	1	4	90	10	100	100	8.5
T2304D	0.5	25	90	400	-50 to 100	10	10	10	10	1	4	90	10	100	100	8.5
T2305B	0.5	25	90	200	-50 to 100	25	25	40	40	1	4	90	10	100	100	8.5
T2305D	0.5	25	90	400	-50 to 100	25	25	40	40	1	4	90	10	100	100	8.5
T41 types																
T4105B	6	100	90	200	-50 to 100	50	50	80	80	5	10	90	30	150	100	1
T4105D	6	100	90	400	-50 to 100	50	50	80	80	5	10	90	30	150	100	1
T4115B	6	100	90	200	-50 to 100	50	50	80	80	5	10	90	30	150	100	1
T4115D	6	100	90	400	-50 to 100	50	50	80	80	5	10	90	30	150	100	1
T4104B	10	100	85	200	-50 to 100	50	50	80	80	5	10	85	30	150	100	1
T4104D	10	100	85	400	-50 to 100	50	50	80	80	5	10	85	30	150	100	1
T4114B	10	100	85	200	-50 to 100	50	50	80	80	5	10	85	30	150	100	1
T4114D	10	100	85	400	-50 to 100	50	50	80	80	5	10	85	30	150	100	1
T4103B	15	100	80	200	-50 to 100	50	50	80	80	5	10	80	30	150	100	1
T4103D	15	100	80	400	-50 to 100	50	50	80	80	5	10	80	20	100	100	1
T4113B	15	100	80	200	-50 to 100	50	50	80	80	5	10	80	30	150	100	1
T4113D	15	100	80	400	-50 to 100	50	50	80	80	5	10	80	20	100	100	1
T64 types																
T6405B	25	300	85	200	-50 to 100	80	80	120	120	2	—	85	30	150	100	0.8
T6405D	25	300	85	400	-50 to 100	80	80	120	120	2	—	85	30	150	100	0.8
T6415B	25	300	80	200	-50 to 100	80	80	120	120	2	—	85	30	150	100	0.9
T6415D	25	300	80	400	-50 to 100	80	80	120	120	2	—	85	30	150	100	0.9
T6404B	40	300	70	200	-50 to 100	80	80	120	120	2	—	70	50	200	110	0.8
T6404D	40	300	70	400	-50 to 100	80	80	120	120	2	—	70	50	200	110	0.8
T6414B	40	300	65	200	-50 to 100	80	80	120	120	2	—	65	50	200	110	0.9
T6414D	40	300	65	400	-50 to 100	80	80	120	120	2	—	65	50	200	110	0.9

lists RCA triacs characterized for operation at 400-Hz.

Of practical interest is the variation of permissible dv/dt at various current levels at one frequency. This variation is illustrated in Fig. 161 for the 2N5442 40-ampere triac. The commutating dv/dt at low currents approaches the static dv/dt capability of the device. It is also apparent that operation under overload conditions is possible, although reduced dv/dt capability must be taken into account.

SNUBBER NETWORKS

As pointed out previously, a snubber network can be placed across a triac to reduce the rate of rise of the voltage across the device. The snubber network, as shown in Fig. 162, consists of a resistance R_s and a capacitance C_s placed in series across the main terminals of the device. For some snubber component values and some types of load, excessive ringing can occur in the circuit. This voltage ringing may exceed

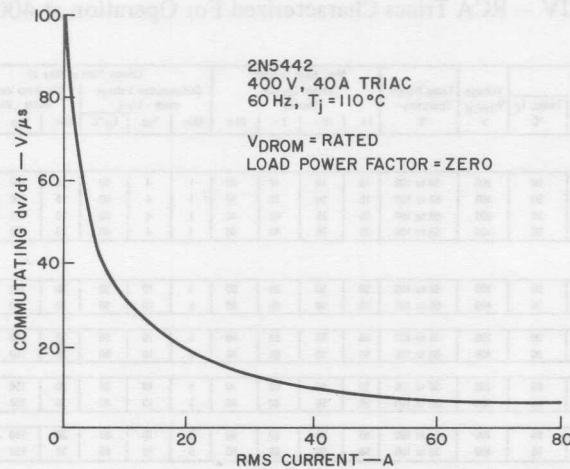


Fig. 161—Maximum commutating dv/dt (Pg. 170) as a function of current.

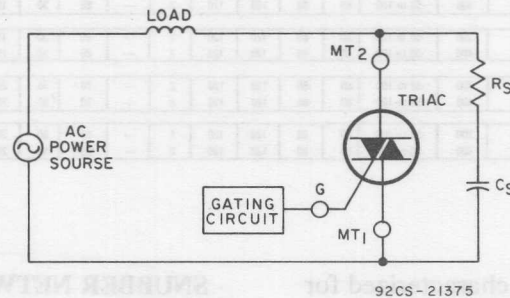
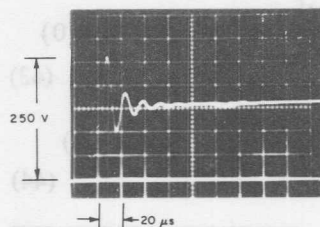


Fig. 162—Triac circuit using a snubber network (R_S and C_S) connected across the triac.

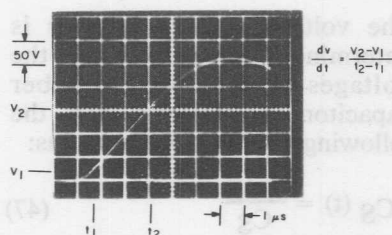
the blocking capability (V_{DROM}) of the triac. Malfunction of the triac then results because of the inability of the device to block the voltage even though it can withstand the dv/dt stress. An example of voltage ringing is shown in Fig. 163(a). Fig. 163(b) shows the same voltage on an expanded time scale.

Basic Circuit Analysis

The suppression network must be designed to limit the dv/dt stress and to have an acceptable voltage overshoot. Fig. 164 shows an equivalent circuit used for analysis, in which the triac has been replaced by an ideal switch.



(a)



(b) 92CS-21376

Fig. 163—(a) Ringing, caused by inductive load, in the principal voltage of triac; (b) principal voltage shown on an expanded scale.

When the triac is in the blocking or nonconducting state, represented by the open switch, the circuit is a standard RLC series network driven by an ac voltage source. The following differential

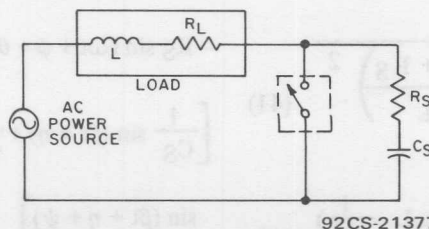
equation can be obtained by summing the voltage drops around the circuit:

$$(R_L + R_S)i(t) + L \frac{di(t)}{dt} + \frac{q_c(t)}{C_S} = V_M \sin(\omega t + \phi) \quad (33)$$

in which $i(t)$ is the instantaneous current after the switch opens, $q_c(t)$ is the instantaneous charge on the capacitor, V_M is the peak line voltage, and ϕ is the phase angle by which the voltage leads the current prior to opening of the switch. After differentiation and rearrangement of terms, the equation can be expressed as a standard second-order differential equation with constant coefficients. With the imposition of the boundary conditions that $i(0)=0$ and $q_c(0)=0$, the equation for the charge on the capacitor can be stated for the three circuit conditions as follows:

Condition I: $(R_L + R_S)^2 < 4L/C$

$$q_c(t) = \frac{-|V_M|}{\omega|Z|} \cos(\omega t + \phi + \theta) + |Q_t| e^{-\alpha t} \sin(\beta t + \eta) \quad (34)$$



92CS-21377

Fig. 164—Equivalent circuit used for analysis of snubber network.

Condition II: $(R_L + R_S)^2 = 4L/C$

$$q_c(t) = \frac{-|V_M|}{\omega|Z|} \cos(\omega t + \phi + \theta) + e^{-\alpha t} [(1 + \alpha t) q_d + i_d t] \quad (35)$$

Condition III:

$(R_L + R_S)^2 > 4L/C$

$$q_c(t) = \frac{-|V_M|}{\omega|Z|} \cos(\omega t + \phi + \theta) + \frac{e^{-\alpha t}}{\beta'} [(\alpha q_d + i_d t) \sinh \beta' t + \beta' q_d \cosh \beta' t] \quad (36)$$

The symbols used in these equations are defined as follows:

$$\phi = \tan^{-1}(\omega L/R_L) \quad (37)$$

$$\theta = -\tan^{-1}[(\omega L - \frac{1}{\omega C_S})/(R_L + R_S)] \quad (38)$$

$$\alpha = \frac{R_L + R_S}{2L} \quad (39)$$

$$\beta' = \sqrt{\left(\frac{R_L + R_S}{2L}\right)^2 - \frac{1}{LC_S}} \quad (40)$$

$$\beta = \sqrt{\frac{1}{LC_S} - \left(\frac{R_L + R_S}{2L}\right)^2} \quad (41)$$

$$Z = (R_L + R_S) + j(\omega L - \frac{1}{\omega C_S}) \quad (42)$$

$$q_d = \frac{|V_M|}{\omega|Z|} \cos(\phi + \theta) + q_c(0) \quad (43)$$

$$i_d = i(0) - \frac{|V_M|}{|Z|} \sin(\phi + \theta) \quad (44)$$

$$|Q_t| = \sqrt{\left[\frac{\alpha q_d + i_d}{\beta}\right]^2 + q_d^2} \quad (45)$$

$$\eta = \tan^{-1}\left(\frac{\beta q_d}{\alpha q_d + i_d}\right) \quad (46)$$

The voltage across the triac is determined by calculating the voltages across the snubber capacitor and resistor from the following fundamental relations:

$$v_{CS}(t) = \frac{q_c(t)}{C_S} \quad (47)$$

$$v_{RS}(t) = R_S \frac{dq_c(t)}{dt} \quad (48)$$

The sum of these two voltages then represents the instantaneous voltage across the triac. The following equations give the instantaneous voltage for the three circuit conditions:

Condition I: $(R_L + R_S)^2 < 4L/C$

$$v(t) = \frac{-|V_M|}{|Z|} \left[\frac{1}{\omega C_S} \cos(\omega t + \phi + \theta) \right. \\ \left. - R_S \sin(\omega t + \phi + \theta) \right] + |Q_t| e^{-\alpha t}$$

$$\left[\frac{1}{C_S} \sin(\beta t + \eta) + \frac{R_S}{\sqrt{LC_S}} \sin(\beta t + \eta + \psi) \right] \quad (49)$$

where ψ is defined by the following expression:

$$\psi = \tan^{-1} \left(\frac{\beta}{-\alpha} \right) \quad (50)$$

Condition II: $(R_L + R_S)^2 = 4L/C$

$$\begin{aligned} v(t) = & \frac{-|V_M|}{|Z|} \\ & \left[\frac{1}{\omega C_S} \cos(\omega t + \phi + \theta) \right. \\ & \left. - R_S \sin(\omega t + \phi + \theta) \right] \\ & + \frac{1}{C_S} [(1 + \alpha t) q_d + i_d t] e^{-\alpha t} \\ & + R_S [(1 - \alpha t) i_d - \alpha 2 t q_d] e^{-\alpha t} \end{aligned} \quad (51)$$

Condition III: $(R_L + R_S)^2 > 4L/C$

$$\begin{aligned} v(t) = & \frac{-|V_M|}{|Z|} \left[\frac{1}{\omega C_S} \cos(\omega t + \phi + \theta) \right. \\ & \left. - R_S \sin(\omega t + \phi + \theta) \right] + \frac{e^{-\alpha t}}{\beta' C_S} \\ & [(\alpha q_d + i_d) \sinh \beta' t + \beta' q_d \cosh \beta' t] \\ & + R_S e^{-\alpha t} \left[\frac{-\alpha i_d - \frac{1}{L C_S} q_d}{\beta'} \right. \\ & \left. \sinh \beta' t + i_d \cosh \beta' t \right] \end{aligned} \quad (52)$$

A computer is used to calculate the voltage across the snubber because hand calculation is time-consuming. The magnitude and time of occurrence of the peak

voltage are found by numerical analysis, and then the values and times of the voltages at 10 per cent and 63 per cent of peak are calculated. These values are used to compute the dv/dt stress as defined by the following equation:

$$dv/dt = \frac{V_2 - V_1}{t_2 - t_1} \quad (53)$$

where V_1 and t_1 are the voltage and time of the 10-per-cent point and V_2 and t_2 are the voltage and time of the 63-per-cent point. This program therefore allows evaluation of various load and snubber combinations in a matter of minutes.

In general, it is most desirable from a cost standpoint to use a device with the lowest possible V_{DROM} capability. For applications involving the control of a load operating on a 120-volt ac line, a device with a V_{DROM} of 200 volts would be desirable; a 400-volt device should be used for operation on a 220-volt line. The use of the lower-voltage device in any application is contingent on the ability of the circuit to limit any possible voltage ringing below the V_{DROM} rating of the device. The snubber can be designed to limit this voltage ringing during the post-commutation period to within this rating. Figs. 165 and 166 show the values of C_S and R_S that limit peak voltage across the triac to specific values. Fig. 165 allows the selection of snubber components that will limit the peak voltage of 200 volts for a zero-power-factor load at the desired dv/dt for an rms line voltage of 120 volts. Fig. 166 shows

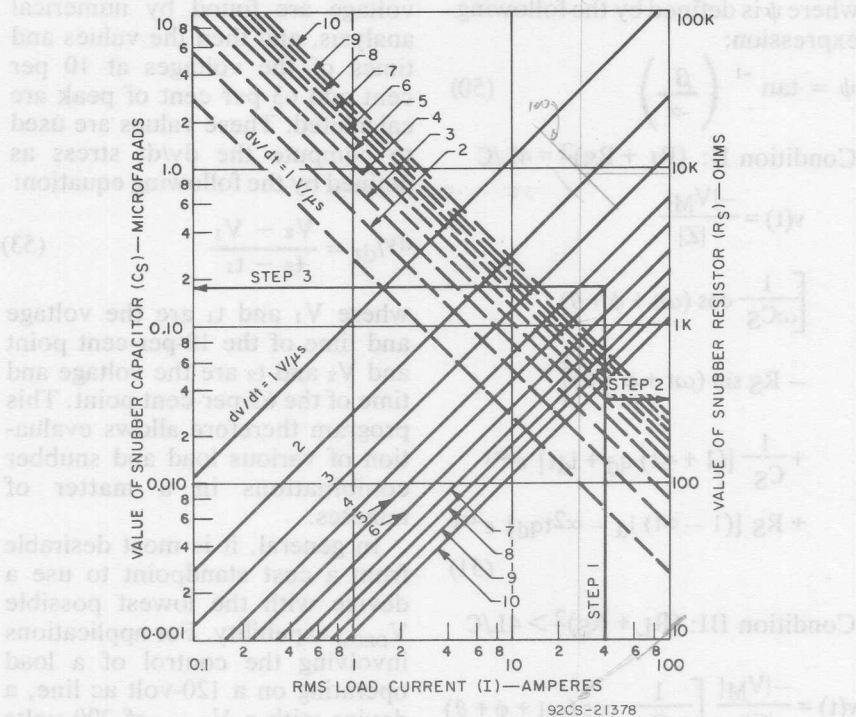


Fig. 165—Design curves for snubber that limits peak voltage to 200 volts for 120-volt ac line and zero power factor.

the components that limit the voltage to 400 volts when the rms line voltage is 220 volts.

Snubber Design Procedure

For use of the graphs, three things must be known: (1) the rms line voltage, (2) the rms load current, and (3) the allowable dv/dt . The following procedure is used to obtain the required snubber components:

- (1) Draw a vertical line on the proper voltage graph at the load current.
- (2) At the intersection of the vertical line and the dashed line that represents the allowable dv/dt , draw a horizontal line

to the right vertical axis. Read the value of R_s from the right vertical axis.

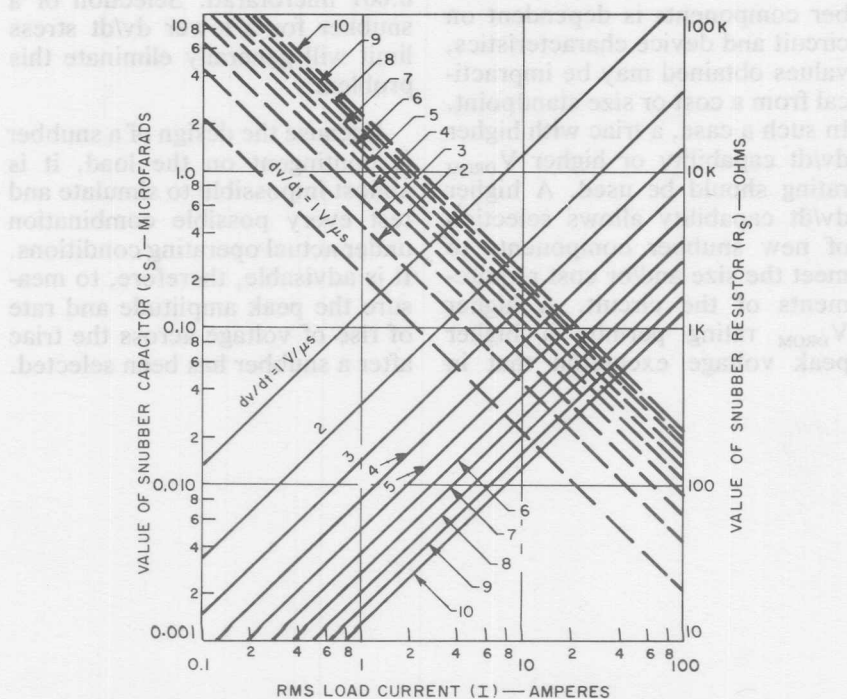
- (3) At the intersection of the vertical line and the solid line that represents the allowable dv/dt , draw a horizontal line to the left vertical axis. Read the value of C_s from the left vertical axis.

As an illustration of the above procedure, Fig. 165 is used to find snubber component values that limit the dv/dt stress to 5 volts per microsecond for a 40-ampere rms current in a 120-volt rms line. From Fig. 165, these values are $R_s = 340$ ohm and $C_s = 0.18$ microfarad.

As previously stated, these graphs were developed to limit the peak voltage for a zero-power-factor load. For the non-ideal load the graphs are used in the same fashion; a reduction in the peak voltage following commutation and a slight reduction in the dv/dt stress are the only effects introduced by the non-ideal load. The reduction in the peak voltage excursion is caused by the decrease in instantaneous voltage at the time of commutation. As the power factor increases, the phase angle between the voltage and current decreases toward 0° . This

decrease in the phase angle shifts the time of commutation in the half-cycle toward the zero-voltage crossing and thus reduces the instantaneous voltage. The reduction in the dv/dt stress is the result of both the reduction in the voltage at commutation and the increasing resistive impedance of the load.

A numerical example shows how a load that is not purely inductive reduces the peak voltage after commutation. The snubber components for 8 volts per microsecond at an rms current of 22.7 amperes are found from Fig. 165



92CS-21379

Fig. 166—Design curves for snubber that limits peak voltage to 400 volts for 220-volt ac line and zero power factor.

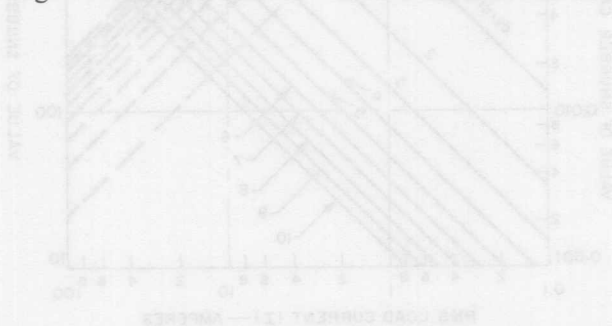
to be 960 ohms and 0.04 microfarad. If the load is purely inductive, the peak voltage is limited to 200 volts. If the load has the same current rating but a power factor of 0.7, this snubber network limits the peak voltage after commutation to 140 volts. The peak voltage is reduced because the instantaneous line voltage at the time of commutation is only 121 volts. The dv/dt stress is also slightly lower than the 8-volts-per-microsecond value. This example demonstrates that the design graphs of Figs. 165 and 166 can be used for loads having any power factor.

Because the selection of snubber components is dependent on circuit and device characteristics, values obtained may be impractical from a cost or size standpoint. In such a case, a triac with higher dv/dt capability or higher V_{DROM} rating should be used. A higher dv/dt capability allows selection of new snubber components to meet the size and/or cost requirements of the circuit. A higher V_{DROM} rating permits a higher peak voltage excursion that in

general will allow selection of a smaller snubber capacitor and smaller resistor.

The analysis given in the preceding paragraphs assumes the effects of the triac to be minimal. Some error is introduced by neglect of the reverse recovery process and the displacement current. The additional current flow tends to increase the instantaneous dv/dt during the first few microseconds following commutation. The over-all effect is to increase slightly the average dv/dt stress across the triac. This effect is most noticeable when the snubber capacitance is less than 0.001 microfarad. Selection of a snubber for a lower dv/dt stress limit will generally eliminate this problem.

Because the design of a snubber is contingent on the load, it is almost impossible to simulate and test every possible combination under actual operating conditions. It is advisable, therefore, to measure the peak amplitude and rate of rise of voltage across the triac after a snubber has been selected.



Thyristor Triggering

Thyristors are excellent devices for use in the control of ac power. In general, thyristors initially assume a blocking, or high-impedance state, and remain in that state until triggered to the on or low-impedance state. Once triggered, the thyristor remains on until the current is reduced to zero. The thyristor then returns to its blocking state. Because the current decreases to zero during every half-cycle in an ac supply, turn-off is guaranteed every half-cycle. All that is necessary for ac power control, therefore, is a trigger circuit to control thyristor turn-on so that whole or partial cycles may be switched to the load.

PHASE CONTROL

In many power-control applications of thyristors, partial cycles of the applied ac voltage are switched to the load. Because the power delivered to the load is controlled by variation of the phase angle at which the thyristor switching initiates current flow, this type of operation is usually referred to as **phase control**. The electrical angle of the applied ac voltage waveform at which thyris-

tor current is initiated is termed the **firing angle** (θ_F). It is usually more important, however, to know and to refer to the **conduction angle** (θ_C), which is the number of electrical degrees of the applied ac voltage waveform during which the thyristor is in conduction. The conduction angle is equal to $180^\circ - \theta_F$ for a half-wave circuit and $2(180^\circ - \theta_F)$ for a full-wave circuit. The voltage waveforms across the thyristor and the load for each type of circuit are illustrated in Fig. 167.

Basic Circuit Arrangements

Phase control of thyristor-and-diode combinations may be employed to provide many different ac and dc output waveforms to a load circuit. Some basic combinations, together with the corresponding voltage waveforms at the load for two complete cycles of operation, are shown in Fig. 168. In general, triac circuits are more economical for full-wave power control than are circuits that use two SCR's. For partial range control when the load is not sensitive to a nonsymmetrical waveform, such as resistive loads,

a control circuit that uses a diode and an SCR is acceptable.

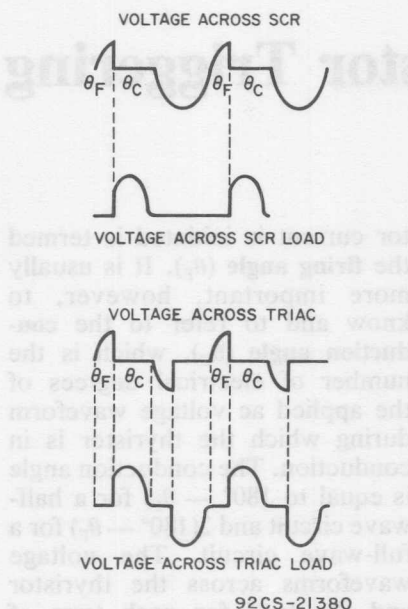


Fig. 167—Voltage waveforms showing conduction angle for half-wave operation (SCR) and full-wave operation (triac) of thyristor phase-control circuits.

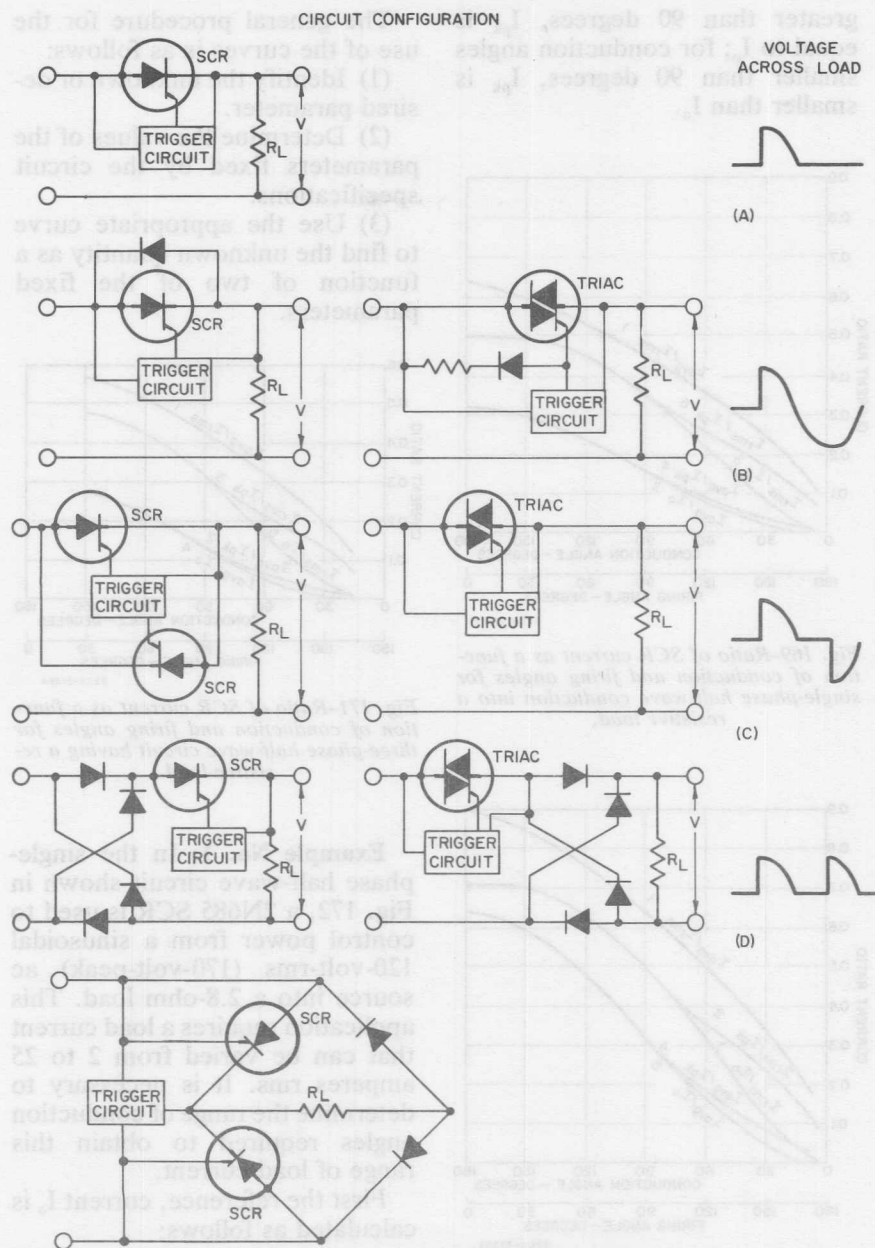
Current Ratios

In the design of thyristor power-control circuits of the types shown in Fig. 168, it is often necessary to determine the specific values of peak, average, and rms current that flow through the thyristors. For conventional rectifiers, these values are readily determined by use of the current ratios shown in Table IX, given in the section on **Silicon Rectifiers**. For thyristors, however, the calculations are more difficult because the current ratios become

functions of the conduction angle and the firing angle of the device.

The curves in Figs. 169, 170, and 171 show several current ratios as functions of conduction or firing angles for three basic SCR circuits. These curves can be used in a number of ways to calculate desired current values. For example, they can be used to determine the peak or rms current in an SCR when a certain average current is to be delivered to a load during a specific part of the conduction period. It is also possible to work backwards and determine the necessary period of conduction if, for example, a specified peak-to-average current ratio must be maintained in a particular application. Another use of the curves in Figs. 169, 170, and 171 is in the calculation of the rms current at various conduction angles when it is necessary to determine the power delivered to a load, or power losses in transformers, motors, leads, or bus bars. Although the curves are presented in terms of device current, they are equally useful for the calculation of load current and voltage ratios.

The curves provide ratios that relate average current I_{avg} , rms current I_{rms} , peak current I_{pk} , and reference current I_o . The reference current is a circuit constant and is equal to the peak source voltage V_{pk} divided by the load resistance R_L . The term I_{pk} refers to the peak current that flows through the SCR during its period of forward conduction. I_o is the maximum possible peak-current value during the peak of the sine wave. For conduction angles



92CM-21381

Fig. 168—Basic circuit configurations for thyristor power controls and voltage waveform across the load.

greater than 90 degrees, I_{pk} is equal to I_o ; for conduction angles smaller than 90 degrees, I_{pk} is smaller than I_o .

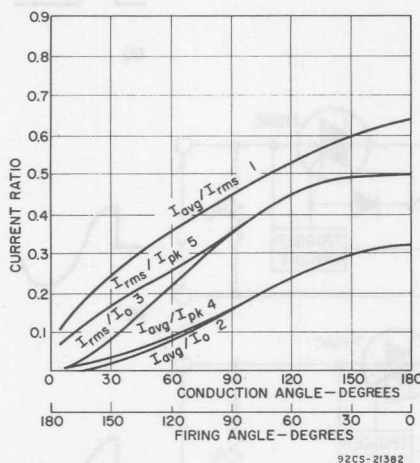


Fig. 169—Ratio of SCR current as a function of conduction and firing angles for single-phase half-wave conduction into a resistive load.

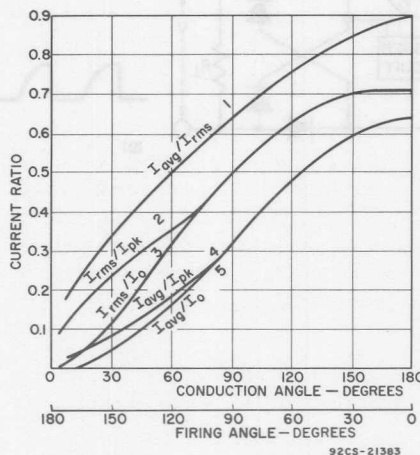


Fig. 170—Ratio of thyristor current as a function of conduction and firing angles for single-phase full-wave conduction into a resistive load.

The general procedure for the use of the curves is as follows:

- (1) Identify the unknown or desired parameter.
- (2) Determine the values of the parameters fixed by the circuit specifications.
- (3) Use the appropriate curve to find the unknown quantity as a function of two of the fixed parameters.

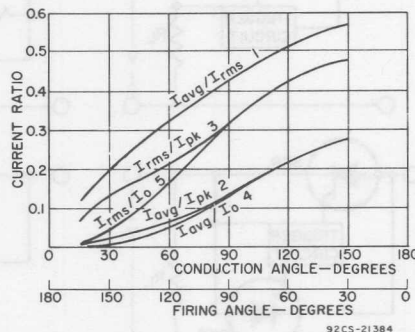
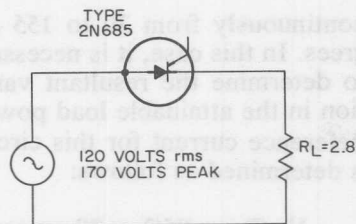


Fig. 171—Ratio of SCR current as a function of conduction and firing angles for three-phase half-wave circuit having a resistive load.

Example No. 1: In the single-phase half-wave circuit shown in Fig. 172, a 2N685 SCR is used to control power from a sinusoidal 120-volt-rms (170-volt-peak) ac source into a 2.8-ohm load. This application requires a load current that can be varied from 2 to 25 amperes rms. It is necessary to determine the range of conduction angles required to obtain this range of load current.

First the reference, current I_o is calculated as follows:

$$I_o = \frac{V_{pk}}{R_L} = \frac{170}{2.8} = 61 \text{ amperes}$$



$$\begin{aligned}
 I &= 0 \quad (0^\circ \leq \theta \leq \theta_f) \\
 I &= I_o \sin \theta \quad (\theta_f \leq \theta \leq 180^\circ) \\
 I_{avg} &= \frac{1}{2\pi} \int_{\theta_f}^{180^\circ} I d\theta \\
 I_{rms} &= \left[\frac{1}{2\pi} \int_{\theta_f}^{180^\circ} I^2 d\theta \right]^{1/2} \\
 I_{pk} &= I_o \quad (0 \leq \theta_f \leq 90^\circ) \\
 I_{pk} &= I_o \sin \theta_f \quad (90^\circ \leq \theta_f \leq 180^\circ)
 \end{aligned}$$

92CS-21385

Fig. 172—Single-phase half-wave circuit that operates into a resistive load and the respective equation for SCR current.

The ratio of I_{rms} to I_o for the minimum and maximum load current values is then calculated as follows:

$$(I_{rms}/I_o)_{min} = 2/61 = 0.333$$

$$(I_{rms}/I_o)_{max} = 25/61 = 0.41$$

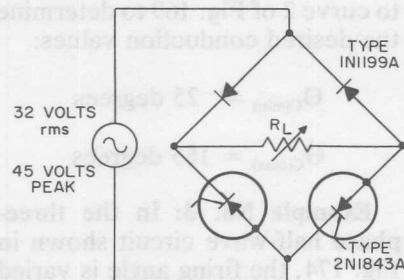
These current-ratio values are then applied to curve 3 of Fig. 169 to determine the corresponding conduction angles:

$$\theta_{C(min)} = 15 \text{ degrees}$$

$$\theta_{C(max)} = 106 \text{ degrees}$$

Example No. 2: In the single-phase full-wave bridge circuit (two legs controlled) shown in Fig. 173, a constant average load current of 7 amperes is to be maintained while the load resistance varies from 0.2 to 4 ohms. In this case, it is necessary to de-

termine the variation required in the conduction angle. The average current through the SCR is one-half the load current, or 3.5 amperes. The applicable current ratios for this circuit are shown in Fig. 169 (the individual device currents are half-wave although the load current is full-wave).



$$\begin{aligned}
 I &= 0 \quad (0^\circ \leq \theta \leq \theta_f) \\
 I &= I_o \sin \theta \quad (\theta_f \leq \theta \leq 180^\circ) \\
 I_{avg} &= \frac{1}{\pi} \int_{\theta_f}^{180^\circ} I d\theta \\
 I_{rms} &= \left[\frac{1}{\pi} \int_{\theta_f}^{180^\circ} I^2 d\theta \right]^{1/2} \\
 I_{pk} &= I_o \quad (0 \leq \theta_f \leq 90^\circ) \\
 I_{pk} &= I_o \sin \theta_f \quad (90^\circ \leq \theta_f \leq 180^\circ)
 \end{aligned}$$

92CS-21392

Fig. 173—Single-phase full-wave bridge circuit that operates into a resistive load and the respective equations for SCR current.

Again, the first quantity to be calculated is the reference current I_o . Because the reference current varies with the load resistance, the maximum and minimum values are determined as follows:

$$I_{o(max)} = V_{pk}/R_{L(min)} = 45/0.2$$

$$= 225 \text{ amperes}$$

$$I_{o(min)} = V_{pk}/R_{L(max)} = 45/4$$

$$= 11.2 \text{ amperes}$$

The corresponding ratios of I_{avg} to I_o are then calculated, as follows:

$$(I_{avg}/I_o)_{min} = 3.5/225 = 0.015$$

$$(I_{avg}/I_o)_{max} = 3.5/11.2 = 0.312$$

Finally, these ratios are applied to curve 2 of Fig. 169 to determine the desired conduction values:

$$\Theta_{C(min)} = 25 \text{ degrees}$$

$$\Theta_{C(max)} = 165 \text{ degrees}$$

Example No. 3: In the three-phase half-wave circuit shown in Fig. 174, the firing angle is varied

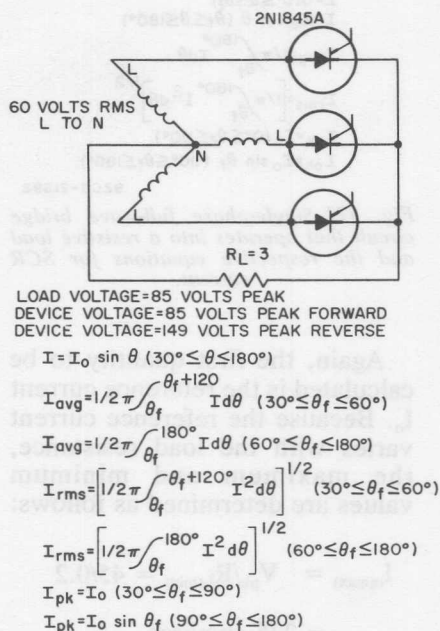


Fig. 174—Three-phase half-wave circuit that uses a resistive load and the respective equation for SCR current.

continuously from 30 to 155 degrees. In this case, it is necessary to determine the resultant variation in the attainable load power. Reference current for this circuit is determined as follows:

$$I_o = V_{pk}/R_L = 85/3 = 28 \text{ amperes}$$

Rectifier current ratios are determined from Fig. 171 for the extremes of the firing range, as follows:

$$\Theta_F = 30 \text{ degrees}; I_{rms}/I_o = 0.49$$

$$\Theta_F = 155 \text{ degrees}; I_{rms}/I_o = 0.06$$

These ratios, together with the reference current, are then used to determine the range of rms current in the rectifiers, as follows:

$$I_{rms(max)} = 0.49 \times 28 = 13.7 \text{ amperes}$$

$$I_{rms(min)} = 0.06 \times 28 = 1.7 \text{ amperes}$$

In this circuit, the rms current in the load is equal to the rms rectifier current multiplied by the square root of three; as a result, the desired power range of the load is as follows:

$$P_{max} = [I_{rms(max)} \sqrt{3}]^2 R_L$$

$$= 1700 \text{ watts}$$

$$P_{min} = [I_{rms(min)} \sqrt{3}]^2 R_L$$

$$= 26 \text{ watts}$$

Phase-control techniques can be used very effectively and efficiently to control ac input power in lamp-dimming, motor-speed-control, low-power electric-

heating, and many other similar types of applications. Phase-control systems generate radio-frequency noise as a result of the random thyristor switching and often must include suppression circuits to minimize radio-frequency interference (RFI) in other electrical systems. In higher-power applications, the RFI is of such magnitude that the suppression circuits become excessively bulky and expensive.

ZERO-VOLTAGE SWITCHING

Power to an ac load may be controlled by switching of complete half-cycles or integral numbers of whole cycles of the ac power to the load. This type of control is usually referred to as **integral-cycle** or **zero-voltage-switching control**. Fig. 175 shows the relationship between line and load voltages for both SCR

circuits is substantially decreased, or even eliminated, because thyristor switching occurs at or near the 0- or 180-degree (zero-voltage) points on the ac line voltage.

In zero-voltage-switching controls, only two levels of input power are delivered to the load. The load receives the full amount of power for a period of time and zero power for a period of time; the average power delivered to the load, therefore, depends upon the ratio of the power-on interval to the power-off interval.

In solid-state power-control systems that employ zero-voltage-switching techniques, two modes of operation are possible. The controlled variable (for example, temperature in a heat-control system) may be sensed and used to turn the power on or off. Because the power-control element is a solid-state device and, therefore, is free of wearout mechanisms,

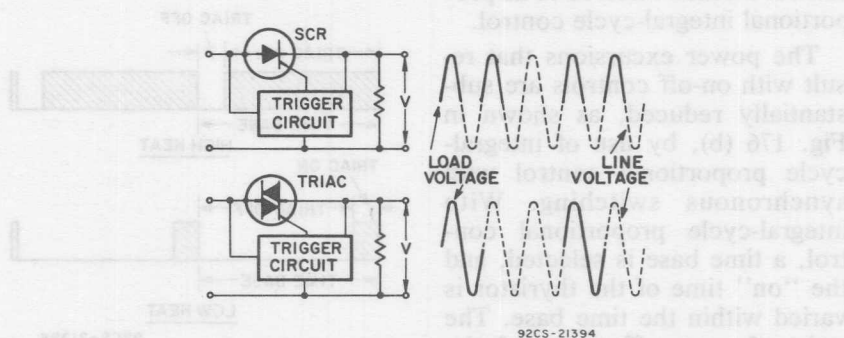


Fig. 175—Integral-cycle thyristor power control circuits

(half-wave) and triac (full-wave) power-control circuits that employ this control technique. With this type of control, the RFI associated with phase-control cir-

cuits is substantially decreased, or even eliminated, because thyristor switching occurs at or near the 0- or 180-degree (zero-voltage) points on the ac line voltage. The power delivered to the load, therefore, depends upon the ratio of the power-on interval to the power-off interval. In solid-state power-control systems that employ zero-voltage-switching techniques, two modes of operation are possible. The controlled variable (for example, temperature in a heat-control system) may be sensed and used to turn the power on or off. Because the power-control element is a solid-state device and, therefore, is free of wearout mechanisms,

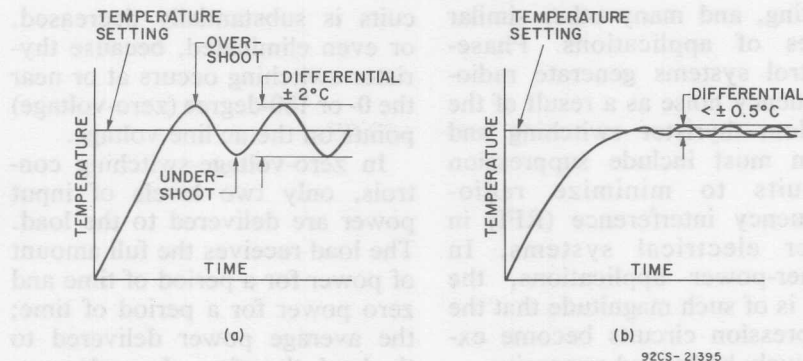


Fig. 176—Transfer characteristics of (a) on-off and (b) proportional control systems.

for a heating system that uses this type of control.

In control systems that have large time constants, such as a home heating system, on-off controls of the type described above may produce relatively large overshoots and undershoots. In this type of system, better regulation may be achieved by use of a control method referred to as proportional integral-cycle control.

The power excursions that result with on-off controls are substantially reduced, as shown in Fig. 176 (b), by use of integral-cycle proportional control with synchronous switching. With integral-cycle proportional control, a time base is selected, and the "on" time of the thyristor is varied within the time base. The ratio of on-to-off times of the thyristor during this interval depends upon the amount of power to the load required to maintain a predetermined average level for the system. As this level is approached (as determined by a sensing element), less power is

delivered to the load (i.e., the duty cycle is reduced). This type of control is usually selected for heating systems.

Fig. 177 shows the on-off-ratio of the triac. Within the time period, the on-time varies by an integral number of cycles from full on to a single cycle of input voltage.

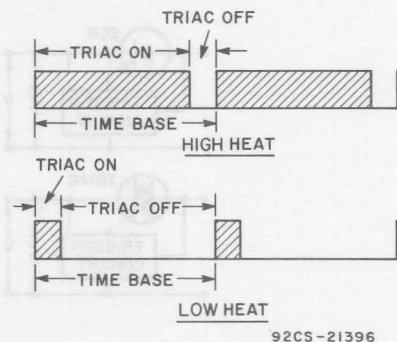


Fig. 177—Triac duty cycle.

One method of achieving integral-cycle proportional control is to use a fixed-frequency sawtooth generator signal which is summed with a dc control signal.

The saw-tooth generator establishes the period or time base of the system. The dc control signal is obtained from the output of the temperature-sensing network. The principle is illustrated in Fig. 178. As the sawtooth voltage increases, a level is reached

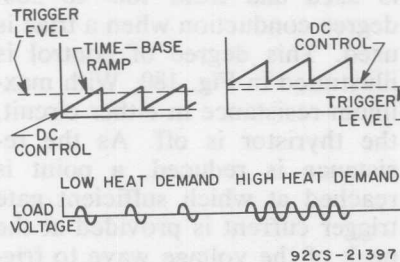


Fig. 178—Proportional-controller wave-shapes.

which turns on power to the heating elements. As the temperature at the sensor changes, the dc level shifts accordingly and changes the length of time that the power is applied to the heating elements within the established time.

When the demand for heat is high, the dc control signal is high and high power is supplied continuously to the heating elements. When the demand for heat is completely satisfied, the dc control signal is low and low power is supplied to the heating elements. Usually a system using this principle operates continuously somewhere between full on and full off to satisfy the demand for heat.

BASIC TRIGGERING TECHNIQUES

When thyristors are triggered, the primary requirement to assure

sustained forward conduction is that the gate current is of sufficient strength to meet all requirements specified in the published data on the thyristor. These triggering requirements are usually stated in terms of dc voltage and current. Because it is often desirable to pulse-fire thyristors, it is also necessary to consider the duration of firing pulse required. A trigger pulse that has an amplitude just equivalent to the dc requirements must be applied for a relatively long period of time (approximately 30 microseconds) to ensure that the gate signal is provided during the full turn-on period of the thyristor. As the amplitude of the gate-triggering signal is increased, the turn-on time of the thyristor is decreased, and the width of the gate pulse may be reduced. When highly inductive loads are used, the inductance controls the current-rise portion of the turn-on time. For this type of load, the gate pulse must be long enough to assure that the principle current rises to a value greater than the latching-current level of the device. The latching current of RCA thyristors is always less than twice the holding current.

The application usually determines the degree of sophistication of the circuit used to trigger a given thyristor. Triggering circuits can be as numerous and as varied as the applications in which they are used; this text discusses the basic types only.

Many applications require that a thyristor be switched full on or full off in a manner similar to the

operation of a relay. The simplest method of accomplishing this type of triggering is illustrated by the circuits shown in Fig. 179.

The resistance R_G maintains the gate current within the rating of the thyristor gate and the associated switch. After firing, the thyristor switches to its low-impedance state; depending on the forward-current magnitude, the voltage drop across the thyristor can be as high as a few volts. It cannot be assumed that if the resistor were removed from the gate circuit, the gate switch would carry only enough current to trigger the device and then decrease to zero. Because the gate has a low impedance, it carries a large percentage of the forward current.

illustrates the use of the SCR-and-diode combination.

When an ac resistive trigger network is used, only a certain degree of phase-angle control can be accomplished. The degree of control varies from 90- to 180-degree conduction when an SCR is used and from 180- to 360-degree conduction when a triac is used. This degree of control is illustrated in Fig. 180. With maximum resistance in either circuit, the thyristor is off. As the resistance is reduced, a point is reached at which sufficient gate trigger current is provided at the peak of the voltage wave to trigger the thyristor. The thyristor initially turns on with a conduction angle θ_C of 90 degrees. A

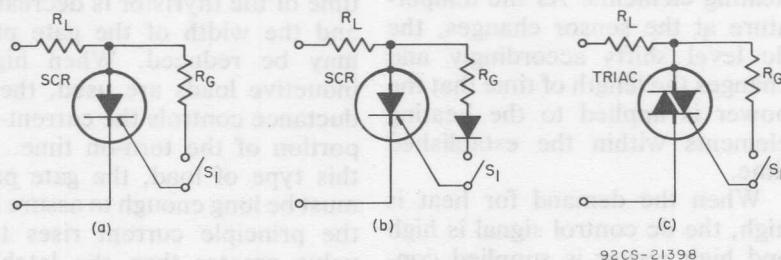


Fig. 179—Simple thyristor triggering methods: (a) resistance triggering of SCR; (b) resistance-diode triggering of SCR; (c) resistance triggering of triac.

The gate resistor R_G assures that the gate current will decrease to a negligible value after the thyristor is fired.

When an SCR is used with an ac supply, a diode may be required to keep the reverse polarity across the SCR from being impressed across the gate circuit. The allowable reverse dissipation is limited to that shown in the published data on the SCR. Fig. 179 (b)

further reduction in resistance increases the conduction angle from 90 degrees toward 180 degrees for an SCR and from 90 degrees and 270 degrees to zero and 180 degrees, respectively, for a triac.

The easiest method to obtain a firing-angle delay greater than 90 degrees for half-wave operation is to use a resistance-capacitance triggering network, which is shown in its simplest form in Fig.

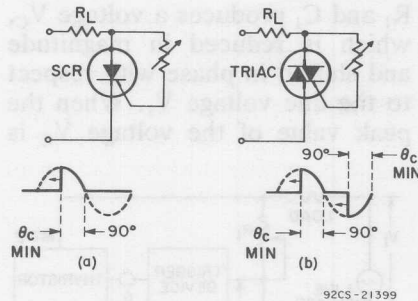


Fig. 180—Degree of control over conduction angles when ac resistive network is used to trigger SCR's and triacs.

181 (a). The polarity of the sine wave which reverse-biases the SCR charges the capacitor in the reverse direction to the peak of the line voltage through a diode. On the next half-cycle, the capacitor charges through the potentiometer to the relatively small positive voltage required to trigger the SCR.

Controls of this type can have conduction angles from 0 to 180 degrees.

Resistance and resistance-capacitance trigger circuits have one great disadvantage: the gate voltage rises slowly to the triggering level. Because of variations in gate characteristics among thyristors (15 to 1 in gate-trigger current, 2 to 1 in gate-trigger voltage, and 4 to 1 with temperature), a given control-potentiometer resistance setting may yield a different conduction angle for different thyristors or temperature conditions. The performance of the circuit is improved somewhat by use of a double RC section, as shown in Figs. 181 (b) and 181 (c), or by use of a negative voltage across the capacitor, as shown in Fig. 181(a). These techniques increase the rate

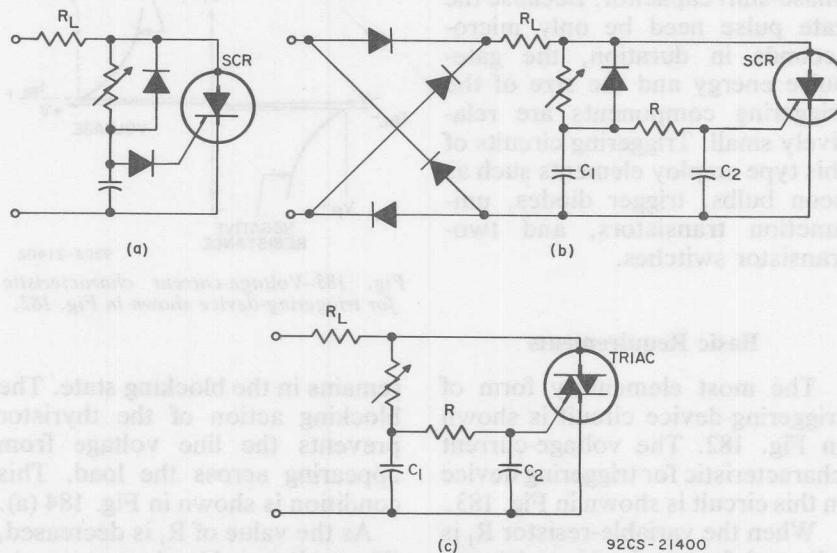


Fig. 181—RC triggering networks used for phase-control triggering of thyristors: (a) series RC network and diode (for SCR); (b) RC lattice network and diode (for SCR); (c) RC lattice network without diode (for triac).

of rise of gate voltage in the vicinity of the triggering potential and, therefore, minimize the effects of gate differences on the conduction angle.

TRIGGERING DEVICES

A variety of thyristor triggering devices are available to overcome the disadvantages noted for simple resistance or resistance-capacitance triggering circuits. These triggering devices have a smaller range of characteristics and are not so temperature-sensitive. Basically, a thyristor triggering device exhibits a negative resistance after a critical voltage is reached, so that the gate-current requirement of the thyristor can be obtained as a pulse from the discharge of the phase-shift capacitor. Because the gate pulse need be only microseconds in duration, the gate-pulse energy and the size of the triggering components are relatively small. Triggering circuits of this type employ elements such as neon bulbs, trigger diodes, unijunction transistors, and two-transistor switches.

Basic Requirements

The most elementary form of triggering-device circuit is shown in Fig. 182. The voltage-current characteristic for triggering device is shown in Fig. 183.

When the variable-resistor R_1 is adjusted for maximum resistance in the circuit, the circuit operates so that the series combination of

R_1 and C_1 produces a voltage V_C , which is reduced in magnitude and shifted in phase with respect to the line voltage V_1 . When the peak value of the voltage V_C is

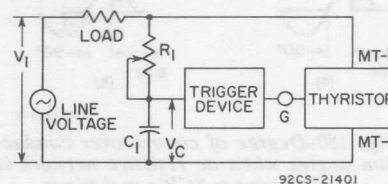


Fig. 182—Thyristor power control in which switching is controlled by basic triggering-device circuit.

less than the triggering-device breakdown voltage V_p , the trigger device does not conduct; the thyristor receives no gate current and

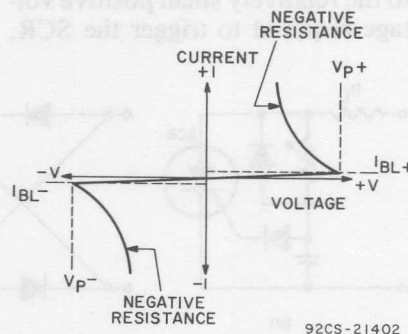


Fig. 183—Voltage-current characteristic for triggering-device shown in Fig. 182.

remains in the blocking state. The blocking action of the thyristor prevents the line voltage from appearing across the load. This condition is shown in Fig. 184 (a).

As the value of R_1 is decreased, the voltage V_C increases in magnitude and changes in phase with respect to the line voltage V_1 .

This change continues as long as the value of R_1 is decreased, and eventually a point is reached at which V_C exceeds V_P . At this point, the trigger device instantaneously breaks down. This

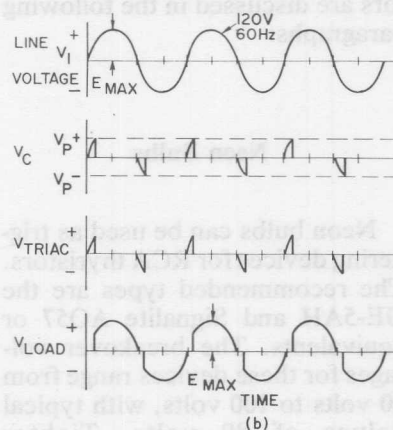
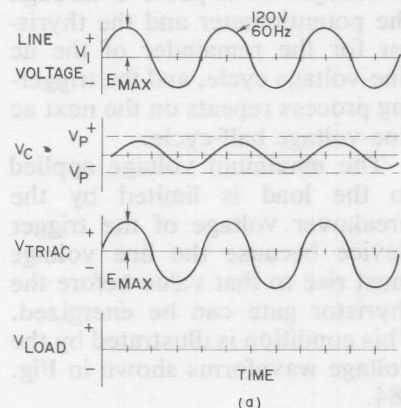


Fig. 184—Voltage waveforms for circuit shown in Fig. 182: (a) thyristor in blocking state; (b) when thyristor is triggered at controlled intervals by triggering-device circuit.

breakdown is accompanied by a sudden discharge of capacitor C_1 , which results in a pulse of gate current into the thyristor. The thyristor is then triggered into conduction and remains in the on state for the rest of that particular half-cycle of line voltage.

The magnitude and duration of the gate-current pulse is determined by the interaction of the capacitor C_1 , the triggering-device characteristics, and the impedance of the thyristor gate. This interaction can be represented by the curves shown in Fig. 185.

The capacitor, which is charged to the voltage V_C , discharges through the negative-resistance slope of the trigger device, and the gate current rises to some magnitude A at which the total voltage drops in the circuit are equal to the voltage source V_C . The capacitor voltage immediately begins to decrease from its initial value V_C , at a rate determined by the current level reached and the size of the capacitor. As it does, the gate current decreases. The load line representation at some later instant is shown by the dashed line in Fig. 185, and gate current at that instant is defined by point B . As this process continues, the circuit enters the unstable negative-slope region of the triggering device characteristic and quickly reverts to a stable point, approximately indicated by C . Fig. 186 shows the typical shape of the gate-current pulse that is produced. (More specific magnitudes are shown in later diagrams for particular triggering devices). The delay in reaching the peak gate

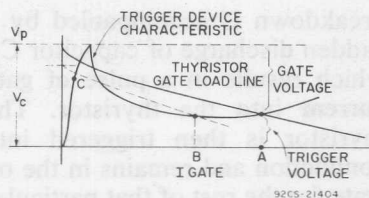


Fig. 185—Load line for the circuit shown in Fig. 182.

current is a function of the speed at which the triggering device is switched from its high-impedance to its low-impedance state. This

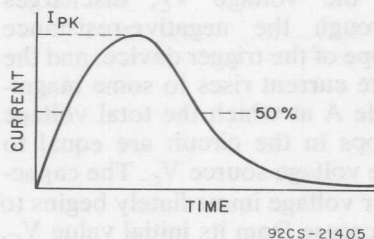


Fig. 186—Typical gate-current waveform for circuit shown in Fig. 182.

delay in effect indicates that there is a dynamic or time-dependent characteristic of the trigger device, which traces out a shape somewhat different from the static characteristic shown in Fig. 185.

The magnitude and duration of the gate pulse produced by the triggering device and the capacitor must be adequate to fire the thyristor. A curve of turn-on time as a function of gate-pulse magnitude, provided in the published data on the thyristor, defines the minimum requirements.

Because the thyristor is triggered to the on state by the rae pulse, and the voltage source for the triggering circuit is taken from across the thyristor, the triggering circuit cannot go through another charge-discharge cycle after the first firing pulse. The capacitor discharges from point C through the potentiometer and the thyristor for the remainder of the ac line-voltage cycle, and the triggering process repeats on the next ac line-voltage half-cycle.

The maximum voltage applied to the load is limited by the breakover voltage of the trigger device because the line voltage must rise to that value before the thyristor gate can be energized. This condition is illustrated by the voltage waveforms shown in Fig. 184.

Several types of devices commonly used to trigger RCA thyristors are discussed in the following paragraphs:

Neon Bulbs

Neon bulbs can be used as triggering devices for RCA thyristors. The recommended types are the GE-5AH and Signalite AO57 or equivalents. The breakover voltages for these devices range from 50 volts to 100 volts, with typical values of 80 volts. Tighter breakover voltage spreads can be obtained by manufacturer's selections. A typical current pulse resulting from a 0.1-microfarad capacitor discharging through a

neon bulb and a thyristor gate is illustrated in Fig. 187.

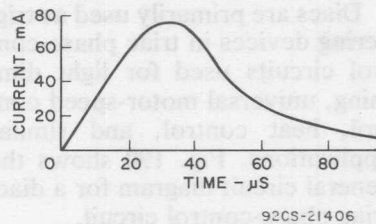


Fig. 187—Typical current pulse that results from the discharge of a 0.1-microfarad capacitor through a neon bulb and a thyristor gate.

Use of a neon bulb as a trigger device does have disadvantages. For example, when this type of device is used as a trigger on a 120-volt-rms ac line, an rms voltage loss as great as 10 per cent can occur at the load. The losses are caused by the relatively high breakdown voltage of the neon bulb. The neon bulb is also sensitive to radiation in that the breakdown point changes. When precise control is required, it may be necessary to shield the bulb or to obtain bulbs specially treated to minimize the effects of radiation. A major advantage of neon triggers is that relatively reliable and long-lived triggers can be obtained for a low price.

Trigger Diodes (Diacs)

A trigger diode is the solid-state replacement for a neon bulb in phase-control triggering circuits. These diodes offer the advantages of reduced requirements for peak-voltage firing, higher pulse-current capability, and

longer life. The solid-state diodes have breakdown voltages in the range of 27 to 37 volts and are designed specifically for triggering triacs.

The trigger diodes, often referred to as **diacs**, are three-layer symmetrical avalanche devices which break over in the negative-resistance region whenever a particular voltage, termed the break-over voltage, is exceeded in either voltage polarity. Fig. 188 shows the junction diagram and schematic symbol for a diac.

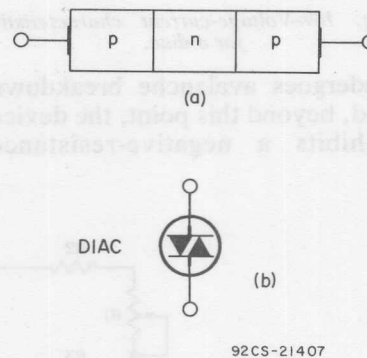


Fig. 188—(a) Junction diagram and (b) schematic symbol for a diac.

This three-layer trigger diode is similar in construction to a bipolar transistor, but differs from it in that the doping concentrations at the two junctions are approximately the same and there is no contact made to the base layer. The equal doping levels result in a symmetrical bidirectional switching characteristic, as shown in Fig. 189. This characteristic is essentially the same as that for the ideal thyristor triggering device shown in Fig. 183. When an in-

creasing positive or negative voltage is applied across the terminals of the diac, a minimum (leakage) current $I_{(BO)}$ flows through the device until the voltage reaches the breakover point $V_{(BO)}$. The reverse-biased junction then

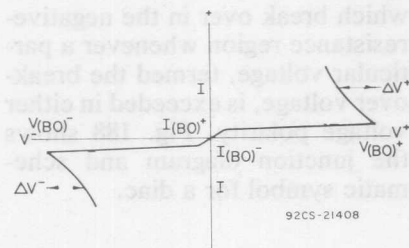


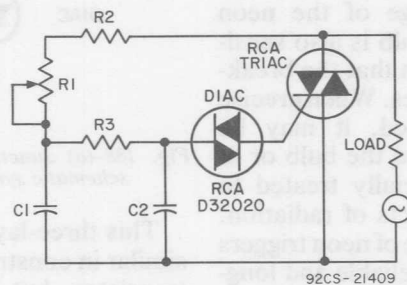
Fig. 189—Voltage-current characteristic for a diac.

undergoes avalanche breakdown and, beyond this point, the device exhibits a negative-resistance

characteristic, i.e., current through the device increases substantially with decreasing voltage.

Diacs are primarily used as triggering devices in triac phase-control circuits used for light dimming, universal motor-speed control, heat control, and similar applications. Fig. 190 shows the general circuit diagram for a diac/triac phase-control circuit.

The magnitude and duration of the gate current pulse are determined by the value of the phase-shift capacitance, the change in voltage across and the dynamic impedance of the trigger diac, and the thyristor gate impedance. The interaction of all circuit impedances and the phase-shift capacitance can best be represented by the curve of peak current as a



AC INPUT VOLTAGE	C ₁	C ₂	R ₁	R ₂	R ₃	RCA TRIAC TYPES
120 V 60 Hz	0.1 μF 200V	0.1 μF 100V	100 KΩ ½ W	2.2 KΩ ½ W	15 KΩ ½ W	T2800B
240 V 50 Hz	0.1 μF 400 V	0.1 μF 100 V	250 KΩ 1 W	3.3 KΩ ½ W	15 KΩ ½ W	T2800D
240 V 60 Hz	0.1 μF 400 V	0.1 μF 100 V	200 KΩ 1 W	3.3 KΩ ½ W	15 KΩ ½ W	T2800D

Fig. 190—Typical triac phase-control circuit for lamp-dimming, heat-control, and motor-speed-control applications.

function of the capacitance shown in Fig. 191.

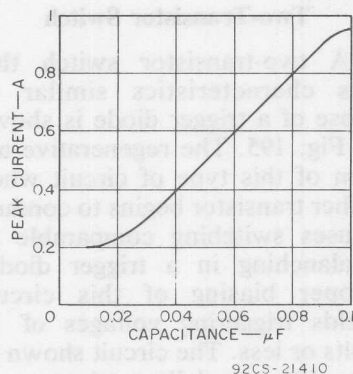


Fig. 191—Peak pulse trigger currents as a function of the phase-shift capacitance.

Unijunction Transistor

The unijunction transistor is a three-terminal two-layer device formed by an emitter and a base, as illustrated in Fig. 192. One lead is connected to the emitter and the other two leads are connected to the base. Between the two base connections there is an "interbase resistance." Fig. 193 illustrates the use of this device in a pulse-triggering circuit.

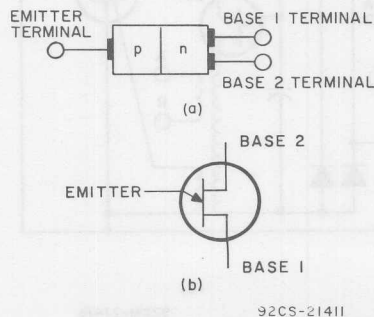
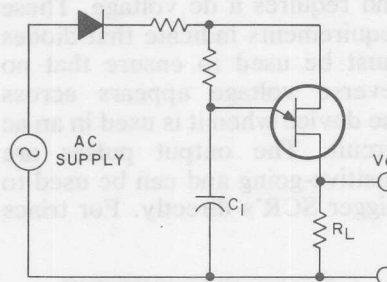


Fig. 192—(a) Junction diagram and (b) schematic symbol for a unijunction transistor.

Proper choice of external biasing resistors, coupled with the interbase resistance, normally serves to reverse-bias the "emitter-to-base-1" diode. This condition holds the emitter-to-base-1 diode in a high-impedance state until the emitter voltage is raised to a value high enough to forward-bias this junction. As the forward-bias point is reached, the same junction switches to a low-impedance state and causes capacitor C_1 to discharge into the load resistance R_L , which may be a thyristor gate. This voltage-sensitive



92CS-21412

Fig. 193—Pulse-triggering circuit that uses a unijunction transistor.

switching characteristic makes unijunction transistors ideal for triggering thyristors. When the biasing resistors and the emitter are connected to the same voltage source, as shown in Fig. 193, there is a degree of self-regulation of supply-voltage variation.

This regulation results because the interbase forward-bias point tracks the variation in emitter voltage V_e as V_e varies with supply voltage. Another advantage of the use of the unijunction

transistor is the way in which it automatically synchronizes to an ac supply. At the end of every cycle, any charge left on the capacitor after firing is discharged when the supply goes to zero. This action occurs because the point or firing voltage is also reduced toward zero. A third advantage is the inherent ability of the device to switch relatively high currents and thus to assure positive triggering of high-gate-current thyristors.

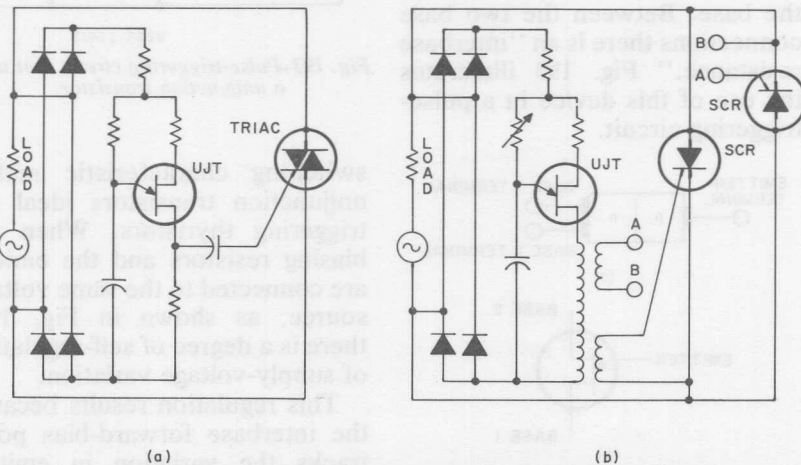
The disadvantage of the unijunction device is that it is unilateral with regard to current flow and requires a dc voltage. These requirements indicate that diodes must be used to ensure that no reverse voltage appears across the device when it is used in an ac circuit. The output pulses are positive-going and can be used to trigger SCR's directly. For triacs

or inverse parallel SCR's, transformer or capacitive coupling is required, as shown in Fig. 194.

Two-Transistor Switch

A two-transistor switch that has characteristics similar to those of a trigger diode is shown in Fig. 195. The regenerative action of this type of circuit when either transistor begins to conduct causes switching comparable to avalanching in a trigger diode. Proper biasing of this circuit yields triggering voltages of 15 volts or less. The circuit shown in Fig. 196 can deliver trigger currents as high as 1 ampere and is more than capable of triggering all RCA thyristors.

Fig. 197 shows an SCR circuit that uses the two-transistor regenerative-trigger network. The phase-shift characteristics are still retained to provide conduction



92CM-21416

Fig. 194—Circuits showing application of unijunction-transistor circuit for pulse triggering of triacs and inverse parallel SCR's: (a) triggering pulse is capacitively coupled to gate of triac; (b) triggering pulse is transformer-coupled to gates of SCR's.

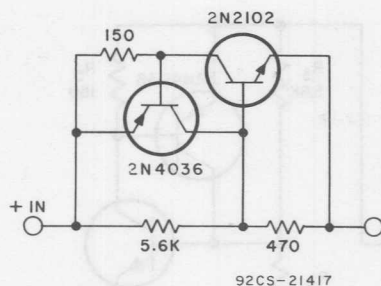


Fig. 195—Two-transistor switch. Characteristics of this circuit are similar to those of a trigger diode.

angles less than 90 degrees through the RC network of R_1 , R_2 , and C_1 . Resistor R_3 provides turn-on current to the base of Q_1 when the voltage across C_1 becomes large enough during the positive half-cycle. The base current in Q_1 turns on this transistor. Transistor

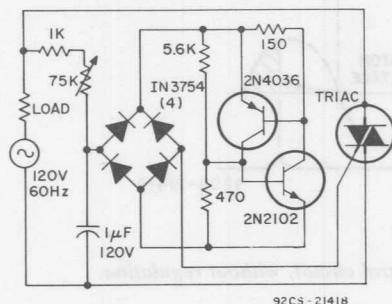


Fig. 196—Circuit showing application of two-transistor switch as thyristor triggering device.

Q_1 then supplies base current to Q_2 . When Q_2 turns on, it supplies more base current to Q_1 . This regenerative action leads to the rapid saturation of transistors Q_1 and Q_2 . Capacitor C_1 discharges through the saturated transistors into the gate of the SCR. When

the SCR fires, the remaining portion of the positive half-cycle of ac power is applied to the motor. Speed control is accomplished by adjustment of potentiometer R_1 . For the component values shown on the schematic diagram in Fig. 197, the threshold voltage for firing the circuit is approximately 8 volts, and the maximum conduction angle is approximately 170 degrees. Table XV shows values for operation of the circuit with various RCA SCR's.

An advantage of the two-transistor trigger circuit is its low threshold triggering voltage. For all practical purposes, a full 180-degree conduction angle can be obtained when an SCR is used. When two SCR's are to be triggered, a transformer must be used to couple a gate signal of the proper polarity to the SCR with the proper anode-to-cathode polarity. A triac, however, can be triggered in either direction with positive-polarity gate signals. The only requirement is that isolation be maintained between the dc and ac current.

Application Guide to Trigger Devices

Table XVI provides a quick reference to the prevalent types of applications for various triggering devices.

ISOLATED TRIGGER CIRCUITS

In many applications, phase control of a thyristor by use of an

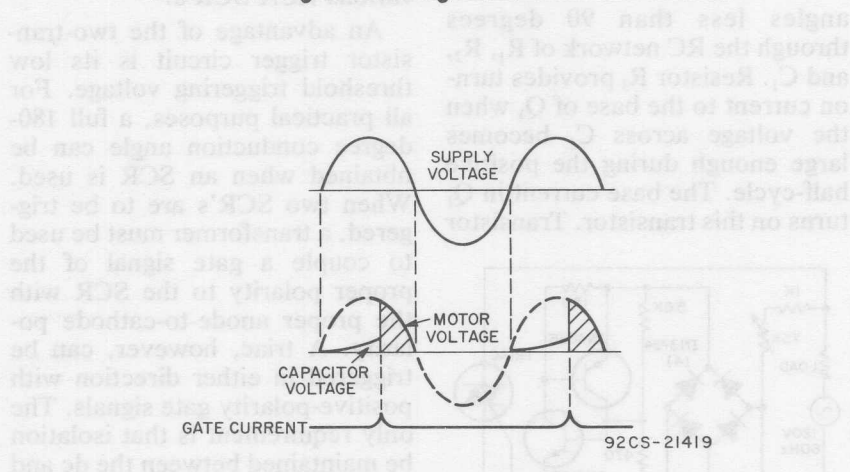
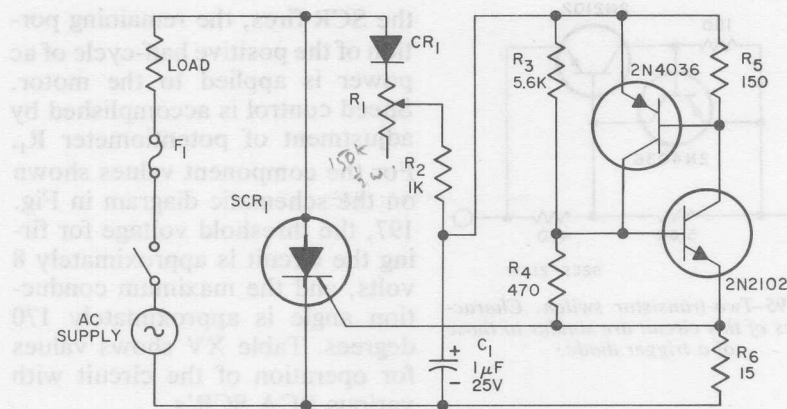


Fig. 197—Half-wave SCR motor control circuit, without regulation.

Table XV—Components For Circuit Shown in Fig. 197

AC SUPPLY	AC CURRENT	F1	CR1	R1	SCR1
120V	1A	3AG, 1.5A, Quick Act	RCA-D1201D	75K, ½W	RCA-2N3528
120V	3A	3Ab, 3A	RCA-D1201D	75K, ½W	RCA-2N3228
120V	7A	3AB, 7A	RCA-D1201D	75K, ½W	RCA-2N3669
120V	25A	3AB, 25A	RCA-D1201D	75K, ½W	RCA-2N3897
240V	1A	3AG, 1.5A, Quick Act	RCA-D1201M	150K, ½W	RCA-2N3529
240V	3A	3AB, 3A	RCA-D1201M	150K, ½W	RCA-2N3525
240V	7A	3AB, 7A	RCA-D1201M	150K, ½W	RCA-2N3670
240V	25A	3AB, 25A	RCA-D1201M	150K, ½W	RCA-2N3898

Function	Manual or Simple On-Off Power Control	Automatically Controlled or Regulated power	Power-Output Stage in Large Electronic or Electro-Mechanical System
Typical Applications	Light Dimmers Tool Speed Controls Appliance Speed Controls Gas Ignition Photoelectric Controls Static On-Off Switches	Regulated Power Supplies Temperature Controls Commercial DC Motor Drives Flashers Time Delays Static On-Off Power Relays	Bulk Power Conversion for Metal Refining and Electrochemical Processes Large Industrial Motor Drives Variable-Frequency Drives Pulse Modulators Precise Process-Temperature Controls Logic-Arrays Power Output eg.—Vending Machines —Signs and Scoreboards Computer Printer—Driver
Common Characteristics of the Application	Frequently Bidirectional Small physical size an asset Low performance demands	Frugal but not poor Both dc and ac loads Thyristor fired is higher cost Technically oriented users and applications Electrical feedback or sensor input in addition to manual control Long firing pulses often required	Firing circuit small percentage of system cost Rigid and extensive performance requirements Firing circuit often merged into other system circuits Custom engineered Primarily electrical inputs from regulators or sensors Often built up from standard logic and waveshaping circuits
Trigger Devices in Approximate Order of Preference or Use	1. Diac 2. Neon bulb 3. Four-layer diode 4. Unijunction transistor 5. Two-transistor regenerative circuit NOTE: For on-off control, a switch contact or single transistor may form the firing circuit	1. Unijunction transistor 2. Transistors 3. Integrated Circuits 4. Magnetic amplifier NOTE: Firing circuit often includes several diodes, a zener, pulse transformers, control power transformers, and numerous passive components	1. Transistors 2. Integrated Circuits

isolated, low-voltage control element is desirable. A number of techniques are available for use in this type of control.

Step-Down Transformers

A suitable step-down transformer can be used as shown in

Fig. 198 to provide isolation between the load and the control element in a thyristor power control circuit. The transformer provides impedance transformation and reflects the transformed value of potentiometer R_1 into the secondary circuit. As the potentiometer is adjusted from a maximum to a minimum value, the voltage at point A in Fig. 198 varies from a minimum to a maximum value.

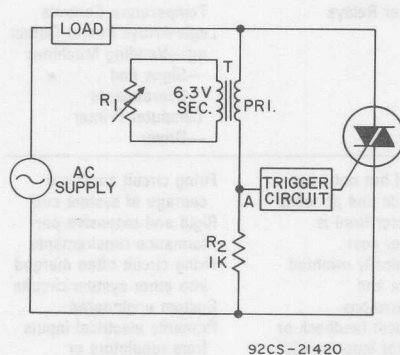


Fig. 198—Triac power-control circuit in which a step-down transformer is used to provide isolation of the control potentiometer.

The trigger circuit may be either a modified diac-resistance-capacitance network or a unijunction

type of circuit. The advantage of the circuit shown in Fig. 198 is that it provides low-voltage potentials and isolation for remote controls in a conductive environment.

Pulse Transformers

When a trigger circuit provides a fast-rising current pulse for gated turn on, a pulse transformer provides a simple form of circuit isolation between the line-voltage system and the control system. Fig. 199 illustrates this application of a pulse transformer.

Reed Relays

For applications in which an on-off switching function is required and isolation is necessary between the control circuit and load circuits, a current reed relay can be used to provide an effective method of control. The contacts of the reed relay carry only a small current, usually less than 100 milliamperes to assure an extended relay contact life. A circuit using this technique is illustrated in Fig. 200.

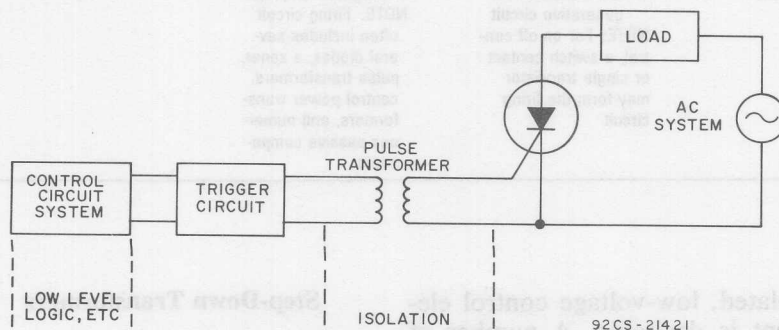


Fig. 199—SCR power-control circuit that uses a pulse transformer to provide isolation between the line voltage and the control circuit.

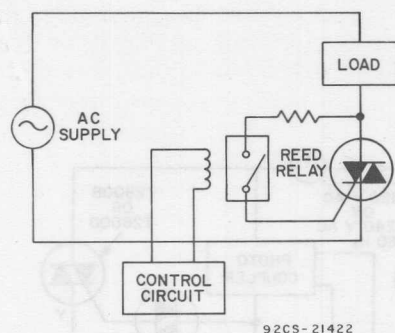


Fig. 200—Triac power-control circuit that uses a reed relay to provide isolation between the control circuit and the load.

Photocell Trigger Circuits

Optical coupling between trigger circuits and load circuits provides complete dc isolation. In addition, this technique permits variable power control as well as on-off switching control functions. The optical control element of this system is a light source of the filament type, gas-discharge type, or the light-emitting-diode (LED) type. The sensing element is a photosensitive resistor, which forms part of the gate circuit.

Photoresistors (photocells) are available in a wide range of dark-to-light resistance ratios and resistance values. Integral photocouplers which use any one of the three types of light sources described above are also available. Variable power control can be achieved by changing the resistance value of the photoresistor by use of a low-power variable-intensity light source. The range of control depends on the type of light source and photoresistor. A photoresistor can be used by itself to sense ambient light intensity for a switching

application or for modulating power as a function of ambient light intensity. Fig. 201 illustrates circuit applications using photo trigger circuits.

INTEGRATED-CIRCUIT ZERO-VOLTAGE SWITCH

The RCA-CA3059 zero-voltage switch is a monolithic integrated circuit used primarily as a trigger circuit for the control of thyristors. The multistage circuit employs a diode limiter, a threshold detector, a differential amplifier, and a Darlington output driver to provide the basic switching action. The dc supply voltage for these stages is supplied by an internal zener-diode-regulated power supply that has sufficient current capability to drive external circuit elements, such as transistors and other integrated circuits. This built-in power supply provides unique solutions to many application problems. An important feature of the CA3059 is that the trigger pulses developed by this circuit can be applied directly to the gate of a silicon controlled rectifier (SCR) or a triac. A built-in fail-safe circuit inhibits the application of these pulses to the thyristor gate circuit in the event that the external sensor for the integrated-circuit switch should be inadvertently opened or shorted.

Basic Circuit Operation

Fig. 202 shows a functional block diagram of the CA3059 integrated-circuit zero-voltage switch. Any triac that is driven directly from the output terminal of this circuit should be charac-

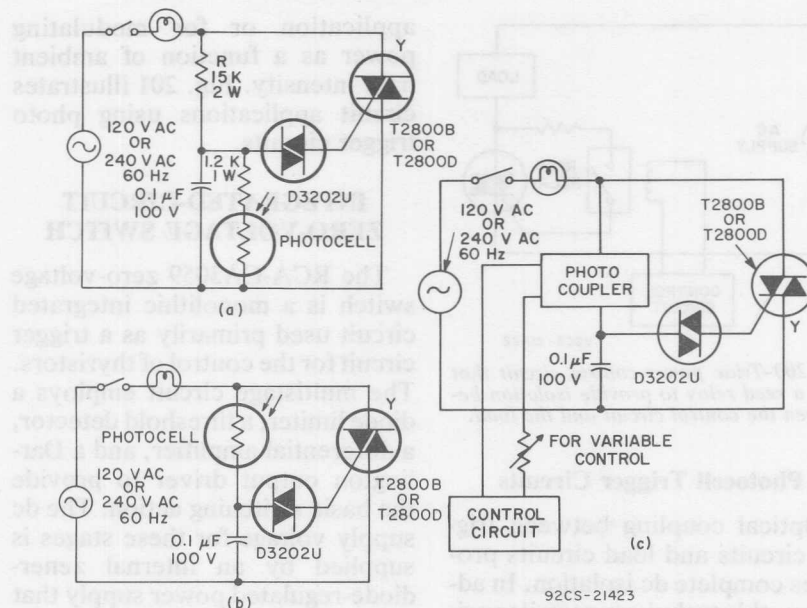


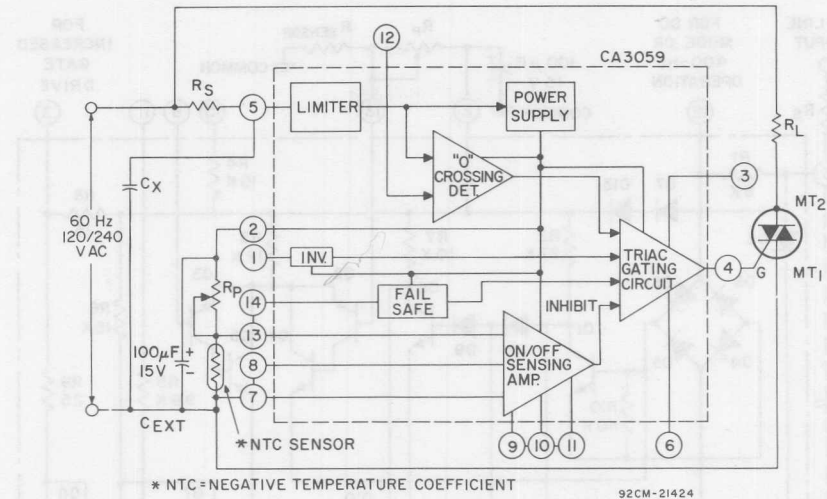
Fig. 201—Triac power-control circuits that use optical coupling to provide complete dc isolation between the control circuit and the load: (a) light-controlled turn-off circuit with photocell sensor; (b) light-control turn-on circuit with photocell sensor; (c) light-controlled turn-off circuit with photocoupler sensor.

terized for operation in the I (+) or III (+) triggering modes, i.e., with positive gate current (current flows into the gate for both polarities of the applied ac voltage).

The limiter stage of the CA3059 clips the incoming ac line voltage to approximately plus and minus 8 volts. This signal is then applied to the zero-voltage-crossing detector, which generates an output pulse during each passage of the line voltage through zero. The limiter output is also applied to a rectifying diode and an external capacitor that comprise the dc power supply. The power supply

provides approximately 6 volts as the V_{CC} supply to the other stages of the CA3059. The on/off sensing amplifier is basically a differential comparator. The triac gating circuit contains a driver for direct triac triggering. The gating circuit is enabled when all the inputs are at a high voltage, i.e., the line voltage must be approximately zero volts, the sensing-amplifier output must be "high", the external voltage to terminal 1 must be a logical "1", and the output of the fail-safe circuit must be "high".

Fig. 203 shows the circuit diagram of the CA3059. The zero-voltage threshold detector consists of diodes D₃, D₄, D₅, and D₆,



AC Input Voltage (Volts) 50/60 or 400 Hz	Series Resistor R_S (k Ω)	Power Rating of R_S (Watts)
24	2	0.5
120	10	2
208/230	20	4
277	25	5

Fig. 202—Functional block diagram of the integrated-circuit zero-voltage switch

and transistor Q_1 . The differential amplifier consists of transistor pairs Q_2 - Q_4 and Q_3 - Q_5 . Transistors Q_1 , Q_6 , Q_7 , Q_8 , and Q_9 comprise the triac gating circuit and driver stage. Diode D_{12} , zener diode D_{15} , and transistor Q_{10} constitute the fail-safe circuit. The power supply consists of diodes D_7 and D_{13} , and an external resistor and capacitor

connected to terminals 5 and 2, respectively, and to ground through pin 7. If the transistor pair Q_2 - Q_4 and transistor Q_1 are turned off, an output appears at terminal 4. Transistor Q_1 is in the off state if the incoming line voltage is less than approximately the voltage drops across three silicon diodes (2.1 volts) for either the positive

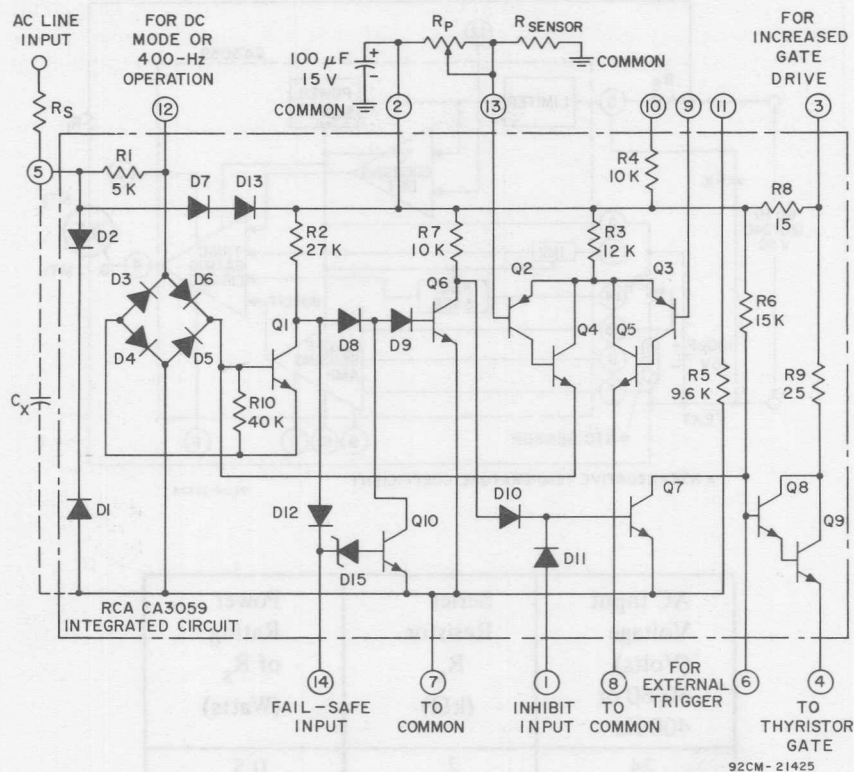


Fig. 203—Circuit diagram for the CA3059 zero-voltage switch.

or negative excursion of the line voltage. Transistor pair Q_2 - Q_4 is off if the voltage across the sensor, connected from terminals 13 to 7, exceeds the reference voltage from 9 to 7. If either of these conditions is not satisfied, pulses are not supplied to terminal 4. Fail-safe operation requires that terminal 13 be connected to 14. The addition of hysteresis and elimination of half-cycling can be obtained by a resistive voltage divider connected from 13 to 8 and from 8 to 7.

Fig. 204 shows the position and width of the pulses supplied to the

gate of a thyristor with respect to the incoming ac line voltage. The

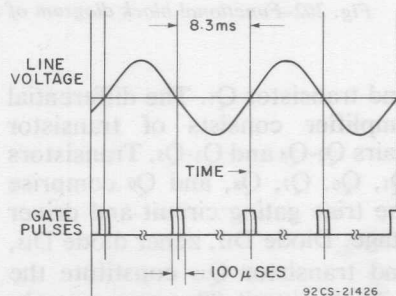


Fig. 204—Timing relationship between the output pulses of the CA3059 and the ac line voltage.

voltage and current to trigger most RCA thyristors at ambient temperatures of 25°C. However, under worst-case conditions (i.e., at ambient-temperature extremes and maximum triggering requirements), selection of the higher-current thyristors may be necessary for particular applications.

Effect of Zero-Voltage Switch on Thyristor Load Characteristics

The CA3059 is designed primarily to gate a thyristor that switches a resistive load. Because the output pulse supplied by the CA3059 is of short duration, the latching current of the triac becomes a significant factor in determining whether other types of loads can be switched. (The latching-current value determines whether the triac will remain in conduction after the gate pulse is removed.) Provisions are included in the CA3059 to accommodate inductive loads and low-power loads. For example, for loads that are less than approximately 4 amperes rms or that are slightly inductive, it is possible to retard the output pulse with respect to the zero-voltage crossing by insertion of the capacitor C_x from terminal 5 to terminal 7 as shown in Fig. 202. The insertion of capacitor C_x permits switching of triac loads that have a slight inductive component and that are greater than approximately 200 watts (for operation from an ac line voltage of 120 volts rms). However, for loads less than 200 watts (for example, 70 watts), it is recommended that the user employ the

with the CA3059 because of the low latching-current requirement of this triac.

For loads that have a low power factor, such as a solenoid valve, the user may operate the CA3059 in the dc mode. In this mode, terminal 12 is connected to terminal 7, and the zero-crossing detector is inhibited. Whether a "high" or "low" voltage is produced at terminal 4 is then dependent only upon the state of the differential comparator within the CA3059 integrated circuit, and not upon the zero crossing of the incoming line voltage. Of course, in this mode of operation, the CA3059 no longer operates as a zero-voltage switch. However, for many applications that involve the switching of low-current inductive loads, the amount of RFI generated can frequently be tolerated.

Fail-Safe Feature

As shown in Figs. 202 and 203, when terminal 13 is connected to terminal 14, the fail-safe circuit of the CA3059 is operable. If the sensor should then be accidentally opened or shorted, power is removed from the load (i.e., the triac is turned off). The internal fail-safe circuit functions properly, however, only when the ratio of the sensor impedance at 25°C, if a thermistor is the sensor, to the impedance of the potentiometer R_p is less than 4 to 1. It is readily apparent that, if the potentiometer is adjusted for 1000 ohms and the sensor is 100,000 ohms, the zener diode D_{15} (shown in Fig. 203)

cycling phenomenon at the control point. Fig. 206 illustrates this phenomenon. The CA3059 senses the zero-voltage crossing every half-cycle, and an output, for example pulse No. 4, is produced to indicate the zero crossing. During the remaining 8.3 milliseconds, however, the differential amplifier in the CA3059 may change state and inhibit any further output pulses. The uncertainty region of

the differential amplifier, therefore, prevents pulse No. 5 from triggering the triac during the negative excursion of the ac line voltage.

Sever oleexist for elimination of the half-cycling phenomenon. If the user can tolerate some hysteresis in the control, then positive feedback can be added around the differential amplifier.

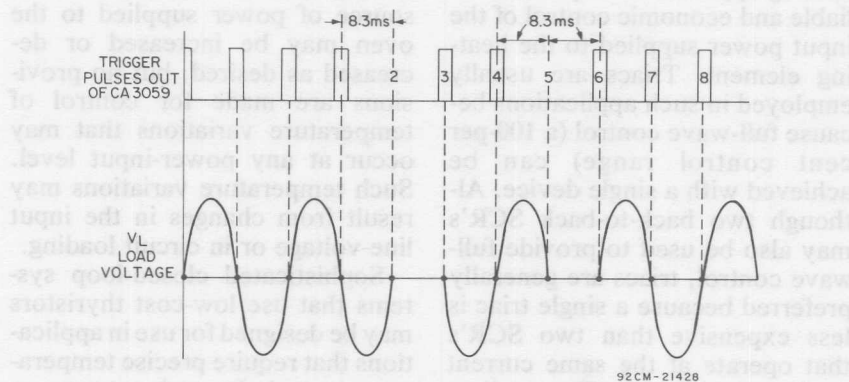


Fig. 206—Half-cycling phenomenon in the CA3059.

Heating Controls

Thyristors may be used in most heating applications to provide reliable and economic control of the input power supplied to the heating element. Triacs are usually employed in such applications because full-wave control (a 100-per cent control range) can be achieved with a single device. Although two back-to-back SCR's may also be used to provide full-wave control, triacs are generally preferred because a single triac is less expensive than two SCR's that operate at the same current performance level. The application of power to the heating element may be controlled by a single SCR for applications in which half-wave control is adequate. An SCR and diode combination is used when only limited control is required and an always-on system is desired.

GENERAL DESIGN CONSIDERATIONS

The temperature of the heat acceptor can be controlled to an accuracy of $\pm 20^{\circ}\text{C}$ by use of relatively simple open-loop systems, i.e., systems in which no feedback is received from the heat acceptor.

A typical example is an oven-heating system in which a variable source of power supplied to the oven may be increased or decreased as desired, but no provisions are made for control of temperature variations that may occur at any power-input level. Such temperature variations may result from changes in the input line voltage or in circuit loading.

Sophisticated closed-loop systems that use low-cost thyristors may be designed for use in applications that require precise temperature control. In such systems, a sensor is used to monitor the temperature of the heat acceptor, and an error (feedback) signal is developed to indicate whether the amount of power delivered to the heating element should be increased or decreased. The system operates in response to the feedback signal to compensate for the effects of any change in line voltage or circuit loading; as a result, variations in the temperature of the heat acceptor can be limited to very small values. With a closed-loop system, a control accuracy within $\pm 0.5^{\circ}\text{C}$ is readily achieved.

An important practical consideration for heating-control sys-

tems is that when power is added to or removed from the ac line, the increments of change in power level should not exceed 5 kilowatts. This limitation is necessary to assure that transient effects produced by the power switching do not interfere with other electronic equipment on the same ac line. These increments of power level can be easily controlled by use of digital circuitry and low-level control circuits.

In heating systems that use air as a heat-transfer medium, modulation of the air flow may be necessary to match the amount of heat energy being produced. With this technique, a minimum amount of heat can be provided at a low speed to reduce the temperature difference between the heated area and the stagnant air.

In many applications, isolation of the sensor and associated circuitry from the triac and ac line are desirable. As explained previously in the section on **Isolated Trigger**

Circuits, either optical or magnetic techniques may be employed to provide this isolation. In polyphase control circuits this type of isolation is essential. Typical isolation circuits and techniques used in such applications are described in the section on **Three-Phase Triac Controls**.

BASIC HEAT-CONTROL TECHNIQUES

Manual adjustment of the output of electrical heaters can be provided over an infinite range by use of the phase-control techniques described in the section on **Thyristor Triggering**. Automatic temperature regulation may be incorporated into phase-control systems by the addition of a firing circuit that adjusts the conduction angle of the thyristor in response to feedback from a temperature sensor, such as a thermistor.

Fig. 207 shows a simple full-

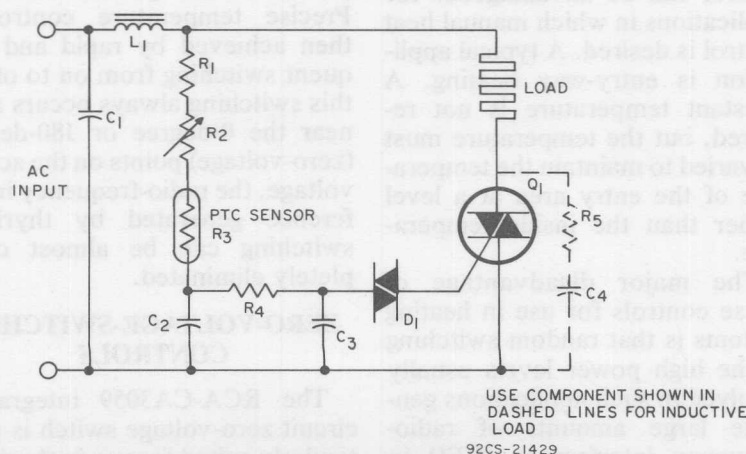


Fig. 207—Phase-control type of triac heat-control circuit.

wave heat-control circuit that employs the phase-control technique. This circuit illustrates a rather crude, but usable approach to heat control that may be employed for hot plates, solder pots, and other non-critical appliances. The circuit employs the basic two-time-constant phase-control configuration. A description of the operation and basic features of this type of circuit configuration is given in the section on **Lighting Controls**.

The range of the positive-temperature-coefficient (PTC) sensor must be sufficient to provide the desired control. Care must be taken to assure that the sensor is not self-heated as a result of the current that flows through it. The triac Q_1 provides full-wave control so that the amount of dc component on the ac line is very small.

If the sensor is replaced by a short circuit, an open-loop control is obtained. (The value of resistor R_2 must be increased.) Open-loop control can be advantageous for applications in which manual heat control is desired. A typical application is entry-way heating. A constant temperature is not required, but the temperature must be varied to maintain the temperature of the entry area at a level higher than the inside temperature.

The major disadvantage of phase controls for use in heating systems is that random switching of the high power levels usually involved in such applications generate large amounts of radio-frequency interference (RFI) in nearby electrical equipment and

particularly in standard AM broadcast-band receivers. In the phase-control circuit shown in Fig. 207, the capacitor C_1 and the inductor L_1 form a filter network that is used to limit the RFI produced by the circuit. The value (and size) of inductor L_1 must be increased as the load is increased. At higher power levels, this requirement often causes packaging difficulties and substantially increases the over-all cost of the circuit. For this reason, zero-voltage switching is used for most heater controls.

The thermal-response time of a heater is generally much longer than the period of the ac line frequency. Modulation of the heater output, therefore, may be accomplished by application of full power to the load for a short time and complete removal of the power for a period of time. If the control circuit is made sufficiently sensitive to temperature changes, an extremely small temperature differential can be maintained between power-on and power-off states. Precise temperature control is then achieved by rapid and frequent switching from on to off. If this switching always occurs at or near the 0-degree or 180-degree (zero-voltage) points on the ac line voltage, the radio-frequency interference generated by thyristor switching can be almost completely eliminated.

ZERO-VOLTAGE-SWITCHED CONTROLS

The RCA-CA3059 integrated-circuit zero-voltage switch is particularly suited for use in thyristor temperature-control applications.

The integrated circuit may be employed as either an on-off type of controller or a proportional controller, depending upon the degree of temperature regulation required. The availability of numerous terminal connections to internal circuit points greatly increases the flexibility of the CA3059 and permits the circuit designer to exercise his creativity to employ the integrated switch in unique ways. A detailed description of the CA3059 and the block diagram (Fig. 202) and schematic (Fig. 203) of this integrated circuit are

provided in the earlier section on **Thyristor Triggering.**

On-Off Control

Fig. 208 shows a simple zero-voltage-switching control that uses a CA3059 and a triac. By selecting the triac for the current level involved, this simple circuit can control heater power at current and voltage levels from 2.5 amperes and 24 volts to 80 amperes and 600 volts. The components that must be changed for operation at different power levels are the series resistor R_S and the

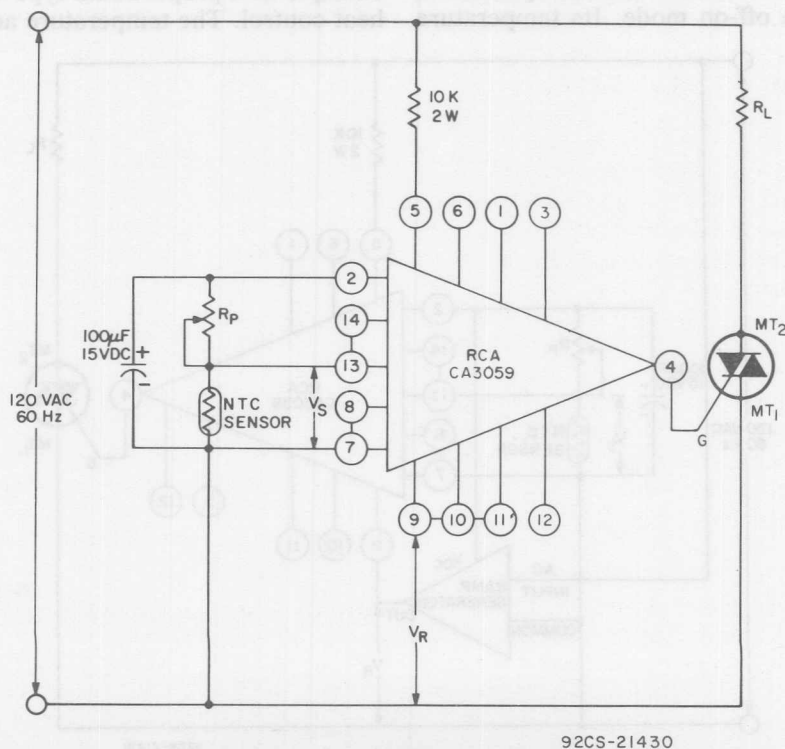


Fig. 208—On-off temperature controller.

triac. The chart shown with the functional diagram of the CA3059 in Fig. 202 illustrates the easy way in which circuits that use this integrated-circuit zero-voltage switch can be changed to accommodate various line voltages.

The circuit shown in Fig. 208 requires a negative-temperature-coefficient (NTC) thermistor for proper operation. If terminals 9 and 13 of the CA3059 are interchanged, positive-temperature-coefficient thermistors can be used, and advantage can then be taken of the shorted- and open-circuit fail-safe provisions of the CA3059.

The heater control operates in the off-on mode. Its temperature

accuracy depends on the differential input sensitivity of the CA3059, or the thermistor used, and, to some extent, on the level of the temperature being controlled. This behavior is controlled by the slope of the decrease in thermistor resistance with increasing temperature. These effects must be accommodated during the design of the circuits.

Proportional Heating Controls

When precise temperature control is required, closed-loop proportional control is recommended. Fig. 209 shows a typical example of a proportional type of heat control. The temperature ac-

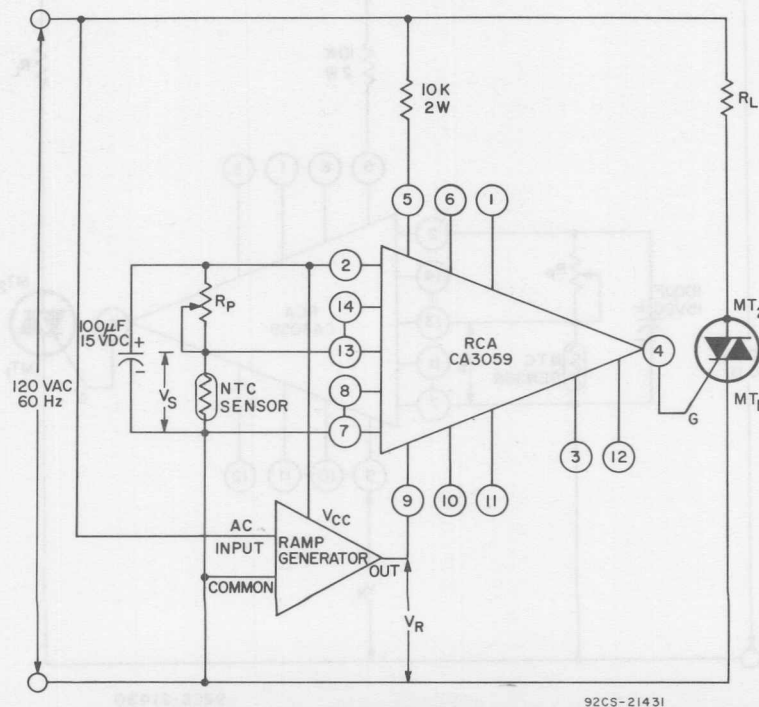


Fig. 209—Proportional temperature controller.

curacy of this circuit, which depends on the input sensitivity of the CA3059, the thermistor used, and the level of temperature being controlled, is in the order of $\pm 0.2^\circ\text{C}$.

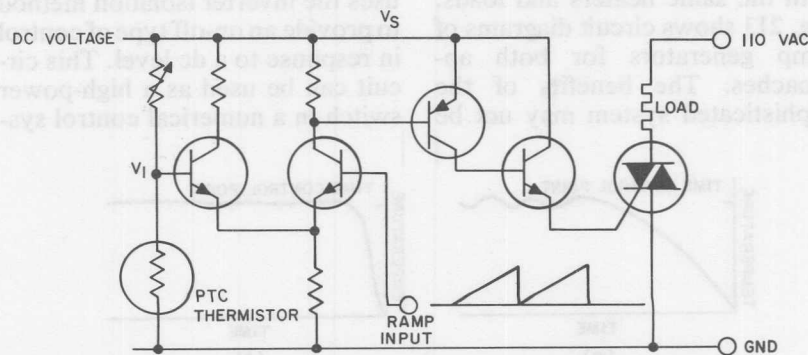
In proportional-control systems, either of two basic approaches may be used depending upon the performance desired. The simpler approach is to use a reference ramp that has an amplitude almost equal to the voltage swing that exists. A more sophisticated approach is to use a limited ramp that covers the set point.

Fig. 210 shows a basic circuit that may be used to perform the comparison between the reference ramp and a voltage divider formed by the sensor and calibration resistor. In the large-ramp approach, the ramp voltage varies from 0 volts to the voltage V_s . With this approach, the triac is not gated when the magnitude of the ramp voltage is less than the voltage V_1 . This mode of oper-

ation produces an "on" period that decreases as the sensor temperature increases, as shown in Fig. 211.

Fig. 211 shows that, as the value of the reference voltage V_1 varies, the length of time the triac is on changes. The triac is never off all the time. The increments of power are based on the number of line voltage half-cycles that occur during the time-based period. A half-second time base allows 60 half-cycle periods of operation. The heat can then be changed in increments of $(1/60)$ 100 or 1.6 per cent; if finer control is desired, the time base must be lengthened. The maximum amount of heating power that can be controlled is easily changed by selection of different triac and heater combinations. The increments of heat produced by this type of circuit are a function of the time base, the heater, and the differential-amplifier resolution.

In the more sophisticated limited-ramp approach, the ramp



92CS-21432

Fig. 210—Basic circuit for comparison of ramp voltage and reference voltage in a proportional temperature controller.

voltage traverses only small increments. In this case, the ramp voltage may vary from 0.4Vs to 0.6Vs. The heater receives full power until the voltage V_1 rises to 0.4Vs. At this point, the power

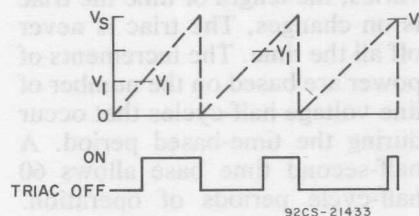


Fig. 211—Waveform showing effect of the relative amplitude of the ramp voltage and the reference voltage on the conduction time of the triac.

supplied to the heater starts to decrease, and the heater is totally off when the voltage V_1 reaches 0.6Vs. This type of operation provides minimum warm-up time and the fastest response to loading. It is particularly useful in temperature-controlled processes. Fig. 212 compares the two approaches to proportional control with the same heaters and loads. Fig. 213 shows circuit diagrams of ramp generators for both approaches. The benefits of the sophisticated system may not be

needed in all applications, and care must be exercised to assure that the added cost is warranted. A complete heater control that uses the sophisticated type ramp generator is shown in Fig. 214.

Heat Controls With Isolated Sensors

In many industrial controls, isolation of the sensor from the thyristor and ac line is required. The main premise is to provide adequate operation and at the same time isolate the input from the power lines. Three schemes for achieving this isolation are shown in Figs. 215, 216, and 217.

Fig. 215 shows an isolation system that uses a low-voltage transformer and pulse transformer to provide sensor isolation and low-voltage operation of the CA3059. This circuit is a typical example of a heat-control circuit used in industrial applications.

Fig. 216 illustrates the use of an inverter stage for input isolation. The circuit shown in Fig. 216 (a) uses the inverter isolation method to provide an on-off type of control in response to a dc level. This circuit can be used as a high-power switch in a numerical control sys-

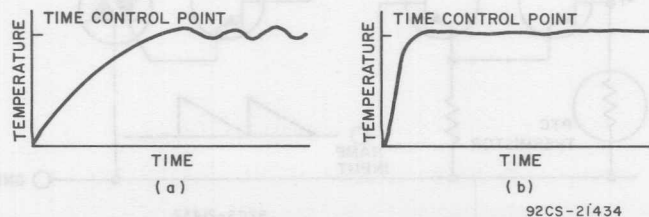
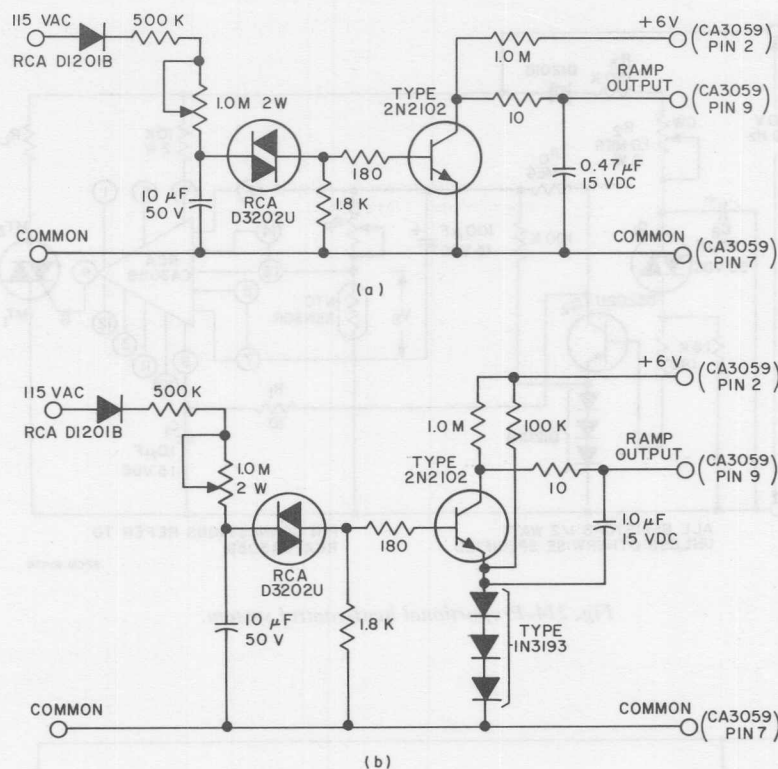


Fig. 212—Response characteristics for (a) elementary and (b) sophisticated proportional heat-control systems.



92CM-21435

Fig. 213—Ramp generators: (a) ramp amplitude from 0 to 6 volts; (b) ramp amplitude limited to 1.5 volts to 6 volts.

tem. In effect, it is simply a form of a solid-state ac relay and may be used for many other types of applications in addition to that of heating control.

Fig. 216 (b) shows the use of an inverter as an interface between a complex control system and the CA3059-triac combination. This type of circuit is usually employed for industrial control circuits in which the sensor is coupled to low-level logic systems. A control circuit of this type may also be used with polyphase systems to

provide isolation between phases. This isolation is accomplished most economically by use of multiple secondary windings. As the output of the inverter is coupled to the differential input of the CA3059, very little output current is required and power consumed by the inverter is basically its inherent losses.

Fig. 217 shows a system in which optical coupling is used to provide input isolation. Incandescent lamps, neon lamps, or light-emitting diodes may be used.

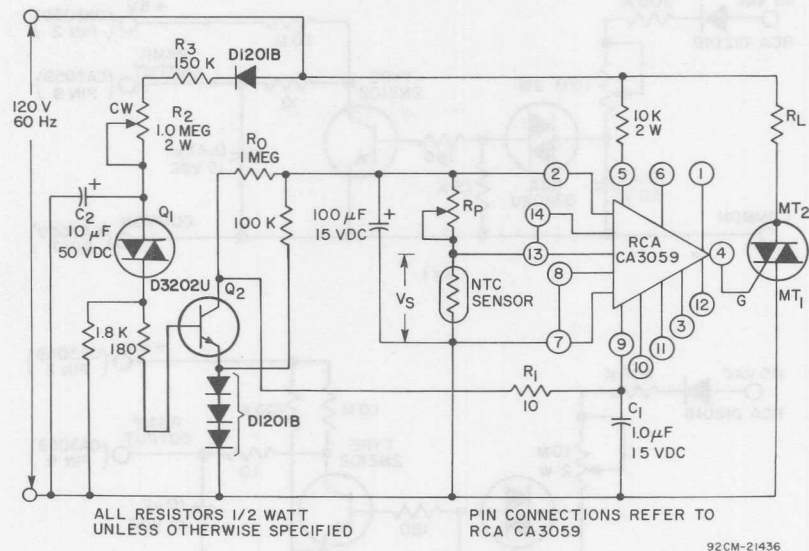


Fig. 214—Proportional heat-control system.

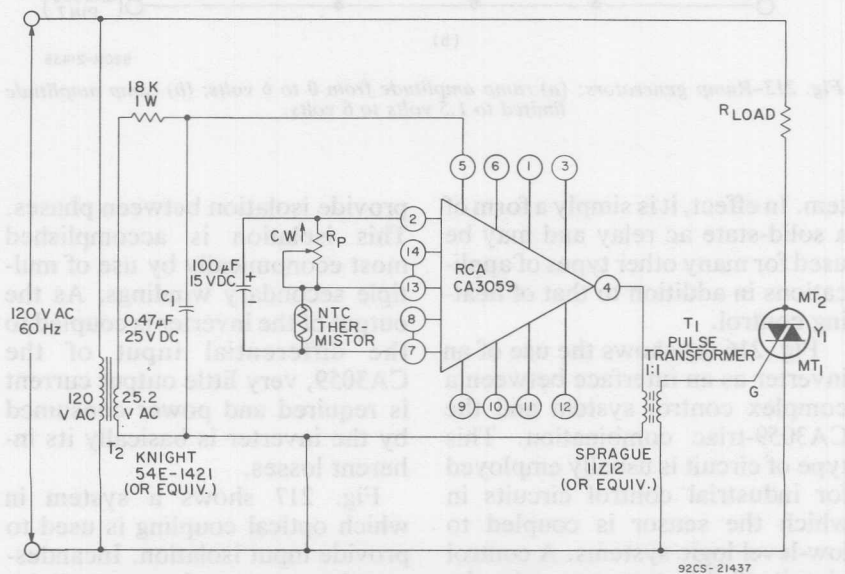


Fig. 215—On-off controller that uses a step-down transformer to provide isolation of the sensor.

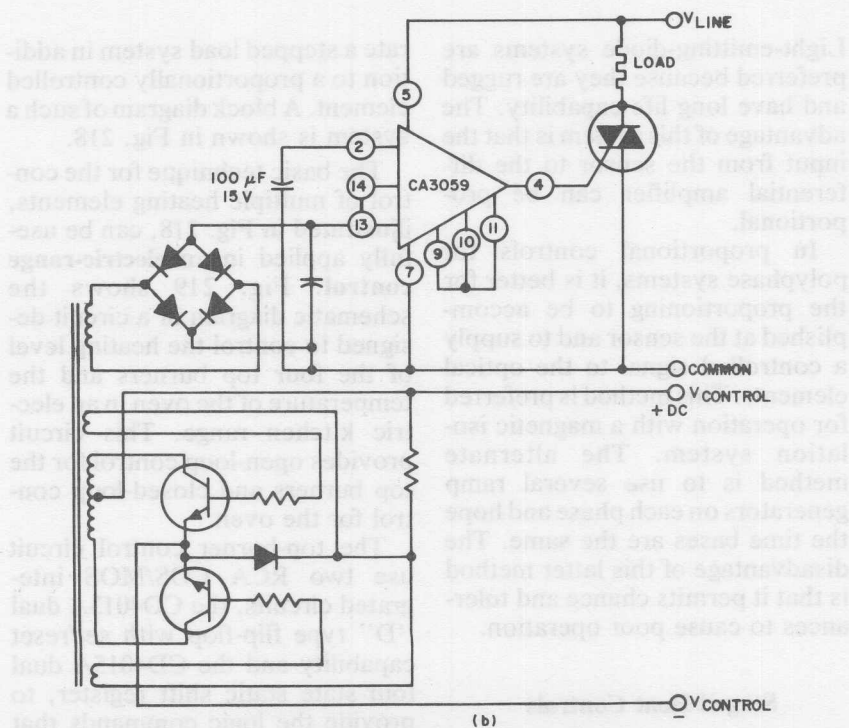
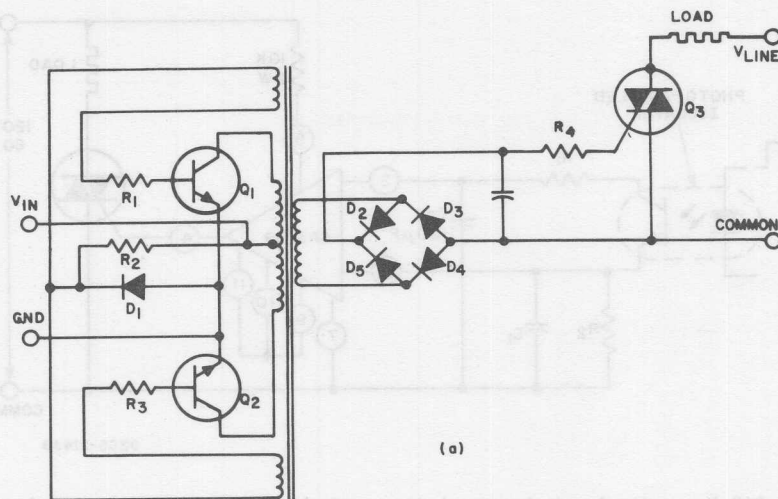


Fig. 216—Proportional heat controls that use an inverter stage to provide input isolation.

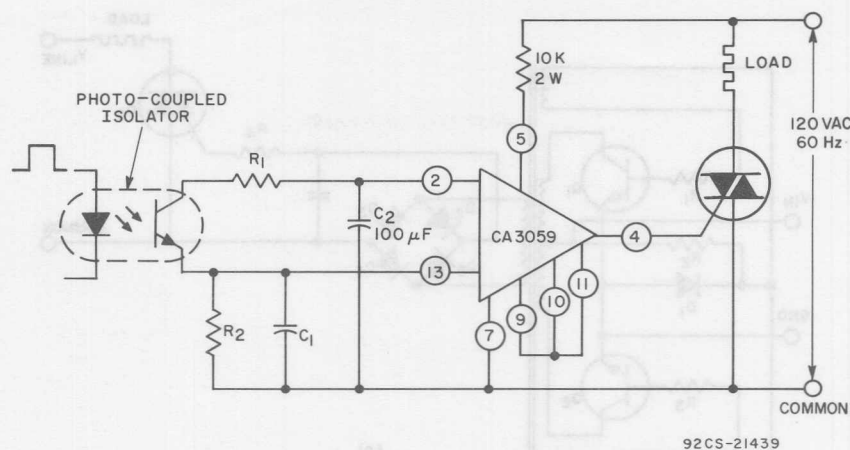


Fig. 217—Proportional control system that uses optical coupling to provide input isolation.

Light-emitting-diode systems are preferred because they are rugged and have long life capability. The advantage of this system is that the input from the sensor to the differential amplifier can be proportional.

In proportional controls for polyphase systems, it is better for the proportioning to be accomplished at the sensor and to supply a controlled signal to the optical elements. This method is preferred for operation with a magnetic isolation system. The alternate method is to use several ramp generators on each phase and hope the time bases are the same. The disadvantage of this latter method is that it permits chance and tolerances to cause poor operation.

Staged Heat Controls

In high-power systems (5 kW or higher), it is advisable to incorpo-

rate a stepped load system in addition to a proportionally controlled element. A block diagram of such a system is shown in Fig. 218.

The basic technique for the control of multiple heating elements, illustrated in Fig. 218, can be usefully applied in an **electric-range control**. Fig. 219 shows the schematic diagram of a circuit designed to control the heating level of the four top burners and the temperature of the oven in an electric kitchen range. This circuit provides open-loop control for the top burners and closed-loop control for the oven.

The top-burner control circuit use two RCA COS/MOS integrated circuits, the CD4013A dual "D" type flip-flop with set/reset capability and the CD4015A dual four-state static shift register, to provide the logic commands that control the application of power to each top-burner heating element.

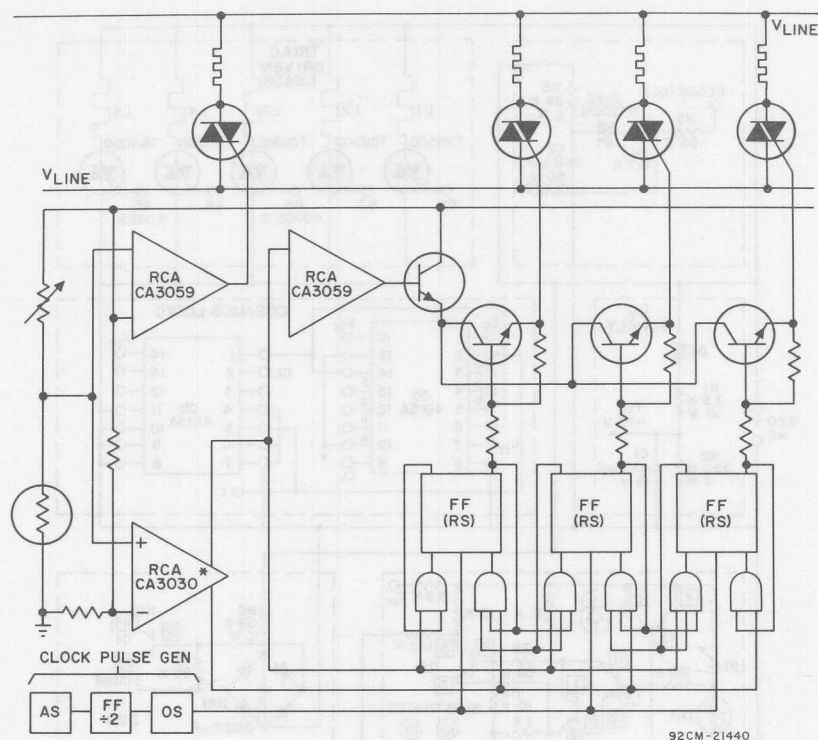


Fig. 218—Non-isolated staged heat control.

The two sections of the CD4015A are serially connected to form an eight-stage register that provides the command signal to initiate the zero-voltage triggering of the triacs in series with each top-burner heating element. The CD4013A flip-flop is used to reset the register. Figs. 220 and 221 show the functional and logic diagrams for the CD4013A and CD4015A COS/MOS integrated circuits. Detailed information on the operation of COS/MOS flip-flops and registers is given in the **RCA COS/MOS Integrated Circuit**

Manual, Technical Series CMS-271, and definitive characteristics and ratings data on the CD4013A and CD4015A are given in the **RCA Solid-State Data Book SSD-203** or Technical Bulletin File No. 279.

As shown in Fig. 219, the top-burner control circuits employ a number of multiplexed functions in which the logic commands for dc zero-voltage triac switching and for register shifts are shared by the four top-burner heating elements (L_1 through L_4). Fig. 222 through 224 shows the output waveforms

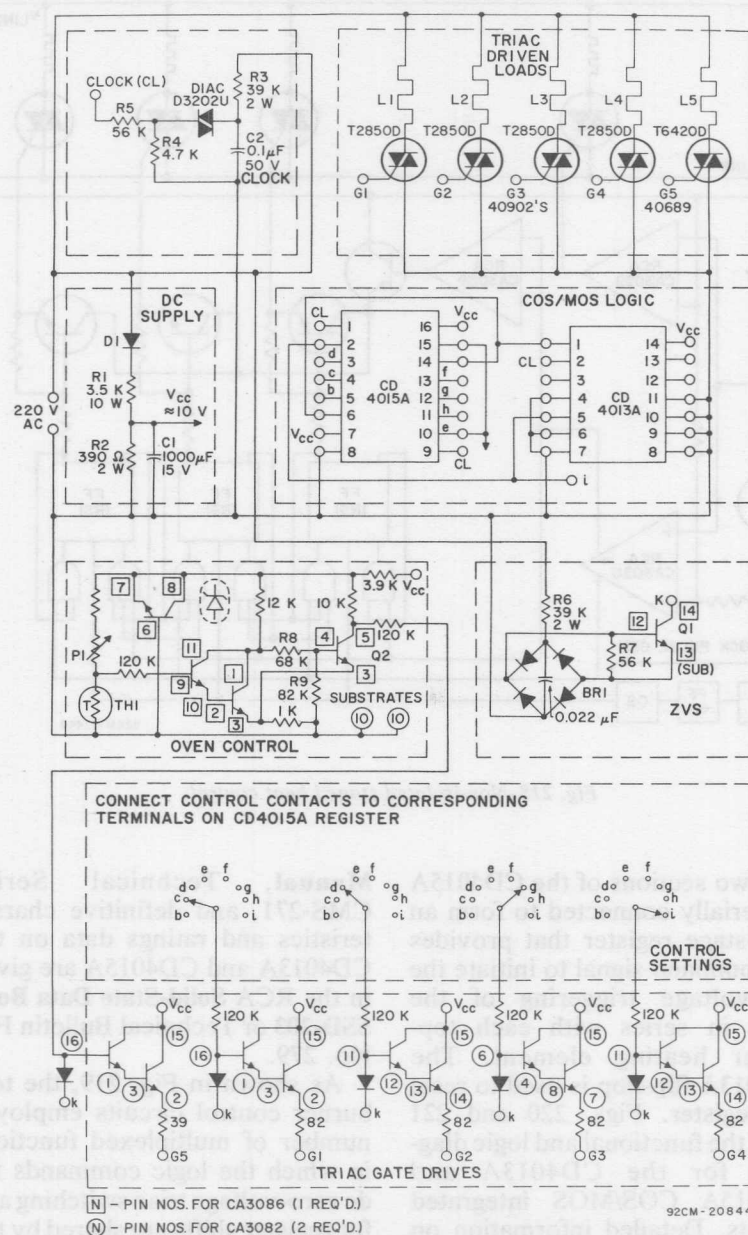


Fig. 219—Electric-range heater control.

7

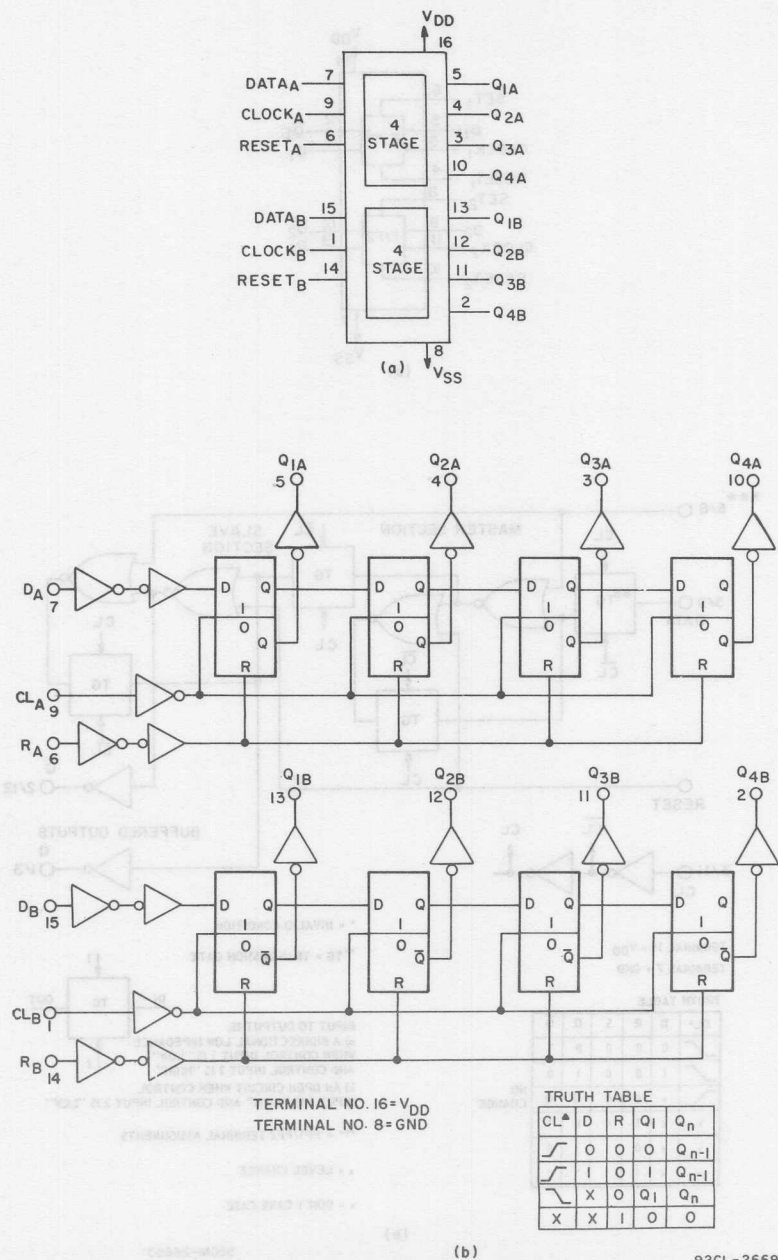


Fig. 221—RCA-CD4015A COS/MOS dual four-stage shift register; (a) terminal-connection diagram; (b) logic diagram and "truth" table.

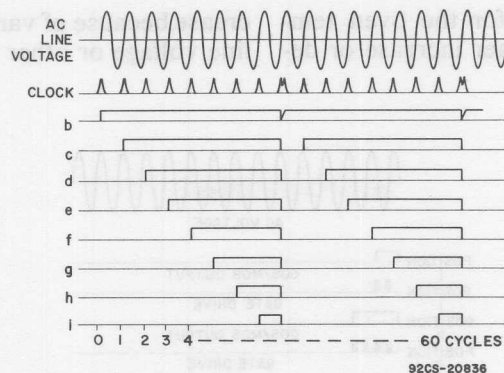


Fig. 222—Output waveforms for COS/MOS logic circuit.

from the COS/MOS circuits, the load-current waveforms, and the gate drive relationships to these waveforms for different settings of the top-burner temperature selectors.

Two RCA-CA3082 integrated-circuit n-p-n transistor arrays are used to develop the gate drive for the top-burner and the oven triacs (T_1 through T_5). Pairs of the array transistors are interconnected in Darlington configurations to supply the required gating signals to

the individual triacs when the proper logic commands are received from the top-burner COS/MOS logic circuits or the oven-control circuits.

The oven-control circuit uses an RCA-CA3086 integrated-circuit n-p-n array interconnected in a closed-loop configuration to develop the command signals that control the application of power to the oven heating element. The dc supply voltage and zero-voltage triac switching in these circuits are also incorporated as multiplexed functions. A negative-temperature-coefficient (NTC) thermistor is used as the feedback sensor element required in a closed-loop system. If the oven temperature varies above or below a preselected value (determined by the setting of the oven-temperature potentiometer), the resistance of the thermistor changes. This change in thermistor resistance results in an error signal that allows the control circuit to compensate automatically for

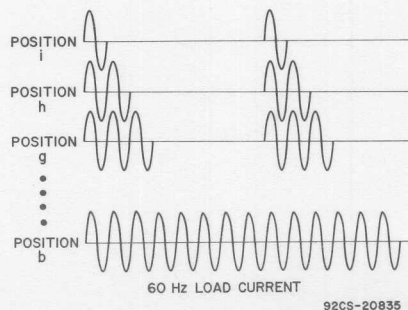


Fig. 223—60-Hz load current waveforms for various positions of temperature selector.

any tendency for the oven temperature to either increase or decrease because of variations in the line voltage or other factors.

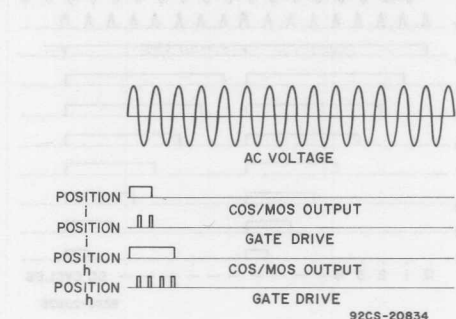


Fig. 224—Gating relationships for electric-range heat control.

Incandescent Lighting Controls

A popular application of thyristors, particularly of triacs, is in controls for incandescent lighting systems, such as lamp dimmers, traffic-signal lights, and warning flasher lights. In addition, triacs may be used to advantage in bulb preheat circuits that are employed to maintain the temperature of lamp filaments at a point just below that required for incandescence. Use of bulb preheat circuits makes it possible to avoid high initial current surges that result when full turn-on power is first applied to an incandescent lamp because of the low resistance of the cold filament.

SURGE-CURRENT CONSIDERATIONS

An important consideration in the design of triac control circuits for incandescent lighting systems is the load and its effect on the requirements of the triac. Obviously, the triac must be capable of handling the steady-state load current. In addition, however, the triac should be capable of withstanding transient current surges that may result from bulb flashover or cold-filament inrush current.

Flashover

A short-duration, extremely high-current surge through the triac is initiated when a lamp filament ruptures. The rupture is most likely to occur as a result of a termination in bulb life; however, it can be caused by a mechanical shock. The mechanism of flashover is initiated by the gap formed when rupturing occurs. The instantaneous value of line voltage across the break sets up an electric field that ionizes the gases in close proximity to the gap. The ionized gases, usually argon and nitrogen, provide an electrical conduction path across the gap, and the resulting current heats and ionizes more gases until an arc is formed across the filament lead-in wires. The arc is maintained as long as the regenerative heating and ionization continue. Finally, because of either increasing arc length or decreasing ac line voltage, or both, the electric field becomes too weak to sustain the arc, and the arc is extinguished.

Fig. 225 shows a flashover current pulse. Its magnitude and duration depend on many factors.

The actual peak magnitude of the source voltage, the voltage phase at the instant of filament rupture, and the impedance of the lead wires and other circuitry (including RFI filters) all affect the duration and magnitude of the surge. Typical values can be given for the stress of flashover at a load center point. For bulbs of less than 75 watts, the duration of the surge can be typically less than 2 milliseconds. For bulbs of 100 to 150 watts, the duration of the surge can be typically less than 4 milliseconds. The magnitude of surge can vary considerably, with

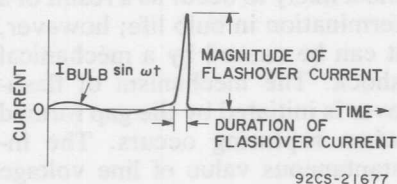


Fig. 225—Flashover current at peak voltage point.

typical peak values ranging from 80 to 200 amperes when the flashover occurs near the maximum voltage point. If the flashover occurs at a zero-voltage crossing, the current surge may be reduced as a result of the dependence of the magnitude on the voltage phase at rupture.

Because of the short duration of the flashover current, it is usually difficult to provide circuit fuse protection against flashover. Most incandescent bulbs are provided with a fuse built into one of the lead-in wires. This built-in fuse is not 100-per-cent effective against

flashover and, therefore, cannot be depended upon to protect the triac.

Inrush Current

In tungsten-filament lamps, the cold filament resistance is approximately $1/18$ to $1/12$ of the hot filament resistance. The actual currents in a circuit under inrush and steady-state conditions do not vary in these ratios, however, because of the inductance and external limiting resistance of the circuitry, including the lead-in wires to the bulb. Furthermore, it is obvious that the highest inrush current will occur at the peak of the voltage sine wave in a lamp load circuit. If switching occurs at any other phase of the voltage sine wave, the peak current through the bulb is less than "worst case." Typically, the maximum inrush peak current can be ten times as great as the steady-state peak current, while the peak inrush current with zero-voltage switching can be approximately five times as great as the steady-state peak current, as shown in Fig. 226. Thus zero-voltage switching of a lamp effects a soft turn-on that reduces the initial peak of inrush current by half and greatly increases bulb life. This increase of bulb life by zero-voltage switching has been verified by test results; an increase in life of approximately ten times, with a 90 per cent confidence level, has been reported. Thus, maintenance costs are reduced and system reliability increased.

Fig. 226 shows how the current in a lamp circuit decreases to the steady-state value. The rate of decrease depends upon the thermal time constant of the tungsten filament. A 100-watt bulb typi-

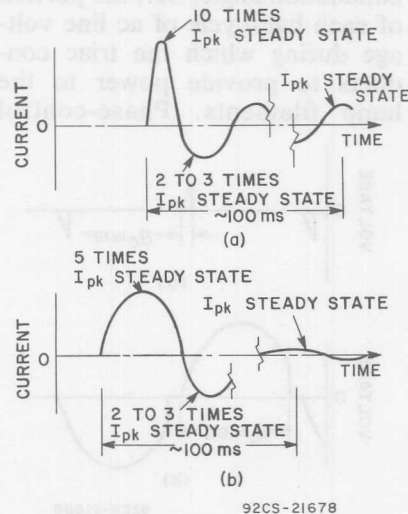


Fig. 226—(a) Inrush current at peak voltage point and (b) inrush current at zero-voltage point.

cally might reach steady-state current within 100 milliseconds after turn-on, while a 1000-watt bulb typically requires 200 milliseconds to reach its steady-state current condition.

Fuses

Flashover and inrush can occur in combination. Because a bulb is exposed to its most severe normal operating stress during inrush, the weakest spot of the filament often ruptures and causes a flashover at turn-on. Most often, switching and flashover occur at some point other than the peak voltage; there-

fore, the resulting peak current is usually within the handling capability of the triac.

Fuses in incandescent-lamp circuits must not blow under the stress of inrush current, yet must blow under flashover current. For low-power bulbs, the flashover current is substantially greater than the peak inrush current, and fuse protection is simple. For example, a 100-watt bulb might have a typical flashover current of 100 to 200 amperes and a typical inrush current of 10 amperes. For large-wattage bulbs, however, fusing is difficult. For a 1000-watt bulb, the peak flashover current might still be between 100 and 200 amperes, while the peak inrush current is approximately 120 amperes. Fuses set to blow at 150 amperes peak flashover current of short duration may also blow under the long-duration, slightly-lower-amplitude stress of inrush. As a result, a fusing solution to the problem of triac protection would be marginally reliable. One solution is to use a 40-ampere triac (available in the RCA-2N5443 series), which has a single-cycle surge capability of 300 amperes, to control this 10-ampere load. Here again, system reliability would be improved, and maintenance costs reduced.

FILAMENT PREHEAT CIRCUIT

Fig. 227 shows a filament preheat circuit that may be used to reduce the initial inrush current of an incandescent lamp. In this circuit, when transistor Q_1 is off, the logic interfacing triac T_1 is also

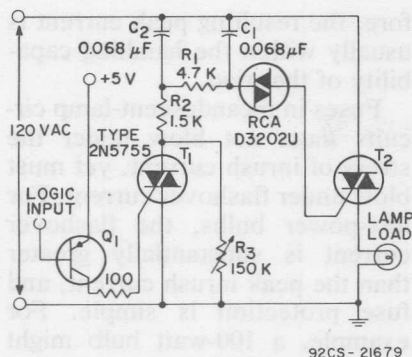


Fig. 227—A circuit including a filament preheat arrangement.

off. Resistor R_3 , which can be a fixed resistor of approximately 98 kilohms, is set so that triac T_2 is fired for only a small portion of the voltage cycle. This firing is accomplished by the standard double-time-constant gate circuitry of triac T_2 . The low-conduction-phase firing of the bulb keeps the tungsten filament warm but not hot enough to radiate any readily visible light. When transistor Q_1 is turned on, triac T_1 is gated on and resistor R_3 is shorted, and the lamp load turns on.

The associated waveforms are shown in Fig. 228. For a 200-watt bulb in the circuit of Fig. 227, the first peak of current through the bulb is 7.5 amperes when the warm-up circuit is used and 25 amperes with cold-filament inrush.

LAMP DIMMERS

The light intensity of an incandescent lamp depends upon the magnitude of the voltage impressed upon the lamp filament.

Changes in the lamp voltage, therefore, vary the brightness of the lamp. When ac source voltages are used, a triac can be employed in series with an incandescent lamp to vary the voltage to the lamp by changing the conduction angle, i.e., the portion of each half-cycle of ac line voltage during which the triac conducts to provide power to the lamp filaments. Phase-control

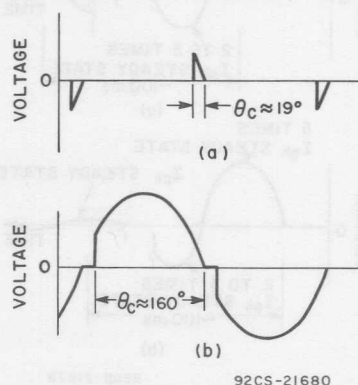


Fig. 228—Waveforms for circuit in Fig. 227: (a) voltage on bulb when Q_1 is off; (b) voltage on bulb when Q_1 is on.

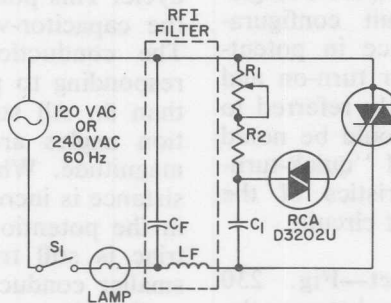
switching of a triac is a very effective and widely used control technique for lamp-dimmer applications.

In 400-Hz (or higher-frequency) power systems, the thermal time constant associated with the lamp filament permits the intensity of an incandescent lamp to be varied (without noticeable flicker) by use of proportional integral-cycle triac controls to change the average power applied the lamp. This type of control may be desirable in high-power 400-Hz systems to reduce RFI components and inrush current surges.

Single-Time-Constant Circuit

Fig. 229 shows the circuit diagram for a single-time-constant phase-control circuit. This circuit represents the most economical type of lamp dimmer. However, it provides a high initial illumination level and exhibits hysteresis in the control-potentiometer setting at low light levels.

gate circuit of the triac. This discharge causes triggering at earlier phase positions on succeeding half-cycles and, because the capacitor charges from a lower potential of opposite polarity, results in a "quick-turn-on" effect which produces fairly high levels of initial illumination. Continued rotation of the potentiometer shaft increases the voltage across the



92CS-21681

AC INPUT VOLTAGE	TRIGGER-CIRCUIT TIME-CONSTANT NETWORK			RFI FILTER		RCA TRIAC TYPES
	C ₁	R ₁	R ₂	L _F (typical)	C _F (typical)	
120 V 60 Hz	0.05 μ F 100 V	250 K ½ W	3.3 K ½ W	100 μ H	0.05 μ F 100 V	T2800B T2802B
240 V 60/50 Hz	0.1 μ F/0.12 μ F 100 V	250 K 1 W	4.7 K ½ W	200 μ H	0.1 μ F 100 V	T2800D T2802D

Fig. 229—Single-time-constant phase-controlled lamp-dimmer circuit.

Initial Brightness—The dimmer control turns on the incandescent lamp with an appreciable initial brilliance for the following reason. The first instantaneous discharge of C₁ reduces the voltage across it by some amount ΔV . This voltage reduction is caused by the instantaneous discharge of C₁ through the trigger device and the

load until the points of maximum load voltage and lamp illumination are reached.

Rotation of the potentiometer shaft in the opposite direction increases the resistance value of R₁ and causes the phase position of the triac triggering to be increasingly delayed from the line-voltage crossover point. This de-

laid triggering reduces the effective load voltage gradually until a point is reached at which a small increment of additional resistance causes the triac to stop conducting. At this point, all voltage is removed from the load and the lamp is turned off. The value of resistance, R_{TO} , required to turn off the triac completely is greater than the value R_{IC} required for the triac to conduct initially. Therefore, $R_{TO} > R_{IC}$ for a single-time-constant circuit configuration. This difference in potentiometer settings for turn-on and turn-off is commonly referred to as **hysteresis**. It should be noted that hysteresis and "quick-turn-on" are characteristics of the single-time-constant circuit.

Hysteresis Effect—Fig. 230 shows the interaction between the RC network and the diac to produce the hysteresis effect. The capacitor voltage and the ac line voltage are shown as solid lines. As the resistance in the circuit is decreased from its maximum value, the capacitor voltage reaches a value which fires the diac. This point is designated A on the capacitor-voltage waveshape.

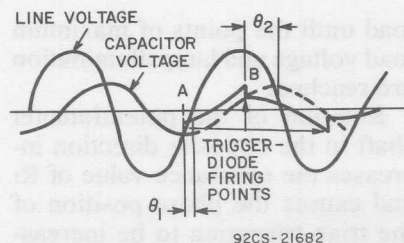


Fig. 230—Waveforms showing interaction of control network and trigger diode.

When the diac fires, the capacitor discharges and triggers the triac at an initial conduction angle θ_1 . During the forming of the gate trigger pulse, the capacitor voltage drops suddenly. The charge on the capacitor is smaller than when the diac did not conduct. As a result of the different voltage conditions on the capacitor, the break-over voltage of the diac is reached earlier in the next half-cycle. This point is labeled B on the capacitor-voltage waveform. The conduction angle θ_2 corresponding to point B is greater than θ_1 . All succeeding conduction angles are equal to θ_2 in magnitude. When the circuit resistance is increased by a change in the potentiometer setting, the triac is still triggered, but at a smaller conduction angle. Eventually, the resistance in series with the capacitance becomes so great that the voltage on the capacitor does not reach the break-over voltage of the diac. The circuit then turns off and does not turn on until the circuit resistance is again reduced to allow the diac to be fired. The hysteresis effect makes the voltage load appear much greater than would normally be expected when the circuit is initially turned on.

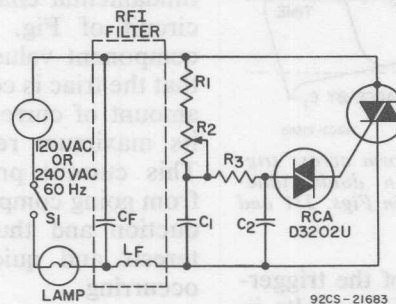
Trigger-Device Characteristics

— Other important factors that influence dimmer performance are the characteristics of the trigger device used in a given circuit configuration. In Fig. 183, the voltage-current characteristics for a triggering device were given, and several important parameters

of the device were shown, including V_p , I_{BL} , and the negative-resistance characteristic R_N . Devices that have high values of V_p and negative resistance produce large hysteresis and high values of V_{IL} . The value of V_p is fundamental in determination of the value of V_{IL} , and the magnitude of the negative resistance R_N is the primary factor in determination of the hysteresis.

Double-Time-Constant Circuit

The hysteresis effect can be substantially reduced by use of a double-time-constant lamp-dimmer control. The two basic forms of the double-time-constant circuit are shown in Figs. 231 and 232. Both these circuits produce less hysteresis and lower initial load voltage V_{IL} than the single-time-constant circuit because the



AC INPUT VOLTAGE	TRIGGER-CIRCUIT TIME-CONSTANT NETWORK					RFI FILTER		RCA TYPES
	C ₁	C ₂	R ₁	R ₂	R ₃	L _F (typical)	C _F (typical)	
120 V 60 Hz	0.1 μ F 200 V	0.1 μ F 200 V	2.2 K ½ W	100 K ½ W	15 K ½ W	100 μ H	0.1 μ F 200 V	T2800B T2802B
240 V 60/50 Hz	0.1 μ F 400 V	0.1 μ F 400 V	3.3 K ½ W	200/250 K 1 W	15 K ½ W	200 μ H	0.1 μ F 400 V	T2800D T2802D

Fig. 231—Basic double-time constant lamp-dimmer circuit in which triac is cut off when potentiometer is set for maximum resistance.

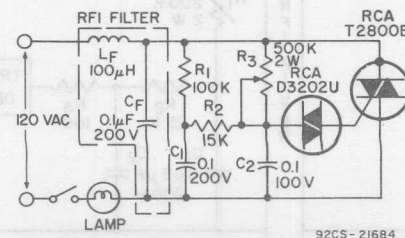


Fig. 232—Double-time-constant lamp-dimmer circuit in which a small amount of triac current flows when potentiometer is set for maximum resistance.

C_2 and thus to reduce the instantaneous voltage drop across C_2 . This technique results in a further reduction of hysteresis and quick turn-on.

Flash at Turn-Off—The performance characteristics of light dimmers which are influenced by the circuit configuration include hysteresis; the voltage across the load at initial turn-on, V_{IL} ; the maximum voltage that can be developed across the load, $V_L(\max)$; and a phenomenon called "flash at turn-off." All of these characteristics were considered previously except flash at turn-off. The flash at turn-off is produced in double-time-constant circuits when the potentiometer is adjusted to turn off the triac. This effect can also be achieved by a reduction in the magnitude of the line voltage applied to the circuit when the potentiometer is set at, or near, maximum resistance. A lower line voltage causes a shift in the phase of gate-triggering voltage to a point where the flashing condition occurs. The fundamental cause of this condition is a phase shift in the triggering voltage beyond the zero crossover point of the line voltage into the early portion of the next successive half-cycle, as shown in Fig. 235. The effective voltage on the load undergoes a transient change that lasts for a few cycles and results in the presence of an appreciable voltage across the load during the transient condition. This transient voltage causes the lamp filament to become brightly illuminated for a number of milli-

seconds and is manifested as a bright flash as the illumination of the lamp is being gradually reduced.

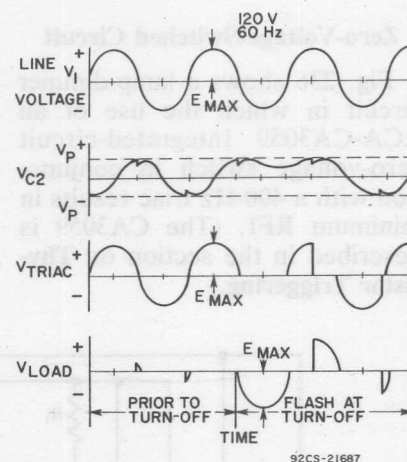


Fig. 235—Waveforms during flash-at-turn-off condition in a double-time-constant phase-control circuit.

The double-time-constant circuit is capable of producing a phase shift of the triggering voltage which is greater than 90 degrees. If the circuit components are chosen to produce this result and, simultaneously, to maintain the voltage magnitude across the triggering capacitor above the trigger-device breakover voltage, then a flash at turn-off occurs. However, if the circuit components are selected to limit the maximum amplitude of the triggering voltage at the 90-degree phase-delay condition below this critical value, there is no flash at turn-off. It should be noted that a trade-off exists between the flash-at-turn-off phenomenon and the hysteresis and V_{IL} phenomena;

i.e., elimination of the flash at turn-off produces slightly greater hysteresis and larger values of V_{IL} .

Zero-Voltage-Switched Circuit

Fig. 236 shows a lamp-dimmer circuit in which the use of an RCA-CA3059 integrated-circuit zero-voltage switch in conjunction with a 400-Hz triac results in minimum RFI. (The CA3059 is described in the section on **Thyristor Triggering**.)

complete or half cycles within a period (typically 17.5 milliseconds) without noticeable flicker. Fourteen different levels of lamp intensity can be obtained in this manner. In the circuit shown in Fig. 237, a line-synced ramp is set up with the desired period and applied to terminal No. 9 of the differential amplifier within the CA3059. The other side of the differential amplifier (terminal No. 13) uses a variable reference level, set by the potentiometer R_2 . A change of the po-

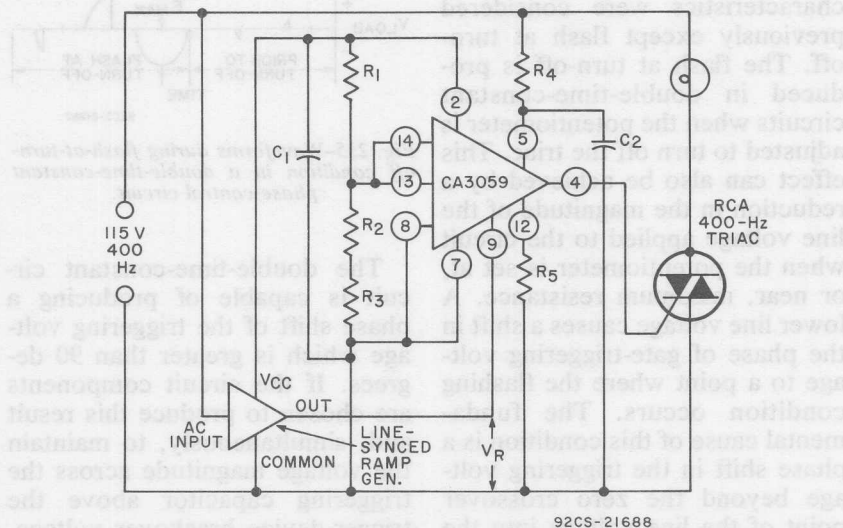


Fig. 236—Circuit diagram for 400-Hz zero-voltage-switched lamp dimmer.

Lamp dimming is a simple triac application that demonstrates an advantage of 400-Hz power over 60 Hz. Fig. 237 shows a means of controlling power to the lamp by the zero-voltage-switching technique. Use of 400-Hz power makes possible the elimination of

tentiometer setting changes the lamp intensity.

In 400-Hz applications, it may be necessary to widen and shift the CA3059 output pulse (which is typically 12 microseconds wide and centered on zero voltage crossing) to assure that sufficient

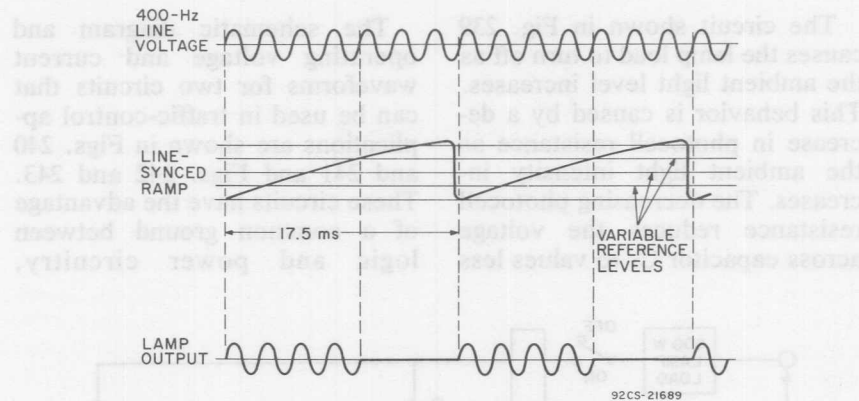


Fig. 237—Waveforms for 400-Hz zero-voltage-switched lamp dimmer.

latching current is available. The resistor R_5 (terminal No. 12 to common) and the capacitor C_2 (terminal No. 5 to common) are used for this adjustment.

PHOTOCELL-OPERATED ON-OFF LAMP CONTROLS

Photocells can be used in conjunction with light-dimmer circuits to provide light-operated controls. These controls can be designed so that the lamp turns on

or off as the ambient light level changes from dark to light, or vice versa. Two photocell control circuits are shown in Figs. 238 and 239.

The circuit shown in Fig. 238 causes the lamp load to turn on gradually as the light impinging on the photocell increases in intensity. As the ambient light intensity increases, the photocell resistance decreases to produce a higher effective voltage across the load.

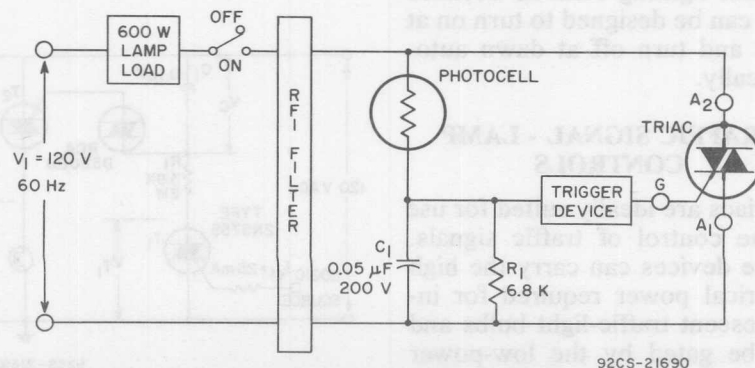


Fig. 238—Photocell-operated on-off lamp control that energizes lamp load when photocell is illuminated.

The circuit shown in Fig. 239 causes the lamp load to turn off as the ambient light level increases. This behavior is caused by a decrease in photocell resistance as the ambient light intensity increases. The decreasing photocell resistance reduces the voltage across capacitor C_1 to values less

The schematic diagram and operating voltage and current waveforms for two circuits that can be used in traffic-control applications are shown in Figs. 240 and 241 and Figs. 242 and 243. These circuits have the advantage of a common ground between logic and power circuitry,

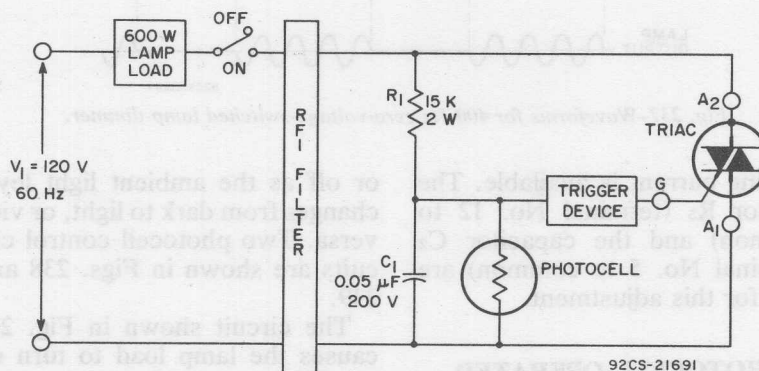


Fig. 239—Photocell-operated lamp control circuit that energizes lamp load when photocell is not illuminated.

than the breakover voltage of the triggering device and prevents the triac from being triggered. Circuits of this type are useful as outdoor lighting controls because they can be designed to turn on at dusk and turn off at dawn automatically.

TRAFFIC SIGNAL - LAMP CONTROLS

Triacs are ideally suited for use in the control of traffic signals. These devices can carry the high electrical power required for incandescent traffic-light bulbs and can be gated by the low-power signals from electronic control timers or monitoring computers.

grounded bulbs, and isolation between the dc logic and the power circuitry afforded by use of the interfacing logic triacs.

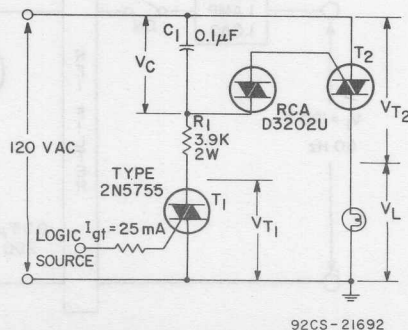


Fig. 240—Positive-logic bulb-switching circuit.

In the positive-logic switching circuit shown in Fig. 240, logic triac T_1 is used to interface between the low-level logic and the load triac T_2 . With triac T_1 gated on, capacitor C_1 is charged through resistor R_1 to the break-over voltage of the diac, at which point triac T_2 and the load are triggered on. As Fig. 241 (d) shows, there is continuous gate power driving triac T_2 whenever triac T_1 is on, and thus the light is on hard.

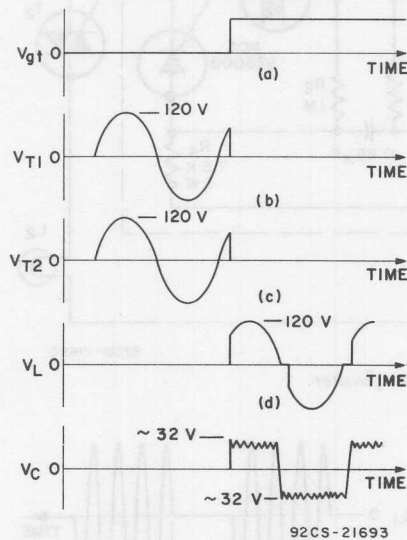


Fig. 241—Waveforms for positive-logic switching.

A variation of this circuit with opposite (negative) logic is shown in Fig. 242. In this circuit, when triac T_1 is triggered on, triac T_2 and the lamp are off. When T_1 is off, capacitor C_1 can charge through resistors R_1 and R_2 to diac breakover, which discharges

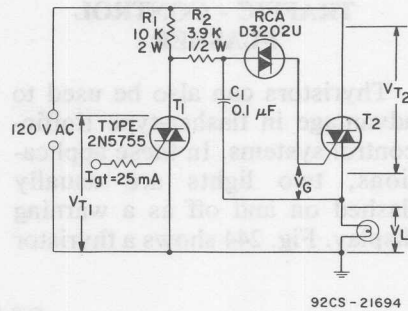


Fig. 242—Negative-logic bulb-switching circuit.

capacitor C_1 into the gate of triac T_2 and energizes the load. Little gate power is dissipated in this circuit because triac T_2 shorts across its gate circuitry when it is on.

Both of these circuits are shown with continuous gate drive into triac T_1 . Logic power could be conserved by use of pulse drive, with no change of power-stage operation; however, the logic circuitry would be more complex.

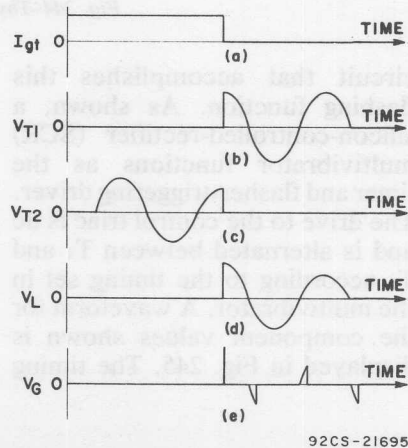


Fig. 243—Waveforms for negative-logic switching.

TRAFFIC - CONTROL FLASHER

Thyristors can also be used to advantage in flasher-type traffic-control systems. In these applications, two lights are usually flashed on and off as a warning display. Fig. 244 shows a thyristor

can be modified by selecting different values for any of the following components: R_1 , R_2 , R_3 , R_4 , C_1 , C_2 . The important features of this circuit are the simple, rugged dc power supply used and the use of SCR's as both timing and memory devices to trigger the triacs.

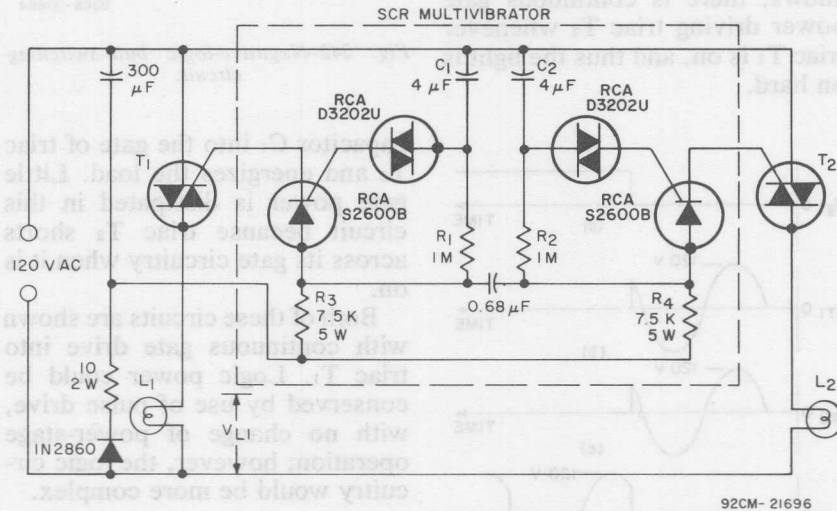


Fig. 244—Thyristor flasher.

circuit that accomplishes this flashing function. As shown, a silicon-controlled-rectifier (SCR) multivibrator functions as the timer and flasher-triggering driver. The drive to the control triac is dc and is alternated between T_1 and T_2 according to the timing set in the multivibrator. A waveform for the component values shown is displayed in Fig. 245. The timing

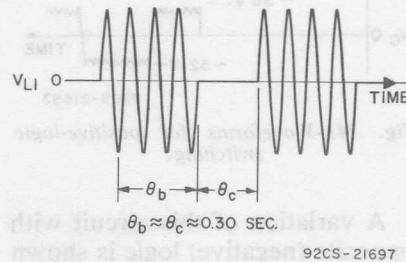


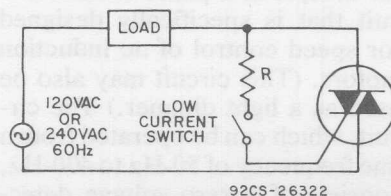
Fig. 245—Timing of thyristor flasher.

Motor Controls

Triacs and SCR's can be used very effectively to apply power to motors and perform switching, or any other desired operating condition that can be obtained by a switching action. Because most motors are line-operated, the triac can be used as a direct replacement for electromechanical switches.

MOTOR SWITCH CIRCUITS

Fig. 246 shows a very simple triac static switch for control of ac motors. The low-current switch used to control the gate trigger current can be any type of transducer, such as a pressure switch, a thermal switch, a photocell, or a magnetic reed relay. This simple type of circuit allows the motor to be switched directly from the transducer switch without any intermediate power switch or relay.

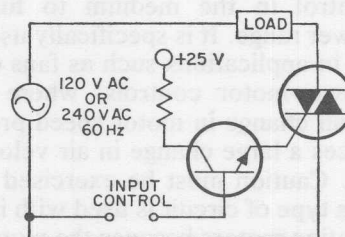


92CS-26322

Fig. 246—Simple triac static switch.

Triacs can also be used to change the operating characteristics of motors to obtain many different speed and torque curves.

For dc control, the circuit of Fig. 247 can be used. By use of the dc



92CS-26323

Fig. 247—AC triac switch control from dc input.

triggering modes, the triac can be directly triggered from transistor circuits by either a pulse or continuous signal.

INDUCTION—MOTOR CONTROLS

Fig. 248 shows a single-time-constant circuit which can be used as a satisfactory proportional speed control for some applications and with certain types of induction motors, such as shaded pole or permanent split-capacitor motors, when the load is fixed.

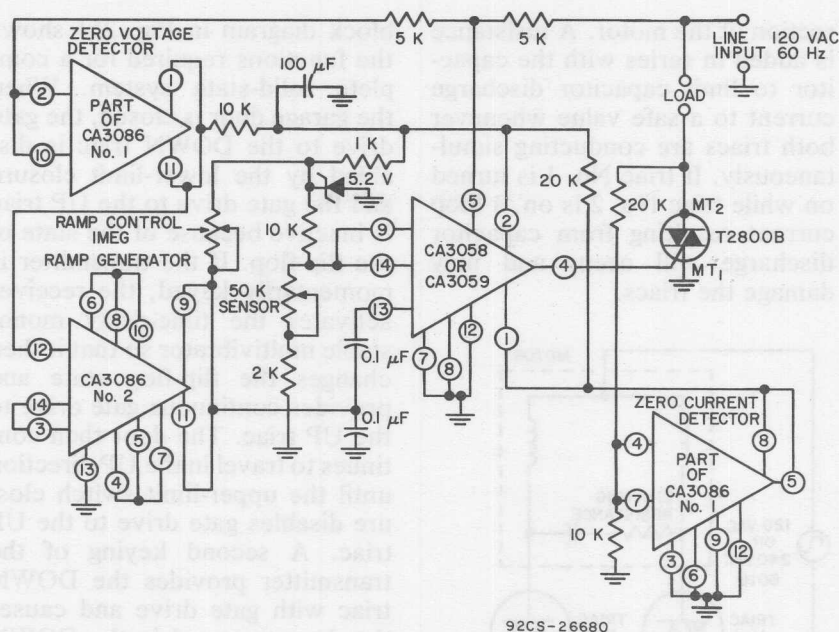


Fig. 249—Phase control using a CA3059 and two CA3086 integrated-circuits.

generator, a zero-current detector, and a line-derived control circuit (i.e., the zero-voltage switch). The zero-voltage detector (part of CA3086 No. 1) and the ramp generator (CA3086 No. 2) provide a line-synchronized ramp-voltage output to terminal 13 of the zero-voltage switch. The ramp voltage, which has a starting voltage of 1.8 volts, starts to rise after the line voltage passes the zero point. The ramp generator has an oscillation frequency of twice the incoming line frequency. The slope of the ramp voltage can be adjusted by variation of the resistance of the 1-megohm ramp-control potentiometer. The output phase can be controlled easily to provide 180° firing of the triac by programming

the voltage at terminal 9 of the zero-voltage switch. The basic operation of the zero-voltage switch driving a thyristor was explained previously in the discussion on **Heat Controls**.

Reversing Motor Controls

In many industrial applications, it is necessary to reverse the direction of a motor, either manually or by means of an auxiliary circuit. Fig. 250 shows a circuit which uses two triacs to provide this type of reversing motor control for a split-phase capacitance motor. The reversing switch can be either a manual switch or an electronic switch used with some type of sensor to reverse the di-

rection of the motor. A resistance is added in series with the capacitor to limit capacitor discharge current to a safe value whenever both triacs are conducting simultaneously. If triac No. 1 is turned on while triac No. 2 is on, a loop current resulting from capacitor discharge will occur and may damage the triacs.

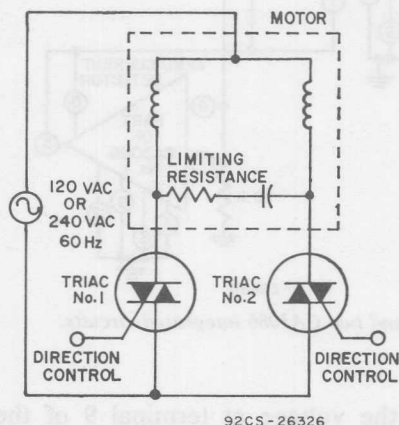


Fig. 250—Reversing motor control.

The circuit operates as follows: when triac No. 1 is in the off state, motor direction is controlled by triac No. 2; when triac No. 2 reverts to the off state and triac No. 1 turns on, the motor direction is reversed.

Electronic Garage-Door System

The triac motor-reversing circuit can be extended to electronic garage-door systems which use the principle for garage-door direction control. The system contains a transmitter and a receiver and provides remote control of door opening and closing. The

block diagram in Fig. 251 shows the functions required for a complete solid-state system. When the garage door is closed, the gate drive to the DOWN triac is disabled by the lower-limit closure and the gate drive to the UP triac is inactive because of the state of the flip-flop. If the transmitter is momentarily keyed, the receiver activates the time-delay monostable multivibrator so that it then changes the flip-flop state and provides continuous gate drive to the UP triac. The door then continues to travel in the UP direction until the upper-limit switch closure disables gate drive to the UP triac. A second keying of the transmitter provides the DOWN triac with gate drive and causes the door to travel in the DOWN direction until the gate drive is disabled by the lower limit closure. The time during which the monostable multivibrator is active should override normal transmit-

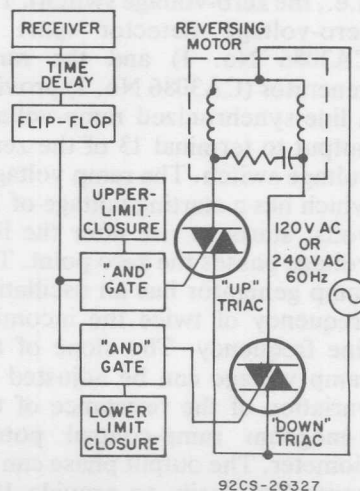


Fig. 251—Block diagram for remote-control solid-state garage-door system.

ter keying for the purpose of eliminating erroneous firing. A feature of this system is that, during travel, transmitter keying provides motor reversing independent of the upper- or lower-limit closures. Additional features, such as obstacle clearance, manual control, or time delay for overhead garage lights can be included very economically.

DC Motor Reversing and Speed Control

Fig. 252 shows a reversing motor speed control which employs a triac to provide variable power to a rectifier bridge, and four SCR's to control and steer

door openers, loading machines, elevators, cranes, and many applications that formerly used ac/dc universal motors. (This circuit may also be used with universal motors.) In addition to a motor reversing function, the circuit provides speed control by adjusting the conduction angle of the ac input to the full-wave bridge. Incremental speed control can be accomplished by the use of a relay or solid-state device to switch the phase-control network at S_1 .

A circuit of this type requires transient protection to prevent false triggering of two SCR's in series, such as Y_1 and Y_3 , which would result in a short-circuit condition. An LC filter at the ac

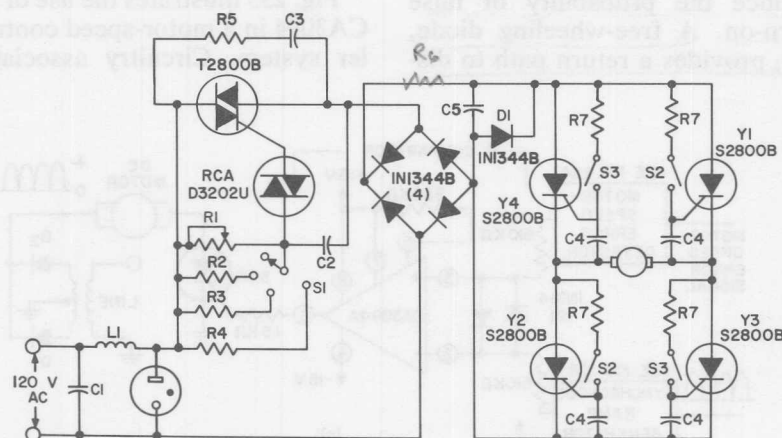


Fig. 252—Typical dc motor reversing and speed control.

the unfiltered full-wave rectified current through a motor load. It is particularly useful for reversing permanent-magnet types of dc motors which may be used on

input filters incoming high-frequency transients and also prevents any RFI generated within the circuit from entering the mains. A voltage-clipping device,

- such as spark gap (SG), prevents high-voltage transients from exceeding the voltage ratings of the triac or the SCR's and rectifiers. The inductor functions with a spark gap to limit surge current in the event of spark-gap conduction. An RC network at the output of the rectifier bridge provides integration of fast-rising transients that enter the circuit from the mains or those generated during the triac switching function. The value of the resistor R_6 , in this network is selected to limit the maximum surge current through all thyristors and rectifiers to a safe level during a faulted turn-on of two series SCR's. The gate-to-cathode capacitors on each SCR enhance static dv/dt capability to reduce the probability of false turn-on. A free-wheeling diode, D_1 , provides a return path to dis-

sipate the inductive energy stored in the motor windings.

Load current is reversed by switching gate drive power from Y_1 and Y_2 to Y_3 and Y_4 . This function can be implemented with mechanical switching, relays, optical devices, pulse transformers, or transistor circuitry. The only requirement is that a delay time greater than $1/2$ cycle occur after the removal of gate drive to the forward SCR pair before gate drive is applied to the reversing pair, to permit the first pair to commutate off at their next current-axis crossing.

SPEED CONTROLLER SYSTEM FOR A DC MOTOR

Fig. 253 illustrates the use of the CA3094 in a motor-speed controller system. Circuitry associated

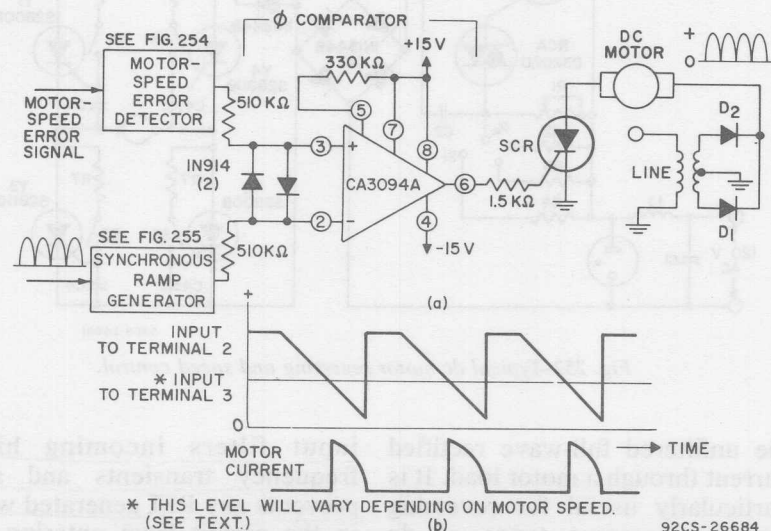


Fig. 253—Motor-speed controller system.

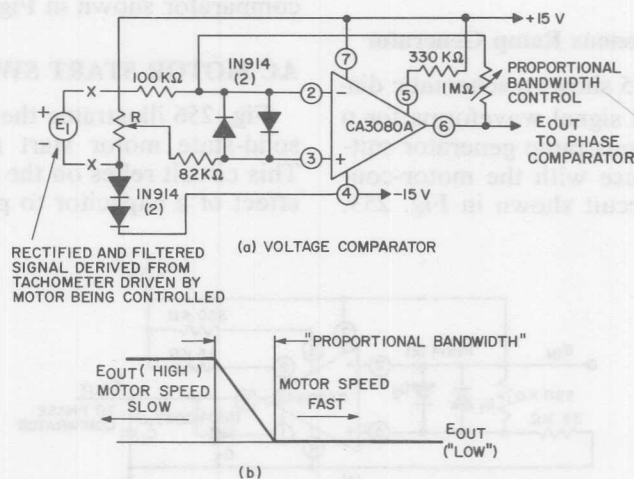
92CS-26684

with rectifiers D_1 and D_2 comprises a fullwave rectifier which develops a train of half-sinusoid voltage pulses to power the dc motor. The motor speed depends on the peak value of the half-sinusoids and the period of time (during each half-cycle) the SCR is conductive. The SCR conduction, in turn, is controlled by the time duration of the positive signal supplied to the SCR by the phase comparator. The magnitude of the positive dc voltage supplied to terminal 3 of the phase comparator depends on motor-speed error as detected by a circuit such as that shown in Fig. 254. This dc voltage is compared to

less than that of the error voltage on terminal 3. The motor-current conduction period is increased as the error voltage at terminal 3 is increased in the positive direction. Motor-speed accuracy of ± 1 per cent is easily obtained with this system.

Motor-Speed Error Detector

Fig. 254(a) shows a motor-speed error detector suitable for use with the circuit of Fig. 253. A CA3080 operational transconductance amplifier is used as a voltage comparator. The reference for the comparator is estab-



92CS-20276

Fig. 254—Motor-speed error detector.

that of a fixed-amplitude ramp wave generated synchronously with the ac-line-voltage frequency. The comparator output at terminal 6 is "high" (to trigger the SCR into conduction) during the period when the ramp potential is

lished by setting the potentiometer R so that the voltage at terminal 3 is more positive than that at terminal 2 when the motor speed is too low. An error voltage E_1 is derived from a tachometer driven by the motor. When the motor

terminal 2 of the voltage comparator is less positive than that at terminal 3, and the output voltage at terminal 6 goes "high". When the motor speed is too high, the opposite input conditions exist, and the output voltage at terminal 6 goes "low". Fig. 254(b) also shows these conditions graphically, with a linear transition region between the "high" and "low" output levels. This linear transition region is known as "proportional band-width". The slope of this region is determined by the proportional bandwidth control to establish the error-correction response time.

Synchronous Ramp Generator

Fig. 255 shows a schematic diagram and signal waveforms for a synchronous ramp generator suitable for use with the motor-controller circuit shown in Fig. 253.

mately +2.7 volts (above the negative supply voltage). The input signal E_{IN} at terminal 2 is a sample of the half sinusoids (at line frequency) used to power the motor in Fig. 253. A synchronous ramp signal is produced by using the CA3094 to charge and discharge capacitor C_1 in response to the synchronous toggling of E_{IN} . The charging current for C_1 is supplied by terminal 6. When terminal 2 swings more positive than terminal 3, capacitor C_1 discharges linearly through the external diode D_3 and the CA3094 to produce the ramp wave. The E_{OUT} signal is supplied to the phase comparator shown in Fig. 253.

AC MOTOR START SWITCHES

Fig. 256 illustrates the use of a solid-state motor start network. This circuit relies on the charging effect of a capacitor to provide a

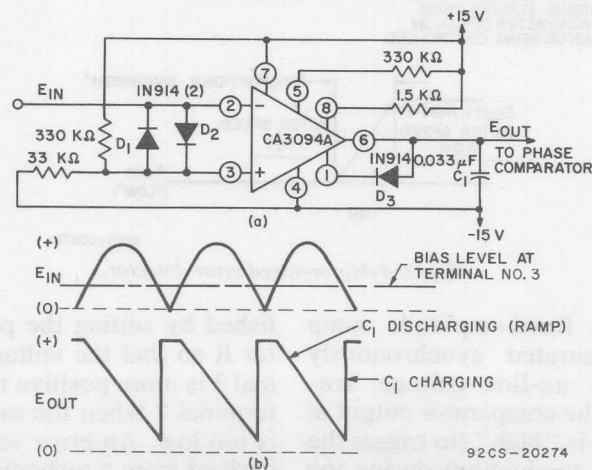


Fig. 255—Synchronous ramp generator with input and output waveforms.

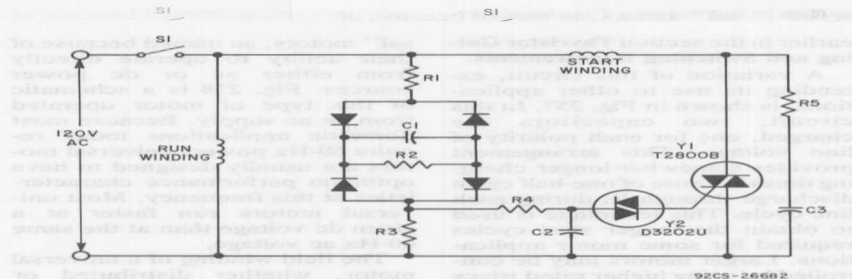


Fig. 256—Basic motor-start switch.

time-dependent decay of trigger signals to gate a triac switch in the start winding of a motor. The start-cycle time and recovery time are variable and adjustable to provide for optimum starting torque when motor loads are known.

At the closing of the power switch S1, capacitor C1 begins to charge because of current flow through R1, R2, and R3. The voltage drop across resistor R3 is the triggering voltage to the diac trigger circuit. This trigger circuit develops pulses early in each half cycle, immediately following the closing of S1. As the charging capacitor voltage increases at an exponential rate, the charging current decreases at a corresponding exponential rate. This effect results in triggering times which become more phase-delayed on subsequent cycles of line voltage. During the charging of C1, a 90 degree firing will be reached after which no additional triggering can

occur, and the start winding becomes inactive. To assure that this point is reached, the values of R1, R2, and R3 must be selected to provide a voltage division at R3 so that the peak voltage across R3 can become less than the minimum diac trigger voltage. The recycle time, or time required after motor turn-off before the motor can be restarted, depends on the R2C1 time constant since C1 discharges through R2. Because the start time is usually in the order of 1 to 2 seconds, a heat sink is generally unnecessary, as the triac package has sufficient thermal capacitance to absorb generated heat and dissipate it through convection and lead wire conduction.

When triacs or SCR's are used to switch ac power in inductive loads, a parallel network, such as that formed by R5 and C3 may be employed to reduce the resulting dv/dt. Use of such networks, called snubbers, was discussed

earlier in the section **Thyristor Gating and Switching Requirements**.

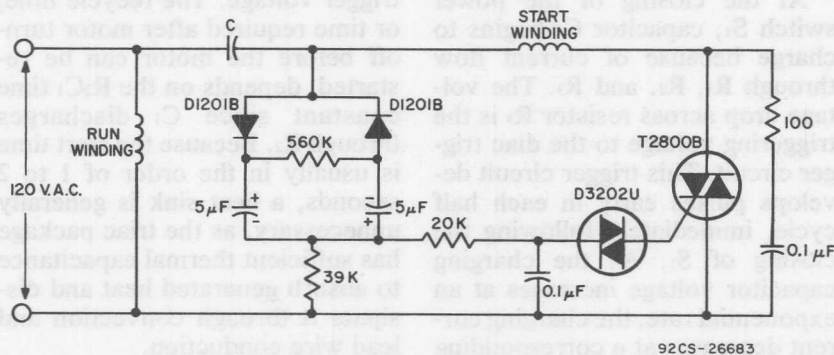
A variation of this circuit, extending its use to other applications, is shown in Fig. 257. In this circuit, two capacitors are charged, one for each polarity of line voltage. This arrangement provides somewhat longer charging times because of one-half cycle discharge through R_2 during each line cycle. This technique is used to obtain the longer start cycles required for some motor applications. Larger motors may be controlled by using higher rated triacs in similar circuits designed for 240 volt ac lines, as suggested in Fig. 257.

SPEED CONTROLS FOR UNIVERSAL MOTORS

Many fractional-horsepower motors are series-wound "univer-

sal" motors, so named because of their ability to operate directly from either ac or dc power sources. Fig. 258 is a schematic of this type of motor operated from an ac supply. Because most domestic applications today require 60-Hz power, universal motors are usually designed to have optimum performance characteristics at this frequency. Most universal motors run faster at a given dc voltage than at the same 60-Hz ac voltage.

The field winding of a universal motor, whether distributed or lumped (salient pole), is in series with the armature and external circuit, as shown in Fig. 258. The current through the field winding produces a magnetic field which cuts across the armature conductors. The action of this field in opposition to the field set up by the armature current subjects the



Motor Rating—HP

Up to ¼
Up to ½
½ to 1
1 to 3
3 to 5

Triac Type

T2801B
T2800B
2N5572
2N5542
T8430D

Fig. 257—Start switch for fractional-horsepower motors.

individual conductors to a lateral thrust which results in armature rotation.

AC operation of a universal motor is possible because of the nature of its electrical connections. As the ac source voltage reverses every half-cycle, the magnetic field produced by the field winding reverses its direction simultaneously. Because the

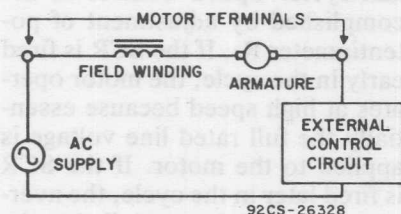


Fig. 258—Series-wound universal motor.

armature windings are in series with the field windings through the brushes and commutating segments, the current through the armature winding also reverses. Because both the magnetic field and armature current are reversed, the direction of the lateral thrust on the armature windings remains constant. Typical performance characteristic curves for a universal motor are shown in Fig. 259.

One of the simplest and most efficient means of varying the impressed voltage to a load on an ac power system is by control of the conduction angle of a thyristor placed in series with the load. Typical curves showing the variation of motor speed with conduction angle for both half-wave and

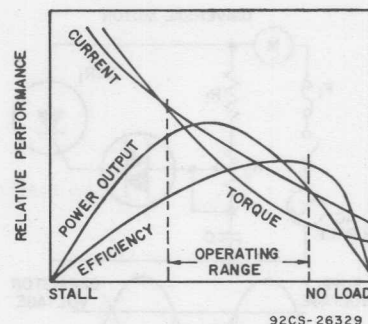


Fig. 259—Typical performance curves for a universal motor.

full-wave impressed motor voltages are illustrated in Fig. 260.

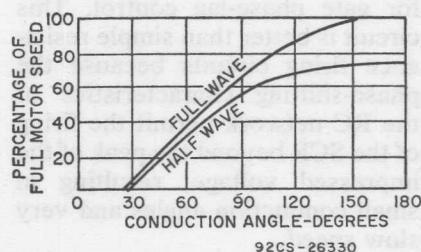


Fig. 260—Typical performance curves for a universal motor with phase-angle control.

Half-Wave Control

There are many good circuits available for half-wave control of universal motors. The circuits are divided into two classes: regulating and non-regulating. Regulation in this instance implies load sensing and compensation of the system to prevent changes in motor speed.

The half-wave proportional control circuit shown in Fig. 261 is a non-regulating circuit that depends upon an RC delay network

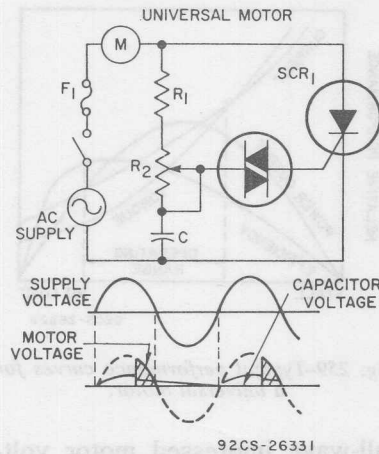


Fig. 261—Half-wave motor control with no regulation.

for gate phase-lag control. This circuit is better than simple resistance firing circuits because the phase-shifting characteristics of the RC network permit the firing of the SCR beyond the peak of the impressed voltage, resulting in small conduction angles and very slow speed.

Fig. 262 shows a fundamental circuit of direct-coupled SCR control with voltage feedback. This circuit is highly effective for speed control of universal motors. The circuit makes use of the counter emf induced in the rotating armature because of the residual magnetism in the motor on the half-cycle when the SCR is blocking.

The counter emf is a function of speed and, therefore, can be used as an indication of speed changes as mechanical load varies. The gate-firing circuit is a resistance network consisting of R_1 and R_2 . During the positive half-cycle of

the source voltage, a fraction of the voltage is developed at the center-tap of the potentiometer and is compared with the counter emf developed in the rotating armature of the motor. When the bias developed at the gate of the SCR from the potentiometer exceeds the counter emf of the motor, the SCR fires. AC power is then applied to the motor for the remaining portion of the positive half-cycle. Speed control is accomplished by adjustment of potentiometer R_1 . If the SCR is fired early in the cycle, the motor operates at high speed because essentially the full rated line voltage is applied to the motor. If the SCR is fired later in the cycle, the average value of voltage applied to the motor is reduced, and a corresponding reduction in motor speed occurs. On the negative half-cycle, the SCR blocks voltage to the motor. The voltage

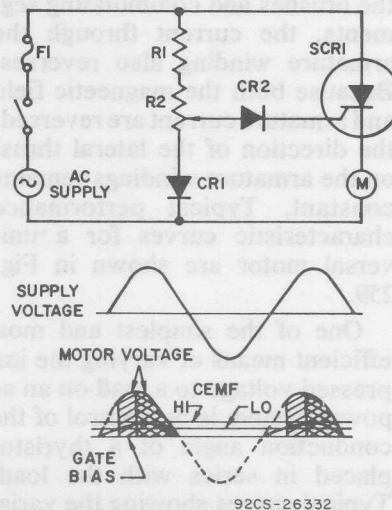


Fig. 262—Half-wave motor control with regulation.

applied to the gate of the SCR is a sine wave because it is derived from the sine-wave line voltage. The minimum conduction angle occurs at the peak of the sine wave and is restricted to 90 degrees. Increasing conduction angles occur when the gate bias to the SCR is increased to allow firing at voltage values which are less than the peak value.

At no load and low speed, skip cycling operation occurs. This type of operation results in erratic motor speeds. Because no counter emf is induced in the armature when the motor is standing still, the SCR fires at low bias-potentiometer settings and causes the motor to accelerate to a point at which the counter emf induced in the rotating armature exceeds the gate firing bias of the SCR and prevents the SCR from firing. The SCR is not able to fire again until the speed of the motor has reduced, as a result of friction losses, to a value at which the induced voltage in the rotating armature is less than the gate bias. At this time the SCR fires again. Because the motor deceleration occurs over a number of cycles, there is no voltage applied to the motor; hence, the term skip-cycling.

When a load is applied to the motor, the motor speed decreases and thus reduces the counter emf induced in the rotating armature. With a reduced counter emf, the SCR fires earlier in the cycle and provides increased motor torque to the load. Fig. 262 also shows variations of conduction angle with changes in counter emf. The

counter emf appears as a constant voltage at the motor terminals when the SCR is blocking.

If a universal motor is operated at low speed under a heavy mechanical load, it may stall and cause heavy current flow through the SCR. For this reason, low-speed heavy-load conditions should be allowed to exist for only a few seconds to prevent possible circuit damage. In any case, fuse ratings should be carefully determined and observed.

Nameplate data for some universal motors are given in developed horsepower to the load. This mechanical designation can be converted into its electrical current equivalent through the following procedure.

Internal motor losses are taken into consideration by assigning a figure of merit. This figure, 0.5, represents motor operation at 50-percent efficiency, and indicates that the power input to the motor is twice the power delivered to the load. With this figure of merit and the input voltage V_{ac} , the rms input current to the motor can be calculated as follows:

$$\text{rms current} = \frac{\text{mechanical horsepower} \times 746}{0.5 V_{ac}} \quad (72)$$

For an input voltage of 120 volts, the rms input current becomes

$$\text{rms current} = \text{horsepower} \times 12.4 \quad (73)$$

For an input voltage of 240 volts, the rms input current becomes

$$\text{rms current} = \text{horsepower} \times 6.2 \quad (74)$$

The motor-control circuits described above should not be used with universal motors that have calculated rms current exceeding the values given. The circuits will accommodate universal motors with ratings up to $\frac{3}{4}$ horsepower at 120 volts input and up to $1\frac{1}{2}$ horsepower at 240 volts input.

In applications in which the hysteresis effect can be tolerated or which require speed control primarily in the medium to full-power range, a single-time-constant circuit such as that shown in Fig. 247 for induction motors can also be used for universal motors. However, it is usually desirable to extend the range of speed control from full-power on to very low conduction angles. The double-time-constant circuit shown in Fig. 263 provides the delay necessary to trigger the triac at very low conduction angles with a minimum of hysteresis, and also provides practically full power to the

load at the minimum-resistance position of the control potentiometer. When this type of control circuit is used, an infinite range of motor speeds can be obtained from very low to full-power speeds.

Full-Wave Control

A very simple SCR full-wave proportional control circuit is shown in Fig. 264. Again, ac phase shifting and neon triggering are used to provide gate phase-angle control; a small pulse transformer is utilized for isolation. The circuit provides a symmetrical output for both halves of the ac input voltage because the same electrical components are used in the phasing network for both SCR gates. Because the SCR gate circuits are completely isolated from each other, the cross-talk problem usually associated with gate firing circuits using transformer coupling and bi-directional trigger devices is avoided. There is a hysteresis effect associated with this circuit because C_1 charges to

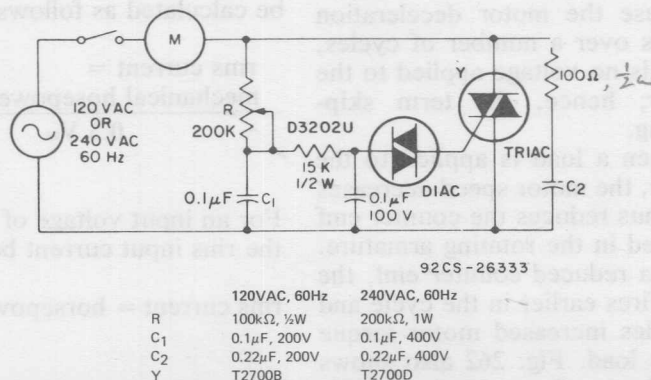
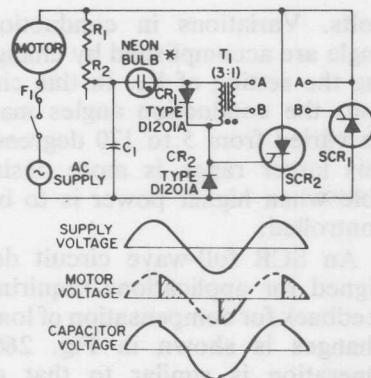


Fig. 263—Universal motor speed control.



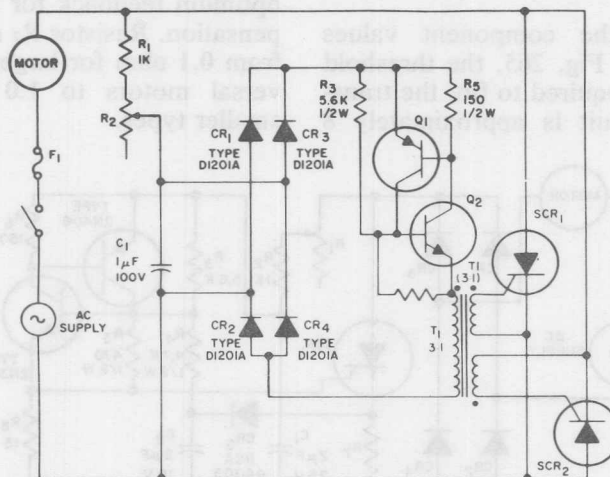
*NE-83, 5AH, A057B, or equiv.
T₁ - Better Coil and Transformer
Co. Type 99A16, or equiv.

92CS-26904

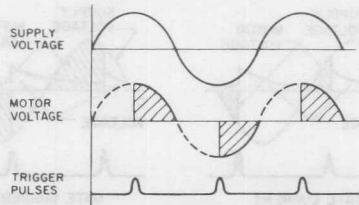
Fig. 264—Full-wave motor control with no regulation.

alternate positive and negative values. For 60-hertz operation, the transformer characteristics are not critical because the magnitude and shape of the current firing pulse are determined primarily by the charge on the capacitor and the characteristics of the neon lamp. Conduction angles obtained with this circuit vary from 30 to 150 degrees; at the maximum conduction angle, the voltage impressed upon the load (universal motor) is approximately 95 per cent of the input rms voltage.

Fig. 265 shows a full-wave control circuit that has increased



Q₁, Q₂ - Complementary pair of general-purpose p-n-p and n-p-n transistor



92CS-26903

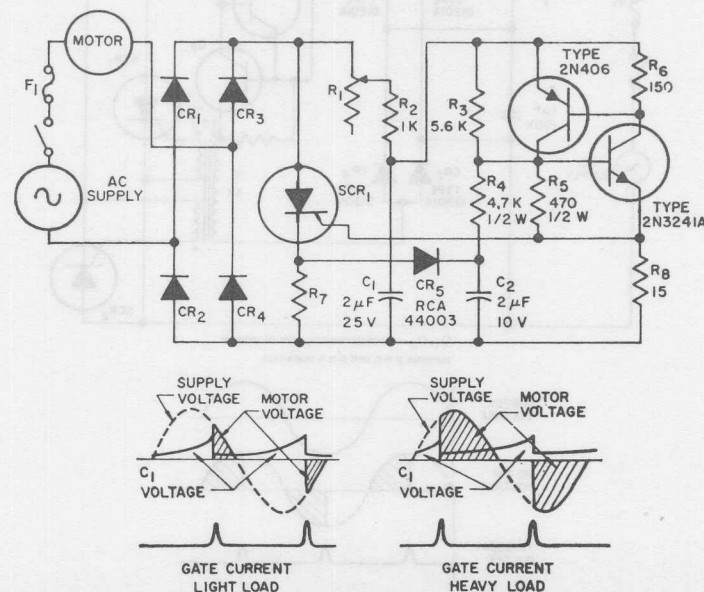
Fig. 265—Full-wave motor control with increased conduction control (no regulation).

conduction-angle capability. Table VI shows the component chart for use of the circuit with various SCR's. The threshold point of the transistor circuit can be changed by varying the value of R_3 . The phase-shift network composed of R_1 , R_2 and C_1 permits the variation of conduction angles from minimum to maximum. An ac potential impressed upon this phase-shifting network eliminates skip-cycling at low conduction angles. The bridge network of CR_1 , CR_2 , CR_3 , and CR_4 rectifies the ac voltage developed across C_1 and provides the switching transistors with dc voltage.

With the component values shown in Fig. 265, the threshold voltage required to fire the transistor circuit is approximately 8

volts. Variations in conduction angle are accomplished by changing the setting of R_2 . In this circuit, the conduction angles may be varied from 5 to 170 degrees; this larger range is more desirable when higher power is to be controlled.

An SCR full-wave circuit designed for applications requiring feedback for compensation of load changes is shown in Fig. 266. Operation is similar to that of the circuits discussed previously except that this circuit has full-wave conduction with proportional control. R_7 must be matched with the motor rating to provide optimum feedback for load compensation. Resistor R_7 may range from 0.1 ohm for larger-size universal motors to 1.0 ohm for smaller types.



92CS-26905

Fig. 266—Full-wave motor control with regulation.

Triac Controls for Three-Phase Power Systems

The growing demand for solid-state switching in heating controls and other industrial applications has resulted in the increasing use of three-phase triac power-control circuits. The following paragraphs describe the use of triacs to control the application of ac power to both three-phase resistive and inductive loads. In the circuits described, the RCA-CA3059 integrated-circuit zero-voltage switch is used as an interface control from the low-power logic circuitry to the high-power load. The requirements of the three-phase triac controls are as follows:

1. The load should be connected in either a three-wire delta or wye configuration. Four-wire wye loads may be handled as three independent single-phase systems.

2. Only one logic command signal is available for the control circuits. This signal must be electrically isolated from the three-phase power system.

3. Three separate triac gating signals are required.

4. With resistive loads, the zero-voltage-switching technique should be used to minimize any RFI/EMI that may be generated.

ISOLATION OF DC LOGIC CIRCUITRY

The dc logic circuitry provides the low-level electrical signal that dictates the state of the load. For temperature controls, the dc logic circuitry includes a temperature sensor for feedback. The RCA integrated-circuit zero-voltage switch, when operated in the dc mode with some additional circuitry, can replace the dc logic circuitry for temperature controls.

Isolation of the dc logic circuitry from the ac line, the triac, and the load circuit is often desirable even in many single-phase power-control applications. In control circuits for polyphase power systems, however, this type of isolation is essential, because the common point of the dc logic circuitry cannot be referenced to a common line in all phases.

In the three-phase circuits described in this section, photo-optic techniques (i.e., photo-coupled isolators) are used to provide the electrical isolation of the dc logic command signal from the ac circuits and the load. The photo-coupled isolators consist of

an infrared light-emitting diode aimed at a silicon phototransistor, coupled in a common package. The light-emitting diode is the input section, and the phototransistor is the output section. The two components provide a typical voltage isolation of 1500 volts. Other isolation techniques, such as pulse transformers, magnetoresistors, or reed relays, can also be used with some circuit modifications.

THREE-PHASE RESISTIVE LOADS

Fig 267 illustrates the basic phase relationships of a balanced three-phase resistive load, such as may be used in heater applications, in which the application of load power is controlled by zero-voltage switching. The following conditions are inherent in this type of application:

1. The phases are 120 degrees

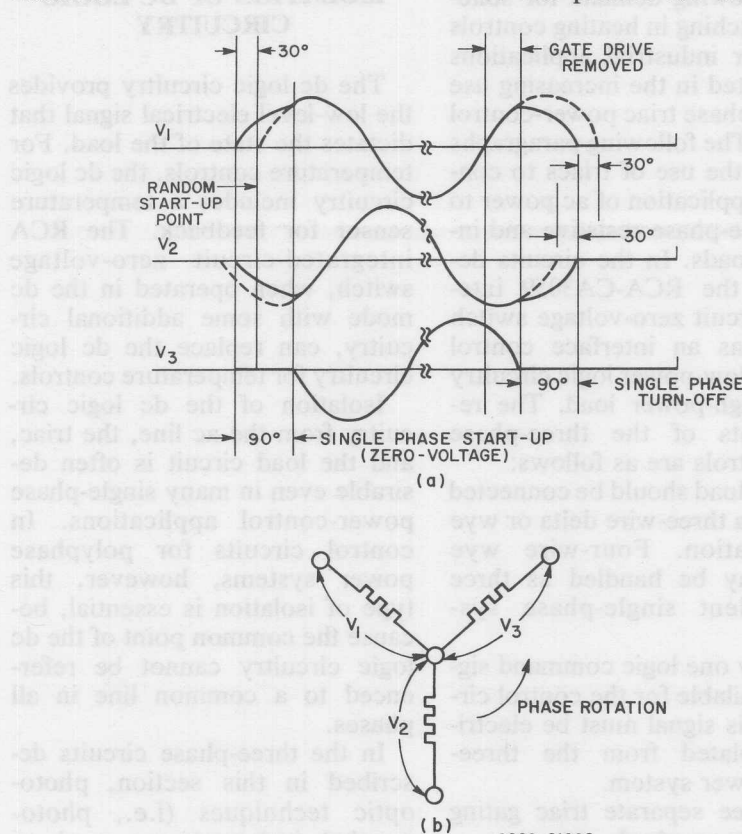


Fig. 267—Voltage phase relationship for a three-phase resistive load when the application of load power is controlled by zero-voltage switching: (a) voltage waveforms, (b) load-circuit orientation of voltages. (The dashed lines indicate the normal relationship of the phases under steady-state conditions. The deviation at start-up and turn-off should be noted.)

apart; consequently, all three phases cannot be switched on simultaneously at zero voltage.

2. A single phase of a three-wire system cannot be turned on.

3. Two phases must be turned on for initial starting of the system. These two phases form a single-phase circuit which is out of phase with both of its component phases. The single-phase circuit leads one phase by 30 degrees and lags the other phase by 30 degrees.

These conditions indicate that in order to maintain a system in which no appreciable RFI/EMI is generated by the switching action, from initial starting through the steady-state operating condition, the system must first be turned on, by zero-voltage switching, as a single-phase circuit and then must revert to synchronous three-phase operation. Fig. 268 shows a simplified circuit configuration of a three-phase heater control that employs zero-voltage synchronous switching in the steady-state operating condition, with random starting. In this system, the logic command to turn on the system is given when heat is required, and the command to turn off the system is given when heat is not required. Time proportioning heat control is also possible through the use of logic commands.

The three photocoupled inputs to the three CA3059 circuits change state simultaneously in response to a "logic command". The CA3059 circuits then provide a positive pulse, approximately 100 microseconds in duration, only at a zero-voltage crossing

relative to their particular phase. A balanced three-phase sensing circuit is set up with the three CA3059 circuits each connected to a particular phase on their common side (pin 7) and referenced at their high side (pin 5), through the current-limiting resistors R_4 , R_5 , and R_6 , to an established artificial neutral point. This artificial point is necessary because the neutral on the load side is not accessible. Because only one triac is pulsed on at a time, the diodes (D_1 , D_2 , and D_3) are necessary to trigger the opposite-polarity triac and, in this way, to assure initial latching-on of the system. The three resistors (R_1 , R_2 , and R_3) are used for current limiting of the gate drive.

In critical applications that require suppression of all generated RFI/EMI, the circuit shown in Fig. 269 may be used. In addition to synchronous operating conditions, this circuit also incorporates a zero-voltage starting circuit. The start-up condition is zero-voltage synchronized to a single-phase, 2-wire, line-to-line circuit, comprised of phases A and B. The logic command engages the single-phase "start-up" CA3059 and three-phase photo-isolators OCI_3 , OCI_4 , and OCI_5 through photo-isolators OCI_1 and OCI_2 . The single-phase CA3059 which is synchronized to phase A and B starts the system at zero voltage. As soon as start-up is accomplished, the three photo-isolators OCI_3 , OCI_4 , and OCI_5 take control, and three-phase synchronization begins. When the "logic command" is

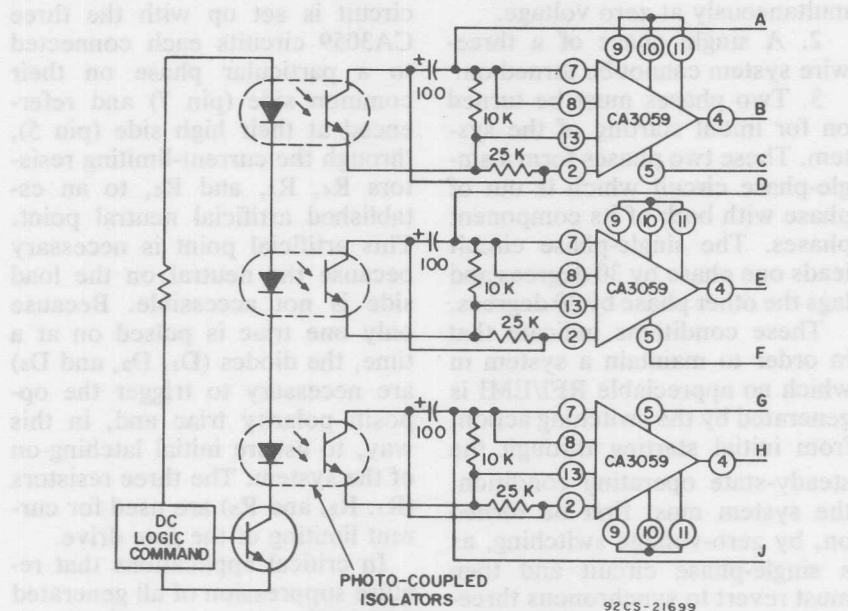


Fig. 268—Simplified diagram of a three-phase heater control that employs zero-voltage synchronous switching in the steady-state operating conditions. (Continued on page 257.)

turned off, all control is ended, and the triacs automatically turn off when the sine-wave current decreases to zero. Once the first phase turns off, the other two will turn off simultaneously, 90° later, as a single-phase line-to-line circuit, as is apparent from Fig. 267.

THREE-PHASE INDUCTIVE LOAD

For inductive loads, zero-voltage turn on generally is not required because the inductive current cannot increase instantaneously; therefore, RFI/EMI generated is usually negligible. Also, because of the lagging nature of

the inductive current, the triacs cannot be pulse fired at zero voltage. There are several ways in which the CA3059 may be interfaced to a triac for inductive-load applications. The most direct approach is to use the CA3059 in the dc mode, i.e., to provide a continuous dc output instead of pulses at points of zero-voltage crossing. This mode of operation is accomplished by connection of terminal 12 to terminal 7, as shown in Fig. 270. The output of the CA3059 should also be limited to approximately 5 milliamperes in the dc mode; and the use of a sensitive-gate triac, such as the RCA T2300D, is recommended

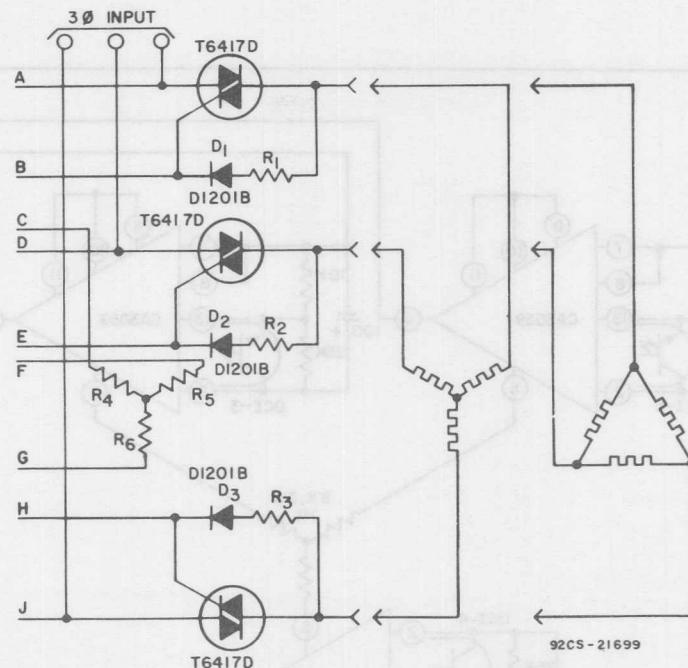


Fig. 268—Simplified diagram of a three-phase heater control that employs zero-voltage-synchronous switching in the steady-state operating conditions. (Continued from page 256.)

for this application. Terminal 3 is connected to terminal 2 to limit the steady-state power dissipation within the CA3059. For most three-phase inductive load applications, the current handling capability of the T2300D triac (2.5 amperes) is not sufficient. Therefore, the T2300D is used as a trigger triac to turn on any other currently available power triac that may be used. The trigger triac is used only to provide trigger pulses to the gate of the power triac (one per half cycle); the

power dissipation in this device, therefore, will be minimal.

Simplified circuits using pulse transformers and reed relays will also work quite satisfactorily in this type of application. The RC networks across the three power triacs are used for suppression of the commutating dv/dt when the circuit operates into inductive loads. A detailed explanation of commutating dv/dt is provided in the basic discussion of **Thyristors** in an earlier section of this Manual.

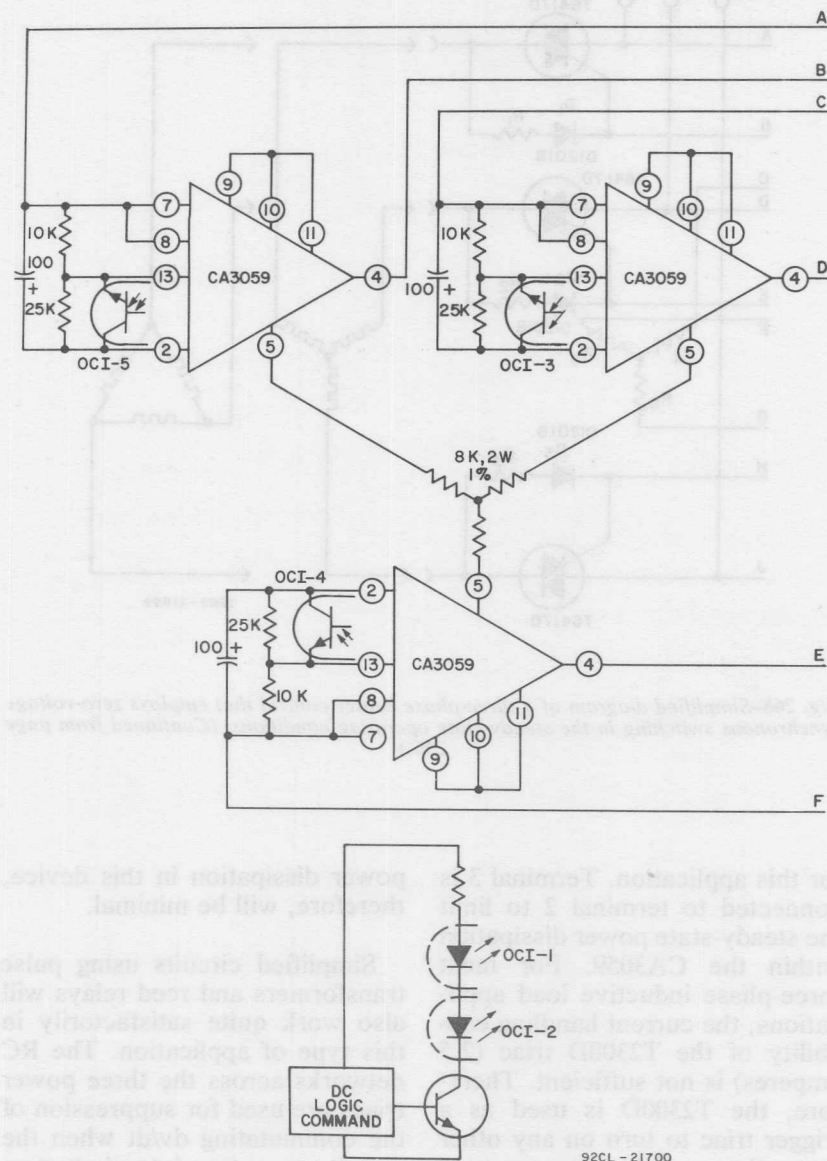
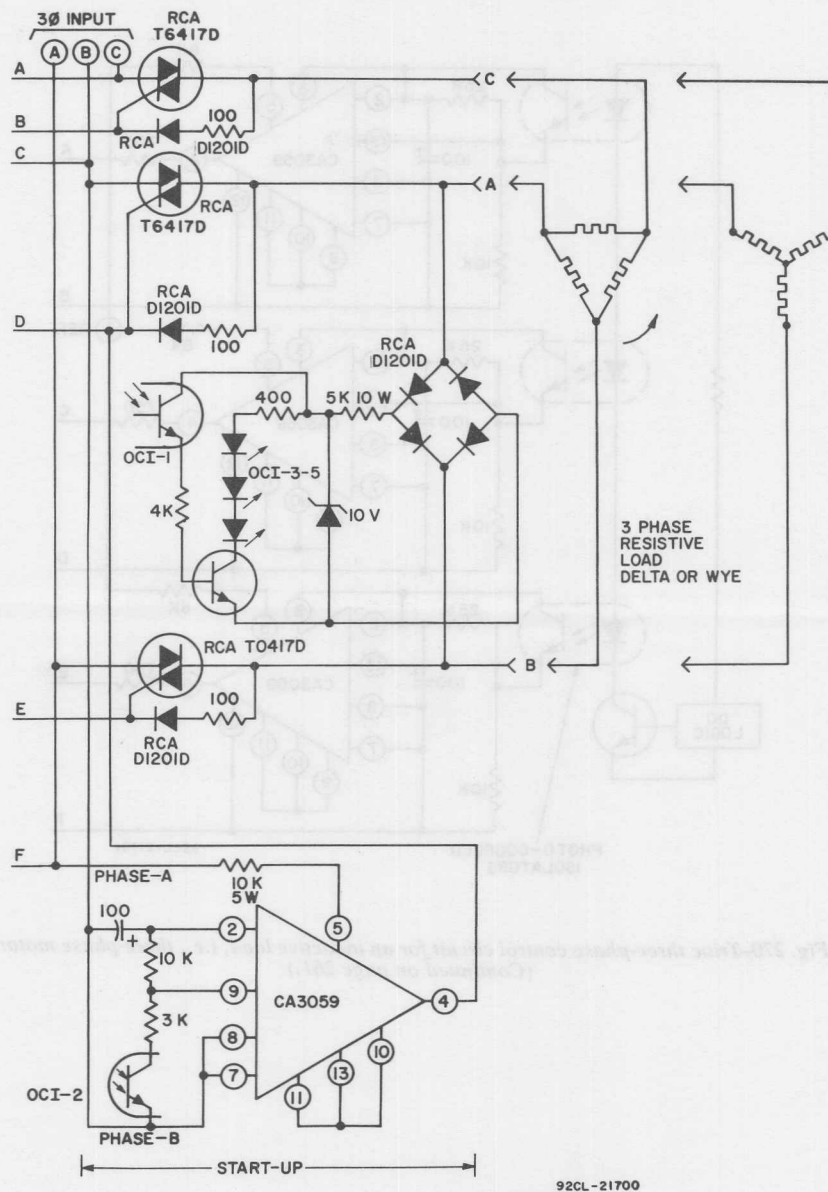
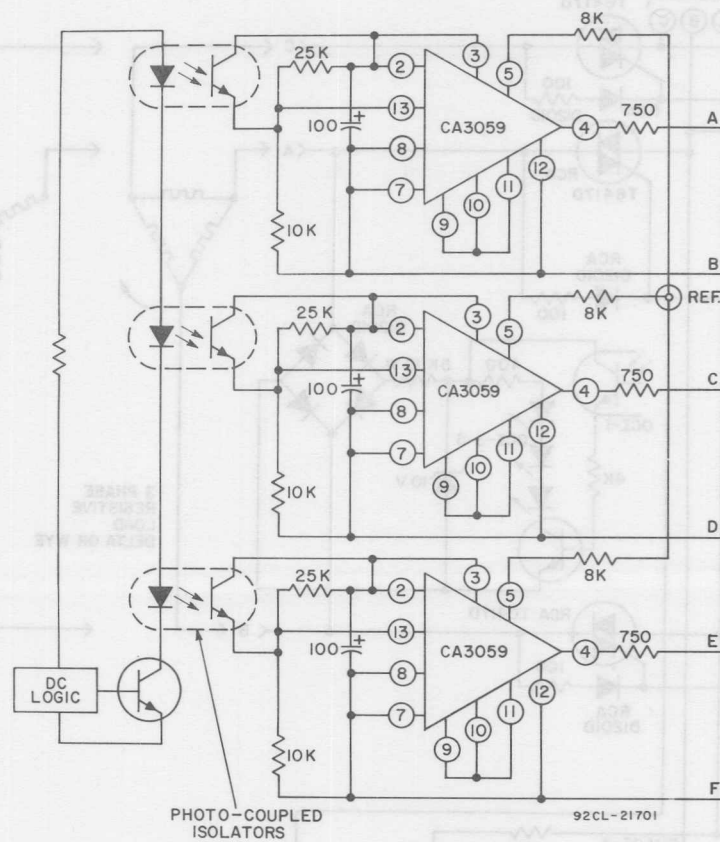


Fig. 269—Three-phase power control that employs zero-voltage synchronous switching both for steady-state operation and for starting. (Continued on page 259.)



92CL-21700

Fig. 269—Three-phase power control that employs zero-voltage synchronous switching both for steady-state operation and for starting. (Continued from page 258.)



*Fig. 270—Triac three-phase control circuit for an inductive load, i.e., three-phase motor.
(Continued on page 261.)*

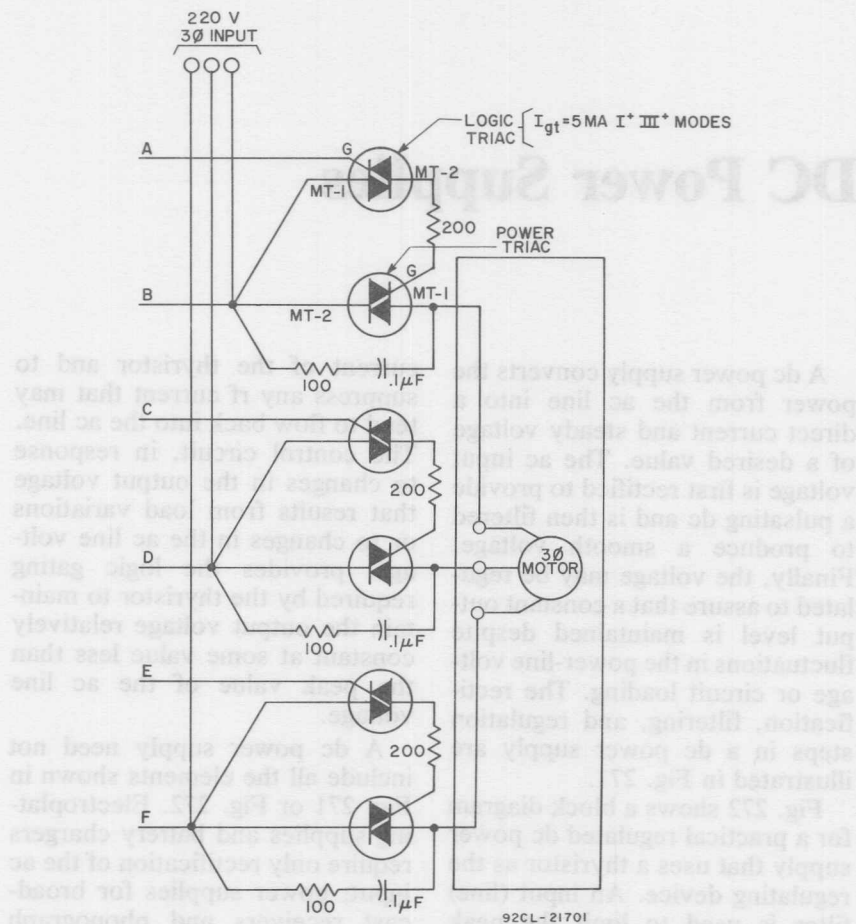


Fig. 270—Triac three-phase control circuit for an inductive load, i.e., three-phase motor.
(Continued from page 260.)

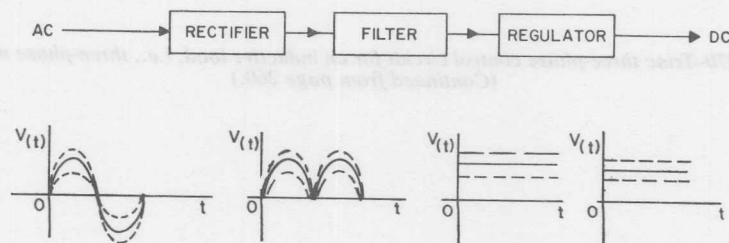
DC Power Supplies

A dc power supply converts the power from the ac line into a direct current and steady voltage of a desired value. The ac input voltage is first rectified to provide a pulsating dc and is then filtered to produce a smooth voltage. Finally, the voltage may be regulated to assure that a constant output level is maintained despite fluctuations in the power-line voltage or circuit loading. The rectification, filtering, and regulation steps in a dc power supply are illustrated in Fig. 271.

Fig. 272 shows a block diagram for a practical regulated dc power supply that uses a thyristor as the regulating device. An input (line) filter is used to limit the peak

current of the thyristor and to suppress any rf current that may tend to flow back into the ac line. The control circuit, in response to changes in the output voltage that results from load variations or to changes in the ac line voltage, provides the logic gating required by the thyristor to maintain the output voltage relatively constant at some value less than the peak value of the ac line voltage.

A dc power supply need not include all the elements shown in Fig. 271 or Fig. 272. Electroplating supplies and battery chargers require only rectification of the ac input; power supplies for broadcast receivers and phonograph



92CS-25819

Fig. 271—Block diagram of a regulated dc power supply. The waveforms show the effects of rectification, filtering, and regulation. (Dashed lines indicate voltage fluctuations as a result of input variations.)

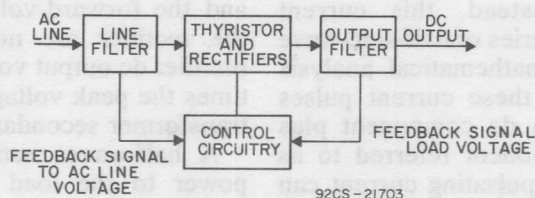


Fig. 272—Block diagram of a regulated dc power supply that uses a thyristor as the main regulating device.

amplifiers require only the rectifier and filter sections. However, circuits such as oscillators, high-gain amplifiers, and low-voltage logic, which have exacting frequency, stability, or output requirements, can be critically affected by variations in dc supply voltages. Some type of regulation, therefore, is frequently required to prevent significant changes in the output of a dc power supply because of line-voltage fluctuations or changes in circuit loading.

RECTIFIER CIRCUITS

The optimum type of rectifier circuit for a particular application depends upon the dc voltage and current requirements, the maximum amount of ripple (undesirable fluctuations in the dc output caused by an ac component) that can be tolerated in the circuit, and the type of power available. Single-phase circuits are used to provide the relatively low dc power required for radio and television receivers, public-address systems, and similar types of electronic equipment. Polyphase rectifier circuits are used to provide the dc power in high-power industrial applications.

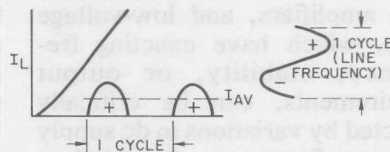
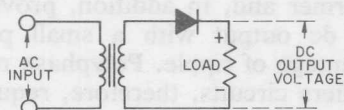
Polyphase circuits more fully take advantage of the capabilities of the rectifier and power transformer and, in addition, provide a dc output with a small percentage of ripple. Polyphase rectifiers circuits, therefore, require less filtering of the dc output voltage than is required for the dc output from single-phase rectifier circuits.

Single-Phase Rectifiers

The following paragraphs describe and show the basic circuit configurations for a variety of different types of single-phase rectifiers. Significant voltage and current waveforms are shown with the circuit diagram for each individual type of rectifier.

Half-Wave Rectifier—Fig. 273 shows the circuit diagram and load-current waveform for a single-phase half-wave rectifier. This circuit allows current to pass only during the positive half-cycle (i.e., during the positive excursions) of the ac input voltage and is blocked during alternate half-cycle (i.e., during negative excursions). Although the load current is always in the same direction, it is not a pure direct

current. Instead, this current flows as a series of half-sine-wave pulses. A mathematical analysis shows that these current pulses consist of a dc component plus an ac component referred to as ripple. The pulsating current can be converted into a true direct current by use of a smoothing filter between the rectifier and the load, as will be explained subsequently in the discussion of **Filter Networks**.



92CS-21704

Fig. 273 - Single-phase half-wave Rectifier and load-current waveform.

As is apparent from Fig. 273, the output current waveform of the half-wave rectifier is an exact replica of the positive alternation of the ac input voltage waveform. The anode current flows through the load impedance and develops a pulsating voltage across this impedance that has exactly the same waveform as the ac input voltage except that only the positive half-cycles are reproduced. Because the negative half-cycles of the input ac voltage are not used, the efficiency of the half-wave rectifier is low.

In a half-wave rectifier circuit, the average value of the rectifier anode current is 0.318 times the peak value. Similarly, if the voltage drop across the internal impedance of the transformer, the voltage drop across the surge-current limiting resistor (if used),

and the forward-voltage drop of the rectifier are neglected, the rectifier dc output voltage is 0.318 times the peak voltage across the transformer secondary winding.

A half-wave rectifier delivers power to the load only during half of the input ac cycle. Consequently, the ratio of peak to average current in this circuit is high, the circuit efficiency is low, and the output voltage regulation is poor. Half-wave rectifiers,

therefore, are used mainly for applications, such as the power supply in ac-dc radio receivers and the high-voltage supply for oscilloscopes and television picture tubes, in which the current drain is relatively small. Half-wave rectifiers are also used occasionally for the power-supply in television receivers. In such applications, an extremely high value of filter capacitance is required to reduce the ripple content to acceptable levels. Another disadvantage of the half-wave rectifier for high-current applications is that the dc component of the rectified output current flows through the secondary winding of the power transformer. This current results in dc magnetization and possible saturation of the power transformer core; consequently, a re-

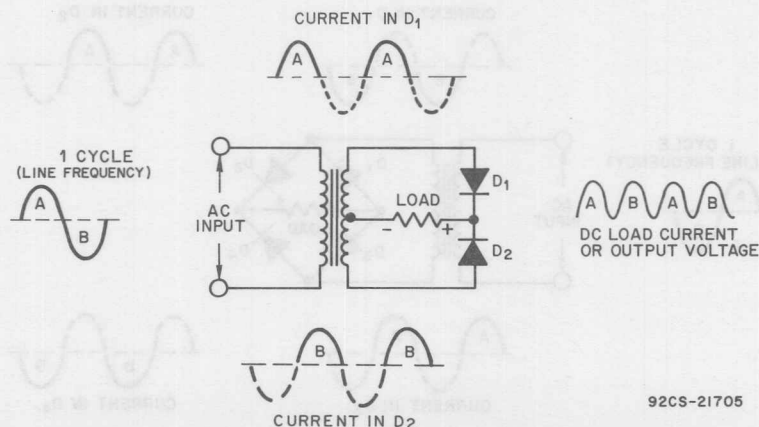
duction in transformer efficiency results.

Full-Wave Rectifier — Two half-wave rectifiers connected back-to-back, as shown in Fig. 274, can be used to provide unidirectional load current during both half-cycles of the applied ac voltage. In this type of circuit, which is referred to as a full-wave rectifier, the two rectifier sections alternately supply current pulses to the load in such a way that the load current always flows in the same direction.

In the full-wave circuit shown in Fig. 274, the cathodes of the two rectifiers are connected together (if a negative output voltage is desired, the anodes are connected together) and one end of the load is connected to the common junction. The other end of the load is connected to the centertap of the transformer secondary winding. Only one-half the transformer secondary winding is con-

nected between the cathode and anode of each rectifier. The total transformer secondary voltage, therefore, must be twice the anode voltage required for each rectifier. In most applications, the dc output voltage required from the power supply is substantially greater than the peak value of the line voltage. In such instances, the power transformer provides a large step-up in voltage from primary to secondary.

As shown in Fig. 274, a full-wave rectifier delivers two pulses of load current for each cycle of the ac input voltage. The average value of the output current (and voltage), therefore, is twice that of the half-wave rectifier, or 0.636 times the peak value. The peak value of the voltage is 1.414 times the RMS value. The output voltage of the full-wave rectifier, therefore, may also be expressed as 1.414 times 0.636, or 0.9, times the rms value of the secondary voltage.



92CS-21705

Fig. 274 — Single-phase Full-wave Rectifier Circuit With Center-tapped Transformer

The individual rectifier currents in the full-wave rectifier circuit flow in opposite directions through the secondary winding of the power transformer. Consequently, the problems of dc magnetization and saturation of the transformer core are avoided, and the permissible current drain from a full-wave rectifier supply is significantly higher than that for the half-wave rectifier supply. In addition, because the full-wave circuit uses both half-cycles of the ac input, this circuit has higher efficiency and less ripple content than the half-wave rectifier circuit. Full-wave rectifiers are widely used for power supplies in applications such as television receivers and large audio amplifiers.

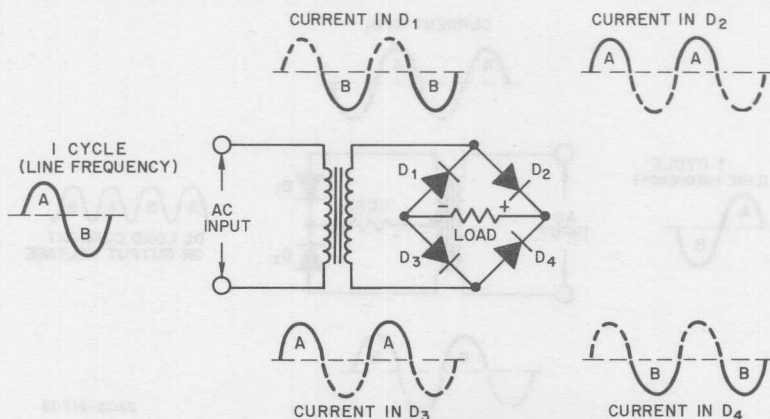
Full-Wave Bridge Rectifier—The full-wave bridge rectifier circuit, shown in Fig. 275, avoids the need for a center-tapped power transformer, and provides twice

the output voltage obtained from a basic full-wave rectifier for the same transformer secondary voltage. Four rectifiers are used in the bridge circuit; separate pairs of series-connected rectifiers carry the current on alternate half-cycles.

Like the basic full-wave rectifier shown in Fig. 274, the bridge rectifier avoids saturation of the power transformer, has only 50 per cent of the load current in each rectifier, and provides a relatively low ripple in the output voltage.

The full-wave bridge rectifier is a popular choice for the power supply in amateur-transmitter systems. This circuit is also used extensively in power supplies for color television receivers.

Voltage-Multiplier Rectifier Circuits—In some power-supply applications, a power transformer that provides the required second-



92CS-21706

Fig. 275 — Full-wave bridge rectifier without center-tapped power transformer.

ary voltage cannot be conveniently provided; and often in low-cost receiver circuits, the power transformer is eliminated as a cost savings. In such cases, a rectifier circuit can be designed to deliver dc output voltage equal to two or more times the peak amplitude of the applied ac input voltage. This voltage multiplication is achieved by the charging of two or more capacitors through the rectifiers on alternate half-cycles in a way such that the dc voltages on the capacitors add in series.

Full-Wave Voltage Doubler: Fig. 276 shows the circuit diagram for a full-wave voltage-doubler type of rectifier circuit. During the positive alternation (period A) of the ac input, rectifier D_1 conducts and capacitor C_1 is charged (in the polarity indicated) to the peak value of the ac input voltage. During the negative half-cycle (period B) of the input ac voltage, rectifier D_2 conducts, and capacitor C_2 is then charged (in the polarity indicated) to the peak

value of the input voltage. Both capacitors (C_1 and C_2), therefore, are charged to the peak value of the input ac voltage in a polarity such that with respect to the load these voltages add together. The output voltage across the load, therefore, is equal to twice the peak value of the input ac voltage. As indicated in Fig. 276, the current through each rectifier in the double circuit flows for less than a complete half-cycle of the ac input. Once capacitors C_1 and C_2 become charged, rectifiers D_1 and D_2 become reversed-biased and can conduct only when the applied ac voltage exceeds the voltage on the capacitors.

The conduction periods for the rectifiers occur near the peaks of the applied ac input. The duration of these conduction periods is a function of the rate at which charge is removed from the capacitors by the current delivered to the load.

Under no-load conditions, the dc output voltage of the full-wave doubler is equal to twice the peak value of the applied ac voltage.

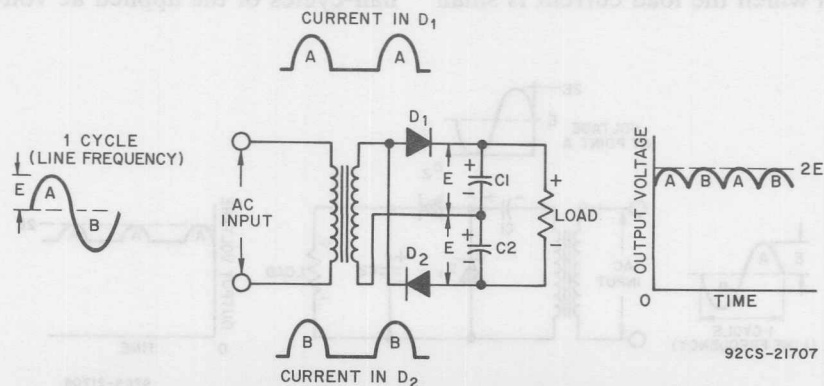


Fig. 276—Full-wave voltage-double circuit.

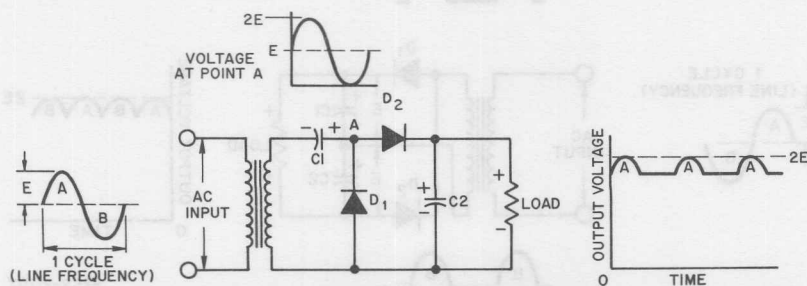
When the load current is drawn, the output voltage decreases. The amount of the decrease depends upon the magnitude of the load current and the values of capacitors C_1 and C_2 . The energy-storage capability of a capacitor is directly proportional to the capacitance value. Very large capacitors, therefore, can maintain the output voltage at a value very near twice the peak of the input ac voltage for relatively large load currents. Large capacitors, however, draw very high peak currents, which may damage the rectifiers. Surge limiting resistors are often placed in series with the rectifiers to reduce the peak currents, but such resistors also limit the charging current to the capacitors. (The selection and use of surge-limiting resistances are described subsequently in the discussion of **Capacitive Load Circuits**.)

Voltage regulation of the full-wave voltage doubler is relatively poor. As a result, use of this type of power-supply circuit is generally limited to applications in which the load current is small

or applications in which high load currents are limited to a few microseconds (i.e., pulse circuits).

Half-Wave Voltage Doubler: In the half-wave voltage doubler, shown in Fig. 277, the negative terminal of the load is common with one side of the ac line. In this circuit, capacitor C_1 charges (in the polarity indicated) through rectifier D_1 to the peak value of the ac input voltage across the secondary of the power transformer during the negative alternation of this voltage. During the positive alternation of the secondary ac voltage, the voltage applied to rectifier D_2 is a dc voltage equal to the peak value of the secondary ac voltage (i.e., voltage on capacitor C_1), plus the ac voltage. The output voltage to which the output capacitor C_2 is charged, therefore, is equal to twice the peak value of the applied ac voltage.

In the half-wave doubler, energy is supplied to the output capacitor C_2 (and current is delivered to the load) only on alternate half-cycles of the applied ac volt-



92CS-21708

Fig. 277—Half-wave voltage-doubler circuit.

age. The ripple frequency of this doubler circuit, therefore, is the same as the frequency of the applied ac voltage. Voltage regulation in this circuit is even poorer than that in the full-wave doubler circuit. The half-wave doubler, however, can be used with the negative terminal of the load connected to one side of the ac line. For this reason, the circuit has been and will continue to be used for low-current applications such as power supplies for ac-dc radio receivers.

***n*-Times Voltage Multipliers:** Additional voltage multiplication can be obtained by "stacking" or

cascading rectifier circuits. The voltage tripler circuit shown in Fig. 278 is derived from the half-wave voltage doubler shown in Fig. 277 by addition of the section that includes rectifier D_3 and capacitor C_3 . Similarly, higher orders of multiplication can be obtained by use of additional half-wave doubler sections in cascade, as indicated in Fig. 279.

High-Voltage Rectifiers for Television Receivers—The dc supply voltage for the picture tube in television receivers is usually derived from the horizontal-scan retrace voltage. This voltage is stepped-up by the high-voltage

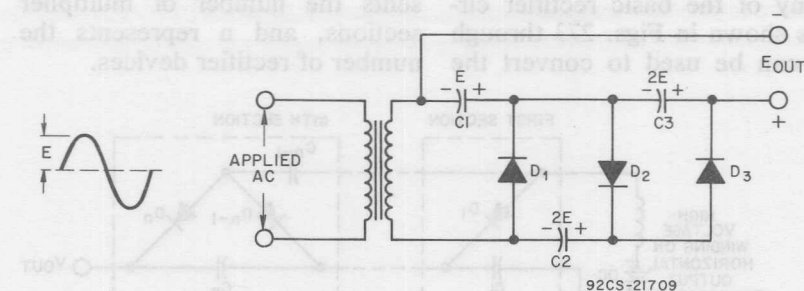


Fig. 278—Half-wave voltage-tripler circuit.

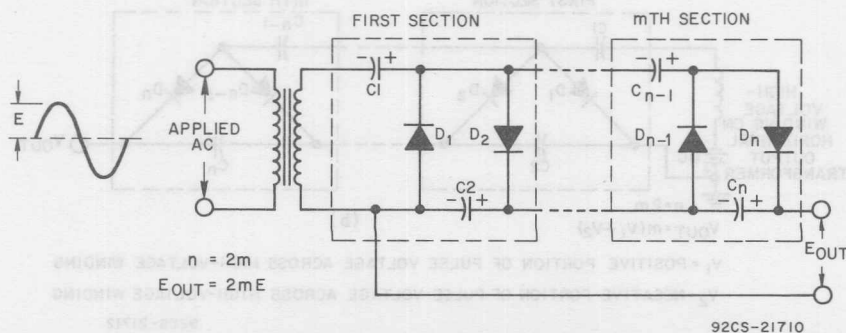


Fig. 279—Half-wave "n" multiplier rectifier circuit.

(flyback) transformer. The retrace voltage waveform consists of a narrow high-amplitude positive pulse followed by a low-amplitude negative excursion, as shown in Fig. 280. The negative excursion, which is very small in comparison to the positive pulse, contributes only slightly to the dc voltage developed for the picture tube.

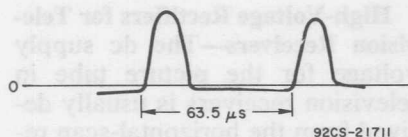


Fig. 280—Retrace voltage.

Any of the basic rectifier circuits shown in Figs. 273 through 279 can be used to convert the

retrace waveform into the high dc voltage required for the picture tube. Voltage-multiplier circuits are frequently used, however, in order to reduce the voltage stresses on the high-voltage transformers, the capacitors, and the rectifiers. Fig. 281 shows the basic configurations for voltage-multiplier circuits used as the high-voltage dc supply in television receivers. The battery shown in the circuit diagrams represents either the low-voltage dc supply in the television receiver or the average voltage on a capacitor connected to the ground side of the high-voltage transformer. In these circuit diagrams, m represents the number of multiplier sections, and n represents the number of rectifier devices.

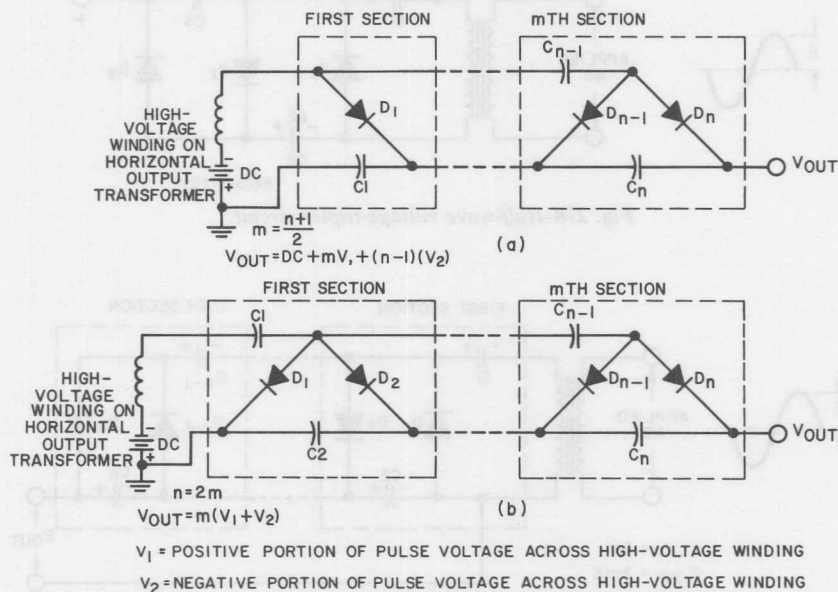
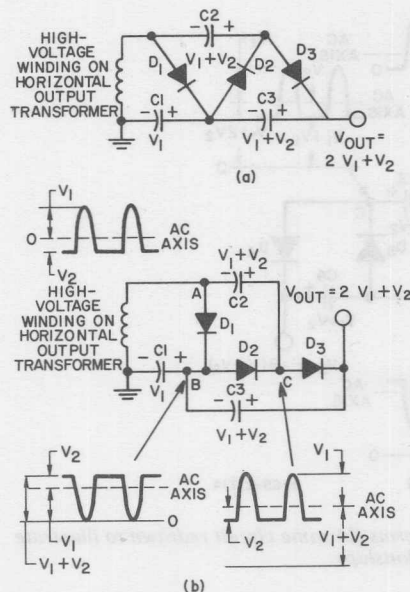


Fig. 281—Basic multiplier circuits: (a) with odd number of diodes; (b) with even number of diodes.

The **three-diode multiplier** shown in Fig. 282 is a practical example of the basic configuration shown in Fig. 281(a). This circuit provides a dc output voltage that is slightly more than twice the



92CS-21713

Fig. 282—Three-diode multiplier (TV voltage doubler). (a) standard form; (b) same circuit redrawn to illustrate voltage relationships.

peak value of the input (retrace) voltage. (The dc voltage at the ground end of the high-voltage transformer is not shown in Fig. 282 because this voltage is normally very small in comparison to the dc output from the high-voltage supply.) The three-diode multiplier shown in Fig. 282, is essentially the same basic circuit as the voltage tripler shown in Fig. 278. However, because the negative excursion of the retrace

voltage obtained from the high-voltage transformer is very small in comparison to the positive pulse, the three-diode circuit is normally referred to a voltage doubler when used in a television-receiver high-voltage supply.

Fig. 283 shows a **four-diode doubler circuit** derived from the basic voltage-multiplier configuration shown in Fig. 281(b). This circuit is identical to the n-type voltage multiplier shown in Fig. 278 for $m=2$. With a sine-wave input, this circuit would quadruple the input voltage.

Figs. 284 and 285 show a **voltage tripler** and a **voltage quadrupler** that are typical of the types of voltage-multiplier circuits used in television receivers. These circuits "tap" the voltage across the capacitor in the lowest-voltage section of the circuit to provide a focus voltage for the picture tube. In the circuit shown in Fig. 285, a resistor is included in series with one of the rectifiers so that the focus voltage more closely tracks the high-voltage output.

The rectifiers used in the voltage multipliers for television high-voltage supplies are specially designed, fast-recovery types that have closely matched characteristics so that the RC compensation is not required. The RC compensation used to achieve voltage equalization in high-voltage rectifier stacks is explained and RCA fast-recovery rectifiers recommended for use in television high-voltage supplies are listed in the section on **Silicon Rectifiers**.

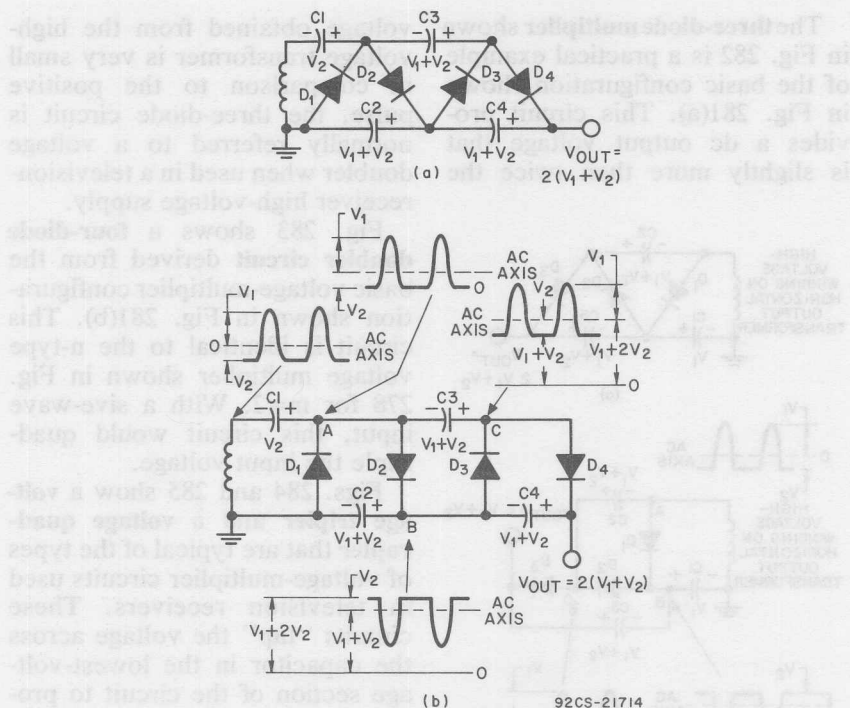


Fig. 283—Four-diode multiplier: (a) standard forms (b) same circuit redrawn to illustrate voltage relationships.

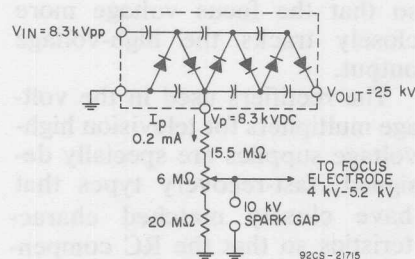


Fig. 284—Typical voltage "tripler" circuit.

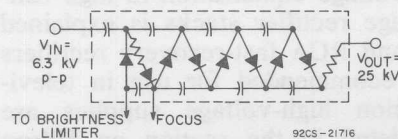


Fig. 285—Voltage-quadrupler circuit.

Polyphase Rectifiers

Modern power-distribution systems transmit ac power over three wires with the voltage between any two wires in the system 120 degrees out of phase with the voltage across the other two pair of wires. This arrangement is referred to as a three-phase system.

Power delivered to private homes normally consists of one phase of the three-phase system. Practically all industrial installations use three-phase power. Direct current is required, however, for many of the processes and equipment used in industrial

plants; polyphase rectifier circuits, therefore, are required. The configurations employed may include three-phase, six-phase, or twelve-phase circuits all of which are derived from the basic three-phase circuits.

Three-Phase, Half-Wave, Delta-Wye Rectifier—Fig. 286 shows the basic configuration and output-voltage waveform for a three-phase, half-wave, delta-wye rectifier circuit. This circuit consists of three half-wave rectifiers, one for each of the three phases.

Each rectifier carries current during the positive half-cycle of its particular phase of the applied ac input; current, therefore, flows for one-third of the time. The ripple frequency of the output is three times the frequency of the ac input so that filtering of the output is relatively easy.

Three-Phase, Full-Wave, Delta-Wye Bridge Rectifier—Fig. 287 shows the circuit diagram and

output-voltage waveform for a three-phase, full-wave, delta-wye bridge rectifier. This circuit requires twice as many rectifiers as the half-wave circuit shown in Fig. 286; however, it also provides twice the dc output voltage for the same transformer secondary voltage.

Three-Phase, Delta-Star (Six-Phase), Half-Wave Rectifier—In the rectifier circuit shown in Fig. 288, the windings of the wye-type secondary are center-tapped to achieve the equivalent of six-phase operation. The voltage across each half of each winding of the "star-connected" secondary is opposite in polarity to the voltage across the other half of the winding. In effect, therefore, this system provides a total of six phases (one phase for each leg of the star.) Each rectifier conducts only during the time when its associated secondary winding is most positive, i.e., 60 electrical degrees.

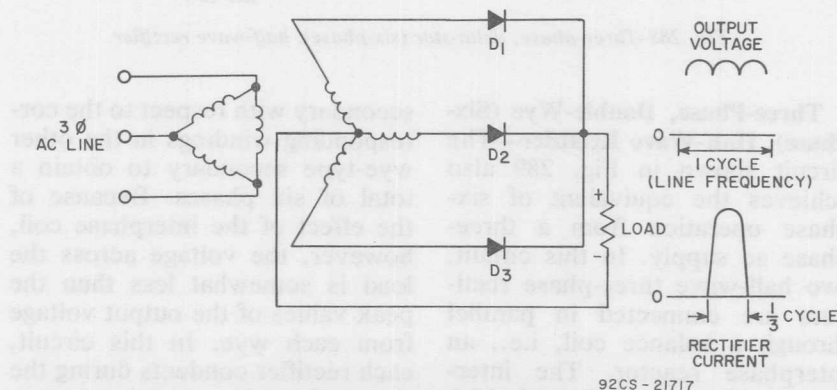


Fig. 286—Three-phase half-wave Delta-Wye circuit.

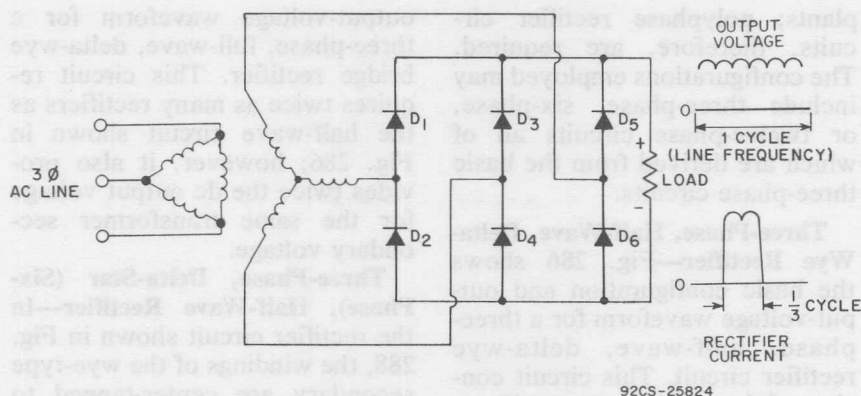


Fig. 287—Three-phase, full-wave, delta-wye bridge rectifier.

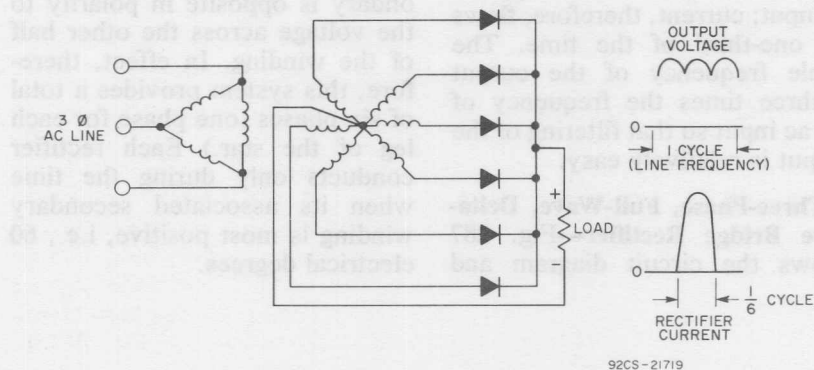
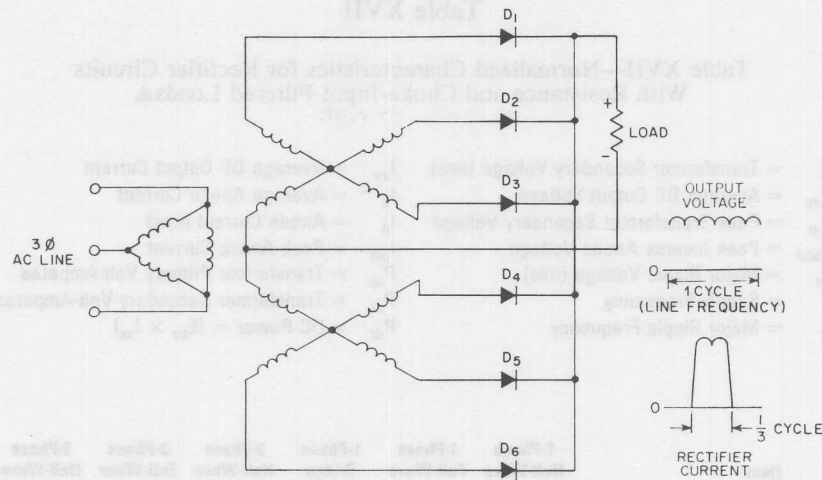


Fig. 288—Three-phase, delta-star (six-phase), half-wave rectifier.

Three-Phase, Double-Wye (Six-Phase), Half-Wave Rectifier—The circuit shown in Fig. 289 also achieves the equivalent of six-phase operation from a three-phase ac supply. In this circuit, two half-wave three-phase rectifiers are connected in parallel through a balance coil, i.e., an interphase reactor. The interphase coil reverses the polarities of the windings in one wye-type

secondary with respect to the corresponding windings in the other wye-type secondary to obtain a total of six phases. Because of the effect of the interphase coil, however, the voltage across the load is somewhat less than the peak values of the output voltage from each wye. In this circuit, each rectifier conducts during the time when its associated secondary winding is the most posi-



92CS-25826

Fig. 289—Three-phase, half-wave, double-wye and interphase transformer circuit.

tive within the wye secondary, i.e., 120 electrical degrees. The output current is shared between the two wye secondaries.

Rectifier Voltage and Current Ratios

Table XVII lists voltage and current ratios for the basic rectifier circuits shown in Figs. 273 through 275 and in Figs. 286 through 289. For most effective use of the rectifiers and power transformers, operation of the rectifier circuits into inductive loads, except for the single-phase half-wave type, is generally recommended. Current ratios given for inductive loads are applicable only when a filter choke (inductance) is used between the output of the rectifier and any capacitor in the filter circuit. The values shown neglect the voltage drops

in the power transformer, the silicon rectifiers, and the filter components that occur when load current is drawn. When a specific type of rectifier has been selected for a specific circuit, the information given in Table XVII can be used to determine the parameters and characteristics of the circuit.

FILTER NETWORKS

In general, the output-voltage waveform of a dc power supply should be as flat as possible (i.e., should approach a pure dc). The objective, therefore, is a voltage waveform that has a peak-to-average ratio of unity. The output of a basic rectifier circuit, however, is a series of positive or negative pulses rather than a pure dc voltage. The rectifier output may be considered as a steady dc

Table XVII

Table XVII—Normalized Characteristics for Rectifier Circuits
With Resistance and Choke-Input-Filtered Loads▲

E	= Transformer Secondary Voltage (rms)	I_{av}	= Average DC Output Current
E_{av}	= Average DC Output Voltage	I_b	= Average Anode Current
E_m	= Peak Transformer Secondary Voltage	I_p	= Anode Current (rms)
E_{bmi}	= Peak Inverse Anode Voltage	I_{pm}	= Peak Anode Current
E_r	= Major Ripple Voltage (rms)	P_{ap}	= Transformer Primary Volt-Amperes
F	= Supply Frequency	P_{as}	= Transformer Secondary Volt-Amperes
f_r	= Major Ripple Frequency	P_{dc}	= DC Power = $(E_{av} \times I_{av})$

Item	1-Phase Half-Wave (Fig. 273)	1-Phase Full-Wave (Fig. 274)	1-Phase Bridge (Fig. 275)	3-Phase Half-Wave (Fig. 286)	3-Phase Full-Wave (Fig. 287)	3-Phase Half-Wave Double-Wye with Bal. Coil (Fig. 289)
Voltage Ratios						
E_m / E_{av}	3.14	1.57	1.57	1.21	1.05	1.05
E / E_{av}	2.22	1.11	1.11	0.854	0.74	0.854
E_{bmi} / E	1.41	2.83	1.41	2.45	2.83	2.45
E_{bmi} / E_{av}	3.14	3.14	1.57	2.09	2.09	2.09
E_r / E_{av}	1.11	0.471	0.471	0.177	0.040	0.04
Frequency Ratio						
■ f_r / f	1	2	2	3	6	6
Current Ratios						
■ I_b / I_{av}	1	0.5	0.5	0.333	0.167	0.167
Resistive Load						
I_p / I_{av}	1.57	0.785	0.785	0.587	0.409	0.294
I_{pm} / I_{av}	3.14	1.57	1.57	1.21	1.05	0.525
I_{pm} / I_b	3.14	3.14	3.14	3.63	6.3	3.14
Inductive Load°						
I_p / I_{av}	*	0.707	0.707	0.577	0.408	0.289
I_{pm} / I_{av}	*	1.00	1.00	1.00	1.00	0.5

Notes:

- ▲ Conditions assume sine-wave voltage supply; zero voltage drop across rectifiers when conducting; no losses in transformer or choke; output load is a pure resistance.
- ° The use of a large filter-input choke is assumed.
- * Single-phase, half-wave, choke-input-filtered load has no practical significance; only a minute pulsating dc current will flow.
- These ratios also apply for the case of capacitor-input filtered load.

voltage with an alternating voltage superimposed on it. For most applications, this alternating voltage (ripple) must be removed (filtered out), or the equipment in which the power supply is used will not operate properly.

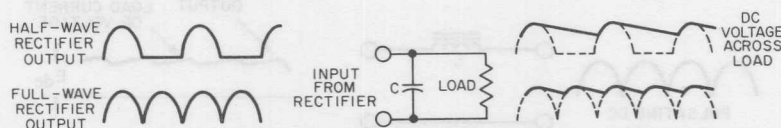
Types of Filters

Filter networks are normally used with rectifier circuits to smooth out the ripple in the dc output. The types of configurations for such networks are as many and as varied as the rectifier circuits with which they are used. Regardless of the type of configuration used, however, the operation of the filter network is based upon the principle that a capacitor will not react to rapid changes in voltage, an inductance opposes any change in the magnitude of the current through it, or a combination of these factors.

Capacitance Filter — The simplest type of power-supply filter consists of a single capacitor in shunt with the load, as shown in Fig. 290. The capacitor charges and stores energy in its electric field when the voltage tends to rise above the average value and discharges to release this energy when current flows into the load and the voltage tends to decrease.

The simple capacitor filter is used in low-current applications, such as high-voltage supplies for television receivers. This simple filter provides poor voltage regulation at high load currents, and even though some smoothing of the output voltage is achieved, as shown in Fig. 290, the ripple content, at best, is still greater than can be tolerated in many circuits. Although the ripple content can be reduced and the regulation can be improved by use of a larger filter capacitor, the charging current may become excessive and cause damage to the rectifiers if the capacitor is made too large. Fig. 291 shows the effect of the filter capacitor on the current and voltage in a half-wave rectifier. As mentioned previously, excessive peak currents in the rectifiers may be avoided by insertion of a surge limiting resistor in series with the rectifiers. The use of surge limiting resistors, however, adversely affects the voltage regulation.

Inductance Filter — Some degree of filtering is obtained when a single inductance is placed in series with the rectifier output, as shown in Fig. 292. The inductor opposes any change in the magnitude of the load current. Energy is stored in the magnetic field of



92CS-21721

Fig. 290—Single capacitor filter.

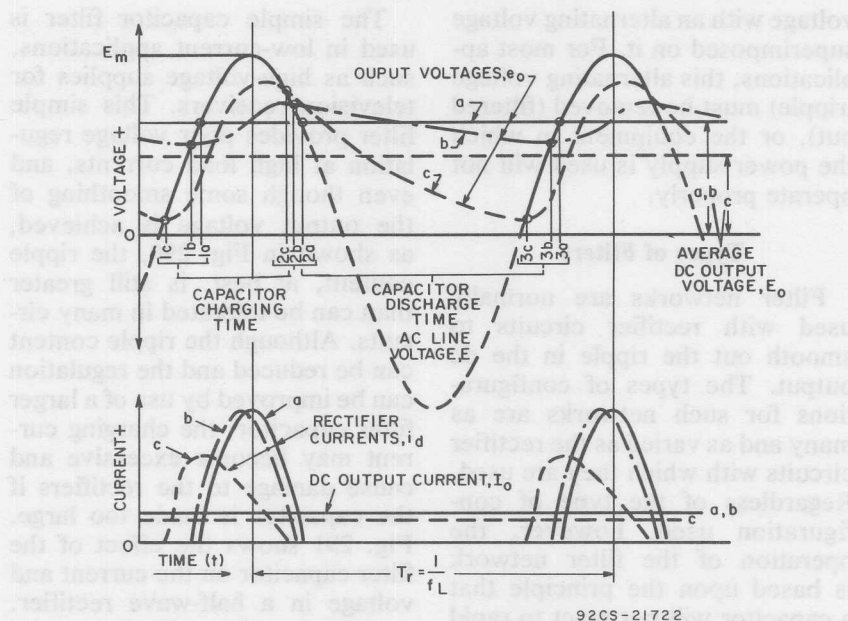


Fig. 291—Effect on Current and Voltage Waveshapes of Changing the Size of the Input-Filter Capacitor in a Half-Wave, Single-Phase Rectifier.

the inductor when the current tends to increase, and this energy is released to maintain the current flow to the load when the current tends to decrease. The result is a substantial reduction in the magnitude of the ripple voltage at the output of the filter.

As shown in Fig. 292, the current through the inductor (and the voltage across the load) lag the rectifier output voltage (input to the filter) by 90 degrees. In addi-

tion, the magnitude of the dc output voltage, however, does not decrease as rapidly with an increase in load current as that of the capacitor filter.

Choke-Input Filter — Fig. 293 shows a choke-input filter with a shunt capacitor output. At zero load current, the dc output voltage of this filter is nearly equal to the peak value of the pulsating dc from the rectifier. For this

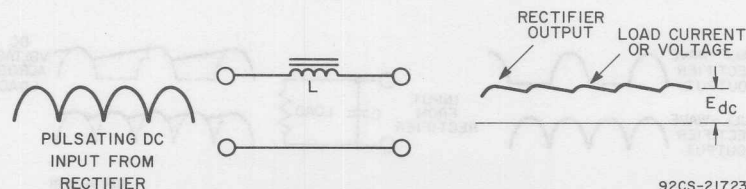


Fig. 292—Simple inductance filter.

condition, no voltage is dropped across the inductor, and the output capacitor can charge to the full peak value. As soon as load current is drawn, however, the dc output decreases to a lower value and is then maintained over a relatively wide range of load current.

where R_L is the load resistance presented to the power supply.

In general, a choke-input filter is not used with a half-wave rectifier because of the extremely low output voltage that would be obtained.

The relationships given for the

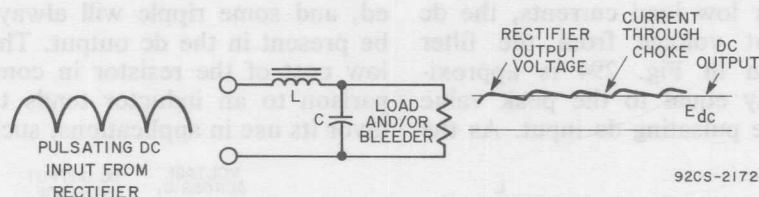


Fig. 293—Choke-input filter.

Frequently, a bleeder resistor is connected across the output of the filter in order to assure that operation starts in the relatively constant portion of the voltage-regulation characteristic. The bleeder also prevents the development of high-voltage surges across the load when the equipment is first turned on.

The inductance of the choke L shown in Fig. 293 must be above a certain critical value in order to maintain a continuous flow of load current. For operation in a 60-Hz supply, the minimum value of the choke inductance can be approximated as follows:

$$L = R_L/1130 \quad (75)$$

For operation in a 50-Hz supply, the minimum value of choke inductance is given by

$$L = R_L/940 \quad (76)$$

minimum value of choke inductance indicate that, if the load current varies, the required value of inductance can vary over a wide range. At extremely low currents, the load resistance R_L becomes very high, and the required value of choke inductance may be excessive in comparison to that required for good filtering at normal load currents. A bleeder resistor may be used to reduce the initial inductance required for the filter choke. If the load current varies over a very wide range, a "swinging" choke may be used. This type of choke has a smaller air gap than that required to maintain a constant inductance at all loads. The inductance of the swinging choke will be high at low load currents and will decrease as load current increases.

Capacitor-Input Filter — The smoothing actions of capacitors and inductors can be combined as

shown in Fig. 294. In such a filter, the capacitors charge and discharge as required to prevent any significant change in voltage, and the magnetic field of the inductor stores or releases energy as required in an effort to prevent changes in the magnitude of the load current.

For low load currents, the dc output voltage from the filter shown in Fig. 294 is approximately equal to the peak value of the pulsating dc input. As the

circuit shown in Fig. 294 can be replaced by a resistor. The resultant resistance-capacitance filter is shown in Fig. 295. The series resistor in the filter offers the same impedance to both the dc and the ripple components of the rectifier output. The effectiveness of the resistor, therefore, is limited, and some ripple will always be present in the dc output. The low cost of the resistor in comparison to an inductor tends to favor its use in applications, such

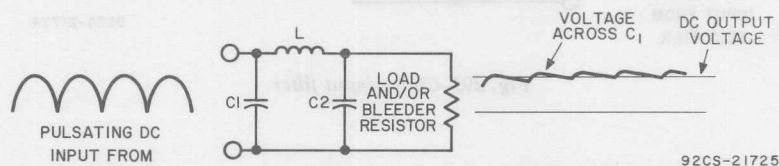


Fig. 294—Capacitor-input LC filter.

load current increases, the capacitors are unable to maintain this peak value, and the output voltage decrease rapidly. A bleeder resistor should always be connected across the output of the capacitor input filter. This resistor improves the voltage regulation and also provides a discharge path for the capacitors when the equipment is turned off.

Resistance-Capacitance Filter —
If load-current requirements are small, the inductance in the filter

as ac-dc receivers, in which cost is a major consideration.

The value of the input capacitor C_1 in the resistance-capacitance filter should be sufficiently large so that its impedance to the ripple-frequency component is very low in comparison to the dc resistance of resistor R . In some applications, the value of resistor R may be restricted to only 10 to 20 ohms in order to minimize the dc voltage drop. In such cases, the capacitance of C_1 may be selected to provide about the

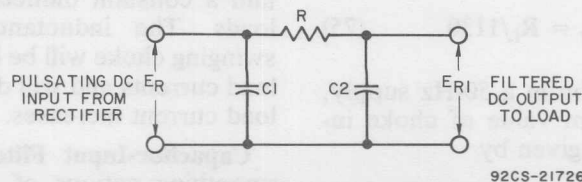


Fig. 295—Resistance-capacitance filter.

same impedance to the ripple-frequency component as that provided by resistor R . The value of the output capacitor C_2 is then chosen to produce the required degree of filtering of the output voltage. The ripple-reduction factor across the load (α) is expressed by the following equation:

$$\alpha = E_R/E_{R1} = 2RC_2 + 1 \quad (77)$$

where E_R is the ripple voltage at the input to the filter and E_{R1} is the ripple voltage at the output of the filter.

The ripple-reduction factor may be read directly from the curves shown in Fig. 296. If several resistance-capacitance filter sections are connected in series, the total reduction factor is approximately equal to the product of the reduction factors of the individual sections.

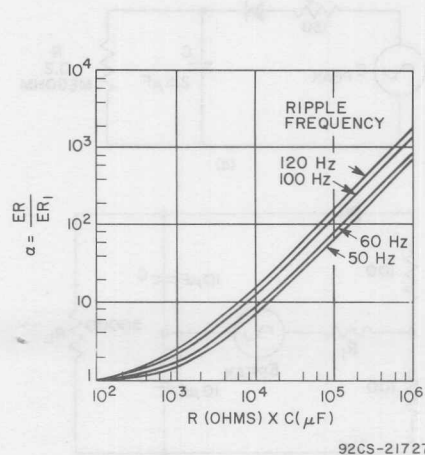


Fig. 296—Curve for determining the value of $\alpha = E_R/E_{R1}$ of a resistance-capacitance type single section filter for frequencies of 50, 60, 100 and 1200 Hz. This curve is based on the formula, $E_R/E_{R1} = \omega CR + 1$.

Combined LC Filters — Any of the filter networks described in the preceding paragraphs may be connected in cascade to obtain better filtering and improved voltage regulation. For example, the filter networks shown in Figs. 293 and 294 are often combined. The resultant filter network is shown in Fig. 297. This network may be considered as two choke-input filters in cascade.

In the design of an LC filter, the filter network is normally assumed to consist of a series inductance and a shunt capacitance. For a capacitor-input filter, such as that shown in Fig. 294, the input capacitor is considered to be part of the rectifier output rather than part of the filter. Consequently, for this design approach, the sections of a capacitor-input LC filter and a choke-input filter become identical. The rectifier output voltage and the ripple voltage applied to the series inductance of the capacitor-input filter (i.e., the voltage across the input filter capacitor) can be obtained directly from the **Design Curves** shown subsequently in the discussion of **Capacitive-Load Circuits**.

The fractional reduction in the ripple voltage provided by a choke-input filter of n identical sections can be determined from the following relationship:

$$\alpha = E_R/E_{R1} = (4^2 f^2 LC - 1)^n \quad (78)$$

where E_R is the ripple voltage at the input to the filter, E_{R1} is the ripple voltage at the output of the

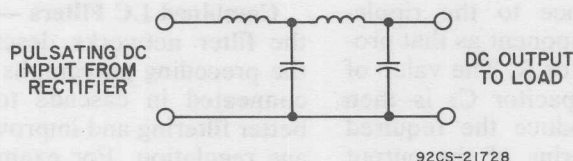


Fig. 297—Combined choke-input and capacitor-input LC filter.

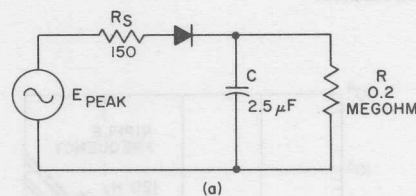
filter, f is the fundamental ripple frequency, LC is the inductance-capacitance product of one filter section, and n is the number of identical filter sections.

If the filter sections are not identical, the ripple-reduction factor α should be calculated separately for each section. (For these calculations, n is equal to unity.) The ripple-reduction factor for the over-all filter is then equal to the product of the individual factors for each section.

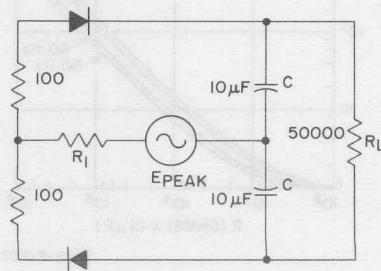
Capacitive-Load Circuits

When rectifiers are used in circuits with capacitive loads, the rectifier current waveforms may deviate considerably from their true sinusoidal shape. This deviation is most evident for the peak-to-average-current ratio, which is somewhat higher than that for a resistive load. For this reason, capacitive-rating calculations are generally more complicated and time-consuming than those for resistive-load rectifier circuits. However, the simplified rating system described below allows the designer to calculate the characteristics of capacitive-load rectifier circuits quickly and accurately.

Surge-Limiting Resistance — Fig. 298 shows typical half-wave and voltage-doubling rectifier circuits that use capacitive loads. In such circuits, the low forward voltage drop of the silicon rectifiers may result in a very high surge of current when the capacitive load is first energized. Although the generator or source impedance may be high enough to protect the rectifier, additional resistance must be added in some cases. The sum of this resistance



(a)



(b)

92CS-21729

Fig. 298—Typical rectifier circuits using capacitive loads: (a) half-wave rectifier circuit; (b) voltage doubler.

plus the source resistance is referred to as the total limiting resistance R_s . The magnitude of R_s required for protection of the rectifier may be calculated from surge rating charts such as those shown in Figs. 299 and 300. Each point of these curves defines a surge rating by indicating the maximum time for which the device can safely carry a specific value of rms current.

With a capacitive load, maximum surge current occurs if the

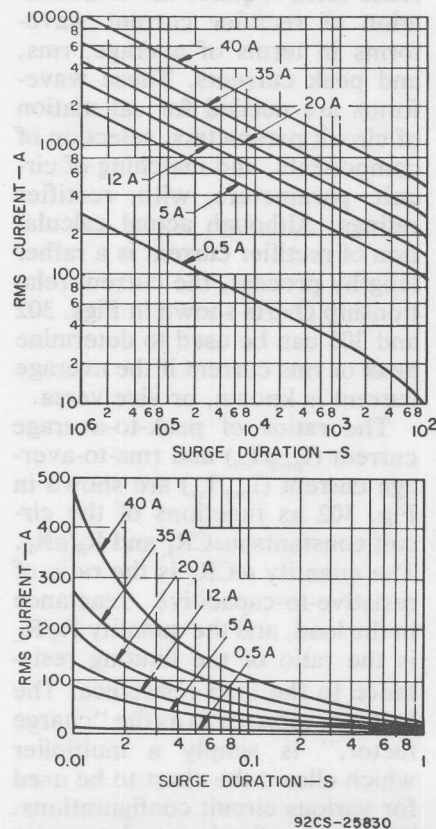


Fig. 299—Universal surge rating charts for RCA rectifiers.

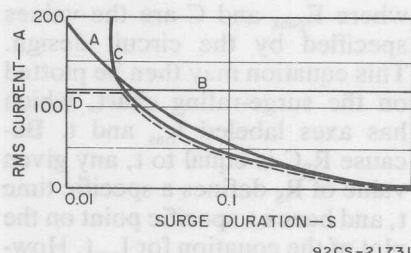


Fig. 300—Typical coordination chart for determination of fusing requirements: Curve A—surge rating for 20-ampere rectifier; Curve B—expected surge current in half-wave circuit; Curve C—opening characteristics of protective device; Curve D—resulting surge current in modified circuit.

circuit is switched on when the input voltage is near its peak value. When the time constant $R_s C$ of the surge loop is much smaller than the period of the input voltage, the peak current I_{peak} is equal to the peak voltage E_{peak} divided by the limiting resistance R_s , and the resulting surge approximates an exponentially decaying current with the time constant $R_s C$.

Surge-current ratings for rectifiers are often given in terms of the rms value of the surge current and the time duration t of the surge. For rating purposes, the surge duration t is defined by the time constant $R_s C$. The rms surge current I_{rms} is then approximated by the following equations:

$$\begin{aligned} I_{\text{rms}} &= 0.7 (E_{\text{peak}} C / R_s C) \\ &= 0.7 (E_{\text{peak}} C / t) \end{aligned} \quad (79)$$

and

$$I_{\text{rms}} t = 0.7 E_{\text{peak}} C \quad (80)$$

where E_{peak} and C are the values specified by the circuit design. This equation may then be plotted on the surge-rating chart, which has axes labeled I_{rms} and t . Because $R_S C$ is equal to t , any given value of R_S defines a specific time t , and hence a specific point on the plot of the equation for $I_{\text{rms}} t$. However, R_S must be large enough to make this point fall below the rating curve for the rectifier used.

The following example illustrates the use of this simplified procedure for the half-wave rectifier circuit shown in Fig. 298(a), which has a frequency f of 60 Hz and a peak input voltage E_{peak} of 4950 volts. The values shown for E_{peak} and C are substituted in the equation for $I_{\text{rms}} t$ as follows:

$$\begin{aligned} I_{\text{rms}} t &= 0.7 (4950) (2.5 \times 10^{-6}) \\ &= 0.0086 \end{aligned}$$

When this value is plotted on the surge-rating chart of Fig. 301, the resulting line intersects the rectifier rating curve at 3.3×10^{-4} second. The minimum limiting resistance which affords adequate

surge protection is then calculated as follows:

$$\begin{aligned} R_S C &\geq 3.3 \times 10^{-4} \\ R_S &\geq \frac{3.3 \times 10^{-4}}{2.5 \times 10^{-6}} = 132 \text{ ohms} \end{aligned}$$

Therefore the value of 150 ohms shown for R_S in Fig. 298(a) provides adequate surge-current protection for the rectifier.

Design Curves — The design of rectifier circuits having capacitive loads often requires the determination of rectifier current waveforms in terms of average, rms, and peak currents. These waveforms are needed for calculation of circuit parameters, selection of components, and matching of circuit parameters with rectifier ratings. Although actual calculation of rectifier current is a rather lengthy process, the current-relationship charts shown in Figs. 302 and 303 can be used to determine peak or rms current if the average current is known, or vice versa.

The ratios of peak-to-average current ($I_{\text{peak}}/I_{\text{av}}$) and rms-to-average current ($I_{\text{rms}}/I_{\text{av}}$) are shown in Fig. 302 as functions of the circuit constants ωCR_L and R_S/nR_L . The quantity ωCR_L is the ratio of resistive-to-capacitive reactance in the load, and the quantity R_S/R_L is the ratio of the limiting resistance to the load resistance. The factor n , referred to as the "charge factor," is simply a multiplier which allows the chart to be used for various circuit configurations. The value of n is equal to unity for half-wave circuits, to 0.5 for

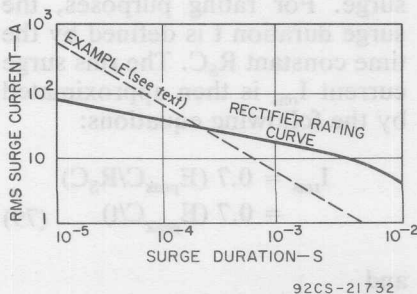


Fig. 301—Surge rating chart for a stack rectifier.

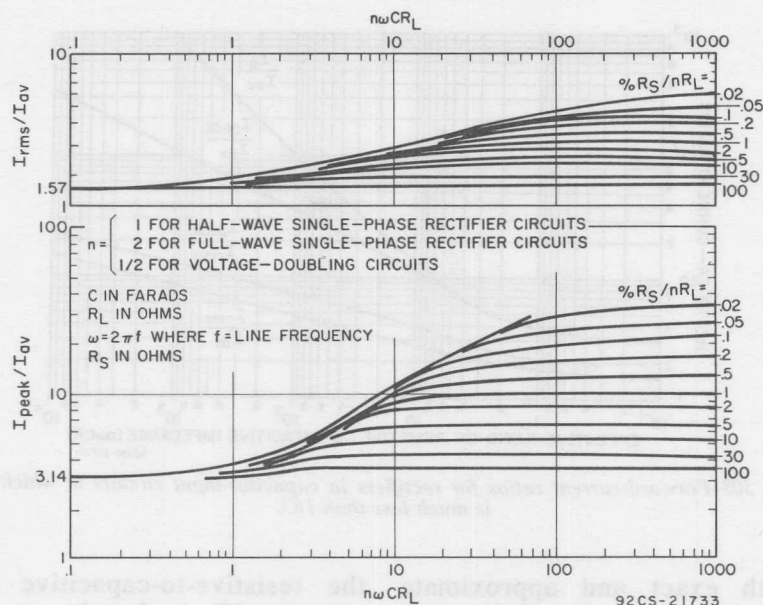


Fig. 302—Relationship of peak, average, and rms rectifier currents in capacitor-input circuits.

doubler circuits, and to 2 for full-wave circuits. (These values actually represent the relative quantity of charge delivered to the capacitor on each cycle.)

In many silicon rectifier circuits, R_s may be neglected when compared with the magnitude of R_L . In such circuits, the calculation of rectifier currents is simplified by use of Fig. 303, which gives current ratios under the limitation that R_s/R_L approaches zero. Even if this condition is not fully satisfied, the use of Fig. 303 merely indicates a higher peak and higher rms current than will actually flow in the circuit, i.e., the rectifiers will operate more conservatively than calculated. As a result, this simplified solution can be used whenever a rough

approximation or a quick check is needed on whether a particular rectifier will fit a specific application. When more exact information is needed, the chart of Fig. 302 should be used.

Average output voltage E_{av} is another important quantity in capacitor-input rectifier circuits because it can be used to determine average output current I_{av} . The relationships between input and output voltages for half-wave, voltage-doubler, and full-wave circuits are shown in Figs. 304, 305, and 306, respectively. Fig. 307 shows curves of output ripple voltage (as a percentage of E_{av}) for all three types of circuits.

The following example illustrates the use of these curves in rectifier-current calculations.

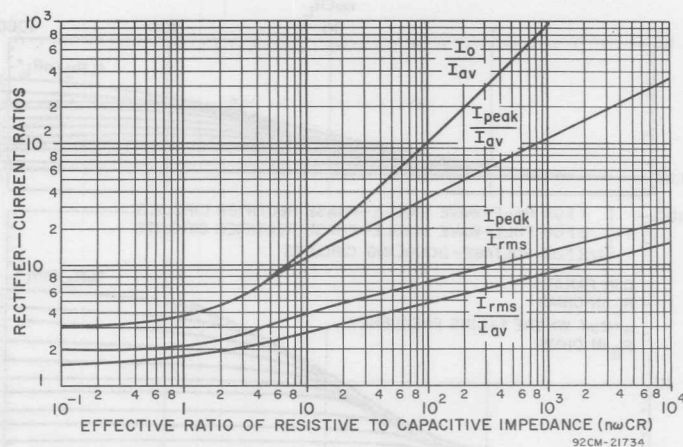


Fig. 303—Forward-current ratios for rectifiers in capacitor-input circuits in which R_s is much less than $1/C$.

Both exact and approximate solutions are given. For the half-wave circuit of Fig. 299(a),

the resistive-to-capacitive reactance ωCR_L is given by

$$\begin{aligned}\omega CR_L &= 2\pi \times 60 \times 2.5 \times 10^{-6} \\ &= \times 200,000 \\ &= 189\end{aligned}$$

For an exact solution using Fig. 302, the ratio of R_s to R_L is first calculated as follows:

$$\frac{R_s}{R_L} = \frac{150}{200,000} = 0.075 \quad (83)$$

The values for ωCR_L and R_s/R_L are then plotted in Fig. 304 to determine the average output voltage E_{av} and the average output current I_{av} as follows:

$$\begin{aligned}E_{av}/E_{peak} &= 98 \text{ per cent} \\ E_{av} &= 0.98 \times 4950 = 4850 \text{ volts} \\ I_{av} &= E_{av}/R_L \\ &= 4850 \text{ volts}/200,000 \text{ ohms} \\ &= 24.2 \text{ milliamperes}\end{aligned} \quad (84)$$

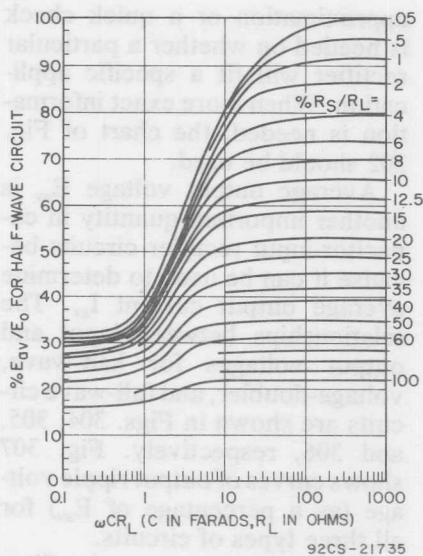


Fig. 304—Relationship of applied ac peak voltage to dc output voltage in half-wave capacitor-input circuit.

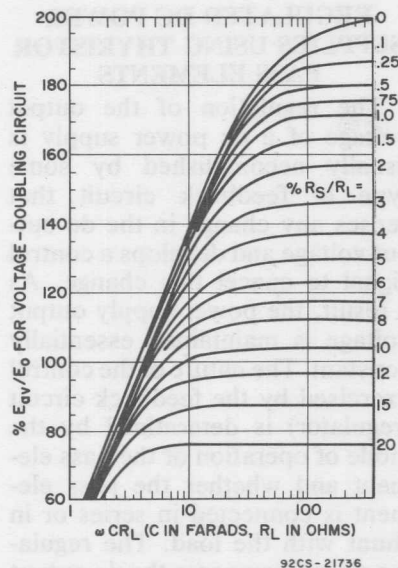


Fig. 305—Relationship of applied ac peak voltage to dc output voltage in capacitor-input voltage-doubler circuit.

This value of I_{av} is then substituted in the ratio of I_{rms}/I_{av} obtained from Fig. 302, and the exact value of rms current I_{rms} in the rectifier is determined as follows:

$$\begin{aligned} I_{rms}/I_{av} &= 4.4 \\ I_{rms} &= 4.4 \times 24.2 \\ &= 107 \text{ milliamperes} \end{aligned} \quad (85)$$

For a simplified solution using Fig. 303, it is assumed that the average output current I_{av} is approximately equal to the peak input voltage E_{peak} divided by the load resistance R_L , as follows:

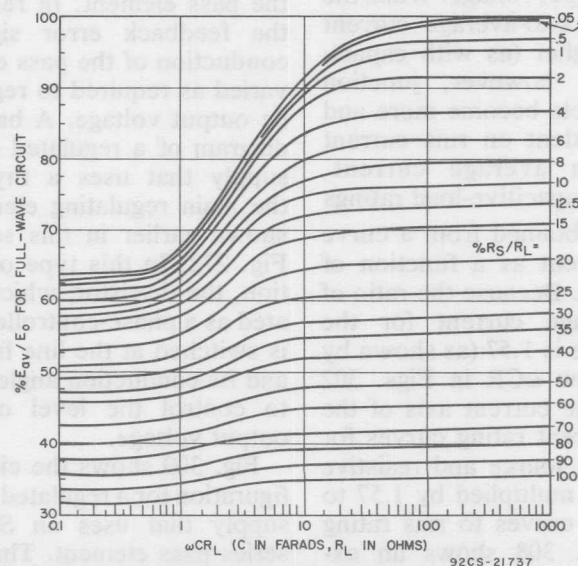


Fig. 306—Relationship of applied ac peak voltage to dc output voltage in full-wave capacitor-input circuit.

$$I_{av} = E_{peak}/R_L$$

$$I_{av} = 4950/200,000$$

$$= 24.7 \text{ milliamperes}$$

(86)

This value of I_{av} is then substituted in the ratio of I_{rms}/I_{av} obtained from Fig. 303, and the approximate rms current is determined, as follows:

$$I_{rms}/I_{av} = 5.7$$

$$I_{rms} = 5.7 \times 24.7$$

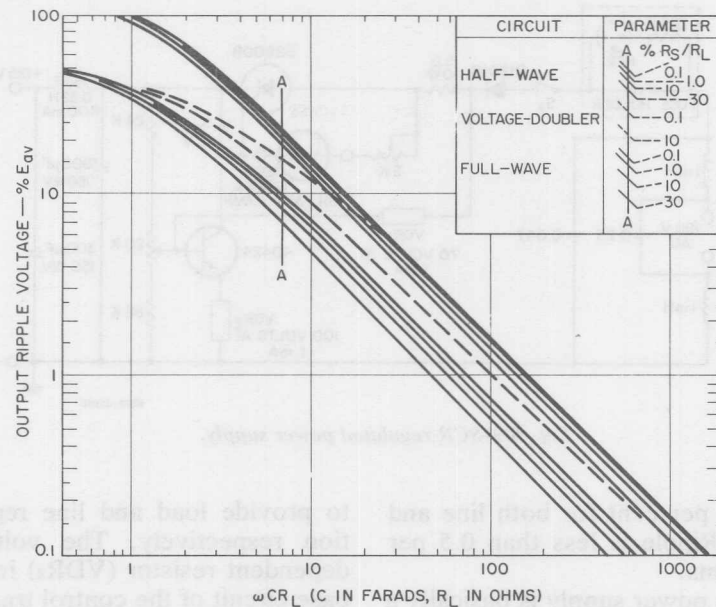
$$= 141 \text{ milliamperes (87)}$$

Current-versus-temperature ratings for rectifiers are usually given in terms of average current for a resistive load with 60-Hz sinusoidal input voltage. When the ratio of peak-to-average current becomes higher (as with capacitive loads), however, junction heating effects become more and more dependent on rms current rather than average current. Therefore, capacitive-load ratings should be obtained from a curve of rms current as a function of temperature. Because the ratio of rms-to-average current for the rated service is 1.57 (as shown by I_{rms}/I_{av} at low ωCR in Figs. 302 and 303), the current axis of the average-current rating curves for a sinusoidal source and resistive load can be multiplied by 1.57 to convert the curves to rms rating curves. Fig. 308 shows an example of this conversion for RCA stack-rectifier rating curves.

REGULATED DC POWER SUPPLIES USING THYRISTOR PASS ELEMENTS

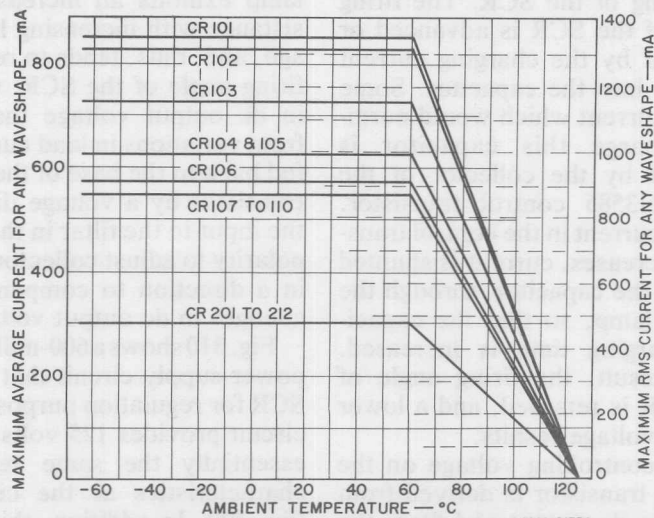
The regulation of the output voltage of a dc power supply is usually accomplished by some type of feedback circuit that senses any change in the dc output voltage and develops a control signal to cancel this change. As a result, the power-supply output voltage is maintained essentially constant. The nature of the control exercised by the feedback circuit (regulator) is determined by the mode of operation of the pass element and whether the pass element is connected in series or in shunt with the load. The regulator circuit compares the dc output voltage from the power supply with a reference voltage and develops a difference (error) signal that is amplified and fed back to the pass element. In response to the feedback error signal, the conduction of the pass element is varied as required to regulate the dc output voltage. A basic block diagram of a regulated dc power supply that uses a thyristor as the main regulating element was shown earlier in this section, in Fig. 272. In this type of application, the thyristor, which is operated as a phase-controlled device, is switched at the line frequency, and its conduction angle is varied to control the level of the dc output voltage.

Fig. 309 shows the circuit configuration for a regulated dc power supply that uses an SCR as a series pass element. This type of circuit is designed to provide approximately 125 volts, regulated



92CS-21738

Fig. 307—RMS ripple voltage in capacitor-input circuits.



92CS-21739

Fig. 308—Current-temperature ratings for silicon stack rectifiers.

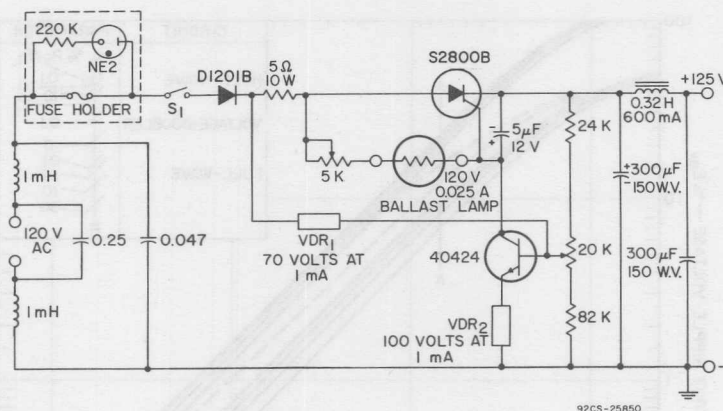


Fig. 309—SCR regulated power supply.

to ± 3 per cent for both line and load. Ripple is less than 0.5 per cent rms.

The power supply is basically a half-wave phase-controlled rectifier. The 5-microfarad capacitor between the cathode and gate of the SCR charges up during half of each cycle and is discharged by the firing of the SCR. The firing angle of the SCR is advanced or retarded by the charging current flowing into the capacitor. Some of the current which would normally charge this capacitor is shunted by the collector of the RCA-2N3585 control transistor. As the current in the control transistor increases, current is shunted around the capacitor, through the ballast lamp, so that the capacitor charging time is increased. As a result, the firing angle of the SCR is retarded, and a lower output voltage results.

The controlling voltage on the control transistor is derived from both the dc output and from the line voltage in such a manner as

to provide load and line regulation respectively. The voltage-dependent resistor (VDR₂) in the base circuit of the control transistor decreases resistance for an increase in line voltage and thus increases base current (and collector current) as line voltage is increased. In addition, the ballast lamp exhibits an increase in resistance with increasing line voltage, and, thus, tends to retard the firing angle of the SCR. Changes in dc output voltage that result from variations in load current are fed back to the base of the control transistor by a voltage divider at the input to the filter in the proper polarity to adjust collector current in a direction to compensate for changes in dc output voltage.

Fig. 310 shows a 600-milliampere power supply circuit that uses an SCR for regulation purposes. This circuit provides 125 volts dc with essentially the same regulation characteristics as the circuit of Fig. 309. In addition, this power supply provides 220 volts that is

unregulated for either line or load variations. A conventional bridge rectifier supplies unregulated dc to the regulator circuit, and a second bridge rectifier provides 120 volts unregulated voltage which is then added to the output of the regulated supply to provide 220 volts.

An isolation transformer (or a polarized line plug) should be used to supply the rectifiers in the power-supply circuit. Otherwise, if the chassis ground becomes connected to earth ground, which is one side of the ac line, a portion of the bridge will be shorted out.

The regulator portion of the circuit shown in Fig. 310 is similar to that of the circuit shown in Fig. 309, except that no ballast lamp is used. Transistor Q_1 governs the conduction angle of the SCR to provide regulation against line voltage changes, and transistor Q_2 provides regulation against changes in output voltage because of load-current variations.

Triacs can also be used in power-supply voltage-regulator applications. A low-voltage line-regulated dc power supply that uses a triac as the main regulating element is described in the section entitled **AC Voltage Regulator**.

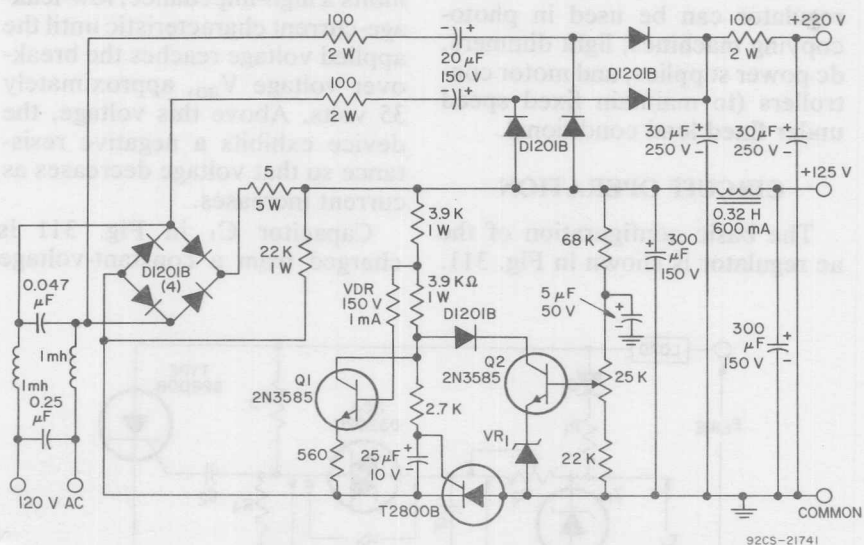


Fig. 310—SCR Power Supply Circuit

AC Voltage Regulator

Thyristors are used in a basic ac-voltage regulating circuit that prevents ac rms or dc voltage from fluctuating more than ± 3 per cent in spite of wide variations in input line voltage. Load voltage can also be held within ± 3 per cent of a desired value despite variations in load impedance through the use of a voltage-feedback technique. The voltage regulator can be used in photocopying machines, light dimmers, dc power supplies, and motor controllers (to maintain fixed speed under fixed load conditions).

CIRCUIT OPERATION

The basic configuration of the ac regulator is shown in Fig. 311.

For simplicity, only a half-wave SCR configuration is shown; however, the explanation of circuit operation is easily extended to include a full-wave regulator that uses a triac.

Thyristor Triggering

The RCA-D3202U diac used as the trigger device in Fig. 311, exhibits a high-impedance, low-leakage-current characteristic until the applied voltage reaches the break-over voltage V_{BO} , approximately 35 volts. Above this voltage, the device exhibits a negative resistance so that voltage decreases as current increases.

Capacitor C_1 in Fig. 311 is charged from a constant-voltage

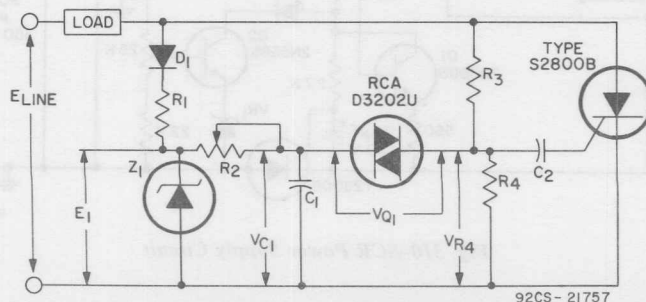


Fig. 311—Basic ac regulator.

source established by zener diode Z_1 . The capacitor is charged, therefore, at an exponential rate regardless of line-voltage fluctuations. A trigger pulse is delivered to the S2800B SCR when the voltage across capacitor C_1 is equal to the trigger voltage of the diac plus the instantaneous voltage drop developed across resistor R_4 during the positive half-cycle of line voltage. When the diac is turned on, the SCR is turned on for the remainder of the positive cycle of source voltage. Control of the conduction angle of the SCR regulates the rms voltage to the load.

Regulation Technique

Regulation is achieved by the following means: When line voltage increases, the voltage across R_4 increases, but the charging rate

of C_1 remains the same; as a result, the voltage across C_1 must attain a larger value than required without line-voltage increase before the diac can be triggered. The net effect is that the pulse that triggers the SCR is delayed, and the rms voltage to the load is reduced. In a similar manner, as line voltage is reduced, the SCR turns on earlier in the cycle and increases the effective voltage across the load.

Voltage Waveforms

Fig. 312 shows the voltage waveforms exhibited by the ac regulator at both high and low line voltage. The charging voltage, E_1 , for capacitor C_1 is equal to the zener voltage and remains constant up to the instant that the

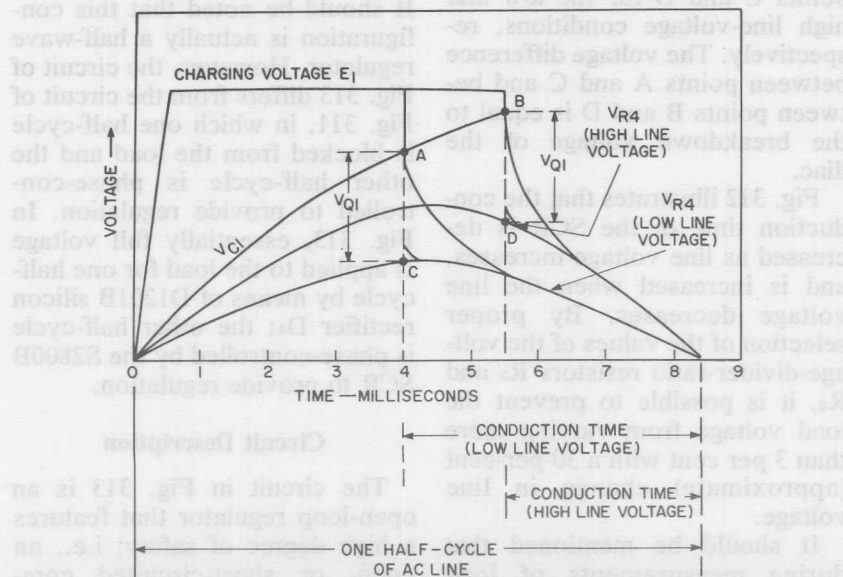


Fig. 312—Voltage waveforms exhibited by the ac regulator in Fig. 311.

SCR is turned on. The capacitor voltage, V_{C1} , increases exponentially because the charging voltage E_1 is constant. The voltage across resistor R_4 conforms to the sinusoidal variations of the 60-Hz line voltage. At any given phase angle, the voltage across R_4 increases if line voltage increases and decreases if line voltage decreases.

The diac and SCR both trigger when the capacitor voltage, V_{C1} , equals the breakover voltage of the diac plus the instantaneous value of voltage developed across R_4 during the positive half-cycle of line voltage. This capacitor voltage is represented by points A and B for the low and high line-voltage conditions, respectively. The instantaneous voltages across resistor R_4 just before the SCR is triggered are represented by points C and D for the low and high line-voltage conditions, respectively. The voltage difference between points A and C and between points B and D is equal to the breakdown voltage of the diac.

Fig. 312 illustrates that the conduction time of the SCR is decreased as line voltage increases, and is increased when the line voltage decreases. By proper selection of the values of the voltage-divider-ratio resistors R_3 and R_4 , it is possible to prevent the load voltage from varying more than 3 per cent with a 30-per-cent (approximate) change in line voltage.

It should be mentioned that during measurements of load voltage careful consideration

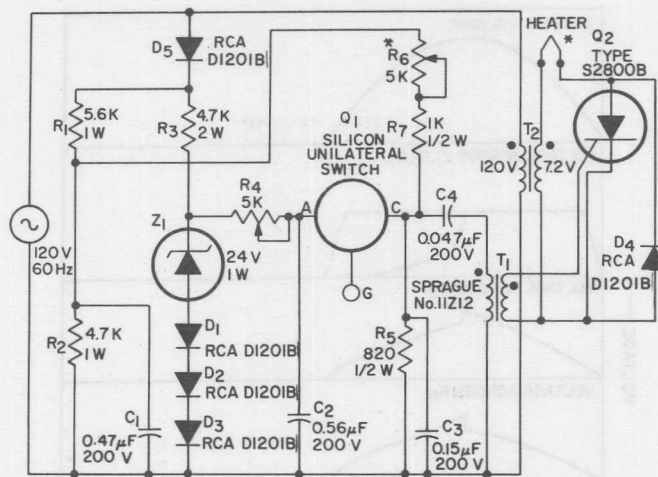
must be given to the measuring instruments. Many circuits produce a non-sinusoidal voltage across the load; the rms value of this voltage can be measured only with a true rms meter, such as a thermocouple meter. It is possible, however, that in certain applications the low input impedance of the thermocouple meter might load down the circuit being measured. In such cases, a high-input-impedance rms meter may be required.

HEATER-VOLTAGE REGULATOR

Fig. 313 shows a basic regulating technique for applications in which it is desired to maintain constant voltage across a load such as a receiving-tube heater, the filament of an incandescent lamp, or possibly a space heater. It should be noted that this configuration is actually a half-wave regulator. However, the circuit of Fig. 313 differs from the circuit of Fig. 311, in which one half-cycle is blocked from the load and the other half-cycle is phase-controlled to provide regulation. In Fig. 313, essentially full voltage is applied to the load for one half-cycle by means of D1201B silicon rectifier D_4 ; the other half-cycle is phase-controlled by the S2800B SCR to provide regulation.

Circuit Description

The circuit in Fig. 313 is an open-loop regulator that features a high degree of safety; i.e., an open- or short-circuited component does not result in an ex-



* IN THE CLOSED-LOOP REGULATOR, R_6 IS REPLACED BY A PHOTOCELL, AND A POTENTIOMETER IN SERIES WITH A 6-VOLT INCANDESCENT LAMP IS CONNECTED IN PARALLEL WITH THE HEATER TERMINALS
NOTE: ALL RESISTOR VALUES ARE IN OHMS

92CS-21759

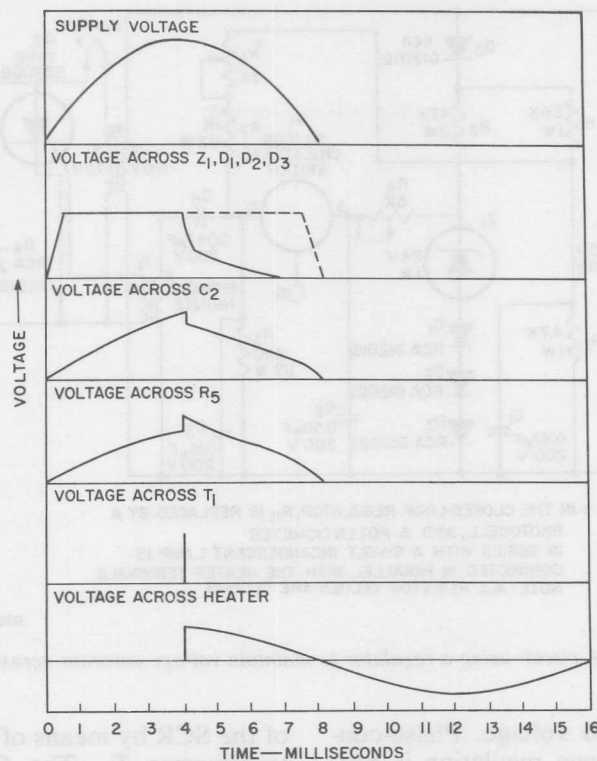
Fig. 313—A circuit using a regulator to maintain voltage constant across a load.

cessive load voltage. Phase-controlled voltage regulation is provided by a silicon unilateral switch* and a control circuit, as follows: Capacitor C_2 is charged from a voltage source that is maintained constant by zener diode Z_1 ; the silicon rectifiers D_1 , D_2 , and D_3 compensate for the change in zener voltage with temperature. The voltage across C_2 increases until the sum of the breakover voltage of Q_1 and the instantaneous voltage across R_5 is exceeded. At this point, a positive pulse is coupled into the gate

of the SCR by means of the pulse transformer T_1 . The SCR then switches on for the remainder of the positive cycle of line voltage. Control of the conduction angle of the SCR varies the rms voltage to the heater.

As line voltage increases, the voltage across resistor R_5 also increases; because capacitor C_2 charges along the same exponential curve, however, the voltage across C_2 must attain a larger value before the SCR is turned on. The net effect is a delay in the trigger pulse and reduced rms voltage across the heater. In a similar manner, as line voltage is reduced, the SCR turns on earlier in the cycle and increases the effective voltage across the heater.

* A silicon unilateral switch is a silicon, planar, monolithic integrated circuit that has thyristor electrical characteristics closely approximating those of an ideal four-layer diode. The device shown switches at approximately 8 volts.



92CS-21760

Fig. 314—Voltage waveforms exhibited by the circuit of Fig. 313.

By proper adjustment of potentiometer R_6 in conjunction with potentiometer R_4 , it is possible to obtain excellent heater-voltage compensation over a range of line voltages. Fig. 314 shows the waveforms associated with the heater-regulator circuit.

Performance Characteristics

Curve A in Fig. 315 shows heater voltage as a function of line voltage for the open-loop regulator circuit shown in Fig. 313. Curve B in Fig. 315 shows a similar curve for a closed-loop regu-

lator using a lamp-photocell module. The lamp, in series with a limiting resistor, is connected across the heater terminals, and the photocell replaces potentiometer R_6 . The lamp unit senses the phase-controlled true rms heater voltage. Changes in lamp brightness produced by heater-voltage variations change the photocell resistance in reverse proportion to the lamp voltage. The remainder of the circuit functions as previously described except that regulation is obtained not only through the monitoring of the instantaneous magnitude of line

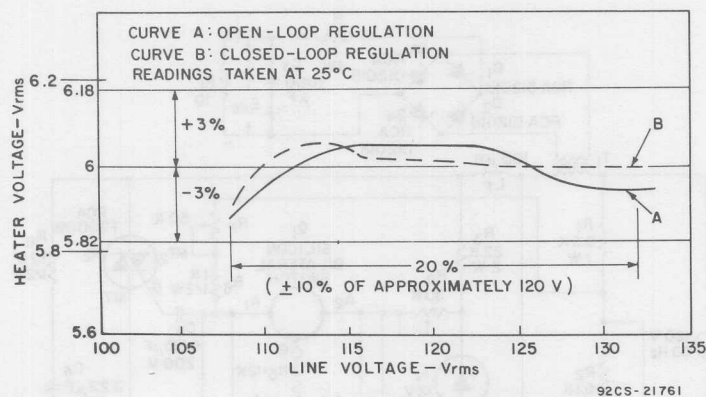


Fig. 315—Heater voltage as a function of line voltage of the open- and closed-loop regulators.

voltage, but also through the sensing of the true rms voltage across the heater. This characteristic identifies the circuit as an ac voltage regulator with closed-loop feedback control. The closed-loop regulator produces less error, is more resistant to the drift effects of components, and is easier to adjust than the open-loop regulator.

The lamp used in the closed-loop regulator is rated at 6 volts, but the series resistor limits the voltage to approximately 2 volts so that extremely long lamp life can be expected. An additional advantage at low voltage is that the light intensity varies linearly with the voltage across the lamp so that a small increase in voltage increases brightness markedly; near rated voltage the intensity does not vary linearly and the variation in brightness is not very apparent. A loss in sensitivity would result if the lamp were operated at its rated voltage.

The open-loop regulator can regulate 6 volts to within ± 3 per

cent within a temperature range from 10 to 40°C with an input-voltage swing of ± 10 per cent. The closed-loop regulator can regulate 6 volts to within ± 2 per cent within a temperature range from 0 to 60°C with an input-voltage swing of ± 10 per cent.

LINE-VOLTAGE-REGULATED DC POWER SUPPLY

A simple but stable dc power supply that uses thyristors for line-voltage regulation is shown in Fig. 316. The power supply is intended for use with a constant load; consequently, no provisions are included for regulation of the dc output voltage against variations in load current. The power-supply section consists of the well-known full-wave bridge with RC filter. A line-voltage transformer is employed to step down the supply voltage of 120 volts rms to approximately 12.5 volts rms. If a dc output voltage greater than 10 volts is desired, a transformer with a lower primary-to-

of 10 ohms. Fig. 318 shows the voltage waveforms associated with the circuit of Fig. 316.

If increased line, temperature, and load compensation are desired in the regulated supply of Fig. 316, closed-loop control can be obtained by use of a photocell in place of potentiometer R_F and connection of a lamp across the output of the supply in such a way that the light from the lamp can impinge on the photocell surface.

During the beginning of each half-cycle of the input ac voltage, the triac is in the off state. The full line voltage, therefore, appears across the main terminals of this device, and no voltage appears across transformer T_1 . The full line voltage is also impressed across the network in parallel with

the triac. The back-to-back series-connected zener diodes D_7 and D_8 conduct when the ac line voltage rises to 12 volts in either direction. These zener diodes maintain the junction of resistors R_3 and R_4 at 12 volts, and capacitor C_2 charges toward this voltage.

The voltage on capacitor C_2 is applied to terminal A_2 of the silicon bilateral switch. Simultaneously, a portion of the ac line voltage is applied to terminal A_1 of the bilateral switch. When the potential difference between terminals A_1 and A_2 reaches the firing potential of the bilateral switch, this device conducts and produces a pulse of current at the gate of the triac. This gate current pulse triggers the triac into conduction. The phase angle at which

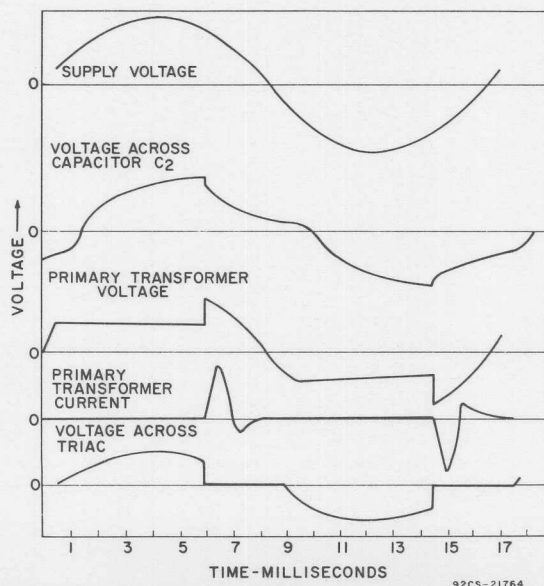


Fig. 318—Voltage waveforms exhibited by the circuit of Fig. 316.

the triac is triggered into conduction is advanced or retarded by varying the time required for the capacitor to charge sufficiently to

increase the potential difference between terminal A_1 and A_2 to the value required to fire the bilateral switch.

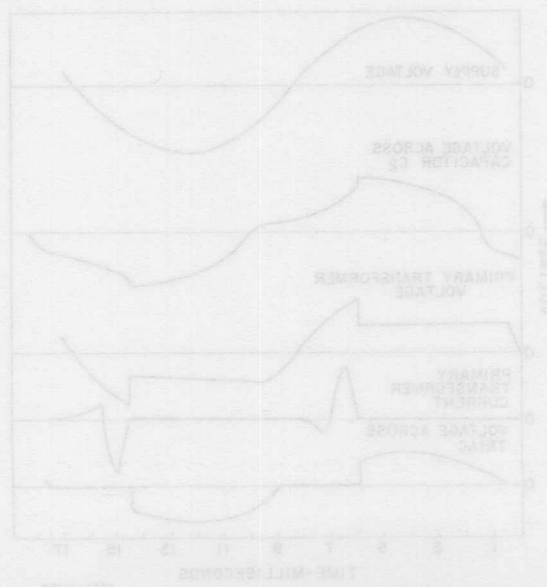


Fig. 315—Voltage waveforms exhibited by the circuit of Fig. 316.

SCR Inverters and Converters

In many applications, the optimum value of voltage is not available from the primary power source. In such instances, dc-to-dc converters or dc-to-ac inverters may be used to provide the desired value of voltage. The "boost" regulator circuit described in the subsequent section on **SCR Horizontal Deflection Systems** is one example of a dc-to-dc converter used to convert a given value of dc voltage to a higher, more optimum value for a specific application.

An inverter is used to transform dc power to ac power. If the ac output is rectified and filtered to provide dc again, the overall circuit is referred to as a converter. The purpose of the converter then, is to change the magnitude of the available dc voltage.

Power-conversion circuits, both inverters and converters, consist basically of some type of "chopper". Fig. 319(a) shows a simple chopper circuit. In this circuit, a switch *S* is connected between the load and a dc voltage source *E*. If the switch is alternately

closed and opened, the output voltage across the load will be as shown in Fig. 319(b). If the on-off intervals are equal, the average voltage across the load is equal to $E/2$. The average voltage across the load can be varied by varying the ratio of the on-to-off time of the switch, by periodically varying the repetition rate, or by a combination of these factors. If a filter is added between the switch and the load, the fluctuations in the output can be suppressed, and the circuit becomes a true dc-to-dc stepdown transformer (or converter).

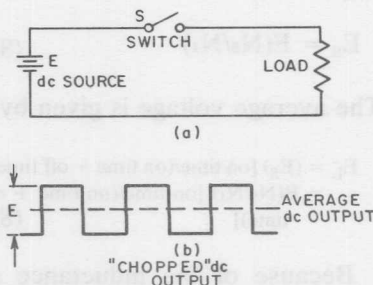


Fig. 319—Simple chopper circuit and output-voltage waveform.

The chopper circuit can easily be used to provide an average voltage to the load which is less than the supply voltage, but another technique is required to "step-up" the voltage. The basic arrangement used to obtain voltages higher than the supply voltage is shown in Fig. 320.

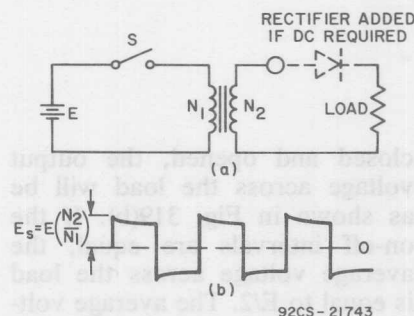


Fig. 320—Simple chopper circuit (inverter) transformer coupled to load and voltage waveform across secondary of output transformer.

In the circuit shown in Fig. 320, the peak voltage across the transformer secondary, except for a transient which occurs at the opening and closing of the switch, is given by

$$E_s = E(N_2/N_1) \quad (88)$$

The average voltage is given by

$$E_L = (E_s) [\text{on time}/(\text{on time} + \text{off time})] \\ = E(N_2/N_1) [\text{on time}/(\text{on time} + \text{off time})] \quad (89)$$

Because of the inductance of the transformer winding, a transient voltage is generated at each opening and closing of the switch.

The spikes in the output waveform shown in Fig. 320(b) result because the inductance of the transformer winding opposes both the sudden increase in current when the switch is closed and the sudden decrease in current when the switch is opened. In practice, the switch cannot open or close in zero time, but it is possible to generate transient voltages which are considerably higher in magnitude than the supply voltage.

The transient voltage generated by the rapidly changing current in the transformer winding can be reduced by connection of a "free-wheeling" diode across the transformer primary, as shown in Fig. 321. When the switch is opened and a high transient voltage tends to develop across the winding, the free-wheeling diode becomes forward-biased, and the energy stored in the magnetic field of the transformer is dissipated by current flow through the diode.

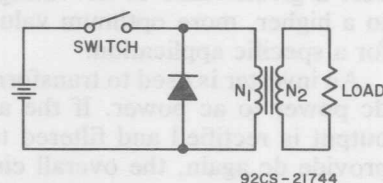


Fig. 321—Simple inverter circuit with a free-wheeling diode added to reduce transient voltages.

In practice, the switch shown in Figs. 319 through 321 may be replaced by a silicon controlled rectifier (SCR). The SCR switch can easily be closed by application of a positive pulse to its gate. Once conduction has been initiated, however, the gate loses

control, and some means must be provided to stop conduction and open the switch.

COMMUTATION OF INVERTERS SCR'S

Circuits that are used to turn off an SCR are commonly called commutating circuits. The commutating circuit normally bypasses the load current around the SCR for a time sufficiently long to permit the SCR to recover its forward-blocking capability.

Parallel-Capacitor Commutation

One of the simplest methods for commutation of an SCR in an inverter circuit is by use of a capacitor connected in parallel with the load, as shown in Fig. 322. If the switch *S* is open at the time the SCR is triggered by a pulse applied to its gate, the negative terminal of capacitor *C* will be connected to the negative terminal of the supply voltage. Capacitor *C* then charges at an exponential rate through resistor *R* toward the dc supply voltage.

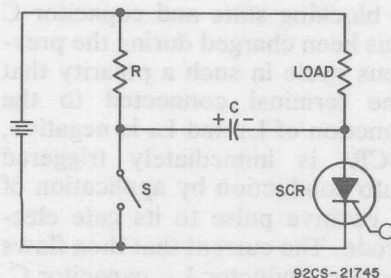


Fig. 322—Parallel-capacitor type of SCR commutation circuit.

When the switch is closed, capacitor *C* will be connected between anode and cathode of the SCR in a polarity such that it provides a negative anode voltage for the SCR. Load current is then diverted through the capacitor, and the SCR turns off. The capacitance of the capacitor and the voltage to which it is charged must be sufficient to bypass the load current around the SCR for the time required for the SCR to recover its forward-blocking capability.

In an actual circuit, the switch *S* shown in Fig. 322 is replaced by a second SCR, as shown in Fig. 323. The resultant circuit is the familiar single-phase capacitor-commutated inverter. Capacitor *C* alternately commutates SCR₁ and SCR₂. The inductor limits the current that flows into *C* during the charging intervals in a manner similar to that of resistor *R* in Fig. 322, but without the I^2R losses that occur in a resistor.

Series-Capacitor Commutation

A basic series-capacitor-commutated circuit is shown in Fig. 324. In this circuit, commutation is achieved through the action of a capacitor connected in series with the load. When the SCR is turned on by a positive pulse applied to its gate, inductor *L* and capacitor *C* are connected in series with the load to the supply voltage. The inductor *L* and the capacitor *C* form a series resonant circuit. Current through this resonant circuit (and the SCR) builds

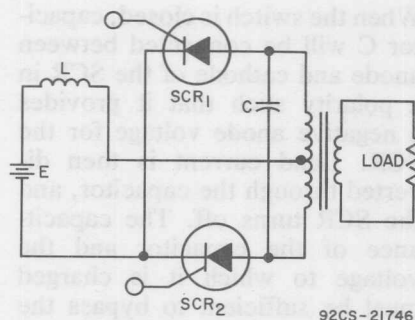


Fig. 323—Single-phase capacitor-commutated SCR inverter.

up sinusoidally to a maximum, decreases to zero, and then attempts to reverse. When the current attempts to reverse, the SCR turns off, and reverse voltage is maintained across it by the charge on capacitor C. With the configuration shown in Fig. 324, a recurrent waveform cannot be maintained because capacitor C will be charged to a voltage equal to or higher than the supply voltage,

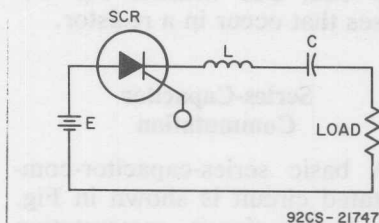


Fig. 324—Basic series-capacitor type of SCR commutation circuit.

and the SCR can never be forward-biased after the initial conduction period has ceased. A more practical circuit for use as an inverter is shown in Fig. 325.

In this circuit, SCR₁ and SCR₂ are gated on alternately, with sufficient time between gating pulses

to permit the LC circuit to commute the conducting SCR. When SCR₁ conducts, the voltage across capacitor C rises to some positive value above the supply voltage. When SCR₂ conducts, the voltage across capacitor C falls to some negative value below the supply voltage. When one SCR is triggered on, forward voltage is immediately applied to the other SCR. Therefore, sufficient delay must be allowed between the end of one half-cycle of load current and the start of another. This

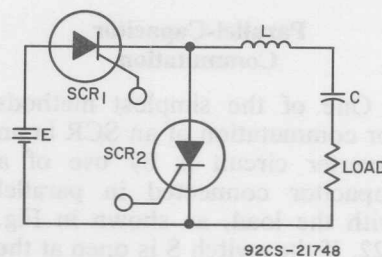


Fig. 325—Basic series-capacitor-commutated SCR inverter.

delay must be at least equal to the turnoff time (t_q) of the SCR. The required delay in triggering can be reduced by the use of an additional inductor, as shown in Fig. 326.

If both SCR₁ and SCR₂ are in a blocking state and capacitor C has been charged during the previous cycle in such a polarity that the terminal connected to the junction of L₁ and L₂ is negative, SCR₁ is immediately triggered into conduction by application of a positive pulse to its gate electrode. The current that then flows through inductor L₁, capacitor C, and the load is a half sine-wave pulse, as shown in Fig. 326(b).

This half sine-wave pulse resonantly charges capacitor C in the opposite polarity. By the end of the current pulse, capacitor C is charged to a value higher than the supply voltage. Current then attempts to reverse through SCR_1 .

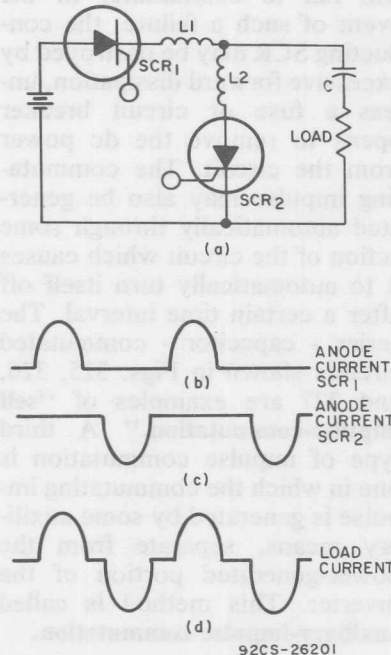


Fig. 326—Basic series-capacitor-commutated SCR inverter circuit with additional inductor.

Some reverse-recovery current flows for a few microseconds, and SCR_1 then reverts to its reverse-blocking state (i.e. turns off). Current remains at zero until a gating pulse is applied to SCR_2 . When SCR_2 is triggered on, capacitor C will discharge through SCR_2 in a half sine-wave pulse. When current attempts to reverse, SCR_2 ,

after a few microseconds of reverse-recovery current, reverts to its blocking state, and the cycle is repeated.

In the circuit shown in Fig. 326, the current carried by SCR_2 is supplied completely by energy stored in capacitor C during the period when SCR_1 is conducting. Because the objective of the inverter is to supply energy to the load, an arrangement that supplies energy from the supply on each half cycle, such as shown in Fig. 327, is desirable.

In the circuit shown in Fig. 327, capacitor C is divided into two equal parts. During the half-cycle that SCR_1 conducts, capacitor C_2 is charged from the supply, and capacitor C_1 is discharged through the load. Both the charging current of capacitor C_2 and the discharging current of capacitor C_1 flow through SCR_1 , inductor L_1 , and the load. On the next half-cycle, a similar action takes place except that SCR_2 conducts, capacitor C_1 charges from

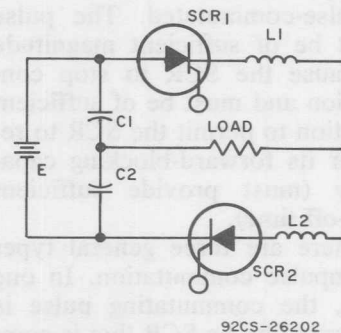


Fig. 327—Series-capacitor-commutated SCR inverter in which energy from the power source is supplied to the load on each half-cycle of inverter operation.

the supply, and capacitor C_2 discharges. If $C_1 = C_2$ and $L_1 = L_2$, one-half the load current on each half cycle is supplied by the power supply, and the other half of the load current is supplied by the capacitor being discharged.

If separate inductors are used for L_1 and L_2 , the maximum operating frequency of the inverter must always be slightly less than the series resonant frequency of L_1C_1 and L_2C_2 . However, if L_1 and L_2 are closely coupled on a common core, the operating range of the inverter can be extended slightly above the resonant frequency of the series LC circuit. If L_1 and L_2 are coupled, when one SCR is turned on, the current that flows in the reactor associated with that SCR induces a voltage in the other reactor that reverses the voltage on the other SCR and causes it to cease conduction.

Impulse Commutation

If a very short pulse is used to reverse the voltage on an SCR briefly, the SCR is said to be impulse-commutated. The pulse must be of sufficient magnitude to cause the SCR to stop conduction and must be of sufficient duration to permit the SCR to recover its forward-blocking capability (must provide sufficient turn-off time).

There are three general types of impulse commutation. In one type, the commutating pulse is generated by an SCR that is complementary to the SCR being turned off. This is called **complementary impulse-commutation**.

The parallel-capacitor commutation circuit shown in Fig. 323 is an example of complementary impulse-commutation. One disadvantage of such a circuit is that if the gating signals are lost for any reason, the conducting SCR will not be turned off, i.e., will fail to commute. In the event of such a failure, the conducting SCR may be destroyed by excessive forward dissipation, unless a fuse or circuit breaker opens to remove the dc power from the circuit. The commutating impulse may also be generated automatically through some action of the circuit which causes it to automatically turn itself off after a certain time interval. The series - capacitor - commutated circuits shown in Figs. 325, 326, and 327 are examples of "**self impulse-commutation**." A third type of impulse commutation is one in which the commutating impulse is generated by some auxiliary means, separate from the power-generated portion of the inverter. This method is called **auxiliary-impulse commutation**.

Self-Impulse Commutation

— Fig. 328 shows a basic "chopped" circuit in which the commutating impulse is generated by action of the circuit. When the SCR is off, but load current has been established during a previous cycle, load current will be maintained by L_2 . Because the SCR is off, the return path for the load current will be through the rectifier D. During the off time of the SCR, capacitor C will charge through inductors L_1 and L_2 and

the load to the supply voltage E . When the SCR is gated on, the voltage at the junction of inductors L_1 and L_2 rises immediately to the supply voltage E .

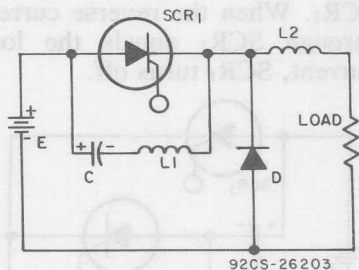


Fig. 328—Basic self-impulse-commutated SCR inverter.

Rectifier D then becomes reverse-biased, and the load current flows through the SCR. Capacitor C also discharges through inductor L_1 and the SCR in an oscillatory manner and reverses its charge within one-cycle. After the first half-cycle the current through inductor L_1 and capacitor C reverses and causes current to flow through the SCR which is in a reverse direction from the load current. The net current through the SCR is then the difference between the load current and the current through L_1 and C . When the current through L and C equals the load current, the SCR current becomes zero, and the SCR turns off. The voltage remaining on capacitor C then appears as inverse voltage across the SCR. Load current continues to flow through C , L_1 , and L_2 until C has been charged back to the supply voltage E . At this time, current through C stops, and load

current is transferred to the rectifier D . The cycle is then repeated.

Fig. 329 shows a circuit that uses another form of self-impulse commutation. This configuration is the well-known Morgan circuit. During the off-time, load current is maintained by L_2 , as in the circuit shown in Fig. 328. However, the current that charges capacitor C during the off time saturates the core of L_1 (positively, it is assumed for this explanation) so that the inductance of this inductor is small. When the SCR is triggered on, the capacitor will be connected directly across L_1 and will drive its core towards saturation in the reverse direction (negative saturation). A finite time interval is required for the core to "switch" from positive saturation to negative saturation. During this time interval, current flows through the SCR, inductor L_2 , and the load.

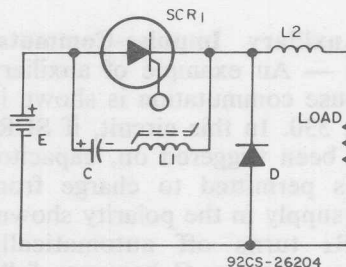


Fig. 329—Basic Morgan type of inverter circuit.

Rectifier D is reverse-biased and therefore does not conduct. When the core of L_1 switches to negative saturation, capacitor C discharges in an oscillatory manner through the SCR. Because the in-

ductance of inductor L_1 is very small at this time, the resonant discharge is very rapid, and the voltage on capacitor C very quickly falls from $+E$ to $-E$. The core of L_1 remains in the negatively saturated condition for a certain time interval and then switches rapidly to the positively saturated condition. During this interval, the SCR continues to conduct current which flows through L_2 and the load. When the core of L_1 becomes positively saturated again, the capacitor C once more discharges in a resonant manner, and current is driven in the reverse direction through the SCR. When the reverse current through the SCR equals the load current, the SCR turns off. In practice, a rectifier is usually connected across the SCR in the circuit shown in Fig. 328 and Fig. 329 to carry the excess reverse current once the reverse current becomes equal to the load current.

Auxiliary Impulse-Commutation — An example of auxiliary impulse commutation is shown in Fig. 330. In this circuit, if SCR_2 has been triggered on, capacitor C is permitted to charge from the supply in the polarity shown. SCR_2 turns off automatically once capacitor C becomes fully charged because of the lack of current. When SCR_1 is triggered on, load current flows through SCR_1 and the load. In addition capacitor C discharges through inductor L , rectifier D , and SCR_1 until it has reversed its charge. The hold-off rectifier D then prevents the current through capaci-

tor C from reversing again. Load current continues to flow through SCR_1 until SCR_2 is triggered on, capacitor C is then allowed to discharge through SCR_2 , and, in a reverse direction, through SCR_1 . When the reverse current through SCR_1 equals the load current, SCR_1 turns off.

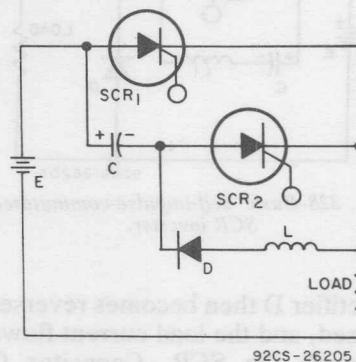


Fig. 330—SCR inverter circuit that employs auxiliary type of impulse commutation of SCR's.

Commutating Capacitors

In all the commutation arrangement discussed in the preceding paragraphs, the commutation current for the conducting SCR must be carried by a capacitor. This fact imposes rather severe requirements on the commutating capacitor. The capacitor must be able to carry the high peak currents necessary for commutation without excessive losses that would reduce circuit efficiency, cause excessive temperature rise, and premature capacitor failure. Also, because the series inductance of the capacitor may limit the width of the commutating pulse and the initial rate of-rise of current in the conducting SCR, capacitor

manufacturers should be consulted as to the current ratings of the commutating capacitors at the operating frequency of the inverter. In addition, life tests should be conducted to assure that operating-temperature ratings of the capacitor are not exceeded after long periods of operation.

SCR INVERTER

Fig. 331 shows a typical high-frequency SCR switching inverter; Fig. 332 shows the waveshapes across each SCR and the output of the transformer. For resistive loads, this inverter is capable of

delivering 500 watts of output power at an operating frequency of 10 kHz, and is provided with regulation from a no-load condition to full load. With proper output derating, this circuit can also accommodate inductive and capacitive loads. Under a capacitive load the power dissipation of the SCR's is increased; under an inductive load, the turn-off time is decreased.

The inverter can be operated at any optional frequency up to 10 kHz provided that a suitable output transformer is used and the timing capacitors are changed in the gate-trigger-pulse generator.

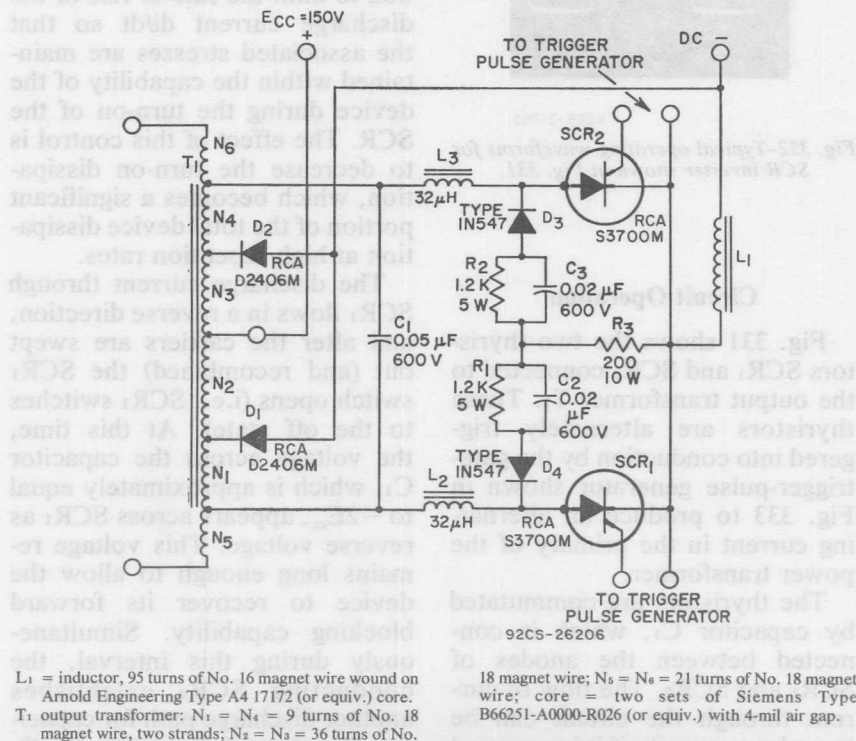
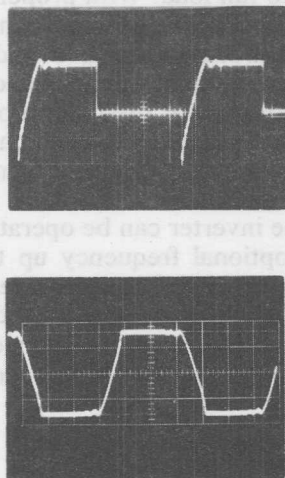


Fig. 331—High-frequency (10-kHz) SCR push-pull switching inverter.

A change in operating frequency, however, does not require any change in the commutating components C_1 and L_1 .



92CS-21755

Fig. 332—Typical operating waveforms for SCR inverter shown in Fig. 331.

Circuit Operation

Fig. 331 shows the two thyristors SCR_1 and SCR_2 connected to the output transformer T_1 . These thyristors are alternately triggered into conduction by the gate-trigger-pulse generator shown in Fig. 333 to produce an alternating current in the primary of the power transformer.

The thyristors are commutated by capacitor C_1 , which is connected between the anodes of SCR_1 and SCR_2 . The flow of current through the circuit can be traced more easily if it is assumed that initially SCR_1 is conducting

and SCR_2 is cut off and that the common cathode connection of the SCR's is the reference point. For this condition, the voltage at the anode of SCR_2 is twice the voltage of the dc power supply, i.e., $2 E_{cc}$. The load current flows from the dc power supply through one-half the primary winding of transformer T_1 , inductor L_2 , SCR_1 , and inductor L_1 . When the firing current is applied to the gate of SCR_2 , this SCR turns on and conducts.

During the on period of SCR_2 , the capacitor C_1 begins to discharge through L_3 , SCR_2 , SCR_1 , and L_2 . Inductors L_2 and L_3 function to limit the rate of rise of the discharge current di/dt so that the associated stresses are maintained within the capability of the device during the turn-on of the SCR. The effect of this control is to decrease the turn-on dissipation, which becomes a significant portion of the total device dissipation at high repetition rates.

The discharge current through SCR_1 flows in a reverse direction, and after the carriers are swept out (and recombined) the SCR_1 switch opens (i.e., SCR_1 switches to the off state). At this time, the voltage across the capacitor C_1 , which is approximately equal to $-2E_{cc}$, appears across SCR_1 as reverse voltage. This voltage remains long enough to allow the device to recover its forward blocking capability. Simultaneously during this interval, the conducting SCR_2 establishes another discharge path for capacitor C_1 through transformer T_1 and inductors L_1 and L_3 . The

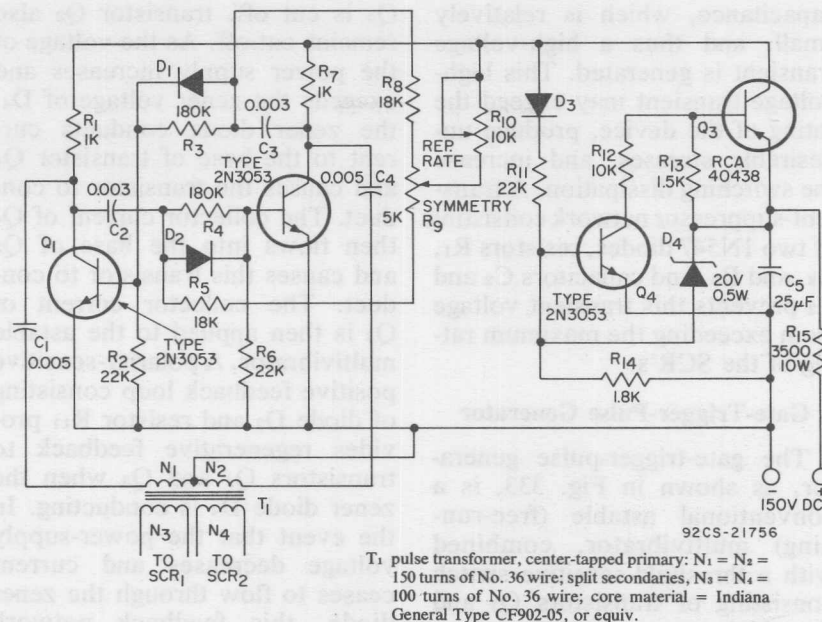


Fig. 333—Gate-trigger pulse generator for SCR inverter shown in Fig. 331.

role of inductor L₁ is to control the rate of discharge of the capacitor to allow sufficient time for turn-off.

After capacitor C₁ is discharged from $-2E_{cc}$ to zero, it starts to charge in the opposite direction to $+2E_{cc}$. When C₁ is charged to $+2E_{cc}$, because of the phase shift between voltage and current the flux at that time in the inductor L₁ is a maximum. This reactive energy stored in the inductor is normally transferred to the capacitor and causes an "overvoltage" or "overcharge", which in this particular case is undesirable. Voltages on the capacitor higher than $2E_{cc}$ produce a negative voltage at the anode of SCR₂ with respect to the negative terminal of the dc power supply. This condition is prevented by use of

a clamping diode D₂ connected to an extra tap on the transformer oriented close to the anode of SCR₂. As a result, the amount of "overcharge" of the capacitor is considerably reduced. The energy stored in inductor L₁ causes current to flow through diode D₂, the N₄ transformer winding inductor L₃, and SCR₂. Transformer windings N₄ and N₃ act as an autotransformer through which the energy stored in the inductor is fed back to the power supply.

When the firing current is applied to the gate of SCR₁, this device conducts and the process described above is repeated.

Each time the SCR's turn off to interrupt the reverse recovery current, a certain amount of energy remains in the inductor. This energy is transferred to the device

capacitance, which is relatively small, and thus a high-voltage transient is generated. This high-voltage transient may exceed the rating of the device, produce undesirable stresses, and increase the switching dissipation. A transient-suppressor network consisting of two 1N547 diodes, resistors R_1 , R_2 , and R_3 , and capacitors C_2 and C_3 prevents this transient voltage from exceeding the maximum rating of the SCR's.

Gate-Trigger-Pulse Generator

The gate-trigger-pulse generator, as shown in Fig. 333, is a conventional astable (free-running) multivibrator, combined with a threshold-sensitive switch consisting of transistors Q_3 and Q_4 which turns the generator on and off. The square-wave output of the generator is differentiated and fed to the gates of SCR₁ and SCR₂ through the N_3 and N_4 windings of pulse transformer T_1 . The threshold-sensitive switch holds the generator off until the required dc level is achieved in the power supply. This minimum level is necessary to maintain a nominal repetition rate and to supply sufficient current to trigger both SCR's. As dc power is applied through resistor R_{15} to charge capacitor C_5 , the gradually increasing voltage at the emitter of transistor Q_3 eventually rises to a value above the zener voltage of the zener diode D_4 connected between the emitter of transistor Q_3 and the base of transistor Q_4 . So long as this voltage is not exceeded, the base current of transistor Q_4 is zero. Because transistor

Q_4 is cut off, transistor Q_3 also remains cut off. As the voltage of the power supply increases and exceeds the zener voltage of D_4 , the zener diode conducts current to the base of transistor Q_4 and causes the transistor to conduct. The collector current of Q_4 then flows into the base of Q_3 and causes this transistor to conduct. The collector current of Q_3 is then applied to the astable multivibrator. A polarity-sensitive positive feedback loop consisting of diode D_3 and resistor R_{11} provides regenerative feedback to transistors Q_4 and Q_3 when the zener diode D_4 is conducting. In the event that the power-supply voltage decreases and current ceases to flow through the zener diode, this feedback network maintains transistor Q_3 in saturation until the voltage in the circuit drops to a few volts.

The collector current through transistors Q_1 and Q_2 does not maintain perfect balance as the base currents of transistors Q_1 and Q_2 increase. Any slight unbalance in collector current is amplified through the positive feedback loops. As a result, one transistor is cut off and the other is turned on at the extreme limit of unbalance. If transistor Q_1 is assumed turned on, the base of transistor Q_2 is driven negative by capacitor C_2 , which is connected to the collector of Q_1 . The negative bias on the base of Q_2 drives the transistor into the cut-off state. Capacitor C_3 connected to the base of Q_1 is then charged through the load resistor R_7 of transistor Q_2 , and the base drive

on transistor Q_1 increases until the capacitor is fully charged. Capacitor C_2 , with its negatively charged plate connected to the base of transistor Q_2 through a resistor divider consisting of R_4 and R_6 , is discharged through resistor R_5 . Resistor R_5 is connected to a potentiometer R_9 which controls the waveshape symmetry and another potentiometer R_{10} which is connected to the positive supply voltage and serves as the repetition-rate control.

When the negative bias decreases to zero and the base of Q_3 becomes positive, transistor Q_2 turns on and causes Q_1 to turn off. The capacitor C_4 which was charged through load resistor R_7 starts to discharge through the N_2 primary windings of the pulse transformer T_1 after Q_2 is turned on. This discharge current is fed to the gate of the SCR, in the appropriate direction to fire the device. During the alternate half-cycle of multivibrator operation, capacitor C_1 discharges through the N_1 primary windings of the

pulse transformer to trigger SCR_1 .

Applications

Some of the applications of the SCR inverter are as follows:

1. DC-to-dc Converters:

Conversion can be accomplished by the use of small light-weight, low-cost transformers, inductors, and capacitors. Applications of the dc-to-dc converter include:

- a. Computer power supplies
- b. Power supplies for telephone equipment
- c. Power supplies for transmitters
- d. Battery chargers

2. High-frequency power source:

Because of the high frequency of operation, the size and weight of equipment is reduced, and often efficiency is improved. Some possible inverter applications include:

- a. Fluorescent lamp supply
- b. Mercury-vapor lamp supply
- c. Inductor heating

SCR Horizontal Deflection Systems

For reproduction of a transmitted picture in a television receiver, the face of a cathode-ray tube is scanned with an electron beam while the intensity of the beam is varied to control the emitted light at the phosphor screen. The scanning is synchronized with a scanned image at the TV transmitter, and the black-through-white picture areas of the scanned image are converted into an electrical signal that controls the intensity of the electron beam in the picture tube at the receiver.

STANDARDS FOR SCANNING AND SYNCHRONIZATION

The National Television Systems Committee (NTSC) has recommended, and the Federal Communications Commission (FCC) has adopted, standards of transmission for a nationally coordinated television system. These standards assure that any television receiver in the United States can produce a satisfactory picture from any U.S. television broadcast (provided that signal strength

is sufficient). The FCC standards for scanning and synchronization form the basis for the television industry in this country.

Scanning

The picture on the face of a television picture tube is formed by rapid movement of a single spot of light in both horizontal and vertical directions. This spot of light is produced when the electron beam strikes the fluorescent screen; the brightness of the spot varies in proportion to the amplitude of the video signal. The electron beam moves under the influence of two magnetic fields. One field causes the beam to move (scan) horizontally across the face of the picture tube; the other field causes the beam to move from top to bottom.

Fig. 334 illustrates the basic scanning principle. This diagram assumes that the beam starts at the upper left corner of the picture area, sweeps rapidly across and simultaneously moves **downward** at a very small slope to the opposite edge of the screen. The

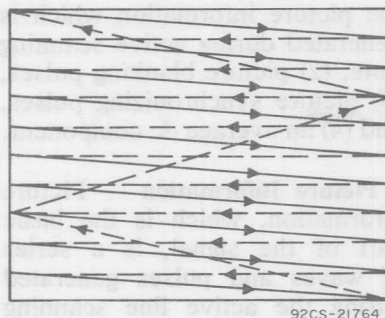


Fig. 334—Non-interlaced scanning.

beam then jumps back, or re-traces, much more rapidly to the left edge, and starts across again at a point lower down as shown.

The two magnetic fields which cause the beam to sweep across the face of the picture tube are so related that the beam scans $262\frac{1}{2}$ times across the face of the picture tube horizontally for every time it scans once across the tube vertically. Each complete picture is "scanned" twice in a time interval of $1/30$ th second. Therefore, the rate at which a complete picture is scanned, or at the frame rate, is 30 frames per second. Persistence of vision makes it practical to portray motion very well with this frame rate.

A picture or "raster" of $262\frac{1}{2}$ lines presents two problems which make it unsatisfactory for commercial television use. First, a line structure of $262\frac{1}{2}$ lines is relatively coarse and can be readily seen at normal viewing distances and, of course, imposes a severe limitation on vertical resolution. Second, although the eye with its persistence of vision averages a succession of still pictures into apparent smooth motion, it does

not filter out the periodic brightness changes as the complete frames are presented and cut off at a 30 frames-per-second rate.

The vertical resolution is improved and the flicker effect is eliminated if the scanning pattern is changed from the simple one first discussed to a pattern called **interlaced scanning**.

In interlaced scanning, as shown in Fig. 335, the beam skips every even numbered line in scanning the entire picture, then jumps back and sweeps over the even-numbered lines. In other words, on its first trip, the beam scans all the off-number lines (1,3,5,7...), on the second trip, the beam scans even-numbered lines (2,4,6,8...). All this action occurs in the time of one frame ($1/30$ second).

Although the eye has received two distinct light impressions for each frame, each spot on the screen has actually been scanned only once. The effect on the eye is the same as though 60 complete pictures per second were transmitted instead of 30, and the eye is quite insensitive to this flicker rate.

It would have been possible to select a frame rate of 24, which

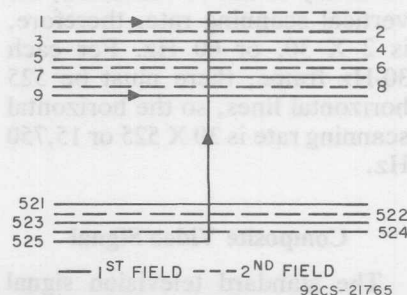


Fig. 335—Interlaced scanning.

has been used for movies, and a flicker rate of 48 would probably be tolerable. However, a frame rate which is an integral multiple or submultiple of the 60-Hz line frequency minimizes the effect of any picture distortion produced by factors such as poor power-supply filtering, wiring pickup, and heater-cathode leakage in the picture tube. Such effects produce a stationary distortion pattern for a 60-Hz flicker rate. If another frame frequency were used, a continuously moving distortion pattern would result. Experiments have shown that a moving distortion pattern is much more annoying than a stationary one.

Although the complete television picture is made up of 525 lines, not all these lines are actually used in forming the picture on the face of the picture-tube. If the lines on the picture tube were counted, only about 480 "active" lines would be visible. The missing lines are blanked out during the retrace period. The reasons for this blanking will become obvious during the discussion on synchronization, later in this section.

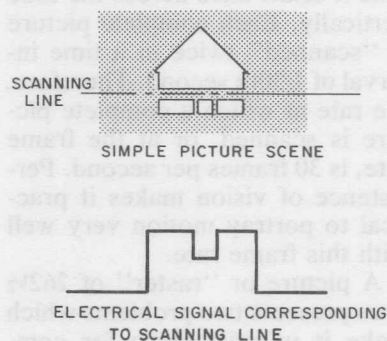
Two complete fields are scanned vertically in one 30-Hz frame, the vertical scanning rate, therefore, is 2×30 , or 60 Hz. For each 30-Hz frame, there must be 525 horizontal lines, so the horizontal scanning rate is 30×525 or 15,750 Hz.

Composite Video Signal

The standard television signal has four major components: (1)

the picture information which is generated during active scanning time, (2) picture blanking pulses, (3) picture synchronizing pulses, and (4) an average dc component.

Picture Information — Picture information, which is the basic part of the signal, is a series of waves and pulses generated during the active line scanning of the camera tube. For a monochrome picture, as the electron beam traverses the face of the camera tube, its amplitude is modulated in accordance with the brightness of the scene it is scanning. Fig. 336 shows a very simple scene being scanned, and the electrical brightness signal from the camera that corresponds to one scanning line.



92CS-21766

Fig. 336—Video signal for one scanning line.

For color pictures, the three color-difference signals are added to the monochrome, or Y, signal, as explained later in the discussion of **Color Synchronization**.

Blanking Signals — During retrace periods, the camera pickup tube may generate spurious signals. Also, during this period, retrace lines in either the camera tube or in the picture-tube in the receiver can detract from the appearance of the picture. Blanking pulses are applied to the scanning beams in both the pickup camera and in the receiver picture tube to eliminate retrace lines and the unwanted information from the picture during retrace.

A standard blanking signal has been agreed upon by the television industry. The blanking signal is actually part of the signal produced by the synchronizing circuit. It is a pulse somewhat longer than the synchronizing pulse, but of smaller amplitude. The magnitude of this pulse is held at the proper value to cut off the scanning beam during retrace. This level is called the black level, because during the time the signal from the transmitter is at that level the beam does not produce any light on the face of the picture tube. Fig. 337 shows how the picture information is combined with the blanking pulses and synchronizing pulses to form the composite video signal. It should be noted that the undesired signals have been pushed down below the black level.

Actually, there are two blanking signals, because the beam must move both vertically and horizontally. The horizontal blanking pulses are transmitted at the end of each line at intervals of $1/15,750$ second ($1/15,374$ second for color broadcasts) and blank the beam

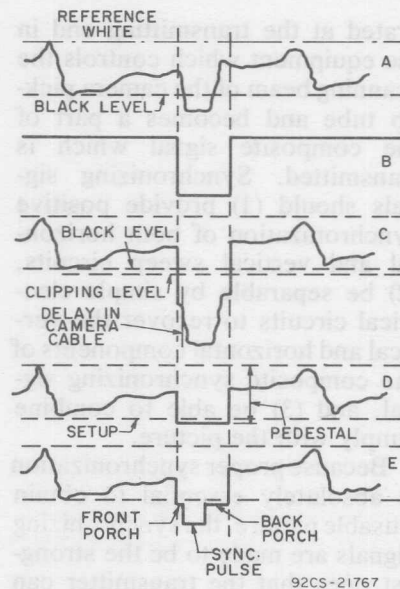


Fig. 337—Steps in synthesis of picture signal.

during the retrace period between lines. Vertical blanking pulses are transmitted at the end of each field, at the bottom of the picture, at intervals of $1/60$ second ($1/59.94$ second for color), and blank the beam during the time required for its return to the top of the picture.

Synchronizing Signals — The attainment of a viewable picture on the face of the picture tube requires that the scanning beams in the camera and the receiver be in exact synchronism at all times. This synchronization is provided in the form of electrical pulses during the retrace interval between successive lines of the picture and between successive pictures. These pulses are gen-

erated at the transmitting end in the equipment which controls the scanning beam of the camera pick-up tube and becomes a part of the composite signal which is transmitted. Synchronizing signals should (1) provide positive synchronization of both horizontal and vertical sweep circuits, (2) be separable by simple electrical circuits to recover the vertical and horizontal components of the composite synchronizing signal, and (3) be able to combine simply with the picture.

Because proper synchronization is absolutely essential to obtain a usable picture, the synchronizing signals are made to be the strongest ones that the transmitter can produce. The level of the picture signal itself is not allowed to exceed 75 percent of the full transmitter power (black level); the full power of the transmitter, however, is used to transmit the sync pulses. The task of separating the sync pulses from the rest of the signal at the receiver, therefore, is simplified. Fig. 338 shows the waveform of a radiated picture signal, together with a horizontal sync pulse. The reference white

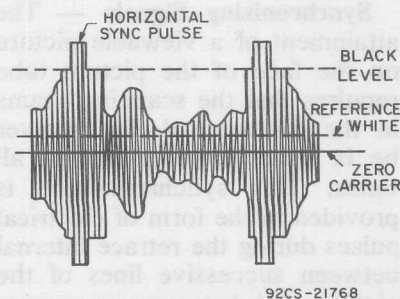


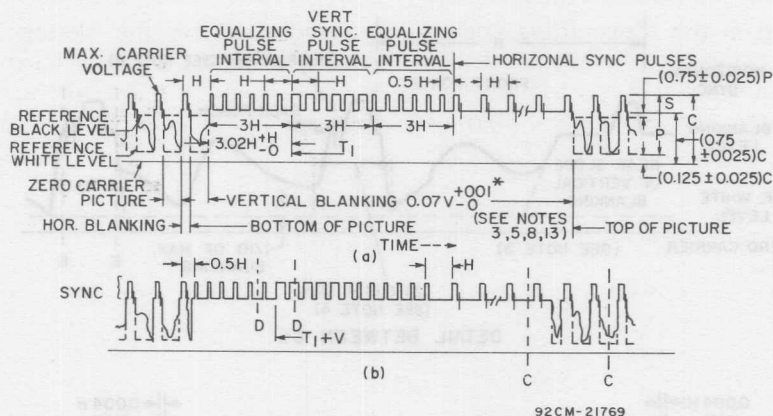
Fig. 338—Waveform of radiated picture signal.

line indicated on the sketch is relatively close to zero carrier level (12.5 percent), the synchronizing pulses, however, are in the "blacker than black" region that represents maximum carrier power. Fig. 339 and 340 shows how the synchronizing signal waveform is added to the picture signal.

The horizontal and vertical synchronizing pulses have the same amplitude, but different wave-shapes and time durations. Frequency discrimination techniques, therefore, can then be used to separate them in the receiver.

The vertical synchronizing pulses are rectangular in shape, but are of much greater duration than the horizontal pulses. The difference in the time duration of the two types of pulses provides a means of frequency discrimination. Each vertical synchronizing pulse has six slots (serrations) in it, so that it appears to be a series of six wide pulses at the horizontal frequency. The width of the slots in the vertical sync pulses is approximately equal to the width of the horizontal sync pulses. Although the slots do not assist in vertical synchronization, they do provide a means of providing uninterrupted synchronizing information to the horizontal oscillator during the vertical sync interval. The slots are spaced one horizontal line apart so that the receiver can use this pulse information to keep the horizontal oscillator in synchronization.

One of the most difficult problems in synchronization is that of maintaining accurate interlacing.



NOTES

1. H = time from start of one line to start of next line.
2. V = time from start of one field to start of next field.
3. Leading and trailing edges of vertical blanking should be complete in less than $0.1 H$.
4. Leading and trailing slopes of horizontal blanking must be steep enough to preserve minimum and maximum values of $(x + y)$ and (z) under all conditions of picture content.
- *5. Dimensions marked with asterisk indicate that tolerances given are permitted only for long time variations and not for successive cycles.
6. Equalizing pulse area shall be between 0.45 and 0.5 of area of a horizontal sync pulse.
7. Color burst follows each horizontal pulse, but is omitted following the equalizing pulses and during the broad vertical pulses.
8. Color bursts to be omitted during monochrome transmission.
9. The burst frequency shall be 3.579545 MHz. The tolerance on the frequency shall be ± 10 hertz with a maximum rate of change of frequency not to exceed 1/10 hertz per second per second.
10. The horizontal scanning frequency shall be 2/455 times the burst frequency.
11. The dimensions specified for the burst determine the times of starting and stopping the burst, but not its phase. The color burst consists of amplitude modulation of a continuous sine wave.
12. Dimension "P" represents the peak excursion of the luminance signal from blanking level, but does not include the chrominance signal. Dimension "S" is the sync amplitude above blanking level. Dimension "C" is the peak carrier amplitude.
13. For monochrome transmissions only, the duration of the horizontal sync pulse between 10 per cent points is specified as $0.08H \pm 0.01$, the period from the leading edge of sync to the 10 per cent point on the trailing edge of horizontal blanking is specified as $0.14H$ min., and the duration of vertical blanking is specified as $0.05V + 0.03V - 0$. All other dimensions remain the same.

Fig. 339—Standard FCC video waveforms.

Variations in either the timing or the amplitude of the vertical scanning of alternate fields will cause a vertical displacement of the interlaced fields. The result

is a nonuniform spacing of the scanning lines. This effect, which is usually called "pairing," reduces the vertical resolution and makes the line structure of the

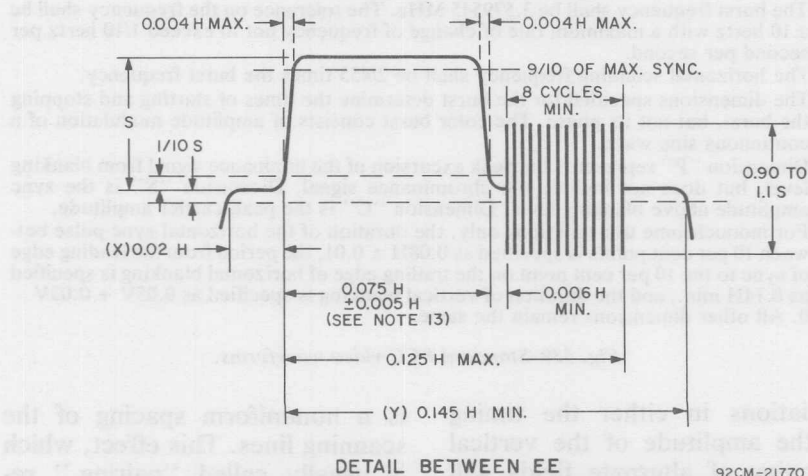
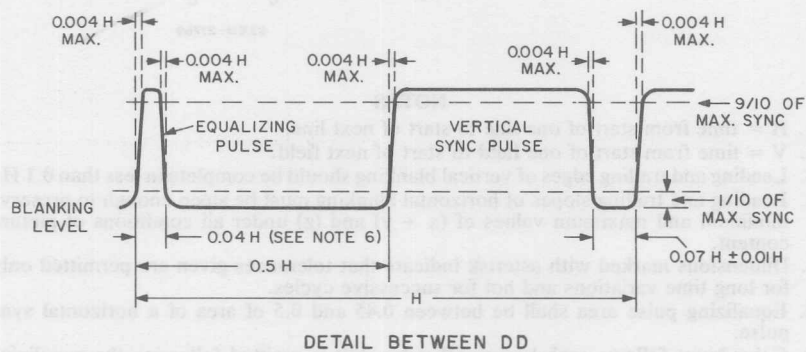
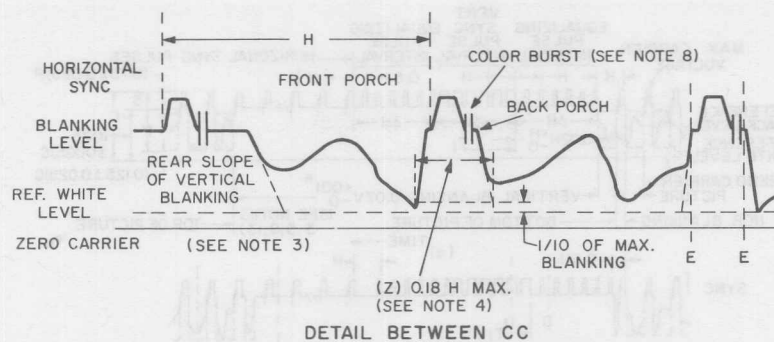


Fig. 340—Expanded view of some of the standard FCC video waveforms shown in Fig. 339.

picture visible at normal viewing distance. Because the two interlaced fields are displaced by half a line with an equivalent frame rate of 30 Hz, there is an inherent 30-Hz component in the synchronizing signal. If even a minute portion of this 30-Hz component gets into the vertical oscillator, it will inevitably cause pairing.

The pairing problem is minimized and continuous horizontal synchronization throughout the vertical sync and blanking intervals is assured by addition of another series of pulses, called "equalizing pulses," just before and just after the vertical sync pulses. The repetition frequency of the equalizing pulses and of the slots in the vertical sync pulse is twice the horizontal rate. Therefore, the pulses are spaced half a horizontal line apart. The horizontal oscillator will "trigger" on every odd pulse in the first field and on every even pulse in the second field and, therefore, provides interlace as shown previously in Fig. 335.

Color Synchronization — For color receivers, an additional synchronizing signal is required. The demodulators must be supplied with locally generated continuous-wave 3.58-MHz signals, which are precisely locked in frequency and in phase with the color subcarrier signals applied to the modulators at the transmitter, in order to function properly and demodulate the proper colors. The 3.58-MHz local oscillator in the receiver is synchronized in frequency and in phase

by a synchronizing signal sent out by the transmitter. This **color-sync signal** consists of a short burst of 3.58-MHz signal transmitted during the horizontal-blanking interval and following the horizontal-synch interval, as shown in Fig. 341. The phase of

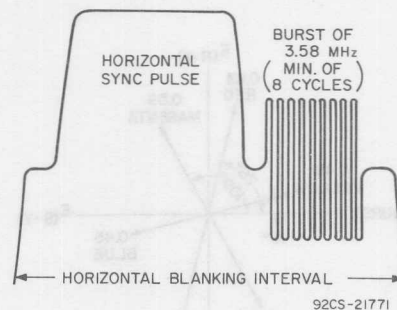


Fig. 341—A synchronizing signal, consisting of about 8 cycles of the subcarrier signal at the reference phase, is transmitted in short bursts following every horizontal sync pulse.

the **burst signal** is the reference phase for the system. It is chosen to coincide with the phase of the — $E_{(B-Y)}$ color-difference signal, as shown in Fig. 342. Fig. 343 shows how the burst signal is used in a color television receiver.

The composite video signal, which includes the burst signal as well as the chrominance signal, is applied to a burst amplifier, which is tuned to 3.58 MHz. In the absence of a keying pulse, this amplifier is cut-off, or nonconducting. A keying pulse, delayed the appropriate amount to be coincident with the burst signal, is derived from the horizontal deflection circuit and drives the burst amplifier into conduction. The burst amplifier, therefore, amplifies the burst signal,

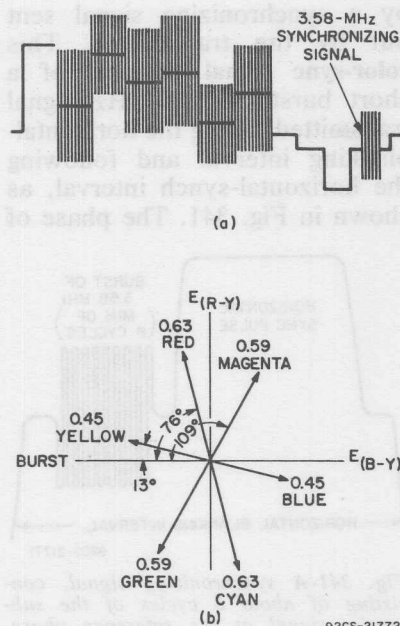


Fig. 342—Addition of burst to color signal.

but is cut-off for most of the composite video signal. After separation in this way, the amplified burst signal is applied to a phase detector in which it is compared with another 3.58-MHz signal obtained from the local subcarrier oscillator. Any error in frequency or instantaneous phase of the locally generated subcarrier produces a dc output from the phase detector. This correction voltage is used to correct the phase of the subcarrier oscillator through a reactance control circuit.

DC Component — Most sound systems, even the best high fidelity systems, use ac coupling and do not reproduce frequencies below 15 to 20 Hz. This limitation does not impose any special problem because the human ear is in-

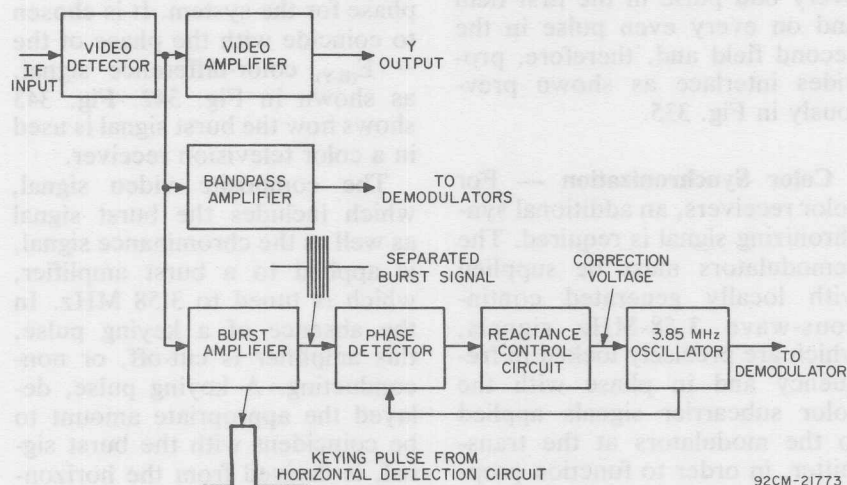


Fig. 343—The color subcarrier synchronizing system. (This system resembles horizontal AFC systems. The oscillator signal is compared with the burst signal and an error in phase produces a dc correction voltage that forces the oscillator to operate at the correct phase.)

capable of responding to frequencies below 15 to 20 Hz. The eye, however, can perceive both absolute intensities of light and very slow variations in intensity. As the frequency of the variations increases, the eye soon loses its ability to follow the changes and tends to respond to the average of the variations. This phenomenon, which is called persistency of vision, makes it possible for the eye to see a rapid succession of still pictures as apparent smooth, uninterrupted motion.

Because the eye can recognize slow changes in light intensity, a television system must be able to transmit these slow changes to the receiver and to the screen of the picture-tube. The system must either pass the entire TV spectrum, including the dc component, through each stage, or the signal must contain information which makes it possible to restore the dc component in the receiver.

The loss of the dc component results in a signal which tends to adjust itself about its own ac axis. Fig. 344(a) shows the video signal when the dc component is present. Fig. 344(b) shows the effect on this signal when the dc component is lost.

Addition of the dc component by means of a dc restorer will restore the signal to its original form, shown in Fig. 344(a). As shown in Fig. 344(b), when the dc component is lost, the peak-to-peak excursions of the signal are considerably increased and require a greater amplitude excursion from the amplifiers through

which the signal must pass. Therefore, it is sometimes desirable to reinsert the dc component at earlier points in the system, in addition to restoring it at the picture tube. DC restoration also tends to reduce hum, switching surges, and some spurious signals.

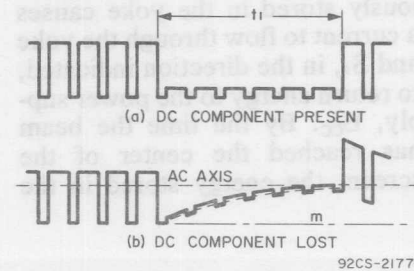


Fig. 344—DC component of video signal.

ANALYSIS OF BASIC DEFLECTION CIRCUIT

When a transmitted picture is reproduced on a television screen, the face of the picture tube is scanned with an electron beam, and simultaneously, the intensity of the beam is varied to produce varying intensities of light emitted from the phosphor screen. This scanning must be synchronized with the scanning of the original image by the camera located at the transmitter.

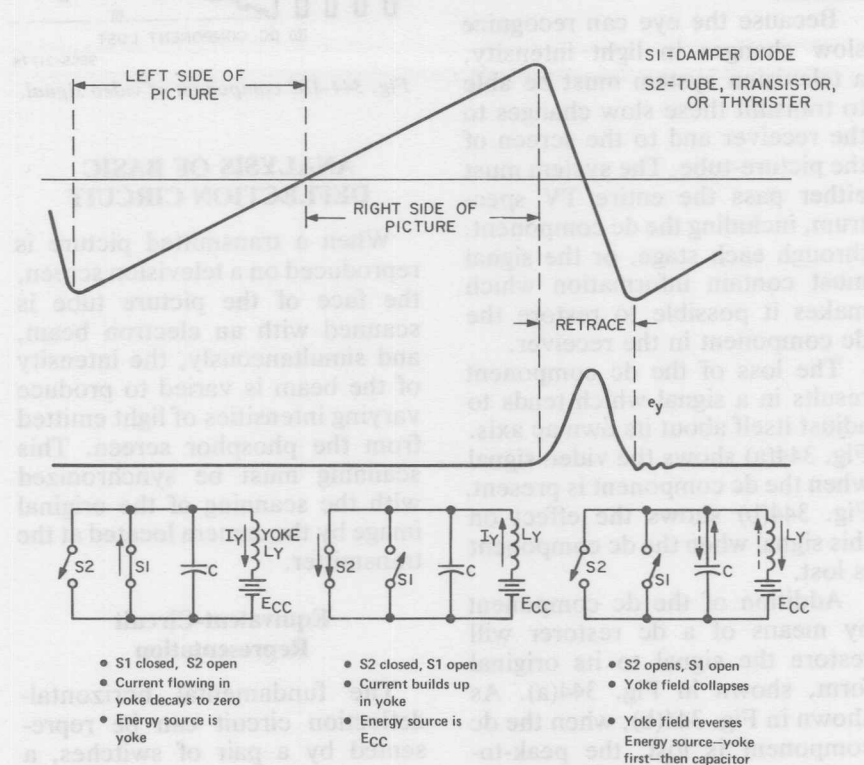
Equivalent-Circuit Representation

The fundamental horizontal-deflection circuit can be represented by a pair of switches, a capacitor, a deflection yoke, and a power supply. Fig. 345 shows such a fundamental circuit, together with the circuit currents

that correspond to the different portions of the scanning cycle.

When the electron beam is at the left edge of the picture (raster), yoke current, which has previously been established, is at a maximum value in the negative direction, switch S_1 is closed, and switch S_2 is open. Energy previously stored in the yoke causes a current to flow through the yoke and S_1 , in the direction indicated, to return energy to the power supply, E_{CC} . By the time the beam has reached the center of the screen, the energy stored in the

yoke has decayed to zero, and yoke current has decayed to zero. Switch S_1 is then opened, and switch S_2 is closed. At this instant, the current through the yoke reverses, and the power supply provides the energy to produce an increasing current through the yoke as shown. When the beam reaches the right hand side of the raster, switch S_2 is opened. The energy stored in the magnetic field of the yoke begins to decay. Because switches S_1 and S_2 are both open at this time, the decaying yoke current (as indicated by



92CS-21775

Fig. 345—Scanning waveforms and circuit diagrams for fundamental horizontal deflection circuit.

the dotted arrows) flows into the capacitor, and the energy previously stored in the yoke is transferred to the capacitor. This transfer of energy occurs fairly rapidly compared to the time required for the previous build-up of current. When the yoke current decays to zero, the direction of current in the yoke reverses because the capacitor then discharges its stored energy through the yoke (in the direction indicated by the solid arrows). The electron beam has now returned to the left side of the raster, and the cycle is repeated.

Because the horizontal scanning rate is 15,750 Hz (15,734 Hz for color systems), mechanical switches obviously cannot provide the required high switching rate. In practice, switch S_1 will be a diode (commonly called a damper diode), and switch S_2 will be an active device, such as an electron tube, a transistor, or a thyristor.

Basic Mathematical Relationships

As shown in Fig. 345, the voltage E_y developed across the yoke winding during retrace is a half-sine wave. The fundamental frequency of this half-sine wave is given by

$$f = \frac{1}{2\pi(L_y C)^{1/2}} \quad (90)$$

The total period of a sine wave is $1/f$, and because the retrace is a half-sine wave, the retrace time ($1/2 f$) can be expressed as follows:

$$t_r = \pi (L_y C)^{1/2} \quad (91)$$

The maximum energy stored in the yoke is determined as follows:

$$E_M = \frac{1}{2} (L_y I_y^2) \quad (92)$$

where I_y is the maximum value of yoke current.

The maximum energy stored in the capacitor is given by

$$E_M = \frac{1}{2} (C V^2) \quad (93)$$

where V is the maximum voltage to which the capacitor C is charged.

If the losses in the circuit are neglected, the maximum energy stored in the yoke is equal to the maximum energy stored in the capacitor. Therefore,

$$\frac{1}{2} (L_y I_y^2) = \frac{1}{2} (C V^2) \quad (94)$$

The maximum voltage developed across the yoke then may be determined from the following relationship

$$V = \frac{L_y I_y^2}{C}^{1/2} \quad (95)$$

Substitution of $C = t_r^2 / L_y$, derived from Eq. (91), into Eq. (95) yields the following result:

$$V = \frac{\pi L_y I_y}{t_r} \quad (96)$$

Eq. 96 expresses the peak voltage as a function of retrace time t_r .

The maximum voltage across switches S_1 and S_2 is equal to the sum of the supply voltage

E_{CC} and the value obtained in Eq. (95) or (96).

The value of E_{CC} , which must be added to the value given by Eq. (95) or (96) to obtain the peak voltage across switches S_1 and S_2 , is not necessarily the B supply voltage. In some circuits, this voltage may be a dc voltage to which a capacitor in series with the yoke is charged. This choice is normally obvious from an inspection of the circuit.

One problem in the use of Eq. (95) is that the correct value of circuit capacitance is not necessarily known, because it includes stray capacitances in addition to any fixed external capacitance. It can be shown that the peak voltage across switches S_1 and S_2 is defined by the following expression:

$$V = E_{CC} \left(1.79 + 1.57 \frac{t_t}{t_r} \right) \quad (97)$$

where t_t is the trace time and, as previously given, t_r is the retrace time

By use of Eq. (97), the peak voltage for various values of retrace time can be predicted. The proper supply voltage and retrace time can then be chosen to stay within the ratings of the available deflection devices. For a range of retrace times from 10 microseconds to 13 microseconds, the quantity $(1.79 + 1.57) t_t/t_r$ varies from 10.2 to 7.9. This range leads to a "rule of thumb" that has been used for transistor horizontal deflection circuits. This "rule" states that the peak voltage on the deflection device(s) is approximately 8 to 10 times the sup-

ply voltage. A safety margin of 10 to 20 per cent should be added to allow for factors such as high-line operation or off-frequency operation.

Third-Harmonic Tuning

The peak voltage across switches S_1 and S_2 of the basic circuit shown in Fig. 345 may be reduced by addition of a tuned circuit resonant at the third harmonic of the yoke circuit, as shown in Fig. 346. This circuit is shock-excited by the retrace pulse across the yoke and develops a third-harmonic signal. The addition of the third-harmonic signal to the retrace pulse reduces the voltage peak by about 20 percent.

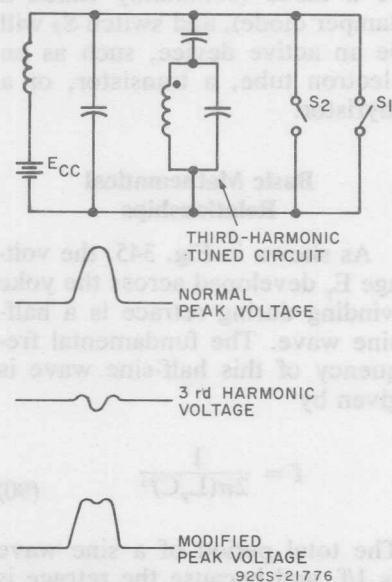


Fig. 346—Effect of third harmonic tuning on peak voltage.

In actual practice, the added circuit usually forms a part of the high-voltage system, and its presence is not obvious from an inspection of the schematic diagram.

Auxiliary Deflection-System Functions

Although the major function of the horizontal deflection system is to deflect the electron beam horizontally across the face of the picture tube, it normally also provides a number of auxiliary functions. These functions may include items such as follows:

- (1) Generation of the high-voltage for the picture tube
- (2) Focus supply voltage for the picture tube
- (3) High-voltage regulation
- (4) Scan-linearity correction
- (5) Convergence waveforms
- (6) Retrace blanking
- (7) Gating pulse for automatic gain control (agc)
- (8) Timing reference for automatic frequency control (afc)
- (9) Bias voltage for grid-No. 2 of the picture tube
- (10) Low voltage supplies for the other sections of the receiver

The voltages for these functions are normally obtained by connection of a transformer in shunt with the yoke. This transformer is called the high-voltage or "fly-back" transformer. This transformer is always a step-up transformer for the high-voltage rectifier and is usually a step-down transformer for the various other

voltages obtained from it. In addition, it may be used as a slight step-up or step down transformer for the yoke, the damper diode, the capacitor, or any combination of these components. Figure 347 shows a deflection circuit that includes a high voltage transformer together with a number of auxiliary functions.

If the low-voltage windings on the transformer are neglected and only the primary and high voltage windings are considered, Fig. 348 shows an the equivalent circuit of the deflection circuit of Fig. 347 during retrace.

L_1 is the equivalent inductance of the transformer windings and deflection yoke referred to the high-voltage side of the transformer. C_1 is the equivalent capacitance of the transformer and yoke windings, the output transistor, and any added circuit capacitance. L_2 is the leakage inductance between the yoke winding and the high-voltage winding. C_2 is the equivalent stray capacitance across L_2 , and C_3 is the capacitance across the high-voltage terminal. It can be shown that during retrace there are two frequencies of oscillation in the current and voltage waveforms. The lower of the two frequencies (which determines the retrace interval) is determined by L_1 resonating in parallel with C_1 and the capacitance path $L_2C_2C_3$. The higher resonant frequency is a result of L_2 resonating with C_2 and the capacitive path $C_3L_1C_1$. By proper design of the high voltage transformer, the leakage inductance and stray capacitance

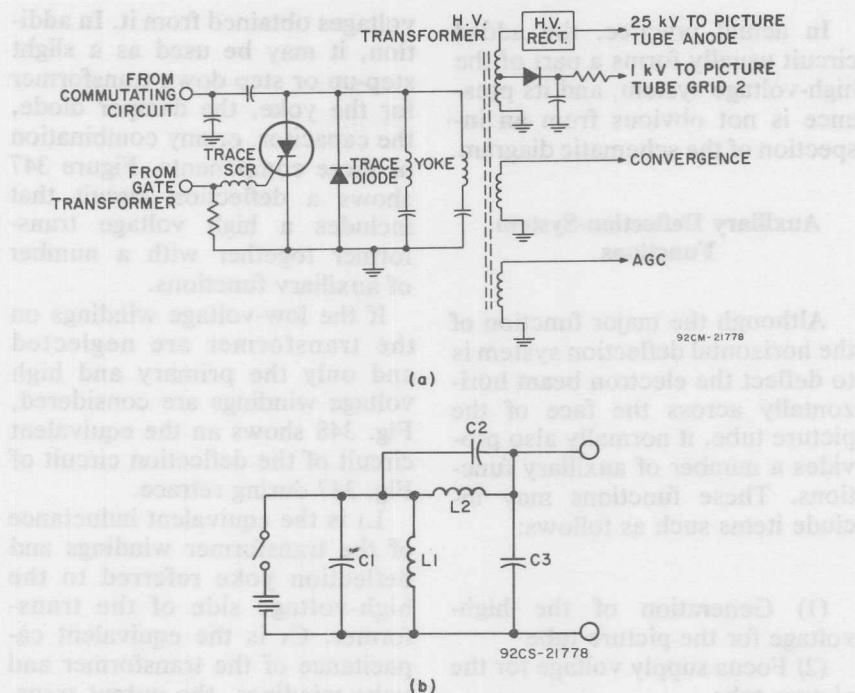


Fig. 347—Horizontal-deflection circuit with high-voltage transformer: (a) over-all schematic diagram; (b) equivalent circuit of high-voltage transformer during retrace.

may be made to resonate at the third harmonic of the retrace frequency to reduce the peak voltage on the horizontal output device, as shown previously in Fig. 346.

High-Voltage Generation

For a high-performance color receiver, a maximum beam current of 1.5 milliamperes at 25 KV is usually provided. This power is normally obtained by rectification of the voltage obtained from a tertiary winding on the high-voltage transformer. The rectifier used may be a vacuum-tube diode, a single "stack" of series-connected solid-state diodes, or

a voltage multiplier made up of several stacks of diodes together with capacitors. A voltage multiplier provides somewhat better voltage regulation with beam current, because the small tertiary high-voltage winding required represents a lower source impedance for the high voltage load.

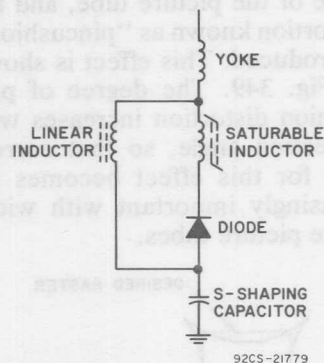
Scan Linearity Correction

For accurate reproduction of pictures, the electron beam must move at a linear rate across the faceplate of the picture tube. If the faceplate were a section of a sphere with its center at the center of deflection, a linear sawtooth of current through the deflection

yoke would be required for linear deflection. Although the faceplate is a section of sphere, its radius is much greater than the distance to the center of deflection. The distance from the center of deflection to the faceplate therefore, is greater at the edges than at the center of the picture tube. Consequently, a given amount of deflection of the beam at the deflection center produces a greater movement of the beam at the edges of the raster than at the center. For this reason, the required current waveform through the deflection yoke should be somewhat "S"-shaped rather than an absolutely linear sawtooth. Much of this S-shaping is accomplished by a capacitor connected in series with the yoke, as shown in Fig. 347.

The yoke and its series capacitor, shown in Fig. 347, make up a series-resonant circuit, with the return path being either the trace SCR, or the trace diode depending on which is conducting. The resonant frequency of this circuit is roughly 10 kHz. The period of one-half cycle, therefore, is approximately the time duration of one scanning line. The current waveform during the scan period, then, is a section of a sine wave and is approximately S-shaped. Unfortunately, the degree of S correction provided by the S-shaping capacitor is often insufficient for good linearity. The radius of curvature of the faceplate may require greater "flattening" of the current waveform at the edges of the raster than the resonance effect can produce

or the resistance of the yoke may distort the waveform. Fig. 348 illustrates a possible method of linearity correction.



92CS-21779

Fig. 348—Variable-inductance linearity correction circuit.

The circuit shown in Fig. 348 acts as a variable inductance in series with the yoke. During the first part of trace, the flow of yoke current through the saturable inductor is blocked by the diode. During the second part of trace, the diode becomes forward-biased, and yoke current is gradually shunted through the self-saturable inductor. With the proper values for the two inductors, the equivalent inductance in series with the yoke varies just the right amount to produce the proper degree of linearity correction.

Raster Correction

The distance from the center of deflection to the outside edge of the raster on the picture tube is greatest at the corners of the raster and decreases to a minimum at the center. Because the electron beam must travel a great-

er distance to reach the corners of the raster, a given deflection of the beam produces a greater movement of the spot on the faceplate of the picture tube, and the distortion known as "pincushion" is produced. This effect is shown in Fig. 349. The degree of pincushion distortion increases with deflection angle, so that correction for this effect becomes increasingly important with wide-angle picture tubes.

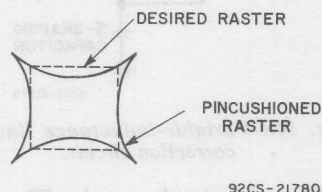


Fig. 349—Effect of pincushion distortion.

In monochrome receivers, correction of pincushion distortion is achieved by imbedding magnets in the forward edge of the deflection yoke assembly. This type of correction, however, would degrade convergence and purity, so it cannot be used in color receivers. The usual method of

achieving pincushion correction is to reduce the yoke current as the beam approaches the corners of the raster. One method of side pincushion correction that uses active devices is shown in Fig. 350.

In this circuit, the collector supply for the transistor Q_2 is the voltage across the 0.68 microfarad capacitor C_1 connected in series with the primary of the high-voltage transformer. Loading of this supply by transistor Q_2 increases the energy being drawn from the high-voltage transformer and thus reduces scan. Transistor Q_2 is driven by a sawtooth derived from the vertical output stage. During the second half of vertical trace, transistors Q_1 and Q_2 , which are driven into conduction by the vertical sawtooth, discharge the 10-microfarad capacitor C_2 . Capacitor C_1 is then loaded with an increasing current from the middle to the end of vertical scan. At the end of vertical scan, transistors Q_1 and Q_2 are turned off. Capacitor C_2 is again charged by

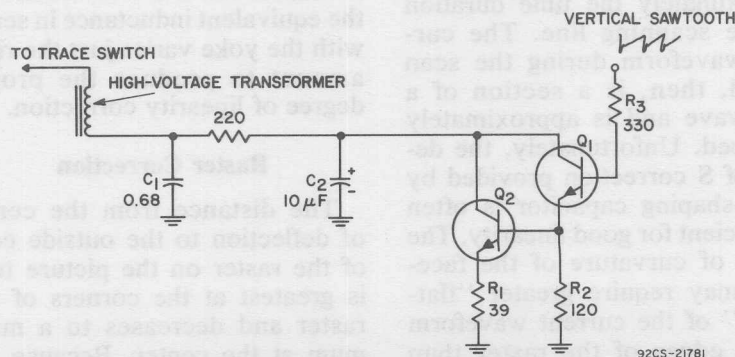


Fig. 350—Active side-pincushion correction circuit.

the energy stored in capacitor C_1 . The loading of C_1 by C_2 is a maximum at the beginning of vertical scan (top of picture), and decreases toward zero from the top toward the middle of vertical scan as capacitor C_2 charges.

Another method for correction of side pincushion distortion is shown in Fig. 351. In this circuit, the control winding of the saturable transformer is supplied

creases from a minimum at the center of vertical scan to a maximum at the end of vertical scan. At the beginning of vertical scan, the current through the control winding is maximum, and the degree of loading of the high-voltage transformer and yoke is maximum. The current in the control winding (and the yoke loading) gradually decreases to a minimum toward the center of scan.

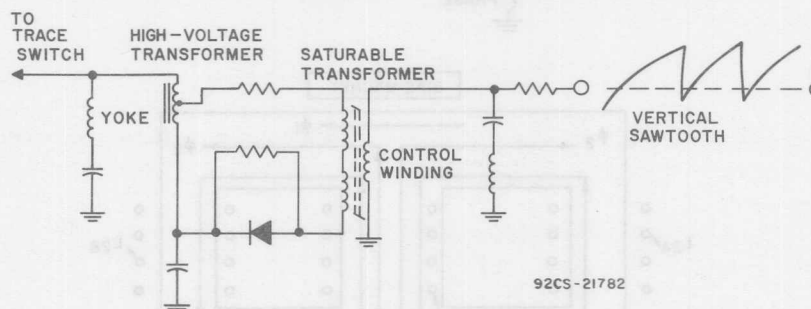


Fig. 351—Saturable reactor side-pincushion correction circuit.

with a vertical sawtooth (preferably somewhat parabolic in shape). This current determines the degree of saturation of the transformer core and, therefore, the impedance of the secondary windings, which are shunted across a portion of the primary of the high-voltage transformer. During the second half of vertical scan, the current through the control winding gradually increases from zero at the center of scan to a maximum value at the end of scan. The degree of core saturation also increases, and the inductance of the windings in shunt with the transformer (and yoke) decreases accordingly. The loading of the high-voltage transformer and yoke gradually in-

Fig. 352 shows a circuit for correction of top and bottom pincushion distortion. In this circuit, T_1 is a saturable-core transformer which has two windings connected in parallel on the center leg of the core and two series-connected windings on the outside legs. A permanent magnet induces a "bias" magnetic flux, ϕ_1 in the direction shown. The vertical yoke current flowing through the transformer windings L_{2A} and L_{2B} produces a flux ϕ_2 , which is proportional in magnitude and polarity to the vertical yoke current. The horizontal current that flows through the windings L_{1A} and L_{1B} produces a flux ϕ_{3A} and ϕ_{3B} . The fluxes ϕ_{3A} and ϕ_{3B} oppose

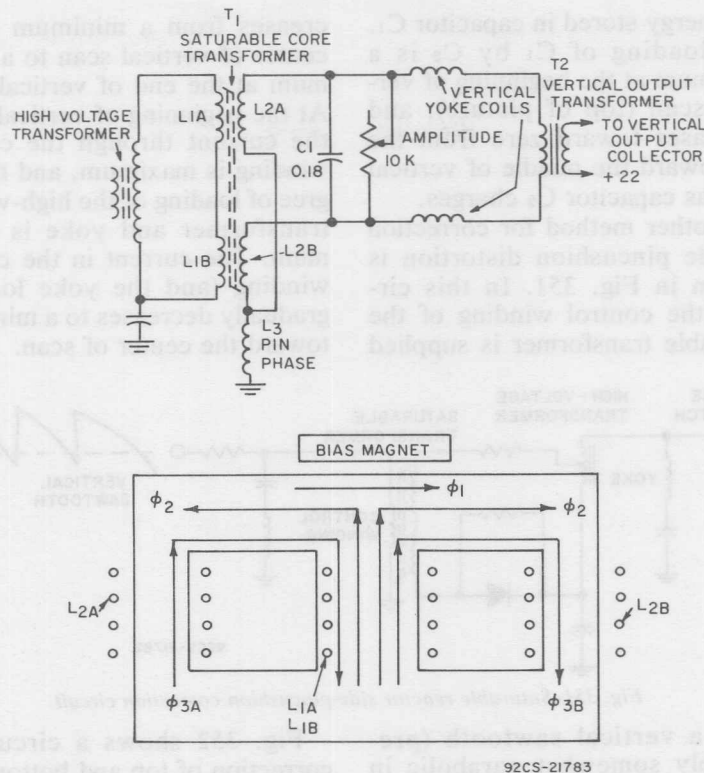


Fig. 352—Top and bottom pincushion correction circuit.

each other because L_{1A} and L_{1B} are connected in phase opposition. When the vertical yoke current is zero, as it is when the electron beam is at the center of the raster, the flux in the outer legs of the transformer is balanced, and $\phi_{3A} = \phi_{3B}$. Therefore, no voltage is induced in L_{2A} or L_{2B} , which are connected in series with the vertical yoke coils. At the other extreme, when the beam is at the top of the raster and vertical current is at its maximum positive value, the net flux ϕ that tends to saturate the core in the left leg of the transformer is

equal to $\phi_1 + \phi_2$, and the flux in the right leg is equal to $\phi_1 - \phi_2$. The fluxes ϕ_{3A} and ϕ_{3B} are no longer equal, and the flux in the center leg is equal to $\phi_{3A} - \phi_{3B}$. A voltage at the horizontal rate, proportional to $\phi_{3A} - \phi_{3B}$, is induced in L_{2A} and L_{2B} . At the bottom of the raster, when vertical yoke current is at its maximum negative value, the induced voltage in L_{2A} and L_{2B} is proportional to $\phi_{3B} - \phi_{3A}$. At all points between these extremes, the difference between ϕ_{3A} and ϕ_{3B} is directly dependent on the magnitude of ϕ_2 or the vertical yoke

current. Therefore, a decreasing correction toward the center of the raster and a reversal in the phase of the correction between the two halves of the raster is achieved.

Transformer windings L_{2A} and L_{2B} are tuned by capacitor C_1 to approximately the horizontal scanning frequency in order to obtain proper phasing of the correction voltage. This tuning results in a correction signal which is sinusoidal in shape rather than the parabolic shape which is required. However, because of the retrace time of the horizontal scan, only a portion of the sine wave is used and this represents an acceptable approximation of a parabolic waveform.

Because it is impractical to adjust capacitor C_1 or coil L_{2A} or L_{2B} in production to obtain proper tuning, the phase coil L_3 is added. This coil is not in the magnetic field of the saturable transformer, and it can be varied to obtain the proper phasing with negligible effect on the amplitude of the correction. A resistive amplitude control is used to adjust the amplitude of the correction.

FUNCTIONAL DESCRIPTION OF SCR DEFLECTION SYSTEM

In an SCR horizontal deflection system, the switching action required to generate the scanning current in the horizontal yoke windings and the high-voltage pulse used to derive the dc operating voltages for the picture tube is controlled by two SCR's that are used in conjunction with associated fast-recovery diodes to

form bipolar switches.

The SCR deflection system operates directly from a conventional unregulated dc supply voltage which may be as low as 140 volts (or as high as 280 volts) and provides full-screen deflection at angles up to 90 degrees at full beam current. The current and voltage waveforms required for horizontal deflection and for generation of the high-voltage are derived essentially from LC resonant circuits. As a result, fast and abrupt switching transients which would impose strains on the solid-state devices are avoided.

A regulator stage is included in the SCR horizontal deflection circuit to maintain the scan and the high-voltage within acceptable limits with variations in line voltage. The equivalent source impedance of the high-voltage system is sufficiently low (about 1.5 megohms) so that variation in high-voltage with beam current is well within commercial limits. The system also contains horizontal linearity and pincushion correction circuits.

Basic Deflection Circuit

The basic SCR deflection circuit is shown in Fig. 353. The trace-switch diode D_T and the trace-switch controlled rectifier SCR_T provide the switching action which controls the current in the horizontal yoke windings L_Y during the trace interval. The commutating-switch diode D_C and the commutating-switch controlled rectifier SCR_C initiate retrace and control the yoke current during the retrace interval. Inductor L_R

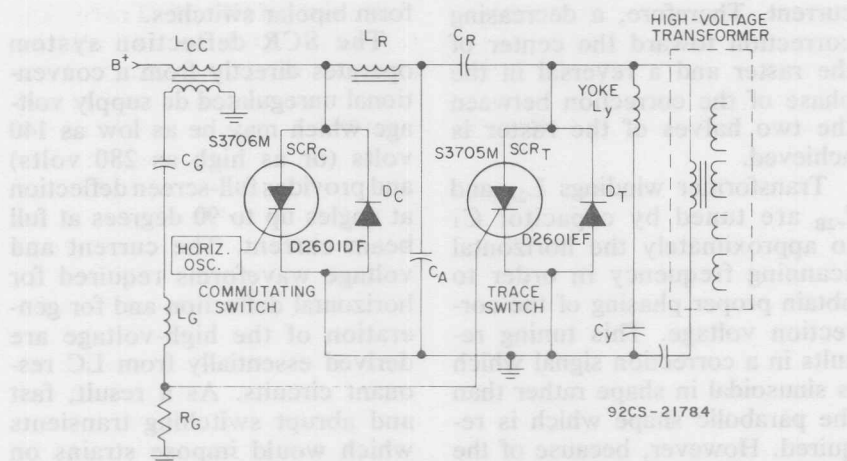


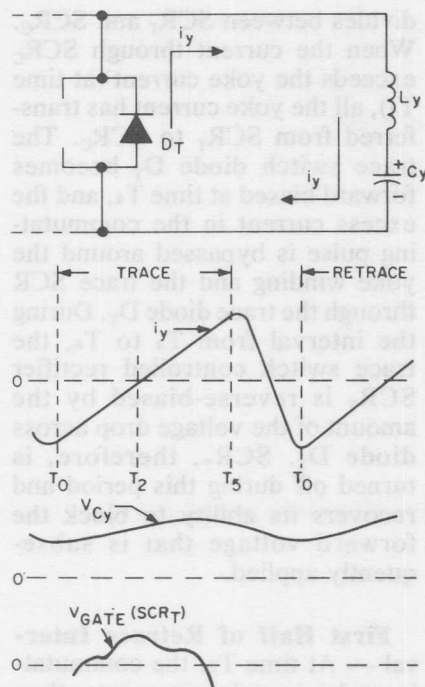
Fig. 353—Basic circuit for generation of the deflection-current waveform in the horizontal yoke winding.

and capacitors C_R , C_A and C_Y provide the necessary energy storage and timing cycles. Inductor L_{CC} supplies a charge path for capacitor C_R from the dc supply voltage ($B+$) so that the system can be recharged from the receiver power supply. The secondary of inductor L_{CC} provides the gate trigger voltage for the trace switch SCR. Capacitor C_R establishes the optimum retrace time by virtue of its resonance with inductor L_R .

The SCR deflection system contains four active devices in addition to a number of passive components. Each device conducts or blocks current at the appropriate time during the trace or retrace interval. In the discussion to follow each discrete interval is considered separately. The effects of the auxiliary capacitor C_A and the high-voltage transformer are initially neglected in order to simplify the explanation.

First Half of Trace Interval — Fig. 354 shows the circuit elements involved and the voltage and current relationships during the first half of the trace interval, time T_0 to T_2 . At time T_0 , the magnetic field has already been established about the yoke by the circuit action during the retrace portion of the preceding cycle (explained in subsequent description of retrace interval). This magnetic field induces a flow of current in the yoke which decays from a maximum negative value at T_0 to zero at T_2 (when the energy stored in the yoke has been depleted). This current charges capacitor C_Y to a positive voltage V_{CY} through the trace switch diode D_T .

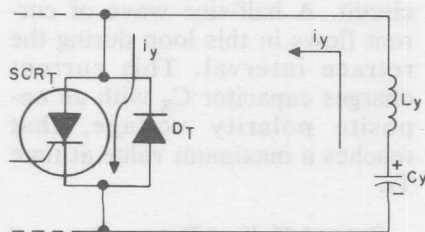
Just prior to time T_2 , the trace-controlled rectifier SCR_T is made ready to conduct by the application of a positive gate voltage pulse V_{GATE} . However, SCR_T is



92CS-21785

Fig. 354—Effective configuration of the deflection circuit during the first half of the trace interval, time T_0 to T_2 , and operating voltage and current waveforms for the complete trace-retrace cycle.

reverse-biased during the first half of trace and does not conduct until the second half of trace.



92CS-21786

Fig. 355—Effective configuration of the deflection circuit during the second half of the trace interval, time T_2 to T_3 , and the complete scan-current waveform.

Second Half of Trace Interval — At time T_2 , all the energy stored in the yoke has been transferred to capacitor C_Y , and yoke current has decayed to zero. Capacitor C_Y then begins to discharge through the yoke. The direction of yoke current is then reversed, and the trace switch diode D_T becomes reverse-biased. SCR_T is now forward-biased by the voltage V_{CT} across the capacitor, and the capacitor discharges through the yoke inductance and SCR_T , as shown in Fig. 355. Capacitor C_Y is sufficiently large so that V_{CY} remains essentially constant throughout the trace and retrace intervals. This constant voltage results in a linear rise of current through the yoke inductance over the entire scan interval from T_0 to T_5 .

Start of Retrace Interval

— Fig. 356 shows the circuit elements involved at the start of retrace. At time T_3 , just prior to the end of the trace interval, the commutating controlled rectifier SCR_C is turned on by a pulse applied to its gate by the horizontal

oscillator. Commutating capacitor C_R then discharges through SCR_C and the commutating inductor L_R . L_R , C_R and the yoke form a series resonant circuit with the series loop being completed by SCR_C . The current in this loop, referred to as the commutating loop, builds up in the form of a half-sine wave pulse. The yoke current which had been flowing in SCR_T now

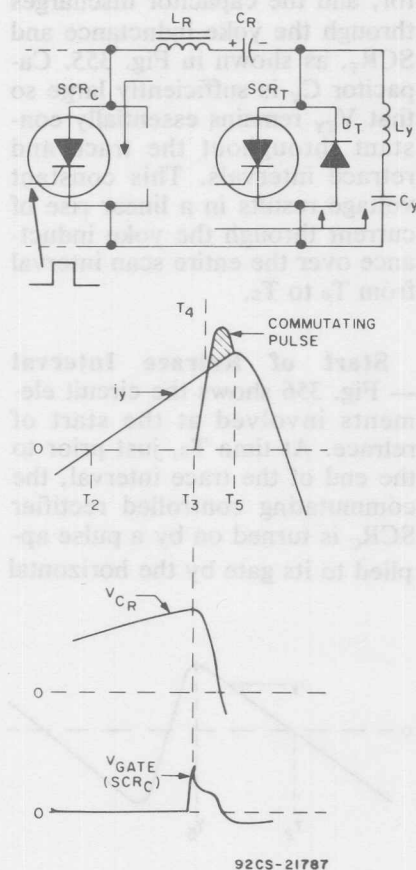


Fig. 356—Effective configuration of the deflection circuit and significant voltage and current waveforms for initiation of retrace, time T_2 to T_5 .

divides between SCR_T and SCR_C . When the current through SCR_C exceeds the yoke current (at time T_4), all the yoke current has transferred from SCR_T to SCR_C . The trace switch diode D_T becomes forward biased at time T_4 , and the excess current in the commutating pulse is bypassed around the yoke winding and the trace SCR through the trace diode D_T . During the interval from T_4 to T_5 , the trace switch controlled rectifier SCR_T is reverse-biased by the amount of the voltage drop across diode D_T . SCR_T , therefore, is turned off during this period and recovers its ability to block the forward voltage that is subsequently applied.

First Half of Retrace Interval — At time T_5 , the commutating pulse is no longer greater than the yoke current, as shown in Fig. 357, and trace-switch diode D_T ceases to conduct. The yoke inductance maintains the flow of yoke current, but with SCR_T in the off-state, this current now flows in the commutating loop formed by L_R , C_R , and SCR_C . Time T_5 is the beginning of trace. L_R , C_R , L_Y , C_Y , and SCR_C form a resonant circuit. A half-sine wave of current flows in this loop during the retrace interval. This current charges capacitor C_R with an opposite polarity voltage, that reaches a maximum value at time T_6 .

Second Half of Retrace Interval — At time T_6 , the energy stored in the yoke inductance is depleted, and the stored energy in the re-

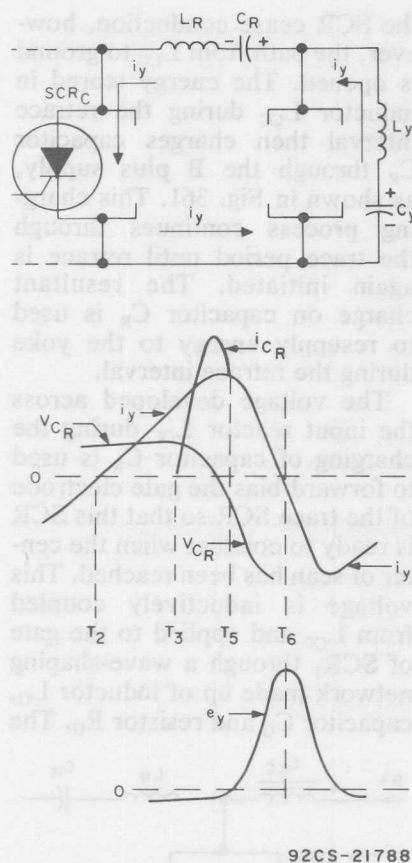


Fig. 357—Effective configuration of the deflection circuit and operating voltage and current waveforms during the first half of retrace, time T_5 to T_0 .

trace (commutating) capacitor is then returned to the yoke. During the reversal of yoke current, the commutating switch diode D_C provides the return path for the loop current as indicated in Fig. 358.

SCR_C is reverse biased by the amount of the voltage drop across diode D_C. This SCR, therefore, turns off and recovers its forward blocking capability. As the yoke current builds up in the negative

direction, the voltage on the retrace capacitor C_R is decreased. At time T_0 , the voltage across capacitor C_R no longer provides a driving voltage for the yoke current to flow in the loop formed by L_R , C_R , and L_Y . The yoke current finds an easier path up through trace switch diode D_T , as shown in Fig. 359. This action represents the beginning of the trace for the yoke current. (i.e. the start of a new cycle of operation), time T_0 .

Once the negative yoke current is decoupled from the commutating loop by the trace switch diode, the current in the commutating

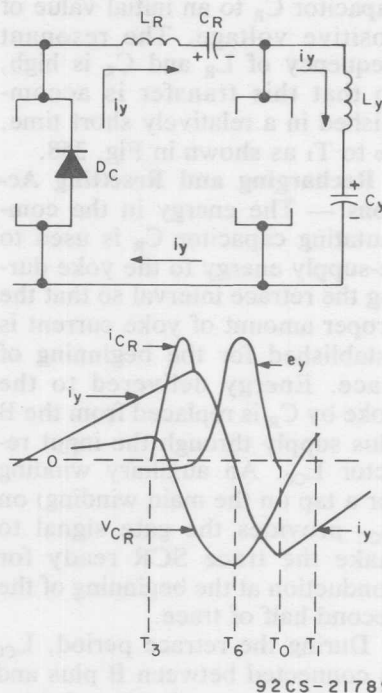
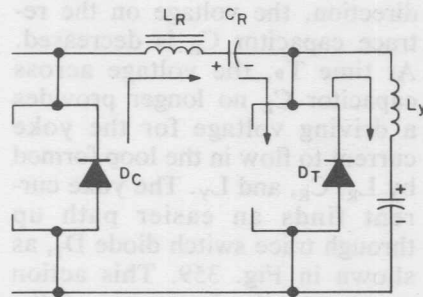


Fig. 358—Effective configuration of the deflection circuit and operating voltage and current waveforms during the second half of retrace, time T_6 to T_0 .



92CS-21790

Fig. 359—Effective configuration of the deflection circuit during the switchover from retrace to trace, time T_0 .

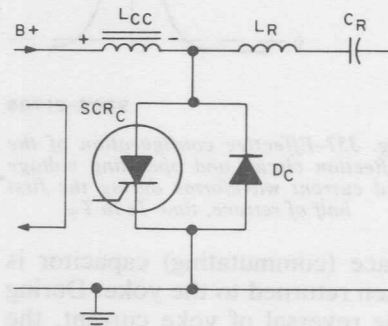
circuit decays to zero. The stored energy in the inductor L_R charges capacitor C_R to an initial value of positive voltage. The resonant frequency of L_R and C_R is high, so that this transfer is accomplished in a relatively short time, T_0 to T_1 as shown in Fig. 358.

Recharging and Resetting Actions — The energy in the commutating capacitor C_R is used to re-supply energy to the yoke during the retrace interval so that the proper amount of yoke current is established for the beginning of trace. Energy delivered to the yoke by C_R is replaced from the B plus supply through the input reactor L_{CC} . An auxiliary winding (or a tap on the main winding) on L_{CC} provides the gate signal to make the trace SCR ready for conduction at the beginning of the second half of trace.

During the retrace period, L_{CC} is connected between B plus and ground by the conduction of either the commutating-switch SCR or diode (SCR_C or D_C), as indicated in Fig. 360. When the diode and

the SCR cease conduction, however, the path from L_{CC} to ground is opened. The energy stored in inductor L_{CC} during the retrace interval then charges capacitor C_R through the B plus supply, as shown in Fig. 361. This charging process continues through the trace period until retrace is again initiated. The resultant charge on capacitor C_R is used to resupply energy to the yoke during the retrace interval.

The voltage developed across the input reactor L_{CC} during the charging of capacitor C_R is used to forward-bias the gate electrode of the trace SCR so that this SCR is ready to conduct when the center of scan has been reached. This voltage is inductively coupled from L_{CC} and applied to the gate of SCR_T through a wave-shaping network made up of inductor L_G , capacitor C_G and resistor R_G . The



92CS-21791

Fig. 360—Circuit elements and current path used to supply energy to the charging choke L_{CC} during period from the start of retrace switching action to the end of the first half of the retrace interval, time T_3 to T_1 .

resulting signal applied to the gate of SCR_T has the proper shape and amplitude so that, when for-

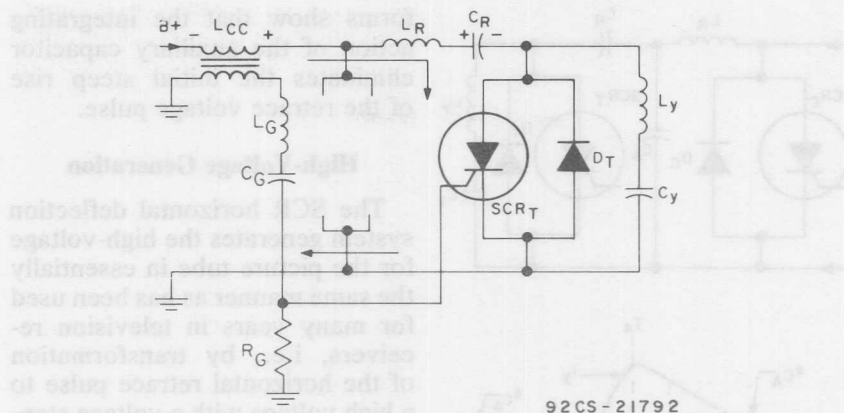


Fig. 361—Effective configuration of the deflection circuit for resetting (application of forward bias to) the trace SCR and recharging the retrace capacitor C_R , during time interval from T_2 to T_3 .

ward voltage is applied between anode and cathode, approximately midway through the trace period, SCR_T conducts.

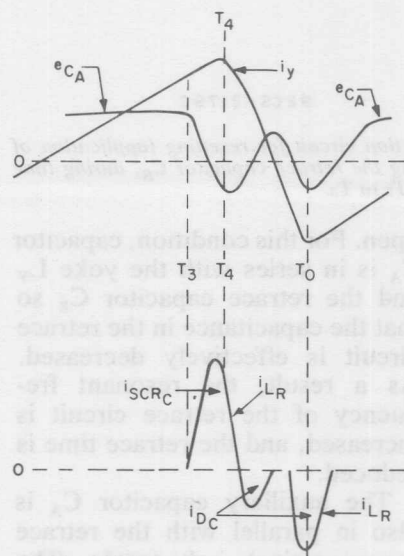
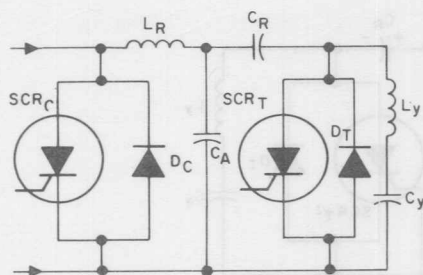
Effect of Auxiliary Capacitor C_A — In the preceding discussion, the effect of capacitor C_A was neglected. This capacitor affects some of the circuit waveforms, as shown in Fig. 362. Capacitor C_A also lengthens the turn off time requirement of the trace SCR, reduces the retrace time, provides additional energy-storage capability for the circuit, and reduces the rise time of the retrace voltage across the trace switch.

During most of the trace interval (from time T_0 to T_4), including the interval during which the commutating pulse occurs, (T_3 to T_4), the trace switch is closed, and capacitor C_A is in parallel with the retrace capacitor C_R . From the start of retrace at time T_4 to the beginning of the next trace interval at time T_0 , the trace switch is

open. For this condition, capacitor C_A is in series with the yoke L_Y and the retrace capacitor C_R so that the capacitance in the retrace circuit is effectively decreased. As a result, the resonant frequency of the retrace circuit is increased, and the retrace time is reduced.

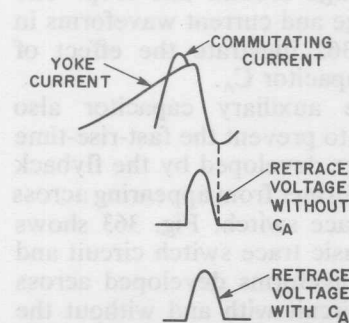
The auxiliary capacitor C_A is also in parallel with the retrace (commutating), inductor L_R . The waveshapes in the deflection circuit are also affected by the resultant high-frequency resonant discharge around this loop. The voltage and current waveforms in Fig. 362 illustrate the effect of the capacitor C_A .

The auxiliary capacitor also helps to prevent the fast-rise-time voltage developed by the flyback transformer from appearing across the trace switch. Fig. 363 shows the basic trace switch circuit and the waveforms developed across this circuit with and without the auxiliary capacitor. These wave-



92CS-21793

Fig. 362—Circuit configuration showing the addition of auxiliary capacitor C_A and current and voltage waveforms showing the effect of this capacitor.



92CS-21794

forms show that the integrating action of the auxiliary capacitor eliminates the initial steep rise of the retrace voltage pulse.

High-Voltage Generation

The SCR horizontal deflection system generates the high-voltage for the picture tube in essentially the same manner as has been used for many years in television receivers, i.e., by transformation of the horizontal retrace pulse to a high voltage with a voltage step-up transformer and subsequent rectification of this stepped-up voltage. In common with other solid-state receiver designs, a solid-state high-voltage multiplier is used as the high-voltage rectifier. A high-voltage rectifier tube, such as the 3CZ3, or a solid-state high-voltage "stack" rectifier could also be used, although the increased source impedance in the high-voltage transformer would result in slightly poorer high-voltage regulation with beam current.

High-Voltage Regulation

The use of a silicon voltage multiplier for the high-voltage rectifier, together with very tight

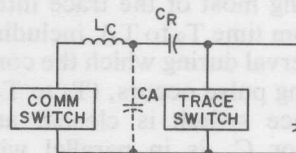


Fig. 363—Simplified schematic of trace-switch circuit and waveforms showing effect of auxiliary capacitor on the rise time of the retrace voltage pulse.

coupling between the primary and secondary of the high-voltage transformer, results in a high-voltage system that has very low internal impedance. As a result, it is necessary to regulate the high-voltage only against changes in line voltage. The regulator shown in Fig. 364 is non-dissipative (reactive), and provides good reliability at low cost.

the line voltage. This pulse is rectified and used as the collector voltage source for the regulator transistor. By means of a resistive voltage divider and a zener diode, it also provides base bias to the regulator transistor when the voltage, as determined by the resistive divider, exceeds the zener voltage. The transistor conducts and current flows through the con-

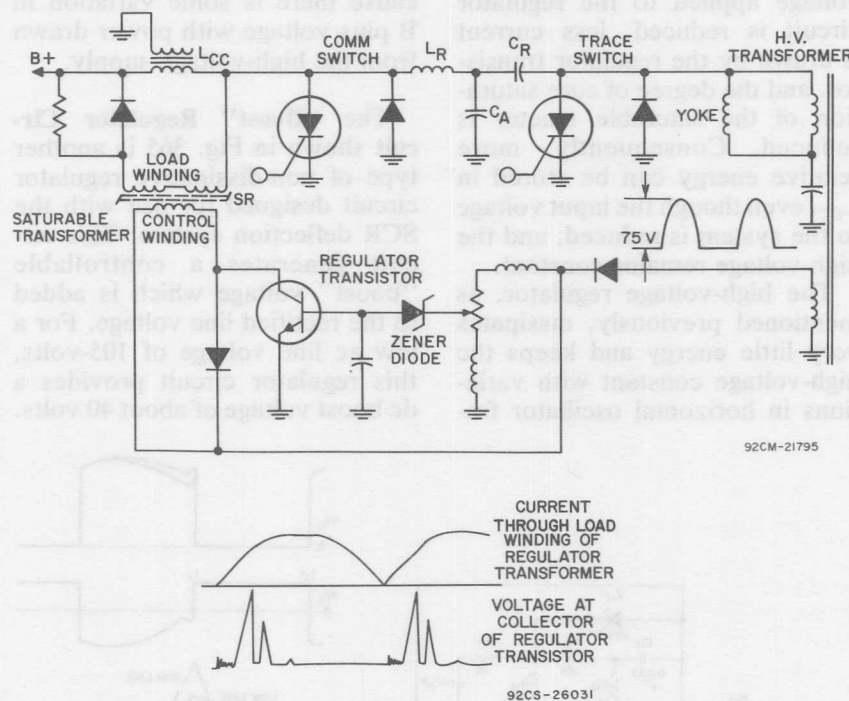


Fig. 364—Schematic diagram and current and voltage waveforms for high-voltage regulator circuit.

A supplementary winding on the high voltage transformer provides a voltage pulse which is proportional to the B plus voltage. The B plus voltage varies directly with line voltage so that the voltage pulse provides an excellent reference for sensing variations in

control winding of the saturable reactor. This current saturates the core of the saturable reactor (to a degree dependent upon the base voltage applied to the regulator transistor), and the inductance of the load winding decreases sharply. The load winding, which is in

As line voltage increases, the boost voltage decreases until at an ac line voltage of 135 volts the dc boost voltage is zero. The effective dc supply voltage E_{CC} , is about 165 volts, regulated for ac line voltages between 105 and 135 volts. An SCR is used for active regulation.

The controllable boost voltage is rectified from winding N_1 on the storage inductor L_{CC} at the time when the commutating switch in closed (L_{CC} is then connected across the supply voltage). The regulator SCR is gated by a positive sawtooth which is formed from the voltage at the winding N_1 . The voltage is first clipped by zener Z_{11} and then integrated by resistor R_{12} and capacitor C_{11} . The ramp voltage on capacitor C_{11} is then amplified by the transistor to provide the trigger current to the regulator SCR. For a line voltage of 105 volts, the composite supply voltage E_{CC} , across C_{10} is less than 160 volts, the conduction time of zener Z_{10} is very short, and the ramp current triggers SCR_R into conduction at time t_0 . The current through SCR_R charges C_{10} . The current that charges C_{10} will increase as long as commutating switch S_C is closed and then decrease when S_C opens (S_C is closed for about 27 microseconds). When SCR_R starts conduction at t_0 , the highest boost voltage is developed to maintain E_{CC}' , at 165 volts at low line voltage. The rate of current rise through SCR_R is controlled by inductor L_{10} and the leakage inductance between winding N_1 and the storage inductor L_{CC} .

For a line voltage higher than 105 volts, the composite supply voltage is greater than 160 volts. This higher voltage then causes Z_{10} to conduct for a longer time. The ramp voltage on capacitor C_{11} is, therefore, reduced, and SCR_R is triggered at a time later than t_0 . As a result, the conduction time for SCR_R is shorter and, consequently, less charge is developed on capacitor C_{10} .

Auxiliary Power Supplies

In solid-state television receivers, several power supply voltages are normally required. These supplies may include those for the horizontal-deflection, vertical-deflection, video-amplifier, and signal-processing stages.

Such supply voltages can be obtained by special windings on a main power transformer with a separate rectifier and filter system for each supply. The power transformer represents a major cost item in a color receiver, so a significant cost-reduction could be made if the power transformer could be eliminated. Elimination of the power transformer can be achieved by deriving the various supply voltages from the deflection system. Figure 366 shows a number of arrangements which can be used to derive auxiliary supply voltages from the SCR deflection system. Because these supplies involve the rectification of the 15-kHz horizontal scanning frequency, filtering is relatively simple. However, since the frequency being rectified is high, fast recovery diodes must be used for the rectifiers.

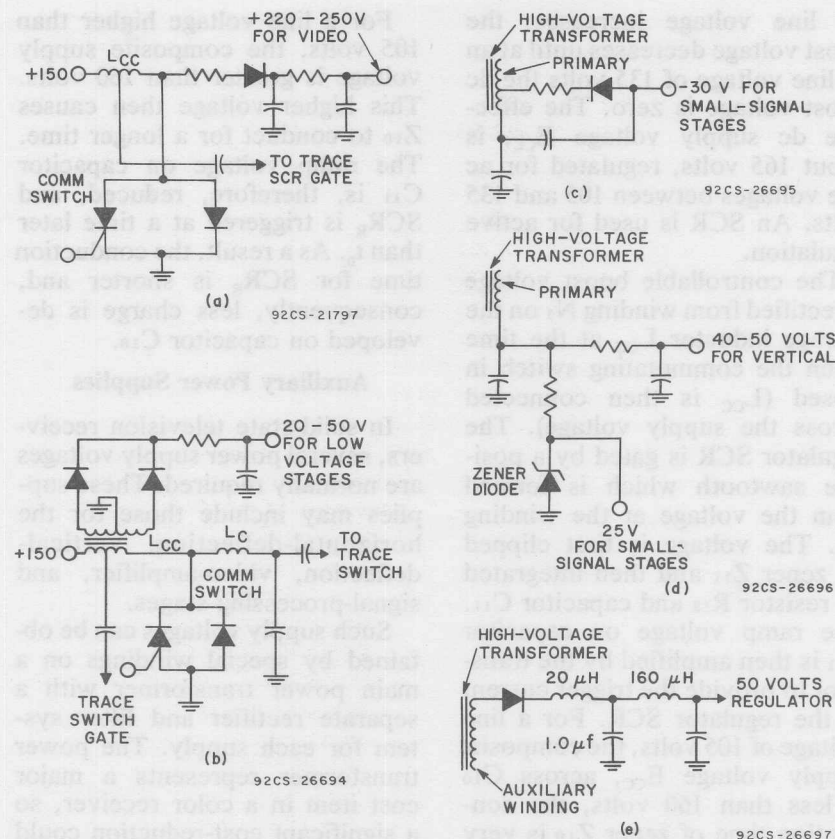


Fig. 366—Various circuit arrangements for developing auxiliary low voltages from the SCR deflection system.

SCR's have much greater power handling capability than that normally required for deflection, so the SCR system is particularly suited to systems which derive auxiliary voltages from the deflection system.

SCR DEFLECTION CIRCUITS FOR COLOR TV RECEIVERS

Fig. 367 shows a complete SCR television horizontal deflection system designed to deflect the beam of a standard 90-degree

color picture tube. In this circuit, a supply voltage of 250 volts for the video output stage is obtained by an "overwind" on the input reactor. A supply voltage of 40 volts is developed for the small-signal stages of the receiver by rectification of a pulse obtained from a supplementary winding on the high-voltage transformer. The linearity-correction circuit is essentially the same as that shown earlier in Fig. 348. The side-pin-cushion correction circuit is basically the same as that shown in

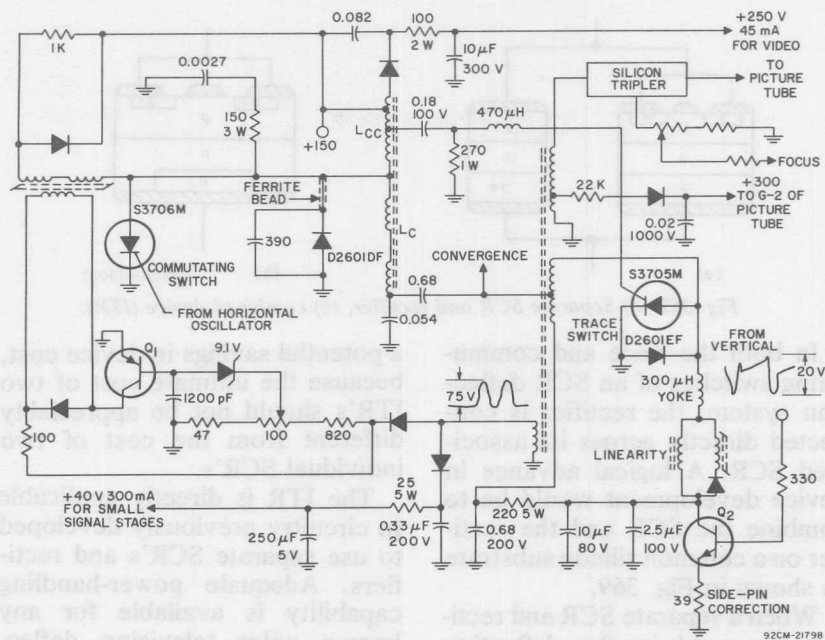


Fig. 367—Line-operated, SCR horizontal-deflection system for 90-degree color picture tubes.

Fig. 350, with the exception that only a single transistor is needed to provide the required correction. The regulator circuit is essentially identical to that shown in Fig. 364.

In the circuit shown in Fig. 367, the commutating coil and the input reactor are combined on a single E-type Ferrite core. Interaction between the input reactor and the commutating coil is avoided by separation of the commutating winding into two equal sections which are wound on the two outside legs of the E-type core. Because each coil contains exactly the same number of turns, the magnetic fields about each winding are such that they cancel in the center leg of the core, as

shown in Fig. 368. The input reactor is wound on the center leg of the stack; consequently, there is no interaction between the commutating coil and the input reactor. If cost is not a major consideration, the input reactor and the commutating coil can be wound on separate cores.

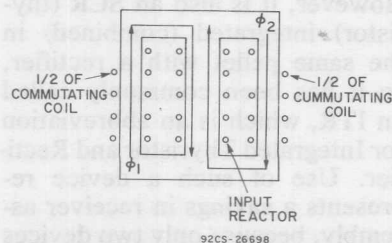


Fig. 368—Cancellation of fields from commutating coil.

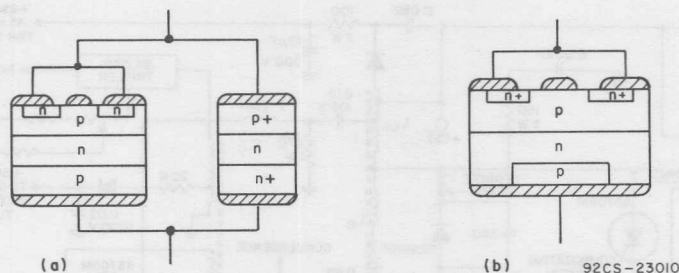


Fig. 369—(a) Separate SCR and rectifier, (b) combined device (ITR).

In both the trace and commutating switches of an SCR deflection system, the rectifier is connected directly across its associated SCR. A logical advance in device development would be to combine the SCR and the rectifier on a common silicon substrate as shown in Fig. 369.

When a separate SCR and rectifier are used in the deflection circuit, the SCR cathode is shorted to the rectifier anode and the SCR anode is shorted to the rectifier cathode by external connections. In the combined device, these elements are shorted together through the lead metallization on the surface of the pellet.

The combined device is really an SCR which conducts in the reverse as well as the forward direction, and might properly be termed a reverse-conducting SCR. However, it is also an SCR (thyristor) integrated (combined) in the same pellet with a rectifier, so it has been commonly called an ITR, which is an abbreviation for Integrated Thyristor and Rectifier. Use of such a device represents a savings in receiver assembly, because only two devices need be wired into the circuit instead of four. It also represents

a potential savings in device cost, because the ultimate cost of two ITR's should not be appreciably different from the cost of two individual SCR's.

The ITR is directly applicable to circuitry previously developed to use separate SCR's and rectifiers. Adequate power-handling capability is available for any known color television deflection application.

Since the announcement of the 90° Precision-in-Line color picture tube with its integral torroidal yoke, the availability of 100° color picture tubes in Europe with the PST torroidal yoke, and the sampling of 110° color picture tubes in the U.S., some work has been done on the development of a "universal" circuit for the two tubes. A simplified schematic of such a circuit is shown in Fig. 370. In this schematic, the component values for the P.I.L. tube which differ from those for the 110° tube are shown in brackets. This particular circuit has been designed for use with the relatively high B-supply voltage which would be available in a European receiver. Some adjustment of the component values would be required for operation in a U.S. receiver

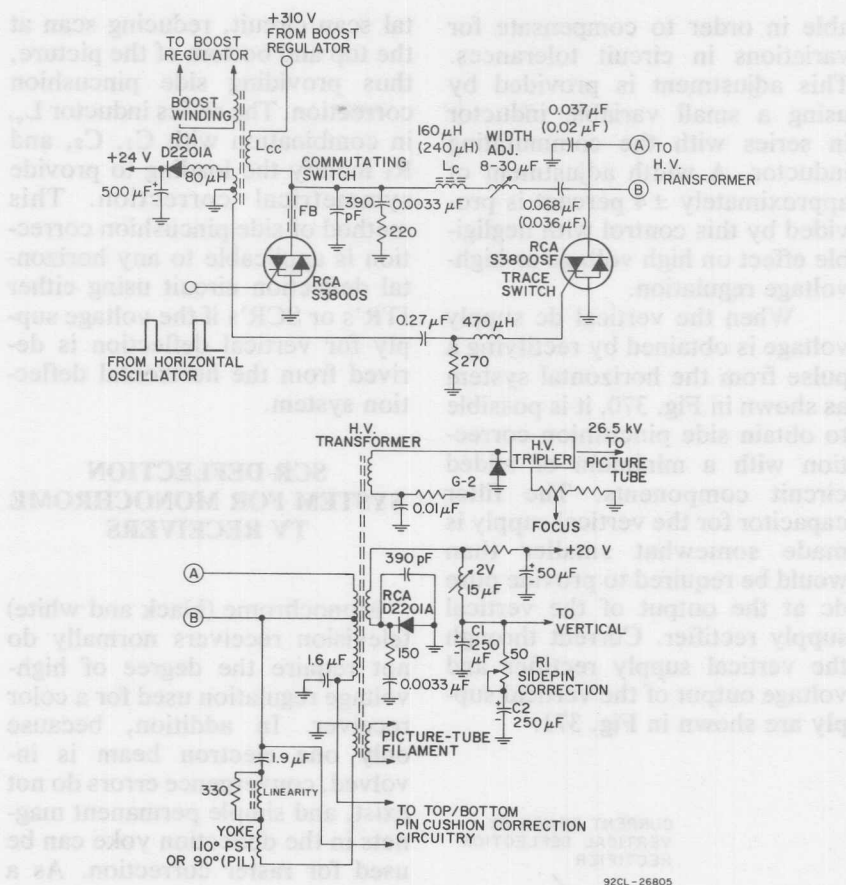


Fig. 370—Simplified schematic diagram of a "universal" circuit adaptable to 90° and 110° picture tubes.

which might have a B-supply of 250 volts. The high-voltage capability of the ITR is an advantage in this circuit, since both trace and commutating switches must be rated above 700 volts.

Fortunately the voltage across the 90° P.I.L. yoke and the 110° PST yoke for full scan is the same. Therefore, the same high-volt-

age transformer can be used for both the 90° and 110° systems. In order to meet the voltage rating on the P.I.L. yoke, the low end of the yoke is returned to ground through a 5-turn bucking winding on the high-voltage transformer. This winding is not used with the 110° yoke.

For a deluxe receiver, provision for adjustment of width is desir-

able in order to compensate for variations in circuit tolerances. This adjustment is provided by using a small variable inductor in series with the commutating inductor. A width adjustment of approximately ± 4 percent is provided by this control with negligible effect on high voltage or high-voltage regulation.

When the vertical dc supply voltage is obtained by rectifying a pulse from the horizontal system as shown in Fig. 370, it is possible to obtain side pincushion correction with a minimum of added circuit components. The filter capacitor for the vertical supply is made somewhat smaller than would be required to provide pure dc at the output of the vertical supply rectifier. Current through the vertical supply rectifier and voltage output of the vertical supply are shown in Fig. 371.

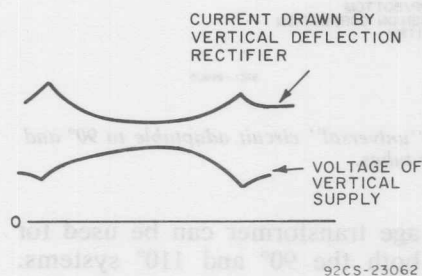


Fig. 371—Current through the vertical supply rectifier and voltage output of the vertical supply.

It can be seen that current drawn by the vertical circuit is a maximum at the beginning and end of scan and a minimum at the center of scan. This current represents a load on the horizon-

tal scan circuit, reducing scan at the top and bottom of the picture, thus providing side pincushion correction. The series inductor L_v , in combination with C_1 , C_2 , and R_1 modify the loading to provide symmetrical correction. This method of side pincushion correction is applicable to any horizontal deflection circuit using either ITR's or SCR's if the voltage supply for vertical deflection is derived from the horizontal deflection system.

SCR DEFLECTION SYSTEM FOR MONOCHROME TV RECEIVERS

Monochrome (black and white) television receivers normally do not require the degree of high-voltage regulation used for a color receiver. In addition, because only one electron beam is involved, convergence errors do not exist, and simple permanent magnets in the deflection yoke can be used for raster correction. As a result, a monochrome deflection circuit can be considerably simplified as compared to one for a color receiver. Fig. 372 shows a horizontal deflection circuit for a monochrome television receiver. This circuit is similar to the color deflection circuits previously discussed except that no regulator circuit is used. High voltage and scan will vary with line voltage in a manner similar to a conventional tube-type receiver. If regulation is desired, one of the regulator circuits previously discussed could be added to the circuit.

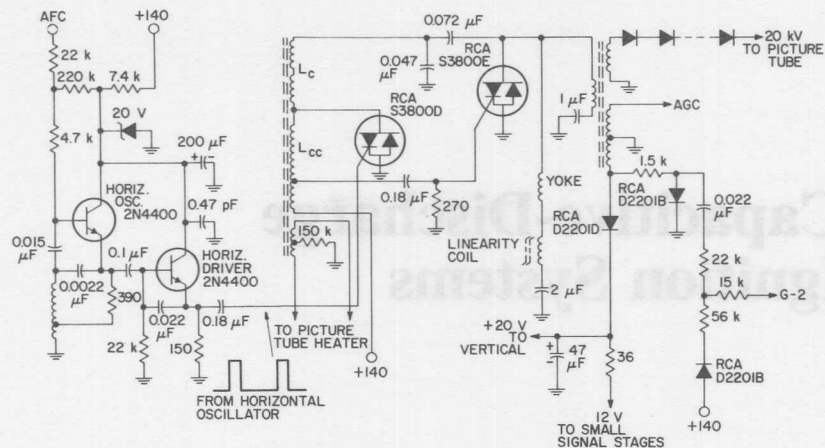


Fig. 372—Schematic diagram of a deflection circuit for a black and white receiver operating from a simple half-wave line rectifier with no regulation.

Capacitive-Discharge Ignition Systems

The increasing use of solid-state ignition systems in the automotive industry has stimulated demands for improved performance, reduction in emissions that results because more accurate spark timing is achieved with magnetic-pickup distributors, and greater reliability. The following discussion covers the basic operation of and the requirements for SCR capacitive-discharge automobile ignition systems and small-engine ignition circuits.

BASIC CONSIDERATIONS FOR AUTOMOTIVE SYSTEMS

Under worst-case conditions, about 22 kilovolts are required to ignite the combustible mixture in the cylinder of an automobile engine. In addition, a minimum energy of about 20 millijoules must be available in the spark to assure propagation of a stable flame front originating at the spark. The exact values of voltage and energy required under all operating conditions depend on

many factors, including those described in the following paragraphs.

Condition of Spark Plugs

Fouled plugs reduce both the voltage and the energy available for ignition. The plug gap also affects both the voltage and the energy required. As the plug gap is increased, the required voltage increases, but the required energy decreases.

Cylinder Pressure

The cylinder pressure depends on both the compression at the point of ignition and the air-fuel mixture. The minimum breakover voltage in any gas is a function of the product of gas pressure and electrode spacing (Paschen's Law). In automobile engines, the minimum voltage increases as this product increases. Therefore, higher pressures also require higher voltages. However, the energy required decreases as the pressure increases and in-

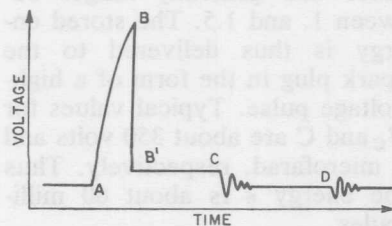
creases as the fuel-air mixture moves away from the optimum ratio. Worst-case conditions occur when the engine is started, at idle speeds, and during acceleration from a low speed because carburetion is poor and the fuel-air mixture is lean. The combination of a lower cylinder pressure and a dilute fuel-air mixture results in a high energy requirement under these conditions.

Plug Polarity

The center electrode of the spark plug is hotter than the outside electrode because of the thermal resistance of the ceramic sleeve that supports it. If the center electrode is made negative, the effect of thermionic emission from this electrode can reduce the required ignition voltage by 20 to 40 per cent.

Spark-Plug Voltage Waveshape

The spark-plug voltage waveshape is shown qualitatively in Fig. 373. The voltage starts to rise at point A, and reaches ignition at point B. The region from B' to C represents the sustaining voltage for ionization across the spark plug. When there is insuffi-



92CS-21803

Fig. 373—Ignition-voltage waveshape.

cient energy left to maintain the discharge (at point C), current flow ceases and the remaining energy is dissipated by ringing. The final small spike at point D occurs when the ignition coil again starts to pass current.

The two most important characteristics of the voltage waveshape are its rise time (from A to B) and the spark duration (from B' to C). A rise time that is too long results in excessive energy dissipation with fouled plugs; a rise time that is too short can lead to radiation losses of the high-frequency voltage components through the ignition harness. The minimum rise time should be about 10 microseconds; a 50-microsecond rise time is acceptable. Conventional systems have a typical rise time of about 100 microseconds. It should be noted that, at an engine speed of 5000 revolutions per minute, one revolution takes 12 milliseconds. Engine timing accuracy is usually no better than 2 degrees, which corresponds to 67 microseconds. The error caused by the rise time is therefore comparable to normal timing errors. At normal cruising speeds (about 2000 revolutions per minute), the 2-degree timing error corresponds to about 165 microseconds and rise-time effects are negligible.

Energy Storage

The energy delivered to the spark plug can be stored in either an inductor or a capacitor. After the storage element is discharged by ignition, it must be recharged before the next spark plug is

fired. For an eight-cylinder engine that has a dwell angle of 30 degrees, the time τ between ignition pulses (in milliseconds) is equal to 15000 divided by the engine rpm, and the time τ_{ON} during which the points are closed is equal to 10000/rpm. When the engine rpm is 5000, τ_{ON} is 2 milliseconds. For either an inductive or a capacitive storage system, therefore, the charging-time constant should be small compared to 2 milliseconds.

BASIC CAPACITIVE-DISCHARGE SYSTEMS

Two basic capacitive-discharge ignition circuits are shown in Fig. 374. It is important to note that the transformer serves simply as a pulse transformer. Therefore, per-

formance at high engine speeds is not affected by the transformer primary inductance but, instead, is governed by the time required to charge capacitor C to the desired voltage level. The dc sources for these basic circuit representations are covered later.

Circuit Operation

The trigger-control circuit (which can be a transistor switch) is controlled by the distributor points. More sophisticated distributor control, such as that available from distributors in which the voltage pulses are derived magnetically or photo-optically, can also be used to control the trigger circuit. The capacitor is charged to the dc voltage; the stored energy ϵ is equal to $C(V)^2/2$, where V_c is the capacitor voltage. At the appropriate time, the trigger-control circuit fires the silicon controlled rectifier (SCR). The capacitor discharges through the transformer, which steps up the voltage to a value V_s equal to KNV_c , where N is the transformer turns ratio and K is a constant that is dependent mainly on the value of the capacitance and of the transformer leakage inductance and generally ranges between 1. and 1.5. The stored energy is thus delivered to the spark plug in the form of a high-voltage pulse. Typical values for V_c and C are about 350 volts and 1 microfarad, respectively. Thus the energy ϵ is about 60 millijoules.

Because the energy dissipated in the spark gap is equal to the

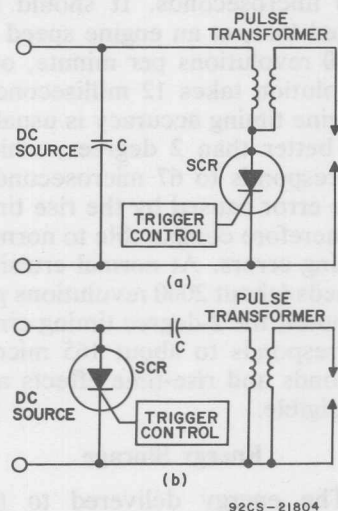


Fig. 374—Basic configuration for capacitive-discharge ignition circuits; (a) storage capacitor connected across input voltage source; (b) storage capacitor connected in series with input voltage source and pulse transformer.

energy stored in the capacitor minus the losses in the transformer and SCR, the energy available in the system is relatively easy to calculate. Examination of the basic circuits shows that the energy is transferred only when the SCR is forward conducting with the gate biased on. However, part of the energy is not available in the basic circuit because the capacitor and inductor form a turned circuit when the SCR is on, and the energy that would normally flow back from the inductor to the capacitor is stopped by the high reverse impedance of the SCR. This energy is, therefore, lost as available spark energy. The duration of the spark is limited, then, to approximately one-half cycle of the natural LC frequency of oscillation. Some of the energy lost can be regained and used to increase the spark duration by installing a diode in the basic circuits of Fig. 374 as shown in Fig. 375. The diode not only bypasses the reverse impedance of the SCR but eliminates the possibility that the SCR might conduct in the reverse direction should the gate of the SCR be biased on at this time. Thus, in addition to improving system low-temperature performance by increasing spark duration, the diode reduces the possibility of excessive heating and damage to the SCR that could accompany reverse conduction, and thereby reduces the over-all cost of the system by reducing the reverse blocking requirement of the SCR. The ratio of spark duration to charging time decreases with in-

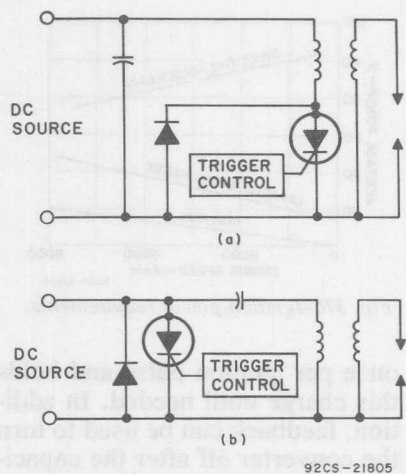


Fig. 375—Basic circuit configurations shown in Fig. 374 modified by the addition of a diode in shunt with the SCR switching device.

creasing RPM so that in some applications an RPM limit may be reached below the desired maximum because of the charging-time requirements.

Technical Features

One significant feature of the capacitive-discharge system is that the input power increases directly with the increased spark-plug power required as engine speed increases. In the inductive-discharge system, on the other hand, the opposite is true, as shown in Fig. 376. The required power is the product of the energy required per ignition pulse and the number of ignition pulses per second.

In the capacitive-discharge system, input power can be made proportional to the required power because the capacitor is charged

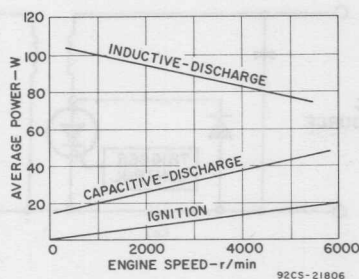


Fig. 376—Ignition power requirements.

once per ignition pulse and holds this charge until needed. In addition, feedback can be used to turn the converter off after the capacitor is charged and thus cut off the input power to the system. The input power can therefore be made proportional to engine speed, and higher efficiency can be achieved at all speeds. The curve shown in Fig. 376 applies for a commercially available capacitive-discharge system. The higher efficiency of this system is apparent.

A second important advantage of the capacitive-discharge system is that faster rise times are more readily obtained because the transformer acts only as a pulse transformer and not as an energy-storage element. Therefore, its high-frequency response characteristic is governed by its leakage inductance, which is much smaller than the primary magnetizing inductance. This advantage is obtained even when a conventional ignition coil is used as the pulse transformer. Secondary-voltage rise times of about 15 to 30 microseconds are readily obtained. As discussed previously, the shorter rise time greatly enhances the

ability of this system to fire fouled plugs.

A major operating point that must be considered in the capacitive-discharge system is when to charge the capacitor. In some systems the capacitor is charged soon after discharge, in others, just before discharge. The second method is the better in that it minimizes the losses resulting from leakage, but this advantage is somewhat negated because of the precise timing required to institute the charge just prior to discharge. This requirement can result in complex mechanical or electrical arrangements.

Component Requirements

In a capacitive-discharge ignition system, the forward blocking voltage of the SCR must be greater than about 400 volts, and its current-handling capability must be about 5 amperes. The SCR firing characteristics as a function of temperature are important, and must be taken into account in the design of the trigger circuit. Because the specifications of the spark coil are usually known, the design of an ignition circuit is usually begun there; capacitor size and voltage are determined from these known quantities. The capacitor chosen determines the spark-gap duration and the charging time required; the reliability of the system is almost directly related to the reliability of this component. No recommendations for this capacitor are made here except that the user is reminded that the high peak current which flows

through the SCR also flows through this capacitor, necessitating that the capacitor be as carefully chosen as the SCR.

The limit on charging time is the dv/dt rating of the SCR. By using the capacitor size and the dv/dt rating of the SCR, the charging current required is determined by applying the formula $L = Cdv/dt$. This formula can also be used to determine the peak current and its duration, and the rate of rise of current. The rate of rise of the current should be checked against the limiting circuit value, the di/dt rating of the SCR.

Table XVIII—SCR Parameter Values of Importance in Ignition Circuits

I_{DROM}	when $V_D = V_{Capacitor} + 20\%$ at a case temperature T_C of 100°C .
I_{RRDM}	when $V_R = 25$ volts when using a diode as in the circuit of Fig. 375 or when $V_R = V_{peak\ reverse}$ due to flywheel effect in the flywheel charged system. In both cases, T_C is 100°C .
V_T	when $I = I_{peak}$, the value of v_T is approximately 2.5 to 4 volts depending on current pulse amplitude, repetition rate, and case temperature.
V_{gate}	at 12 volts with $R_A = 30$ ohms. V_{gate} and I_{gate} will be maximum or minimum limits depending on trigger-circuit requirements. Higher limits help prevent spurious firing as a result of noise.

The SCR parameter values that must be specified to assure reliable device operation in ignition circuit applications are shown in Table XVIII.

The ignition coil used in the capacitive-discharge circuit can be a specially wound low-inductance unit or the existing coil. The existing coil has an advantage in that it can be used with a breaker-point distributor to provide the ignition function in the event of an electronic failure. The major disadvantage of the use of the existing coil is that the benefits of ignition pulses with sharp rise times, the type of pulses needed to fire fouled spark plugs, are reduced because of the inductance of the coil. Because of the ease of obtaining a trigger pulse and the circuit simplicity, the SCR capacitor-discharge system is used almost exclusively on small engines.

TYPES OF CAPACITIVE-DISCHARGE SYSTEMS

There are three systems in which capacitor-discharge ignition circuits can be used to good advantage; the flywheel-charged small-engine system, the line-charged ignitor used with gas-operated appliances such as dryers and furnaces, and the inverter-charged system such as that used in automotive and stationary engine systems. All of these systems are operated similarly in that energy stored in a capacitor is transferred to a spark gap through a transformer and SCR.

The circuit of Fig. 377 is typical of that used in the three systems. The ac potential across transformer T_1 is rectified by diode D_2 , and charges capacitor C_1 to the required voltage. Resistor

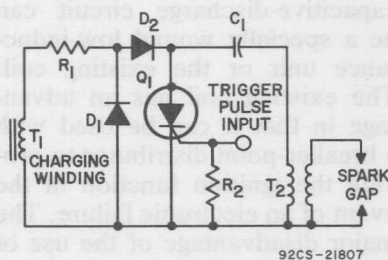


Fig. 377—Typical circuit configuration for a capacitor-discharge ignition system.

R_1 limits the current and prevents the SCR from firing as a result of the imposition of a dv/dt value in excess of the capability of the SCR. The combination of diodes D_1 and D_2 prevents the charging winding of transformer T_1 from impressing a high reverse voltage across the SCR. Resistor R_2 damps variations in the input impedance of the SCR. The SCR is triggered at the appropriate time, and the energy stored in the capacitor is transferred into the primary of T_2 , thus causing a spark at the spark gap. The voltage required to break down the spark gap is a function of the spacing of the electrodes and pressure in the cylinder in the vicinity of the gap. The spark in the gap lasts until the value of current passing through the SCR is below its holding current. When the SCR stops conducting, D_1 and D_2 start conducting in the reverse direction and lengthen spark duration. After the SCR turns off, C_1

is discharged, and the circuit is ready to repeat the cycle.

Flywheel-Charged Systems

Some of the simplest ignition systems are constructed using the flywheel-charging method as this method affords a reliable circuit with a minimum of active components. The system makes use of a rotating magnetic field to charge the capacitor and to trigger the SCR; mechanical position determines timing. The designer has several options in the determination of when the charging of the capacitor takes place in the flywheel system. The most advantageous time occurs just before the capacitor is to be discharged. However, some voltage regulation problems must be considered. Because $V = Nd\phi/dt$ where $d\phi$ and N are constant, the voltage produced across the charging winding varies with RPM. At low flywheel speeds, there may not be enough voltage available to produce the energy required; at high flywheel speeds, it is possible to have too high a voltage and therefore to exceed the voltage breakdown rating of the SCR and cause premature triggering. If the breakdown voltage rating of the capacitor is also exceeded, the capacitor will be damaged. Therefore, some means of accommodating or regulating the voltage must be considered.

The design of the trigger coil is also important. It must be capable of providing voltages and currents high enough to gate the SCR into conduction at all

temperatures and RPM. In addition, consideration should be given to the fact that the gate pulse should end before the current through the SCR ceases to flow so that the device is not gated during the period of reverse voltage.

As is evident in the above discussion, a major factor in the performance of the flywheel ignition circuit is the design of the magnetic components used for the triggering and charging functions. A typical example of a flywheel-charged ignition circuit is shown in Fig. 378.

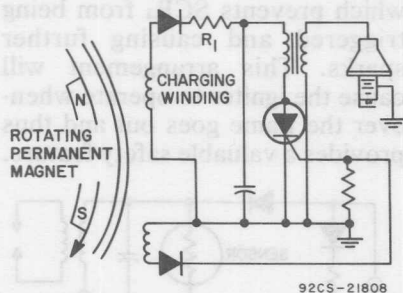


Fig. 378—Flywheel-charged igniter circuit.

Inverter-Charged Systems

A system that eliminates the dependence on the rotational speed of the flywheel magnetics is the inverter-charged system. This system is used where a battery is available, such as in an automobile.

There are some practical considerations which limit the use of the inverter system. The first limitation is starting under low temperature. At an ambient temperature of -40°C , the available battery voltage in a "12-volt" au-

tomotive system (12-volts nominal at 25°C) may be as low as 6 volts dc because of the starter current required at this temperature and the reduced battery capability. In addition, at this temperature, the fuel-air mixture is wet, particularly in a two-cycle engine. For reliable starting, the full spark energy must be available immediately. This means that the inverter must be capable of producing the full energy at low supply voltages. The voltage step-up ratio of the system transformer is constant and therefore cannot be increased as the temperature decreases; such an action would assure sufficient voltage at low temperatures, but would subject the capacitor and SCR to voltages in excess of their ratings under normal conditions and after starting. The problem of starting at low temperature may be circumvented by regulating the voltage on the capacitor or by using a transformer with a higher step-up ratio than required and then shutting down or removing the inverter, with its transformer, from the circuit at a time that will prevent any voltages from becoming a problem.

As the maximum RPM of the engine increases, the demands on the inverter also increase; this variation in demand can be alleviated by ballasting. When ballasting of the ignition is accomplished by means of a regulator circuit, external ballasts are not needed. A typical example of an inverter-type ignition system with regulator ballasting is shown in Fig. 379. The trigger

circuit shown in the figure is subject to the same variations in potential as the inverter circuit in addition to others arising from the need to gate the SCR with a high-current at low temperature when the available voltage is low. This gating problem can only be solved by a compromise between overdriving of the gate at high

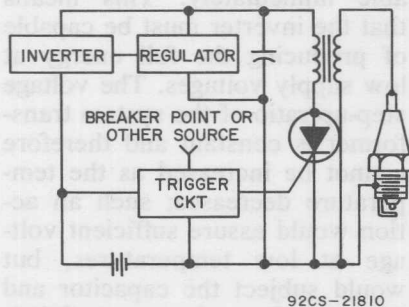


Fig. 379—Block diagram of an inverter-charged ignition system.

temperature and maintaining only an adequate drive at low temperatures; there are many circuits that can be used to achieve this compromise. The gate current could also be regulated with respect to temperature with a substantial increase in circuit cost and complexity.

The inverter must be capable of handling a power level, typically between 20 and 50 watts, representing an energy level of 80 millijoules per pulse, for a 4-cycle, 8-cylinder engine. The inverter circuit should operate at a frequency high enough to make use of smaller transformer-core sizes and yet be able to incorporate low-cost power devices. The RCA line of home-taxial power transistors is generally very reliable and economical in inverter ignition systems.

Line-Charged Igniter

The line-charged ignition circuit finds greatest use in heating systems and large gas-operated appliances. Normally, circuits of this type charge at the line voltage that produces the lowest-cost circuit. The gate trigger pulse is derived by using a diac and an RC phase-shift network such as that shown in Fig. 380. This figure represents an ignition circuit with a flame sensing feature added.

On each positive half-cycle of the ac line, the circuit operates once until the flame is burning; the sensor then turns on SCR₂ which prevents SCR₁ from being triggered and causing further sparks. This arrangement will cause the igniter to operate whenever the flame goes out and thus provides a valuable safety feature.

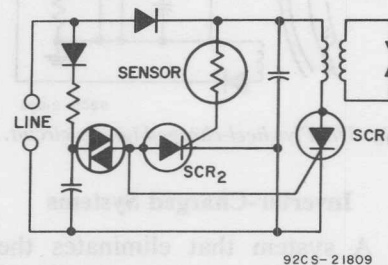


Fig. 380—Line-charged ignition circuit.

AUTOMOTIVE IGNITION SYSTEM

Fig. 381 shows the circuit diagram for a low-cost transistor/SCR capacitor-discharge ignition system for passenger automobiles. This system offers the advantages of reduced maintenance, smaller current drain on the automobile battery, full output volt-

All the resistors are ½W unless otherwise indicated.

Fig. 381—An SCR capacitor-discharge automobile ignition circuit.

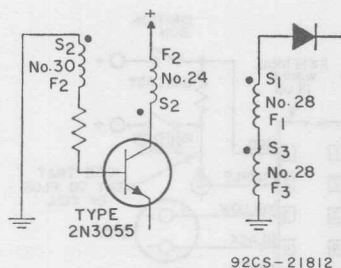


Fig. 382—Details of inverter transformer (T₁) shown in Fig. 381.

age at low battery voltage (down to 4 volts), and a high-voltage output pulse that has a rapid rate of rise. As pointed out previously, this latter factor provides greater assurance of the firing of fouled spark plugs.

The SCR ignition system is essentially a combination of eight basic circuit units, as follows: (1) A single-ended, self-oscillating swinging-choke inverter is used to provide the dc-to-ac inversion and the step-up of the battery voltage. (2) An output circuit that includes an SCR, a storage capacitor, an ignition coil (a standard automotive ignition coil is used), and a commutating diode develops the fast-rising high-voltage pulse for the spark plugs. (3) The commutating diode and a single rectifying diode form a capacitor-charging circuit to transfer energy from the inverter to the output-circuit storage capacitor. (4) A regulator stage controls the frequency of the inverter stage to provide efficient regulation of the voltage across the storage capacitor. (5) A protection circuit (limiting inductance and resistance) prevents damage

to the system by transients that may be developed in the case of an open or shorted ignition coil or because of high-voltage arcing to either primary terminal of the ignition coil. (6) A shut-down circuit holds the inverter inoperative when the ignition breaker points are open. (7) A trigger circuit suppresses the normal bounce of the breaker points and also prevents SCR triggering by the residual voltage across the closed points. (8) A method of SCR commutation is used that involves the interplay of several parts of the overall system.

Inverter, Regulator, and Capacitor-Charging Circuit

The inverter uses a 2N3055 transistor (Q₁) in a single-ended output stage, a 2N3053 transistor (Q₂) in an emitter-follower driver stage, and a 2N2102 transistor (Q₃) in a control stage that is part of the shutdown circuit which holds the inverter inoperative when the ignition breaker points are open. Regenerative feedback is coupled from the feedback winding of the inverter output transformer T₁ back to the bases of the driver and output transistors. The high gain provided by the combination of transistors Q₁ and Q₂ assures oscillation and low drive-power requirements for the inverter. The starting resistor R₅ provides a forward bias that drives transistors Q₁ and Q₂ into conduction to initiate oscillation in the inverter. The regenerative action of the circuit very quickly drives the output transistor Q₁ into

conduction, and essentially the full battery voltage is then applied across the primary of the inverter output transformer T_1 . The resultant current increase in the transformer primary winding induces a voltage across the feedback winding that supplies sufficient current through resistors R_1 and R_4 and diode D_1 to maintain the output transistor Q_1 in saturation. During this part of the operating cycle (i.e., during the conduction of transistor Q_1 , the voltage across the secondary winding of transformer T_1 reverse-biases the rectifying diode D_2 in the capacitor-charging circuit, and no energy is transferred to the output circuit of the ignition system.

With transistor Q_1 operating with fixed base current (in saturation), its collector current rises to a value beyond which it cannot increase. As a result, the feedback voltage is decreased, and no longer maintains base drive to transistor Q_1 , and the transistor starts to turn off. The regenerative action of the inverter circuit causes a rapid reversal of the base drive for transistors Q_1 and Q_2 . These transistors, therefore, are quickly cut off, and a "flyback" voltage pulse is generated at the collector of the output transistor Q_1 . Diode D_3 blocks the reverse voltage and limits the reverse base drive. The reverse-bias current that turns off transistors Q_1 and Q_2 is applied through resistors R_3 and R_1 , respectively. The flyback-pulse voltage is stepped up across the secondary of trans-

former T_1 . The polarity of this pulse, however, is such that the rectifying diode D_2 becomes forward-biased. As a result, the energy previously stored in the primary winding of transformer T_1 is transferred through the secondary winding, rectifying diode D_2 , and commutating diode D_3 to charge the output-circuit storage capacitor C_2 . The capacitor C_1 connected across transistor Q_1 reduces the amplitude of the leakage-inductance pulse and restricts the rate of rise of the collector voltage of transistor Q_1 . The charging current for capacitor C_2 is shunted around the ignition coil by the commutating diode D_3 so that no energy is transferred into the ignition coil and from there to the spark plugs.

When the collector voltage of transistor Q_1 decrease to a value less than the battery voltage, it again begins to conduct, and the cycle is repeated to charge the storage capacitor C_2 to a higher voltage. Until the voltage across the storage capacitor rises above a predetermined value, the voltage applied to the zener diode D_4 from the voltage divider formed by resistors R_6 and R_8 is insufficient to cause the zener diode to conduct. If the ignition breaker points are closed during this time, resistor R_7 is returned to ground and transistor Q_3 cannot conduct. When the capacitor voltage rises to a level high enough to cause zener diode D_4 to conduct, transistor Q_3 turns on and shunts base drive current from transistor Q_2 . This effect

tor to pull out of saturation at a lower collector-current level which, in turn, increases the frequency of oscillation. The cut-back in peak primary current reduces the charging rate of the storage capacitor C_2 to the level required to replenish circuit losses and prevents further rise in the output voltage.

Transistor Q_3 also holds the inverter inoperative when the ignition breaker points are open. When these points open, the current fed from the voltage at the breaker points through resistor R_7 causes transistor Q_3 to conduct heavily. This effect shorts the base of transistor Q_2 and stops the oscillation.

Fig. 383 shows that the collector voltage of transistor Q_1 swings alternately between the saturation level and the peaks of flyback pulses of increasing amplitude. The change in frequency that results from regulator action is apparent in the voltage waveform. The collector voltage

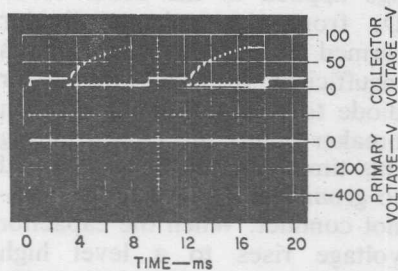
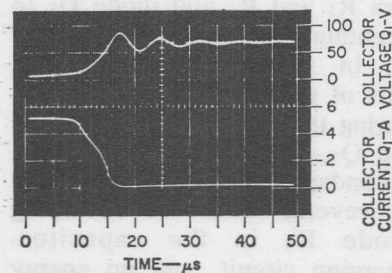


Fig. 383—Collector voltage of the inverter output transistor Q_1 (top) and ignition-coil primary voltage (bottom) as functions of time (2000 rpm; $V_{CC} = 12V$.)

points open and shut down the inverter. Fig. 384 shows an expanded view of the turn-off and flyback characteristics of transistor Q_1 at a point when the storage capacitor is being charged.



92CS-21814

Fig. 384—Expanded collector voltage (top) and current (bottom) of the inverter output transistor (Q_1) as functions of time during turn off when the storage capacitor (C_2) is being charged ($V_{CC} = 12V$).

Output Circuit

When a high-voltage pulse is required, the RCA-S2620D SCR in the output circuit is gated on. As a result, the anode voltage of the SCR decreases to approximately zero, and the voltage across the charged storage capacitor is applied to the primary of the ignition coil. (The value of the inductance L_1 is negligible in comparison to the inductance of the ignition coil and is not considered in this analysis.) The ungrounded (+) side of the ignition-coil primary (terminal 3 on the connecting plug) is driven negative with respect to the capacitor potential. Diode D_3 , in parallel with the coil, is reverse-biased at this time. The discharge

of the capacitor into the primary of the ignition coil generates a high-voltage pulse across the secondary.

The capacitor discharges into the primary inductance of the ignition coil and builds up the primary current in the coil. When the voltage across the capacitor (and coil primary) decreases to zero and starts to reverse, the commutating diode D_3 becomes forward-biased and begins to conduct. The current through the primary of the ignition coil is at a peak at the time the diode begins to conduct. The current then suddenly switches out of the SCR and into the diode. The primary-coil voltage remains clamped at zero, and the primary current decays at a rate determined by the L/R ratio of the coil. Because of the clamping action of the commutating diode D_3 , the duration of the spark in the spark plug is lengthened.

When the SCR is on, it effectively places a short across the secondary of the inverter transformer. However, the inverter is off when the SCR is on (because of the shut-down circuitry); the inverter, therefore, does not operate into the short.

Figs. 385 and 386 show the SCR voltage and current as a function of time. The starting point of the waveform shown in Fig. 385 occurs at the instant the ignition points open. The anode voltage of the SCR decreases to zero and the anode current builds up to the peak value in a quarter cycle. The current is then switched out of

the SCR, and SCR current decreases suddenly almost to zero.

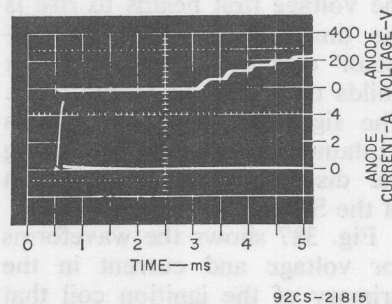


Fig. 385—SCR voltage (top) and current (bottom) as a function of time (2000 rpm; $V_{CC} = 12V$).

The small residual current is a result of the energy stored in the inverter transformer during the period that the inverter is inoperative. This stored energy causes a current to circulate from the secondary of the transformer through the SCR. When the ignition points close and the capacitor recharges, the SCR blocks the voltage on the capacitor.

The starting point for the waveform shown in Fig. 386 occurs at the instant that the igni-

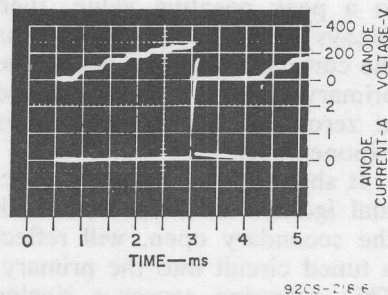
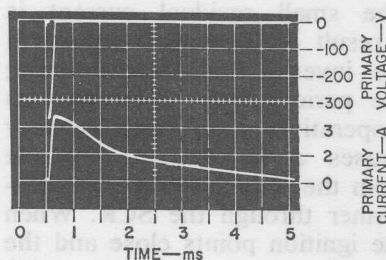


Fig. 386—SCR voltage (top) and current (bottom) as a function of time (oscilloscope sweep triggered at instant ignition breaker points are closing; 4000 rpm; $V_{CC} = 12V$).

tion points close. The period between the instant at which the points close and that at which the voltage first begins to rise is the time during which the collector current of transistor Q_1 builds up to the switching level. The significance of this time is explained subsequently during the discussion on commutation of the SCR.

Fig. 387 shows the waveforms for voltage and current in the primary of the ignition coil that result when a 7-millihenry inductor is used to simulate the



92CS-21817

Fig. 387—Primary voltage (top) and current (bottom) as a function of time (1-mH coil used in place of standard ignition coil; 2000 rpm; $V_{CC} = 12V$).

primary of the ignition coil. The primary voltage increases rapidly to a peak negative value, then decays sinusoidally to zero as the current builds to a peak. The primary voltage is then clamped at zero, and the current decays exponentially.

It should be noted that an actual ignition coil, operated with the secondary open, will reflect a tuned circuit into the primary. This operation causes a ringing on top of the waveforms, as shown in Fig. 387. The anode voltage of the SCR may actually

reverse for a short time because of this ringing. The SCR essentially blocks this reverse voltage except for a small current that flows because of the presence of positive gate signal. As a result, some instantaneous dissipation occurs in the reverse-blocking function of the SCR. The SCR can safely withstand this dissipation for the short period of time required. The gate signal is kept positive through the ringing cycle so that the SCR continues to conduct when the anode voltage rings back positive. This ringing does not occur when the secondary voltage fires a plug because the ionized plug shorts the secondary winding.

Protection Circuit

Inductance L_1 is used to protect the system against a shorted primary in the ignition coil. The limiting inductance controls the rate of change of current (di/dt) and peak current that occurs when the SCR is turned on with a short across the primary of the ignition coil. Resistance R_{13} is used to assure that the voltage across the primary of the ignition coil is not negative when the coil is open. If this voltage were not clamped, the regulator would not operate properly, and the peak collector voltage of transistor Q_1 would exceed the limits specified for the device.

Trigger Circuit

The triggering circuit performs the following functions: (1) trig-

gers and holds the SCR on when the ignition points open (at battery voltage down to 4 volts), (2) applies a signal back into the inverter shutdown circuitry when the ignition points are open, (3) suppresses the inverter signal that rides on the power supply so that it does not trigger the SCR, (4) prevents the residual voltage across the closed points from triggering the SCR, (5) prevents normal point bounce that occurs when the points close, and (6) maintains proper operation whether or not the capacitor is present across the breaker points. The 2N2102 transistor Q_4 is used to perform these functions.

The trigger current for the gate of the SCR is initiated when the base voltage of transistor Q_4 reaches approximately 0.6 volt above the emitter voltage. The trigger current flows from the supply through resistor R_{11} , transistor Q_4 , and capacitor C_3 to the gate of the SCR.

When the ignition points open, capacitor C_4 (and the capacitor across the points) charges because of the current through resistor R_3 . If the points are open long enough (without bouncing), the voltage across capacitor C_4 becomes high enough to turn on transistor Q_4 . The voltage required to turn on transistor Q_4 is the sum of the gate-cathode voltage of transistor Q_5 , the voltage across capacitor C_3 , the emitter-base voltage of transistor Q_4 , and the voltage drop across resistor R_{10} . (Resistor R_{10} ensures that the voltage across the open ignition points

rises to a value high enough to supply sufficient current through resistor R_7 to shut down the inverter.) At normal engine speeds, the average voltage level across capacitor C_3 keeps both the gate-cathode junction of the SCR and the emitter-base junction of the transistor reverse-biased until capacitor C_4 charges high enough to turn on transistor Q_4 . Because transistor Q_4 is off and the gate of the SCR is reverse-biased when the points are closed, the desired suppression of inverter signal and residual point voltage is achieved.

If the points bounce during normal operation, they discharge C_4 (and the distributor capacitor) almost instantly each time they close. Thus, each time they bounce open, these capacitors must recharge from zero toward the triggering level. With normal bouncing, the points do not stay open long enough for the triggering level to be reached, so the SCR is not triggered. If severe bouncing occurs at very high speeds, the points can stay open long enough to cause triggering of the SCR.

Better filtering is achieved when the automobile distributor capacitor is retained, but satisfactory operation is achieved without this capacitor. With the capacitor left in the distributor, it is possible to switch back to standard ignition by switching the plug shown in Fig. 381.

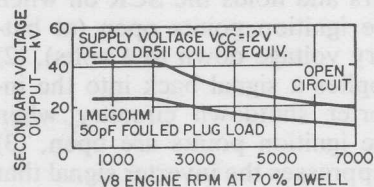
Commutation of SCR

All the parts of the system work together in such a manner as to

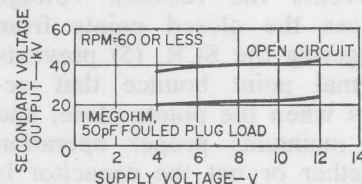
cause the SCR current to go to zero for a sufficient length of time to cause commutation (turn off). As explained earlier, the current through the primary of the ignition coil is switched from the SCR and into the commutating diode when the primary voltage decreases to zero. From that time on, the diode keeps the coil current clamped out of the SCR. The SCR then conducts only the small current that results from the energy stored in the inverter transformer. When the points close again, the inverter restarts and, as explained previously, the rectifying diode D_2 is reverse-biased during the time the collector current of transistor Q_1 builds back up to the switching level. No current then flows in the SCR, and the SCR is allowed to turn off. Fig. 385 shows that the current is zero for about 300 microseconds before anode voltage is re-applied at a rate of 0.5 volt per microsecond. A worst-case SCR commutates in less than 100 microseconds at a temperature of 100°C under these operating conditions.

Performance Data

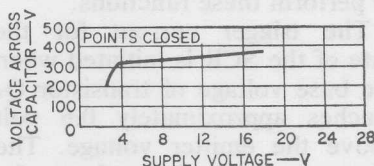
Fig. 388 shows several performance curves for the SCR capacitor-discharge ignition system. Fig. 389 shows the open-circuit output voltage as a function of time, and Fig. 390 shows the output voltage when the load on the secondary consists of a 1-megohm resistor in parallel with a 50-picofarad capacitor.



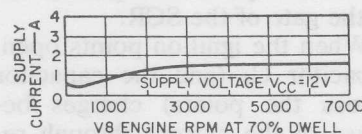
(a) Output voltage as a function of engine rpm at 12 volts for both an open secondary and a fouled-plug load.



(b) Output voltage as a function of battery voltage at cranking speeds for both an open secondary and a fouled-plug load.



(c) Regulation curve showing peak capacitor (and SCR) voltage as a function of battery voltage.

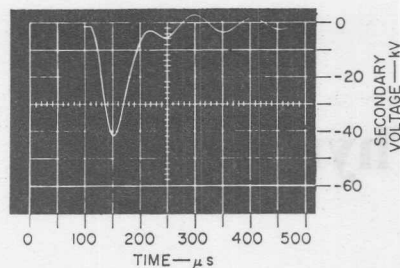


(d) Battery drain as a function of engine rpm at a battery voltage of 12 volts.

92CS-21818

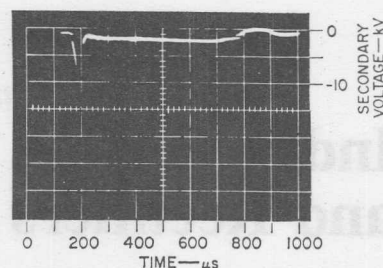
Fig. 388—Performance of the capacitor-discharge ignition circuit.

Figs. 391 and 392 show the secondary voltage under sparking conditions. Arc duration, as shown in Fig. 391, is 300 microseconds (single polarity) under wide-gap conditions. The narrower-gap conditions shown in Fig. 392 result in an arc duration of 400 microseconds.



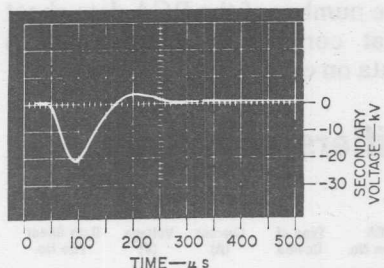
92CS-21819

Fig. 389—Open-circuit output voltage (standard ignition coil, Delco D511 or equivalent; 2000 rpm; $V_{CC} = 12V$).



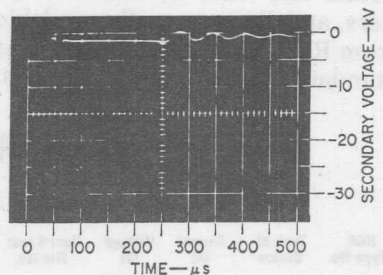
92CS-21821

Fig. 391—Output voltage showing duration of spark arc (standard ignition coil, Delco D511 or equivalent; 2000 rpm; $V_{CC} = 12 V$).



92CS-21820

Fig. 390—Output voltage with fouled spark plugs (standard ignition coil, Delco D511 or equivalent; 50-pF load in parallel with 1-megohm resistance; 2000 rpm; $V_{CC} = 12 V$).



92CS-21822

Fig. 392—Output voltage with spark gap shortened (standard ignition coil, Delco D511 or equivalent; 2000 rpm; $V_{CC} = 12V$).

Mounting Considerations

The SCR ignition circuit must be protected from moisture. Heat-generating components, however, should not be enclosed in non-circulating atmosphere. Still air has a thermal-resistance 12,000 times that of copper, and generation of heat in this high thermal resistance could cause the inside ambient temperature to rise above the specified limits. All components subject to high temperature rise (marked in Fig.

381 with a small circle) should be thermally connected to a low-thermal-resistance path to the outside environment. For example, the SCR may be mounted to an aluminum plate on a mica insulating washer. This plate should then be fastened to the inside of the chassis wall that provides the thermal path to the outside environment. The resistors and diodes which require a heat sink should be attached to the chassis with a thermally conductive epoxy.

Index to RCA Thyristors and Rectifiers

This section lists thyristors (triacs and SCR's), silicon rectifiers, and diacs currently available from RCA Solid State Division as standard commercial products.

Current and voltage ratings are included for each type, and the file number of the RCA data sheet that contains detailed technical data on each device is also shown.

RCA Thyristors, Rectifiers and Diacs

RCA Type No.	Type of Device	Current (A)	Voltage (V)	Data Sheet File No.	RCA Type No.	Type of Device	Current (A)	Voltage (V)	Data Sheet File No.
1N248C	Rectifier	20	50	6	1N1203A	Rectifier	12	300	20
1N249C	Rectifier	20	100	6	1N1204A	Rectifier	12	400	20
1N250C	Rectifier	20	200	6	1N1205A	Rectifier	12	500	20
1N440B	Rectifier	0.75	100	5	1N1206A	Rectifier	12	600	20
1N441B	Rectifier	0.75	200	5	1N1341B	Rectifier	6	50	58
1N442B	Rectifier	0.75	300	5	1N1342B	Rectifier	6	100	58
1N443B	Rectifier	0.75	400	5	1N1344B	Rectifier	6	200	58
1N444B	Rectifier	0.75	500	5	1N1345B	Rectifier	6	300	58
1N445B	Rectifier	0.75	600	5	1N1346B	Rectifier	6	400	58
1N536	Rectifier	0.75	50	3	1N1347B	Rectifier	6	500	58
1N537	Rectifier	0.75	100	3	1N1348B	Rectifier	6	600	58
1N538	Rectifier	0.75	200	3	1N1763A	Rectifier	1	400	89
1N539	Rectifier	0.75	300	3	1N1764A	Rectifier	1	500	89
1N540	Rectifier	0.75	400	3	1N2858A	Rectifier	1	50	91
1N547	Rectifier	0.75	600	3	1N2859A	Rectifier	1	100	91
1N1095	Rectifier	0.75	500	3	1N2860A	Rectifier	1	200	91
1N1183A	Rectifier	40	50	38	1N2861A	Rectifier	1	300	91
1N1184A	Rectifier	40	100	38	1N2862A	Rectifier	1	400	91
1N1186A	Rectifier	40	200	38	1N2863A	Rectifier	1	500	91
1N1187A	Rectifier	40	300	38	1N2864A	Rectifier	1	600	91
1N1188A	Rectifier	40	400	38	1N3193	Rectifier	0.75	200	41
1N1189A	Rectifier	40	500	38	1N3194	Rectifier	0.75	400	41
1N1190A	Rectifier	40	600	38	1N3195	Rectifier	0.75	600	41
1N1195A	Rectifier	20	300	6	1N3196	Rectifier	0.5	800	41
1N1196A	Rectifier	20	400	6	1N3253	Rectifier	0.75	200	41
1N1197A	Rectifier	20	500	6	1N3254	Rectifier	0.75	400	41
1N1198A	Rectifier	20	600	6	1N3255	Rectifier	0.75	600	41
1N1199A	Rectifier	12	50	20	1N3256	Rectifier	0.5	800	41
1N1200A	Rectifier	12	100	20	1N3563	Rectifier	0.4	1000	41
1N1202A	Rectifier	12	200	20	1N3879	Rectifier	6	50	726

RCA Thyristors, Rectifiers, and Diacs (cont'd)

RCA Type No.	Type of Device	Current (A)	Voltage (V)	Data Sheet File No.	RCA Type No.	Type of Device	Current (A)	Voltage (V)	Data Sheet File No.
1N3880	Rectifier	6	100	726	2N3228	SCR	5	200	114
1N3881	Rectifier	6	200	726	2N3525	SCR	5	400	114
1N3882	Rectifier	6	300	726	2N3528	SCR	2	200	114
1N3883	Rectifier	6	400	726	2N3529	SCR	2	400	114
1N3889	Rectifier	12	50	727	2N3650	SCR	35	100	408
1N3890	Rectifier	12	100	727	2N3651	SCR	35	200	408
1N3891	Rectifier	12	200	727	2N3652	SCR	35	300	408
1N3892	Rectifier	12	300	727	2N3653	SCR	35	400	408
1N3893	Rectifier	12	400	727	2N3654	SCR	35	50	724
1N3899	Rectifier	20	50	728	2N3655	SCR	35	100	724
1N3900	Rectifier	20	100	728	2N3656	SCR	35	200	724
1N3901	Rectifier	20	200	728	2N3657	SCR	35	300	724
1N3902	Rectifier	20	300	728	2N3658	SCR	35	400	724
1N3903	Rectifier	20	400	728	2N3668	SCR	12.5	100	116
1N3909	Rectifier	30	50	729	2N3669	SCR	12.5	200	116
1N3910	Rectifier	30	100	729	2N3670	SCR	12.5	400	116
1N3911	Rectifier	30	200	729	2N3870	SCR	35	100	578
1N3912	Rectifier	30	300	729	2N3871	SCR	35	200	578
1N3913	Rectifier	30	400	729	2N3872	SCR	35	400	578
1N5211	Rectifier	1	200	245	2N3873	SCR	35	600	578
1N5212	Rectifier	1	400	245	2N3896	SCR	35	100	578
1N5213	Rectifier	1	600	245	2N3897	SCR	35	200	578
1N5214	Rectifier	0.75	300	245	2N3898	SCR	35	400	578
1N5215	Rectifier	1	200	245	2N3899	SCR	35	600	578
1N5216	Rectifier	1	400	245	2N4101	SCR	5	600	114
1N5217	Rectifier	1	600	245	2N4102	SCR	2	600	114
1N5218	Rectifier	0.75	800	245	2N4103	SCR	12.5	600	116
1N5391	Rectifier	1.5	50	478	2N5441	Triac	40	200	593
1N5392	Rectifier	1.5	100	478	2N5442	Triac	40	400	593
1N5393	Rectifier	1.5	200	478	2N5443	Triac	40	600	593
1N5394	Rectifier	1.5	300	478	2N5444	Triac	40	200	593
1N5395	Rectifier	1.5	400	478	2N5445	Triac	40	400	593
1N5396	Rectifier	1.5	500	478	2N5446	Triac	40	600	593
1N5397	Rectifier	1.5	600	478	2N5567	Triac	10	200	457
1N5398	Rectifier	1.5	800	478	2N5568	Triac	10	400	457
1N5399	Rectifier	1.5	1000	478	2N5569	Triac	10	200	457
2N681	SCR	25	25	96	2N5570	Triac	10	400	457
2N682	SCR	25	50	96	2N5571	Triac	15	200	458
2N683	SCR	25	100	96	2N5572	Triac	15	400	458
2N684	SCR	25	150	96	2N5573	Triac	15	200	458
2N685	SCR	25	200	96	2N5574	Triac	15	400	458
2N686	SCR	25	250	96	2N5754	Triac	2.5	100	414
2N687	SCR	25	300	96	2N5755	Triac	2.5	200	414
2N688	SCR	25	400	96	2N5756	Triac	2.5	400	414
2N689	SCR	25	500	96	2N5757	Triac	2.5	600	414
2N690	SCR	25	600	96	2N6394	SCR	12	50	891
2N1842A	SCR	16	25	28	2N6395	SCR	12	100	891
2N1843A	SCR	16	50	28	2N6396	SCR	12	200	891
2N1844A	SCR	16	100	28	2N6397	SCR	12	400	891
2N1845A	SCR	16	150	28	2N6398	SCR	12	600	891
2N1846A	SCR	16	200	28	2N6400	SCR	16	50	892
2N1847A	SCR	16	250	28	2N6401	SCR	16	100	892
2N1848A	SCR	16	300	28	2N6402	SCR	16	200	892
2N1849A	SCR	16	400	28	2N6403	SCR	16	400	892
2N1850A	SCR	16	500	28	2N6404	SCR	16	600	892

RCA Thyristors, Rectifiers, and Diacs (cont'd)

RCA Type No.	Type of Device	Current (A)	Voltage (V)	Data Sheet File No.	RCA Type No.	Type of Device	Current (A)	Voltage (V)	Data Sheet File No.
D1201A	Rectifier	1	100	495	G5002M	GTO	8.5	600	867
D1201B	Rectifier	1	200	495	G5002A	GTO	8.5	100	867
D1201D	Rectifier	1	400	495	G5002B	GTO	8.5	200	867
D1201F	Rectifier	1	50	495	G5002D	GTO	8.5	400	867
D1201M	Rectifier	1	600	495	G5002M	GTO	8.5	600	867
D1201N	Rectifier	1	800	495	G5003A	GTO	8.5	100	867
D1201P	Rectifier	1	1000	495	G5003B	GTO	8.5	200	867
D1300A	Rectifier	0.25	100	784	G5003D	GTO	8.5	400	867
D1300B	Rectifier	0.25	200	784	G5003M	GTO	8.5	600	867
D1300D	Rectifier	0.25	400	784	S122A	SCR	8	100	889
D2101S	Rectifier	1	700	522	S122B	SCR	8	200	889
D2103S	Rectifier	3	700	522	S122C	SCR	8	300	889
D2103SF	Rectifier	3	750	522	S122D	SCR	8	400	889
D2201A	Rectifier	1	100	629	S122E	SCR	8	500	889
D2201B	Rectifier	1	200	629	S122F	SCR	8	50	889
D2201D	Rectifier	1	400	629	S122M	SCR	8	600	889
D2201F	Rectifier	1	50	629	S122S	SCR	8	700	889
D2201M	Rectifier	1	600	629	S2060A	SCR	4	100	654
D2201N	Rectifier	1	800	629	S2060B	SCR	4	200	654
D2406A	Rectifier	6	100	663	S2060C	SCR	4	300	654
D2406B	Rectifier	6	200	663	S2060D	SCR	4	400	654
D2406C	Rectifier	6	300	663	S2060E	SCR	4	500	654
D2406D	Rectifier	6	400	663	S2060F	SCR	4	50	654
D2406F	Rectifier	6	50	663	S2060M	SCR	4	600	654
D2406M	Rectifier	6	600	663	S2060Q	SCR	4	15	654
D2412A	Rectifier	12	100	664	S2060Y	SCR	4	30	654
D2412B	Rectifier	12	200	664	S2061A	SCR	4	100	654
D2412C	Rectifier	12	300	664	S2061B	SCR	4	200	654
D2412D	Rectifier	12	400	664	S2061C	SCR	4	300	654
D2412F	Rectifier	12	50	664	S2061D	SCR	4	400	654
D2412M	Rectifier	12	600	664	S2061E	SCR	4	500	654
D2520A	Rectifier	20	100	665	S2061F	SCR	4	50	654
D2520B	Rectifier	20	200	665	S2061M	SCR	4	600	654
D2520C	Rectifier	20	300	665	S2061Q	SCR	4	15	654
D2520D	Rectifier	20	400	665	S2061Y	SCR	4	30	654
D2520F	Rectifier	20	50	665	S2062A	SCR	4	100	654
D2520M	Rectifier	20	600	665	S2062B	SCR	4	200	654
D2540A	Rectifier	40	100	580	S2062C	SCR	4	300	654
D2540B	Rectifier	40	200	580	S2062D	SCR	4	400	654
D2540D	Rectifier	40	400	580	S2062E	SCR	4	500	654
D2540F	Rectifier	40	50	580	S2062F	SCR	4	50	654
D2540M	Rectifier	40	600	580	S2062M	SCR	4	600	654
D2600M	Rectifier	0.5	600	839	S2062Q	SCR	4	15	654
D2601A	Rectifier	1	100	723	S2062Y	SCR	4	30	654
D2601B	Rectifier	1	200	723	S2400A	SCR	4.5	100	567
D2601D	Rectifier	1	400	723	S2400B	SCR	4.5	200	567
D2601E	Rectifier	1	500	839	S2400D	SCR	4.5	400	567
D2601F	Rectifier	1	50	723	S2400M	SCR	4.5	600	567
D2601M	Rectifier	1	600	723	S2600B	SCR	7	200	496
D2601N	Rectifier	1	800	723	S2600D	SCR	7	400	496
D3202U	Diac	2 (pk)	25-40	577	S2600M	SCR	7	600	495
D3202Y	Diac	2 (pk)	29-35	577	S2610B	SCR	3.3	200	496
G5001A	GTO	8.5	100	867	S2610D	SCR	3.3	400	496
G5001B	GTO	8.5	200	867	S2610M	SCR	3.3	600	496
G5001D	GTO	8.5	400	867	S2620B	SCR	7	200	496

RCA Thyristors, Rectifiers, and Diacs (cont'd)

RCA Type No.	Type of Device	Current (A)	Voltage (V)	Data Sheet File No.	RCA Type No.	Type of Device	Current (A)	Voltage (V)	Data Sheet File No.
S2620D	SCR	7	400	496	S6230D	SCR	20	400	877
S2620M	SCR	7	600	496	S6230M	SCR	20	600	877
S2710B	SCR	1.7	200	266	S6240A	SCR	20	100	877
S2710D	SCR	1.7	400	266	S6240B	SCR	20	200	877
S2710M	SCR	1.7	600	266	S6240D	SCR	20	400	877
S2800A	SCR	10	100	890	S6240M	SCR	20	600	877
S2800B	SCR	10	200	890	S6250A	SCR	20	100	877
S2800C	SCR	10	300	890	S6250B	SCR	20	200	877
S2800D	SCR	10	400	890	S6250D	SCR	20	400	877
S2800E	SCR	10	500	890	S6250M	SCR	20	600	877
S2800F	SCR	10	50	890	S6400N	SCR	35	800	578
S2800M	SCR	10	600	890	S6410N	SCR	35	800	578
S2800S	SCR	10	700	890	S6420A	SCR	35	100	578
S3700B	SCR	5	200	306	S6420B	SCR	35	200	578
S3700D	SCR	5	400	306	S6420D	SCR	35	400	578
S3700M	SCR	5	600	306	S6420M	SCR	35	600	578
S3701M	SCCR	5	600	476	S6420N	SCR	35	800	578
S3702S	SCR	5	700	522	S6430A	SCR	35	100	877
S3703SF	SCR	5	750	522	S6430B	SCR	35	200	877
S3704A	SCR	5	100	690	S6430D	SCR	35	400	877
S3704B	SCR	5	200	690	S6430M	SCR	35	600	877
S3704D	SCR	5	400	690	S6430N	SCR	35	800	877
S3704M	SCR	5	600	690	S6440A	SCR	35	100	877
S3704S	SCR	5	700	690	S6440B	SCR	35	200	877
S3705M	SCR	5	600	839	S6440D	SCR	35	400	877
S3706E	SCR	5	500	839	S6440M	SCR	35	600	877
S3714A	SCR	5	100	690	S6440N	SCR	35	800	877
S3714B	SCR	5	200	690	S6450A	SCR	35	100	877
S3714D	SCR	5	400	690	S6450B	SCR	35	200	877
S3714M	SCR	5	600	690	S6450D	SCR	35	400	877
S3714S	SCR	5	700	690	S6450M	SCR	35	600	877
S3800D	ITR*	5	400	639	S6450N	SCR	35	800	877
S3800E	ITR*	5	500	639	S6493M	SCR	35	600	247
S3800EF	ITR*	5	550	639	S7410M	SCR	35	600	408
S3800M	ITR*	5	600	639	S7412M	SCR	35	600	724
S3800MF	ITR*	5	650	639	T2300A	Triac	2.5	100	470
S3800S	ITR*	5	700	639	T2300B	Triac	2.5	200	470
S3800SF	ITR*	5	750	639	T2300D	Triac	2.5	400	470
S5210B	SCR	10	200	757	T2301A	Triac	2.5	100	431
S5210D	SCR	10	400	757	T2301B	Triac	2.5	200	431
S5210M	SCR	10	600	757	T2301D	Triac	2.5	400	431
S6200A	SCR	20	100	418	T2302A	Triac	2.5	100	470
S6200B	SCR	20	200	418	T2302B	Triac	2.5	200	470
S6200D	SCR	20	400	418	T2302D	Triac	2.5	400	470
S6200M	SCR	20	600	418	T2304B	Triac	0.5	200	441
S6210A	SCR	20	100	418	T2304D	Triac	0.5	400	441
S6210B	SCR	20	200	418	T2305B	Triac	0.5	200	441
S6210D	SCR	20	400	418	T2305D	Triac	0.5	400	441
S6210M	SCR	20	600	418	T2306A	Triac	2.5	100	406
S6220A	SCR	20	100	418	T2306B	Triac	2.5	200	406
S6220B	SCR	20	200	418	T2306D	Triac	2.5	400	406
S6220D	SCR	20	400	418	T2310A	Triac	1.6	100	470
S6220M	SCR	20	600	418	T2310B	Triac	1.6	200	470
S6230A	SCR	20	100	877	T2310D	Triac	1.6	400	470
S6230B	SCR	20	200	817	T2311A	Triac	1.6	100	431

*Integrated thyristor and rectifier

RCA Thyristors, Rectifiers, and Diacs (cont'd)

RCA Type No.	Type of Device	Current (A)	Voltage (V)	Data Sheet File No.	RCA Type No.	Type of Device	Current (A)	Voltage (V)	Data Sheet File No.
T2311B	Triac	1.6	200	431	T4106M	Triac	15	600	406
T2311D	Triac	1.6	400	431	T4107B	Triac	10	200	406
T2312A	Triac	1.9	100	470	T4107D	Triac	10	400	406
T2312B	Triac	1.9	200	470	T4107M	Triac	10	600	406
T2312D	Triac	1.9	400	470	T4110M	Triac	15	600	458
T2313A	Triac	1.9	100	414	T4111M	Triac	10	600	457
T2313B	Triac	1.9	200	414	T4113B	Triac	15	200	443
T2313D	Triac	1.9	400	414	T4113D	Triac	15	400	443
T2313M	Triac	1.9	600	414	T4114B	Triac	10	200	443
T2316A	Triac	2.5	100	406	T4114D	Triac	10	400	443
T2316B	Triac	2.5	200	406	T4115B	Triac	6	200	443
T2316D	Triac	2.5	400	406	T4115D	Triac	6	400	443
T2500B	Triac	6	200	615	T4116B	Triac	15	200	406
T2500D	Triac	6	400	615	T4116D	Triac	15	400	406
T2506B	Triac	6	200	406	T4116M	Triac	15	600	406
T2506D	Triac	6	400	406	T4117B	Triac	10	200	406
T2700B	Triac	6	200	351	T4117D	Triac	10	400	406
T2700D	Triac	6	400	351	T4117M	Triac	10	600	406
T2706B	Triac	6	200	406	T4120B	Triac	15	200	458
T2706D	Triac	6	400	406	T4120D	Triac	15	400	458
T2710B	Triac	3.3	200	351	T4120M	Triac	15	600	458
T2710D	Triac	3.3	400	351	T4121B	Triac	10	200	457
T2716B	Triac	3.3	200	406	T4121D	Triac	10	400	457
T2716D	Triac	3.3	400	406	T4121M	Triac	10	600	457
T2800B	Triac	8	200	838	T4126B	Triac	15	200	406
T2800C	Triac	8	300	838	T4126D	Triac	15	400	406
T2800D	Triac	8	400	838	T4126M	Triac	15	600	406
T2800E	Triac	8	500	838	T4127B	Triac	10	200	406
T2800M	Triac	8	600	838	T4127D	Triac	10	400	406
T2801B	Triac	6	200	837	T4127M	Triac	10	600	406
T2801C	Triac	6	300	837	T4130B	Triac	15	200	878
T2801D	Triac	6	400	837	T4130D	Triac	15	400	878
T2801E	Triac	6	500	837	T4130M	Triac	15	600	878
T2802B	Triac	8	200	838	T4131B	Triac	10	200	878
T2802C	Triac	8	300	838	T4131D	Triac	10	400	878
T2802D	Triac	8	400	838	T4131M	Triac	10	600	878
T2802E	Triac	8	500	838	T4140B	Triac	15	200	878
T2802M	Triac	8	600	838	T4140D	Triac	15	400	878
T2806B	Triac	8	200	406	T4140M	Triac	15	600	878
T2806D	Triac	8	400	406	T4141B	Triac	10	200	878
T2850A	Triac	8	100	540	T4141D	Triac	10	400	878
T2850B	Triac	8	200	540	T4141M	Triac	10	600	878
T2850D	Triac	8	400	540	T4150B	Triac	15	200	878
T2856B	Triac	8	200	406	T4150D	Triac	15	400	878
T2856D	Triac	8	400	406	T4150M	Triac	15	600	878
T4100M	Triac	15	600	452	T4151B	Triac	10	200	878
T4101M	Triac	10	600	457	T4151D	Triac	10	400	878
T4103B	Triac	15	200	443	T4151M	Triac	10	600	878
T4103D	Triac	15	400	443	T4700B	Triac	15	200	300
T4104B	Triac	10	200	443	T4700D	Triac	15	400	300
T4104D	Triac	10	400	443	T4706B	Triac	15	200	406
T4105B	Triac	6	200	443	T4706D	Triac	15	400	406
T4105D	Triac	6	400	443	T6400N	Triac	40	800	593
T4106B	Triac	15	200	406	T6401B	Triac	30	200	459
T4106D	Triac	15	400	406	T6401D	Triac	30	400	459

RCA Thyristors, Rectifiers, and Diacs (cont'd)

RCA Type No.	Type of Device	Current (A)	Voltage (V)	Data Sheet File No.	RCA Type No.	Type of Device	Current (A)	Voltage (V)	Data Sheet File No.
T6401M	Triac	30	600	459	T6427B	Triac	30	200	406
T6404B	Triac	40	200	487	T6427D	Triac	30	400	406
T6404D	Triac	40	400	487	T6427M	Triac	30	600	406
T6405B	Triac	25	200	487	T6430B	Triac	40	200	878
T6405D	Triac	25	400	487	T6430D	Triac	40	400	878
T6406B	Triac	40	200	406	T6430M	Triac	40	600	878
T6406D	Triac	40	400	406	T6430N	Triac	40	800	878
T6406M	Triac	40	600	406	T6431B	Triac	30	200	878
T6407B	Triac	30	200	406	T6431D	Triac	30	400	878
T6407D	Triac	30	400	406	T6431M	Triac	30	600	878
T6407M	Triac	30	600	406	T6440B	Triac	40	200	878
T6410N	Triac	40	800	593	T6440D	Triac	40	400	878
T6411B	Triac	30	200	459	T6440M	Triac	40	600	878
T6411D	Triac	30	400	459	T6440N	Triac	40	800	878
T6411M	Triac	30	600	459	T6441B	Triac	30	200	878
T6414B	Triac	40	200	487	T6441D	Triac	30	400	878
T6414D	Triac	40	400	487	T6441M	Triac	30	600	878
T6415B	Triac	25	200	487	T6450B	Triac	40	200	878
T6415D	Triac	25	400	487	T6450D	Triac	40	400	878
T6416B	Triac	40	200	406	T6450M	Triac	40	600	878
T6416D	Triac	40	400	406	T6450N	Triac	40	800	878
T6416M	Triac	40	600	406	T6451B	Triac	30	200	878
T6417B	Triac	30	200	406	T6451D	Triac	30	400	878
T6417D	Triac	30	400	406	T6451M	Triac	30	600	878
T6417M	Triac	30	600	406	T8410B	Triac	80	200	894
T6420B	Triac	40	200	593	T8410D	Triac	80	400	894
T6420D	Triac	40	400	593	T8410M	Triac	80	600	894
T6420M	Triac	40	600	593	T8411B	Triac	60	200	725
T6420N	Triac	40	800	593	T8411D	Triac	60	400	725
T6421B	Triac	30	200	459	T8411M	Triac	60	600	725
T6421D	Triac	30	400	459	T8420B	Triac	80	200	894
T6421M	Triac	30	600	459	T8420D	Triac	80	400	894
T6426B	Triac	40	200	406	T8420M	Triac	80	600	894
T6426D	Triac	40	400	406	T8421B	Triac	60	200	725
T6426M	Triac	40	600	406	T8421D	Triac	60	400	725
					T8421M	Triac	60	600	725

Index

- A**bsolute Maximum System 105
 Absolute Maximum Ratings 105
 AC Voltage Regulator 292
 Circuit Operation 292
 Amperes Squared-Seconds (I^2t) 80
 Analysis of Basic Deflection Circuit 323
 Anode 9
 Application Guide to Trigger Devices 195
 Automotive Ignition System 358
 Basic Considerations For 350
 Capacitive-Charging Circuit 360
 Circuit Diagram 359
 Inverter 360
 Mounting Considerations 367
 Output Circuit 362
 Performance Data 362
 Protection Circuit 364
 Regulator 360
 SCR Commutation 365
 Trigger Circuit 364
 Auxiliary Capacitor C_A , Effect of 339
 Auxiliary Deflection-System Functions 327
 Auxiliary Power Supplies 343
 Avalanche 73
 Avalanche Breakdown 107
 Average Current 77
- B**asic Energy Relationships 11
 Basic Heat-Control Techniques 207
 Basic Thermal System 29
 Basic Thyristor Design and Rating Factors 99
 Basic Thyristor Triggering Techniques 185
 Blanking Signals 317
 Blocking Current 102
 "Boost" Regulator Circuit 342
 Breakdown 73
 Burst Signal 321
- C**apacitive-Discharge Ignition Systems 350
 Capacitive-Load Circuits 282
 Surge-Limiting Resistance 282
 Design Curves 284
 Case-to-Ambient Thermal Capacitance 40
 Case-to-Ambient Thermal Resistance 39
 Cathode 9
 Circuit Commutated Turn-Off Time 152
 Color Synchronization 316, 321
 Color-Sync Signal 321
 Commutating Capacitors 308
 Commutating di/dt 165
 Commutating dv/dt Capability (of Triacs) 163
 Commutation of Inverters SCR's 303
 Parallel-Capacitor 303
 Series-Capacitor 303
 Impulse 306
 Self-Impulse 306
 Auxiliary Impulse 308
 Composite Video Signal 316
 Concentrated Turn-On Losses 154
 Conduction 43
 Conduction Angle 177
 Controlled Solder Process 51
 Convection 43
 Conventional SCR's and Triacs 146
 Critical rate of rise of Commutation Voltage 163
 Current and Dissipation Ratings (GTO's) 118
- Current Flow 7
 Current Ratios 178
 Cylinder Pressure 350
- D**amper Diode 93
 DC Component 322
 DC Power Supplies 262
 DC Logic Circuitry, isolation of 253
 Diffusion Current 6
 Diode Biasing Network 98
 Doping Level 13
 Double-Time-Constant Circuit 229
 Drift Current 7
 Dynamic Resistance 73
- E**lectric-Range Control 216
 Energy Barrier 7
 Energy Storage 351
 External Heat Sink, Effect of 41
 External Heat Sinks, Selection of 43
- F**ailure Analysis 130
 Fast-Recovery Rectifiers 85
 Federal Communications
 Commission (FCC) 314
 Feedback Diode 93
 Fermi Energy Level 11
 Filament Preheat Circuit 225
 Filter Networks 275
 Filters, Type of 277
 Capacitance 277
 Inductance 277
 Choke-Input 278
 Capacitor-Input 279
 Resistance-Capacitance 280
 Combined LC 281
 Firing Angle 177
 Flash at Turn-Off 231
 Flashoner 223
 Flyback Diode 93
 Flywheel-Charged Ignition Systems 356
 Flywheel Diode 93
 Forbidden-Energy Region 12
 Forward-Bias Conditions 15
 Forward-Blocking State 16
 Forward-Conducting State 16
 Forward Current 77
 Forward Voltage Drop 72
 Four-Diode Doubler Circuit 271
 Forward breakover voltage 102
 Forward On-State Voltage 102
 Fuses 225
- G**ate 10
 Gate Characteristics 138
 Gate Nontrigger voltage 139
 Gate Signal, Effect of on Breakover Voltage 104
 GTO Characteristic 103
 Gate-Controlled Turn-Off 22
 General Mathematical Relationships 35
 General Physical Theory 3
 GTO Devices 148
 Gate Turn-Off SCR's (GTO's) 10
- H**eat Control, Basic Techniques 207
 Heat Controls with Isolated Sensors 212

- Heater-Voltage Regulator 294
 Circuit Description 294
 Performance Characteristics 296
 Heating Controls 206
 General Design Considerations 206
 Heat Sinks 45
 Performance Criteria 45
 Physical Criteria 44
 Types of 44
 Typical Examples 48
 Heat-Sink Insulators, Effect of 42
 Heat-Sink Mounting, General Procedures 54
 Heat-Sinks, Types of 44
 Cylindrical Horizontal-Finned 45
 Cylindrical or Radial Vertical-Finned 45
 Flat Vertical-Finned 44
 Heat-Transfer Methods 43
 High-Voltage Generation 328, 340
 High-Voltage Rectifiers for TV Receivers 269
 Holding and Latching Currents 122
 Hysteresis Effect 228
- I**dling 98
 Ignition Systems, Capacitive Discharge 350
 Basic Systems 352
 Circuit Operation 352
 Component Requirements 354
 Technical Features 353
 Types of 355
 Impurities 4
 Incandescent Lighting Controls 223
 Surge-Current Considerations 223
 Inductive Load, Three-Phase 259
 Initial Brightness 227
 Inrush Current 224
 Integrated-Circuit Zero-Voltage Switch 199
 Basic Circuit Operation 199
 Effects on Thyristor
 Load Characteristics 203
 Fail-Safe Feature 203
 Half-Cycling and
 Hysteresis Characteristics 204
 Interlaced Scanning 315
 Inverter-Charged Ignition Systems 357
 Isolated Trigger Circuits 195
- J**unction-to-Case Thermal Impedance 36
- L**amp Dimmers 226
 Lead-Bending Techniques 53
 Line-Charged Igniter 358
 Line-Voltage-Regulated DC Power Supply 297
 Logic Circuitry, DC, Isolation of 253
- M**agnitude and Rate of Rise of
 Reapplied Forward Voltage 153
 Maximum Average Forward-Current
 Rating $I_F(AV)$ 78
 Maximum Average On-State Current 116
 Maximum Junction Temperature 32
 Maximum Ratings 74
 Absolute Maximum System 74
 Design Center System 75
 Design Maximum System 75
 Maximum rms On-State Current Rating 116
 Maximum Junction Temperature 111
 Multiple Rectifier Connections 84
 Parallel Arrangements 84
 Series Arrangements 85
 Multiplier, Three-Diode 271
- N**ational Television Systems
 Committee (NTSC) 314
 Negative Gate Bias 153
 Neon Bulbs 190
 Nonrepetitive Peak Off-State Voltage 110
 Nonrepetitive Peak Reverse Voltage 111
- O**ff-State Voltage, Critical Rate of Rise of 124
 Off-State Voltage, Total 110
 On-Off Control 209
 On-State Current 152
 On-State Current, Critical Rate of Rise of 123
 On-State Current Ratings (SCR's and Triacs) 113
 Off-State Voltage Ratings 109
- P**ackages, Handling and Mounting 52
 Peak Current 77
 Peak OFF/State Voltages 109
 Peak Reverse Voltage 75
 Pellet Structures 99
 Phase Control 177
 Photocell-Operated ON-OFF
 Lamp Controls 233
 Photocell Trigger Circuits 199
 Picture Information 316
 p-n Junction 6
 Polyphase Rectifiers 272
 Three-Phase, Half-Wave,
 Delta-Wye Rectifier 273
 Three-Phase, Full-Wave,
 Delta-Wye Bridge Rectifier 273
 Three-Phase, Delta-Star
 (Six-Phase), Half-Wave Rectifier 273
 Three-Phase, Delta-Wye
 (Six Phase), Half-Wave Rectifier 274
 Press-Fit Packages 62
 Principal Voltage-Current Characteristics 101
 Product Matrices 132
 Proportional Heating Controls 210
 Pulse Transformers 198
 Pulse Triggering 140
- R**adiation 43
 Raster Correction 329
 Ratings and Limiting Characteristics 105
 RCA Thyristors, Rectifiers, and Diacs,
 Index to 368
 Recovery Characteristics, Types of 87
 Recovery-Time Test Circuit 89
 Rectifier Circuits 263
 Single-Phase 263
 Half-Wave 263
 Full-Wave 265
 Full-Wave Bridge 266
 Voltage-Multiplier 266
 Full-Wave Voltage Doubler 267
 Half-Wave Voltage Doubler 268
 n-Times Voltage Multipliers 269
 Rectifier Diode 7
 Rectifier Packages, Low- and
 Medium Power 55
 Rectifier Potential-Energy Analysis 13
 Rectifier Product Matrix 70, 71
 Rectifier Voltage and Current Ratios 275
 Reed Relays 198
 Regulated DC Power Supplies Using
 Thyristor Pass Elements 287
 Regulation Technique 293
 Reliability 127
 Reliability Testing 127

Repetitive Peak Forward-Current Rating I_{FRM}	78	Thermal Impedances	30, 35
Repetitive Peak Reverse Voltage	110	Thermal Resistance	30
Resistive Load, Three-Phase	254	Thermal Runaway	32
Resistivity	4	Thermal-Stability Requirements	32
Reverse-Bias Conditions	15	Thermal Systems, Basic	29
Reverse-Blocking Thermal Runaway	73	Third-Harmonic Tuning	326
Reverse Blocking Voltage	154	Three-Diode Multiplier	271
Reverse Voltages	110	Three-Phase Inductive Load	259
Reverse Current	73	Three-Phase Resistive Load	254
Reverse-Recovery Current	74	Thyristor Equivalent-Model Analyses	24
Reverse-Recovery Time	73, 152	Thyristor Gating and Switching Requirements	138
RMS Current	77	Thyristor Packages,	56
S can Linearity Correction	328	Flexible-Lead (TO-5-Style)	56
Scanning	314	Flanged-Case	56
SCR Characteristic	102	Versawatt (Molded-Plastic)	63
SCR Horizontal Deflection Systems	314	Thyristor Potential-Energy Analysis	15
For Color TV Receivers	344	Thyristor Structures	9
For Monochrome TV Receivers	348	Thyristor Triggering	177, 207, 292
Functional Description	333	Thyristors	9
SCR Inverter	309	Thyristors and Rectifiers,	368
Circuit Operation	310	Index to RCA Types	6
Gate-Trigger-Pulse Generator	312	Transition Region	236
Applications	313	Traffic Control Flasher	234
SCR Inverters and Converters	301	Traffic Signal Lamp Controls	76
SCR Turn-Off Time, Effect of on	152	Transient Reverse Voltage Rating	11
Operation Conditions	10	Triacs	103
Silicon Controlled Rectifiers (SCR's)	9, 70	Triac Characteristic	253
Silicon Rectifiers	72	Triac Controls for Three-Phase	141
Electrical Characteristics	3	Power Systems	191
Semiconductor Materials	230	Trigger-Circuit Requirements	228
Series Gate Resistor, Effect of	227	Trigger Diodes (Diacs)	188
Single-Time-Constant Circuit	173	Trigger-Device Characteristics	188
Snubber Design Procedure	169	Triggering Devices	139
Snubber Networks	53	Basic Requirements	18
Soldering Methods	350	Turn-Off	156
Spark Plugs	351	Turn-Off Switching (For GTO's)	151
Condition of	351	Turn-Off Time (For SCR's)	155
Polarity	95	Turn-Off Time Text Circuit	145
Voltage Waveshape	95	Turn-On Time	26
Special-Function Rectifiers	96	Two-SCR Analogy of a Triac	24
Controlled-Avalanche Rectifiers	97	Two-Transistor Analogy of an SCR	194
Voltage-Reference Diodes	216	Two-Transistor Switch	193
Compensating Diodes	314	U nijunction Transistor	63
Staged Heat Controls	114	V ersawatt Thyristor Packages	63
Standards for Scanning and Synchronization	197	Lead-Forming Techniques	65
Steady-State Ratings	58	Mounting	65
Step-Down Transformers	78	Special Thermal Considerations	68
Stud Packages	79	Cleaning After Mounting	106
Surge Current	117	Voltage Breakdown	271
Surge-Current Rating Curve	145	Voltage Quadrupler	271
Surge Ratings	317	Voltage Tripler	293
Switching Characteristics	152	Voltage Waveforms	73
Synchronizing Signals	50	Z ener	232
T emperature	30	Zero-Voltage-Switched Circuit	208
Thermal Fatigue	29	Zero-Voltage-Switched Controls	183
Thermal-Fatigue Considerations		Zero-Voltage Switching	
Thermal Capacitance			
Thermal Considerations			